3C empresa
Investigación y pensamiento crítico

Ed. 51_Iss. 12_N.1
January - March, 2023

ISSN: 2254-3376

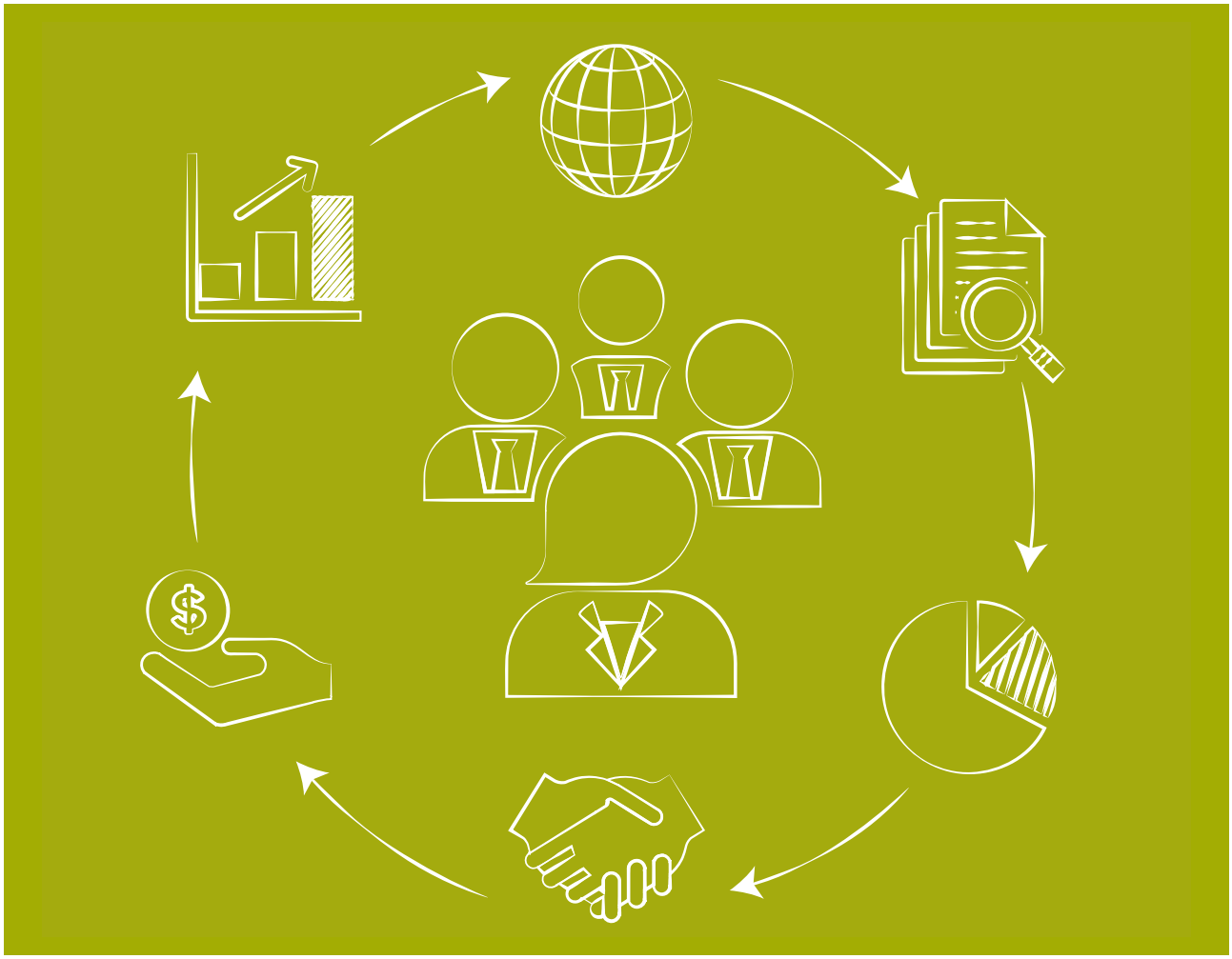

https://doi.org/10.17993/3cemp.2023.120151

3C Empresa. Investigación y pensamiento crítico.

Quarterly periodicity.

Edition 51, Volume 12, Issue 1 (January - March, 2023).

National and internacional circulation.

Articles reviewed by the double blind peer evaluation method.

ISSN: 2254 - 3376
Legal: A 268 - 2012
DOI: https://doi.org/10.17993/3cemp.2023.120151

Edita:
Área de Innovación y Desarrollo by UP4 Institute of Sciences, S.L.
info@3ciencias.com _ www.3ciencias.com

https://doi.org/10.17993/3cemp.2023.120151

https://doi.org/10.17993/3cemp.2023.120151

EDITORIAL BOARD

https://doi.org/10.17993/3cemp.2023.120151

AIMS AND SCOPE

PUBLISHING GOAL

3Ciencias wants to transmit to society innovative projects and ideas. This goal is reached thought the publication of original articles which are subdue to peer review or thorough the publication of scientific books.

TEMATIC COVERAGE

3C Empresa is a scientific - social journal, where original works are spread, written in English, for dissemination with empirical and theoretical analyzes on financial markets, leadership, human resources, market microestructure, public accounting and bussines management.

OUR TARGET

- Research staff.
- PhD students.
- Professors.
- Research Results Transfer Office.
- Companies that develop research and want to publish some of their works.

SUBMISSION GUIDELINES

3C Empresa is an arbitrated journal that uses the double-blind peer review system, where external experts in the field on which a paper deals evaluate it, always maintaining the anonymity of both the authors and of the reviewers. The journal follows the standards of publication of the APA (American Psychological Association) for indexing in the main international databases.

Each issue of the journal is published in electronic version (e-ISSN: 2254-3376), each work being identified with its respective DOI (Digital Object Identifier System) code.

STRUCTURE

The original works will tend to respect the following structure: introduction, methods, results, discussion/conclusions, notes, acknowledgments and bibliographical references.

The inclusion of references is mandatory, while notes and acknowledgments are optional. The correct citation will be assessed according to the 7th edition of the APA standards.

https://doi.org/10.17993/3cemp.2023.120151

PRESENTATION WORK

All the information, as well as the templates to which the works must adhere, can be found at:

https://www.3ciencias.com/en/journals/infromation-for-authors/

https://www.3ciencias.com/en/regulations/templates/

ETHICAL RESPONSIBILITIES

Previously published material is not accepted (they must be unpublished works). The list of signatory authors should include only and exclusively those who have contributed intellectually (authorship), with a maximum of 4 authors per work. Articles that do not strictly comply with the standards are not accepted.

STATISTICAL INFORMATION ON ACCEPTANCE AND INTERNATIONALIZATION FEES

- Number of accepted papers published: 20.
- Level of acceptance of manuscripts in this number: 66,7%.
- Level of rejection of manuscripts: 33,3%.
- Internationalization of authors: 3 countries (India, Spain, China).

Guidelines for authors: https://www.3ciencias.com/en/regulations/instructions/

https://doi.org/10.17993/3cemp.2023.120151

INDEXATIONS

https://doi.org/10.17993/3cemp.2023.120151

INDEXATIONS

https://doi.org/10.17993/3cemp.2023.120151

/SUMMARY/

https://doi.org/10.17993/3cemp.2023.120151

https://doi.org/10.17993/3cemp.2023.120151

https://doi.org/10.17993/3cemp.2023.120151

https://doi.org/10.17993/3cemp.2023.120151

/01/

KEY TECHNOLOGIES OF SMART FACTORY MACHINE VISION BASED ON EFFICIENT DEEP NETWORK MODEL

Fangfang Zhang*

School of Fine Arts, Weifang College, Weifang, Shandong, 261061, China

20110738@wfu.edu

Kunfan Wang

College of Grammar, Northeast Forestry University, Harbin, Heilongjiang, 150040, China

Reception: 12/11/2022 **Acceptance:** 26/12/2022 **Publication:** 10/01/2023

Suggested citation:

Z., Fangfang and W., Kunfan (2023). **Key technologies of smart factory machine vision based on efficient deep network model**. *3C Empresa. Investigación y pensamiento crítico, 12(1)*, 15-35. https://doi.org/10.17993/3cemp.2023.120151.15-35

https://doi.org/10.17993/3cemp.2023.120151.15-35

ABSTRACT

Most of the existing smart space machine vision technologies are oriented to specific applications, which are not conducive to knowledge sharing and reuse. Most smart devices require people to participate in control and cannot actively provide services for people. In response to the above problems, this research proposes a smart factory based on a deep network model, which is capable of data mining and analysis based on a huge database, enabling the factory to have self-learning capabilities. On this basis, tasks such as optimization of energy consumption and automatic judgment of production decisions are completed. Based on the deep network model, the accuracy of the model for image analysis is improved. Increasing the number of hidden layers will cause errors in the neural network and increase the amount of calculation. The appropriate number of neurons can be selected according to the characteristics of the model. When the IoU threshold is taken as 0.75, its performance is improved by 1.23% year-on-year. The residual structure composed of asymmetric multiple convolution kernels not only increases the number of feature extraction layers, but also allows the asymmetric image details to be better preserved. The recognition accuracy of the trained deep network model reaches 99.1%, which is much higher than other detection models, and its average recognition time is 0.175s. In the research of machine vision technology, the smart factory based on the deep network model not only maintains a high recognition accuracy rate, but also meets the real-time requirements of the system.

KEYWORDS

Smart factory; Deep network model; Machine vision; Image processing; Model optimization

https://doi.org/10.17993/3cemp.2023.120151.15-35

PAPER INDEX

https://doi.org/10.17993/3cemp.2023.120151.15-35

1. INTRODUCTION

With the development and innovation of computer science and communication technology, the degree of intelligence of computing is also getting higher and higher. Smart space is a typical distributed system, so the acquired situational data has distributed characteristics [1, 2]. Context-aware applications need to synthesize distributed context data and perform appropriate storage management for the collected context data. On this basis, the data is analyzed to provide usable information for the users of the smart space [3,4]. Smart factory is a typical application of smart space, which realizes the application of situational awareness in smart factory [5]. Its main task is to proactively eliminate the fault and prompt the cause of the fault when a fault occurs in the operation of the smart factory. Introduce the sources of contextual data and use ontology-based hierarchical modeling methods to model application scenarios [6]. Finally, the rule setting of situational reasoning is explained, and the reasoning result is analyzed. A smart factory is defined as a factory that can intelligently perceive situational information and use situational awareness technology to help people and machines perform tasks. Industrial robots have the characteristics of high work efficiency, high work quality, and high repeat positioning accuracy. It is a development trend for industrial robots to replace manual labor. However, the robot does not have the developed human brain and visual system, and cannot adjust the movement trajectory according to the specific environment. These problems can be well solved by robot vision, and machine vision technology is the key to the transformation from traditional production to intelligent production [7].

The information of the entire production process is collected by sensors and smart devices in the smart factory, and transmitted to the upper computer for development and utilization [8]. Zhang et al. [9] used the graph-optimized SLAM algorithm to construct a two-dimensional grid map of the physical simulation environment of the printing smart factory, and designed a combined navigation scheme combining the SLAM algorithm and the dynamic window method (DWA). The simulation results verify the accessibility of global path planning and the feasibility of local path obstacle avoidance. , Jerman et al. [10] proposed a case study on the impact of Industry 4.0 on the business model of smart factories for the key elements of smart factories. Its main objective will be that the roles of employees working in production will be primarily to express their creativity, to make emergency interventions and to perform process custody. The key factors influencing smart factory business models are top management and leadership orientation, employee motivation, collective intelligence, creativity and innovation. The study provides useful guidance for the strategic management of innovative companies in the early stages of the decision-making process. SHANTHIKUMAR et al. [11] have a limited level of operational control in scheduling for each factory, assigning different types of products to different factories. In a dedicated factory, only similar products are produced in the same factory. A multi-server, multi-job-class queuing model is established, and the model is used to form a centralized factory to handle similar tasks. In intelligent manufacturing, machine vision is the "eye" of the machine and the "brain" of vision. The machine vision module is composed of cameras, light sources, brackets, computers, etc., and can meet the

https://doi.org/10.17993/3cemp.2023.120151.15-35

needs of rich vision applications such as visual positioning, measurement, detection and identification. Machine vision is used to collect images, which can carry out continuous acquisition and external control acquisition. [12] expounded the role and importance of machine vision systems in industrial applications. The intended function of a vision machine is to exploit and impose the environmental constraints of the scene, capture images, analyze the captured images, and identify certain objects and features in each image. and initiate follow-up actions to accept or reject the corresponding object. Application areas include automated visual inspection (AVI), process control, part identification, and play an important role in the guidance and control of robots. Looking ahead to the development of manufacturing, it is possible to improve reliability, improve product quality, and provide technical support for new production processes. Chen et al. [13] studied the hardware and software requirements and recent developments of machine vision systems, focusing on the analysis of multispectral and hyperspectral imaging in modern food inspection. Future trends in the application of machine vision technology are discussed. Robie et al. [14] investigated the development of machine vision techniques for the automated quantitative analysis of social behavior, greatly improving the scale and resolution at which we analyze interactions between members of the same species. Several components of machine vision-based analysis are discussed: high-quality video recording methods for automated analysis, video-based tracking algorithms for estimating the position of interacting animals, and machine learning methods for identifying interaction patterns. The applicability of these methods is very general, reviewing the successful application to biological problems in several model systems with very different types of social behavior. [15] studied the Lambert diffuse model for computational vision applications, and the Lambertian model can be shown to be a very inaccurate approximation of the diffuse component. The brightness of Lambertian surfaces is independent of the viewing direction, whereas the brightness of rough diffuse surfaces increases as the observer approaches the source direction. The model takes into account complex geometric and radiation phenomena such as masking, shadowing and inter-reflection between surface points. The resulting reflectance measurements are in strong agreement with the model-predicted reflectance values. Davies et al. [16] studied the application progress of machine vision in the field of food and agriculture since 2000. It involves applying different wavelengths of radiation to the material, not only looking at the surface but also the internal structure. With its powerful feature learning capabilities, deep networks have been widely used in machine vision such as face recognition [17], semantic segmentation [18], and human pose detection [19]. Among them, convolutional neural network has become one of the most successful image analysis models and is widely used in the field of computer vision. In addition to training deep neural networks in a single feed-forward manner, recurrent neural networks, a deep model that captures temporal information, are more suitable for prediction of sequence data of arbitrary length. Agarwal et al. [20] proposed a new deep neural network-based approach that relies on coarse-grained sentence modeling. Use convolutional neural network and recurrent neural network (RNN) models combined with specific fine-grained word-level similarity matching models. The proposed deep paraphrase-based method achieves

https://doi.org/10.17993/3cemp.2023.120151.15-35

good results in both types of text and is thus more robust and general than existing methods. Tai et al. [21] made great breakthroughs in the field of computer vision by using deep learning for the obstacle avoidance problem of mobile robots, especially in recognition and cognitive tasks. Taking the original depth image as input, generating control commands as network output and realizing model-free obstacle avoidance behavior. [22] proposed an end-to-end trainable deep network structure based on a Gaussian Conditional Random Field (GCRF) model for image denoising. The proposed deep network explicitly models the input noise variance and is able to handle a range of noise levels. Experiments on the Berkeley segmentation and PASCALVOC datasets show that the proposed method produces the same results as the state-of-the-art without training a separate network for each individual noise level. Bai et al. [23] studied a novel comprehensive solution for the compression and acceleration of visual question answering systems. The algorithm uses long and short-term memory to compress convolutional neural networks to improve processing speed. To further compress this parameter, a tensor shrinking layer is used to compress the feature flow between layers.

To sum up, in the traditional fault diagnosis, the production efficiency of the factory is reduced due to the poor communication of information. It is difficult for the management of the factory to get the fault information of the factory and make a response at the first time. Smart factories can provide an intelligent fault detection service that supports dynamic collection of abnormal event information, real-time transmission, and abnormal response-level monitoring. The smart factory machine vision technology built with the help of efficient deep network model provides a guarantee for troubleshooting events and improving the operating efficiency of the factory. When equipment in the smart factory fails, the factory control center can quickly obtain abnormal information. At the same time, relevant maintenance personnel can obtain real-time warnings and fault-related information through mobile devices such as mobile phones.

2. DEEP NETWORK MODEL

Deep learning, which attempts to capture high-level abstract features through multiple nonlinear transformations and hierarchical representation structures, has become a hot research topic. According to the input of the network and the function of the network, it is divided into four categories: convolutional neural network, recurrent neural network, graph convolutional network and binary network. The input of the first three networks is static image or vector, sequence and graph data respectively. The binary network is based on the existing deep model, and further quantifies the network weights and activations.

2.1. CONVOLUTIONAL NEURAL NETWORK

Convolutional neural networks are currently one of the most successful image analysis models and are widely used in various computer vision tasks [24, 25]. The design of its model was first inspired by biologists' research on the biological functions

https://doi.org/10.17993/3cemp.2023.120151.15-35

of human brain nerve cells. Convolutional neural network has made great progress in the field of deep learning and is the mainstream in the field of image related. Different from the traditional neural network, its original image can be directly input into the convolutional neural network for calculation. Simplified image preprocessing is a feedforward neural network. The main structure of the convolutional neural network layer is: input layer, convolutional layer, pooling layer and fully connected layer.

In practical applications, the experience of human-computer interaction is often at the millisecond level. Only by solving the efficiency problem of convolutional neural networks can convolutional neural networks be more widely used in various mobile devices. The usual method is to perform model compression, that is, to perform compression on the already trained model, so that the network carries fewer network parameters. The mathematical formula for the convolutional layer is as follows:

$$X_j^L = f\left(\sum_{i=1}^{M} W_{ij}^L * X_i^{L-1} + W_b\right) \tag{1}$$

where X_j^L is the output feature of the convolutional layer, f(•) is the activation function, W_{ij}^L is the convolution kernel weight matrix, X_i^{L-1} is the input image feature, and W_b is the bias value.

2.2. RECURRENT NEURAL NETWORK

There are many sequential data in real-world problems, such as text, speech, and video, which have obvious temporal correlations [26]. The output and input of traditional neural networks (such as CNN) are independent of each other, have no memory ability, and cannot use the correlation in time series. For this reason, as early as 1986, the Jordan network proposed by Bilski et al. directly feeds the final output of the entire network back to the input layer of the network through the delay module, so that all layers of the entire network are recursive. Recurrent Neural Network (RNN) is a network designed for sequence signal processing and is suitable for predicting sequence data of arbitrary length. The state of the hidden layer inside the RNN is cyclic, and the state of the hidden layer depends not only on the current input but also on the state of the previous hidden layer.

$$\begin{aligned} \boldsymbol{o}_t &= g\left(\mathbf{V}\boldsymbol{s}_t\right) \\ \boldsymbol{s}_t &= f\left(\mathbf{U}\boldsymbol{x}_t + \mathbf{W}\boldsymbol{s}_{t-1}\right) \end{aligned} \tag{2}$$

where V is the output weight matrix, U is the weight matrix of the input x_t, W is the weight matrix of the input s_{t-1} at the previous moment, and f(·), g(·) are the activation functions.

Each memory unit module uses three gate structures: input gate, output gate and forget gate to control the hidden state at different times, and to model the temporal correlation in the sequence. Great success in automatic speech recognition, music creation, grammar learning, and even image tagging. At present, LSTM has been

https://doi.org/10.17993/3cemp.2023.120151.15-35

widely used in classification-based tasks, and combined with convolutional neural networks, images can be automatically annotated.

2.3. DEEP GRAPH CONVOLUTIONAL NEURAL NETWORKS

Existing convolutional neural networks utilize a large amount of trainable data to efficiently accelerate computing resources (GPU).

The unique network structure and efficient training mechanism can effectively extract data feature representations from Euclidean space data such as images, texts and videos for various tasks [27, 28]. Graph convolutional networks well-designed for different tasks continue to emerge, including attention graph neural networks, graph autoencoders, graph generative networks, and graph spatiotemporal networks. The attention mechanism has proved useful in multiple tasks, and the essence of the attention map neural network is to assign weights to different neighbors when aggregating feature information. The goal is to embed node feature representations into a low-dimensional vector space through neural networks, and utilize decoders to reconstruct the nearest neighbor statistics of nodes. Use a graph neural network to generate probabilistic dependencies between nodes and edges of a graph. The input to each node changes over time, and the graph spatiotemporal network captures both the temporal and spatial dependencies of the spatiotemporal graph. The spectral domain-based graph convolution and the spatial domain-based graph convolution introduce convolution kernels from the perspective of graph signal processing to define graph convolution. The feature extraction of nodes is realized by the feature decomposition of the Laplacian matrix of the graph, and the information of adjacent nodes in the graph is aggregated.

Spatial features in graph data have the following characteristics:

1) Node characteristics: each node has its own characteristics;

2) Structural features: Each node in the graph data has structural features, that is, there is a certain relationship between nodes and nodes. Graph data needs to consider both node information and structural information. Graph convolutional neural networks can automatically learn not only node features, but also the association information between nodes.

Suppose there is a set of graph data, which has N nodes (nodes), each node has its own characteristics. Let the features of these nodes form an N×D-dimensional matrix X, and then the relationship between each node will also form an N×N-dimensional matrix A. The way it propagates from layer to layer is:

$$H^{(l+1)} = \sigma\left(\hat{D}^{-\frac{1}{2}} \hat{A} \hat{D}^{-\frac{1}{2}} H^{(l)} W^{(l)} \right). \tag{3}$$

Among them, A wave=A+I, I is the unit matrix, D wave is the degree matrix of A wave, H is the feature of each layer, and for the input layer, H is X_{σ} is the nonlinear activation function.

https://doi.org/10.17993/3cemp.2023.120151.15-35

2.4. MODEL TRAINING AND EVALUATION METRICS

When testing the performance of deep learning models, the smaller the memory occupied by the model, the faster the detection speed and the higher the accuracy, the stronger the performance. The evaluation index is a quantitative index for the performance of the model. One evaluation index can only reflect part of the performance of the model. If the selected evaluation index is unreasonable, wrong conclusions may be drawn. Therefore, different evaluation indexes should be selected for specific data and models. For the trained model, a model evaluation coefficient is required to measure the accuracy of the model. The mean absolute error MAE and the coefficient of determination are widely used in the evaluation of model accuracy, and the expressions are:

$$MAE = \frac{1}{m}\sum_{j=1}^{m}\left|y_j^{'} - y_j\right| \tag{4}$$

$$R^2 = 1 - \frac{\sum_{j=1}^{m}\left(y_j - y_j^{'}\right)^2}{\sum_{j=1}^{m}\left(y_j - \bar{y}\right)^2} \tag{5}$$

In the formula, $y_j^{'}$ and y_j represent the predicted value and the true value of the j th sample respectively; $\bar{y}$ represent the average value of the true value of the sample; m represent the number of samples. The smaller the value of the mean absolute error MAE, the smaller the error of the model and the better the effect: the coefficient of determination R^2 is a value from 0 to 1, which indicates the goodness of fit, and the closer its value is to 1, the better the model fitting effect. the better.

In target detection, IOU is used to represent the coincidence area of the predicted detection frame and the real frame. The larger the value, the more accurate the algorithm positioning is. The mathematical formula is as follows:

$$\mathrm{IOU} = \frac{A \cap B}{A \cup B} \tag{6}$$

3. SMART FACTORY VISION TECHNOLOGY APPLICATION

A smart factory is a complex production system that requires the high precision, immediacy and reproducibility of machine vision perception control technology [29-30]. The systematic scheme of machine vision perception control in smart factories relies on the actual production needs to design the intelligent vision imaging system and the automatic image acquisition part in sequence. Images of objects are collected. The second-step processing is performed on the obtained clear and high-

https://doi.org/10.17993/3cemp.2023.120151.15-35

quality images. The image content is judged and classified and screened according to the pre-set information base to complete the identification, inspection, measurement and calculation of the detection object. The information obtained in the processing of the image allows for appropriate optimization control.

3.1. MACHINE VISION DEVELOPMENT PRINCIPLES

The machine vision system performs the detection function of the measured object based on the computer, and the functional composition of the machine vision system is divided into three parts[31-32]. Collect images of the object under test, process and analyze the images, and output or display the test results, respectively. The imaging system of machine vision is mainly composed of a light source, a lens and a camera, which is the basis for the system to perform the detection function. Therefore, the final imaging quality of the measured object of the machine vision imaging system has a direct impact on the detection result of the system. Due to the influence of factors such as light intensity, surrounding environmental factors and the image acquisition equipment itself, there must be many interference signals and noises in the images captured by the book sorting system. These disturbances and noises make the image mainly show the imbalance of light and dark contrast, and the noise drowns out some important information. In order to improve the signal-to-noise ratio of the image, the image enhancement method is used to process the machine vision image. Due to the high real-time nature of spatial filtering, the spatial filtering method is used to realize the filtering processing of the collected images. The principle of spatial filtering is shown in the following formula.

$$G(x,y) = \sum_{a}\sum_{b} F(x,y)K(x-a,y-b) \tag{7}$$

Among them, F(x, y) is the original gray value; G(x, y) is the gray value after filtering; K is a filter kernel function used in image processing.

Morphological operations can remove image noise and also highlight the localization of regions of minimum and maximum values in the image. Image erosion is to find the local minimum value of the image, the main purpose is to make the area of minimum value cover the area of other maximum value. The expansion of the image is to find the local maximum value of the image, the main purpose is to make the area of maximum value cover the area of minimum value. Table 1 is a comparison of the standard deviation of pixel values of different algorithms.

Table 1 Comparison of standard deviations of pixel values in different algorithms

Filtering algorithm	a	b	c	d
Mean filter	49.83	49.09	48.03	48.83
Gaussian filter	49.83	47.56	47.83	48.65
Median filter	46.48	46.98	45.46	46.78
Bilateral filtering	44.41	44.58	45.48	44.32

https://doi.org/10.17993/3cemp.2023.120151.15-35

The specific implementation steps are as follows:

(1) Image edge detection: First, edge detection is performed on the tilt-corrected book image. Complete detection of image edges facilitates analysis of object detection, localization, and recognition.

(2) Image binarization: The problem in the previous step can be solved by the operation of image binarization. All pixels in the image are judged and screened to complete the retention of the image part.

(3) Morphological processing: According to the obtained binarized image, the barcode area becomes the largest rectangular area through erosion and expansion processing. Other areas in the image background are basically removed, and the largest area of the image can be selected.

3.2. RESEARCH ON MACHINE VISION BASED ON DEEP NETWORK

With the continuous development of deep learning, especially the emergence of deep neural networks based on ensemble learning. Complex network models emerge in an endless stream, and although the prediction accuracy of the models continues to improve, it is difficult to apply them to real-world scenarios.

The image distortion correction of the machine vision system based on the deep network proposed in this paper is divided into two parts: the solution of the image nonlinear distortion model and the image correction. Firstly, a large number of images with different degrees of distortion of the machine vision system are simulated based on MATLAB, and then the structure of the deep network is designed, and the obtained distorted images are used as the data set to train the deep network. When correcting the distorted images of the system, the trained deep network model can be applied to machine vision systems with different degrees of image distortion. Solve the distortion parameters of its image nonlinear distortion model.

In a deep network, the input feature image is convolved, pooled, and the output feature image of each hidden layer is obtained. Each hidden neuron corresponds to a region of its input feature map, then this region is the receptive field of the corresponding neuron. The local receptive field of the feature image is used as the input of the lowest layer of the deep network structure, and the information of the local receptive field is transmitted to different layers in turn. Each layer obtains the relevant features of the data through the convolution operation of the convolution kernel, and integrates the global information at the high level. This mode can reduce the number of network parameters and the calculation speed is faster. A lens in a machine vision system consists of a set of lenses, when light enters the lens parallel to the main optical axis. The point where all rays converge is the focal point, and the distance between the focal point and the center of the lens is the focal length.

The conversion relationship between the image coordinate system and the pixel coordinate system is:

https://doi.org/10.17993/3cemp.2023.120151.15-35

$$\begin{cases} u = \dfrac{x}{dx} + u_0 \\ v = \dfrac{y}{dy} + v_0 \end{cases} \quad (8)$$

The conversion of the image coordinate system and the camera coordinate system is:

$$\begin{cases} x = \dfrac{fXc}{Zc} \\ y = \dfrac{fYc}{Zc} \end{cases} \quad (9)$$

The distance from the origin of the camera coordinate system to the image plane. The above relationship is expressed as a matrix in homogeneous coordinates as:

$$Zc\begin{pmatrix} x \\ y \\ 1 \end{pmatrix} = \begin{pmatrix} f & 0 & 0 & 0 \\ 0 & f & 0 & 0 \\ 0 & 0 & 1 & 0 \end{pmatrix}\begin{pmatrix} Xc \\ Yc \\ Zc \\ 1 \end{pmatrix} \quad (10)$$

The transformation of the camera coordinate system and the world coordinate system is:

$$\begin{pmatrix} Xc \\ Yc \\ Zc \\ 1 \end{pmatrix} = \begin{pmatrix} \mathbf{R} & t \\ 0^T & 1 \end{pmatrix}\begin{pmatrix} Xw \\ YW \\ Zw \\ 1 \end{pmatrix} \quad (11)$$

The generation of the data set is mainly by changing the distortion parameters in the nonlinear model to randomly generate images with different degrees of distortion. Therefore, using the regression function of the deep network, the distorted images in the dataset do not need to be classified.

Based on Matlab, the program to generate the data set was programmed, and the LABEL function was used to record the distortion parameter matrix corresponding to the distorted image. Table 2 shows the matching time and matching degree under different parameters.

Table 2 Matching time and matching degree under different parameters

https://doi.org/10.17993/3cemp.2023.120151.15-35

MinScore	Match time (ms)	Can match
0.5	24	Yes
0.6	19	Yes
0.7	14	Yes
0.88	10	Yes
0.96	/	No

3.3. REALIZATION OF VISION TECHNOLOGY IN SMART FACTORY

The deep learning network structure designed in this paper consists of an input layer, four convolutional layers, four pooling layers, two fully connected layers and an output layer, and each convolutional layer applies a relu activation function. After this series of layers, the output of the last pooling layer is flattened and fed into the fully connected layer. The final output result is each distortion parameter of the image nonlinear distortion model, which is the complete training model. Use the Flatten layer to convert the feature image into one-dimensional features and then input them into the fully connected layer. Deep learning is a special kind of neural network that can remember spatial information, so flattening the feature image input to the fully connected layer does not affect the positional relationship between the features.

Smart factory is a complex system engineering, using the results of visual inspection and identification as well as the results of positioning and attitude determination as a reference. Smart factories can control robots to accurately complete very complex tasks such as positioning, picking, and classification. The visual control rate is defined by visual error to confirm the control amount. Control the robot to move, and then achieve the specified work tasks. The manipulator is used in the smart factory to serve the products. During the work of the manipulator, the manipulator may overheat (overHeat), run out of battery (batteryDie) and stop working (breakDown). There are three levels of failures in the factory: low, medium, and high, corresponding to the three conditions described above.

3.4. VISION APPLICATION OF SMART FACTORY BASED ON DEEP NETWORK

Machine vision systems are widely used in the field of industrial product quality inspection, especially in workpiece size measurement and appearance defect detection. By systematically measuring the size of large-scale workpieces and inspecting workpieces for defects, the system distinguishes between good and non-conforming products. The image distortion correction algorithm for machine vision system based on deep network proposed in this paper is suitable for installed machine vision systems with different degrees of image distortion. In this paper, the

https://doi.org/10.17993/3cemp.2023.120151.15-35

standard template is used as the measured object of the system in the scene demonstration of the machine vision system, and the obtained distorted template image is input into the trained deep network model. The distortion parameters of the system are obtained, and then the system is used to capture an image of the workpiece to be measured, and the distortion image of the workpiece is corrected based on MATLAB. The PTZ module is a support device specially used to install and fix the camera, and it can also expand the scanning range of the camera. Automatically adjust the camera's level, up and down angles on the PTZ, and only need to adjust the mechanism to make the camera achieve the best working position and posture. The system is used to test and identify 120 different images containing components, and these 120 images have different tilt angles. During the test, the book images are divided into 4 categories according to the different tilt angles, with an average of 30 book images for each category. The collected images of books with different inclination angles are one in the range of 0~90°, 90°~180°, 180°~270°, and 270°~360°, respectively, from left to right. Table 3 is the image recognition system test.

Table 3 Image recognition system testing

Angle	Number of tests	Unrecognized	Recognition rate	Processing time	Recognition time
0~90	30	0	100%	1.43s	0.57s
90~180	30	1	96.67%	1.31s	0.62s
180~270	30	0	100%	1.60s	0.44s
270~360	30	0	100%	1.53s	0.59s

4. RESULTS AND DISCUSSION

4.1. THE EFFECT OF THE NUMBER OF NEURONS ON THE PERFORMANCE OF DEEP NETWORKS

The sample images in the dataset need to be preprocessed, and the head poses corresponding to the images should be marked. There are some parameters in the network that need to be set manually. All network parameters are set as follows: the number of iterations is 80, the total number of batch training samples is 1000, and the learning rate η is 0.0002. Figure 1 shows the training performance of the neural network under R2 to obtain a high coefficient of determination R2. When the number of neurons in the hidden layer increases from 5 to 10, MAE gradually decreases and R2 increases first, indicating that increasing the number of neurons is conducive to improving the performance of the neural network; when the number of neurons increases from 10 to 15 , MAE gradually increases and R2 gradually decreases, indicating that excessively increasing the number of neurons will cause overfitting of

https://doi.org/10.17993/3cemp.2023.120151.15-35

the neural network, thereby reducing the performance of the neural network. As shown in Figure 1, the neural network has the best performance when the number of neurons is 10. At this time, R2 is 0.981 and MAE is 25. Increasing the number of hidden layers will cause errors in the neural network and increase the amount of computation, which is not conducive to model training. Therefore, it is necessary to select the appropriate number of neurons according to the characteristics of the model.

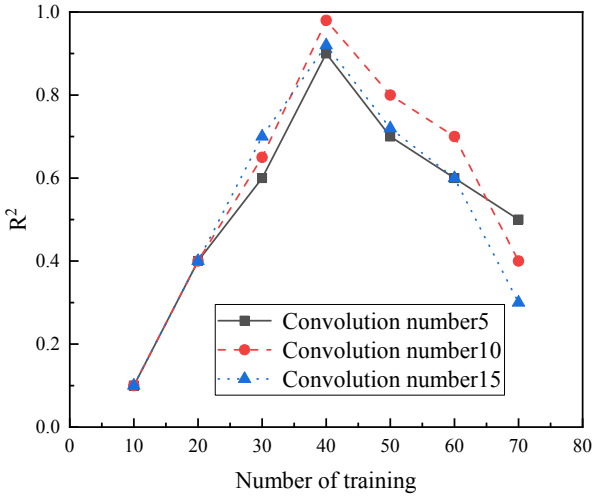

Figure 1 R^2 trained with different numbers of neurons

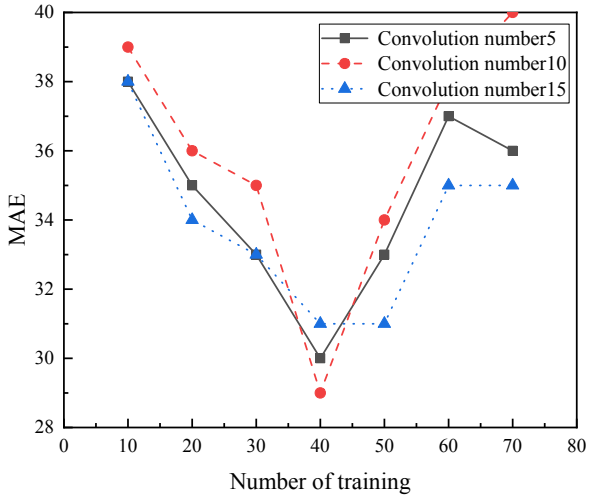

Figure 2 MAE under training with different numbers of neurons

4.2. DEEP NETWORK MODEL OPTIMIZATION FOR SMART FACTORIES

According to the application scenario of the factory, the data in the factory is dynamically obtained in real time, the amount of data generated is large and most of the data is in the normal range. For the factory inspection dataset, a total of three inspection models are trained. The model trained by the original convolutional network is used as the base model. First replace the convolution default regression loss function MSE loss with the GIoU loss function. Then use the GIoU loss as the regression loss, and the last group uses the

https://doi.org/10.17993/3cemp.2023.120151.15-35

The proposed deep network algorithm completes the bounding box regression task. When testing the performance of the model, the mAP value when the IoU thresholds were 0.5 and 0.75 were mainly calculated as the model evaluation index. The model trained using the MSE loss function is used as the benchmark, although using the GIoU function under the AP75 standard improves the model performance by 0.15%. When the IoU value is less than 0.6, the detection model based on AIoU loss function is slightly lower than the detection accuracy based on MSE loss function. However, when the value is greater than or equal to 0.6, its model performs better, and from the overall trend, the model test results using the AIoU loss function are significantly better than the other three groups. When the IoU threshold is taken as 0.75, its performance improvement is the highest, which is improved by 1.23%. The residual structure composed of asymmetric multiple convolution kernels not only increases the number of feature extraction layers, but also allows the asymmetric image details to be better preserved. And it can normalize the image features, thereby ensuring the stability of the network learning process.

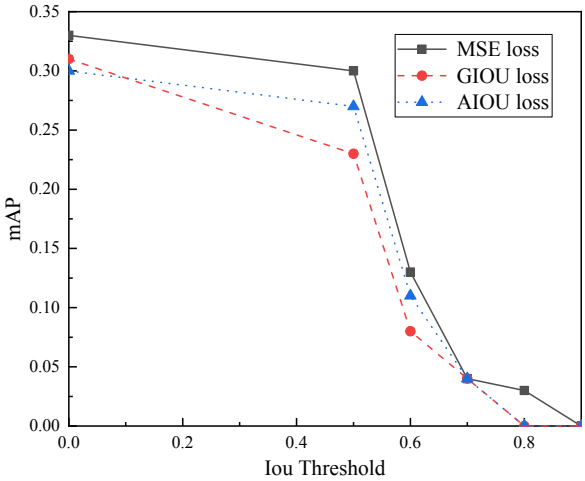

Figure 3 mAP of different detection models

4.3. DEVELOPMENT OF KEY VISUAL TECHNOLOGIES FOR SMART FACTORIES

The deep network is an algorithm designed for image processing. The number of input samples is in picture format, and the sample data provided in this paper is the node data collected by the system camera. The feature data (numerical type) extracted by the operation, so in order to meet the requirements of the convolutional neural network framework, there will be no lack of dimension when the data enters the operation of each convolutional layer and pooling layer. By setting the learning rates to be 0.1, 0.01, and 001 for training, the loss of all 8 learning rates decreases rapidly during the training process. But relative to the learning rate of 0.01 and 0.001, when the learning rate is 0.001. The training loss decreases the fastest, that is, the learning speed of the model is the fastest, so the training model in this experiment chooses a learning rate equal to 0.001. Continuously collect 300s image node data to construct

https://doi.org/10.17993/3cemp.2023.120151.15-35

600 detection samples. Input the trained deep network model and compare it with the detection results of thresholding, support vector machine, strong separator, decision tree, k-nearest neighbor model. Its recognition accuracy reaches 99.1%, which is much higher than other detection models. The average recognition time is 0.175s, which is much faster than several other machine learning detection algorithms. The detection model not only maintains a high recognition accuracy rate, but also meets the real-time requirements of the system.

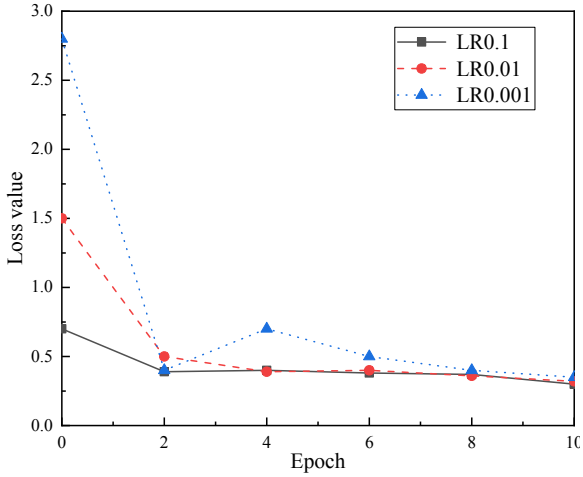

Figure 4 Training loss at different learning rates

The quality of the saliency map can be measured by the target localization evaluation. By extracting the maximum point from the saliency map to observe whether the point falls within the target bounding box, the extraction of the maximum point is extended to the entire saliency map. Determine how much of the saliency map can fall within the target bounding box. Table 4 shows that the method in this paper is significantly better than the comparison method in the target localization performance. The numerical results show that more than 60% of the pixels in the saliency map obtained by the method in this paper fall within the target detection frame. It shows that the target noise of the saliency map of the method in this paper is small, which is consistent with the previous subjective visualization analysis results. First, the image and the target category bounding box are binarized, where the inner region is assigned a value of 1, and the outer region is assigned a value of 0. It is then multiplied point-by-point with the generated saliency map and summed to get the energy in the target bounding box. The larger the Location value, the better the localization performance of the saliency map.

Table 4 Target positioning evaluation comparison test results

Method	Locatioin
Grad-CAM	0.45
Grad-CAM++	0.47
Score-CAM	0.54
XGrad-CAM	0.57

https://doi.org/10.17993/3cemp.2023.120151.15-35

Ablation-CAM	0.52

5. CONCLUSION

In the traditional fault diagnosis, the production efficiency of the factory is reduced due to the poor communication of information. It is difficult for the management of the factory to get the fault information of the factory and make a response at the first time. Smart factories can provide an intelligent fault detection service that supports dynamic collection of abnormal event information, real-time transmission, and abnormal response-level monitoring. This research proposes a deep learning algorithm, and this research proposes a smart factory based on a deep network model, which is capable of data mining and analysis based on a huge database, enabling the factory to have self-learning capabilities. Based on the deep network model, the accuracy of the model for image analysis is improved. In the research of machine vision technology, the smart factory based on the deep network model not only maintains a high recognition accuracy rate, but also meets the real-time requirements of the system. It has great development prospects and determines that the deep network model has a significant impact on smart factories. and came to the following conclusions:

(1) When the number of neurons in the hidden layer is 10, the increase of R2 indicates that increasing the number of neurons is beneficial to improve the performance of the neural network. When the number of neurons is 15, the gradual decrease of R2 indicates that excessively increasing the number of neurons will cause overfitting of the neural network, thereby reducing the performance of the neural network. Therefore, it is necessary to select the appropriate number of neurons according to the characteristics of the model.

(2) When the IoU value is less than 0.6, the detection model based on AIoU loss function is slightly lower than the detection accuracy based on MSE loss function. When the value is greater than or equal to 0.6, its model performs better, and from the overall trend, the model test results using the AIoU loss function are significantly better than the other three groups. When the IoU threshold is taken as 0.75, its performance improvement is the highest, which is improved by 1.23%.

(3) The deep network is an algorithm designed for image processing. The number of input samples is in picture format, and the sample data provided in this paper is the node data collected by the system camera. Continuously collect 300s image node data to construct 600 detection samples. Its recognition accuracy rate of 99.1% is much higher than other detection models, and the average recognition time is only 0.175s.

6. DATA AVAILABILITY

The data used to support the findings of this study are available from the corresponding author upon request.

https://doi.org/10.17993/3cemp.2023.120151.15-35

7. CONFLICT OF INTEREST

The authors declare that the research was conducted in the absence of any commercial or financial relationships that could be construed as a potential conflict of interest.

8. ACKNOWLEDGMENTS

The writing process was strongly supported by other teachers.

REFERENCES

(1) Selvarajah K, Zhao R, Speirs N. **Building Smart Space Applications with Pervasive Computing in Embedded Systems (PECES) Middleware[J]**. *GSTF Journal on Computing (JoC)*, 2014, 1(4):12-15.1.

(2) Shi Y, Xie W, Xu G. **Smart remote classroom: Creating a revolutionary real-time interactive distance learning system[M]**. *Advances in Web-Based Learning. Springer Berlin Heidelberg*, 2002: 130~141.

(3) Berhe G, Brunie L, Pierson J M. **Content Adaptation in distributed multimedia system[J]**. *Journal of Digital Information Management*, 2005, 3(2): 95~100.

(4) DengL,YuD. **Deep learning: methods and applications[J]**. *Foundations and trends® in signal processing*, 2014, 7(3–4):197-387.

(5) J Chen H, Perich F, Finin T, et al. **Soupa: Standard ontology for ubiquitous and pervasive applications[C]**. in: *Mobile and Ubiquitous Systems: Networking and Services*, 2004: 258~267

(6) Wang, Georgette and Yi-Ning Katherine Chen. **Collectivism, relations and Chinese communication**. (2010):1-9.

(7) FangT, FaureGO. **Chinese communication characteristics: A Yin Yang perspective[J]**. *International Journal of Intercultural Relations*, 2011, 35(3):320-333.

(8) LeCunY, BengioY, HintonG. **Deep learning [J]**. *nature*,2015,521(7553):436-444.

(9) Zhang Y F, Zhang W, Liu S H, et al. **Research on AGV Navigation Simulation in Printing Wisdom Factory[C].** *2021 IEEE 5th Advanced Information Technology, Electronic and Automation Control Conference (IAEAC). IEEE*, 2021, 5: 2312-2316..

(10) Jerman A, Bertoncelj A, Erenda I. **The influence of critical factors on business model at a smart factory: A case study[J]**. *Business Systems Research: International journal of the Society for Advancing Innovation and Research in Economy*, 2019, 10(1): 42-52.

(11) SHANTHIKUMAR J G, Xu S H. **Strong Asymptotic Optimality Of Focused Factory[J]**. 1999.

(12) Golnabi H, Asadpour A. **Design and application of industrial machine vision systems[J]**. *Robotics and Computer-Integrated Manufacturing*, 2007, 23(6): 630-637.

https://doi.org/10.17993/3cemp.2023.120151.15-35

(13) Chen Y R, Chao K, Kim M S. **Machine vision technology for agricultural applications[J]**. *Computers and electronics in Agriculture*, 2002, 36(2-3): 173-191.

(14) Robie A A, Seagraves K M, Egnor S E R, et al. **Machine vision methods for analyzing social interactions[J]**. *Journal of Experimental Biology*, 2017, 220(1): 25-34.

(15) Oren, Michael, and Shree K. Nayar. **Generalization of the Lambertian model and implications for machine vision**. *International Journal of Computer Vision* 14.3 (1995): 227-251.

(16) Davies E R. **The application of machine vision to food and agriculture: a review[J]**. *The Imaging Science Journal*, 2009, 57(4): 197-217.

(17) HaoX, ZhangG, MaS. **Deep learning[J]**. *International Journal of Semantic Computing*, 2016,10(03):417-439.

(18) KimP. Matlab deep learning[J]. **With machine learning, neural networks and artificial intelligence, 2017, 130 (21 AFRAMA, JANABI-SHARIFIF. Review of modeling methods for HVAC systems[J]**. *Applied Thermal Engineering*, 2014,67(1-2):507-519.

(19) GulliA, PalS. **Deep learning with Keras[M].** *Packt Publishing Ltd*, 2017.

(20) Agarwal B, Ramampiaro H, Langseth H, et al. **A deep network model for paraphrase detection in short text messages[J]**. *Information Processing & Management,* 2018, 54(6): 922-937.

(21) Tai L, Li S, Liu M. **A deep-network solution towards model-less obstacle avoidance[C].** *2016 IEEE/RSJ international conference on intelligent robots and systems (IROS). IEEE*, 2016: 2759-2764.

(22) Vemulapalli R, Tuzel O, Liu M Y. **Deep gaussian conditional random field network: A model-based deep network for discriminative denoising[C].** *Proceedings of the IEEE conference on computer vision and pattern recognition.* 2016: 4801-4809.

(23) Bai Z, Li Y, Woźniak M, et al. **DecomVQANet: Decomposing visual question answering deep network via tensor decomposition and regression[J]**. *Pattern Recognition*, 2021, 110: 107538.

(24) Schmidhuber J. **Deep learning in neural networks: An over view[J].** *Neural networks*, 2015,61:85-117.

(25) WangH, RajB. **On the origin of deep learning[J]**. *arXiv preprint arXiv*: 1702.07800,2017.

(26) RenM, ZengW, YangB, etal. **Learning to reweight examples for robust deep learning[C]**. *International conference on machine learning.* PMLR, 2018:4334-4343.

(27) Lamport L. **On interprocess communication[J]**. *Distributed computing,* 1986, 1(2): 86-101.

(28) Luhmann N. **What is communication?[J]**. *Communication theory*, 1992, 2(3): 251-259.

(29) Chen G M. A**n introduction to key concepts in understanding the Chinese: Harmony as the foundation of Chinese communication[J]**. 2011.

https://doi.org/10.17993/3cemp.2023.120151.15-35

(30) Smith T W, Colby S A. **Teaching for deep learning[J]**. *The clearing house: A journal of educational strategies, issues and ideas*, 2007, 80(5): 205-210.

(31) Horani M. O., Najeeb, M., y Saeed, A. (2021). **Model electric car with wireless charging using solar energy**. *3C Tecnología. Glosas de innovación aplicadas a la pyme*, 10(4), 89-101. https://doi.org/10.17993/3ctecno/2021.v10n4e40.89-101

(32) Chen Shuang & Ren Yuanjin.(2021). **Small amplitude periodic solution of Hopf Bifurcation Theorem for fractional differential equations of balance point in group competitive martial arts**. *Applied Mathematics and Nonlinear Sciences* (1). https://doi.org/10.2478/AMNS.2021.2.00152.

https://doi.org/10.17993/3cemp.2023.120151.15-35

/02/

MANAGEMENT AND CONTROL OPTIMIZATION BASED ON DEEP LEARNING MODEL

Jingjing Dai

Nanjing University of Technology, Nanjing, Jiangsu, 210023, China

c18905175401@163.com

Reception: 19/10/2022 **Acceptance**: 26/12/2022 **Publication**: 19/01/2023

Suggested citation:

D., Jingling (2023). **Management and control optimization based on deep learning model**. *3C Empresa. Investigación y pensamiento crítico, 12(1)*, 37-49. https://doi.org/10.17993/3cemp.2023.120151.37-49

ABSTRACT

Microgrid technology is a key solution to improve distributed power consumption, complementary utilization of multiple energy sources, and power supply reliability. To guarantee the reliability of the microgrid system, a realistic strategy must be created. This work takes the microgrid as an object and uses simulation technology to construct a microgrid system. Then, using this simulation system and the double deep Q-learning, the goal is to minimize the 24-hour electricity consumption cost from the external power grid to meet the requirements of voltage deviation. Power balancing and energy storage loads for microgrid systems. Under the constraints of the electrical state and other constraints, the control variable is the energy storage's capacity for charging and discharging, and the optimization strategy of energy storage control is obtained through training. The results demonstrate that the DDQN algorithm will save 26.95% of the electricity purchase cost, which is significantly more than the MPPT algorithm's 12.43% savings. As a result, this work examines the efficacy of the charging and releasing approach for energy storage and confirms the potential of the suggested approach to reduce the cost of purchasing electricity.

KEYWORDS

Deep reinforcement learning; DDQN; Microgrid technology; Optimization strategy; Electricity

PAPER INDEX

https://doi.org/10.17993/3cemp.2023.120151.37-49

1. INTRODUCTION

The power system's development of the energy structure has advanced significantly in recent years toward a clean and sustainable development due to the widespread availability of renewable energy. Because of structural changes on the energy supply side and the 2030 carbon peaking target, the amount of renewable energy in the power grid will increase even more[1]. The grid-connected use of large-scale renewable energy is faced with a significant problem because distributed renewable energy is highly volatile and intermittent due to the influence of natural factors [2]. A microgrid is a compact power generation [3]. Configuring an energy storage device is important to preserve the microgrid's power balance and lessen the effect that distributed energy output uncertainty has on the microgrid. A typical microgrid so typically consists of a variety of power-producing equipment, energy storage devices, loads, and other components [4]. At present, there are many studies on the microgrid, and the energy storage control strategy has attracted much attention as a hot spot for optimal regulation of energy dispatch.

Microgrid scheduling is a popular topic in research connected to microgrids and is a crucial tool for ensuring the safe, dependable, and cost-effective operation of microgrids [5]. Traditional microgrid optimization scheduling is usually based on optimization theories and methods. First, each component in the microgrid is modeled, then the model is simplified and processed, and finally, the model is solved by researching the related solution algorithm. Typically, the model's primary goal is to minimize operational costs, and there are also related studies that comprehensively consider the economic, environmental, and social benefits to establish a multi-objective optimization model [6]. Commonly used model modeling methods include mixed integer programming [7, 8], dynamic programming [9], model predictive control [10, 11], distributed optimization [12], Lyapunov optimization, etc.; commonly used model solving algorithms include Genetic algorithm [13, 14], particle swarm algorithm [15, 16], active evolution algorithm [17], Lagrangian relaxation method, etc.

The uncertainty of microgrid operation has greatly increased during the past few years because of the rising number of renewable energy sources. The common solution to such problems is to convert uncertain problems into deterministic problems for modeling and solving, mainly including scene-based stochastic optimization[18], Opportunity Constrained Optimization [19], Robust optimization [20], etc. However, these methods all have certain limitations, which are mainly reflected in: the refined modeling of each component of the microgrid is difficult, and the simplified model is difficult to describe the physical characteristics of the actual operation of the components, resulting in the optimization results may be sub-optimal; the established model It is generally nonlinear and non-convex, and its solution is a typical non-deterministic polynomial problem, and the solution efficiency is low; the establishment of the model needs to be completed according to the topology structure and operation mode, and the adaptability to the change of topology structure and the access of new power equipment Not strong; the pre-planned control based on "offline calculation and online matching" is difficult to adapt to complex and changeable system conditions.

https://doi.org/10.17993/3cemp.2023.120151.37-49

Artificial intelligence has developed rapidly in recent years. As a typical timing control problem, the microgrid energy control problem conforms to the deep reinforcement learning solution framework, and there are many outstanding works at present. Hua et al. [21] used a deep learning algorithm with asynchronous advantages to solve the multi-microgrid energy dispatch control problem. Zhang et al. [22] gave the composite energy storage coordination control strategy of the microgrid through the deep reinforcement learning algorithm. Liu et al. [23] established a microgrid framework model based on energy buses and compared the advantages of a deep Q-learning algorithm in energy scheduling control problems compared with the heuristic algorithm. Du et al. [24] gave retail pricing strategies through Monte Carlo reinforcement learning algorithms to reduce the demand-side peak ratio and protect user privacy. Mocanu et al.[25] explored the use of deep learning to refine the usability of building energy management systems in a smart grid environment and was successfully validated on a large database.

When addressing the energy storage charging and releasing control technique with deep learning, in contrast to prior work, the training data is real-time data occurring while the microgrid simulation environment is running. By adding state information about voltage, current, phase angle, and other state information in the simulation environment to achieve a simulation that is closer to the real state, the results are more reliable. This paper firstly presents the composition of the microgrid objects studied, and then mainly introduces the deep reinforcement learning algorithm framework used and its application process in the energy storage control problem. Finally, the comparison with the existing method illustrates the usefulness of the algorithm flow in this research.

2. SYSTEM MODEL

2.1. MICROGRID COMPONENTS

A significant component of distributed energy in the microgrid system is photovoltaic power generation. The photovoltaic power can be given by equation (1)

$$P_{PV}(t) = R(t) S \eta_{PV} \tag{1}$$

S is the area of the placed solar panels, and R(t) is the amount of solar radiation at time t, expressed in W/m^2. The power of photovoltaic energy generation at time t is calculated by multiplying the solar radiation power by the conversion efficiency η_{PV}, which is the product of the solar radiation power and the panel area.

The battery is a popular kind of high-efficiency energy storage, and its internal energy state satisfies the equation (2)

$$E_{bat}(t) = E_{bat}(t-1) + P_{bat}(t)\bar{}\, t \tag{2}$$

https://doi.org/10.17993/3cemp.2023.120151.37-49

$P_{bat}(t)$ is the battery's charging and discharging capacity at time t; Δt is the time interval between two charging and discharging operations.

Load. Load is the general term for the part that consumes electric energy in a microgrid system. For a fixed microgrid system, the load demand is determined by the local climate environment and the properties of the microgrid, so it is usually not adjustable. In the energy scheduling problem in this paper, the load curve is input to the microgrid as a fixed quantity. network system.

The external power supply used in this paper is replaced by the three-phase AC power supply module that comes with Simulink. The parameter settings of the module need to be given according to the actual simulation requirements. Then, it is connected with the internal module of the microgrid system through the varistor module to provide the required power for the system. In this study, a microgrid system that uses grid connectivity is taken into account. The three-phase dynamic load is also used to produce the PQ control effect since the energy storage system model that needs to be developed can be modified. In the simulation experiment, due to the randomness of the load, the microgrid load usually consists of two parts, one of which is a variable load and the other is a fixed load, which is directly acted by the resistance module in Simulink in the simulation model. The simulation modules of each distributed energy source are regulated by the PQ control strategy to guarantee the stability and controllability of the interaction between the microgrid system and the external power. Based on the simulation model, this paper conducts deep reinforcement learning training. As a result, the energy storage system's charging and releasing control approach is optimized. Compared to traditional reinforcement learning training based on mathematical formulas, the influence of more abundant state variables on the control objective can be comprehensively considered.

2.2. DEEP REINFORCEMENT LEARNING ALGORITHM

Reinforcement learning is aimed at maximizing the expected return. The mapping relationship between the environment's state variable and the agent's action variable is discovered through the agent and the environment's ongoing interaction. The agent provides an optimized action policy. Deep reinforcement learning uses deep neural networks to create a correspondence between state variables and action variables. Due to the powerful expressive ability of deep neural networks, deep reinforcement learning can deal with more complex and practical policy decision-making problems. In the disciplines of optimum control, robot control, and autonomous driving, deep reinforcement learning has made significant strides in recent years. Deep reinforcement learning is derived from MDP. The traditional MDP process consists of 4 elements, consisting of (S, A, R, μ), which stand for the set of environmental conditions, the set of actions the agent is capable of taking, the reward function, and the policy set, respectively.

Solving algorithms for reinforcement learning optimization strategies includes three categories: value function-based solutions, policy gradient-based solutions, and search and supervision-based solutions [26]. This paper focuses on the solution

https://doi.org/10.17993/3cemp.2023.120151.37-49

method based on the value function. Among them, the dynamic programming algorithm is suitable for solving the situation with models and dimensions. The Monte Carlo technique has the drawback of requiring entire state sequences, which is challenging in many systems. Without the entire state sequence, the time series difference approach can estimate the value function. The classic time series difference methods include the SARSA and the Q-Learning algorithm. Both approaches keep a Q-table to address tiny reinforcement. The size of the Q-table that needs to be kept increases when the state and action spaces are continuous or discrete at very large scales, which will bring difficulties to storage. However, the development of deep neural networks has solved this problem. Using a deep neural network instead of Q-table results in a deep reinforcement learning algorithm that is more suitable for complex problems. A typical algorithm is the deep Q-Learning (deep Q network, DQN) algorithm.

The Q-Learning algorithm is responsible for formula-based updates to the defined Q function (3).

$$Q(S,A)=Q(S,A)+\alpha\left(R+\gamma\, maxQ(S',a)-Q(S,A)\right) \quad (3)$$

$Q(S,A)$ is a function of action value; α is the learning rate. When the update formula converges, the optimal control strategy for reinforcement learning can be obtained.

DQN replaces the Q function in Q-Learning with a deep neural network $Q(S,A|\ )$.

Formula (3) is then used to determine the current goal Q value, and the Q network updates the parameter ω of the neural network.

The DDQN algorithm is based on DQN with two improvements. The first is to introduce two networks, one is the target network $Q'(S,A|\ )$ to calculate the target Q value, and the other is the update network $Q(S,A|\ )$ to update the Q value, which can reduce the Dependencies between small target Q-values and updated network parameters. The target network has the same structure as the Q-value network, and the timing is synchronized with the parameters from the Q-value network.

The second is to decouple the action selection of the target Q and the calculation process of the target Q in the target formula (3), thereby reducing the overestimation caused by the greedy algorithm. The specific method is that when calculating the target Q, the maximum Q corresponding to the action is no longer found in the target Q network, but the action corresponding to the maximum Q value is first found in the update network:

$$a(S'|\ ) = argmax_{aeA} Q(S' A'\ ) \quad (4)$$

Then use this action $a(S'|\ )$ to calculate the target Q value:

https://doi.org/10.17993/3cemp.2023.120151.37-49

$$Q' = R + \gamma Q'(S', a' | S' |) \quad (5)$$

Through the above two improvements, the DDQN algorithm solves the strong dependence and overestimation problems of the traditional DQN algorithm, and other algorithm processes are the same as DQN.

3. RESULTS AND DISCUSSION

3.1. NETWORK SETTINGS

The implementation of the DDQN algorithm in solving the microgrid energy storage control problem is demonstrated in this part, along with a comparison to the MPPT control to demonstrate the efficacy of the DDQN method.

To speed up the simulation speed, in the simulation experiment verification, this paper does not consider other distributed generation modules such as wind power generation.

The upper and lower bound constraints in constraint (8) are set as:

$$P_{bat}^{min} = -4 \times 10^5 W, \ P_{bat}^{max} = 4 \times 10^5 W \ S_{soc}^{min} = 0.19 \ S_{soc}^{max} = 0.85$$

Another important setting is the setting of the Q-value estimation neural network in the DDQN algorithm. According to experience and continuous debugging and verification, the neural network used in this paper is a fully connected layer with 4 layers and 24 nodes, and the relu function is employed as the middle layer activation function.

3.2. NUMERICAL RESULTS

When training the DDQN algorithm, it is necessary to normalize each component of the state variable and then substitute it into the target network of DDQN for training. Given that the control objective of this paper is to reduce the cost of purchasing electricity, this paper multiplies the electricity price state variable by a 2-fold amplification factor during training to increase the impact of electricity price fluctuations on the control objective. The training time step is 300s, so a training cycle is 288 steps. The results of this experiment were obtained under 100,000 training cycles (Table 1).

Table 1. Hyperparameter settings for target network training

Hyperparameter	value
Batch size	300
Learning rate	0.001
No. of training epochs	100000
No. of layers	4

https://doi.org/10.17993/3cemp.2023.120151.37-49

No. of neurons	24
Optimization	Adaptive Moment Estimation (Adam)

Combined with the real-time electricity price table in Fig.1, it can be seen that in 24 hours, the electricity price from 16 to 21 hours is the highest, followed by the electricity price from 5 to 6 hours. The energy storage charging and discharging strategy obtained by the DDQN algorithm is, between 0 and 2h, when the photovoltaic power generation does not work, the energy storage is discharged first, from 50% to below 20%, after the SOC of the energy storage reaches the lower limit, the External grid power generation. The energy storage begins to charge around 7 to 11 hours after the photovoltaic system starts to produce power, at which point any excess power is stored and the SOC rises from 20% to roughly 80%. The energy storage will stop working after being fully charged between 11 and 17 hours, and the excess photovoltaic power generation will be fed back to the external power grid. Then at a peak time of electricity consumption from 17 to 22 hours, when the electricity price increases, the cost of electricity increases, the energy storage is discharged during this period for the use of the microgrid load, and the SOC of the energy storage at this time is similar to that at 5 hours. level, that is, below 20%. In summary, this control strategy is to store solar energy during the day for use at night, to achieve the purpose of saving electricity purchase costs. Therefore, logically, this control strategy is reasonable. Compared with the control strategy obtained by the DDQN algorithm, the control strategy obtained by the DQN algorithm in the same training period is to discharge the energy storage in 0-1h, and then the energy storage has been in an idle state until about 14h to start charging the energy storage, and the same charging To a similar level to DDQN, that is, the SOC is about 80%, and when the price of electricity starts to increase in 18 hours, the energy storage is then released. The data results showed that the control strategy obtained by the DDQN algorithm, compared with the DQN algorithm, considers the power consumption characteristics at different times in more detail, and allocates the charge and discharge capacity more reasonably, thus achieving a better control effect than the DQN algorithm.

https://doi.org/10.17993/3cemp.2023.120151.37-49

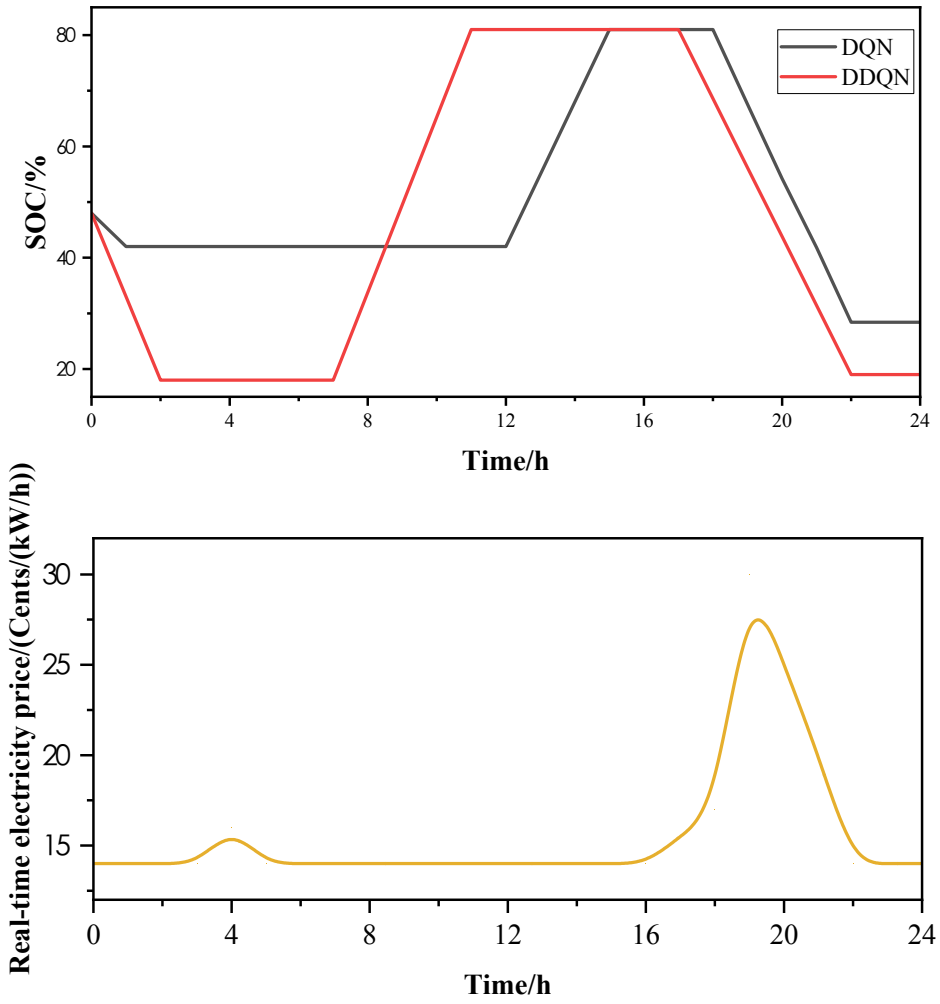

.

Fig.1 Comparison of energy storage SOC and real-time electricity price

The previous results give a qualitative analysis of the energy storage control strategy, and Fig. 2 and Table 2 give quantitative data results to illustrate that the control strategy trained by the DDQN algorithm is more optimized than the traditional control method and the DQN algorithm. The traditional MPPT control based on photovoltaic power generation is a simple state machine control method, that is, it judges the positive or negative power difference between the load and the power in the microgrid, and when the energy storage meets the given SOC state, according to the photovoltaic maximum power tracking principle. It is possible to obtain the energy storage's charging and discharging power. See the literature [27] for more information on the specific algorithm process.

Fig. 2 and Table 2 show the purchased electricity and the corresponding expenses in different situations. For the case without energy storage, when the electricity purchased is 4344.6 kWh, the cost is $840.1; for the MPPT control method, when the electricity purchased is 4003.6 kWh, the cost is $735.7; for the DQN control method, when the electricity purchased for 3833.5 kWh, the cost is $626.9; for the DDQN

https://doi.org/10.17993/3cemp.2023.120151.37-49

control method, when the purchased electricity is 3762.4 kWh, the cost is $613.7. From the data in Fig. 2 and Table 2, compared with the MPPT algorithm, the control strategy obtained by the reinforcement learning algorithm training saves the electricity purchase cost, and under the same training period, the DDQN algorithm is cheaper than the DQN algorithm[28-29]. Compared with the microgrid operation without energy storage, the DDQN algorithm will save 26.95% of the electricity purchase cost, which is much greater than 12.43% of the MPPT algorithm, which fully demonstrates the effectiveness of the DDQN algorithm.

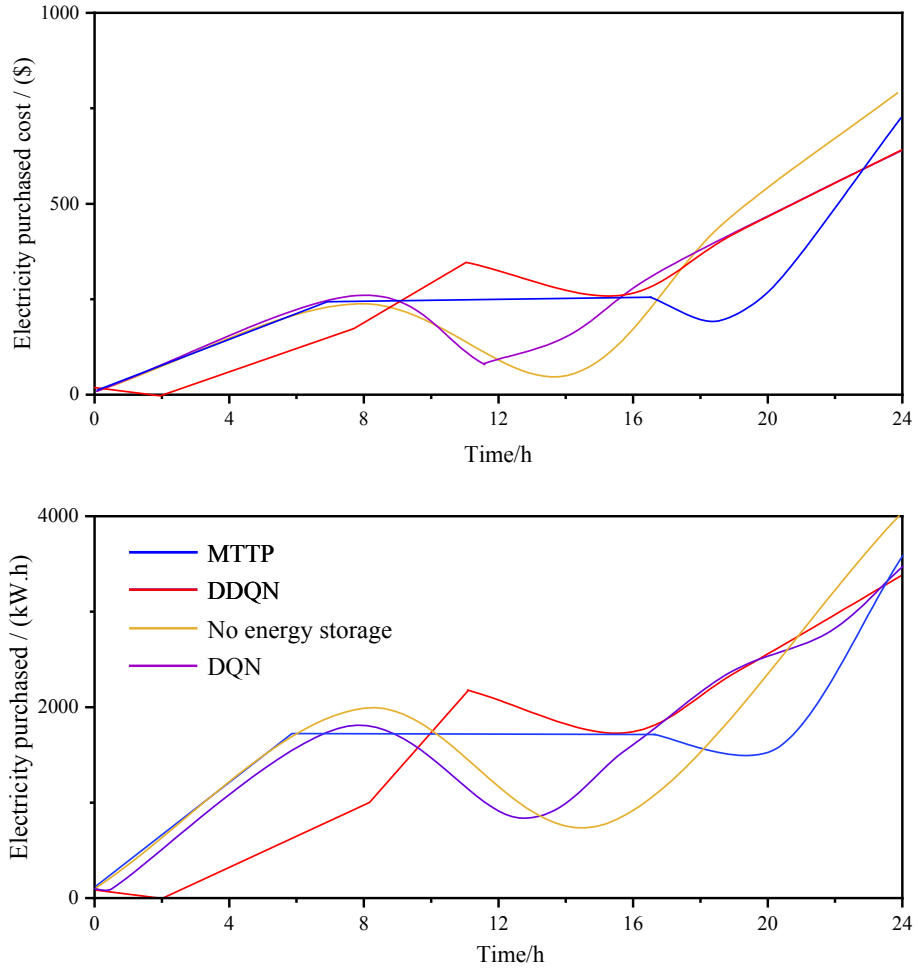

Fig 2. Comparison results of DDQN, DQN, MPPT, and no energy storage.

https://doi.org/10.17993/3cemp.2023.120151.37-49

Table 2 Data results for DDQN, DQN, MPPT, and no energy storage

Method	Electricity purchased/(kW.h)	Cost / $
No energy storage	4344.6	840.1
MPPT	4003.6	735.7
DQN	3833.5	626.9
DDQN	3762.4	613.7

4. CONCLUSION

This research presents an optimum method for the microgrid energy storage control problem based on the simulation model and the deep learning algorithm. The specific conclusions of this study are as includes:

(1) Due to the advantages of deep reinforcement learning in solving model-free problems, this study does not need to know the link between the control objectives, control variables, and state information of grid-connected microgrids. The Q-value function approximated by the neural network can be trained to identify the correlation between the control goal and the state variables using the micro-state network's data.

(2) In the same operation cycle, the energy storage discharge time of the control strategy of the DQN algorithm is 0-1h and 18-22h, while the discharge time of DDQN is 0-2h and 17-22h. The data results demonstrated that the DDQN algorithm's control strategy effect is superior to that of the DQN algorithm.

(3) The results of numerical verification show that the DDQN algorithm will save 26.95% of the electricity purchase cost, which is much greater than 12.43% of the MPPT algorithm, which fully demonstrates the effectiveness of the DDQN algorithm. The method proposed can be extended to a variety of microgrid energy control scenarios, such as adding or deleting different distributed generation modules in the simulation model, changing different control objectives, setting different control variables, and so on.

REFERENCES

(1) Yunhui, J., **Optimal Allocation of Distributed Energy Storage Capacity in Power Grid With High Proportion of New Energy**. *IOP Conference Series: Earth and Environmental Science*, 2021. 827(1).

(2) Na, L., W. Chengdong and G. Cailian, **Research and Application of Energy Storage Battery on Stabilizing Fluctuation Characteristics of Photovoltaic Power System**. *International Journal of Hybrid Information Technology*, 2016. 9(5).

(3) LvZhipeng, Y.X.S.J., **Overview on micro-grid technology**. *Proceedings of the CSEE*, 2014. 1(31): p. 57-70(in Chinese).

(4) Amjad, A., et al., **Overview of Current Microgrid Policies, Incentives and Barriers in the European Union, United States and China**. *Sustainability*, 2017. 9(7): p. 1146.

https://doi.org/10.17993/3cemp.2023.120151.37-49

(5) Domínguez-Barbero, D., et al., **Optimising a Microgrid System by Deep Reinforcement Learning Techniques**. *Energies*, 2020. 13(11): p. 2830.

(6) Liheng Liu, Miaomiao Niu, Dongliang Zhang, Li Liu and Dietmar Frank. **Optimal allocation of microgrid using a differential multi-agent multi-objective evolution algorithm**. *Applied Mathematics and Nonlinear Sciences*, 2021. 6(2): p. 111-124.

(7) **Energy; Data on Energy Detailed by Researchers at Department of Energy (Optimization Models for Islanded Micro-Grids: A Comparative Analysis between Linear Programming and Mixed Integer Programming)**. *Energy & Ecology*, 2017.

(8) Dolara, A., et al., **Optimization Models for Islanded Micro-Grids:A Comparative Analysis between Linear Programming and Mixed Integer Programming**. *Energies*, 2017. 10(2).

(9) Gazijahani, F.S. and J. Salehi, **Stochastic multi-objective framework for optimal dynamic planning of interconnected microgrids**. *IET Renewable Power Generation*, 2017. 11(14).

(10) **Energy - Renewable Energy; New Renewable Energy Study Findings Reported from Shenzhen University (Optimal Scheduling of Multiple Multi-energy Supply Microgrids Considering Future Prediction Impacts Based On Model Predictive Control)**. *Journal of Robotics & Machine Learning*, 2020.

(11) Duchaud, J., et al., **Trade-Off between Precision and Resolution of a Solar Power Forecasting Algorithm for Micro-Grid Optimal Control**. *Energies*, 2020. 13(14).

(12) Wang, Y., et al., **A Wasserstein based two-stage distributionally robust optimization model for optimal operation of CCHP micro-grid under uncertainties**. *International Journal of Electrical Power and Energy Systems*, 2020. 119(C).

(13) Fossati, J.P., et al., **Optimal scheduling of a microgrid with a fuzzy logic controlled storage system**. *International Journal of Electrical Power and Energy Systems*, 2015. 68.

(14) Provata, E., et al., **Development of optimization algorithms for the Leaf Community microgrid**. *Renewable Energy*, 2015. 74.

(15) Fengdao, Z., B. Siyu and W. Dan, **Optimal Dispatching of Microgrid Based on Improved Particle Swarm Optimization**. *Journal of Physics: Conference Series*, 2021. 1871(1).

(16) Yuvaraja, T. and G. M, **Artificial intelligence and particle swarm optimization algorithm for optimization problem in microgrids**. *Asian Journal of Pharmaceutical and Clinical Research*, 2015. 8(3).

(17) Bifei, T. and C. Haoyong, **Stochastic Multi-Objective Optimized Dispatch of Combined Cooling, Heating, and Power Microgrids Based on Hybrid Evolutionary Optimization Algorithm**. *IEEE Access*, 2019. 7.

(18) Luo, Y., et al., **Optimal configuration of hybrid-energy microgrid considering the correlation and randomness of the wind power and photovoltaic power**. *IET Renewable Power Generation*, 2020. 14(4).

(19) Sefidgar-Dezfouli, A., M. Joorabian and E. Mashhour, **A multiple chance-constrained model for optimal scheduling of microgrids considering**

https://doi.org/10.17993/3cemp.2023.120151.37-49

normal and emergency operation. *International Journal of Electrical Power and Energy Systems*, 2019. 112.

(20) **Energy - Electric Power; Study Findings on Electric Power Are Outlined in Reports from North China Electric Power University (A Wasserstein Based Two-stage Distributionally Robust Optimization Model for Optimal Operation of Cchp Micro-grid Under Uncertainties)**. *Energy Weekly News*, 2020.

(21) Hua, H., et al., **Optimal energy management strategies for energy Internet via deep reinforcement learning approach**. *Applied Energy*, 2019. 239(APR.1): p. 598-609.

(22) Dongxia, Z.Z.Q.C., **A coordinated control method for hybrid energy storage system in microgrid based on deep reinforcement learning**. *Power System Technolog*, 2019. 6(43): p. 1914-1921(in Chinese).

(23) Xiaosheng, L.J.C.J., **Energy management and optimization of multi-energy grid based on deep reinforcement learning**. *Power System Technology*, 2020. 10(44): p. 3794-3803(in Chinese).

(24) Du, Y. and F. Li, **Intelligent Multi-Microgrid Energy Management Based on Deep Neural Network and Model-Free Reinforcement Learning**. I*EEE Transactions on Smart Grid*, 2019. PP(99): p. 1-1.

(25) Mocanu, E., et al., **On-line Building Energy Optimization using Deep Reinforcement Learning**. *IEEE Transactions on Smart Grid*, 2017: p. 1-1.

(26) Xionglin, L.J.G.F., S**urvey of deep reinforcement learning based on value function and policy gradient**. *Chinese Journal of Computers*, 2019. 6(42): p. 1406-1438(in Chinese).

(27) Xiong, L., W. Peng and P.C. Loh, **A Hybrid AC/DC Microgrid and Its Coordination Control**. *IEEE Transactions on Smart Grid*, 2011. 2(2): p. 278-286.

(28) Medina, R., Breña, J. L., y Esenarro, D. (2021). **Efficient and sustainable improvement of a system of production and commercialization of Essential Molle Oil (Schinus Molle)**.*3C Empresa. Investigación y pensamiento crítico*, 10(4), 43-75. https://doi.org/10.17993/3cemp.2021.100448.43-75

(29) Meng Siyu & Zhang Xue.(2021).**Translog function in government development of low-carbon economy**. *Applied Mathematics and Nonlinear Sciences* (1). https://doi.org/10.2478/AMNS.2021.2.00138

https://doi.org/10.17993/3cemp.2023.120151.37-49

/03/

RESEARCH ON E-COMMERCE CUSTOMER SATISFACTION EVALUATION METHOD BASED ON PSO-LSTM AND TEXT MINING

Qin Yang*

School of Marxism, Jinling Institute of Science and Technology, Nanjing, Jiangsu, 211169, China

yang2161980@sina.com

Reception: 13/11/2022 **Acceptance**: 29/12/2022 **Publication**: 13/01/2023

Suggested citation:

Y., Qin (2023). **Research on E-commerce Customer Satisfaction Evaluation Method Based on PSO-LSTM and Text Mining**. *3C Empresa. Investigación y pensamiento crítico, 12(1)*, 51-66. https://doi.org/10.17993/3cemp.2023.120151.51-66

ABSTRACT

With the increase of social technology, e-commerce platforms have entered a period of rapid development. Improving customer satisfaction and purchase rate is the key to the survival of e-commerce platforms. Text mining and analysis of customer evaluation data will help to grasp the focus of customers and optimize the e-commerce platform. To this end, through text mining technology, the text comment data of five e-commerce platforms such as Amazon, eBay, Alibaba, Jingdong, and Taobao are collected, and the cleaned text is analyzed by particle swarm algorithm (PSO)-long short-term memory (LSTM) model. The data is subject to time scale extraction, and the extraction results are visualized and interpreted. The research shows that the logistics, price, freshness, quality and packaging of e-commerce platform merchants are important factors that affect the evaluation of e-commerce customer satisfaction.

KEYWORDS

text mining; PSO-LSTM; particle swarm algorithm; long short-term memory network

PAPER INDEX

https://doi.org/10.17993/3cemp.2023.120151.51-66

1. INTRODUCTION

Online shopping has become an important form of shopping. Not only are more and more consumers choosing to shop online, but also more and more categories of consumers are shopping online. After several years of development, various e-commerce platforms are in full swing, but fresh food e-commerce, known as the "last blue ocean" in the e-commerce industry, is still in its infancy. The biggest difference between fresh e-commerce and other e-commerce is that the products pay more attention to freshness and are not easy to preserve. Data from Research shows that the e-commerce market is developing rapidly, with an average annual growth rate of more than 50%. However, due to the constraints of many factors, the overall service of e-commerce is still in the immature stage, its business model is still developing, and the service level is also mixed. The degree is not optimistic [1-3]. The epidemic in 2020 has brought great opportunities to e-commerce [4-6]. Therefore, how to seize this opportunity requires in-depth analysis of the factors affecting customer satisfaction on e-commerce platforms, improving e-commerce products and services, increasing customer satisfaction, and enhancing user stickiness, thereby promoting the development of e-commerce.

For the analysis of e-commerce customer satisfaction evaluation methods, scholars at home and abroad mainly use the text mining method based on sentiment analysis, classify the vocabulary contained in the customer evaluation content, and quantify the emotional trend in the text content through weighted assignment. Based on this method, Susan et al. established an evaluation help degree model to describe the enthusiasm of the evaluation, but did not consider the difference between the evaluation of professional buyers and ordinary customers, and lacked accuracy. The problem of simple evaluation content sentiment analysis has been basically solved, but the evaluation of evaluation content is affected by the additional functions of the e-commerce platform, and a variety of restrictive factors must be comprehensively considered. Yang Ligong et al. [7] used Markov Logic Network to combine sentence context and emotional features for sentiment analysis, and realized cross-domain text analysis. Ming Junren [8] applied the association rule method to text mining analysis, and designed a text data analysis method integrating semantics and association mining, which improved the accuracy of text analysis. Cai Xiaozhen et al. [9] selected 4 indicators as the basis for online user comments, and constructed a text mining model to solve the problem of uneven quality of online user comments. Tang Xiaobo et al. [10] combined co-word analysis and polarity transfer method for text analysis, which overcomes the shortcomings of traditional text analysis and has better text analysis results. Liu L[11] and others proposed to combine the feature vector model and the weighting algorithm of product review sentiment analysis for text analysis. Walaa Medhat [12] proposed that the conventional analysis steps for commodity text analysis are commodity review, emotion recognition, feature selection, emotion classification, and emotion polarity judgment. The above studies have improved the accuracy and efficiency of text analysis, and laid the foundation for the use of particle swarm algorithm to mine intelligence value in text.

https://doi.org/10.17993/3cemp.2023.120151.51-66

With the rapid development of society, accurate e-commerce customer satisfaction prediction is becoming more and more important. The accurate prediction of e-commerce customer satisfaction not only plays an irreplaceable role in the long-term stable operation of e-commerce platforms and sellers, but also plays an important role in reducing the cost of e-commerce platforms, improving product quality and market planning. With the emergence of deep learning, many scholars have turned their attention to deep belief networks, convolutional neural networks, and recurrent neural networks. The related research progress is shown in Figure 1.

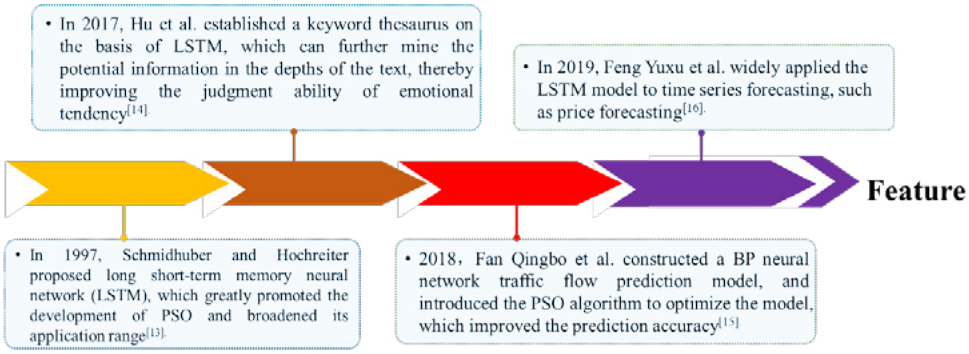

Figure 1 Research progress of LSTM model

As a special form of regular recurrent neural network (RNN), long short-term memory network (LSTM) was first proposed by Hochreiter et al. in 1997, and it is widely used in text mining data prediction. In order to improve the prediction accuracy of e-commerce customer satisfaction, particle swarm optimization (PSO) optimization of long short-term memory (LSTM) neural network hyperparameters for e-commerce customer satisfaction prediction model (PSO-LSTM) is widely used. Aiming at the problem that LSTM hyperparameters are difficult to select, the PSO algorithm can effectively find the global optimal solution to optimize the hyperparameters of the LSTM model, and continuously train to find suitable hyperparameters and verify them. Therefore, this paper combines the PSO-LSTM algorithm with text mining technology to study and analyze the factors that affect the evaluation of e-commerce customer satisfaction.

2. RESEARCH ON TEXT MINING AND ANALYSIS METHODS

Online reviews of e-commerce customers are messy but valuable unstructured or semi-structured data. The information contained in online reviews has an important impact on the strategic decision-making of merchants and the purchasing decisions of consumers [13-14]. At present, the academic community has recognized the importance of online reviews, but the research on online review willingness has not received much attention. It is necessary to link online reviews with Internet word-of-mouth, and study consumers' review willingness from the perspective of Internet word-of-mouth dissemination willingness. This paper directly studies the influencing factors of customer satisfaction evaluation, and uses the method of text mining in the

https://doi.org/10.17993/3cemp.2023.120151.51-66

research to explore which factors will affect consumers' evaluation behavior and willingness [15].

Text mining analysis has a strong foundation under the support of network data. Sem Eval, an international evaluation expert, defines evaluation objects as expressions that can be used to express the characteristics of evaluation entities in specified texts. When evaluating an entity as a commodity, the evaluation object at this time may be the product features, functions, and parts corresponding to the entity. For product reviews on e-commerce platforms, the evaluation objects include express delivery, services, etc. in addition to the inherent attributes of the product. For example: "The phone looks tall and the system runs very fast, but the power is not durable, so I'm a little disappointed." For this comment, "appearance" and "battery" are the evaluation objects, "tall", "Running very fast" and "Not durable" are the comments corresponding to the three evaluation objects. Therefore, the extraction of evaluation objects and comments plays an important role in the analysis of commodity evaluation texts. By analyzing the above comments, it can be found that the comments corresponding to the first two evaluation objects are positive, while the comments corresponding to the third evaluation object are negative. In the actual analysis process, whether the reviews are classified as positive, negative or neutral will affect the accuracy of text mining analysis of product reviews [16-17]. Therefore, the text mining process will extract the evaluation objects and their corresponding comments in each product review, and analyze them, which increases the accuracy of text mining analysis to a certain extent, and can be better applied to e-commerce customer satisfaction. Under evaluation. In addition, it helps e-commerce companies understand their competitive environment and position, discover the breakthrough points of the industry, and further adjust their own development strategies, so that consumers' purchasing experience in merchants can be optimized, and it is also helpful to improve the overall industry. performance level. Taking computer furniture, seafood and aquatic products, fruits and vegetables, and daily necessities as examples, some data of specific customer full score evaluation are shown in Table 1.

Table 1 Some product review data

E-commerce customer	Comment	product category
M***P	I received the phone, and the pink color is too beautiful. I really like this phone. Can last all day on a single charge	phone
Little***j	The logistics is very fast, and the lining protection of the packaging is very characteristic. The dual graphics cards work together, and the video and audio effects are good~~~	computer

https://doi.org/10.17993/3cemp.2023.120151.51-66

Call***girl	The vegetables are very fresh and the price is affordable. There are also garlic moss and eggplants that are currently scarce in the market. It is really good. Thank you for the efforts made by the ** platform for us!	vegetable and fruit
OH***!	The platform is fast, I place an order in the morning and arrive in the afternoon. After the logistics arrives, the frozen state is kept well, and the fish is very fresh.	seafood
See***door	My son loves reading books very much, he bought a lot of books on the e-commerce platform, the quality is very good, very beautiful	book
MY***baby	All solid wood furniture, no glue, no paint, with a touch of pine fragrance, I like it very much	furniture
YOU***left	The fabric and form are really, really good! Bought it for my husband, the e-commerce customer service is very greasy and loving! Buy with confidence!	clothing

The process of text mining analysis method includes text feature extraction, text data cleaning, high-frequency text selection and processing. The feature representation of text refers to a method that can use words, words, phrases or sentences as feature items to represent the entire text, and complete unstructured text processing by processing these feature items. Text features can generally be accurately expressed by words, words and phrases, while sentences and paragraphs can be further divided into words, words and phrases. The text representation method is currently uncommon. Commonly used text feature representation types are as follows:

(1) Words. Individual numbers, letters, spaces, special symbols, and Chinese characters that constitute the structural units of phrases, phrases, and concepts cannot reflect the characteristic meaning and emotional expression of the text, and need to be effectively combined. Therefore, word-based text feature representation requires Extraction and optimization of text words [18-19].

(2) Phrases. To a certain extent, it can be used as a combination of words at the most basic semantic level. Phrase-based text feature representation In a certain limited field, the phrase feature space may contain tens of thousands or even millions of phrases, which requires special dimensionality reduction processing.

https://doi.org/10.17993/3cemp.2023.120151.51-66

(3) Phrases. Single words or compound phrases extracted from the original corpus directly by entity extraction methods are generally composed of specific words, and most of them exist in typical text dictionaries.

(4) Concept. Based on rules or hybrid classification methods, through preprocessing procedures, specific unit combinations are formed by manual counting, identifying individual words, compound phrases, entire sentences and even larger syntactic units.

This text mining analysis collects text comment data from five e-commerce platforms such as Amazon, eBay, Alibaba, JD.com, and Taobao. The product types include furniture, home appliances, digital products, fresh fruits, seafood and meat, and daily necessities[20-22]. The collected text data is processed by data cleaning, word segmentation, etc., and text mining analysis is performed on the data to construct high-frequency words in comments to study the customer satisfaction evaluation of e-commerce platforms.

1) Use web crawler technology to capture customer comment texts of merchants on various e-commerce platforms, filter and clean the data, remove word segmentation and other preprocessing.

2) Perform text mining analysis on the preprocessed data. This stage mainly includes the following steps: ① Select an appropriate method to determine the number of topics (because the number of topics is too large or too small will affect the interpretation of text analysis results); ② Use text mining analysis to extract topics, and thus generate document-topic Distribution matrix and topic-vocabulary distribution matrix; ③Simple sorting and interpretation of the extracted topics; ④Visually display the results of text analysis.

3) Through the interpretation of the text analysis results, it is finally verified how the merchants of the e-commerce platform affect the satisfaction evaluation of consumers, and whether there are other factors in the influence process that mediate or moderate the influence process [23-24].

In order to study the e-commerce customer satisfaction evaluation criteria more accurately, the text topics identified by text mining analysis are in common: logistics, price, service, quality, and packaging. Based on the five types of e-commerce platforms such as Amazon, eBay, Alibaba, Jingdong and Taobao, the text analysis method is used to calculate the five text themes in the five categories of furniture, home appliances, digital products, fresh fruits, seafood and meat, and daily necessities. The weight occupied, and the radar chart is drawn according to the weight, as shown in Figure 2.

https://doi.org/10.17993/3cemp.2023.120151.51-66

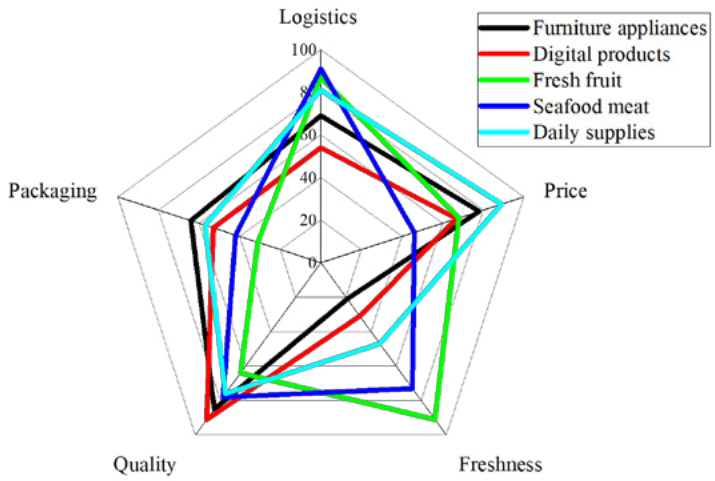

Figure 2 Radar chart of various themes of various e-commerce platforms

It can be seen from Figure 2 that customers value different characteristics of different types of products on the e-commerce platform. For example, for commodities such as fresh fruits, seafood and meat, consumers place the most importance on freshness and quality, and for other types of products, consumers place the most importance on quality. On the whole, consumers pay more attention to the quality, price and logistics of the products of the e-commerce platform. According to the research results, for the major e-commerce platforms, the following suggestions are put forward to improve customer satisfaction:

quality. The above e-commerce platforms all have stable brand suppliers and controllable product sources. There are certain advantages in terms of quality. E-commerce platforms can also achieve quality traceability through technologies such as blockchain and the Internet of Things. After the information is visualized, consumers have more trust in the quality of the products, and the platform will pay more attention to the quality problems in the production process. Price [25]. Some products of the above-mentioned e-commerce platforms are directly sourced, and some products have established their own product bases, so they can provide relatively favorable prices. E-commerce platforms can also compare multiple parties when selecting suppliers. Under the premise of ensuring quality, they can cooperate with suppliers for a long time. At the same time, they can optimize logistics, warehousing and other solutions to reduce costs, so as to give customers the best price.

3. E-COMMERCE CUSTOMER SATISFACTION EVALUATION METHOD BASED ON PSO-LSTM AND TEXT MINING

In the previous section, we conducted text mining on e-commerce customer satisfaction evaluation texts to explore how e-commerce platforms affect consumer satisfaction evaluation behavior, and to find important factors that affect e-commerce

https://doi.org/10.17993/3cemp.2023.120151.51-66

customers' satisfaction evaluation behavior. The factor is single, only high-frequency words are counted, and the time changes of customer evaluations are not considered, so the accuracy is low. The PSO-based LSTM algorithm transforms its structure on the basis of the traditional artificial neural network algorithm, so as to achieve the purpose of enabling the network to remember past time information, so that the network can not only realize the connection from bottom to top (input-output), but also It can also realize information transmission and recording from left to right (time t-time t+1). Therefore, the combination of PSO-LSTM calculation and text mining analysis can more accurately study the satisfaction evaluation of e-commerce customers. The algorithm flow of PSO-LSTM will be discussed in depth below.

1 The forward propagation process

(1) Input-hidden layer

The PSO-LSTM algorithm is a two-dimensional feature algorithm. After the input layer-hidden layer-output layer operation, the local features of the input data are extracted. In this paper, ft is used to represent the channel input of the PSO-LSTM algorithm model, yt is the output weight of the PSO-LSTM algorithm model, Wf is the bias vector of the input layer, and Vht is the receptive field of the output layer on the input data. The algorithm process is shown in formulas (1)-(2):

$$f_t = \sigma\left(W_f h_{t-1} + U_f x_t + b_f\right). \quad (1)$$

(2) Hidden layer - output layer

$$y_t = \sigma\left(V h_t + b_y\right). \quad (2)$$

2. Backpropagation process

(1) Define the error function of the sequence

At time t, the actual output of the LSTM is $y_t = \left\{y_1(t), y_2(t), \ldots, y_p(t)\right\}^T$, while the expected output is $d_t = \left\{d_1(t), d_2(t), \ldots, d_p(t)\right\}^T$, Then the loss function of the entire time series is

$$L = \sum_{t=1}^{T} L_t. \quad (3)$$

Therefore,

$$L_t = \frac{1}{2}\left(y_t - d_t\right)^2. \quad (4)$$

(2) Define the error term at time t

That is, the partial derivative of the loss function to the output value. First, define the error term of the output layer at time t as $\delta y_t = \frac{\partial L_t}{\partial y_t}$, Second, define the error term in the hidden layer at time t.

https://doi.org/10.17993/3cemp.2023.120151.51-66

Error in output gate:

$$\delta h_t = \frac{\partial L_t}{\partial h_t} = \frac{\partial L_t}{\partial y_t}\frac{\partial y_t}{\partial h_t} = \delta y_t \cdot y_t \quad (1 - y_t) \quad \cdot$$

$$\delta o_t = \frac{\partial L_t}{\partial o_t} = \frac{\partial L_t}{\partial h_t}\frac{\partial h_t}{\partial o_t} = \delta h_t \cdot \tanh(C_t). \tag{5}$$

Because the information of all moments is stored in the memory cell state, the error term δCt needs to be accumulated at each moment, and the error returned to the memory cell is divided into two parts, the first part is returned from the output ht of the hidden layer The second part is the error returned from the memory cell state at the next moment Ct+1:

$$\delta C_t = \frac{\partial L_t}{\partial C_t} = \frac{\partial L_t}{\partial h_t}\frac{\partial h_t}{\partial C_t} = \delta h_t \cdot \left[1 - \tanh(C_t)^2\right] \quad \cdot \tag{6}$$

First calculate the error term of the memory cell state in the hidden layer at the previous moment:

$$\delta C_{t-1} = \frac{\partial L_t}{\partial C_{t-1}} = \frac{\partial L_t}{\partial C_t}\frac{\partial C_t}{\partial C_{t-1}} = \delta C_t \cdot f_t, \tag{7}$$

From this formula, the error returned from the memory cell state at time t+1 Ct+1:

$$\delta C_t = \delta C_{t+1} \cdot f_{t+1}, \tag{8}$$

Combining (6) and (8), the error term of the memory cell state is obtained as:

$$\delta C_t = \delta C_{t+1} \cdot f_{t+1} + \delta h_t \quad \left[1 - \tanh(C_t)^2\right] \quad \cdot \tag{9}$$

Error in input gate:

$$\delta i_t = \frac{\partial L_t}{\partial i_t} = \frac{\partial L_t}{\partial C_t}\frac{\partial C_t}{\partial i_t} = \delta C_t \cdot C_t',$$

$$\delta C_t' = \frac{\partial L_t}{\partial C_t'} = \frac{\partial L_t}{\partial C_t}\frac{\partial C_t}{\partial C_t'} = \delta C_t \cdot i_t. \tag{10}$$

Error in output gate:

$$\delta f_t = \frac{\partial L_t}{\partial f_t} = \frac{\partial L_t}{\partial C_t}\frac{\partial C_t}{\partial f_t} = \delta C_t \cdot C_{t-1}. \tag{11}$$

(3) Calculate the error gradient of the weight coefficient matrix

The first step is to calculate the error gradient of the weight matrix V from the hidden layer to the output layer, and the two sides of the loss function L take the partial derivative of V to get:

$$\frac{\partial L}{\partial V} = \sum_{t=1}^{T}\frac{\partial L_t}{\partial V} = \sum_{t=1}^{T}\frac{\partial L_t}{\partial y_t}\frac{\partial y_t}{\partial V} = \sum_{t=1}^{T}\delta y_t \cdot y_t \quad (1 - y_t) h_t^T. \tag{12}$$

https://doi.org/10.17993/3cemp.2023.120151.51-66

The next step is to calculate the error coefficient in the hidden layer:

$$\frac{\partial L}{\partial W_f} = \sum_{t=1}^{T} \frac{\partial L_t}{\partial W_f} = \sum_{t=1}^{T} \frac{\partial L_t}{\partial f_t} \frac{\partial f_t}{\partial W_f} = \sum_{t=1}^{T} \delta f_t \square f_t \quad \square - f_t) h_{t-1}^T. \tag{13}$$

The error gradient from the input layer to the output layer weight matrix can also be obtained in the same way:

$$\frac{\partial L}{\partial U_f} = \sum_{t=1}^{T} \frac{\partial L_t}{\partial U_f} = \sum_{t=1}^{T} \frac{\partial L_t}{\partial f_t} \frac{\partial f_t}{\partial U_f} = \sum_{t=1}^{T} \delta f_t \square f_t \quad \square - f_t) x_t^T. \tag{14}$$

(4) Update of the weight matrix

$$V_{new} = V + \eta \frac{\partial L}{\partial V}. \tag{15}$$

In this paper, the PSO-LSTM algorithm uses an activation function in the neurons and the final prediction layer, which can combine the linear input nonlinearly, so that the PSO-LSTM algorithm has nonlinear factors, and the prediction is more accurate. The commonly used activation functions are Sigmoid function, Relu function, Tanh function. The activation functions of the LSTM network at the neurons are the Relu function and the Tanh function, which are often used because of their simple calculation and fast iteration speed [26-27]. The Sigmoid function is used in the output layer for binary classification probability calculation.

The mathematical formula for the sigmoid function is：

$$sigmoid(x) = \frac{1}{1 + e^{-x}} \tag{16}$$

The mathematical formula for the Tanh function is:

$$\tanh(x) = \frac{1 - e^{-2x}}{1 + e^{-2x}} \tag{17}$$

The mathematical formula for the Relu function is：

$$f(x) = \max(0, x) \tag{18}$$

According to the traditional method of training deep models, the LSTM model in this paper uses the stochastic gradient descent algorithm to train parameters. Choose a cross-entropy loss function according to the classification target definition：

$$E^N = -\frac{1}{N} \sum_{n=1}^{N} \sum_{k=1}^{c} t_k^n \log y_k^n \tag{19}$$

Among them, N represents the number of samples, and c represents the number of categories. tkn represents the true category of the nth sample, and ykn represents the prediction result of the nth sample. The purpose of training the model is to minimize the loss function. Define the output of layer Z as：

https://doi.org/10.17993/3cemp.2023.120151.51-66

$$x^l = f\left(u^l\right)$$
$$u^l = \omega^l x^{l-1} + b^l \quad (20)$$

Among them, f represents the activation function, xl−1 represents the output of the L-1 layer, and for the L layer, it is also its input, l represents the weight of the L layer, and b represents the L layer bias. In the process of error back propagation algorithm, this model uses gradient descent method to update the weight of the calculation network. The update calculation formula of gradient descent method is as follows:

$$\omega_{\text{new}}^l = \omega_{\text{old}}^l - \eta \frac{\partial E}{\partial \omega_{\text{old}}^l}$$
$$b_{\text{new}}^l = b_{\text{old}}^l - \eta \frac{\partial E}{\partial b_{\text{old}}^l} \quad (21)$$

Among them, represents the learning rate in the gradient descent calculation, and the update formula of the weight of each layer can be obtained according to the chain derivation rule. In the process of classifying information texts, there are many situations in the classification results. The following four possibilities exist for the classification results:

(1) True class True positives (TP): The number of positive samples that were successfully identified;

(2) False positives (FP): The number of negative samples that are misidentified;

(3) False negatives (FN): The number of positive samples that are incorrectly identified;

(4) True negatives (TN): The number of negative samples that are correctly identified;

Based on the method of text mining in Chapter 3, and the high-frequency vocabulary logistics, price, freshness, quality and packaging it excavated are the text positive classification data of PSO-LSTM. The sample data are customer evaluations of furniture appliances, digital products, fresh fruits, seafood and daily necessities of the five major e-commerce platforms, from March 2017 to March 2021. The essence of the experiment in this paper is to classify information texts, so only the text and category labels in the collected forum data are extracted as experimental data. The purpose of selecting category labels is to distinguish normal information and spam information with 0 and 1 respectively, the class labels in the category are verified manually, so the labels of the data are true and reliable. The total number of collected data is 83,961 texts, including 14,678 spam messages and 69,283 normal messages. Formulas (1)-(15) are the calculation equations for filtering text data by PSO-LSTM, and the activation function is used in the neurons and the final prediction layer, which can combine the linear input nonlinearly, so that the PSO-LSTM algorithm has non-linear combination. Linear factor, the prediction is more accurate, and the high-frequency words of text mining are classified and calculated according to formulas (22)-(25). Through the previous theoretical research basis and data processing

https://doi.org/10.17993/3cemp.2023.120151.51-66

process, the time division of the weights of high-frequency vocabulary logistics, price, freshness, quality and packaging is carried out, as shown in Figure 3

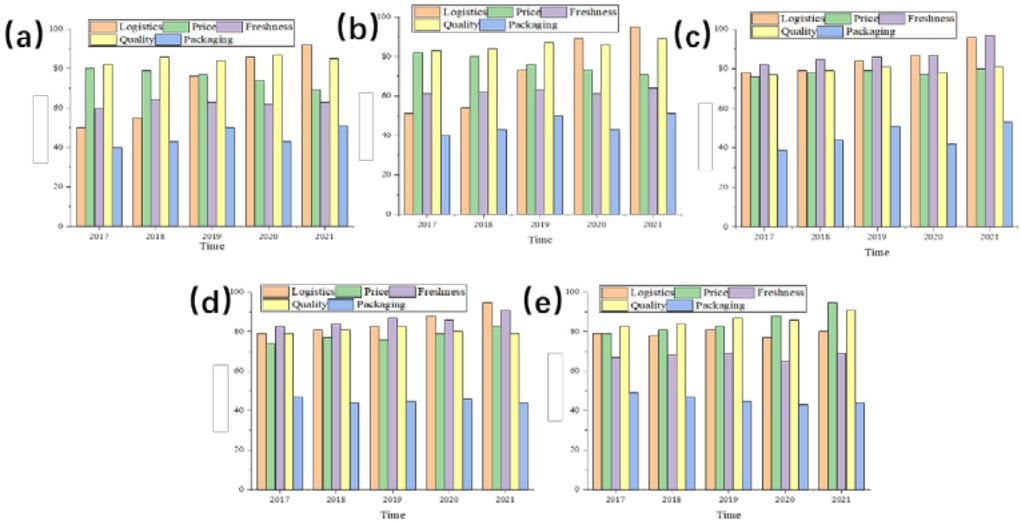

Figure 3 The relationship between the characteristics of various e-commerce platforms (a) furniture and home appliances (b) digital products (c) fresh fruit (d) seafood and meat (e) daily necessities over time

As can be seen from Figure 3(a), with the increase of time, the highest change rate of high-frequency words in e-commerce customers' satisfaction with furniture and home appliances is logistics speed, and its weight is 52 in 2017, and gradually increases to 91 in 2021. This also means that when other factors remain unchanged, the faster the logistics of furniture and home appliances on the e-commerce platform, the higher the customer satisfaction rating; as shown in Figure 3(b), as time goes by, e-commerce customers are more interested in The highest rate of change in the high-frequency words of satisfaction of digital products is also the logistics speed, and its weights from 2017 to 2021 are 51, 54, 73, 89 and 95 respectively; as can be seen from Figure 3(c)-(d), With the increase of time, the most frequent change rate of e-commerce customers' satisfaction with fresh fruits, seafood and meat is their freshness, followed by logistics. The weight of the freshness of the subject word was 82 in 2017 and gradually increased to 97 in 2021. This also means that when other factors remain unchanged, the faster the freshness of fresh fruits and seafood on the e-commerce platform, the higher the customer satisfaction rating; as shown in Figure 3(d), with the increase of time, E-commerce customers' satisfaction with daily necessities has the highest change rate of high-frequency words in price, followed by quality.

In summary, in 2017, the development of e-commerce platforms was relatively weak, the number of e-commerce shoppers was relatively small, and customer satisfaction at that time was more inclined to price, which also meant that the higher the product prices of the merchants on the e-commerce platform. When it is low, the customer satisfaction rating is higher. With the development of e-commerce platforms, customers pay more and more attention to the speed of logistics and the freshness of products. Through data processing through the PSO-LSTM algorithm, it can be seen that in 2018, the proportion of logistics and freshness has increased significantly,

https://doi.org/10.17993/3cemp.2023.120151.51-66

which also means that e-commerce The faster the product logistics speed of the merchants on the platform and the higher the freshness, the higher the customer satisfaction rating. With the advent of the epidemic, the e-commerce platform has entered an ice age, but through data analysis, it can be seen that from 2019 to 2021, product orders on the e-commerce platform will still grow steadily.

4. CONCLUSION

This paper mainly studies the analysis process of e-commerce customer satisfaction evaluation based on PSO-LSTM and text mining, and conducts analysis and research according to the obtained results. The text data of the text all come from five categories of products such as furniture, home appliances, digital products, fresh fruits, seafood and meat, and daily necessities on the five e-commerce platforms of Amazon, eBay, Alibaba, Jingdong, and Taobao. When using text mining technology to analyze the evaluation of e-commerce customer satisfaction, five subject words that have the highest impact on customer satisfaction evaluation are obtained: logistics, price, freshness, quality and packaging.

Since the text mining technology does not consider the time factor, the accuracy of the measured factors is low. In order to more accurately study the factors affecting the evaluation of e-commerce customer satisfaction on the time scale, the text analysis technology and the PSO-LSTM model were combined to further analyze the five types of high-frequency words that affect the evaluation of e-commerce customer satisfaction, and to analyze Its proportion is analyzed. Analyzed the proportion of factors affecting the evaluation of e-commerce customer satisfaction in each time period. For furniture and home appliances, with the increase of time, the highest change rate of high-frequency words in e-commerce customers' satisfaction with furniture and home appliances is logistics speed, the maximum weight is 91 in 2021, and the minimum weight is 52 in 2017; E-commerce customers who buy fresh fruit or seafood are more concerned about the freshness of the goods, and their weight will gradually increase from 82 in 2017 to 97 in 2021. Through the data processing of PSO-LSTM algorithm, it can be seen that due to the impact of the epidemic, the logistics speed and quality have shown a trend of substantial improvement. On the whole, consumers pay more attention to the quality, price and logistics of the products of the e-commerce platform. The evaluation method of e-commerce customer satisfaction based on PSO-LSTM and text mining designed in this paper can effectively solve the imbalance of information datasets, and is exp

REFERENCES

(1) Le S , Wu Y , Guo Y , et al. **Game Theoretic Approach for a service function chain routing in NFV with coupled constraints[J]**. *Circuits and Systems II: Express Briefs, IEEE Transactions on*, 2021, PP(99):1-1.

(2) Mitsuru, Toyoda, Yuhu. **Mayer-Type Optimal Control of Probabilistic Boolean Control Network With Uncertain Selection Probabilities.[J]**. I*EEE transactions on cybernetics*, 2019.

https://doi.org/10.17993/3cemp.2023.120151.51-66

(3) Wu Y, Guo Y, Toyoda M. **Policy Iteration Approach to the Infinite Horizon Average Optimal Control of Probabilistic Boolean Networks[J]**. I*EEE Transactions on Neural Networks and Learning Systems*, PP(99):1-15.

(4) Zhang Y, Qian T, Tang W. **Buildings-to-distribution-network integration considering power transformer loading capability and distribution network reconfiguration[J]**. *Energy*, 2022, 244.

(5) Li, H., Deng, J., Feng, P., Pu, C., Arachchige, D., and Cheng, Q., (2021) **Short-Term Nacelle Orientation Forecasting Using Bilinear Transformation and ICEEMDAN Framework**. *Front. Energy Res*. 9, 780928.

(6) Li, H., Deng, J., Yuan, S., Feng, P., and Arachchige, D., (2021) **Monitoring and Identifying Wind Turbine Generator Bearing Faults using Deep Belief Network and EWMA Control Charts**. *Front. Energy Res*. 9, 799039.

(7) Yang Ligong, Tang Shiping, Zhu Jian. **Sentence Love Based on Markov Logic Network Sense Analysis Method [J]**. *Journal of Beijing University of Technology*, 2013, 33(6): 600-604.

(8) Ming Junren. **Research on Text Sentiment Analysis Algorithm Integrating Semantic Association Mining [J]**. *Library and Information Work*, 2012, 56(15): 99-103.

(9) Cai Xiaozhen, Xu Jian, Wu Sizhu. **Research on User Comment Filtering Model for Sentiment Analysis [J]**. *Modern Library and Information Technology*, 2014, 30(4): 58-64.

(10) Tang Xiaobo, Xiao Lu. **Research on Comment Mining Model Based on Sentiment Analysis [J]**. *Intelligence Theory and Practice*, 2013, 36(7): 100-105.

(11) Liu L, Song W, Wang H, et al. **A novel feature-based method for sentiment analysis of Chinese product reviews[J]**. *China Communications (English version)*, 2014, 11(3): 154-164.

(12) Medhat W, Hassan A, Korashy H. **Sentiment analysis algorithms and applications: A survey[J]**. *Ain Shams Engineering Journal*, 2014, 5(4): 1093-1113.

(13) Hochreiter S, Schmidhuber J. **Long Short-Term Memory[J]**. *Neural Computation*, 1997, 9(8): 1735-1780.

(14) Zhou Ying , Liu Yue , Cai Jun . **Sentiment Analysis of Weibo Based on Attention Mechanism [J]**. *Intelligence Theory and Practice*, 2018,41(03):89-94

(15) Fan Qingbo, Jiang Fucai, Ma Quandang, et al. **BP Neural Network-Markov Ship Traffic Prediction Model Based on PSO [J]**. *Journal of Shanghai Maritime University*, 2018, 39(2): 22-27, 54.

(16) Feng Yuxu, Li Yumei. **Research on CSI 300 Index Prediction Model Based on LSTM Neural Network [J]**. *Practice and Understanding of Mathematics*, 2019, 49(7): 308-315.

(17) Zhao Jingpeng. **Research on hierarchical Web service classification method based on deep learning [D]**. *North China Electric Power University (Beijing)*, 2021.

(18) Luo Zhengjun, Ke Mingsong, Zhou Dequn. **Research on Text Sentiment Analysis Model Based on Improved LSTM [J]**. *Computer Technology and Development*, 2020, 30(12): 40-44.

https://doi.org/10.17993/3cemp.2023.120151.51-66

(19) Li Qichao. **Analysis of web data mining technology based on cloud computing environment [J]**. *Information Technology and Informatization*, 2020(09):54-56.

(20) Kong Jia, Deng Sanhong, Zhang Yue, Zhang Yiwei. **Thematic mining of science and technology news in the Web environment: Taking the field of international polar expeditions as an example [J]**. *Science and Technology Management Research*, 2020, 40(17): 173-179.

(21) Liu Yong. **Design and implementation of substation equipment defect management system based on Web technology [D]**. *University of Electronic Science and Technology of China*, 2020. https://doi.org/10.27005/d.cnki.gdzku.2020.004586.

(22) Yang Mengda. **Temperature prediction based on improved PSO-LSTM neural network [J]**. *Modern Information Technology*, 2020, 4(04): 110-112.

(23) Xia Maosen, Jiang Lingling. **Analysis of "Maker" Hot Words Based on Web Text Mining [J]**. *Journal of Hubei University of Science and Technology*, 2019, 39(05): 56-62.

(24) He Yun. **Research on intelligent traffic flow prediction based on PSO-LSTM algorithm [J]**. *Qinghai Transportation Science and Technology*, 2019(04):76-79.

(25) Zhou Zhou. **Analysis and Research on the Curriculum Setting of Secondary Vocational E-commerce Majors Based on Web Text Mining [D]**. *Guangdong Normal University of Technology*, 2019.

(26) Frayssinet, M., Esenarro, D., Juárez, F. F., y Díaz, M. (2021). **Methodology based on the NIST cybersecurity framework as a proposal for cybersecurity management in government organizations**. *3C TIC. Cuadernos de desarrollo aplicados a las TIC*, 10(2), 123-141. https://doi.org/10.17993/3ctic.2021.102.123-141

(27) Che Xiangbei,Li Man,Zhang Xu,Alassafi Madini O. & Zhang Hongbin.(2021). **Communication architecture of power monitoring system based on incidence matrix model**. *Applied Mathematics and Nonlinear Sciences (1)*. https://doi.org/10.2478/AMNS.2021.1.00098.

https://doi.org/10.17993/3cemp.2023.120151.51-66

/04/

RESEARCH ON LOGISTICS DISTRIBUTION ROUTE OPTIMIZATION BASED ON DEEP LEARNING MODEL AND BLOCK CHAIN TECHNOLOGY

Xiaoshan Yang*

Student Work Division, Nantong Institute of Technology, Nantong, Jiangsu, 226000, China

yxs15262754327@163.com

Weiwei Guan

College of Business, Nantong Institute of Technology, Nantong, Jiangsu, 226000, China

Reception: 28/10/2022 **Acceptance**: 29/12/2022 **Publication**: 24/01/2023

Suggested citation:

Y., Xiaoshan and G., Weiwei (2023). **Research on logistics distribution route optimization based on deep learning model and block chain technology** . *3C Empresa. Investigación y pensamiento crítico, 12(1)*, 68-85. https://doi.org/10.17993/3cemp.2023.120151.68-85

ABSTRACT

The growing data age is reflected in all aspects of today's society. In the field of logistics, especially when the road conditions in urban areas are complex, how to select the optimal distribution path and reduce the distribution time is a problem worthy of attention. Aiming at the problems faced by traditional algorithms in solving the distribution of logistics vehicles in urban areas, however, the method based on regional chain technology can better solve the path optimization problem. A deep reinforcement learning algorithm based on attention mechanism and LSTM model is designed and applied to the distribution path planning of logistics vehicles. The distribution optimization path of logistics vehicles is obtained through sample training experiments, Thus, it provides a new idea for the optimization of logistics distribution path.

KEYWORDS

Regional chain technology; Logistics distribution route; Optimization; Attention mechanism; LSTM model

PAPER INDEX

https://doi.org/10.17993/3cemp.2023.120151.68-85

1. PREFACE

With the rapid development of modern information technology and the arrival of the era of big data, a large amount of scientific and technological information has different values, which can promote the development of human science and technology to a certain extent [1-4]. With the in-depth development of cross-border e-commerce, people's demand for logistics efficiency has increased rapidly, and modern information technology has gradually entered the logistics field in this region. As one of the cutting-edge modern information technologies, blockchain technology is also trying to enter, but its applicability needs in-depth research. At the same time, economic cooperation has widened the gap between supply and demand of regional logistics services. In order to alleviate this contradiction, exploratory research is carried out on the applicability of blockchain technology in this field. From the component perspective, the regional logistics subject and the current situation of logistics demand make the blockchain technology applicable at the theoretical level. Based on the application scheme of each component, the applicability of blockchain technology at the practical level is further verified with the combination of simulation and analytic hierarchy process. This technology helps to improve the transparency of regional logistics services and build an efficient logistics mechanism [5-6].

At the same time, with the progress of science and technology society, people also put forward higher requirements for logistics distribution services, the most important of which is the punctuality of logistics distribution [7-8]. Therefore, for this requirement, it is required that the logistics distribution path should be optimized as much as possible. However, at present, specific urban areas such as communities and schools have complex characteristics such as dense customer nodes and fixed areas, so the optimization of distribution path is in an important research position. However, from the perspective of domestic research, there is little research on solving methods based on artificial intelligence. At present, domestic scholars mainly focus on heuristic algorithm, meta heuristic algorithm and its improved algorithm. Wei Xiaodi et al [9] used an improved algorithm of discrete flower pollination algorithm and discrete flower pollination algorithm, the flower pollination operator is redefined and combined with the improved genetic operator. Su Xinxin et al [10] relaxes the vehicle capacity and customer time window, adds the penalty to the objective function, uses the greedy algorithm to generate the initial solution, and then uses the tabu search algorithm to solve it. Four operators are used to search the solution of the neighborhood. In order to further expand the search range, they use the perturbation operator. At present, foreign research on VRP has successively emerged artificial intelligence methods such as pointer network and decoder network to optimize vehicle route. Mao et al [11] proposed a more practical mathematical model of vehicle routing problem with pick-up and delivery, and used the double termination criterion to generate a new solution by adding storage function and using intra line and inter line exchange.Cordeau et al [12] adopts a unified tabu search heuristic method: periodic and multi site vehicle routing problem with time window. The performance of the heuristic algorithm is evaluated by comparing it with the alternative method of benchmark instance with the characteristics of VRPTW problem.

https://doi.org/10.17993/3cemp.2023.120151.68-85

We mainly elaborate the problem of logistics distribution path optimization, clarify that the main form of path optimization in logistics distribution is the problem of determining the starting and ending points, and introduce the method of deep learning in view of the shortcomings of the implementation process of traditional evolutionary algorithm in path optimization and the difficulties of logistics distribution path optimization in complex road conditions. The attention mechanism model based on deep reinforcement learning algorithm is improved, and the model is applied to the logistics distribution vehicle distribution path optimization problem. The strategy network model is built through model components such as delivery length memory neural network, decoder and attention mechanism module, and the logistics distribution path optimization problem is handled through numerical experimental training, verification, test and analysis, so as to promote the development of the logistics field.

2. ANALYSIS OF LOGISTICS DISTRIBUTION ROUTE OPTIMIZATION

2.1. LOGISTICS DISTRIBUTION PATH OPTIMIZATION

Logistics distribution path optimization is a complex problem, which is mainly to solve the problem of path selection in logistics distribution. Usually, the logistics distribution path optimization problem needs to consider the transportation capacity of vehicles, limited time, transportation cost and other conditions. In the actual logistics distribution activities, the proportion of these factors will change. Therefore, the research on the logistics distribution path optimization problem is also divided into many aspects, and the algorithms used are also various. When selecting the algorithm, we should combine the cost constraints such as distribution capacity and time, and fully consider the problems encountered in the actual distribution, so that the algorithm can get an excellent distribution route solution [13-14].

(1)Concept of logistics distribution route optimization

The rapid economic development of our country also brings the leapfrog development of animal logistics industry, especially the rocket development of e-commerce, which has played a great role in promoting the development of logistics industry. The research on the optimization of logistics distribution has become increasingly important [15-16]. However, the current research mainly focuses on the small cars of trucks or express brothers. In the urban transportation network, the optimal route is solved according to the set algorithm model. The optimal route usually needs to consider five conditions [17-19]. The first is the means of transport, which needs to consider the types of means of transport and the cargo carrying capacity of the means of transport. The appropriate selection and allocation of means of transport is an important premise in the rationalization of transport. The second is the transportation link. At the beginning of transportation, goods need to be sorted and loaded. When the type and quantity of goods are large, this work will take up a lot of

https://doi.org/10.17993/3cemp.2023.120151.68-85

operation time and increase labor and packaging costs. Therefore, the distribution link shall be minimized in the distribution, so as to reduce the cost. The third is transportation time. In today's logistics, transportation time becomes more and more important. There are strict time requirements for the distribution of many items, such as perishable fresh food, items that must be delivered within a specified time limit, etc. Distribution time is not only the requirement of distribution, but also the intuitive embodiment of the distribution ability of logistics companies, which affects the satisfaction of customers. Reducing transportation time is very important to the development of logistics companies. How to reduce the delivery time is the focus of logistics distribution path optimization. The fourth is the transportation distance. Compared with the above factors, the transportation distance has less and less impact on the optimization of logistics distribution path in today's fast traffic environment. However, the increase of transportation distance will also lead to the increase of uncontrollable factors. Now the high incidence of traffic accidents and the increase of road obstacles make the risk cost greatly increase when the transportation distance becomes longer. Therefore, in the optimization of logistics distribution path, we should also try to shorten the transportation distance. The fifth is the transportation cost, which is the key of logistics distribution. After all, logistics distribution is a business activity that pursues the maximization of benefits. The transportation cost mainly includes human cost and loss cost. Now the human cost is getting higher and higher. This problem can be effectively solved by improving the work efficiency of logistics personnel [20-24].

According to different constraints, distribution problems can be roughly divided into the following categories: traveling salesman problem (TSP), collection and forwarding problem, time limited path optimization, multi vehicle path optimization, path optimization with loading capacity constraints, path optimization with compatibility constraints, etc [25-29]. Some literatures are divided into static path optimization problem SVRP and dynamic path optimization problem DVRP according to the treatment methods of the changes of influencing factors in logistics distribution. In today's logistics distribution links, most of the logistics distribution path optimization problems can be regarded as the traveling salesman problem and the problem of determining the starting and ending points. The continuous and rapid growth of traffic flow leads to complex and changeable traffic conditions. Therefore, in the logistics distribution path optimization problem, the research on the logistics distribution path optimization problem based on dynamic road conditions has very important research significance and application value.

(2)Logistics distribution path optimization

In modern logistics distribution, goods are often sent directly to customers from distribution centers or stores. At this time, the form of logistics distribution path optimization is: knowing the departure and arrival places, selecting the best transportation route in the urban transportation network, delivering goods in the shortest time and improving distribution efficiency. The specific form is shown in Figure 1.

https://doi.org/10.17993/3cemp.2023.120151.68-85

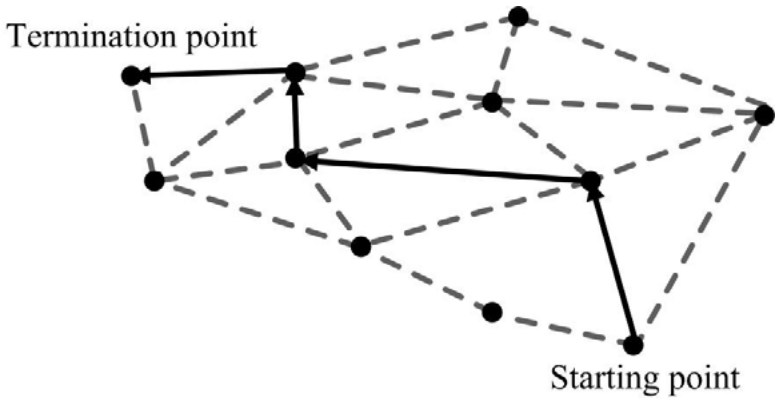

Figure 1 Schematic diagram of starting and ending points of distribution

As can be seen from Figure 1, distribution vehicles start from the starting point, each line represents a road section, and nodes represent intersections. The optimization process is to select the route with the lowest weight value in the urban transportation network to reach the distribution terminal.

2.2. COMPLEXITY OF LOGISTICS DISTRIBUTION ROUTE OPTIMIZATION

In recent years, great changes have taken place in the way, environment and requirements of logistics distribution in China, such as the intelligent management of modern logistics, the changes of logistics transportation tools, customers' higher requirements for logistics distribution standards and increasingly complex traffic conditions. It also puts forward new requirements for the algorithm of logistics distribution path optimization. The traditional algorithm mainly exists in today's logistics distribution path optimization: the solution mode is single, the research on the change of path in path optimization is not accurate enough, and the distribution route cannot be changed flexibly when the traffic conditions change [30].

(1) Complexity of road condition changes

Road conditions many accidents will have a serious impact on road traffic. For example, accidents, road construction, infrastructure construction, abnormal weather, holidays and other events will reduce the road capacity or make it impassable. The traditional algorithm does not consider or deal with these influencing factors. The method is simple and rough, and the calculation accuracy of the influence value on the road condition is very low. In the route optimization, congestion and section gradient are taken into account, and the equivalent consumption is transformed into a flat road with a certain length, which is optimized by the traditional algorithm [31-33]. There is also a logistics distribution route optimization algorithm based on travel time prediction by using the historical average method to predict the road travel time [34-35]. The processing of these algorithms is relatively simple, and the complexity of road conditions is not fully considered.

(2) Complexity of logistics distribution

https://doi.org/10.17993/3cemp.2023.120151.68-85

In the actual logistics distribution link, the driver in the distribution process, the route selection mainly depends on past experience or colleagues' suggestions, which can deliver the goods quickly and effectively [36]. Or in large logistics companies, provide traffic flow guidance services to drivers through intelligent logistics software. These methods have achieved good results in practical application, but there are also some problems. In a new distribution area, drivers need to spend a lot of time getting familiar with the road, which seriously affects the efficiency of distribution. And listening to the experience of others can not guarantee the correct and timely choice in the complex road. In addition, it is difficult for the distribution personnel to understand and analyze the huge and updated information such as the surge of logistics business volume and the expansion of service area, the large-scale construction of cities and the new planning of road construction. The huge logistics distribution network has difficulty in memorizing information.

3. RESEARCH ON OPTIMIZATION OF LSTM LOGISTICS DISTRIBUTION PATH BASED ON BLOCKCHAIN

3.1. INTRODUCTION TO REGIONAL CHAIN TECHNOLOGY

Blockchain technology is a decentralized distributed database. A continuous record storage structure is formed on the block with time stamps. The block contains various recording applications, such as clearing, smart contract, etc. the data recording node calculates the hash through a specific algorithm, and the current hash, previous block hash, data record, etc. are recorded in the block. Such a data system is credible, so blockchain is a tool for manufacturing credit, and the irreversibility and irreversibility of blockchain technology are all highlighted.

However, regional chain technology has many advantages. Blockchain adopts distributed accounting and storage, and there is no centralized hardware or management organization. Therefore, the rights and obligations of any node are equal. Moreover, the blockchain system is open in nature. In addition to the private information of the trading parties being encrypted, the data of the blockchain is open to all. In the blockchain, any human intervention will not work, changing the trust in "people" to the trust in machines [37]. It enables all nodes in the whole system to exchange data freely and safely in the untrusted environment. In addition, once the information is verified and added to the block in the blockchain, it will be permanently stored and cannot be modified, which improves the corresponding security. In addition, there are regular changes in the changes of urban traffic conditions in a certain period of time. There must be the characteristics of road condition information in this large amount of traffic data. Compared with the traditional neural network, the regional chain technology has a stronger ability to extract the characteristics of traffic data through the setting of multi hidden layer parameters. After the self coding learning and training of road information features, the internal correlation of road information features is closer, so that the prediction of future road conditions is more accurate. Provide accurate road condition parameters for logistics distribution path

https://doi.org/10.17993/3cemp.2023.120151.68-85

optimization. Compared with traditional algorithms, the optimization results in actual distribution are more accurate.

3.2. INTRODUCTION TO LSTM MODEL

LSTM is an improved version of sample RNN. RNN will be affected by short-term memory, but LSTM can remember longer sequences. During back propagation, RNN will disappear gradient. If the gradient value becomes very small, it will not continue to learn. LSTM can solve this series of problems. Figure 2 shows a unit structure of LSTM model σ And tanh represent the feedforward network layer, where σ The activation function in is sigmoid.

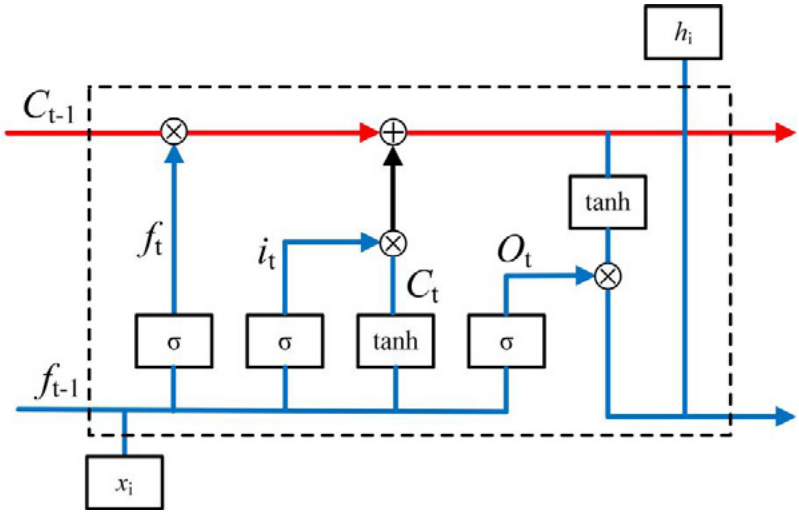

Figure 2 Structure diagram of LSTM model unit

The LSTM model has the characteristics of "long-term and short-term memory", which can be analyzed in this way. It can be seen from Figure 2 that the part shown by the red line is long-term memory. There is only a small amount of linear interaction on this line, which can realize the passage of information from the whole cell structure without change. The part shown by the blue line is short-term memory, which has three parts. The first part is the forgetting gate, It will use ht-1 and Xt to determine which information in the previous unit state Ct-1 is removed. The function formula used is (1):

$$f_t = sigmoid(W_{fx}X_t + W_{fh}h_{t-1} + b_f), \quad (1)$$

The second part is the input gate, which determines which information is put into the unit state, mainly including two steps. The first is that the tanh layer generates the candidate value $C_t^{'}$ that can be added to the state, where $C_t^{'}$ is shown in formula (2). The second is that the sigmoid layer generates the activation value it of the input gate based on ht-1 and Xt, where it is shown in formula (3):

$$C_t^{'} = \tanh(W_{cx}X_t + W_{ch}h_{t-1} + b_c), \quad (2)$$

$$i_t = sigmoid(W_{ix}X_t + W_{ih}h_{t-1} + b_i), \quad (3)$$

https://doi.org/10.17993/3cemp.2023.120151.68-85

The results of the first and second parts jointly determine the new cell state Ct, where Ct is shown in formula (4):

$$C_t = f_t \square C_{t-1} + i_t \square C_t^{'}, \quad (4)$$

The third part is the output gate, which determines which information in the unit state is used for production output. The function used is shown in formula (5) (6):

$$o_t = sigmoid(W_{Gx} X_t + W_{Gh} h_{t-1} + b_G), \quad (5)$$

$$h_t = o_t \square \tanh(C_t). \quad (6)$$

3.3. LOGISTICS DISTRIBUTION VEHICLE ROUTING PLANNING MODEL

All learning algorithms are learned through data. By analyzing the data characteristics of customer requirements, customer location information and demand information, we quantify the location information and demand information of customer nodes, and use the deep reinforcement learning method to design an end-to-end framework to solve the logistics vehicle routing problem [38]. In this method, the training strategy network and value network model only observe the reward signal and follow the feasibility rules to find the near optimal solution for the problem samples sampled from the given distribution. It can be simply explained as a parameterized probability estimation model based on attention mechanism or actor strategy network [39]. The structure of strategy network model is shown in Figure 3.

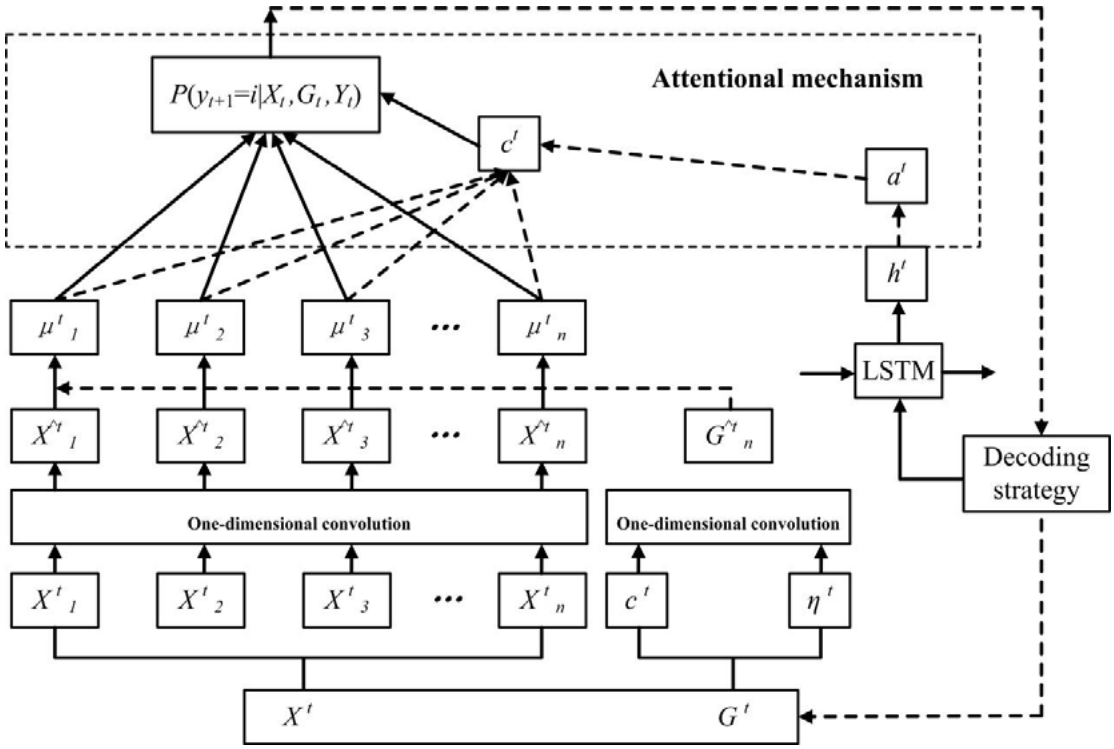

Figure 3 Attention mechanism model based on deep learning reinforcement learning algorithm

https://doi.org/10.17993/3cemp.2023.120151.68-85

This model includes three parts: customer state information fusion module, attention mechanism module and LSTM module. The customer state information fusion module can transform the structured local and global data information into high-dimensional vectors and fuse the information. The attention mechanism module can estimate the probability of each node I. The LSTM module can remember a longer sequence of customer nodes and improve the solution quality of the model to deal with the customer scale of unmanned fleet and distribution path.

(1)The first part of the model is to map the local and global state information of reinforcement learning into a high-dimensional vector space through one-dimensional convolution operation. In this process, the abstract features of customer location time interval, customer goods demand and unmanned vehicle loading are extracted through deep neural network, as shown in Figure 4.

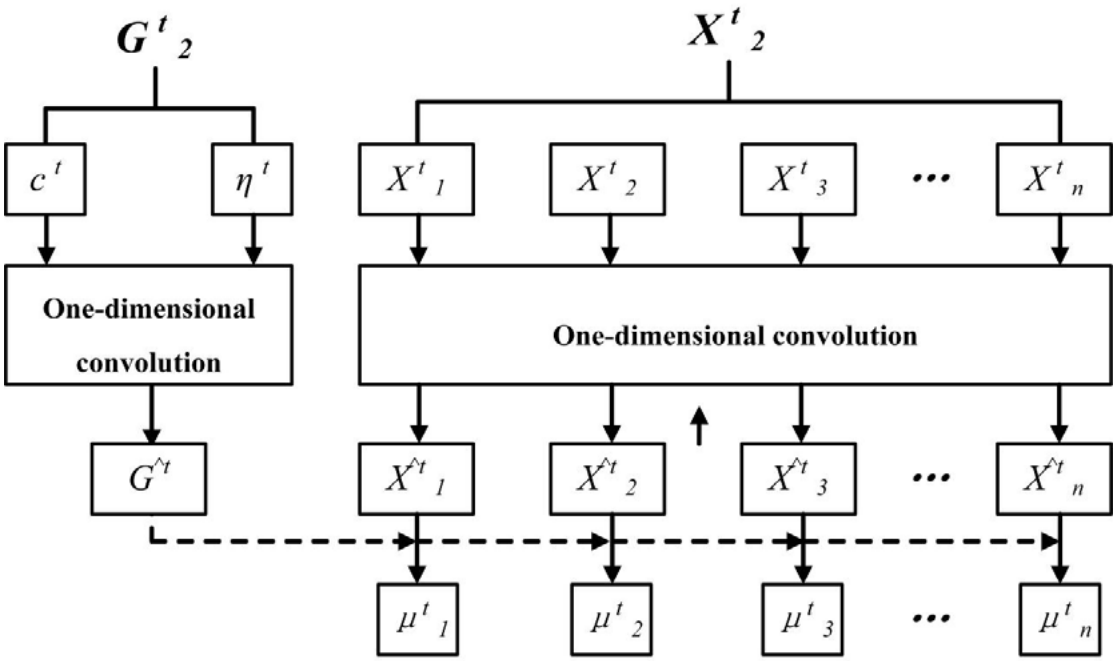

Figure 4 Reinforcement learning state input information fusion module

For customer i, its local information can be expressed by formula (7) and mapped into $\hat{X}_i^t$ vector with ξ dimension through one-dimensional convolution. In order to reduce the amount of parameters, all customers share the weight of one-dimensional convolution. Another one-dimensional convolution layer is used to map the global variable to the $\hat{G}^t$ vector space of dimension ξ, where the global variable is shown in equation (8).The dynamic and static elements contained in local information and global information learn their characteristics in two different convolution layers, and finally fuse them, just like multi-layer information fusion in supervised learning resnet50, and $\hat{G}^t$ and $\hat{X}_i^t$ are combined in a weighted linear way through the ReLU activation function, and finally the fusion information μ_i^t of customer node i is obtained. As shown in equation (9), it contains both global information and local information.

https://doi.org/10.17993/3cemp.2023.120151.68-85

$$X_i^t = (x_i, y_i, e_i, l_i, d_i^t) . \quad (7)$$

$$G^t = \{\eta^t, c^t\} . \quad (8)$$

$$\mu_i^t = \mathrm{Re}\, LU(\theta_1 \hat{X}_i^t + \theta_2 \hat{G}^t) . \quad (9)$$

The attention mechanism can effectively deal with the expansion of the scale of customer nodes. When decoding customer node i, we pay more attention to the part of customers entering the customer node. The processing ability of the attention mechanism in the face of the expansion of the scale of customer nodes is used to calculate the access probability of each node i. Firstly, the attention weight is calculated. Firstly, the similarity between the hidden state ht of the recurrent neural network and the fusion information μ_i^t of each node I is calculated to obtain v_i^t. Then, after obtaining the similarity between each customer node i and the hidden state, the attention weight a_i^t is obtained by softmax normalization transformation, and the obtained attention weight is used to calculate the weighted sum of the input information μ_i^t to obtain ct, and then the probability distribution of each customer node I is obtained [40]. The calculation diagram of attention mechanism for solving the route planning of unmanned logistics distribution fleet is shown in Figure 5, and the calculation process is shown in formulas (10) - (16).

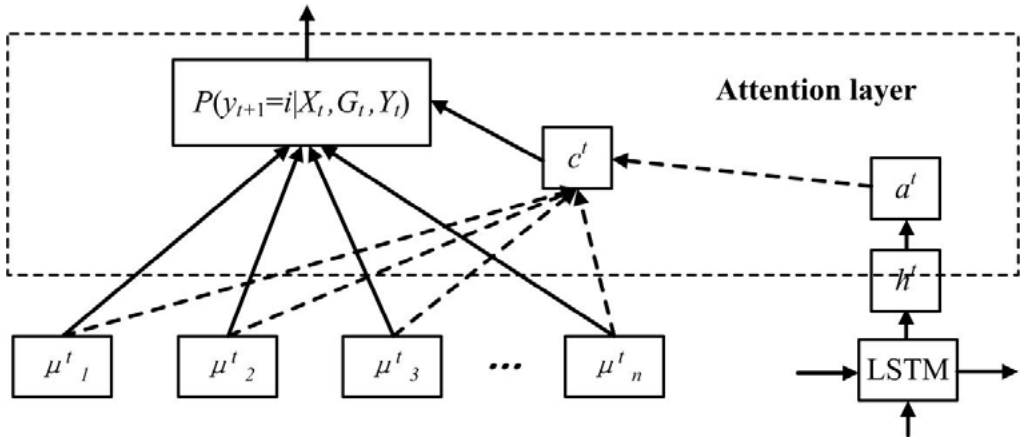

Figure 5 Calculation diagram of attention mechanism for solving logistics distribution path planning

$$v_i^t = \theta_v yanh(\theta_u [\mu_i^t, h^t]) , \quad (10)$$

$$a_i^t = Soft\max(v^t) , \quad (11)$$

$$c^t = \sum_{i=0}^{|V_c|+1} a_i^t \mu_i^t , \quad (12)$$

here ht is the hidden state output of recurrent neural network LSTM, v_i^t is the i-th term of vector v^t, tanh is a nonlinear activation function, θ_v, θ_u are a trainable variable, $|V_c|$ is the number of customer nodes, among them are:

https://doi.org/10.17993/3cemp.2023.120151.68-85

$$\tanh(x) = \frac{e^{x} - e^{-x}}{e^{x} + e^{-x}}, \quad (13)$$

$$Soft\max(x_i) = \frac{e^{xi}}{\sum_{k} e^{xk}}, \quad (14)$$

Then calculate the probability estimate of each customer, where g_i^t is the i-th element of g^t, θ_g, θ_c are trainable variables:

$$g_i^t = \theta_g \tanh(\theta_c[\mu_i^t, c_t]), \quad (15)$$

$$p_i^t = Soft\max(g^t). \quad (16)$$

(3) In Section 3.1, the long-term and short-term memory neural network is introduced. Its input has three parts. In the specific application here, the hidden state output ht-1 at the previous time, the cell state ct-1 at the previous time. The input of LSTM is $\hat{X}_{y^t}^t$ representing the information of customer node yt and the hidden state ht-1 of the previous time. The output hidden state ht is used as the input of attention mechanism to calculate attention weight.

3.4. REINFORCEMENT LEARNING ALGORITHM

Deep reinforcement learning algorithm based on round trajectory reward is used to train strategy network and value network model [41-43], the main algorithms are as follows: first initialize the network weight parameters θ,j, generate N VEPTW training instances and iterate circularly epoch→∞, regenerate into a batch of training samples (M training samples from N) $X_{[1]}, X_{[2]}, \ldots, X_{[M]}$, loop n=1,2,...M, select $y_{[n]}^{i_{n+1}}$ according to the model probability distribution $P_\theta(y_{[n]}^{i_{n+1}} | X_{[n]}^{i_n}, | G_{[n]}^{i_n}, | Y_{[n]}^{i_n})$, until all node requirements are 0, then calculate track reward R [44-45]. The training results are obtained according to equations (17) - (18):

$$d\theta = \frac{1}{M}\sum_{t=1}^{M}[R(Y_{[i]}) - v_\varphi(X_{[i]})]\nabla \log P_\theta(Y_{[i]} | X_{[i]}), \quad (17)$$

$$d\varphi = \frac{1}{M}\sum_{t=1}^{M}\nabla_\varphi\left[R(Y_{[i]}) - v_\varphi(X_{[i]})\right]^2. \quad (18)$$

4. EXPERIMENTAL RESULTS AND ANALYSIS

This experiment considers the practical problems of urban logistics distribution, such as the loading capacity of logistics vehicles. For different sizes of distribution tasks, use distribution vehicles with different loading sizes to carry out numerical simulation experiments on the distribution tasks with customer sizes of 5, 15 and 25 in the end area of the city, and select the distribution vehicle models with unmanned

https://doi.org/10.17993/3cemp.2023.120151.68-85

vehicle loading capacity of 15, 25 and 35 respectively. The experimental results will give the optimized distribution path.

Using the training set to verify the test set data, 18000 instances are generated as the training set, 180 instances are the verification set and 180 instances are the test set. Each instance is a logistics vehicle distribution task problem with fixed customer size and distribution center. The customer node data of verification set and test set are generated in the same way as the data of training set. The information of customer i is expressed by equation (19):

$$X_i^t = (x_i, y_i, e_i, l_i, d_i^t), \quad (19)$$

The customer demand is randomly selected from the discrete number {1,2,3,4,5,6} and the location x_i, y_i of the customer and the distribution center is randomly generated in the surface space of $[0,1]\times[0,1]$. This study uses this to simulate the urban area. For the three customer scale distribution tasks, logistics distribution vehicles with loading capacity of 15, 25 and 35 are selected respectively.

Table 1 Vehicle information of different customer sizes

Task	Loading capacity C	Vehicle speed V
VRPTW-5	15	v
VRPTW-15	25	v
VRPTW-25	35	v

The training set generates 18000 instances. Each iteration batch selects 180 vrptw-5 from 18000 instances as a training batch. Each training batch makes a gradient update to the strategy network and evaluation network. After completing all the instance data, it is used as an iterative epoch. After each epoch is completed, the model is tested with the verification set. The verification set of this study is composed of 180 instances. The running time of the verification set is collected, Average fleet, total distribution mileage, average reward and other information to evaluate the model. Set 25 epochs for iterations, and each iteration completes one epoch to verify the verification set. When 25 iterations are completed, the model training is completed, and the test model stage is entered. 180 instances are randomly generated from the data of the test set and the verification set in the same way, and finally the optimal logistics distribution path is obtained.

The global and local information studied are mapped into 128 dimensional vectors through two different one-dimensional convolutions, and the hidden state output of LSTM is 128 dimensions. All trainable variables begin to officially enter the training stage after a period of pre training. In order to make the model have generalization ability, let the agent contact more environmental conditions and diversify the situations that the model may encounter, In training, this study adopts the strategy of random sampling. When testing, it adopts random decoding and greedy decoding, and compares the advantages of the two decoding strategies. Experiments are carried out on three VRPTW problems. The scale of customer service nodes are 5, 15 and 25

https://doi.org/10.17993/3cemp.2023.120151.68-85

respectively. For the problem of each customer scale, 180 examples are tested and solved.

After the model training, the test set data is used to test the model. The test decoding strategy adopts random decoding and greedy decoding. Figure 6 shows different distribution route schemes to achieve the optimal logistics distribution route. Due to the different tasks to be performed by different distribution vehicles and the different capacity of distribution vehicles, the optimal route will also be different. Three recommended routes are generated from each different logistics distribution starting point to the destination. Due to the complexity of the road and the problems of selection, it can be seen that figure 6 (a) shows three logistics vehicle distribution routes under vrptw-5: blue line {1,2,3,4}, red line {5,6,7,8}, green line {9,10,11}, and blue line is the optimal logistics vehicle distribution route; Figure 6 (b) shows three logistics vehicle distribution paths under vrptw-15: blue line {1,2,3,4}, red line {5,6,7,8}, green line {9,10,11,12,13}. Red line is the optimal logistics vehicle distribution path; Figure 6 (c) shows three logistics vehicle distribution paths under vrptw-25: red line {1,2,3,4,5}, blue line {6,7,8,9}, green line {10,11,12,13}. Blue line is the optimal logistics vehice distribution path.

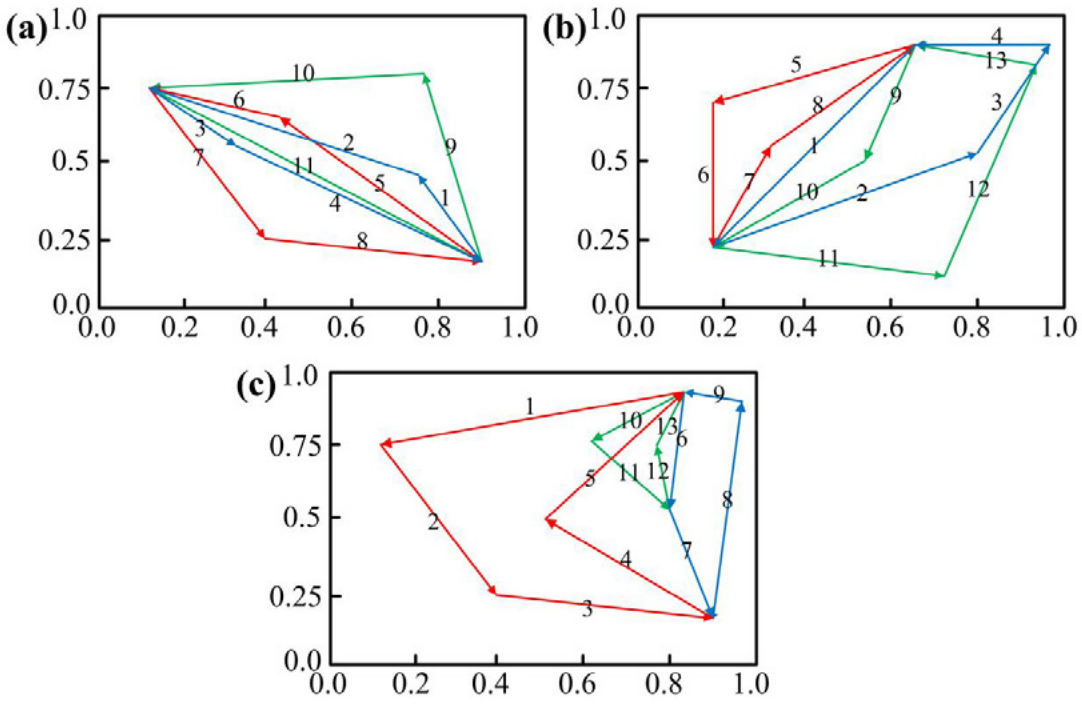

Figure 6 Logistics distribution optimization path with (a)VRPTW-5; (b)VRPTW-15; (c)VRPTW-25

5. IN CONCLUSION

With the rapid development of modern society and entering the Internet era, online shopping has become people's daily life, which makes the logistics industry more and more prosperous. At the same time, it will also put forward higher requirements for logistics distribution, especially in path planning, the logistics distribution method of

https://doi.org/10.17993/3cemp.2023.120151.68-85

applying science and technology has played a more and more important role. The research results of in-depth learning and reinforcement learning have gradually appeared in the research of artificial intelligence method in vehicle routing problem. Compared with the traditional problem-solving algorithm, the method based on regional chain technology to solve the path optimization problem is more attractive. Therefore, a deep reinforcement learning algorithm based on attention mechanism and LSTM model is designed and applied to the distribution path planning problem of logistics vehicles. The training set is designed for sample test training. 18000 examples are generated from the training set. Experiments are carried out on three VRPTW problems, and then iterative calculation is carried out. Each of them obtains three recommended paths of logistics distribution vehicles, Finally, the shortest optimized logistics distribution path is obtained, which promotes the logistics distribution technology in the information age.

REFERENCES

(1) Chen, J., Xu, S., Chen, H., Zhao, C., & Xue, K. (2020, May). **Research on optimization of food cold chain logistics distribution route based on internet of things**. *In Journal of Physics: Conference Series* (Vol. 1544, No. 1, p. 012086). IOP Publishing.

(2) ZHAO, Z. X., & LI, X. M. (2020). **Electric Vehicle Route Optimization for Fresh Logistics Distribution Based on Time-varying Traffic Congestion**. *Journal of Transportation Systems Engineering and Information Technology*, 20(5), 218.

(3) Liu B. **Logistics Distribution Route Optimization Model Based on Recursive Fuzzy Neural Network Algorithm[J]**. *Computational Intelligence and Neuroscience*, 2021, 2021.

(4) Xiong H. **Research on cold chain logistics distribution route based on ant colony optimization algorithm[J]**. *Discrete Dynamics in Nature and Society*, 2021, 2021.

(5) Liu W. **Route optimization for last-mile distribution of rural E-commerce logistics based on ant colony optimization[J]**. *IEEE Access*, 2020, 8: 12179-12187.

(6) Zhao Z, Li X, Zhou X. **Distribution route optimization for electric vehicles in urban cold chain logistics for fresh products under time-varying traffic conditions[J]**. *Mathematical Problems in Engineering*, 2020, 2020.

(7) Sun R, Liu M, Zhao L. **Research on logistics distribution path optimization based on PSO and IoT[J]**. *International Journal of Wavelets, Multiresolution and Information Processing*, 2019, 17(06): 1950051.

(8) Yuanguo Y, Shengyu H. **Research on optimization of distribution route for cold chain logistics of agricultural products based on traffic big data[J]**. *Management Review*, 2019, 31(4): 240.

(9) Wei Xiaodi, Zheng Hongqing **Improved discrete flower pollination algorithm for solving vehicle routing problem with time window [J].** *Practice and understanding of mathematics*, 2020, 50 (02): 195-202.

https://doi.org/10.17993/3cemp.2023.120151.68-85

(10) Su Xinxin, Qin Hu, Wang Kai **Tabu search algorithm for solving vehicle routing problem with time window and multiple distribution personnel [J].** *Journal of Chongqing Normal University (NATURAL SCIENCE EDITION)*, 2020, 37 (1): 22-30.

(11) DENG A M, MAO C, ZHOU Y T. **Optimizing research of an improved simulated annealing algorithm to soft time windows vehicle routing problem with pick-up and delivery[J]**. *Systems Engineering-Theory & Practice*, 2009, 29(5):186-192.

(12) CORDEAU J F, LAPORTE G, MERCIER A. **A unified tabu search heuristic for vehicle routing problems with time windows[J]**. *Journal of the Operational Research Society*, 2001, 52(8):928-936.

(13) Wang H, Li W. **Study on logistics distribution route optimization by improved particle swarm optimization[J]**. *Computer Simulation*, 2012, 29(5): 243-246.

(14) Chen Y, Huang Z, Ai H, et al. **The impact of GIS/GPS network information systems on the logistics distribution cost of tobacco enterprises[J]**. *Transportation Research Part E: Logistics and Transportation Review*, 2021, 149: 102299.

(15) Zhao Y, Zhou Y, Deng W. **Innovation mode and optimization strategy of B2C e-commerce logistics distribution under big data[J]**. *Sustainability*, 2020, 12(8): 3381.

(16) Liu T, Yin Y, Yang X. **Research on logistics distribution routes optimization based on ACO[C].** *2020 5th International Conference on Information Science, Computer Technology and Transportation (ISCTT). IEEE*, 2020: 641-644.

(17) Liu H, Pretorius L, Jiang D. **Optimization of cold chain logistics distribution network terminal[J]**. *EURASIP Journal on Wireless Communications and Networking*, 2018, 2018(1): 1-9.

(18) Ouyang F. **Research on port logistics distribution route planning based on artificial fish swarm algorithm[J]**. *Journal of Coastal Research*, 2020, 115(SI): 78-80.

(19) Li J. **Logistics distribution route optimization based on chaotic cuckoo algorithm[C].** *Advanced Materials Research. Trans Tech Publications Ltd*, 2014, 1049: 1681-1684.

(20) Ding D, Zou X. **The optimization of logistics distribution route based on Dijkstra's algorithm and CW savings algorithm[C].** *6th International conference on machinery, materials, environment, biotechnology and computer (MMEBC 2016)*, Tianjin, China. 2016: 11-12.

(21) Bosona T, Gebresenbet G, Nordmark I, et al. **Integrated logistics network for the supply chain of locally produced food, Part I: Location and route optimization analyses[J]**. *Journal of service science and management*, 2011, 4(02): 174.

(22) Lozano Murciego Á, Jiménez-Bravo D M, Pato Martínez D, et al. **Voice assistant and route optimization system for logistics companies in depopulated rural areas[J]**. *Sustainability*, 2020, 12(13): 5377.

https://doi.org/10.17993/3cemp.2023.120151.68-85

(23) He R, Ma C, Ma C, et al. **Optimisation algorithm for logistics distribution route based on Prufer codes[J]**. *International Journal of Wireless and Mobile Computing*, 2015, 9(2): 205-210.

(24) Konstantakopoulos G D, Gayialis S P, Kechagias E P. **Vehicle routing problem and related algorithms for logistics distribution: A literature review and classification[J]**. *Operational research*, 2020: 1-30.

(25) Bin Z, Xiao-Jun L. **Study on logistics distribution route optimization based on clustering algorithm and ant colony algorithm[J]**. *The Open Cybernetics & Systemics Journal*, 2015, 9(1).

(26) Sun Y, Geng N, Gong S, et al. **Research on improved genetic algorithm in path optimization of aviation logistics distribution center[J]**. *Journal of Intelligent & Fuzzy Systems*, 2020, 38(1): 29-37.

(27) Fan Q, Nie X X, Yu K, et al. **Optimization of logistics distribution route based on the save mileage method and the ant colony algorithm[C].** *Applied Mechanics and Materials. Trans Tech Publications Ltd*, 2014, 448: 3683-3687.

(28) Damayanti T R, Kusumaningrum A L, Susanty Y D, et al. **Route optimization using saving matrix method–A case study at public logistics company in Indonesia[C].** *International Conference on Industrial Engineering and Operations Management*. 2020: 1583-1591.

(29) Wang C, Zhou J, Xiao B, et al. **Uncertainty Estimation for Stereo Matching Based on Evidential Deep Learning**. *Pattern Recognition*, 2021. https://doi.org/10.1016/j.patcog.2021.108498

(30) C. Yan, G. Pang, X. Bai, et al., **Beyond triplet loss: person re-identification with finegrained difference-aware pairwise loss**, *IEEE Trans. Multimedia* (2021), https://doi.org/10.1109/TMM.2021.3069562.

(31) Zhang K, Qiu B, Mu D. **Low-carbon logistics distribution route planning with improved particle swarm optimization algorithm[C].** *2016 International Conference on Logistics, Informatics and Service Sciences (LISS). IEEE*, 2016: 1-4.

(32) Zheng C, Gu Y, Shen J, et al. **Urban Logistics Delivery Route Planning Based on a Single Metro Line[J]**. *IEEE Access*, 2021, 9: 50819-50830.

(33) Yao C. **Research on logistics distribution path analysis based on artificial intelligence algorithms[J]**. *International Journal of Biometrics*, 2020, 12(1): 100-108.

(34) Bai X, Zhou J, Ning X, et al. **3D data computation and visualization[J]**. *Displays*, 2022: 102169.

(35) Zhang Wenguang. **Research on terminal distribution mode and route optimization of e-commerce logistics based on ant algorithm [D].** *Guizhou Normal University*, 2016.

(36) W Cai, B Zhai, Y Liu, et al., **Quadratic polynomial guided fuzzy C-means and dual attention mechanism for medical image segmentation.** *Displays*, vol. 70, no. 102106, 2021. https://doi.org/10.1016/j.displa.2021.102106.

(37) X. Ning, P. Duan, W. Li, and S. Zhang, **Real-time 3D face alignment using an encoder-decoder network with an efficient deconvolution layer**, *IEEE Signal Processing Letters*, vol. 27, pp. 1944–1948, 2020. https://doi.org/10.1109/LSP.2020.3032277.

https://doi.org/10.17993/3cemp.2023.120151.68-85

(38) Jiao Yunlong. **Research on logistics transportation vehicle routing optimization based on travel time prediction [D]**. *Dalian Maritime University*, 2015.

(39) Martins L B, Iori M, Moreira, Mayron César O, et al. **On Solving the Time Window Assignment Vehicle Routing Problem via Iterated Local Search**. 2021.

(40) J. Miao, Z Wang, X. Ning, X. Nan, W. Cai, R. Liu. **Practical and Secure Multifactor Authentication Protocol for Autonomous Vehicles in 5G**. *Software:Practice and Experience*, 2022. https://doi.org/10.1002/SPE.3087

(41) X. Ning, K. Gong, W. Li, and L. Zhang, **JWSAA: Joint Weak Saliency and Attention Aware for person re-identification**, *Neurocomputing*, 2021, vol. 453, pp. 801-811. https://doi.org/10.1016/j.neucom.2020.05.106.

(42) Shan W. **Digital streaming media distribution and transmission process optimisation based on adaptive recurrent neural network[J]**. *Connection Science*, 2022, 34(1): 1169-1180.

(43) Ying L, Qian Nan Z, Fu Ping W, et al. **Adaptive weights learning in CNN feature fusion for crime scene investigation image classification[J]**. *Connection Science*, 2021, 33(3): 719-734.

(44) Medina, R., Breña, J. L., y Esenarro, D. (2021). **Efficient and sustainable improvement of a system of production and commercialization of Essential Molle Oil (Schinus Molle)**. *3C Empresa. Investigación y pensamiento crítico*, 10(4), 43-75. https://doi.org/10.17993/3cemp.2021.100448.43-75

(45) Ma Yanran,Chen Nan & Lv Han.(2021). **Back propagation mathematical model for stock price prediction**. *Applied Mathematics and Nonlinear Sciences(1)*. https://doi.org/10.2478/AMNS.2021.2.00144.

/05/

VISUALIZATION OF COMPUTER-SUPPORTED COLLABORATIVE LEARNING MODELS IN THE CONTEXT OF MULTIMODAL DATA ANALYSIS

Jianqiang Mei*

School of Electronic Engineering, Tianjin University of Technology and Education, Tianjin, 300222, China - Tianjin Engineering Research Center of Fieldbus Control Technology, Tianjin, 300222, China

meijianqiang@tute.edu.cn

Wanyan Chen

School of Electronic Engineering, Tianjin University of Technology and Education, Tianjin, 300222, China

Biyuan Li

School of Electronic Engineering, Tianjin University of Technology and Education, Tianjin, 300222, China - Tianjin Engineering Research Center of Fieldbus Control Technology, Tianjin, 300222, China

Shixin Li

School of Electronic Engineering, Tianjin University of Technology and Education, Tianjin, 300222, China. Tianjin Engineering Research Center of Fieldbus Control Technology, Tianjin, 300222, China

Jun Zhang

School of Electronic Engineering, Tianjin University of Technology and Education, Tianjin, 300222, China - Tianjin Engineering Research Center of Fieldbus Control Technology, Tianjin, 300222, China

Reception: 06/11/2022 **Acceptance**: 01/01/2023 **Publication**: 23/01/2023

Suggested citation:

M., Jianqiang, C., Wanyan, L., Biyuan, L., Shixin and Z. Jun (2023). **Visualization of computer-supported collaborative learning models in the context of multimodal data analysis**. *3C Empresa. Investigación y pensamiento crítico, 12(1)*, 87-109. https://doi.org/10.17993/3cemp.2023.120151.87-109

ABSTRACT

Deep learning evaluation is a new direction formed by the intersection of multiple domains, and the core issue is how to visualize collaborative learning models to motivate learners. Therefore, this paper realizes real-time knowledge sharing and facilitates learners' interaction through computer-supported collaborative learning (CSCL) technology. In this paper, we collect, label, and analyze data based on five modalities: brain, behavior, cognition, environment, and technology. In this paper, a computer-supported collaborative learning process analysis model is developed under the threshold of multimodal data analysis. The model is based on roles and CSCL for intelligent network collaboration. This paper designs and develops an interactive visualization tool to support online collaborative learning process analysis. In addition, this paper conducts a practical study in an online classroom. The results show that the model and the tool can be effectively used for online collaborative learning process analysis, and the test model results fit well. The entropy index of the test model took a value of about 0.85, and about less than 10% of the individuals were assigned to the wrong profile. During the test, the participation of participants gradually increased from 5% to about 25%, and the participation effect improved by about 80%. This indicates the strong applicability value of the computer-supported collaborative learning process analysis model under the multimodal data analysis perspective.

KEYWORDS

multimodality; computer-supported collaborative learning; visualization; process analysis model; online classroom

https://doi.org/10.17993/3cemp.2023.120151.87-109

PAPER INDEX

https://doi.org/10.17993/3cemp.2023.120151.87-109

1. INTRODUCTION

Computer-supported collaborative learning (CSCL) is the theory and practice of learners supported by computer network technology for the purpose of improving learning performance. It enables collaborative cognition, exchange of emotions, and development of collaborative skills in shared activities and interactions. In online collaborative learning supported by technology, learners are able to ask questions to a greater extent. They are able to express ideas clearly, exchange ideas with each other, and share information. They can negotiate meaning. Ultimately, learners are able to improve their collaborative learning skills. They can promote the development of their cognitive skills and critical thinking [1]. Studies have shown that good collaborative learning will have a positive effect on learning outcomes [2]. However, the most central issue of collaborative learning in current research is how to visualize models and thus motivate learners. Moreover, deep learning evaluation is a new direction formed by the intersection of multiple domains. It can collect and build a deep learning database and create a deep learning evaluation analysis model. Ultimately, it can achieve the purpose of optimizing educational evaluation.

In the field of research and practice, there is a growing interest in computer-supported collaborative learning (CSCL). An educational practice in which students form learning groups and learn through social interaction via computers or the Internet [3].CSCL can take place in classroom or online learning environments and can be synchronous or asynchronous [4]. However, there are still many substantial problems with collaborative learning [5]. For example, learners have uneven participation in the learning process, lack of deep interaction, and biased support tools. Since collaborative learning is a complex social process. Learners in CSCL are different individuals. They have unique personality, cognitive, and affective characteristics. They do not actively and voluntarily collaborate with other members [6]. Individual differences and diversity, as well as the complexity of the learning environment, may negatively affect cognition, emotion, and motivation. During collaboration, it is difficult for learners to collaborate on complex problems or concepts through high-quality cognitive mapping, active interaction, and sharing [7]. sotani, Mizoguchi, and Jaques et al [8-9] argued that to improve collaboration in CSCL settings, students' engagement needs to be increased to increase their interaction rate. This implies that issues such as the allocation of responsibilities and resources and the mode of interaction need to be addressed. There is variation in learners' interactive engagement in CSCL, but it is not clear what causes this variation [10]. It has been suggested that differences in engagement during interaction may stem from students' motivation to participate in CSCL [11]. Therefore, a new generation of researchers has begun to seek to identify the causes and mechanisms hidden behind the positive collaborative outcomes. They focus on the process of collaborative interaction among members and try to analyze the collaborative learning process in depth. They understand the internal mechanisms by which effective collaboration occurs and build long-lasting analytical models. In recent years, due to the main properties of deep learning, it is increasingly used to solve several 3D visual problems [12-16], and these collaborative learning analytical models are based on different theoretical

https://doi.org/10.17993/3cemp.2023.120151.87-109

perspectives such as cognition or metacognition, knowledge construction, and critical thinking. The models construct various analytical frameworks oriented towards artifacts, contexts, interactions, and knowledge development. Based on different theoretical perspectives, the analytical frameworks also cover elements such as participants, interaction behaviors, cognitive and metacognitive, affect, learning output, social support, and topic space. Models have focused on different aspects of collaborative learning. Some models emphasize the importance of social interaction for collaboration. Some models focus on elements of collaboration related to interaction such as engagement, affect, and structural features of interaction (size, density, intensity). For example, the models proposed by Fahy [17] and Veldhuis [18]. Some models emphasize the important role of cognition in collaborative analysis. Some models focus on factors related to cognitive involvement, considering whether new ideas are presented in the discussion, whether the problem space is clarified, etc., such as Henri [19] and Newman [20]. There are also models that emphasize the importance of conversational behavior and focus on elements such as questions, answers, arguments, and comments, such as the analytical model constructed by Zhu [21]. However, knowledge construction in groups in collaborative learning is a process in which multiple factors are organically combined and interact with each other. Collaborative learning has the limitation of narrow perspective in examining the process of collaborative learning from a single side. From the analysis of the literature, though, researchers have tried to construct as comprehensive a dimension as possible to analyze the collaborative learning process. There are also researchers who have enhanced their understanding of the internal mechanisms of collaboration and the process of knowledge construction. For example, Li Yanyan's [22] model uses knowledge construction as the theoretical basis and messages as the minimum unit of analysis. The model quantitatively analyzes the collaborative learning process from three aspects: topic space, topic intention, and social network. the model of Paul [23], on the other hand, is based on knowledge construction theory and explores the collaborative learning process based on content analysis from three aspects: cognitive, social, and motivational. However, in general, the model construction and analysis of multidimensional perspectives are still incomplete and scarce. Moreover, along with the continuous development of the online collaborative learning environment, the model needs to be constantly revised and improved in new scenarios. Models to fit the analytical requirements of online collaborative learning. In this paper, after comparing numerous existing collaborative learning models such as: Web-based 1CAI model [24], Intermet-based intelligent teaching system ITS, and intelligent agent-based model of online collaborative environment [25], it is found that each of these virtual learning environment models is constructed with defects. Some models are limited to only two roles, teacher and student, and students are in a passive state. Some models emphasize the active role of students, but ignore the collaboration between teachers and the role of teachers as learners. The models are poorly interactive, lack intelligence, and do not allow for good collaborative learning. Considering that the roles of teachers and students participating in collaborative learning are dynamic and changing in CSCL, we introduced the role mechanism. Therefore, according to the current research base and research questions. In this

https://doi.org/10.17993/3cemp.2023.120151.87-109

paper, we collect, label, and analyze data based on five modalities: brain, behavior, cognition, environment, and technology, based on a deep learning database. In this paper, deep learning evaluation based on multimodal data is implemented and improved in terms of automating data collection, integrating predictive models, deepening educational applications, unifying mechanisms, and enhancing decision wisdom. This paper realizes real-time knowledge sharing and promotes interactive mutual assistance of learners through computer-supported collaborative learning (CSCL) technology. This paper establishes a model for analyzing the process of computer-supported collaborative learning in the context of multimodal data analysis. Based on this model, an interactive visualization tool is designed and developed to support online collaborative learning process analysis, and a practical study is conducted in an online classroom.

In this paper, we propose and build an intelligent network collaboration model RICLU based on role and CSCL, which focuses on role-based interaction, collaboration and negotiation mechanisms among multiple agents in a collaborative learning environment. The intelligent Agent takes on a role in learning on behalf of the client user and interacts with other users and the management Agent on the server side. This is a dynamic and open virtual learning environment, which better reflects the characteristics of autonomy, interactivity, collaboration and distribution transparency. This paper provides a good model for online education. In particular, the introduction of multi-role mechanism better reflects the personalization of user learning while promoting extensive cooperation among users.

2. ROLE-BASED AND CSCL MODELS FOR COLLABORATIVE WEB-BASED LEARNING

2.1. APPLICATION OF ROLE MECHANISM

A role is a unity of responsibilities and rights and has four attributes: responsibilities, rights, activities and agreements. As a reasonable criterion for classifying things, roles are abstracted by grouping participants according to their skills, abilities and other elements of the activity. A single participant may fill multiple roles. A class of roles can also be filled by multiple users. A collaborative organization can be considered as a collection of roles. There are specific relationships between roles. In the collaborative process, a role is an active, relatively independent abstraction unit. A role has a certain goal and can perform a series of operations in a sequential manner. At different moments, roles can be in different states. A role R is usually defined as a mapping f: (O,Ts)→action. O is the object on which the role acts. Ts is the task to be performed. Action is the action of the object. The role-based collaboration process is defined as a binary: P:=<Role, Relation>. Role denotes the set of role spaces, and Relation denotes the collaborative relationship between roles.

The CSCL-based web-based learning environment is a distributed web-based system. Users are located on the client side. Intelligent Agents represent users in their

https://doi.org/10.17993/3cemp.2023.120151.87-109

learning roles. Interacts with other users and the server-side Management Agent. Teachers and students are the most basic roles. Group managers, system managers, resource managers, and message carriers assist in learning as secondary roles to achieve better interactivity. All these roles are performed by the Smart Agent. Each role has different authority according to its task: Management Agent controls and manages all collaborative activities, shared resources, network communication, etc. in the virtual environment; Collaboration Group Agent manages the activities of all members of the group; Resource Management Agent manages the resource repository; Routing Agent is responsible for inter-member messaging. In the role-based and CSCL collaborative learning model, the following relationships exist among the roles: active relationship (equal relationship). The relationship between the collaborative agents is equal, and there is no controlling party and controlled party. They can engage in free learning and mutual learning. For example, the interactions between Student Agent and Student Agent and between Teacher Agent and Teacher Agent during group learning and free discussion are equal. They all have equal access to resources and privileges. One of the collaborators is the controlling party, who is responsible for management and supervision. The other party is the controlled party, whose actions are constrained by the control of one of the subjects. For example, the interaction between the Teacher Agent and the Student Agent reflects the relationship between teaching and learning. The Teacher supervises the students and guides them in their learning. The Environment Management Agent is the master when interacting with other subjects, and the other subjects are the controlled parties. For example, the Student Agent requests services from it (registration, access to a group, access to a repository, exit). The passive relationship is also manifested in the collaborative learning between the Group Agent and the Member Agent, where the latter is controlled by the former.

2.2. MODEL FRAMEWORK

From the perspective of application, collaborative learning can be divided into 3 layers: resource layer, functional layer, and management layer. The resource layer provides a large amount of basic resource data for building the learning environment, including text, audio and video, and WWW. These resources form the basic databases such as the book database, audio and video database, and test bank. The functional layer provides a friendly user interface to interact directly with learners and realize specific application functions. Such as electronic forums, online groups, e-mail, real-time video playback and evaluation of students' learning effects. The management implements effective monitoring of resource data in the resource layer and ensures data security. It performs daily maintenance of the functions in the learning environment and manages the basic information of registered students and teachers.

These management functions can be implemented through software and hardware. Four types of Agents in collaborative learning can be defined based on three characteristics of Agents: Autonomy, Cooperation, and Learning: Cooperative Agent, Learning Agent, Interface Agent, and Decision Agent. It establishes negotiations with

https://doi.org/10.17993/3cemp.2023.120151.87-109

other Agents and performs limited role learning. The Learning Agent emphasizes autonomy and learning. It observes the user's behavior, learns from the patterns it finds, and takes actions based on the user's preferences. The Interface Agent retrieves information intelligently. It finds data automatically and quickly. Decision Agent automatically performs tasks using intelligent mechanisms. It helps the user to learn.

The model is represented by a seven-tuple: F=(A,R,T,Task,Source,D,K). Where A is the set of Agents involved in the environment. A is represented by their internal identifier Aid. r = {Teacher, Student, Manager, Facilitator}, is the set of roles. t = {T1,T2,...Tn} is the set of collaborative groups Ti(1≤i≤n). Task is a set of collaborative tasks, indicating the tasks that each role in the group completes together. source is a collection of system resources, including multimedia database, courseware library, test bank, etc. D represents the database, describing system information such as student management information, resource management information, teacher information, etc. K is the knowledge base, which stores the collaboration rules and guides the collaborative learning activities of the collaborative groups. Based on the role analysis, the model defines Interface Agent (Student Agent and Teacher Agent), Routing Agent, Group Agent, Management Agent, and CORBA-based Object Requirements Agent, where Interface Agent is the functional layer. The Group Agent and the Management Agent belong to the management layer. CORBA-based Object Requirements Agents belong to the resource layer. Agents collaborate with each other over a network (Internet, Intranet or small local area network). Learners can take on the role of teachers or students. Common Object Request Broker Architecture CORBA can provide security services, naming services, lifetime services and external services. This facilitates distributed computing applications in a network environment and effectively describes the dynamic nature of the Agent. This is a better representation of object-oriented features. Combining the functions and roles of each Agent, a unified model is used to describe the basic framework and internal structure of the Agent in the network environment. The intelligent Agent in the model is defined as a nine-tuple: Ag=(M,A,R,B,I, D,V,K,T). M - describes the activities such as methods, executable behaviors and processes that the Agent has. A - describes the type of Agent, the intent to perform the activity and the status information of the cohort collaborators. R - Describes the role of the Agent in a collaborative activity. B - describes the Agent's personal workspace. It is the equivalent of a network blackboard and stores interaction information. I - Reasoning and problem processing system, which controls the behavior of the Agent. It is responsible for the interpretation and execution of domain knowledge, pattern matching, interaction information processing, and result evaluation. D - The basic elements and data sets of the problem solving domain. V - describes the domain knowledge (models, rules) and collaborative interaction communication behavior. K - a knowledge system consisting of domain-specific knowledge. It includes algorithms, models, generative rules and semantic networks, etc. T - the communication mechanism with other Agents. Each Agent performs the following functions in the model:

https://doi.org/10.17993/3cemp.2023.120151.87-109

(1) Interface Agent: Interacts with other Agents on behalf of learners. It exchanges requests, goals, resources, commitments, etc. to achieve the purpose of collaborative learning. It includes user interface layer, semantic understanding layer, operation layer and interaction layer. The operational layer includes behavior control, goal or rule base, information retrieval and reasoning engine. The operational layer corresponds to the belief set and knowledge base of the Agent. It learns the mindset of the user (teacher or student) and understands their preferences. It automatically perceives the learning environment and makes requests to other Agents (e.g., to the administrative Agent to register, exit, enter a group, request a resource, etc.). The Teacher Agent has the same functions as the Student Agent, and in the role of the Teacher, it is responsible for making decisions about teaching and learning issues, making inquiries about teaching and learning situations, and controlling and monitoring the Student Agent.

(2) Group Agent: A special kind of interface agent who supervises the activities of the members of the collaborative group and coordinates their activities as necessary. Tutor all members during group instruction. Responsible for the distribution of speaking rights during free discussion. It is responsible for assigning and coordinating tasks when learning together. It can be elected by the Interface Agent or assigned by the Management Agent. It is created when a group is created and disappears when a task is completed. When intergroup learning occurs, it acts as a representative of the group and negotiates with other group Agents about joint intentions.

(3) Management Agent: It is responsible for coordinating and supervising the activities of members and the allocation of resources in the entire dynamic environment, and any request for resources must be approved by it. It is the super user of the learning environment, and any Agent can communicate with it directly. It is connected to the Resource Module for data storage and retrieval. It can assign a member as a group leader and assign teachers to individual and group instructional activities. It can also record relevant information (including user joins, logins, processing interactions, collaboration information, student information, teacher information).

(4) Routing Agent: Responsible for communication between Interface Agent, between Group Agent and Member Agent, and between Group Agents. He is responsible for passing resource requests, task requests, goals, negotiation requests, information feedback, etc. It can also communicate directly with the Management Agent. It has mobility and is a mobile Agent.

(5) CORBA-based Object Requirements Agent: It follows the CORBA specification and provides CORBA-based public request services, and is connected with resource repositories (multimedia repository, courseware repository, test repository, answer repository), databases (student management information, teacher information, collaborative activity information), and knowledge repositories (collaborative rule repository and goal planning repository). The Management Agent accesses the repository by making resource access requests to it. It can also read, write, and update the database and knowledge base.

https://doi.org/10.17993/3cemp.2023.120151.87-109

2.3. DESCRIPTION OF THE COLLABORATION PROCESS

Collaborative learning includes individual instruction, group instruction, free discussion, and joint learning (collaborative lesson preparation and collaborative practice). In group instruction, the Teacher Agent is the controlling party, supervising and guiding the learning activities of each Agent. Free discussion uses the group Agent's web board as the workspace. The group uses a voice mechanism for collaboration. All members have equal relationships and are learners. However, each member is supervised and managed by the Group Agent. In joint learning, the Teacher Agent breaks down the learning task into subtasks. These subtasks are performed by a number of group members, with each task corresponding to a role. The assignment of tasks is based on a combination of assignment and voluntariness. Each member chooses whether to accept the task according to his or her ability and willingness.

The mechanisms of co-operative learning are conflict and competition, self-explanation, internalization, apprenticeship, shared cognitive tasking, and shared rules. We take co-learning as an example. Combining the above mechanisms and role mechanisms, a formal description of collaborative learning is given. The language system V uses predicates to represent collaborative interaction activities, and defines the interaction activities in task assignment as follows:

State (Ai): indicates the state of a member Agent Ai in the collaborative group. There are three kinds of states: idle (idle), waiting (waiting), and busy (working).

Ask (T, A_i, T_i): Teacher Agent T asks if A_i can complete the task T_i.

Cando (T, A_i, T_i):Ai tells T that it can do the task T_i alone.

Notcand (o T, A_i, T_i): A_i tells T that it cannot complete the task T_i alone.

Assig (n T, A_i, T_i): T assigns the task T_i to A_i.

Needhelp (T, A_i, A_j, T_i): A_i can complete the task assigned to it by T only with the help of A_j.

Askhelp (T, A_i, A_j, T_i): A_i asks A_j for help in completing the task assigned to it by T.

Help (T, Ai, A_j, T_i): A_j is willing to help A_i to complete the task assigned to it by T.

Refusehelp (T, A_i, A_j, T_i):A_j refuses to help Ai to complete the task assigned to it by T.

Do (A_j, A_j, T_i): A_j and A_j work together to complete the task T_i.

Report (A_i,T,result): A_i submits the execution result to T.

For a given task Ti, the interactions in the task assignment process are described by the following algorithm:

FOR each team member Agent A_i

IF State (A_i)=idle

{Ask (T, A_i,T_i);

https://doi.org/10.17993/3cemp.2023.120151.87-109

IF Cando (T, A_i,T_i)

{Assign (T, A_i, T_i); Stat (e A_i)= busy; return; }

ELSE

IF Needhelp (T, A_i, A_j, T_i)

{State(A_i)=waiting;

REPEAT

Askhelp (T, A_i, A_j, T_i);

UNTIL (find an A_j, satisfying: Help (T, A_i, A_j, T_i), or ask all A_j);

IF find A_j Do (A_j, A_j, T_i) that satisfy the condition;

ELSE {State (A_i)=idle; return;}}}

3. VISUAL COLLABORATIVE LEARNING ANALYTICS MODEL CONSTRUCTION

3.1. CSCL-KBS LEARNING ANALYSIS MODEL

Although there are many models on collaborative learning analysis, however, existing research still lacks a systematic and global perspective to overview the dimensions of collaborative process analysis [26]. A review of the current literature on collaborative learning process analysis. We were able to identify some new research perspectives that are gradually gaining attention in the study of collaborative learning process analysis. One of the important aspects is the research on knowledge processing in the collaborative learning process. Knowledge processing plays an important role in the collaborative process [27]. Knowledge processing is concerned with the process of knowledge creation and generation in collaborative learning. This process allows learners to organize knowledge into coherent structures and to generate new knowledge using existing knowledge. Studies have shown that the measurement of knowledge processing can measure whether a cluster is successfully engaged in collaborative problem solving [28]. Another important aspect is the research on social relationships in collaborative learning. Numerous studies point out that active online participation is a key factor in the success of student learning. In online collaborative learning, individuals in a group interact effectively for the common learning goals of the group. Social relationships among members can influence the process and quality of knowledge construction [29]. In addition, the analysis of behavioral patterns of collaborative processes is an important topic of current CSCL research. Group members accomplish activities with specific goals through interaction. This can be seen as consisting of a series of intentional interaction behaviors. Abstracting the sequence of interactions of these behaviors can lead to different behavioral patterns. The different behavioral patterns reflect the collaborative interaction strategies embodied by the collaborative group during the interaction activities.

https://doi.org/10.17993/3cemp.2023.120151.87-109

In order to provide a comprehensive portrayal of learning analysis in CSCL. On the basis of the findings of Li et al. [22]. This paper proposes an improved multidimensional analysis model. The model explores student knowledge construction in collaborative learning discussion activities. The model contains three analytical dimensions: knowledge processing (K), behavioral patterns (B), and social relationships (S). The model is designed for three different levels of study: individual, group, and community. The model is named as KBS model.

3.2. ANALYTICAL MODEL-BASED TOOL DESIGN AND PRACTICE

3.2.1. PARTICIPATION ANALYSIS

It is quite obvious that the basic activity in collaborative learning is to participate in discussions [30-31]. This in a way implies that the participants externalize and share the sense of information or knowledge. This is one of the most important manifestations of active interdependence of individuals. Social construction theory suggests that our knowledge and experience is not objectively "discovered". It is discussed, negotiated, and constructed by participants in group interaction. From the perspective of social construction theory, the process of understanding is not driven by natural forces. It is the result of the active, collaborative work of people in certain relationships. Therefore, participation in a collaborative group is the most basic requirement and behavior.

Researchers have argued that a participant's engagement can be measured by his/her interaction with peers or the teacher. Previous research has shown that participant engagement is a positive predictor of actual learning, individual retention in continuous learning, and learning satisfaction. In general, individual engagement in computer-supported collaborative learning refers to the number of individual perspectives the length of posts in the online environment or whether the perspectives are social rather than focusing on content creativity. Researchers have argued that the number of participants' perspectives is a better indicator of how engaged participants are in the computer-supported collaborative learning process. In this study a viewpoint is primarily a sentence of an individual.

Let C denote the sequence of viewpoints and C_r denote the tth viewpoint in the sequence. n denotes the length of the sequence of viewpoints. Since views vary over time, the variable 1 will be used to index individual views, also called "time" (the value of 1 ranges from 1 to n).

$$1 \leq t \leq n \tag{1}$$

Let P be a set of individuals. The variables a and b will be used to refer to any member (individual) of this set. To determine the initiator (or individual) of each viewpoint, we define the following participation function as shown in Equation (2):

https://doi.org/10.17993/3cemp.2023.120151.87-109

$$P_a(t) = \begin{cases} 1, \\ 0, \end{cases} \tag{2}$$

is denoted as 1 if participant a ∈ P contributes view c, and 0 otherwise. The participation function of any participant (a), can be defined as a sequence:

$$P_a = \{P_a(t)\}_{t=1}^{n} = \{P_a(1), P_a(2), P_a(3)_{,\ldots,}, P_a(n)\} \tag{3}$$

where n is the same length as the sequence of viewpoints C. It takes the value 1 when participant a initiates the corresponding viewpoint in C, and 0 otherwise. Using this participation function, several useful descriptive measures of participation in the discussion can be defined in a relatively simple way. The number of points of view of any participant is:

$$\|Pa\| = \sum_{t=1}^{n} P_a(t) \tag{4}$$

In addition, during the discussion, participants may have "pandering" opinions. These are single-word opinion sentences such as "um", "ah", "yes", and "yes". Treating these as equivalent to longer sentences may result in higher participation by participants who are not seriously engaged in the discussion. This would affect the accuracy of the later analysis. Therefore, it is also necessary to calculate the length of the opinions expressed by the participants. The length W_a of any participant (a) expressing an opinion can be considered as:

$$\|W_a\| = \sum_{t=1}^{n} w_a(t) \tag{5}$$

where $W_a(\mathrm{t})$ is denoted as the length of opinions published by participant a at time t. and the total opinion length W is:

$$W = \sum_{1}^{k} \|W_a\| \tag{6}$$

where k is the number of individuals in the group. The participation of participants can be estimated by the sum of the relative proportions of their participation to the total number of participants and the relative proportions of the total number of words (its variation with rounds is shown in Figure 1):

$$\hat{p}a = \frac{\left(\frac{\|P_a\|}{n} \frac{\|W_a\|}{W}\right)}{2} \tag{7}$$

https://doi.org/10.17993/3cemp.2023.120151.87-109

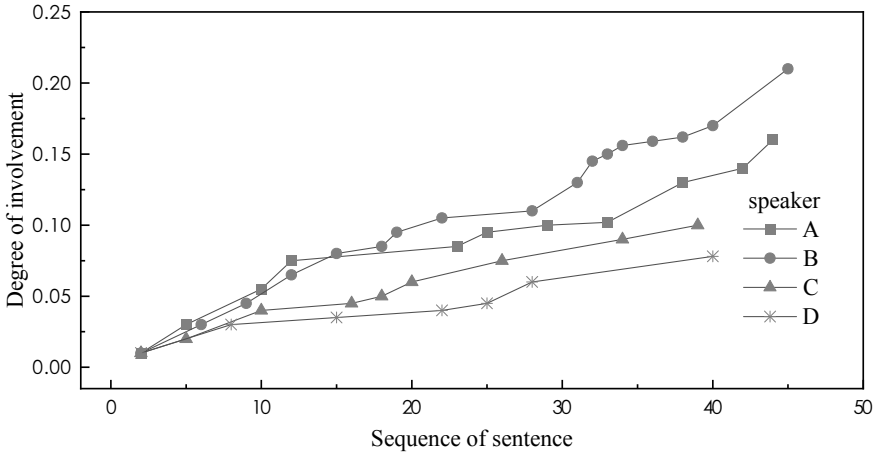

Figure 1 Changes in participant engagement over time

3.2.2. VISUALIZATION DESIGN AND RESULTS PRESENTATION

In the context of knowledge processing, knowledge and the connections between knowledge are important assessment criteria. Students form new knowledge structures by integrating and linking knowledge, thus facilitating knowledge processing. Therefore, it is important to be able to monitor in real time the development of key knowledge points during student discussions. This is important for teachers to keep track of the development of students' cognitive engagement and to effectively monitor the teaching process. In the operationalization analysis of knowledge processing, natural language syllabification techniques were used. The Chinese word-sorting system of CAS was used to keyword-sort the discussion texts during the collaborative process and identify the keywords during the students' discussions. This paper matches with the knowledge concept map provided by experts about the collaborative discussion problem. Meanwhile, this paper measures the cognitive involvement in the collaborative process from the perspective of cluster or student knowledge structure formation. As shown in Figure 2, the knowledge point development change map presents teachers with the development change and distribution pattern of cluster knowledge points from the time dimension. When the mouse hovers over a knowledge point, it also automatically shows back the content of the post where the knowledge point is located, the poster and the time of the posting. Using this visual information, teachers can help discover in-depth information about the process of group discussion. For example, how the group knowledge points were generated over time, whether any group had problems with off-topic or stagnant discussions, and whether relationships between knowledge points were established. This makes the development process of cognitive engagement easier to monitor. However, knowledge processing can only focus on cognitive engagement during collaborative discussions. This lacks a clear indication of the behavioral interactions of the cluster. The developmental changes in cognitive processes are influenced by the behavioral aspects of the cluster interactions themselves. Therefore, further, the visual presentation of behavioral patterns can be used to explore the strategies and patterns of students' behavioral interactions during collaborative knowledge construction.

https://doi.org/10.17993/3cemp.2023.120151.87-109

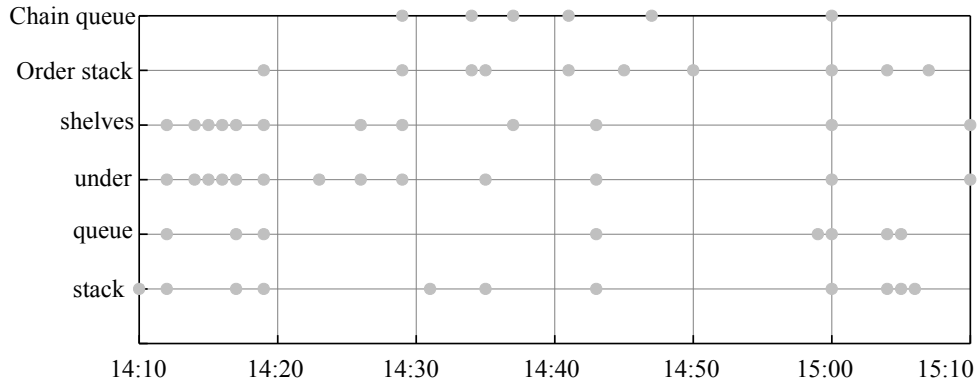

(a) Group 1

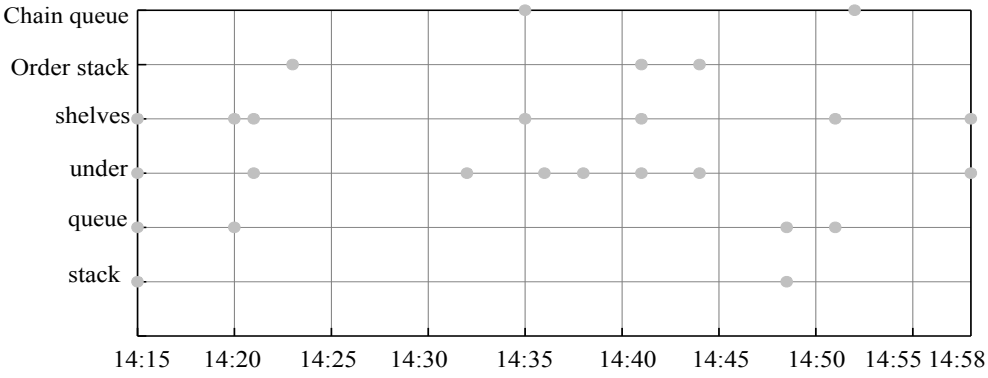

(b) Group 5

Figure 2 Development of knowledge points

In terms of behavioral patterns, to dig deeper into the influence of group behavioral patterns on students' collaborative learning. This paper investigates the characteristics of discussion-based online collaborative learning. In this paper, collaborative behaviors are coded into five first-level categories: presentation (C1), negotiation (C2), questioning (C3), management (C4), and emotional communication (C5), and each category is further refined into 14 second-level categories (C11: gives ideas/ options; C12: further explains ideas; C13: revises ideas/options; C14: summarizes ideas/options. C21: agrees; C22: Agree, give evidence/reference; C23: Disagree; C24: Disagree, give evidence.C31: Ask questions; C32: Ask follow-up questions. C41: Organize/assign tasks; C42: Coordinate management/reminders). Embed these codes in the posting area of the Moodle platform. The selection of behavioral categories can be made when students submit postings. This can support the automated processing of analytics tools. Finally, the association rule approach to data mining in learning analytics is used through the analytics system. This method calculates the probability that each behavior will be accompanied by the next behavior and the intensity of the next behavior, extracts behavior transition pairs that occur at high frequencies, and finally forms behavior sequence transition patterns. These behavior patterns characterize the different behavior patterns of the collaborative group in the collaborative interaction.

In terms of social relationship analysis, the analysis of social interactions will help teachers to better understand who are the central participants in the knowledge

https://doi.org/10.17993/3cemp.2023.120151.87-109

construction dialogue. It can see if there are some undesirable social relationships that can have an impact on the motivation for collaborative learning. The visualization diagram based on the interactions can graphically represent the characteristics of the interaction network structure. It can effectively support teachers in qualitatively analyzing the attributes of the interactive network structure and discovering whether there are distinct central, peripheral, and isolated figures in the network.

3.2.3. POTENTIAL PROFILE ANALYSIS

For potential profile models, the most important issue is to determine the number of their profiles. Currently, researchers still determine the model mainly based on its fit indices. These fit indices include the Akaike Information Criterion (AIC), Bayesian Information Criterion (BIC), and likelihood ratio test. The better the model fit is, the smaller the values of these indices are. In addition, the entropy index has a value range from 0 to 1. This can be used to measure the accuracy of the model in classifying profiles (classes). The higher the value is, the more accurate the classification is. For example, when it is 0.6, about 20% of the individuals may be classified into the wrong profiles (potential classes). While when Entropy=0.8, about less than 10% of the individuals were classified into the wrong profiles (potential classes). As shown in Figure 3, the model results fit well (when choosing a model, it is important to consider not only the statistical indicators but also the substantive significance of each class).

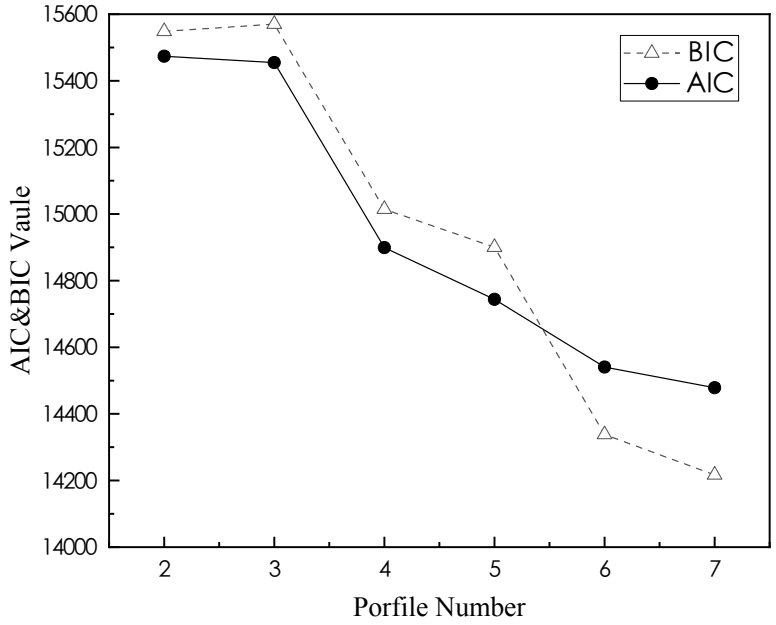

Figure 3 Fitting index gravel plot for potential profile analysis

For the model with six categories of potential profile analysis, the results showed that engagement differed significantly on participant categories ($F(6,164) = 74.22$, $p < 0.01$). Social influence differed significantly across participant categories ($F(6,164) = 76.80$, $p < 0.01$). Overall response rate was significantly different on participant categories ($F(6,164) = 97.89$, $p < 0.01$). Intrinsic correlation was significantly different across participant categories ($F(6,164)= 32.85$, $p<0.01$). Communication density

https://doi.org/10.17993/3cemp.2023.120151.87-109

differed significantly across participant categories ($F(6,164)= 86.89$, $p< 0.01$). Response rate was significantly different across participant categories ($F(6,164) = 86.89$, $p < 0.01$).

4. DISCUSSION OF PRACTICE RESULTS

Through the analysis of the three important dimensions in the model and the visualization of the results based on tool support, it can be seen that the use of learning analytics improves the subjective drawbacks of the mainstream manual coding-based analysis of the original collaborative learning process. The technique overcomes the shortcomings of manual analysis, which is time-consuming and laborious and can only be used for post-collaboration analysis, and provides implementation feedback on the collaborative process. The technique enhances the evaluation, feedback, perception and adaptation of collaborative learning. At the same time, the presentation of visualizations based on tool analysis transforms the data generated by the collaborative process into a friendly visual form. This brings to the fore some important features, patterns, and anomalies. Thus, visual presentation supported by analytical tools can be a key feature. It is used to gain insight into the learning process as well as to provide basic support for monitoring, feedback, and evaluation. It is important for teachers to monitor their teaching, researchers to uncover large-scale teaching patterns, and process evaluation.

4.1. PERCEPTIVENESS OF THE COLLABORATIVE ACTIVITY PROCESS

Model-based visual presentation can improve teachers' perception of the process of collaborative activities. When multiple groups are discussing online at the same time, it can be difficult for teachers to monitor problems with group collaboration in real time without the help of tools. With visual information, it is easier for teachers to identify problems such as digressions and stagnation in the discussion. Teachers can gain a deeper understanding of the discussion process. As can be seen from the comparative display of the two groups in Figure 2, Group 1 had more discussion on the six knowledge points selected by the teacher during the discussion time. There was no deviation or stagnation in the middle of Group 1. In contrast, the discussion in Group 5 was fragmented and disorganized, without establishing relationships among related knowledge points. Further, when the teacher hovers over a particular bullet point, the tool automatically displays more detailed information about that knowledge point. For example, which student mentioned the point at that point in time, and the original text content of their discussion of the point. With this information, teachers can more easily find out at what point the group entered into the discussion of a particular issue. It is also possible to discover how the group gradually builds knowledge-to-knowledge connections in the discussion that facilitate problem solving. In other words, presenting the distribution patterns of knowledge over time makes the traditional "black box" collaborative process of knowledge processing visible. This will provide teachers with sufficient information to better observe the discussion process.

https://doi.org/10.17993/3cemp.2023.120151.87-109

It can provide additional evidence for researchers to conduct ongoing inquiry into the internal mechanisms of collaborative processes.

4.2. IMPACT OF VISUAL PRESENTATION ON THE PATTERN OF COLLABORATIVE ACTIVITIES

Model-based visual presentation can provide powerful support for exploring the patterns of collaborative activities. In large-scale online education scenarios, the visual presentation of behavioral sequence patterns in behavioral models can be used to flexibly explore the behavioral transition patterns of online collaborative activities. The visual presentation helps teachers gain deeper insight into the internal patterns of group interaction behaviors. In Group 1, the self-loop of C11→C11 during the collaborative discussion to complete the task shows that each member can continuously put forward his or her own point of view. Members actively think about the problem and express their suggestions. In addition, the transitions from C11→C32, C11→C23, and C11→C13 show that the members of Group 1 presented their ideas accompanied by further follow-up questions from other members, questioning with evidence, and revision to improve their ideas. This indicates that the members of the group were able to argue the issue sufficiently to keep moving the task forward to completion. Moreover, the transformation of C32→ C12 shows that when a member pursues a point of view, he or she is given a more detailed explanation by other members. This indicates that the group is very interactive. In contrast, after a member of group 5 raises a viewpoint, other members give questions (C11→C21), but the questions are not followed by corresponding explanations. c31→C11 and C32→C11 show that members of the group do not give explanations or revise their views after facing questions or follow-up questions, but continue to raise new views. From the later analysis of the content based on knowledge processing and the synthesis of the interaction structure, it is clear that Group 5 did not reach the pattern of deep interaction of questioning-pursuing-questioning. This is related to its group members' lack of attention to other people's viewpoints and the fact that group members' discussions are more about posting only rather than engaging in dialogue.

Extraction results using real-time behavioral sequence transformation provided by the tool. Teachers or researchers can conduct the mining of online collaborative learning behavioral patterns in various scenarios. For example, in terms of the characteristics of group behavior patterns, the behavioral characteristics of collaborative groups with regular patterns in the process of collaborative knowledge construction can be found. Their effects on knowledge construction can also be found. Also, the similarities and differences in behavioral patterns presented by high and low quality groups can be examined to help teachers explore important positive influences in high quality discussions as well as potential limitations present in low quality groups. This will provide a valuable reference for teachers to design better online collaborative activities and teaching strategies. Using real-time process information from the visualization tool, it can also be explored to obtain comparisons of differences in behavior patterns at different stages. By analyzing the different behavioral patterns of collaborative groups at the beginning, unfolding, and concluding

https://doi.org/10.17993/3cemp.2023.120151.87-109

stages of collaboration, the changes of behavioral development in the collaborative knowledge construction process can be explored. The results can provide a basis for exploring the internal mechanism of the knowledge construction process.

4.3. EVIDENCE SUPPORT FOR PROCESS EVALUATION

Model-based visual representations can provide comprehensive evidence to support process evaluation. Collaborative assignments within online classrooms often involve a large amount of participation and contribution. This makes monitoring and evaluation by tutors time-consuming, tedious, and error-prone. It is nearly impossible for tutors to manually process the hundreds of sequences of contributions in a discussion topic and the relationships between these contributions. As a direct consequence, most online learning environments use simple metrics based on the number of posts, reads, topics created, and average length of statements. These measures are very useful in capturing the dynamics of online collaborative activity. However, they ignore the essential feature of the need to continuously consider the process of knowledge construction. This does not serve the core of process-based evaluation of clusters. Thus, using the three dimensions of the multidimensional model to complement and explain each other will help teachers to comprehensively evaluate the group collaboration process in terms of multiple dimensions, including cognitive engagement, interactive behaviors, and social relationships.

By observing the behavioral transition pattern, it can be found that Group 5 mainly reflected more behavioral strategies of questioning or pursuing in the interaction pattern of behavior. However, group 5 did not show more meaningful negotiation processes such as arguing in the process of question reaching. Further, a deeper examination of the content revealed by the mouse locating knowledge points shows that Group 5 lacked sufficient motivation in the content of their statements to explain their views or to discuss alternative options. Group 5 prefers to seek ultimate help, such as being told the answer directly. In other words, the knowledge processing dimension was further combined. The analysis of the content provides an understanding of the micro-level of online collaborative discussions. Exploring the relationship between the influence of social network structure on knowledge construction can explore the internal causes affecting the effectiveness of collaborative learning from multiple dimensions. This can provide more robust evidence to support process evaluation.

5. CONCLUSION AND OUTLOOK

In this paper, we use computer-supported collaborative learning (CSCL) technology to share knowledge in real time and promote interactive learning. In this paper, we collect, annotate and analyze data based on five modalities: brain, behavior, cognition, environment and technology, and establish a model of computer-supported collaborative learning process analysis in the context of multimodal data analysis. The model is based on the intelligent network collaboration of roles and CSCL, and an interactive visualization tool is designed and developed to support the analysis of

https://doi.org/10.17993/3cemp.2023.120151.87-109

online collaborative learning process. In addition, this paper conducts a practical study in an online classroom. The study shows that the model and tool can be effectively used for online collaborative learning process analysis. It can help teachers monitor the discussion process in real time, identify problems in collaboration, and provide timely intervention and guidance. The following conclusions were obtained:

(1) In this paper, we elaborate the application of role theory in online learning environment, and propose a new intelligent CSCL model by combining the three-layer structure of application perspective. The model is personalized and intelligent, with good practicality, and well reflects the dynamic distribution of multiple roles in collaborative learning. Especially, the multiple roles of teachers in the environment better realize the unity of teaching and learning.

(1) The intelligent network collaboration model based on roles and CSCL is proposed in this paper. The model combines the theory of CSCL, intelligent agent technology and role theory, and has good application value. The model results fit well according to the Akaike Information Criterion (AIC), Bayesian Information Criterion (BIC) and likelihood ratio test. When the entropy index takes a value of about 0.85, about less than 10% of the individuals are assigned to the wrong profile.

(1) Model-based visualization enhances teachers' perception of the process of collaborative activities. It provides powerful support for exploring the patterns of collaborative activities and provides comprehensive evidence to support process evaluation. Visual presentation improves the effectiveness of monitoring the discussion process in real time. During the test, the participation of participants gradually increased from 5% to 25%, and the participation effect increased by about 80%.

In this paper, we study the interaction, cooperation and coordination among role-based multi-intelligent Agents from the perspective of multiple roles. This paper proposes and describes the collaboration and coordination mechanism among role-based intelligent agents. In particular, the role mechanism is studied in the application of open and dynamic network environment. The article greatly enriches the multi-agent system (MAS) theory. The mechanism, if combined with adaptive knowledge mining algorithms, will greatly contribute to the progress of distributed data mining research. The next step is to apply the role-based cooperation and coordination negotiation mechanism among intelligent agents and adaptive knowledge mining of intelligent agents to distributed data mining systems with knowledge orientation. This has good application prospects and is the direction we need to study in the future.

REFERENCES

(1) LI Y, DONG M, HUANG R. Toward a semantie forum for active collaborative learning [J]. Educational technology & society, 2009, 12(4):71-86.

(2) ALAVI M, DUFNER D. Technology-mediated collaborative learning: a research perspective [M/]/Learning together online: research on asynchronous learning networks. Mahwah, NJ: Lawrence Erlbaum Associates, 2005 :191-213.

https://doi.org/10.17993/3cemp.2023.120151.87-109

(3) Soualah-Alila, F., Nicolle, C., & Mendes, F. (2015). **Towards a methodology for semantic and context-aware mobile learning [M/EB]**.[2019-4-26]

(4) Stahl, G., Koschmann, T. D., & Suthers, D. D. (2006). **Computer-supported collaborative learning: An historical perspective [C]** *R. K. Sawyer(Ed.). Cambridge handbook of the learning sciences. Cambridge, UK: Cambridge University Press*:409-426.

(5) Heimbuch, S., Ollesch, L., & Bodemer, D. (2018). **Comparing effects of two collaboration scripts on learning activities for wiki-based environments [J]**. *International Journal of Computer-Supported Collaborative Learning*, 13(3):331-357.

(6) Kreijns, K, Kirschner, P. A., & Jochems, W. (2003). **Identifying the pitfalls for social interaction in computer-supported collaborative learning environments: A review of the research [J]**. *Computers in Human Behavior*, 19(3):35-353.

(7) Ludvigsen, S., Cress, U, Law, N., Stahl, G., & Rose, C. P. (2017). **Future direction for the CSCL field: Methodologies and eight controversies [J]**. *International Journal of Computer-Supported Collaborative Learning*, 12(4):337-341.

(8) Isotani, S., Mizoguchi, R., Isotani, S., Capeli, 0. M., Isotani, N., Albuquerque, A. R., & Jaques, P. (2013). **A semantic web- based authoring tool to facilitate the planning of collaborative learning scenarios compliant with learning theories [J]**. *Computers & Education*, 63(2):267-284.

(9) Reis, R. C. D., Isotani, S., Rodriguez, C. L., Lyra, K. T, Jaques, P. A., & Bittencourt, I. I. (2018). **Affective states in computer-supported collaborative learning: Studying the past to drive the future [J]**. *Computers & Education*, (120): 29-50.

(10) Rienties, B., Tempelaar, D., Van den Bossche, P, Gijselaers, W., & Segers, M. (2009). **The role of academic motivation in computer-supported collaborative learning [J]**. *Computers in Human Behavior*, 25(6):1195-1206.

(11) Koops, W., & Van der Vleuten, C. (2018). **A computer-supported collaborative learning environment in medical education: The importance for educators to consider medical students' motivation [J]**. *Journal of Contemporary Medical Education*, 8(1): 10-17.

(12) Xiang, W. A. , et al. **Multi-view stereo in the Deep Learning Era: A Comprehensive Review**. (2021).

(13) W. Cai, D. Liu, X. Ning, et al., **Voxel-based Three-view Hybrid Parallel Network for 3D Object Classification**, *Displays* 69 (1) (2021).

(14) Bai X, Zhou J, Ning X, et al. **3D data computation and visualization**. *Displays*, 2022: 102169.

(15) X. Ning, P. Duan, W. Li, and S. Zhang, **Real-time 3D face alignment using an encoder-decoder network with an efficient deconvolution layer**, *IEEE Signal Processing Letters*, vol. 27, pp. 1944–1948, 2020.

(16) Wang C, Zhou J, Xiao B, et al. **Uncertainty Estimation for Stereo Matching Based on Evidential Deep Learning**. *Pattern Recognition*, 2021.

https://doi.org/10.17993/3cemp.2023.120151.87-109

(17) Fahy P J , Gail C , Mohamed A . **Patterns of Interaction in a Computer Conference Transcript[J]**. *International Review of Research in Open and Distance Learning*, 2001, 2(1).

(18) VELDHUIS-DIERMANSE A E. **CSC Learning: participation, learning, activities and knowledge construction in computer-supported collaborative learning in higher education[D]**. *Netherlands: Wageningen University*, 2002.

(19) HENRI F. **Computer conferencing and content analysis [M],** *Collaborative learning through computer conferencing. Springer BerlinHeidelberg,* 1992:117-136.

(20) NEWMAN D R, OTHERS A. **A content analysis method to measure critical thinking in face-to-face and computer supported group learming[J],** *Interpersonal computing & technology*, 1995, 3(2) :56-77.

(21) ZHU E. **Meaning knowledge construction and mentoring in a distance leaming course [C],** *National convention of the association for educational communications and technology, Indianopolis*, 1996; 821-844.

(22) LI Y Y, LIAO J,WANG J, et al. **CSCL interaction analysis for assessing knowledge building outcomes: method and tool [C],** *Proceedings of the 8th iternational conference on Computer supported collaborative learning. Intemational Society of the Learning Sciences*, 2007 :431-440.

(23) PAUL A, ERKENS G. **Toward a framework for CSCL research[J]**. *Educational Psychologist*, 2013, 48(1):1-8.

(24) LI. Yanda et al. **Distance Learming.Proceedings of the international Conference on Distance Education,Distance Learning and 215t Century Education Development**. April 12~15,1999,Beijing,China.

(25) Ayala, G and Yano, Y. **Intelligent Agents to Support the Effective Collaboration in a CSCL Environment**. *Proceedings of the ED-TELECOM 96 World Conference on Educational Communications, Boston, Mass. AACE, Patricia Carlson and Fillia Makedon (eds.)*, pp.19-24, June,1996.

(26) KIM M, LEE E. **A multidimensional analysis tool for visualizing online interactions [J]**. *Educational technology & society*, 2012, 15 (3):89-102.

(27) ZHENG L, HUANG R, HWANG G J, et al. **Measuring knowledge elaboration based on a computer -assisted knowledge map analytical approach to collaborative learning[J]**. *Educational technology & society*, 2015, 18(1):321-336.

(28) Eryilmaz E , Pol J , Ryan T , et al. **Enhancing student knowledge acquisition from online learning conversations[J]**. *International Journal of Computer-supported Collaborative Learning*, 2013, 8(1):113-144.

(29) TIRADO R, ANGEL HERNANDO, AGUADED J I. **The effect of centralization and cohesion on the social construction of knowledge in discussion forums Interactive learning environments**, 2015, volume 23(3):1-24.

(30) Julca A. B., Tapia, C. D., Hilario, F. M., y Corpus, C. M. (2021). **Qualitative benchmarking study of software for switch performance evaluation**. *3C Tecnología. Glosas de innovación aplicadas a la pyme*, 10(4), 35-49. https://doi.org/10.17993/3ctecno/2021.v10n4e40.35-49.

https://doi.org/10.17993/3cemp.2023.120151.87-109

(31) Li Zhengjian & Li Lifeng (2021). **Mathematical statistics algorithm in the bending performance test of corroded reinforced concrete beams under fatigue load**. *Applied Mathematics and Nonlinear Sciences* (1). https://doi.org/10.2478/AMNS.2021.2.00142.

https://doi.org/10.17993/3cemp.2023.120151.87-109

/06/

CONSTRUCTION OF AN EFFICIENT EVALUATION MODEL FOR ATHLETIC ATHLETES' COMPETITIVE ABILITY BASED ON DEEP NEURAL NETWORK ALGORITHM

Yuhan Niu*

School of Human Settlements and Civil Engineering, Xi'an Jiaotong University, Xi'an, Shaanxi, 710000, China - Xi'an Jiaotong University City College, Xi'an, Shaanxi, 710000, China

18602977530@163.com

Reception: 05/11/2022 **Acceptance**: 01/01/2023 **Publication**: 01/02/2023

Suggested citation:

N., Yuhan (2023). **Construction of an efficient evaluation model for athletic athletes' competitive ability based on deep neural network algorithm**. *3C Empresa. Investigación y pensamiento crítico, 12(1)*, 111-131. https://doi.org/10.17993/3cemp.2023.120151.111-131

ABSTRACT

This paper analyzes the data of this year's athletes' physical fitness test scores and manages the classification of different physical qualities of the farmer. In order to reduce the manual calculation and increase the prediction efficiency, as well as to unify the scoring criteria of previous years, this paper proposes a comprehensive performance prediction model based on deep neural network algorithm. First, principal component analysis is used to transform multiple attributes with strong correlation into independent attributes that are not related to each other, and to reduce the time and space for model training by eliminating redundancy. Second, a back propagation (BP) neural network algorithm is used to build a physical fitness test prediction model, and the model is applied to the test dataset for model performance evaluation. Finally, the physical fitness test model was applied to other years for comprehensive performance prediction, and the differences between the model prediction results and the actual teachers' manual calculation results were observed. The results showed very good prediction results for 2021, in which 92.95% of the data had an absolute value of error less than 2 and only 0.06% had an absolute value of error greater than 4, which indicated that the prediction performance of the model was extremely significant. At the same time, a new athletic athletic scoring standard was also developed based on the neural network BP model to provide a more scientific theoretical basis and guidance for the evaluation of athletic ability of athletes.

KEYWORDS

BP neural network; athletic ability; track and field; prediction; evaluation

https://doi.org/10.17993/3cemp.2023.120151.111-131

PAPER INDEX

https://doi.org/10.17993/3cemp.2023.120151.111-131

1. INTRODUCTION

Athletics is a sport with a long history, with the largest number of gold medals in the Olympic Games and the most widely practiced sport in the world [1, 2]. Therefore, track and field is known as the mother of sports, and it plays a pivotal role in the development of each sport. Track and field is the cornerstone of the Olympic movement and best embodies the Olympic concept of "faster, higher, stronger". In the 2008 Beijing Olympic Games, China's athletes fought hard and achieved very impressive results, ranking first in the world with 51 gold medals, 21 silver medals and 28 bronze medals, achieving a historic breakthrough and reflecting the strong strength of a major sports nation. But at the same time, we should also clearly see that China's track and field projects, such as men's 110m hurdles, women's middle and long distance running, women's chain ball, etc. have been declared defeated in this Olympic Games, which is a big regret for Chinese sports in this Olympic Games.

Athletics is an important constraint to the progress of Chinese sports from a large sports country to a strong sports country [3]. For this reason, an ambitious goal of Chinese sports in the post-Olympic era is to accelerate the pace of revitalizing Chinese athletics and promoting the perfection of Chinese sports [4]. Athletics can be studied from several perspectives, such as the study of competition performance. Athletic performance is the result of athletes' participation in the competition, which is the substantial reflection of athletes' comprehensive ability, especially the reflection of athletic ability, and also the direct reflection of training results. The intuitive nature of athletic performance fully demonstrates the results of coaches in the whole sports training and competition activities, which is an objective criterion for scientific diagnosis of training and competition results, as well as a basis for the implementation of scientific training methods [4]. Therefore, the analysis of track and field results can provide coaches with an objective basis for training control, which is of great significance for the development of indoor track and field in China [5]. zheng et al. used gray theory and methods to analyze the results of Chinese and foreign outstanding decathletes by multi-level correlations, revealing the correlations between total performance and speed, jumping, throwing, and endurance categories, between each classification, and between total performance and each constituent item. Yu [6] et al. compared and analyzed the factor loading matrices of the top 150 athletes in the world in 2006, and concluded that the intrinsic factors limiting the development of the athletes' performance were the relatively weak basic quality of the athletes, especially the significant differences in the strength factor, and the overall low level. Chen [7] established a multiple regression prediction model for decathlon based on the data of the decathlon competition in track and field championships. The predicted values extrapolated from the dynamic trends of athletes' performance in each individual sport were highly correlated with the actual values with high accuracy and no variability.

Artificial neural networks, also known as neural networks, have their origin in neurobiology [8, 9]. Neural networks, which are composed of a large number of nerve cells, are a simplification, abstraction and simulation of the human brain [10]. Researchers have built artificial neural models by simulating the response processes of nerve cells [11]. A neural network is a parallel interconnected network composed of

https://doi.org/10.17993/3cemp.2023.120151.111-131

simple units that can simulate the interactive responses of the biological nervous system to the real world [12]. In recent years several studies have tried to apply neural networks to sports and athletic ability analysis, i.e., to improve the original algorithm combined with BP neural networks for modeling and combining it with practical applications, mainly for prediction or evaluation of some indicators [13]. As yan et al. provided a basis for the use of neural network modeling in biomechanics, opening a wide prospect of research in this area. They explored the problem of generalized inverse transformations of information in sports biomechanics by using neural network techniques to model the transformation of the characteristic quantities and the original information, taking shot put sports as an example.

The purpose of this paper is to trace the characteristics of various nonlinear functions by analyzing each physical test ability of track and field athletes and the all-around analysis standard published by IAAF, and then select the appropriate function for progressive scoring, so that the progressive method is not constrained by the average performance of athletes, i.e., it is universal. Based on the decathlon scoring scale developed by the progressive scoring method, the scoring criteria were revised based on the neural network method, and its good nonlinear mapping ability was used to try to make the scoring of each item more scientific and reasonable. Based on the successful establishment of the evaluation model of athletic ability of track and field athletes, it provides help for athletes to develop targeted training plans.

2. RESEARCH METHODS AND MODELS

2.1. KEY DATA PROCESSING THEORY

2.1.1. DATA STANDARDIZATION

Along with the progress of human society, the fields of study that humans are involved in have become more and more complex. In fact it has become very difficult to describe things in detail using individual attributes, and it is necessary to consider the problem from a holistic point of view, thus giving birth to the method of multi-indicator evaluation. In the system of multi-indicator evaluation, there are different units of attributes, and there are significant differences in magnitude and order of magnitude between them. Therefore, it is necessary to standardize each attribute of the original data, thus ensuring the reliability of the analysis results.

Currently, there are various methods of data standardization [14, 15], among which the most typical method is data normalization, which is to map the data to the [0, 1] interval uniformly. In this paper, the z-score standardization method is used to standardize the athlete physical measurement data to eliminate unit restrictions and dimensional relationships between variables and also to reduce the prediction time and increase the prediction accuracy [15, 16]. z-score standardization is based on the mean and standard deviation of the original data to standardize the data (Equation 1). This standardization method mainly converts the original data into standard normally

https://doi.org/10.17993/3cemp.2023.120151.111-131

distributed data with mean 0 and variance 1, and is suitable for scenarios with large data volumes.

$$x = \frac{x_i - \mathrm{E}(x)}{s_i} \quad (1)$$

where x_i is the original data, $\mathrm{E}(x)$ is the mean of the data, and s_i is the standard deviation of the data. The conversion of raw data into dimensionless evaluation index values by standardization makes the values of each index at the same level and facilitates the ability to sum weight attributes of different units or magnitudes.

2.1.2. DATA CORRELATION ANALYSIS

In today's era of big data, data correlation analysis can quickly and efficiently discover the intrinsic connections that exist between different things [17, 18]. Correlation, which refers to the pattern that exists between two or more variables in some sense, aims to explore the intrinsic information hidden in the data set. The correlation coefficient can be used to describe the relationship between variables, where the sign of the correlation coefficient indicates whether the direction of the relationship is positive or negative, and the magnitude of its value represents the strength of the relationship between the two variables, where the correlation coefficient is 0 when there is no correlation at all and 1 when there is a perfect correlation. There are various methods for calculating correlation coefficients in correlation analysis, including Pearson correlation coefficient [19], Spearman correlation coefficient [20], partial correlation coefficient [21], Kendall correlation coefficient [22], and so on. In this paper, the Pearson correlation coefficient is used to calculate the magnitude of correlation between the attributes. Standardization of the original data does not change the correlation between the attributes of the original data. Therefore, the standardized data can be used to directly calculate the correlation between the attributes. The correlation coefficient is calculated as shown in Equation 2:

where xi and yi are the data of the two attributes involved in the calculation, and $\bar{x}$ and $\bar{y}$ are the mean values of the corresponding attributes.

$$r = \frac{\sum_{i=1}^{n}(x_i - \bar{x})(y_i - \bar{y})}{\sqrt{\sum_{i=1}^{n}(x_i - \bar{x})^2}\sqrt{\sum_{i=1}^{n}(y_i - \bar{y})^2}} \quad (2)$$

2.1.3. PRINCIPAL COMPONENT ANALYSIS ALGORITHM

Principal component analysis is a commonly used technique for reducing the dimensionality of a data set, allowing exploration and simplification of certain complex

https://doi.org/10.17993/3cemp.2023.120151.111-131

relationships between variables. It can transform several original variables with strong correlation characteristics into several uncorrelated variables through coordinate transformation, and the uncorrelated ones calculated as principal components. The principal component is a linear combination of the original variables, and its model is shown in Figure 1.

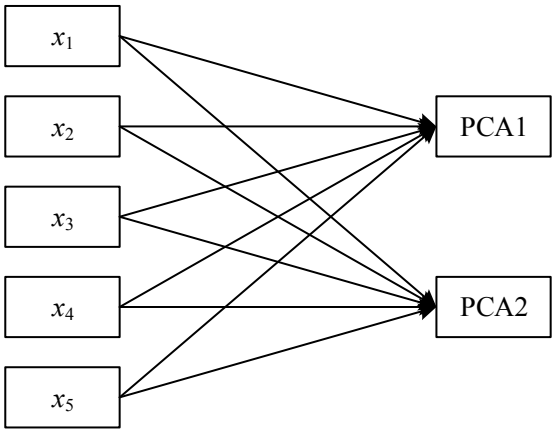

Figure 1 Principal component analysis (PCA) model

The principal components reflect most of the characteristics of the primitive variables and can remove strong correlations between the primitive variables. The principal components are linear combinations of the original variables. The first principal component explains the most variance of the primitive variables, while the second principal component explains the second variance of the original variables and is orthogonal to the first principal component, which means it is completely uncorrelated. By analogy, the remaining principal components are all orthogonal to each other. Suppose, there exist p variables in the original data, namely x_1, x_2,…,, which are linearly combined to form a new p mutually independent principal component variable y_p, whose mathematical model expression is shown in Equation (3).

$$\begin{cases} y_1 = \mu_{11}x_1 + \mu_{12}x_2 + \boxed{?} + \mu_{1i}x_i + \boxed{?}\mu_{1p}x_p \\ y_2 = \mu_{21}x_1 + \mu_{22}x_2 + \boxed{?} + \mu_{2i}x_i + \boxed{?}\mu_{2p}x_p \\ \boxed{?} \\ y_i = \mu_{i1}x_1 + \mu_{i2}x_2 + \boxed{?} + \mu_{ii}x_i + \boxed{?}\mu_{ip}x_p \\ \boxed{?} \\ y_p = \mu_{p1}x_1 + \mu_{p2}x_2 + \boxed{?} + \mu_{pi}x_i + \boxed{?}\mu_{pp}x_p \end{cases} \quad (3)$$

The model is changed into matrix form as shown in Equation (4):

$$y = \begin{bmatrix} \mu_{11} & \mu_{12} & \boxed{?} & \mu_{1p} \\ \mu_{21} & \mu_{22} & \boxed{?} & \mu_{2p} \\ \boxed{?} & \boxed{?} & \boxed{?} & \boxed{?} \\ \mu_{p1} & \mu_{p2} & \boxed{?} & \mu_{pp} \end{bmatrix} \begin{bmatrix} x_1 \\ x_2 \\ \boxed{?} \\ x_p \end{bmatrix} = Ux \quad (4)$$

https://doi.org/10.17993/3cemp.2023.120151.111-131

where the sum of squares of the principal component coefficients μ_{pp} is 1, as shown in Equation (5):

$$\mu_{i1}^{\ 2} + \mu_{i2}^{\ 2} + \boxed{?} + \mu_{ip}^{\ 2} = 1 \tag{5}$$

Next, to obtain the principal component values y_p, the principal component coefficients μ_{pp} are to be calculated, and first the covariance matrix is calculated from the original data as shown in Equation (6):

$$\mathrm{cov} = \frac{1}{n}\sum_{i=1}^{n}(x_i - \bar{x})(y_i - \bar{y}) \tag{6}$$

Since the data have been standardized, then the variance s^2 of the original data is 1 see equation (7), the

$$s^2 = \frac{1}{n}\sum_{i=1}^{n}(x_i - \bar{x})^2 = 1 \tag{7}$$

Changing equation (7) to equation (8), the

$$\sum_{i=1}^{n}(x_i - \bar{x})^2 = ns^2 = n \tag{8}$$

At this point, we can obtain equation (9)

$$r = \frac{\sum_{i=1}^{n}(x_i - \bar{x})(y_i - \bar{y})}{\sqrt{\sum_{i=1}^{n}(x_i - \bar{x})^2}\sqrt{\sum_{i=1}^{n}(y_i - \bar{y})^2}} = \frac{\sum_{i=1}^{n}(x_i - \bar{x})(y_i - \bar{y})}{\sqrt{n}\sqrt{n}} = \mathrm{cov} \tag{9}$$

From Equation (9), the correlation coefficient matrix of the original data is actually equivalent to the covariance matrix. The eigenvalue λ_i of the covariance matrix represents the variance of the principal components, while the eigenvalue of the covariance matrix with the principal component coefficients μ_{pp} is calculated from the correlation coefficient matrix and the eigenvalue y is calculated by the formula $y = x\mu^T$. Theoretically, a smaller number of principal components is selected to replace the original full data based on the contribution of principal components, and the number of principal components with a contribution of 90% is generally selected, but in this paper, the same number of principal components as the number of original variables will be selected, which does not throw away the information of the original data and removes the influence of strong correlation between the original variables on the model training. Next, the neural network model is built using eight new variables that are not correlated with each other, which increases the persuasiveness of the model accuracy and excludes the influence of the data itself factors on the model building and parameter optimization.

2.2. BP NEURAL NETWORK MODEL OPTIMIZATION

https://doi.org/10.17993/3cemp.2023.120151.111-131

BP neural network as a part of neural network is a supervised learning algorithm [23]. It is a multilayer nonlinear feedforward network trained by an error back propagation learning algorithm. The network consists of an input layer, an implicit layer and an output layer. The BP learning algorithm consists of two processes, a forward propagation of the data and a backward propagation of the error signal.

2.2.1. FORWARD PROPAGATION OF DATA

The interconnection pattern between neural networks is formed by interconnecting neurons, and the initial weights between each connection are randomly assigned by the computer. The forward propagation phase of the data signal is the process of the original data signal from the input layer through the implicit layer to the output layer, i.e., the output of the upper layer nodes is used as the input of the lower layer nodes. The basic structure of the forward propagation of the BP neural network is shown in Figure 2.

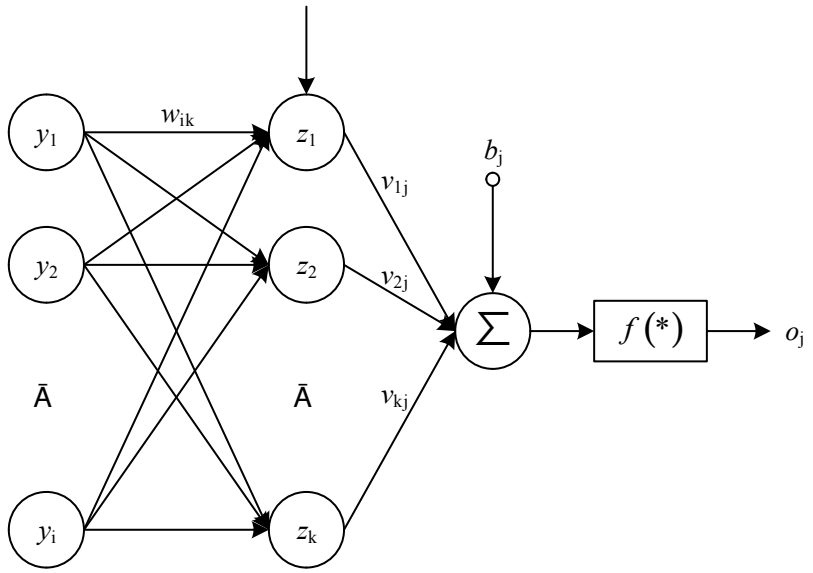

Figure 2 Basic structure of forward propagation stage BP neural network

Figure 2 shows that each neuron cell y_i has a corresponding computational weight w_{ik}. The output value of the input layer in the hidden layer $net1_k$ is obtained by summing and weighting the input values, connection weights and threshold b_k, calculated as Equation (10) shows:

$$net1_k = \sum_{i=1}^{n} w_{ik} y_i + b_k = w_{1k} y_1 + w_{2k} y_2 + \boxed{?} w_{nk} y_n + b_k \qquad (10)$$

In the process of prediction, better prediction accuracy can be obtained by applying activation function processing. There are many kinds of activation functions, such as step function, Sigmoid function, tanh function, and ReLU function. In this project, the Sigmoid function is used to activate the output information. The output value of the input layer is activated by the activation function as ($net1_k$), then the implicit layer z_k is obtained by Equation (11).

https://doi.org/10.17993/3cemp.2023.120151.111-131

$$z_k = f\left(net1_k\right) = \frac{1}{1+\exp\left(-net1_k\right)} \tag{11}$$

Next, the implicit layer data is passed to the output layer as an input layer. The output value $net2_j$ is obtained from the weighted sum of the implied layer value and the connection weight v_{kj} between the implied layer and the output layer, plus the threshold b_j as shown in Equation (12):

$$net2_j = \sum_{k=1}^{n} v_{kj} z_k + b_j = v_{1j} z_1 + v_{2j} z_2 + \boxed{?} v_{nj} y_n + b_j \tag{12}$$

Equation (13) activates the output values to obtain the data of the final output layer.

$$o_j = f\left(\text{net}\,2_j\right) = \frac{1}{1+\exp\left(-net2_j\right)} \tag{13}$$

2.2.2. ERROR BACK PROPAGATION

The error function is used to detect whether the training process of the neural network is finished when the signal is passed to the output layer. The condition for the neural network to stop is that the error function limit is satisfied or a set maximum number of iterations is reached. When the output error function is less than the predefined value, the training will stop. If the condition is not satisfied, the error will be back-propagated. The error function (E) is used to measure the magnitude of the error between the actual output d_j and the desired output o_j, which is calculated as shown in Equation (14).

$$\mathrm{E} = \frac{1}{2}(d-o)^2 = \frac{1}{2}\sum_{j=1}^{n}\left(d_j - o_j\right)^2 \tag{14}$$

The error signal obtained at each layer is used to adjust the weights of the connections between neurons. Equation (3.15) simulates the process of error back propagation.

$$\mathrm{E} = \frac{1}{2}(d-o)^2 = \frac{1}{2}\sum_{j=1}^{n}\left(d_j - o_j\right)^2 \tag{15}$$

The error is reduced along the gradient direction by continuously adjusting the connection weights and thresholds. After calculating the change value Δv_{jk} of the weight connection value between the implicit layer and the output layer, each connection weight is updated as shown in Equation (16) and Equation (17).

$$\Delta v_{kj} = -\eta \frac{\partial E}{\partial v_{kj}} = -\eta \frac{\partial E}{\partial net2_j}\frac{\partial net2_j}{\partial v_{kj}} = -\eta \frac{\partial E}{\partial net2_j} z_k \tag{16}$$

https://doi.org/10.17993/3cemp.2023.120151.111-131

$$v_{kj} = v_{kj} + \Delta v_{kj} \tag{17}$$

Further extending the error to the input layer as in equation (18)

$$E = \frac{1}{2}\sum_{j=1}^{n}\left(d_j - f\left(\sum_{k=1}^{n} v_{kj} z_k\right)\right)^2 = \frac{1}{2}\sum_{j=1}^{n}\left(d_j - f\left(\sum_{k=1}^{n} v_{kj} f\left(\sum_{i=1}^{n} w_{ik} y_i\right)\right)\right)^2 \tag{18}$$

The connection weights between the input layer and the implied layer are updated as shown in Eqs. (19) and (20).

$$\Delta w_{ik} = -\eta \frac{\partial E}{\partial w_{ik}} = -\eta \frac{\partial E}{\partial net1_k}\frac{\partial net1_k}{\partial w_{ik}} = -\eta \frac{\partial E}{\partial net1_k} y_i \tag{19}$$

$$w_{ik} = w_{ik} + \Delta w_{ik} \tag{20}$$

After all the weights are readjusted, signal forward propagation will continue to be executed. When the model reaches the convergence criterion, the training is stopped, the model is built, and the model parameters are adjusted to optimize the model. The established model is used to predict the physical fitness test data, and the error magnitude between the predicted and actual values is calculated to verify the feasibility of the model, and then the model is applied.

3. RESULTS AND DISCUSSION

3.1. VALIDATION OF THE PHYSICAL TEST SCORE PREDICTION MODEL

The physical fitness test data were preprocessed and standardized, and principal component analysis was used to eliminate strong correlations between the data. The model was built using BP neural network after transforming the original data using principal component analysis method. In this project, the physical fitness test data of a provincial track and field team in 2019 were selected to build the model, in which 80% of the athlete samples were used as the training set and the remaining 20% were used as the test set to evaluate the model. The scoring criteria and methods for male and female distance athletes are different, so the male and female distance athletes test data were separated and separate models were built for prediction. The model was continuously adjusted and optimized using 80% of the training set, and the final model parameters are shown in Table 1.

https://doi.org/10.17993/3cemp.2023.120151.111-131

Table 1 The parameters of model

Parameter Name	Parameter Value
Number of neurons in the input layer	8
Number of neurons in the output layer	1
Number of neurons in the hidden layer	11
Threshold	0.005
Learning rate	0.1
Maximum number of iterations	1.0e10
Training algorithm	rprop+
Error function	sse
Activation function	logistic

As shown in Table 1, the threshold value is used as a conditional value for training stop, which specifies the predetermined value in the error function. The maximum number of iterations forces the training to stop when the predetermined value is not always reached and the iteration cannot be stopped. The algorithm used for training, "rprop+", is the error back propagation algorithm with weights, also known as BP neural network algorithm [24]. The error function "sse" is used to calculate the magnitude of the error at the end of the forward propagation. The activation function uses the parameter "logistic" for the Sigmoid activation function. Where the number of neurons in the hidden layer is determined by the mean square error (MSE) with equation (21).

$$h = \sqrt{m+n} + \alpha \tag{21}$$

Where m in equation (21) is the number of input neurons, n is the number of output neurons, and α is a constant in the range 1 to 10, so the number of hidden layers h takes values in the range 4 to 13.

In order to increase the accuracy of the model, prediction models for male and female students were built separately, and the accuracy of the model was evaluated using the data from the test set. The test set data that were not involved in the model training process were brought into the model for prediction separately, and the prediction results for both boys and girls were finally combined to observe the overall model prediction performance. A sample of 40 athletes was randomly selected from the test set of 2019 data, and the difference between the actual values of these 40 athlete samples and the predicted values of the model was compared as shown in Figure 3. The line graph shown in Figure 3 shows the comparison between the predicted and actual values of the randomly selected sample of 40 athletes in the test set. The solid line is the actual value and the dashed line is the predicted value. It is obvious that the two lines have a high overlap rate and only a few samples can be

https://doi.org/10.17993/3cemp.2023.120151.111-131

viewed with significant errors. The results show that the prediction model established in this project is very accurate and has good performance, and the value of mean square error MSE of the model is 1.361713.

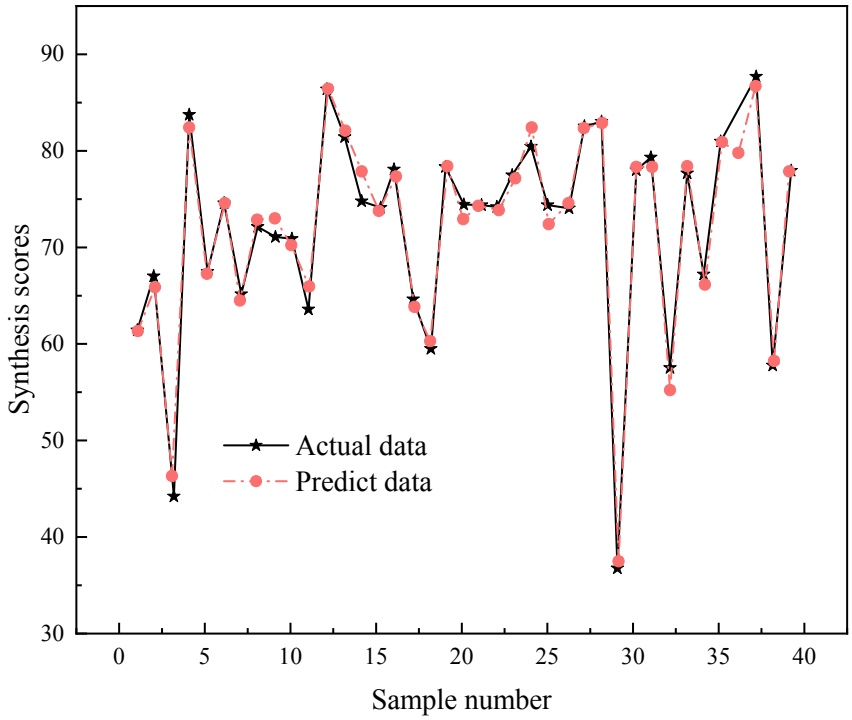

Figure 3 Comparison of predict data with actual data samples

3.2. APPLICATION OF PHYSICAL TEST PERFORMANCE PREDICTION MODEL

After the performance evaluation of the model, the next step is to observe the practical application of the model. In this paper, we chose to apply the model developed from the 2019 athletes to the 2021 athletes to predict the overall performance of the 2019 students, to better observe the changes in the overall performance of the 2019 athletes under a uniform grading scale, and to observe the actual application of the 2019 model in another year. The 2021 athletes' test scores were pre-processed and standardized, and the strong correlation was reduced using principal component analysis. The data of male and female students were separated and brought into the model of male and female students built from the 2019 data separately to obtain the model prediction results. The absolute values of the absolute errors between the 20% test set of 2019 and the predicted results of 2021 data were boxed into six intervals, [0,1), [1,2), [2,3), [3,4), [4,5), [5,∞), and their distributions are shown in Table 2.

https://doi.org/10.17993/3cemp.2023.120151.111-131

Table 2 Percentage of absolute error distribution predicted by the model established 2019 data

	[0,1)	[1,2)	[2,3)	[3,4)	[4,5)	[5,∞)
2016	63.38	27.57	5.27	1.7	0.04	0.02
2019	39.84	28.16	15.71	8.06	4.06	4.17

As shown in Table 2, the prediction results for 2021 are very good, in which 92.95% of the data have an absolute error value less than 2, and only 0.06% have an absolute error value greater than 4. This indicates that the prediction performance of the model is very high. When the model built from the 2021 scoring criteria is applied to 2021, the accuracy of the model prediction decreases, and the percentage of absolute error distribution in the range of 0 to 1 decreases by 23.54%, but the overall prediction result is still considerable. If the scoring criteria of previous years are strictly adhered to, the model criteria of 2019 must be fully applicable to 2021, and the accuracy of the model prediction will be very close to the prediction results of the 2019 test set, while the significant decrease in prediction results indicates that there is a difference between the scoring criteria of 2019 and 2021 due to human calculation.

This model was built based on data from 2019, and the weights between models used the 2019 scoring criteria. When the 2019 scoring scale was used to predict the 2021 composite score, the results showed differences in the scoring scale. Apparently, the scoring criteria for the composite scores of the physical fitness tests were not uniform due to the manual involvement of the coaches in the calculations. The different scoring standards in previous years resulted in the composite score of the physical fitness test not accurately reflecting the changes in the basic physical fitness of the farrier, and it was difficult to infer whether the physical fitness of the farrier had improved or decreased over time, which obviously did not maximize the value of the physical fitness test data from previous years. Using the model to predict the composite score, the constant relationship between the measured item data and the composite score is explored through the learning ability of the model, which can well avoid the whole complicated process of traditional physical fitness test calculation while saving the time of composite score calculation. It is necessary to use the model for predicting the physical fitness test scores because it is possible to see the changes in the physical fitness of the farriers more clearly by classifying them according to the composite score levels after the uniform scoring criteria and combining the radar chart visualization data information.

3.3. ANALYSIS OF TRACK AND FIELD SCORING CORRECTION SCHEME

This section first analyzes the problems of the current decathlon scoring scale published by the IAAF, then proposes our basic correction scheme and develops a new scoring scale using the progressive scoring method and the neural network model. Finally, the existing scoring scale, the scoring scale developed by the

https://doi.org/10.17993/3cemp.2023.120151.111-131

progressive scoring method, and the scoring scale developed based on the neural network model are compared and analyzed, and finally a more scientific and reasonable set of scoring scale is screened and determined.

3.3.1. SCORING REASONABLENESS ANALYSIS

As the level of all-around sports continues to improve, the more difficult it is to improve, the more time and energy athletes pay, in order to motivate athletes and promote the development of all-around sports performance to a higher level, so it should be reflected and rewarded through the incremental value. That is, the all-around performance of each single item from low to high points of the corresponding coordinate points of the line, should be a positive parabolic type with the sports performance and the score increases rapidly. At present, some of the projects with the improvement of the level of sports, but the value of the corresponding linear growth relationship, and even some of the project sports performance incremental rate is gradually reduced.

Scoring from a low score loses its meaning in all-around sports competitions. Because its score is too low and rarely used, then the score of that part of the performance becomes unused and makes the score sheet too large. For example, men's decathlon such as 100m starting point is 17.83s, shot put 1.53m, high jump 0.77m, pole vault 1.03m. Such results can be achieved for children and teenagers with a little training, not to mention for adult professional athletes. If the scoring table is also applicable to children and teenagers, but the IAAF decathlon is quite difficult, and most of its individual events are beyond the physical ability of children and teenagers due to competition conditions and equipment specifications, so a separate scoring table should be developed to meet the needs of children and teenagers. Thus, it seems that the IAAF scale has no meaningful use for children and teenagers. Secondly, the scoring table has certain restrictions, and with the improvement of the level of all-around sports, the scoring table must be constantly widened, but the wide application of the object extends the minimum score of the scoring table, the result is that the original scoring table is too wide to become even wider, making the scoring table more massive, bringing difficulties to the reasonable preparation of the scoring table, bringing trouble to the evaluation of the scoring table.

Some of the projects due to technical innovation, improvement of equipment, the use of more scientific training methods and means, so that the level of sports to improve quickly, while some of the projects training science and technology and means development is slow, so that the difficulty of the individual scoring is not balanced. In the decathlon, a more reasonable score should be equal or approximate scores for different items of equal difficulty, so as to avoid some athletes to get good results, too biased towards an easy to score items, thus not really promote the development of the decathlon in the direction of the whole. For example, some subjects can be achieved with a little training in a certain scoring section, while some items require some effort.

https://doi.org/10.17993/3cemp.2023.120151.111-131

3.3.2. SELECTION OF SCORING INCREMENTAL FUNCTIONS

According to the progressive idea, with the improvement of sports performance, the corresponding score should be increased sharply to encourage the improvement of the sports level of excellent members. That is, sports performance at low levels and high levels to improve the same interval, the increase in score should not be the same, high levels because of the difficulty, the score increased more, the score should be progressive trend with the improvement of performance. Next, we try to describe this phenomenon by using mathematical functions to find out the correspondence between grades and scores. In higher mathematics, monotonicity is actually the portrayal of some functions when the self-varying process is the change of the dependent variable from small to large changes in a given range when the change in the dependent variable presents a special law. There are generally the following four cases: ① from small to large ② from large to small ③ suddenly large and small ④ unchanged. Which has ①, ② these two special laws of the function is an important type of function - monotonic function. Therefore, the monotonicity of a function is a concept used to describe the tendency of a function to change in a certain range. By studying the monotonicity of the function can be reduced to the study of complex functions to some of the more typical, simple types of functions. This phenomenon can be described as monotonically increasing. A monotonically increasing mathematical function can be used to implement the process of increasing.

Definition of increasing monotonicity: Let there be a function y=f(x), x is called the independent variable and y is the dependent variable. If for any x1, x2 $\in$ [a, b] contained in M, if when x1 < x2, there is y1 < y2, that is, f(x1) < f(x2), y increases as x increases, the image of the function rises from left to right, then f(x) is said to be increasing on [a, b], said y is the increasing function on the interval, [ab] is called the monotonic increasing interval of y = f(x). In the interval greater than 0, incremental functions in the primary functions are power functions (such as y = xn), exponential functions (such as y = ex), logarithmic functions (such as y = lnx), tangent functions (such as y = tanx). The four types of functions are shown in Figure 4. From the figure, we can see that as x increases, except for the tangent function, which increases periodically, the y values of the other three types of functions increase to varying degrees, with the exponential function growing the fastest, followed by the power function, and the slowest being the logarithmic function. From Figure 4, we can see that the tangent function periodically increasing, and even appear to calculate the y-value appears negative, so it is not suitable for the development of the score table. We chose the power function, exponential function, and logarithmic function to participate in the initial fitting of the scoring table.

https://doi.org/10.17993/3cemp.2023.120151.111-131

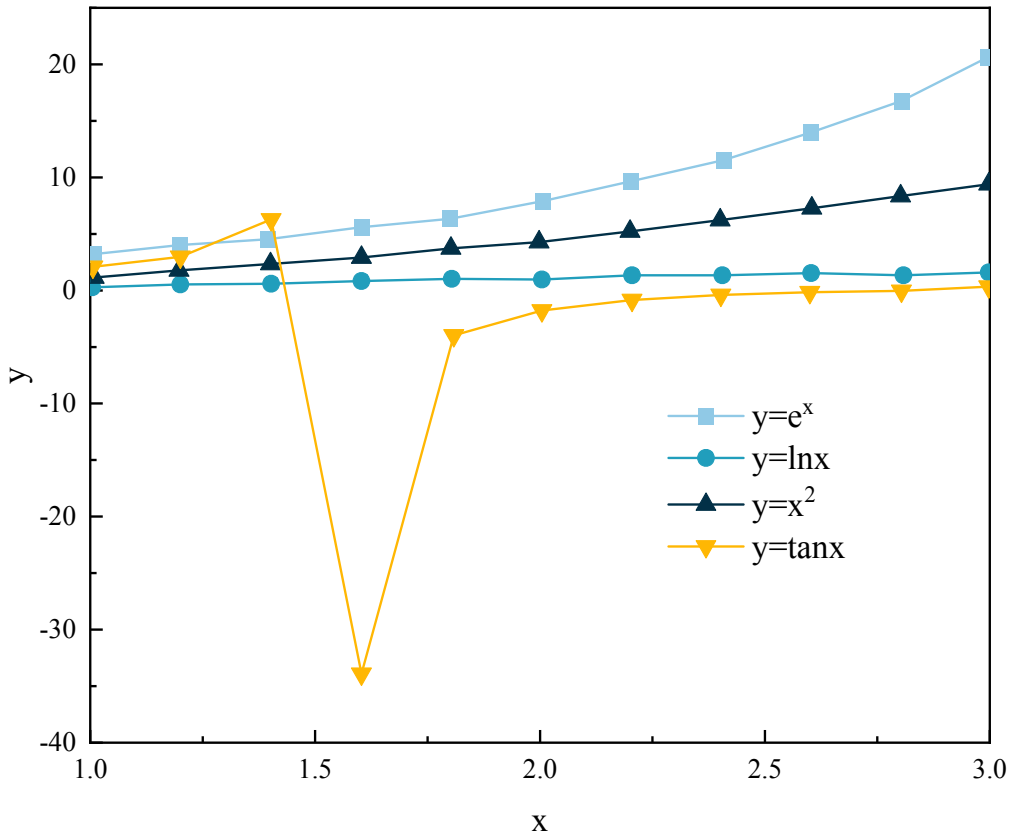

Figure 4 Incremental function diagram

3.4. NEURAL NETWORK DEVELOPMENT OF THE ALLOMETRIC RATING SCALE

Artificial neuronal network is a theorized mathematical model of the neural network of the human brain, an information processing system based on imitating the structure and function of the neural network of the brain [25, 26]. It is an artificially constructed neural network capable of achieving certain functions based on the existing human understanding of the neural network of the brain, which absorbs many advantages of biological neural networks and thus has its special characteristics: (1) highly parallel computing and distributed storage functions: artificial neural networks are composed of many identical basic processing units grouped in parallel, and although the function of each unit is simple, both each Although the function of each unit is simple, both the small unit and the whole neural network have the dual capability of processing and storing information, and these two functions are naturally integrated in the same network, which makes its processing capability and effect on information amazing [27, 28]. (2) Highly nonlinear global action: An artificial neural network is a large-scale nonlinear dynamical system in which each neuron can receive inputs from a large number of other neurons and produce outputs that affect other neurons through parallel networks. It has a strong nonlinear processing capability. Globally, the overall performance of the network is not a simple superposition of local performance, but some kind of collective behavior that exhibits the characteristics of complex nonlinear dynamical systems in general [29]. (3) Good fault tolerance and associative memory function: Artificial neural networks can store information in the weights between

https://doi.org/10.17993/3cemp.2023.120151.111-131

neurons, and through their own network structure can achieve memory of information. This storage is distributed and the extraction of information is collaborative as a whole, each information processing unit contains both a contribution to the collective and cannot determine the overall state of the network, so a failure of the local network does not affect the correctness of the overall network output, which makes the network fault-tolerant [30].

From Figure 4, we can see that the exponential function and the power function are more in line with our design purpose. Therefore, We take the starting and ending points of the new scale initially formulated in the section, remove the ultra-low achievement segments below the starting point, and remove the ultra-high score segments above the stopping point, and use the exponential function and power function to fit the simplified scale in origin9.0, and take the best fitting effect among the many fitting results [31-32]. Then use the function with the best fit, still using the interval of each score segment in the original score table, and bring the scores of the original score table into the fitting function to find the corresponding score, which is the result we get in this section using the progressive idea. The results of the optimal exponential and power function fitting for each item are shown in Tables 3 and 4.

Table 3 Best-fit exponential function

Project	Best-fit function
100m	$y=1+27583.7556*e^{(-0.3196*x)}$
Long Jump	$y=1+71.8068*e^{(0.3345*x)}$
Shot Put	$y=1+149.3857*e^{(0.1071*x)}$
High Jump	$y=1+43.2982*e^{(1.2941*x)}$
400 m	$y=1+17297*e^{(-0.0637*x)}$
110m hurdles	$y=1+10352.2147*e^{(-0.1258*x)}$
Discus	$y=175+27.1458*e^{(-0.0566*x)}$
Pole vault	$y=1+68.0512*e^{(0.4288*x)}$
Javelin	$y=135+38.4222*e^{(0.0528*x)}$
1500m	$y=1+13345.0214*e^{(-0.0208*x)}$

https://doi.org/10.17993/3cemp.2023.120151.111-131

Table 4 Best-fit power functions

Project	Best-fit function
100m	$y= 8359871.4050* x^{-3.7534}$
Long Jump	$y= 10.8651* x^{2.2154}$
Shot Put	$y= 26.9875* x^{1.2345}$
High Jump	$y=128.5425* x^{2.3545}$
400 m	$y= 225487521* x^{-3.3125}$
110m hurdles	$y= 14715841* x^{-2.8412}$
Discus	$y= 6.2514* x^{1.2587}$
Pole vault	$y= 40.2512* x^{1.8998}$
Javelin	$y= 3.5413* x^{1.3087}$
1500m	$y= 38965007571* x^{-3.1875}$

4. CONCLUSION

In this paper, we propose a model for predicting the overall performance of physical fitness test, and successfully apply the machine learning algorithms such as BP neural network and principal component analysis to predict the overall performance of physical fitness test. The following conclusions were obtained:

(1) The use of the prediction model for predicting the composite scores reduces the calculation time of the scores and solves the problem of inconsistent scoring standards due to manual calculation in previous years. The results show that the prediction results for 2021 are very good, with 92.95% of the data having an absolute value of error less than 2 and only 0.06% having an absolute value of error greater than 4, which indicates that the prediction performance of the model is very high.

(2) In addition, this paper also explores the rationality of the athletics scoring method, and by training the existing samples and building a BP neural network model to obtain the expected output, the nonlinear relationship between the score and the athletic performance is better resolved.

(3) By comparing the IAAF scoring scale, the exponential fitting scoring scale, and the scoring scale based on the neural network model, it is shown that the neural network scoring method is better than the former two in terms of scoring progressivity and item balance.

REFERENCES

(1) H Li, **Research on the Status Quo and Countermeasures of Scientific Training of Track and Field Sports**, (2020).

https://doi.org/10.17993/3cemp.2023.120151.111-131

(2) H Cheng, J Lv, T Yuan, **Forecasting Chinese Athletics Performance in Tokyo Olympics from the World Top 20 Athletics Countries in 2018**, *Bulletin of Sport Science & Technology* (2020).

(3) J G Zhan, **Research on Measures Taken for Development of Track & Field Socialization**, *Marketing and Professionalization in China, Journal of Beijing University of Physical Education* (2002).

(4) D Chen, **Cultivation of Athletes' Non-intelligence Factors in Track and Field Training Based on Sports Training Management**, 2019.

(5) Y Ren, J Li, **The Conception of Application of Computer Virtual Reality Technology in Sports Training**, *Journal of Physics: Conference Series* 1861(1) (2021) 012110-.

(6) L Yu, Y He, X Kong, et al., **Projected estimation for large-dimensional matrix factor models, Journal of Econometrics** 229 (2022).

(7) X Chen, R Tu, M Li, et al., **Prediction models of air outlet states of desiccant wheels using multiple regression and artificial neural network methods based on criterion numbers**, *Applied Thermal Engineering* 204 (2022) 117940-.

(8) A A April, J K Basu, D Bhattacharyya, et al., **Use of Artificial Neural Network in Pattern Recognition**, *Springer Berlin Heidelberg* (2020).

(9) S Knight, N Gadda, **Spatiotemporal Patterns in Neurobiology: An Overview for Future Artificial Intelligence** (2022).

(10) H Bagherinezhad, A Farhadi, M Rastegari, **Lookup-based convolutional neural network**, *IEEE*, 2020.

(11) G Jin, M Wang, J Zhang, et al., **STGNN-TTE: Travel time estimation via spatial–temporal graph neural network**, *Future Generation Computer Systems* 126 (2022) 70-81.

(12) I Danihelka, N E Kalchbrenner, G D Wayne, et al., **Associative long short-term memory neural network layers**, 2021.

(13) Z Xing, P Hamilton, A K Story, **Reduction of computation complexity of neural network sensitivity analysis**, 2021.

(14) L Ogiela, M R Ogiela, M Takizawa, **Safety and Standardization of Data Sharing Techniques and Protocols for Management of Strategic Data**, *2017 IEEE 31st International Conference on Advanced Information Networking and Applications (AINA)*, 2017.

(15) X Yang, J Bai, W Sun, **Research on AutoCAD Data Standardization in Coordinate Transformation**, *Urban Geotechnical Investigation & Surveying* (2019).

(16) P Chandio, A B Talpur, **An Assessment of Financial Stability of Textile Sector of Pakistan: An Altman Z Score Approach**, *Sustainable Business and Society in Emerging Economies* 3 (2021).

(17) [P J Schreier, L L Scharf, **Statistical Signal Processing of Complex-Valued Data: Correlation analysis** (2010).

(18) Y Kan, **A Cloud Computing Resource Optimal Allocation Scheme Based on Data Correlation Analysis** (2021).

https://doi.org/10.17993/3cemp.2023.120151.111-131

(19) L Egghe, L Leydesdorff, **The relation between Pearson's correlation coefficient r and Salton's cosine measure**, *Journal of the American Society for Information Science & Technology* 60(5) (2014) 1027-1036.

(20) Y Han, A D Hutson, **A Robust Spearman Correlation Coefficient Permutation Test** (2020).

(21) Y Yan, C Jiang, **Construction of Network Model Based on Partial Correlation Coefficient**, *Journal of Longyan University* (2019).

(22) J Zhou, X Su, H Qian, **Research on Fusion of Dependent Evidence Based on Kendall Correlation Coefficient**, *CSAE 2020: The 4th International Conference on Computer Science and Application Engineering,* 2020.

(23) Y Li, D Zhao, S Yan, **Research on Travel Agency Human Resource Crisis Early Warning Model based on BP Neural Network and Computer Software**, *Journal of Physics Conference Series* 1744(4) (2021) 042061.

(24) S Horikawa, T Furuhashi, Y Uchikawa, **On fuzzy modeling using fuzzy neural networks with the back-propagation algorithm**, *IEEE Transactions on Neural Networks* (1992).

(25) A Lebedeva, A Mironov, A Pisarchik, et al., **Integration technology for replacing damaged brain areas with artificial neuronal networks**, *IEEE 4th Scientific School on Dynamics of Complex Networks and their Application in Intellectual Robotics (DCNAIR)*, 2020.

(26) Y Gao, G A Ascoli, L Zhao, **BEAN: Interpretable and Efficient Learning With Biologically-Enhanced Artificial Neuronal Assembly Regularization**, *Frontiers in Neurorobotics* 15 (2021).

(27) P Meier, K Rohrmann, M Sandner, et al., **Compensation of Measurement Errors for a Magnetoresistive Angular Sensor Array using Artificial Neuronal Networks**, *IEEE Access* (99) (2020) 1-1.

(28) X Yang, T Levi, T Kohno, **Digital Hardware Spiking Neuronal Network with STDP for Real-time Pattern Recognition**, *Journal of Robotics Networking and Artificial Life* 7(2) (2020).

(29) M T Barros, H Siljak, P Mullen, et al., **Objective Multi-variable Classification and Inference of Biological Neuronal Networks** (2020).

(30) J B Bardin, G Spreemann, K Hess, **Topological exploration of artificial neuronal network dynamics**, *Network Neuroscience* (2019) 1-28.

(31) Medina, R., Breña, J. L., y Esenarro, D. (2021). **Efficient and sustainable improvement of a system of production and commercialization of Essential Molle Oil (Schinus Molle)**.3*C Empresa. Investigación y pensamiento crítico*, 10(4), 43-75. https://doi.org/10.17993/3cemp.2021.100448.43-75

(32) Meng Siyu & Zhang Xue.(2021). **Modelling and Simulation of Collaborative Innovation System in Colleges and Universities Based on Interpreted Structural Equation Model**. *Applied Mathematics and Nonlinear Sciences* (1). https://doi.org/10.2478/AMNS.2021.2.00151.

https://doi.org/10.17993/3cemp.2023.120151.111-131

/07/

ENGINEERING APPLICATION OF BIM IN SAVING WATER AND ENERGY CONSERVATION

Xiangbin Wen*

Guangzhou University of Chinese Medicine, Guangzhou, Guangdong, 510006

wenxiangbin2022@163.com

Zhenghui Wang

Guangdong Teachers College of Foreign Language and Art, Guangzhou, Guangdong, 510640

Reception: 06/11/2022 **Acceptance**: 06/01/2023 **Publication**: 28/01/2023

Suggested citation:

W., Xiangbin and W., Zhenghui (2023). **Engineering application of BIM in saving water and energy conservation**. *Journal, Volume (Numer)*, 133-163. https://doi.org/10.17993/3cemp.2023.120151.133-163

ABSTRACT

With the improvement of living standards, people are more and more eager to improve the efficiency of energy conservation and emissions reduction of buildings. Pursuant to this, the application of BIM technology in the water supply and drainage engineering of green buildings is proposed. Firstly, the BIM model is built to draw the axis network and axis height and transform the spatial position of family components, which is conductive to addressing the problem of the loss of engineering information. Then, the energy-saving pathways of green building water supply and drainage projects are analyzed, Concretely, the drainage energy consumption can be reduced by decreasing the overall head of the water pump. The pipe resistance and drainage efficiency can be respectively reduced and improved through reasonable selection of parallel drainage pipelines. Also, the principle of "avoiding the peak and filling valley" can be adopted to reduce pump operation in peak period and water draining in valley period, thereby saving drainage cost. By optimizing the control strategy of the drainage system and improving the utilization rate of water resources, the final results of the study show that BIM technology can realize 69% energy saving of the total savings in water supply and drainage engineering of green buildings, decrease cost consumption and improve the quality of water supply and drainage system, so as to make full use of limited water resources to achieve the effect of energy conservation and emission reduction.

KEYWORDS

BIM technology; Green building; Energy conservation and emissions reduction; Drainage engineering; Avoidance peak and fulling valley

https://doi.org/10.17993/3cemp.2023.120151.133-163

PAPER INDEX

https://doi.org/10.17993/3cemp.2023.120151.133-163

1. INTRODUCTION

Under the promotion of vigorous economic development [1], China's urbanization process is accelerating thereupon, and there are more and more high-rise buildings in the city [2]. In the construction of high-rise buildings, generally speaking, the funds used for water supply and drainage projects only account for about 10% of the overall investment funds [3], but the construction of water supply and drainage projects is crucial for high-rise buildings [4]. To evaluate the grade of a building, the planning and construction of its water supply and drainage system is a vital criterion [5]. Usually, the requirements for water supply and drainage pipelines depend on whether they are planned and arranged reasonably and whether they have an impact on the overall aesthetics of the building [6]. In addition to aforementioned requirements, the basic requirements for the design and arrangement of water supply and drainage pipelines are to be able to meet the requirements of safe water use for all residents, as well as the economic and energy-saving requirements of water supply and drainage pipelines [7].

However, there are also a lot of problems in the design of the water supply and drainage pipelines at the present stage [8]. For instance, the software commonly used by designers is two-dimensional CAD design software, which itself increases the difficulty in the design of water supply and drainage pipelines [9]. Designers, in this regard, need to conceive the three-dimensional structure of pipelines [10], and then express them through two-dimensional drawings. Again, the design of water supply and drainage pipelines generally involve in all kinds of basic Settings, but designers primarily have complicated work, and do not have enough time to optimize the design [11]. In addition to the difficulties in design, the fact that the data and specifications designed can only be completed by manpower, and a unified management system cannot be established also increases the difficulty in data management [12]. At the same time, the waste of resources in the construction of water supply and drainage engineering is extraordinary serious as well [13]. In 2000, some economists surveyed the waste of the global construction industry, and found that the waste of resources in the construction industry reached 30% [14].

Building information modeling (BIM) technology, as a fast-developing information technology can better solve these problems, which is mostly used in project management, known as the construction industry model of the rule changer [15], and capable of assuming a role in all phases of an engineering project (design, construction, operation and maintenance) [16]. According to 2015 Autodesk survey report [17], over the past three years, the use of BIM in the United States has increased by 35%[18], the use of BIM among engineers has increased by 64% [19], and the use of BIM technology in countries around the world has being on the rise. As a modern and efficient building construction technology, the application of BIM technology has a profound impact on the quality of architectural engineering design and construction quality [20]. Precisely, for the construction of energy-saving design, the application of BIM technology can not only achieve the improvement of its energy-saving design effect and level, but also have a significant impact on the green and sustainable development of the building field [21].

https://doi.org/10.17993/3cemp.2023.120151.133-163

With the improvement of urbanization development efficiency, water supply and drainage engineering has played an increasingly prominent role and gradually become the core element of urban development, attracting widespread attention [22]. In the construction process of water supply and drainage engineering of green buildings, it is necessary to carry out the construction without affecting the surrounding environment [23]. This is because the construction scope of water supply and drainage engineering is wide, and once it affects the surrounding environment, it will affect the urban development [24]. However, with the increase in the number of urban construction projects, water supply, and drainage projects also increase, resulting in a large consumption, and a desperate shortage of water resources [25]. Under such context, in order to reduce the consumption of water resources, it is urgent to apply energy-saving and water-saving technology to the construction of water supply and drainage engineering [26].

Literature [27] describes the characteristics of hydrogeology in rainy areas, points out the current situation of hydrogeology in rainy areas, and explains the main damage types and causes of the drainage system, including that water erosion causes structural damage, soil collapse at the outlet of drainage ditch causes damage to drainage structures, the overall instability of the jet channel slides along the bottom contact surface under the action of gravity, etc. Finally, the engineering prevention and control measures are given, including paying attention to adding stilling pool, emphasizing the comprehensive consumption of various forms along the stream channel, strengthening slope scatter flow drainage and vegetation ecological regulation, enhancing the canal seepage prevention and safety design, as well as reinforcing the natural slope ditch, and appropriately constructing sand dam, and flood peak retention pond. Through the research and analysis, some references and guidance may be brought about to the highway-related workers in rainy areas, so as to guarantee the good maintenance of the highway in rainy areas, promote the good use and operation of the highway in rainy areas, and bring better traffic conditions in rainy areas. Literature [28] puts forward a three-year action plan for improving the quality and efficiency of sewage treatment, focusing on the sewage collection system, that is, based on in-depth investigation, it focuses on solving the problems such as direct sewage discharge, indiscriminate sewage removal, full pipe flow of drainage pipes in dry days, low concentration of sewage treatment plant inlet water, and excessive mud accumulation in pipes, so as to ensure that sewage does not enter rivers, clean water does not enter pipes, overflow causes less pollution, and the control and elimination effect of black and smelly water bodies in cities and is improved. In literature [29], it is expounded that the installation and construction technology of water supply and drainage systems affect the service function of buildings, especially high-rise buildings, which is related to the construction cost and determines whether the construction plan can be carried out smoothly. Therefore, according to the actual requirements of the building, it is necessary to clear water supply and drainage system installation points, and improve the relevant technical level. Wherefore, this paper analyzes the installation of the water supply and drainage system and the problems of the construction clock, and puts forward countermeasures, hoping to provide help for the relevant personnel. Literature [30]

https://doi.org/10.17993/3cemp.2023.120151.133-163

comes up with a double-membrane water treatment technology, which is widely applied to the making of soft water and desalted water relying on the advantages of steady water quality, small environment pollution, small coverage area and high degree of automation. Generally, due to the limitation of process conditions, system water consumption will become the key to decrease the water consumption of per ton steel in steel industry. For this, combined with the water quality of water supply and drainage system, the double membrane water treatment technology is adopted to optimize water supply and drainage system, recycle ultrafiltration backwash water, reverse osmosis concentrated water and other kinds of drainage according to the water quality, which not only reduces the treatment cost, but also reduce the system water consumption, achieving a good performance..

At present, people's living conditions are getting better and better, making people more and more aware of the significance of energy conservation and environmental protection. In order to meet the needs of social and economic development and people's requirements for green building, this paper proposes the application of BIM technology in water saving and energy conservation of green building water supply and drainage engineering, and constructs a BIM model, aiming to effectively analyze the energy-saving ways of green building water supply and drainage engineering, and greatly improve the water resource utilization rate and work efficiency of the whole drainage engineering by avoiding waste and optimizing control. Rational use of BIM technology is able to achieve the purpose of energy conservation, and environmental protection, and improve the overall efficiency of construction.

2. BIM DESIGN

2.1. BIM MODEL

From the present stage of water supply and drainage pipeline design and management, the most important design of water supply and drainage is to meet the needs of the owners, which lacks the optimal selection of water supply and drainage design and construction, so it often leads to the waste of cost and energy consumption in the actual construction of water supply and drainage design scheme. With the continuous development of The Times, the water supply and drainage system is more and more complex, pipeline equipment involved in water supply and drainage system is more and more increasing, and the connection between these two is more and close. However, local optimization of water supply and drainage systems cannot ensure the optimization of the whole system.

In addition, with the continuous development of productivity, the social division of labor is becoming more and more obvious. From the perspective of the construction industry, the most important problem is the separation of design and construction. In the present stage of the construction industry, the designers mainly act as the providers of technology and drawings in the project, and the construction party generally serves as the executor of the design Party 's thinking. Due to the above

https://doi.org/10.17993/3cemp.2023.120151.133-163

reasons, there are a lot of problems in the actual production, such as the difficult implementation of the design scheme or increased project costs.

BIM is an important platform that can provide an advanced platform for all project participants to collaborate and communicate with each other. In order to demonstrate the superiority of BIM technology in water supply and drainage management of high-rise buildings, this paper takes a project as an example [31]. Figure 1 is the flow chart of BIM 3D modeling.

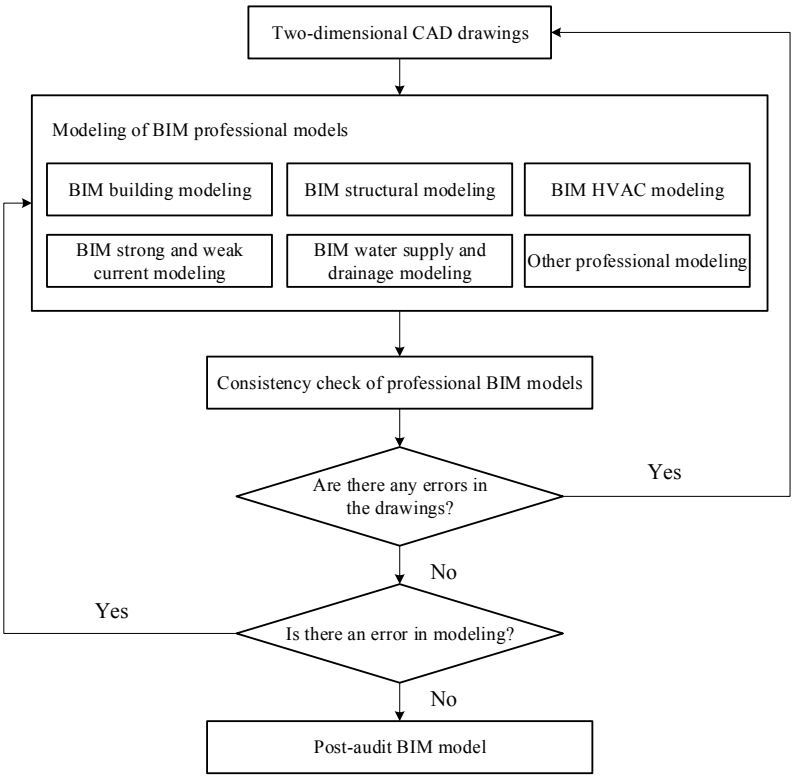

Figure 1 Flow chart of BIM 3D modeling

The establishment of various pipeline models of BIM technology is based on buildings and structural models, so is the establishment of water supply and drainage pipeline models used in this study. The assembly and construction of the model is the last step of the whole BIM model creation, as well as a specific application of the previous creation family. Since Revit family components are parameterized components, the transformation of family components can be realized only by calling the family components in the family library and modifying the parameters of family components or directly editing the model, so as to meet the requirements of the model construction.

2.2. LAYOUT OF MODEL AXIS NETWORK

After building the family components of each hydropower project, it is necessary to create a "construction sample" project in Revit and load the required family components to assemble and build the model. In the process of model assembly, the first thing is to build the axis pairs and elevations of the building in the Revit "structural template" according to various drawings, so as to determine the exact spatial position

https://doi.org/10.17993/3cemp.2023.120151.133-163

of each pressure pipe, corridor, control gate, workshop, and other auxiliary constructions in the whole model [32]. For this, the first is to find "axis network" option in the "baseline" menu under the "construct" tab. Then, it is to click the "modify/place axis network" tab, and draw the required axis network in the working interface according to the type of surface axis network in the "draw" tab, as shown in Figure 2. Similarly, elevations are drawn on the working interface according to the drawings, as shown in Figure 3.

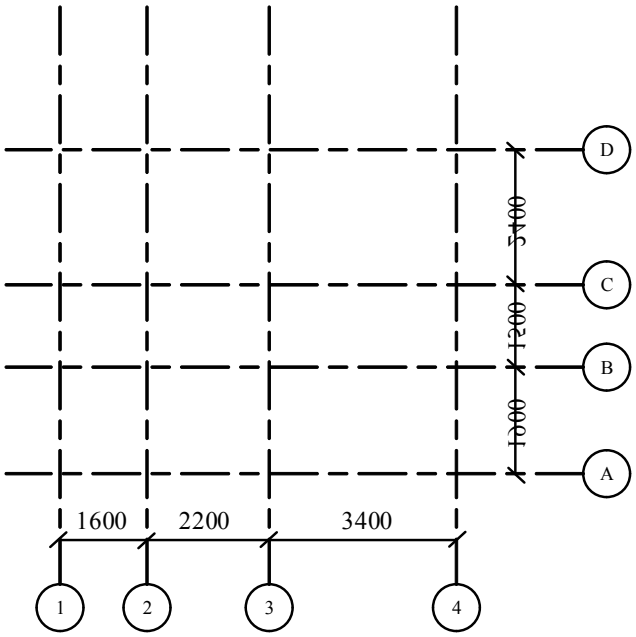

Figure 2 Model construction project axis network

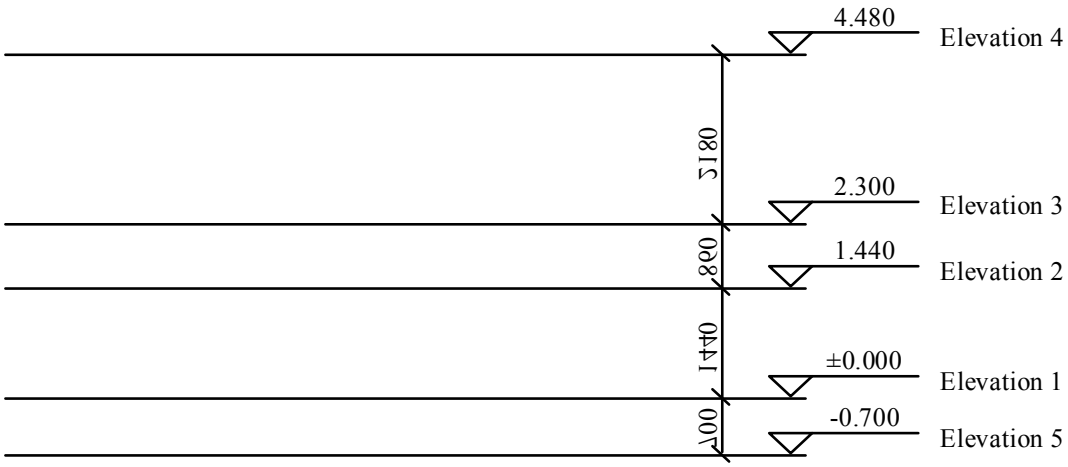

Figure 3 Model construction project axis height

Later, Revit will number each axis as a form of number. If a form of letter is necessary, it just needs to change the number of the first axis to a letter, and then the other axis will automatically be represented as a form of letter. When drawing a grid, you can enable the heads and tails of the axes to be aligned with each other, so that if you move the grid, all the aligned axes will move thereupon.

2.3. SPATIAL POSITION TRANSFORMATION

https://doi.org/10.17993/3cemp.2023.120151.133-163

When loading families or making nested families in the Revit project, it is sometimes necessary to change the spatial position relationship between them to complete the model construction. At the same time, there are also various constraints, such as alignment, rotation and movement. Using these constraint relations, different family components can be nested or assembled to appropriate positions quickly, and the changes of components can be realized through digital drive and constraint transmission.

In principle, the construction and nesting process of family components in the project is the process of exchange between the coordinate system of assembly space and family components, which can be obtained by a 4x4 pose matrix transformation:

$$(x_1, y_1, z_1, 1)^T = A(x, y, z, 1)^T$$

(1)

where, $(x_1, y_1, z_1, 1)^T$ is the global coordinate position of space, and $(x, y, z, 1)^T$ is the local coordinate position of space. The transformation matrix is A.

In translation change, the transformation matrix is expressed as:

$$A = \begin{bmatrix} 1 & 0 & 0 & dx \\ 0 & 1 & 0 & dy \\ 0 & 0 & 1 & dz \\ 0 & 0 & 0 & 1 \end{bmatrix}$$

(2)

where, dx, dy, and dz all are translation variables.

The expression of the rotation matrix around the x-axis in the rotation transformation is:

$$A = \begin{bmatrix} 1 & 0 & 0 & 0 \\ 0 & \cos\alpha & \sin\alpha & 0 \\ 0 & -\sin\alpha & \cos\alpha & 0 \\ 0 & 0 & 0 & 1 \end{bmatrix}$$

(3)

The expression of the rotation matrix around the y-axis in the rotation transformation is:

$$A = \begin{bmatrix} \cos\beta & 0 & \sin\beta & 0 \\ 0 & 1 & 0 & 0 \\ -\sin\beta & 0 & \cos\beta & 0 \\ 0 & 0 & 0 & 1 \end{bmatrix}$$

(4)

The expression of the rotation matrix around the z-axis in the rotation transformation is:

https://doi.org/10.17993/3cemp.2023.120151.133-163

$$A = \begin{bmatrix} \cos\theta & \sin\theta & 0 & 0 \\ -\sin\theta & \cos\theta & 0 & 0 \\ 0 & 0 & 1 & 0 \\ 0 & 0 & 0 & 1 \end{bmatrix}$$

(5)

The above formulas are the matrix of rotational transformations around the x, y, and z axes in a rotational transformation. Any spatial transformation of family components can be obtained by a certain amount of translation and rotation transformation combination. Concretely, firstly, it is to classify the family components to be applied to the "construction template" project of the elevation and axis network created, and formulate the name and number of the family in the project. Then, it comes to determine the position of each dam section in space according to elevation and shaft network, and place it in the appropriate position by changing the direction of family components (translation, rotation), aligning the shaft network and setting it at the appropriate elevation and elevation view. Next, it is to adjust position to align and lock the network. Precisely, according to position of the dam section placed before, its corresponding equipment family (such as generator factory family") is respectively placed. If it can't be moved in the project, you can adjust the start and end points in properties through digital elevation to control the upper and lower position of families, so as to make the model to accurately position, and lock alignment. Finally, after all the assembly is completed, it is to check whether the components of each family are aligned and locked and whether the logical relationship of each family member is correct.

3. APPLICATION OF ENERGY-SAVING AND WATER-SAVING IN WATER SUPPLY AND DRAINAGE ENGINEERING OF GREEN BUILDING

3.1. ANALYSIS OF ENERGY-SAVING APPROACHES FOR DRAINAGE ENGINEERING

The total amount of electricity consumption by green building drainage is determined by the total amount of drainage and the efficiency of equipment operation. The level of energy consumption can be measured by operating efficiency such as water pump efficiency, transmission efficiency, motor efficiency, etc. Also, the circuit power factor can be improved by using reactive compensation capacitors, and the motor's performance can determine the motor efficiency. Therefore, the main factor affecting the drainage operation efficiency depends on the water pump and pipeline [33]. The drainage pump is connected with the motor by the shaft joint, and its efficiency is as follows:

$$\eta = \eta_d \cdot \eta_g \cdot \eta_s$$

(6)

https://doi.org/10.17993/3cemp.2023.120151.133-163

Where, η represents the system efficiency, η_d represents the motor efficiency, η_g represents the pipeline efficiency, and η_s represents the pump efficiency.

It can be seen from the above analysis that the efficiency of pipeline and pump mainly affects the efficiency of system operation, and the peak-valley division of industrial electricity consumption will also affect the consumption of the drainage system. Generally speaking, the consumption of electricity in the valley period will be much smaller than that in the peak period.

There are six basic elements in the centrifugal pump, namely flow Q, head H, power P, speed n, efficiency η and suction height H_t, of which n is usually set as a constant, and all the parameters taken have a certain relationship with each other. This relationship is expressed by curves $H-Q$, $N-Q$ and $\eta-Q$ as the pump characteristic curve.

The pump head is expressed as:

$$H_t = \frac{u_2^2}{g} - \frac{u_2 Q}{g A_2} \cot \beta_{2A} \quad (7)$$

The liquid flow power of the pump is expressed as:

$$P_s = \rho g Q H_t \quad (8)$$

The pump efficiency is defined as:

$$\eta_s = \frac{\rho g Q H}{P_s} \quad (9)$$

In the actual operation of the water pump, when the water flows through the pipeline, there will be mechanical losses due to friction and diffusion of the guide, as follows:

$$h_m = k_{mq} \cdot Q^2 \quad (10)$$

where, Q represents the flow rate and k_{mq} represents the friction diffusion coefficient. Again, in the process of water flow, there is a deviation between the flow direction of liquid flow and the flow direction of water wheel blade design, thus resulting in impact loss, which is shown as follows:

$$h_g = k_g \left(Q_e - Q\right)^2 \quad (11)$$

https://doi.org/10.17993/3cemp.2023.120151.133-163

where, Q_e is the theoretical flow rate and k_g is the impact loss coefficient. It can be deduced that the actual head of the pump is directly proportional to the square of the flow rate:

$$H = H_t - h_m - h_g = KQ^2$$

(12)

where, K is the sum loss coefficient. When the water flows through in the pipe network, there is a certain resistance of the pipe network needing to be overcome. The pipeline characteristic equation is:

$$H_W = R \cdot Q^2$$

(13)

where, R is the pipe network resistance coefficient. When R is constant, the resistance H_W is proportional to the square of the flow rate Q. Flow regulation has a serious effect on resistance. Among them, the loss of pipe network includes local resistance loss and resistance loss along the pipeline, for which the reduced value of R is needed to improve the operation efficiency.

After the selection and installation of the pump unit, the basic parameters have been determined. The operation condition of the pump can only be adjusted by adjusting the valve opening, but this way increases the additional power loss. The analysis shows that there are several ways to improve the working efficiency of drainage projects through optimization control:

(1) High-level drainage

Water pump drainage energy consumption is closely related to the head, the higher the head, the more work the pump does to lift the same amount of water inflow, and the greater the energy consumption is. Therefore, it is necessary to try to reduce the operating head when the operating conditions permit.

It can be concluded from Formula (8) that water pump drainage energy consumption P_s is related to flow rate Q and head H_t. If the drainage flow rate is fixed in unit time, then the head is an important factor affecting energy consumption. If conditions permit, reducing head can reasonably reduce energy consumption. The pump head is mainly composed of pump head and pressure-head head, so reducing the pump running head can be considered from these two aspects, that is, changing the inherent parameters of the pump (speed, impeller, etc.) to adjust the size of the pressure-head, and raising the water level of tank operation.

For the former idea, after the installation, the pump parameters has been shaped, and can't be adjusted through optimization control. Instead, pump motor frequency control operation can better adjust the operation performance, the feasibility of which will be dedicated to exploring in the following chapter.

Increasing the water level of the tank is also an effective way to improve the operation efficiency of the unit. Under the condition that working conditions permit, the storage water can be fully used to reduce the suction head by increasing the working

https://doi.org/10.17993/3cemp.2023.120151.133-163

water level, thus reducing the overall head of the pump and reducing the energy consumption of drainage.

(2) Reasonable optimization of drainage pipe combination

According to the pipeline characteristic equation (13), the head loss of the pipeline is proportional to the square of the flow rate, so, the greater the displacement of a coal mine, the greater the energy consumption. In this regard, the standby pipeline can be put into parallel operation to increase pipeline diameter and reduce pipeline resistance.

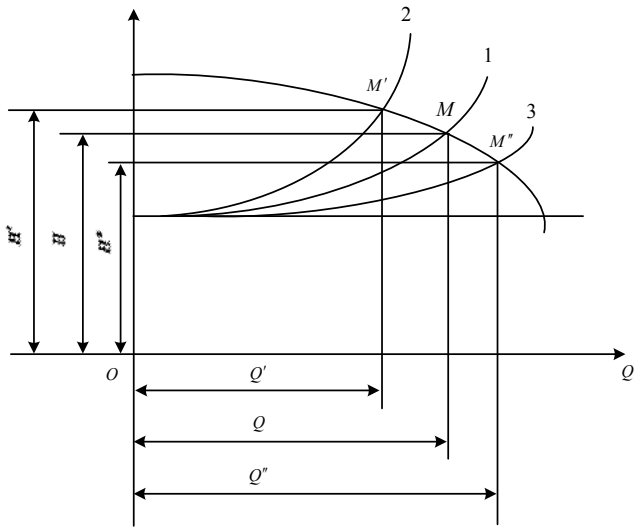

Figure 4 Pipeline parallel characteristic curve

It can be seen from Figure 4 that curves 1, 2 and 3 are performance curves of drainpipes, and other curves are pump head curves. Moreover, curve 3 is the parallel superposition of one pipe characteristic curve 1 and another pipe characteristic curve 2. The working point of the pump changes from M or $M^{'}$ to $M^{"}$, and the flow rate of the pump increases from Q or $Q^{'}$ to $Q^{"}$. When the actual pump head H is constant, the efficiency of the pipeline is improved, and the useless energy consumption to overcome the pipeline resistance is reduced.

According to the above analysis, when a single pump is running, a reasonable selection of drainage pipes in parallel drainage can effectively reduce pipe resistance and improve drainage efficiency.

(3) Avoidance peak and fulling valley

In the past few years, many buildings have focused on the drainage system optimization and energy saving on the operating efficiency of the system, looking for the optimal coordination among the factors that affect the efficiency, so as to achieve the purpose of reducing drainage electricity consumption. Currently, because the power supply department has adjusted the peak and valley price in some areas, the price difference varies widely thereby, and even in some areas, the valley price is only 1/5 of the peak price. Therefore, when draining water, it is best to try to avoid the peak period and make full use of the valley to drain water, which has been strongly proved that this method is an effective way to save energy.

https://doi.org/10.17993/3cemp.2023.120151.133-163

3.2. DRAINAGE SYSTEM OPTIMIZATION CONTROL STRATEGY

In commonly used control systems, controllers are established in accurate mathematical models, but in practical industrial applications, there are many factors affecting the operation of the system, and not all systems are linear, so it is quite difficult to establish an accurate model [34]. Aiming at this, the application of BIM technology can not only realize the improvement of its energy-saving design effect and level, but also have a significant impact on the green and sustainable development of the construction field.

The drainage system mainly controls the water pump unit, and the control parameters include the water storage quantity Q and the water inflow rate Q', in which the water storage quantity Q is a function of the water inflow rate Q'. Therefore, during control, attention should be paid to water storage Q and water inflow rate Q' at that moment. In addition, the randomness of the water inflow rate is very strong, so the appropriate control strategy should be selected based on the change in the water inflow rate Q'.

When the water inflow rate Q' is very small, it is necessary to fully combine high drainage with peak avoidance and valley filling, and dynamically decide the optimal pump opening time through optimal control theory, so as to reduce the consumption of drainage.

In the rainy season and peak season, or the process of mining, the water inflow rate Q' is large. When the water inflow rate Q' is greater than the drainage capacity of one pump, the drainage in the valley section can no longer meet the needs. Sometimes, multiple pumps are required to work 24 hours a day underground. Under this circumstances, the optimization control should focus on how to select the number of pump openings and determine the high drainage target water level. For the randomness and nonlinearity of the system, fuzzy control is chosen in this paper to realize optimization.

The drainage system is generally equipped with multiple water pumps. According to different water inflow conditions, it is necessary to determine the number of operating units, so as to improve the pump efficiency, as well as adopt the principle of "avoiding the peak and filling valley", reducing pump operation in peak period and draining water fully in valley period, so as to save drainage cost.

The research object of dynamic programming is the optimization of the decision process. According to the principle of optimality, regardless of the initial state and the initial decision, the remaining decisions must constitute an optimal strategy for the first decision. Combined with the drainage characteristics of the drainage system, the drainage process can be divided into several interrelated stages, in which decisions need to be made to achieve the best dynamic effect of the whole drainage process. The choice of decisions at each stage depends on the current situation and also affects future development. When the decision of each stage is determined, the decision sequence is thereby formed.

https://doi.org/10.17993/3cemp.2023.120151.133-163

Each drainage cycle is divided into N sections $(o:N-1)$, and the operation of units in each section remains unchanged. Assuming that the water level of the tank in section k is $X(k)(X_1 \le X(k) \le X_h)$, and k is a discrete-time variable. The function relation between water inflow and water level of the tank is:

$$f(k) = F[X(k)]$$

(14)

Suppose the water pump room has n pumps working in parallel, and the running state of the pump i at time k is $u_{i(k)}$, where $u_i(k) = 0$ means shutdown, and $u_i(k) = 1$ means operation.

Then, the control decision vector of the water pump room is:

$$U(k) = \{u_1(k).u_2(k), Lu_n(k)\}$$

(15)

The drainage capacity vector of the water pump is:

$$\Gamma = \{\gamma_1, \gamma_2, \Lambda, \gamma_n\}$$

(16)

The power consumption vector of the pump in each period is:

$$\theta = \{\theta_1, \theta_2, \Lambda, \theta_n\}$$

(17)

The electricity price $c(k)$ within a cycle (24h) is a function that changes with time, so the formula is:

$$c(k) = c(k+N)$$

(18)

The optimal control of the water pump room can be described as that in the drainage cycle, the optimal control vector $U^* = \{U^*(0), U^*(1), U^*(N-1)\}$ is selected to minimize the electricity expense in a cycle, then, the cost function is:

$$J = \sum_{k=0}^{N-1} c(k)U(k)\theta^T = \sum_{k=0}^{N-1} c(k)\left\{\sum_{i=1}^{n} u_i(k)\theta\right\}$$

(19)

$$(k = 0,1,\Lambda N-1, i = 1,\Lambda n)$$

(20)

The optimal performance functional expression is described as:

https://doi.org/10.17993/3cemp.2023.120151.133-163

$$J^* = \min\left\{\sum_{k=0}^{N-1}\sum_{i=1}^{n} c(k)u_i(k)\right\}$$

(21)

The optimal control process of drainage is regarded as a multi-order decision-making process, and then the multi-order decision-making process is shown as follows:

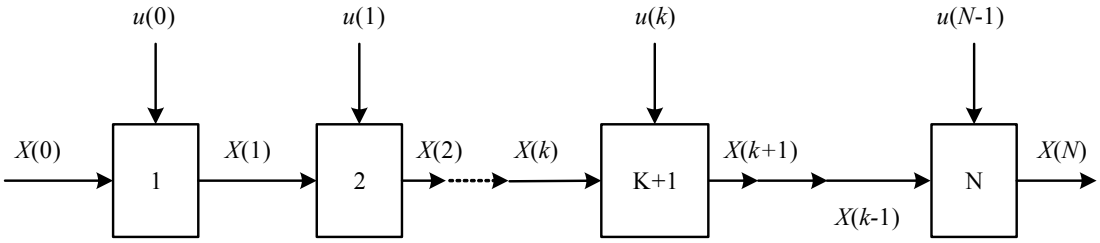

Figure 5 Schematic diagram of a multi-decision process

According to the optimality principle, the process of implementing an optimal decision by dynamic programming method is as follows. First of all, multi-stage decision problems are transformed into a series of single-stage decision problems, starting at the last state and ending till working backward to the beginning state.

With respect to drainage strategy, the system takes the tank water volume, water inflow rate and peak-valley period as dynamic variables of the dynamic programming method, and the working condition, efficiency and flow rate of the pump unit as static constants, where the dynamic variables refers to variable parameters of the control vector determined by the principle of optimality, and the optimal solution is to constantly optimize the control strategy through the change of variables. When the security conditions are met, the solution of the optimal control function is to minimize the energy consumption of the drainage system.

In connectiont o calculation of water inflow rate, considering that water inflow is a nonlinear function, the solution method of water inflow rate in the linear equation is not applicable here. Then, the piecewise method can be used to approximately fit the change curve of water inflow into a combination of countless linear curves, so as to solve the change rate of water inflow in a single period, which can be used as the prediction parameter of dynamic programming.

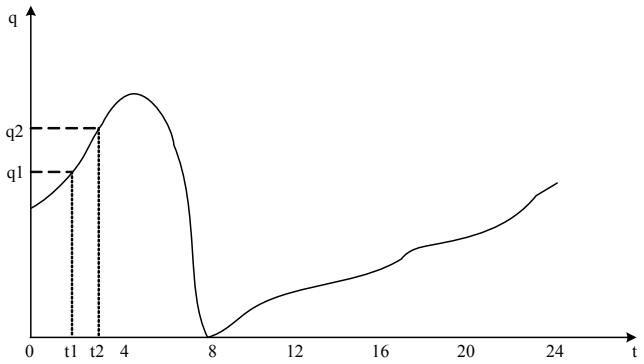

Figure 6 water inflow curve

https://doi.org/10.17993/3cemp.2023.120151.133-163

As can be seen from the figure, the variation of water inflow between t_1 and t_2 can be approximately regarded as a short straight line, and the water inflow rate at t_2 is approximately $v = (q_2 - q_1)/(t_2 - t_1)$.

Then, in terms of control logic, the optimal control process takes into account the present value of variables and the stored value of the previous moments, and makes a reasonable prediction, so as to give the optimal strategy. The underground drainage system is different from other units, which is mainly reflected in the uncertainty of the task (nonlinear change of water inflow and the limit of water level safety, etc.). Therefore, the system adopts multi-level decision-making and judgment step by step to give a reasonable strategy.

Layer 1: security

Coal mine safety production is the premise for the reasonable implementation of other optimization strategies. In order to ensure the normal discharge of water inflow, the upper limit of the water level is set. In this way, no matter in peak or valley period, as long as the upper limit is reached, the water pump will be started for drainage to prevent accidents.

This decision is an unconditional interrupt decision. If only the condition is met, the system will transform to the control interruption of water level over limit, and other control strategies will not override this decision.

Layer 2: warning

The estimated value of the water inflow rate is updated every 20 minutes during the operation of the system. If there is a sudden increase in water inflow rate, the system will transform to the corresponding interruption to determine the number of pumps that need to be started according to the water inflow volume and water inflow rate, and start the corresponding pumps to drain water in advance, so as to prevent accidents caused when the water volume suddenly increases and the personnel on duty cannot find it in time.

Layer 3: economic drainage

On the premise that the control policies of the first two priorities are met, the system is in a normal economic drainage state, revising the control strategy according to the updated tank water volume and water inflow rate every 20 minutes and giving the optimal control scheme.

Concretely, when it is at peak time, the electricity price is the highest, so it is better to try to store water.

When it is at a normal time, the first is to make a logical prediction, and then according to the current water inflow volume and water inflow rate, predict whether it is enough to drain out the water inflow in the tank within the valley time.

Then, when it comes to valley time, after reaching valley time, an appropriate pump start time shall be selected, and the best pump start time shall be calculated every 20 minutes, so that it is feasible to open the corresponding pump according to the

https://doi.org/10.17993/3cemp.2023.120151.133-163

principle of uniform wear, and drain out the water inflow before the end of the valley time.

For this, assume that the time required to start the drainage of water inflow in the tank at t_2 is t, then:

$$t = \frac{V + v\Delta t}{nQ} \quad (22)$$

Where, t is the drainage time, V is the water volume in the water tank, v is the water inflow rate, and Δt is the time difference between 7 o 'clock and the end of valley time. Then, a judgemnet for t is performed, in which $t > 7$ indicates that if two water pumps run together in the valley time, they cannot drain out all the water inflow, so it is necessary to start the water pump to drain water in advance, specifying the drainage time is at the moment when $\Delta t - t < 0.5$, that is, starting to drain water 30 minutes in advance. To ensure that the water inflow is drained out before the arrival of the peak time, it is better to store water as far as possible at the peak time. $t \leq 7$ means that the water inflow can be discharged out within the valley time, without the need for drainage in advance.

The optimal pump starting time can be obtained by substituting $t = \frac{V + v\Delta t}{nQ}$ into the above formula, where n is judged according to the water inflow rate. When the water inflow is small, a water pump is started. Taking into account the power supply capacity of the pipeline and substation, a maximum of seven water pumps can be installed in parallel operation.

In order to increase the drainage rate of the drainage system, in the process of automatic control, the system can choose the pump with the highest efficiency to drain water. The real-time operating efficiency of pump during pump operation is defined as:

$$\eta = \frac{N[?]}{3600[?]} \quad (23)$$

During each operation, the system should store the current operating efficiency of the pump to ensure that the results of the comparison are updated in real-time, and that the whole system can run efficiently.

3.3. AVOID OVER-PRESSURE FLOW

Over-pressure flow refers to the hydrostatic pressure generated by the water supply components exceeding the water inflow head, so that the actual flow is much larger than the rated flow. The flow beyond the rated flow will not bring normal benefits, only a waste. At present, more than half of the ordinary faucets have the problem that the actual flow exceeds the rated flow, that is, the over pressure flow, where the maximum of the actual flow of ordinary faucet can reach more than two

https://doi.org/10.17993/3cemp.2023.120151.133-163

times of the rated flow [35]. In this regard, the following techniques can be adapted to address it.

Limit the actual water pressure at water distribution point. Precisely, over-pressure flow may cause water resources and there is no attention on it. Although current specification provides the maximum pressure limit, it is only to aim at the point of view that too much pressure will cause damages, without attaching real importance to over pressure flow. Less strict demands for over pressure flow can not have a expected restriction effect. Therefore, it is necessary to strictly limit the pressure according to the specific conditions of the water supply system.

Adopt decompression technology. Installing decompression device to the existing water supply system can realize effective control of water pressure, and enable the water pressure to be in an allowable range, so as to avoid the occurrence of over pressure flow phenomenon. The pressure-reducing device comprises a pressure-reducing valve, a pressure-reducing orifice plate and a throttle plug. Among them, pressure reducing valve is generally installed in the household branch pipe. After its installation, the actual water output of each floor is reduced, and the flow and water pressure of each outlet point are also maintained evenly. Installation of pressure-reducing valve can play a significant decompression effect so that the flow on the basis of meeting the requirements is significantly reduced. Compared with the pressure reducing valve, the pressure reducing hole plate is simpler to reduce investment and easier to manage. Practice shows that its installation can bring remarkable water-saving effects. However, it can only reduce the dynamic pressure, where static pressure remains unchanged, and the downstream pressure changes with the change of upstream pressure. It lacks stability, and its structure is also prone to blockage. Now it is mainly used when the water quality is good and the water supply pressure remains stable.

Set water-saving faucet. When the pressure is the same, using a water-saving faucet can effectively improve the water-saving effect, such as touching-type water-saving faucet. Its switch control is shown in Figure 7.

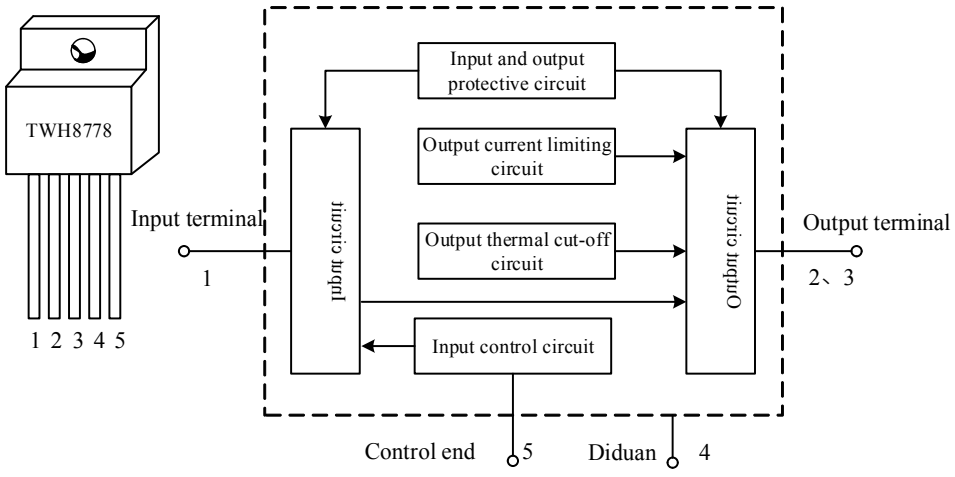

Figure 7. Touch-type water-saving faucet switch control

The maximum water-saving amount can reach 50%, generally being kept in the range of 20%~30%. If the static pressure is high, the use of an ordinary faucet will

https://doi.org/10.17993/3cemp.2023.120151.133-163

have a large amount of water, and at this time switching to water-saving faucet, will bring a huge amount of water saving.

3.4. AVOID EXCESSIVE INEFFECTIVE COLD WATER PRODUCED BY HOT WATER SYSTEM

Nowadays, people's living standards are getting higher and higher, and the functions of buildings are gradually improved. Hot water supply has become a basic function and even needs to be regarded as an important part of the water supply system. The results of the survey show that most hot water supplies have water wastage, `manifesting itself as that a lot of cold water is drained before hot water flows out. The cold water discharged has no benefits and belongs to invalid cold water, resulting in water waste [36]. Its causes include many aspects, which need to be considered from different links, so as to reduce its generation and emissions.

For new buildings, a branch pipe and riser pipe circulation model shall be chosen. Current specifications state that hot water circulation should be selected from the following modes, main pipe, riser pipe and branch pipe. At the same time, in the public bathroom, it is unnecessary to set circulating pipes. The choice of circulation mode largely determines the amount of invalid cold-water production. The water-saving amount of the riser pipe is less than that of the branch pipe, but its water-saving effect is better than that of the main pipe, and its investment can be recovered in 12.5 years. Pursuant to this, the use of riser pipes provides better water-saving effect than main pipes, and is more economical than branch pipes[37-38].

Although the main pipe has relatively low cost in terms of a backwater, its water-saving effect is not obvious, and its investment needs to be recovered after 12.7 years, longer than that of the riser pipe. Therefore, main pipes are not recommended, either with respect to cost or water-saving effect.

When the circulating pipe is not used, a lot of invalid cold water will be produced, which not only fails to meet the requirements of water-saving and energy-saving, but also affects the normal use, so it should be eliminated in the future design.

Based on the above analysis, and in view of the basic national conditions of China, the hot water system must adopt the circulation mode and abandon the main pipe mode for green buildings, and the existing hot water system without circulating pipe should be rapidly transformed. Now, there is still the phenomenon that the bathroom of a lot of buildings has no circulation mode in China, needing to produce and waste a lot of invalid cold water every day. The main reason for this is that the circulation - free systems are relatively simple and can reduce the cost, but in fact, they will increase the operation cost, reduce the service effect, and leads to the loss is outweighed by the gain. In this regard, we should speed up the transformation, and generally, there are the following solutions.

First of all, shorten the local pipeline length and do a good job of pipeline insulation. In current green building projects, local hot water supply is designed to have no return pipe in the system. When the distance between water heater and toilet is relatively far,

https://doi.org/10.17993/3cemp.2023.120151.133-163

before using hot water, a lot of cold water in retention at pipeline will be discharged. In addition, the hot water pipe lacks insulation measures, so that the water in the pipe quickly dissipates heat, and a lot of lower temperature water is releases when the water heater is started once more after a period of time of shutdown. On this account, ,the longer the length of the hot water pipeline is, the more the water wastes. To cope with this, the following measures can be adopted. Firstly, in the design process, not only the use function and layout of the building should be fully considered, but also the water-saving factors should be paid great attention to, and the hot water pipeline should be shortened on the basis of meeting the basic requirements. Secondly, a good job of thermal insulation of hot water pipeline is done, configuring backwater system.

Then, strictly implement the relevant technical specifications and design requirements, and build a sound management system. In addition to the suitable circulation mode, design, construction and management will also affect the discharge of invalid cold water. For this, during the design process, circulating pipes should be arranged in parallel, and when the project is a high-rise building, cold and hot water systems need to be zoned.

In order to avoid the waste of water caused by temperature regulation, it is recommended to set up a single system for bathrooms in public areas, and enable the temperature control installation assume a key role in water temperature control. Currently, many temperature-controlled units lack sensitivity, causing hot water to be too cold or too hot, and thus leading to a waste.. In this regard, it is recommended to popularize the use of new faucets with thermostat elements, so as to ensure that users can obtain the water meeting their requirements in the shortest time and to avoid water waste in the process of temperature regulation.

3.5. AVOID WATER WASTE CAUSED BY SECONDARY POLLUTION

Once secondary pollution occurs, not only the operation of the water supply system will be affected, but the entire system structures will also be affected by sewage. Coupled with, that a lot of tap water is used when cleaning the water supply system, it will inevitably leads to the waste. Therefore, effective measures should be taken to avoid secondary pollution.

For instance, to introduce variable frequency speed regulating pump, as well as pool, water pump and high-water tank,realizes water supply in a high-rise building, as shown in Figure 8. Pressurized water supply is the most commonly used water supply method for high-rise buildings at present, but the water quality of this method is poor because the water will be polluted during storage and transportation. After the introduction of frequency conversion speed regulating pump, pump can be directly sent to the users, without setting water tank, so as to avoid secondary pollution. The details are shown in Figure 9. At present, many areas in China have adopted this new measure, and the effect is very remarkable, being favored by owners.

https://doi.org/10.17993/3cemp.2023.120151.133-163

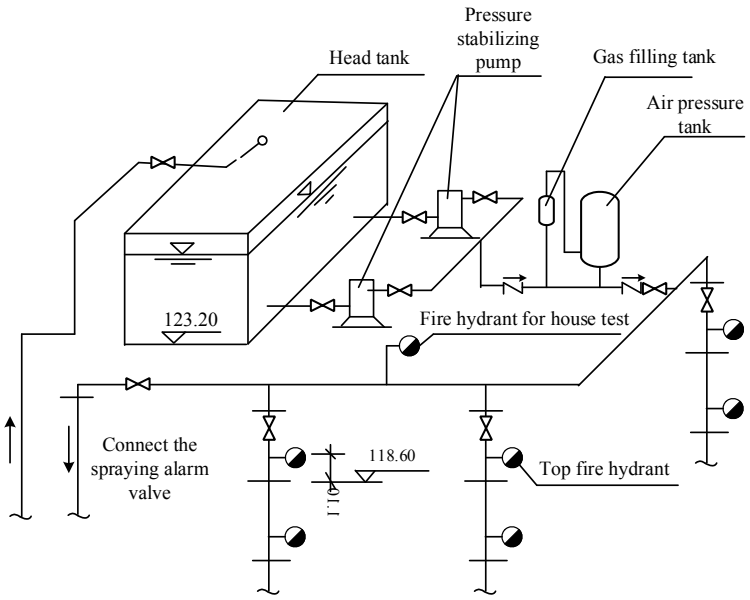

Figure 8. high-water tank

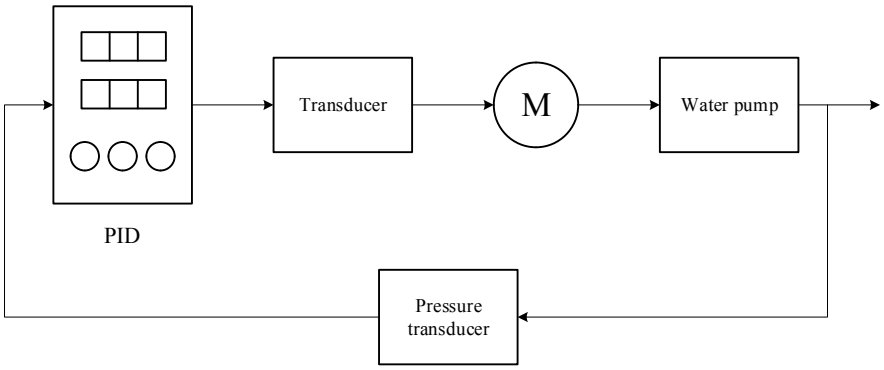

Figure 9. Simplified circuit of frequency conversion speed regulating pump

Separate living pool and fire pool area. Previously, many buildings prefer to merge two pools, which will make the volume of the pool become larger, and the actual water use volume is less than 1/5 of its total use volume. In this way, a large amount of domestic water will be stored for a long time, resulting in water quality changes. The results show that the water temperature is relatively high in summer, and the residual chlorine in the water will become zero after the water is stored in the water for more than 12 h, which enables the rapid breeding and reproduction of bacteria. Therefore, it is necessary to separate the living pool from the fire pool. For the volume of the pool, it is determined according to the actual water use situation.

Although the water supply mode of pool coupled with pump and tank has the problem of secondary pollution, the water quantity and water pressure are relatively stable, and the technology is mature and experienced, so it is impossible to abandon such mode. In this case, as long as the current standards and provisions having put forward are strictly implemented, we can effectively control the secondary pollution, ensure water quality, avoid waste, and achieve the effect of energy-saving and water-saving. These specifications primarily include material selection, piping design, construction design, backwash pollution control, etc.

https://doi.org/10.17993/3cemp.2023.120151.133-163

In summary, energy saving and water saving is the main goal of green buildings, which should be used in practical work to avoid over pressure flow, avoid excessive ineffective cold water in the hot water system and prevent waste of water caused by secondary pollution, so as to improve the utilization rate of water resources and get rid of energy waste on the basis of meeting the requirements of water supply.

4. RESULTS AND ANALYSIS

The construction engineering industry is an important support for China's economic development. In recent years, the number of green building projects has been increasing, and the scale of construction has been expanding, which has effectively driven the development of the regional economy. However, in the construction process, due to the influence of factors such as design and construction concepts, environmental pollution and waste of resources, the issues of construction engineering are becoming increasingly prominent. And also, in the new era, the improvement of energy-saving design quality of green building projects has become an inevitable requirement for the development of construction industry. Therefore, in this paper, combined with the existing literature and the current situation of water resources in a city, a risk evaluation system is established on the basis of hierarchical, systematic, representative and scientific principles, as shown in Table 1.

The development and utilization of water resources is a multi-level and complex problem involving ecological, economic and human activities. Therefore, the selection of evaluation indicators should not only consider the quantity and social economy of water resources but also involve the efficiency and level of development and utilization of water resources. Based on the existing literature and the current situation of water resources in a city, this paper establishes a risk evaluation system based on the principles of hierarchy, systematicness, representativeness and scientificity, as shown in Table 1.

Table 1. Risk evaluation system of water resources development and utilization

Target layer	Criterion layer	Index layer	Index connotation	Attribute
Risk evaluation of water resources development and utilization A	Current situation of water resources B_1	C_{11}/mm	Annual average precipitation	+
		C_{12}/(m³/people)	Per capita occupancy	+
		C_{13}/(m³/m²)	Water consumption modulus	+
	Development and utilization level B_2	C_{21}/%	Development and utilization degree	_
		C_{11}/(m³/people)	Water consumption per capita	_
		C_{11}/(m³/mu)	Irrigation water consumption per mu	_

https://doi.org/10.17993/3cemp.2023.120151.133-163

		C_{11}/(m³/GDP)	Water consumption per 10000 yuan GDP	_
	Socioeconomic level B_3	C_{31}/%	GDP growth rate	_
		C_{32}/%	Population growth rate	_

At present, since there is no systematic and perfect risk evaluation standard for water resources development and utilization, this paper divides the risk level into five standard systems, as shown in Table 2.

Table 2. Risk grade standards of water resources development and utilization

Risk level	I	II	III	IV	V
comprehensive value	<0.3	0.3~0.5	0.5~0.8	0.8~0.95	>0.95
Risk level	micro degree	light	moderate	high	extreme

According to the water resources report, government work report, statistical yearbook and other data in a city, initial values of the above indexes are extracted, and then based on the basic connotation and its properties, the corresponding formula is respectively adopted for the normalized processing, which is as follows. For the positive indicators, that is, the larger the evaluation value, the lighter the risk of water resources development and utilization, the normalization processing formula is:

$$r_{ij} = \frac{x_{ij} - \left(x_{ij}\right)_{\min}}{\left(x_{ij}\right)_{\max} - \left(x_{ij}\right)_{\min}} \quad (24)$$

For the negative index, that is, the smaller the evaluation value, the lower the risk of water resources development and utilization, the normalized treatment formula is as follows:

$$r_{ij} = \frac{x_{\max} - x_{ij}}{\left(x_{ij}\right)_{\max} - \left(x_{ij}\right)_{\min}} \quad (25)$$

Where, r_{ij} represents the standard value of the i evaluation index in the j evaluation sample, and $\left(x_{ij}\right)_{\max}$ and $\left(x_{ij}\right)_{\min}$ are the maximum and minimum values of the same evaluation index x_{ij} in different evaluation samples respectively.

The initial values of each indicator are normalized by using Equations (24) and (25) respectively, and the membership degree of the risk indicators of water resources development and utilization in each region of a city can be obtained, as shown in Figure 10.

https://doi.org/10.17993/3cemp.2023.120151.133-163

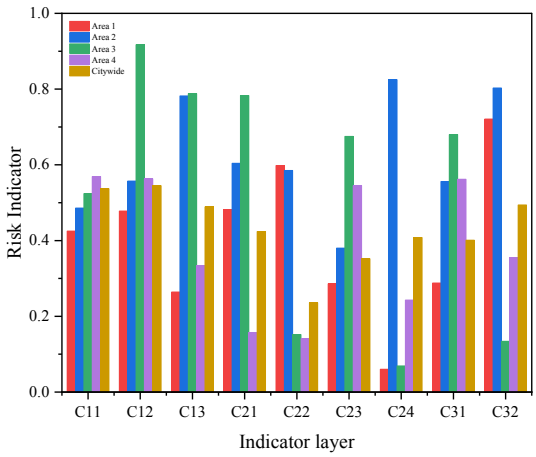

Figure 10. Membership degree of risk index of water resources development and utilization

According to the correlation and importance criteria between indicators , recursive calculation is carried out in the order from bottom to top to obtain the risk degree of each level of the evaluation system. The results are shown in Figure 11.

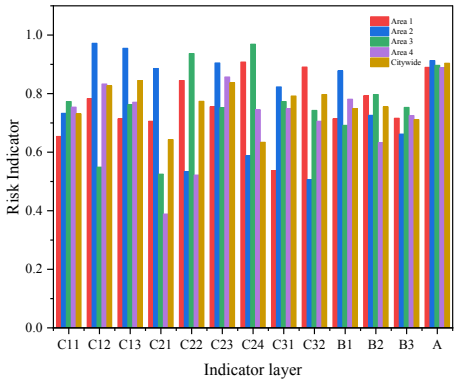

Figure 11. Evaluation results of development and utilization risk value

It can be seen from Figure 11 that the evaluation index C_{12} is 0. 971 in Area 2, which is extremely risky, indicating that the per capita water resources in this region are low and the level of development and utilization is weak. This index is in the range of 0. 548 ~ 0. 830 in other areas, which is wholly in the moderate level. Similarly, the level of other indicators in each region is analyzed successively. The index A, namely risk evaluation of water resources development and utilization is in the range of 0.88 ~ 0.91 in the whole evaluation samples, with that of Area 2 of the most prominent one, indicating that it is in a high-risk state. Besides, the comprehensive risk evaluation value in the citywide is 0.905, also indicating a high risk.

In order to better illustrate the application value of BIM technology in water supply and drainage management, this study evaluates and analyzes the application of BIM technology in water supply and drainage management. The project of this study is mainly based on the data of an engineering project. In order to protect the investment data of the project, percentage method is used in the analysis. After obtaining the summary of effective collision reports, in-depth analysis is made on all kinds of

https://doi.org/10.17993/3cemp.2023.120151.133-163

collisions, mainly analyzing their impact on the project cost, and finally, the cost loss caused by the collision is summarized and counted. Through the study of statistical data, it is found that if each detected collision can be solved perfectly, the return rate of investment of BIM technology in water supply and drainage management is higher. The figure below shows the proportion of cost savings for four different types of collisions involving water supply and drainage pipes.

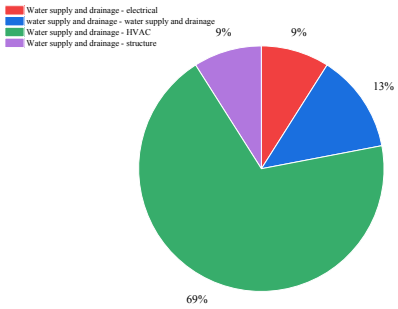

Figure 12. Cost saving ratio of four different types of collision

From Figure 12, it is not difficult to find that the collision cost saving of water supply, drainage and HVAC is the highest, accounting for 69% of the total savings, and the cost saving ratio of other collisions is similar. This also indicates that the design of water supply and drainage pipes should be strengthened in collaboration with HVAC professionals, so as to reduce costs and improve the quality of water supply and drainage system of the project.

BIM technology can play a optimization role at all life stages of green building projects. For this, we mainly divide the optimization analysis of BIM technology to water supply and drainage management into four stages for comparison. The first stage is the design phase, the second phase is construction deepening stage, the third stage is construction preparation stage, and the fourth phase is maintenance stage after operation.

In the first stage, BIM technology is mainly applied in the design of water supply and drainage project. To guarantee the valve of BIM technology in the first stage, after this stage is optimized, if there is still collision in other several stages, the value optimized will not be recorded in this stage.

The second phase is essentially a further deepening design with construction as the purpose. To further eliminate the collision problem of water supply and drainage pipes, the statistics still follow the principle in the first stage, that is, if the subsequent construction is affected, the value optimized will not be recorded in this stage.

The third stage is to formally perform construction management of water supply and drainage engineering after the optimization of the first two stages. In this stage, BIM technology is not only the collision optimization of water supply and drainage pipeline, but also includes the cost management and schedule management of water supply and drainage construction, and the optimization of construction scheme.

https://doi.org/10.17993/3cemp.2023.120151.133-163

The fourth stage is the management optimization of BIM technology in the maintenance stage of the overall operation of the building, including the optimization of data monitoring of all kinds of pipeline information.

5. DISCUSSION

This paper simply studies and analyzes the use of BIM technology in water supply and drainage management of high-rise buildings, and obtains the value of BIM technology in water supply and drainage management of high-rise buildings. However, there are still many applications of BIM technology to be studied and discovered.

Water saving and energy conservation is a major goal of green buildings. For this, it is recommended to feasible new technology and new measures to address the issues such as over pressure flow in the actual work, excessive invalid cold water caused by hot water system and the secondary pollution, so that on the basis of meeting the requirement of water supply, the utilization of water resources is improved, and the waste is avoided. Today, green building has become a major trend in the construction industry, but there is still a long way to go before it is truly universal.

6. CONCLUSION

Based on relevant data and regional water resources states, this paper establishes an evaluation system from the aspects of development and utilization, current situation of water resources and social and economic level, and applies catastrophe theory to perform scientific research on the risk of water resources development and utilization. Finally, the following conclusions are drawn:

(1)By studying the cost consumption at various stages of water supply and drainage engineering management of high-rise buildings pursuant to BIM technology, it can be drawn out that BIM technology has a great use value and assumes a significant optimization function in the water supply and drainage engineering management of high-rise buildings, where its cost saving accounts for 69% of the total.savings.

(2) By optimizing the design having been completed, it is found that the evaluation index C_{12} is 0.971 in Area 2, which is extremely risky, indicating that the per capita water resources in this region are low and the level of exploitation and utilization is weak. This index is in the range of 0.548 ~ 0.830 in other regions, which is wholly in the moderate level. Besides, the comprehensive risk evaluation value in the citywide is 0.905, indicating a high risk, and the index is in the range of 0.88 ~ 0 in other regions.

(3) Water saving and energy conservation is an important part of green building engineering design, and the deep application of BIM technology in its design process not only helps to improve the quality of energy-saving design, but also has a significant impact on the economic benefits of construction enterprises and the

https://doi.org/10.17993/3cemp.2023.120151.133-163

sustainable development of the construction industry. Additionally, in the process of practice, the maximum volume of and energy conservation of green buildings can reach 50%. In this regard, designers should fully recognize the advantages of BIM technology design, and do a good job in the specific application of BIM technology in the design process, so as to achieve the improvement of BIM technology application level, to ensure the quality of energy-saving design at the same time, and to promote the further development of construction projects.

7. DATA AVAILABILITY STATEMENT

The original contributions presented in the study are included in the article/ supplementary material, further inquiries can be directed to the corresponding author.

8. AUTHOR CONTRIBUTIONS

Wei Zheng, Yong Ye and Hongbing Zang conceived this idea. Wei Zheng established the BIM model, conducted data analysis with Yong Ye and Hongbing Zang, and then wrote a paper. All authors read and approve the final draft.

REFERENCES

(1) Gladkih, A M; Yu Konyuhov, V; Galyautdinov, I I; Shchadova, E I. **Green building as a tool of energy saving**. *IOP Conference Series: Earth and Environmental Science*. (2019).

(2) Ayinla, Kudirat Olabisi,Adamu, Zulfikar. **Bridging the digital divide gap in BIM technology adoption.** *ENGINEERING CONSTRUCTION AND ARCHITECTURAL MANAGEMENT*. (2018):1398---1416.

(3) Galieva, Anna; Galiev, Denis; Alekhin, Vladimir; Chirkova, Maria; Boswell, Laurence; Pruškova, K.; Vochozka, M.; Juhásová Šenitková, I.; Fariborz, H.; Váchal, J.; Kulhánek, F.; Juhás, P.; Mareček, J.; Oláh, J.; Flimel, M.; Melcher, J.; Šilarová, S. **Application of BIM technology for surveying heritage buildings**. *MATEC Web of Conferences*. (2019).

(4) Wu Y, Guo Y, Toyoda M. Policy **Iteration Approach to the Infinite Horizon Average Optimal Control of Probabilistic Boolean Networks[J]**. *IEEE Transactions on Neural Networks and Learning Systems*, (99):1-15.

(5) Zhang Y, Qian T, Tang W. B**uildings-to-distribution-network integration considering power transformer loading capability and distribution network reconfiguration[J]**. *Energy*, 2022, 244.

(6) Li, H., Deng, J., Feng, P., Pu, C., Arachchige, D., and Cheng, Q., (2021) **Short-Term Nacelle Orientation Forecasting Using Bilinear Transformation and ICEEMDAN Framework**. *Front. Energy Res*. 9, 780928.

(7) Li, H., Deng, J., Yuan, S., Feng, P., and Arachchige, D., (2021) **Monitoring and Identifying Wind Turbine Generator Bearing Faults using Deep Belief Network and EWMA Control Charts**. *Front. Energy Res*. 9, 799039.

https://doi.org/10.17993/3cemp.2023.120151.133-163

(8) Slavina, Anastasiia; Bychkov, Aleksej; Komarov, Aleksandr; Belyaev, Anton; Zheltenkov, A **BIM technology and environment management conditions**. *E3S Web of Conferences*. (2019).

(9) Qiu, Shiyu; Xu, Hao; Jin, Ju; Zhang, Hao; Sun, Kai. **Application of BIM Technology in Construction Engineering**. *IOP Conference Series: Earth and Environmental Science*. (2019).

(10) Zhang Yang,Guo Xuefei,Zhang Hongwei,Wang Lanzhi. **Application of BIM technology in refrigeration station design.** *Computer Aided Drafting, Design and Manufacturing*. (2017):65-69.

(11) Wen, Zhen. **Application Research of BIM Technology in Engineering Cost Management**. *IOP Conference Series: Earth and Environmental Science*. (2019).

(12) Xiao, Liangli; Du, Zhuang; Liu, Yan; Yang, Zhao; Xu, Kai; Deng, W. **Application Research of BIM Technology in Green Building Construction**. *MATEC Web of Conferences*. (2019).

(13) Mohamed, Mady A.A. **Saving Energy through Using Green Rating System for Building Commissioning**. *Energy Procedia*. (2019).

(14) Liu, Gi-Ren; Lin, Phone; Awad, Mohamad Khattar **Modeling Energy Saving Mechanism for Green Routers**. *IEEE Transactions on Green Communications and Networking*. (2018).

(15) Dahal, Madhu Sudan,Shrestha, Jagan Nath,Shakya, Shree Raj. **Energy saving technique and measurement in green wireless communication**. *ENERGY*. (2018):21---31.

(16) Hou, Yuhan. **Reasonable Use of Artificial Lighting in Building Energy Saving**. *MATERIALS SCIENCE, ENERGY TECHNOLOGY AND POWER ENGINEERING II (MEP2018)*. (2018).

(17) Puleo, Valeria, Notaro, Vincenza, Freni, Gabriele, La Loggia, Goffredo. **Water and Energy Saving in Urban Water Systems: The ALADIN Project**. *Procedia Engineering*. (2016):396-402.

(18) None. **Eco-friendly textile processing: saving time, water, energy. Focus on Surfactants**. (2016):6.

(19) Milad Ashouri,Fariborz Haghighat,Benjamin C.M. Fung,Amine Lazrak,Hiroshi Yoshino. **Development of building energy saving advisory: A data mining approach**. *Energy and Buildings*. (2018):139-139.

(20) Arshad, Rushan,Zahoor, Saman,Shah, Munam Ali,Wahid, Abdul,Yu, Hongnian. **Green IoT:An Investigation on Energy Saving Practices for 2020 and Beyond**. *IEEE ACCESS*. (2017):15667---15681.

(21) Bloul, Albe,Sharaf, Adel,El-Hawary, Mohamed. **An Energy Saving Green Plug Device for Nonlinear Loads**. *2017 INTERNATIONAL CONFERENCE ON RENEWABLE ENERGY AND ENVIRONMENT (ICREE 2017)*. (2018).

(22) Escriva-Bou, A.; Lund, J. R.; Pulido-Velazquez, M. **Saving Energy from Urban Water Demand Management**. *Water Resources Research*. (2018).

(23) Yu, Wenhong,Jiang, Chaowen,Li, hui. **Study on intelligent adjustment blinds and building energy saving**. *IOP Conference Series: Earth and Environmental Science*. (2018).

https://doi.org/10.17993/3cemp.2023.120151.133-163

(24) Tong, Zhineng. **Review of the Application of Green Building and Energy Saving Technology**. *IOP Conference Series: Earth and Environmental Science*. (2017)

(25) Le S, Wu Y, Guo Y, et al. **Game Theoretic Approach for a service function chain routing in NFV with coupled constraints[J]**. *Circuits and Systems II: Express Briefs, IEEE Transactions on*, 2021, PP(99):1-1.

(26) Mitsuru, Toyoda, Yuhu. **Mayer-Type Optimal Control of Probabilistic Boolean Control Network With Uncertain Selection Probabilities[J]**. *IEEE transactions on cybernetics*, 2019.

(27) Caozhendong **Water damage and prevention of highway drainage system in rainy areas**. *East China Science and Technology (comprehensive)* (2018).

(28) Tang Jianguo, Zhang Yue, Mei Xiaojie **Methods and measures for improving the quality and efficiency of urban drainage systems.** *Water supply and drainage* (2019):31-39.

(29) Fan Zeying **Talking about the installation and construction technology of building water supply and drainage system**. *Construction engineering technology and design* (2018):2015.

(30) Chenxiaoqing **Optimization of water supply and drainage system for double membrane water treatment process**. *China's science and technology* (2018):4-5.

(31) Zhang, Haiying. **Construction of water supply and drainage engineering**. *MATEC Web of Conferences*. (2018).

(32) Lia, Yuting; Jing, Mingxia **Application research of BIM technology in water supply and drainage engineering**. *Journal of Physics: Conference Series*. (2019).

(33) Hassanain, Mohammad A., Fatayer, Fady, Al-Hammad, Abdul-Mohsen. *Journal of Performance of Constructed Facilities*. (2015):04014082.

(34) Elshkaki, Ayman,Reck, Barbara K.,Graedel, T. E. **Anthropogenic nickel supply, demand, and associated energy and water use**. *RESOURCES CONSERVATION AND RECYCLING*. (2017):300---307.

(35) He, Guohua, Zhao, Yong, Wang, Jianhua, Li, Haihong, Zhu, Yongnan, Jiang, Shang. **The water–energy nexus: energy use for water supply in China**. *International Journal of Water Resources Development*. (2018):1-18.

(36) Wei, Tianyun, Chen, Guiqing, Wang, Junde. **Application of BIM Technology in Building Water Supply and Drainage Design**. *IOP Conference Series: Earth and Environmental Science*. (2017):012117.

(37) Horani M. O., Najeeb, M., y Saeed, A. (2021). **Model electric car with wireless charging using solar energy**. *3C Tecnología. Glosas de innovación aplicadas a la pyme*, 10(4), 89-101. https://doi.org/10.17993/3ctecno/2021.v10n4e40.89-101

(38) Meng Siyu & Zhang Xue.(2021). **Translog function in government development of low-carbon economy**. *Applied Mathematics and Nonlinear Sciences* (1). https://doi.org/10.2478/AMNS.2021.2.00138.

10. CONFLICT OF INTEREST

The authors declare that the research was conducted in the absence of any commercial or financial relationships that could be construed as a potential conflict of interest.

https://doi.org/10.17993/3cemp.2023.120151.133-163

/08/

DEVELOPMENT OF ECOLOGICAL MANAGEMENT SYSTEM FOR PLANTED FOREST BASED ON ELM DEEP LEARNING ALGORITHM

Zhe Wang*

School of Electronic and Electrical Engineering, Shanghai University of Engineering Science, shanghai, 201620, China

whospurp@163.com

Reception: 18/11/2022 **Acceptance**: 07/01/2023 **Publication**: 27/01/2023

Suggested citation:

W., Zhe (2023). **Development of ecological management system for planted forest based on ELM deep learning algorithm**. *3C Empresa. Investigación y pensamiento crítico, 12(1)*, 165-184. https://doi.org/10.17993/3cemp.2023.120151.165-184

ABSTRACT

Plantations play a central and lever role in maintaining the ecological balance of the earth, maintaining the overall function of the terrestrial ecosystem, and promoting the coordinated development of economic society and ecological construction. In order to strengthen the ecological management of plantation forests and improve the ecological level of forest region, the C/S framework is taken as the basic structure, and the programming mode of business model-user interface controller is used, on J2EE platform. The ecological management system of a planted forest is constructed by the evaluation module, the principal component comprehensive analysis module of ecological function value and the demand prediction module of planted forest based on extreme learning machine and deep learning algorithm, and runs under the support of windows system, oracle 15G and above database software. The indexes and factors affecting the ecological function of plantation forests were evaluated and analyzed, and the final management decision was given by the prediction module. The results showed that the plant density significantly affected plant biomass, organic carbon storage, water content and nutrient accumulation, and the comprehensive evaluation indexes of four ecological functions increased from 32.69, 31.84, 33.71 and 35.46 to 86.18, 89.46, 89.83 and 88.76, respectively. Although the degree of influence of the system on lemon strip plants, herbaceous plants, surface litter and soil varies, it still has good feasibility, effectiveness and practicality, and can assist the scientific ecological management of artificial plantation forests.

KEYWORDS

Extreme learning machine; Deep learning algorithm; Plantation forests; Ecological management system; Principal component analysis

https://doi.org/10.17993/3cemp.2023.120151.165-184

PAPER INDEX

https://doi.org/10.17993/3cemp.2023.120151.165-184

1. INTRODUCTION

As the main body of the terrestrial ecosystem, the forest has always been the focus of debate [1-2]. The function of the forest ecological environment can be direct or indirect. It can be tangible or intangible [3]. The function of forest ecology refers to the natural environmental conditions and effects that are formed by the forest ecosystem and ecological process and maintained by human survival [4].

The management of forest ecology is a systematic and complex project. At present, soil erosion, biodiversity reduction, wetland degradation, land desertification, and other problems are still serious, and the important role of forests in maintaining national ecological security has not been fully played [5-8]. With the development of industrial civilization and the aggravation of global warming, the ecological functions of forests, such as soil and water conservation, water conservation, carbon fixation and oxygen release, air purification and environment beautification, have attracted people's attention [9-10].

Recently, there have been many reports on forest ecological functions, especially on water conservation, carbon sequestration and oxygen release. Therefore, managing forest ecology objectively, dynamically and scientifically can deepen people's environmental awareness, strengthen the leading position of forestry construction in the ecological environment of the national economy, and improve the level of forest ecological environment. It is of great practical significance to accelerate the integration of the environment into the national economic accounting system and correctly handle the relationship between social-economic development and ecological environmental protection [11-13].

Based on the above research background, researchers in related fields are trying to achieve good research results in forest ecological management. Such as literature [14] according to Ukraine and the EU regulatory filing modern requirements for environmental protection and biodiversity conservation and the suggestion, proposing to overcome the ecological problems of radioactive pollution of forest ecosystems from the perspective of environmental management, and create a fire prevention and forest management system based on science, to prevent the personnel and the public excessive exposure from various sources, Prevention of secondary diffusion of radionuclides to relatively clean areas by fire is achieved through the use of hydrodynamic active water extinguishers and the laying of a polyethylene guanidine based barrier in front of the fire line. Literature [15] used mixed methods to conduct ecological management of tropical dry forests on 11079 hectares of land in Colombia. With the participation of 64 experts, the Delphi method was applied to conduct quantitative research on the ecological situation from 2018 to 2020. The results showed that all knowledge management practices identified had a certain impact on ecological management. It also contributes to the generation, transformation, and mobilization of scientific knowledge on each component of the ecological restoration process of tropical dry forests. Literature [16] aims at how to realize the maximization of the value of forest ecological resources to provide theoretical reference to the sustainable development of the global forest resources, using the theory of ecological capital is discussed how to define the concept of forest ecological resources

https://doi.org/10.17993/3cemp.2023.120151.165-184

capitalization, analyzed from two aspects of forest ecological resources capitalization of inner motivation, and how people change the use of forest resources, the results show that the realization path of capitalization of forest ecological resources can provide theoretical reference for maximizing the value of forest ecological resources and realizing the sustainable development of global forest resources. Literature [17] in 30 provinces as a sample, constructed the index system of forest ecological security and the efficiency of forest management, with the help of the CCR model, the coupling coordination model and the spatial panel model, from 2003 to 2017 China's provincial forest ecological safety and the management efficiency of the forestry coupling coordination degree and its temporal pattern characteristics and influence factors in the measurement and analysis, The results show that, in terms of forest ecological security, the index increases as a whole, and the coupling coordination degree changes from near uncoordinated to intermediate coordinated. This study can provide a theoretical reference framework for China's forest ecological management decisions. According to the consensus on the ecological environment in previous studies and the characteristics of the study area. Literature [18] established a quantitative evaluation index system for the comprehensive ecological environment of forest ecosystem nature reserve based on water, air, soil and biological environment, constructed a weightless cloud model, and provided a weightless evaluation mechanism. The results showed that the results of this study can provide theoretical support for the evaluation of forest ecosystem nature reserves and general evaluation when the weight is difficult to determine or uncertain. Literature [19] in human forest botanical garden as the research object, from the regional environmental quality, development conditions and the scenic area characteristic value of three standard level selected 23 indicators, to evaluate the ecological tourism development potential, using the analytic hierarchy process (AHP) to determine the weight of each index, and using the fuzzy comprehensive evaluation method to three standard level and evaluate the ecological tourism development potential, The conclusion suggested that scenic spots should maintain their advantages, enhance tourism characteristics, strengthen ecological civilization construction, and promote the in-depth development of ecological tourism. The above research results have established a relatively comprehensive and applicable forest ecological evaluation index system from different emphases, which has a certain promoting effect on improving the forest ecological environment and enhancing the ecological level.

Human initial afforestation is mainly in order to production needs, as a part of the agricultural production, with the progress of social productivity, timber demand increasing, under the natural state of forest resource components are insufficient to satisfy the human production and life, people began planting plantation, planted forest ecological level and function is becoming more and more attention [20]. Therefore, this article is based on C/S architecture and the J2EE platform, in the Struts framework with the business model - user interface - controller programming model, under the support of construct artificial planting forest ecological management system, through the synergy evaluation module, the ecological function value of the principal component comprehensive analysis module and the depth of the extreme learning machine learning algorithm of planted forests demand forecast module, Various

https://doi.org/10.17993/3cemp.2023.120151.165-184

indicators and factors affecting the ecological function of planted forests were evaluated and analyzed in order to better understand the biodiversity of planted forests and its regulation approaches and mechanisms on ecological function and to provide scientific basis and technical means for guiding the ecological management and sustainable management of planted forests [21].

2. DEVELOPMENT AND DESIGN OF ECOLOGICAL MANAGEMENT SYSTEM FOR ARTIFICIAL PLANTATION FOREST

Based on the C/S framework and J2EE platform, the business model -user interface-controller programming mode of the struts framework is adopted and design the environmental management system for artificial planting forests as shown in Figure 1. The system includes an evaluation module, principal component comprehensive analysis module of ecological function value and planting forest demand prediction module of extreme learning machine deep learning algorithm. The three modules work together to evaluate and analyze the indicators and factors that affect the ecological function of planted forests and provide management and support for decision-makers. The evaluation unit mainly includes three units: single ecological function value evaluation of all planted forest species, total ecological function value evaluation of single planted forest species, and total ecological function value evaluation of all planted forest species. The system server uses windows system, oracle 15G or above database, Tomcat6.0.67 or above server, JDK2.0 or above development package; The client uses IE 9.0 or higher.

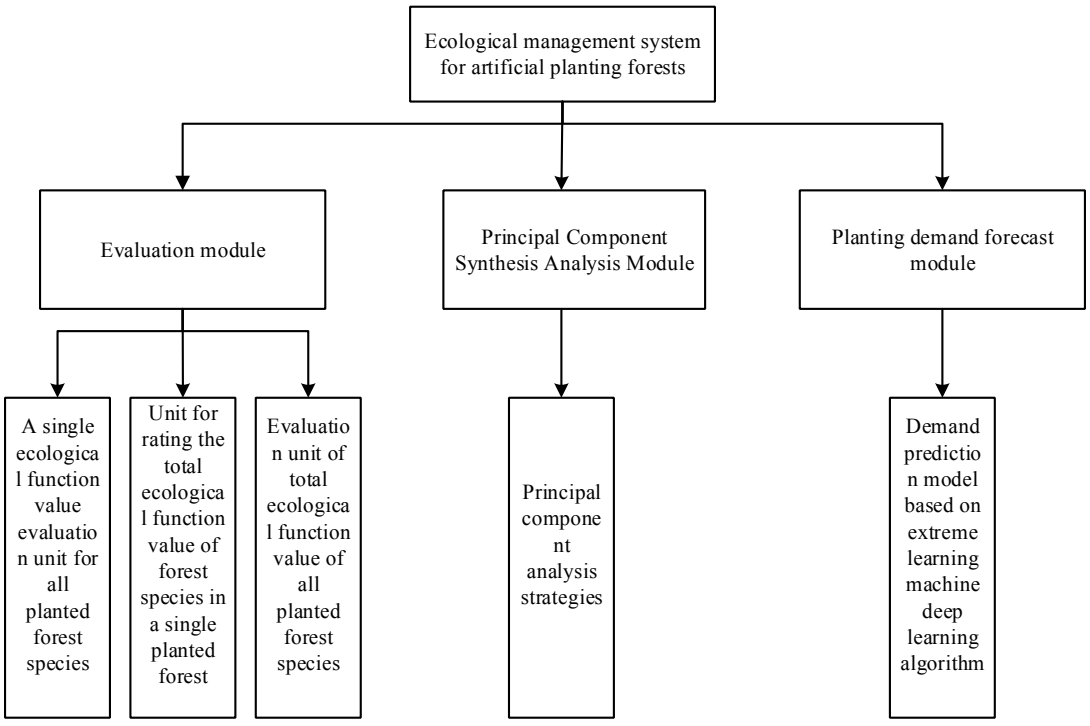

Figure 1. architecture diagram of the environmental management system of artificial plantation forest

https://doi.org/10.17993/3cemp.2023.120151.165-184

2.1. EVALUATION MODULE DESIGN

The ecological function value evaluation algorithm of the four units of the evaluation module is described as follows:

(1) Single ecological function value evaluation unit of all planted forest species: this unit includes the ecological function of water conservation, soil conservation, and carbon dioxide fixation of planted forest species. The value evaluation formulas of different ecological functions are as follows:

$$M_{hysy} = \sum_{i=1,2,\ldots,n} V_i \tag{1}$$

Where, V_i is the ecological function value of water conservation of n dominant tree species in artificial plantation forests.

$$M_{bytr} = \sum_{i=1,2,\ldots,n} T_i \tag{2}$$

Where, T_i is the ecological function value of soil conservation of n dominant tree species in artificial plantation forests.

$$M_{co_2} = \sum_{i=1,2,\ldots,n} Q_{1i} \tag{3}$$

Where, Q_{1i} is the ecological function value of fixed carbon dioxide of n dominant tree species in artificial plantation forests.

(2) Total ecological function value evaluation of monoculture forest species: this unit contains the total ecological function of different dominant tree species, and the value evaluation formula is as follows:

$$M_{dy} = V_i + T_i + Q_{1i} + Q_{2i} + E_i + K_i \tag{4}$$

Where, Q_{2i} is the corresponding ecological function value of oxygen release of dominant tree species in the planted forest. E_i is the ecological function value of biological storage energy of each dominant tree species in the planted forest; K_i is the ecological function value of biodiversity of each dominant tree species in the plantation.

(3) Total ecological function value evaluation of all planted forests and species: the total ecological function value evaluation algorithm of this unit is as follows:

$$M_z = \sum_{i=1,2,\ldots,n} V_i + \sum_{i=1,2,\ldots,n} T_i + \sum_{i=1,2,\ldots,n} Q_{1i} + \sum_{i=1,2,\ldots,n} Q_{2i} + \sum_{i=1,2,\ldots,n} E_i + \sum_{i=1,2,\ldots,n} K_i \tag{5}$$

Evaluation module by running the business model - user interface - controller programming software, all sorts of forest of planted forest respectively calculated single, single planting forest ecological function value of total sorts of forest ecological function value and all sorts of forest of planted forest ecological function value of three indicators, namely the complete management system of planted forest ecological function value assessment, the evaluation function of ecological management system of artificial plantation forest was realized.

https://doi.org/10.17993/3cemp.2023.120151.165-184

2.2. DESIGN OF PRINCIPAL COMPONENT COMPREHENSIVE ANALYSIS MODULE

The principal component analysis method [22] was adopted to comprehensively and systematically understand the comprehensive strength of the ecological function value of different planted forest types, and many indicators reflecting the ecological function value characteristics of planted forest types were considered from different aspects. The program flow chart of the principal component analysis algorithm is shown in Figure 2. The specific description is as follows:

(1) Data standardization of ecological value evaluation index;

(2) The correlation between ecological value evaluation indicators;

(3) Calculate the covariance matrix of standardized data;

(4) Calculate all the eigenvalues of the covariance matrix, calculate the eigenvectors, determine the number of principal components according to the cumulative ratio of eigenvalues;

(5) Calculate principal component load value and factor score coefficient matrix to determine the principal component expression; To calculate the comprehensive score is to carry out the principal component score, sort the scores according to the size of the score value, and output the most important first several ecological value evaluation indicators.

With the support of Windows system, Oracle 15G or above database, Tomcat6.0.67 or above server, JDK2.0 or above development package and other software, the algorithm program of principal component analysis can run according to the process shown in Figure 2. Principal component scoring is carried out according to the obtained comprehensive score. Several important evaluation indexes of ecological value were obtained, and the analysis function of ecological management system of artificial plantation forest was realized.

https://doi.org/10.17993/3cemp.2023.120151.165-184

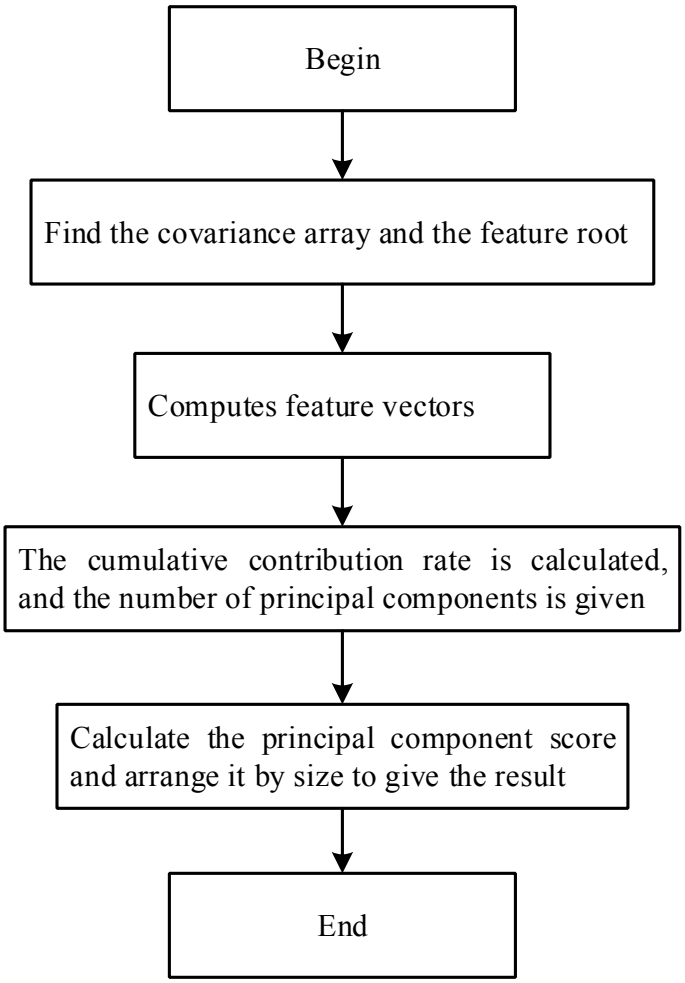

Figure 2. program flow chart of principal component analysis algorithm

2.3. DESIGN OF DEMAND PREDICTION MODULE OF PLANTED FOREST BASED ON EXTREME LEARNING MACHINE DEEP LEARNING ALGORITHM

The prediction module is mainly used for quantitative prediction and analysis of the demand for artificial plantation forests. The change in plantation density is influenced by the social economy, population, natural environment and other factors [23]. So choose gross GDP ($one hundred million), at the end of the total population (ten thousand people), non-agricultural population (ten thousand people), fiscal revenue (one hundred million yuan), financial expenditure (one hundred million yuan), the first industry (one hundred million yuan), the second industry (one hundred million yuan), the third industry (one hundred million yuan), the output value of industrial output value ($one hundred million), construction (one hundred million yuan), the per capita net income (yuan), fixed asset investment ($one hundred million), Urban input (100 million yuan), rural input (100 million yuan), annual precipitation (100 million cubic meters) and other indicators constitute the driving index system of the change of artificial planting forest density (10 thousand trees/ha). There is no simple linear relationship between each driving factor and the density of the planted forest, and there is a correlation in time. Therefore, an extreme learning machine deep learning

https://doi.org/10.17993/3cemp.2023.120151.165-184

algorithm is adopted to build the demand time series prediction model with the nearest neighbor domain theory [24] as the core, as shown in Figure 3. The prediction process is described as follows:

(1) Extraction of training samples: in order to complete the prediction of planting forest density Y_{t+s} at time $t+s$, k samples most similar to the prediction sequence Q of Y_{t+s} should be extracted from all training samples as the recombination samples, and k recombination samples should be used as the input of the local model. The process of finding the nearest neighbor is the process of measuring the similarity between the prediction sequence Q and all the training samples. Through this step, the best prediction model of planting forest density can be built.

In order to select k nearest neighbors of Q from set S as recombination samples, a method is needed to calculate the similarity of two sets of sequences. Assume that A_1 and A_2 are two time series:

$$\begin{cases} A_1 = \left[X_a, Y_a, X_{a+1}, Y_{a+1}, \cdots \quad _{a+q-1}, Y_{a+q-1}, X_{a+q}, Y_{a+q}\right] \\ A_2 = \left[X_b, Y_b, X_{b+1}, Y_{b+1}, \cdots \quad _{b+q-1}, Y_{b+q-1}, X_{b+q}, Y_{b+q}\right] \end{cases} \tag{6}$$

F_1 and F_2 are difference sequences of two time series A_1 and A_2 respectively:

$$\begin{cases} F_1 = \left[X_{a+1} - X_a, Y_{a+1} - Y_a, \cdots \quad _{a+q} - X_{a+q-1}, Y_{a+q} - Y_{a+q-1}\right] \\ F_2 = \left[X_{b+1} - X_b, Y_{b+1} - Y_b, \cdots \quad _{b+q} - X_{b+q-1}, Y_{b+q} - Y_{b+q-1}\right] \end{cases} \tag{7}$$

Assuming that $N_E(A_1, A_2)$ is the standardized Euclidean distance between A_1 and A_2 [25], $N_E(F_1, F_2)$ is the standardized Euclidean distance between F_1 and F_2, we use the mixed Euclidean distance to calculate the similarity of the two groups of time series:

$$N_H(A_1, A_2) = \frac{N_E(A_1, A_2) + N_E(F_1, F_2)}{2} \tag{8}$$

$N_H(A_1, A_2)$ is the mixed Euclidean distance of A_1 and A_2. We calculated the mixed Euclidean distance of each element in the set S and Q, finally obtained z mixed Euclidean distances, and selected k elements $\{S_i\}_{i=1}^{k}$ with the shortest distance as the extracted training samples.

(2) Prediction model derivation of extreme learning machine deep learning algorithm: the deep learning algorithm of extreme learning machine integrates the idea of self-coding [26] and encodes the output by minimizing reconstruction error so that the output can approach the original input infinitely. This structure provides an abstract representation of the input and thus captures the deep features of the original input. Figure 3 describes the prediction modeling process of the algorithm for the output planting forest density Y_{t+s} at time $t+s$. The extracted training sample $\{S_i\}_{i=1}^{k}$ is

https://doi.org/10.17993/3cemp.2023.120151.165-184

taken as the input of the network. It is assumed that the network is composed of the hidden layer of h layer, and $W = \{W_1, W_2, \cdots W_{h+1}\}$ represents the weight parameters to be learned in the network.

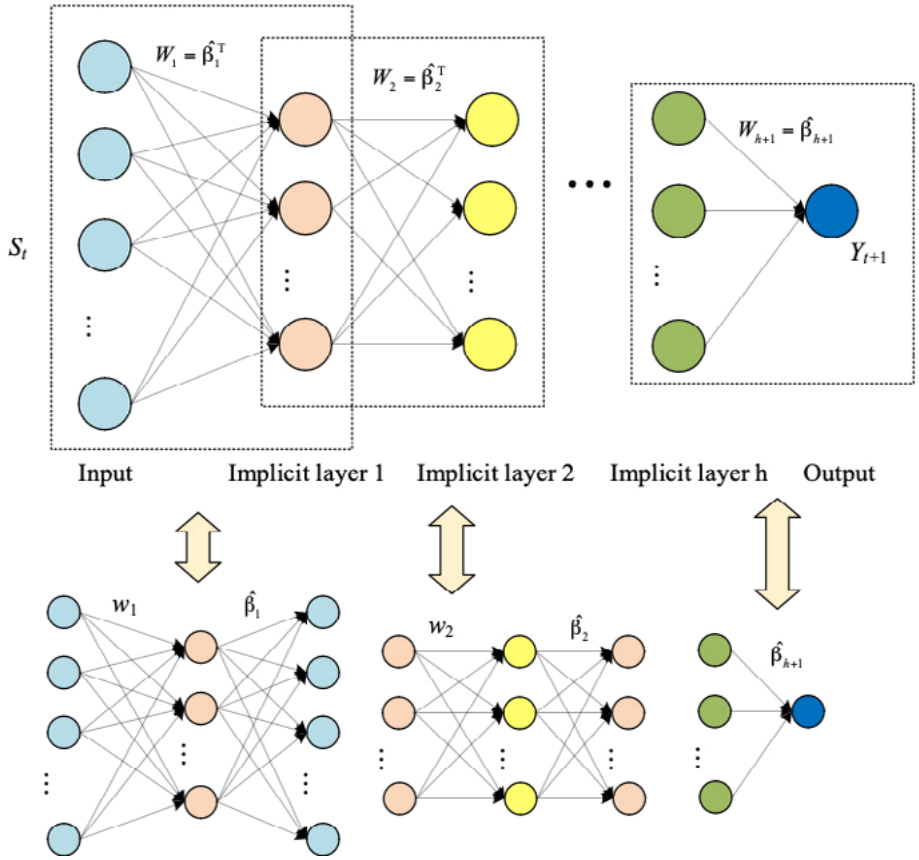

Figure 3. architecture diagram of a prediction model based on extreme learning machine deep learning algorithm

Each layer in the network can be decoupled as an independent extreme learning machine [27], and the target output of each extreme learning machine is equal to the input of the extreme learning machine. In this way, the low-dimensional representation of the input data can be obtained, that is, the hidden layer output of the extreme learning machine, and this output can be used as the input of the next extreme learning machine. The output weight $\hat{\beta}$ of the extreme learning machine is calculated by the following formula:

$$\hat{\beta} = H^T \left(\frac{I}{\lambda} + H^T H \right)^{-1} T \tag{9}$$

Where, λ is the rule item; H is the output matrix of the hidden layer of an extreme learning machine.

Then the weight parameter $W_k \left(k = 1, \cdots\right)$ is calculated by the following formula:

$$W_k = \hat{\beta}_K^T \left(k = 1, \cdots\right) \tag{10}$$

https://doi.org/10.17993/3cemp.2023.120151.165-184

Finally, the feature expression is obtained, that is, the output of the hidden layer of layer h, as the hidden layer of an independent extreme learning machine, and the output weight $\hat{\beta}_{h+1}$ of the extreme learning machine is obtained by similar calculation. The weight parameter W_{h+1} of the network is calculated by the following formula:

$$W_{h+1} = \hat{\beta}_{h+1} \tag{11}$$

According to the obtained network weight parameter $W = \{W_1, W_2, \cdots, W_{h+1}\}$, the prediction model architecture of extreme learning machine deep learning algorithm is defined. After the training sample data is input into the input layer of the prediction model, layer by layer calculation is carried out according to the determined network structure, and Y_{t+s} of planted forest density can be calculated, which provides decision basis for ecological management of planted forest.

3. APPLICATION OF THE SYSTEM

3.1. OVERVIEW OF THE STUDY AREA

An artificial plantation forest area with an area of about 2,000 square kilometers and a planting density of 9.64 million trees per hectare in 2017 was selected as the research target. The research area is located at 110°13 '~111°35' east longitude and 36°46 '~37 °52' north latitude, 983-1684m altitude and mountainous area. It is a typical hilly and gully region with complex terrain and closed traffic. The main type of soil is the yellow soil developed from the parent material of loess, with fine particles and deep soft soil, which is conducive to farming. The main vegetation types include agricultural land crops, grasslands, and shrubland. The main grassland species are alfalfa, long miscanthus, thyme, ice grass, iron pole, pig hair down, Chinese asparagus herb, two cracks, and so on. Shrub species mainly include Salix psammophila, peach, apricot, caragana korshinskii. Caragana korshinskii is widely planted in this region because of its drought resistance, cold resistance, sand resistance and good soil and water conservation. There are large typical experimental and demonstration areas of the caragana korshinskii plantation. The system was put into use in 2018. According to the prediction model of extreme learning machine deep learning algorithm, the reasonable planting density of artificial planting forest in this region is 23.24 million trees/ha. Caragana korshinskii will be planted in 2021.

3.2. SELECTION, MEASUREMENT AND CALCULATION OF ECOLOGICAL FUNCTION EVALUATION INDEX OF PLANTED FOREST

In order to verify the ecological management effect of the system on the region, the ecological function of the forest region is evaluated from four aspects [28-31]: plant biomass, organic carbon storage, nutrient accumulation, and water retention capacity.

https://doi.org/10.17993/3cemp.2023.120151.165-184

The evaluation system and the measurement method of secondary indicators are shown in Table 1. The first-level indicators include (1) plant biomass: caragana korshinskii and herbaceous aboveground biomass and litter biomass; (2) organic carbon storage: the aboveground and ground litter of caragana korshinskii and herbaceous plants and soil organic carbon storage; (3) total nitrogen and total phosphorus reserves of caragana korshinskii plants and herbaceous plants aboveground and litters; soil nutrient index: soil total nitrogen, nitrate nitrogen, ammonium nitrogen, and available phosphorus contents; (4) water content of caragana korshinskii plants and herbaceous plants aboveground, litter and soil.

Table 1. evaluation system and component determination method

Primary indicators	secondary indicators	Determination method
biomass	Aboveground biomass	Model estimation method
	Aboveground and litter biomass	Weighing method
Organic carbon storage	Aboveground and surface litter and soil organic carbon storage	The external heating method of potassium dichromate oxidation
Accumulation of nutrients	Total nitrogen storage in aboveground and litter	Concentrated sulfuric acid - hydrogen peroxide digestion
	Total phosphorus storage in aboveground and litter	Vanadium molybdenum yellow colorimetry
	Contents of total nitrogen, nitrate nitrogen and ammonium nitrogen in soil	Semi-trace Kjeldahl nitrogen determination
	Soil available phosphorus content	Sodium bicarbonate extraction - molybdenum antimony resistance colorimetric method
Water retention	Water content of aboveground and litter	Weighing method
	Soil moisture content	

The contents of different components were determined, and the first-order index of ecological function was measured using average value method[32-33]. Assuming that the actual measured value of the j secondary index of sample plot i is Xij, and the mean value and standard deviation of the j secondary index among all sample plots of the same factor are uj and σj respectively, the calculation formula for the score of the j secondary index of sample plot i is as follows:

$$Zij = \left(Xij - uj\right)/\sigma j \tag{12}$$

Thus, the ecological functional comprehensive index of each level index can be deduced:

$$EMFi = \sum_{1}^{f} Zij / f \tag{13}$$

Where, f is the number of all second-level indicators contained in plot i.

4. RESULTS AND ANALYSIS

https://doi.org/10.17993/3cemp.2023.120151.165-184

4.1. PLANT BIOMASS, ORGANIC CARBON STORAGE AND WATER CONTENT OF ARTIFICIAL PLANTATION FOREST

The aboveground biomass of caragana korshinskii, herbaceous plants and litters were selected as the parameters to evaluate the plant biomass of the planted forest. Figure 4 shows that plant biomass is significantly affected by planting density of planted forests. Before the application of ecological management system, the aboveground biomass and litter biomass of caragana korshinskii and herbage were only 8.19t/hm^2, 6.47t/hm^2 and 5.84t/hm^2, respectively. After applying the system for ecological management, through comprehensive evaluation of the ecological function of the sample land, they are 10.67t/hm^2, 2.51t/hm^2, 1.34t/hm^2, 12.55t/hm^2, respectively. After the application of ecological management system, organic carbon storage increased significantly, reaching 30.43t/hm^2 in 2021, the aboveground biomass and litter biomass of herbage increased, and the aboveground biomass and litter biomass of herbage increased, reaching 40.64t/hm^2, 8.76t/hm^2 and 7.66t/hm^2 in 2021, respectively. The aboveground organic carbon storage of caragana korshinskii and herbage, litter organic carbon storage and soil organic carbon storage were selected as parameters to evaluate the ecological function of organic carbon storage. Caragana korshinskii, herbage, litter and soil organic carbon storage were 7.19t/hm^2, 6.48t/hm^2, 26.71t/hm^2, respectively. Water retention is an important ecological function of planted forests. In this study, four indexes of caragana korshinskii plants, herbaceous plants, ground litters and soil water content were selected as parameters to evaluate the water retention capacity of caragana korshinskii plantations. As shown in figure 4, you can see that plantation planting density of caragana korshinskii and plant litter moisture content is less affected, there was no significant difference before and after the application in the system, but the herbs and soil moisture content in 2017 and 2021 significant difference under different planting density and planting density increase, herbaceous plants and soil water content is increased greatly, in 2021, they will reach 62.58% and 59.43% respectively. To sum up, the environmental management system is based on the results of the evaluation of the single ecological function value of all planted forests, the total ecological function value of all planted forests and the total ecological function value of all planted forests. By reasonably adjusting the planting density in the forest region, the coverage rate of surface vegetation was expanded, and the ecological function indexes were improved. The comprehensive indexes of plant biomass, organic carbon storage and water content of the planted forest increased from 32.69, 31.84 and 35.46 in 2017, respectively. Increasing to 86.18, 89.46 and 88.76 in 2021, there is an obvious synergistic effect between planting density and ecological function in the forest region, and artificial planting forest has a better ability to provide and maintain multiple ecological functions simultaneously.

https://doi.org/10.17993/3cemp.2023.120151.165-184

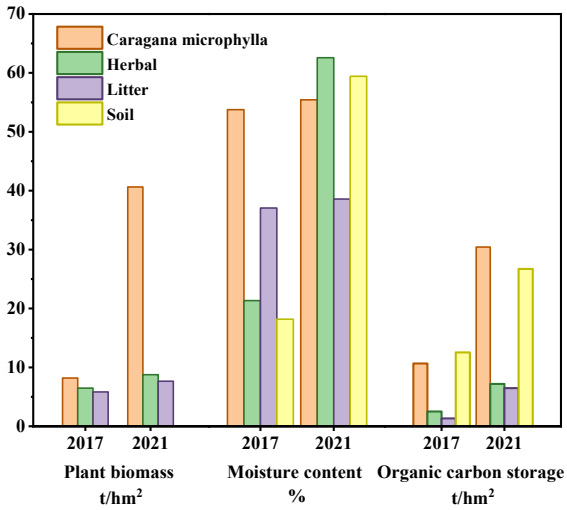

Figure 4. schematic diagram of ecological function change of plantation forest

4.2. NUTRIENT ACCUMULATION IN PLANTATION FORESTS

Total nitrogen and total phosphorus reserves of caragana korshinskii and herbaceous plants, total nitrogen and total phosphorus reserves of litters, and soil nutrient content indexes (soil total nitrogen, available phosphorus, nitrate-nitrogen, ammonium nitrogen) were selected as the parameters to evaluate the ecological function of nutrient accumulation in planting areas. Figure 5 (a) shows that the planting density of caragana korshinskii significantly affected the plant total nitrogen storage of the planted forest. The total nitrogen storage of caragana korshinskii was significantly higher than that of herbaceous plants and litters. Before the system was put into use, the planting density was small, and the total nitrogen reserves of caragana korshinskii, herbaria korshinskii and litters were low, only 135.46kg/hm^2, 11.13kg/hm^2 and 8.54kg/hm^2. However, after the system was put into use, the total nitrogen reserves of three kinds of plants were greatly increased. In 2021, the ecological function of total nitrogen accumulation was 763.08kg/hm^2, 25.66kg/hm^2 and 51.73kg/hm^2, respectively. The ecological function of caragana korshinskii was the most obvious before and after application of the system. Compared with total nitrogen, the total phosphorus reserves of plants in the planted forests with different planting densities changed more gently, but the functional degree of plants was still that the total phosphorus reserves of caragana korshinskii were significantly higher than that of herbaceous plants and litters. Before the use of systematic management of forest ecology, the total phosphorus reserves of the three are 8.46kg/hm^2, 1.23kg/hm^2 and 0.64kg/hm^2, respectively. After management, total phosphorus reserves reach 36.16kg/hm^2, 1.43kg/hm^2 and 2.22kg/hm^2, respectively. There was no significant difference in total phosphorus storage of herbaceous plants and litters under different planting densities.

It can be seen from Figure 5 (b) that with the increase in plantation density, soil total nitrogen content also showed a corresponding upward trend, but the increase was not

https://doi.org/10.17993/3cemp.2023.120151.165-184

obvious, only increased by 0.08g/kg. Therefore, the application of an ecological management system had no significant effect on soil total nitrogen content. Before the application of the system, the contents of soil available phosphorus, nitrate-nitrogen, and ammonium nitrogen content were only 1.03mg/kg, 3.11mg/kg and 0.37mg/kg. When the system gave a reasonable planting density and implemented it, the contents of the three nutrients in the soil were as high as 13.56mg/kg, 18.38mg/kg and 10.84mg/kg, respectively. This is because, with the support of a principal component analysis strategy and extreme learning machine deep learning algorithm, the management system reasonably increases the number of caragana korshinskii plants per unit area, and makes the biomass of caragana korshinskii and litters at a high level. Therefore, it directly promotes the increase of total nitrogen and total phosphorus reserves of caragana korshinskii plants and litters. In addition, by increasing the surface vegetation coverage and improving the input of soil resources, the nutrient contents of soil such as nitrogen and phosphorus were increased, and the nutrient accumulation ecological functional composite index of the cultivated forest increased from 33.71 in 2017 to 89.83 in 2021.

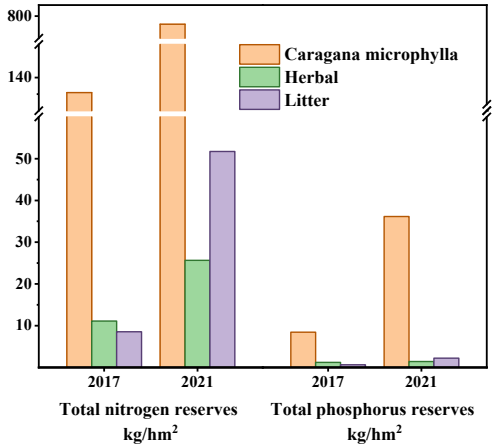

(a) plant and litter nutrient content

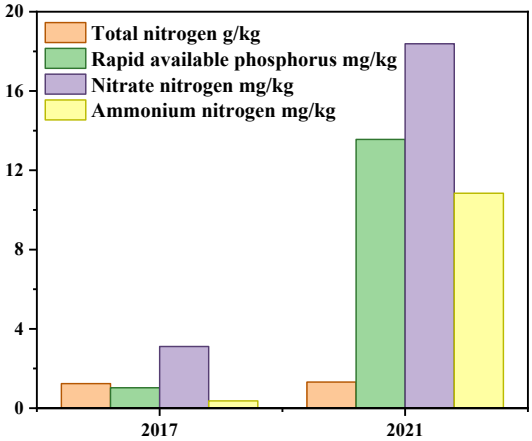

(b) soil nutrient content

Figure 5. schematic diagram of nutrient accumulation

https://doi.org/10.17993/3cemp.2023.120151.165-184

5. DISCUSSION

This study focuses on the study of the environmental management system of artificial planting forests. The data input into the system, through the function evaluation and prediction, helps to achieve the best combination of forest species selection, planting area and ecological environmental benefits. The next step for further in-depth research is as follows:

(1) Combined with 3S technology, global positioning system is used for real-time positioning, remote sensing for data collection and update, geographic information system for spatial analysis and comprehensive processing, so as to rapidly update ecological related data and reduce the cost of manpower and material resources;

(2) For the model base of this study, optimization model and early warning model need to be added in the future. From the perspective of ecological economics, it is expected to think about how to arrange the species structure of planted forest and analyze the optimization between its related functions and generated services. Forewarning of the loss of ecological function of plantation forest;

(3) For the system, there is currently a lack of expert experience and practical knowledge, which needs to be enriched and strengthened in the future. In addition, artificial intelligence technologies such as neural networks, support vector machines and time series analysis can also be used to acquire knowledge in the system.

6. CONCLUSION

Afforestation is one of the main ways of ecological restoration and land reclamation. Whether the restoration mode is suitable or not needs long-term observation to see its restoration effect. The ecological health of the planted forest also varies with the recovery time. Therefore, this paper takes C/S as the basic framework and J2EE as the development platform. With the support of principal component analysis method and extreme learning machine deep learning algorithm, the Struts framework and business model-user-interface controller programming mode are adopted in this paper. An environmental management system consisting of an evaluation module, principal component comprehensive analysis module and planting demand prediction module has been developed. Through carrying out experimental research activities on the effect of ecological management of forest region by the system in the study area, the following three conclusions have been obtained:

(1) Single system USES all sorts of the forest of planted forest ecological function value evaluation, the single planting Lin total sorts of forest ecological function value evaluation, all sorts of the forest of planted forest ecological function value evaluation three units constructing evaluation module, to provide better practice ecological management database and decision basis, and planted forest density and obvious synergistic effect between different ecological functions.

(2) Using principal component analysis comprehensive system understanding of different sorts of the forest of planted forest ecological function value of

https://doi.org/10.17993/3cemp.2023.120151.165-184

comprehensive strength, help considering from different sides reflects growing forest category characteristics of many types of ecological function value indicators, the artificial planting forests can have better ability to provide and maintain multiple ecological functions at the same time.

(3) Based on the extreme learning machine deep learning algorithm, the demand prediction module of planted forest designed by extreme learning machine takes the nearest neighbor domain theory as the core, making the output infinitely close to the original input, and giving the reasonable planting density of planted forest in this region as 23.24 million trees/ha. The biomass, organic carbon storage, nutrient accumulation and water content in the study area were increased to 57.06t/hm^2, 70.81t/hm^2, 924.38kg/hm^2 and 216.03% from 20.5t/hm^2, 27.07t/hm^2, 171.21kg/hm^2 and 130.35%. The corresponding ecological functional composite index increased from 32.69, 31.84, 33.71, 35.46 to 86.18, 89.46, 89.83, 88.76, respectively.

7. DATA AVAILABILITY STATEMENT

The original contributions presented in the study are included in the article/ supplementary material, further inquiries can be directed to the corresponding author.

REFERENCES

(1) Vinnepand M, Fischer P, Zeeden C, et al. **Decoding geochemical signals of the Schwalbenberg Loess- Palaeosol-Sequences -A key to Upper Pleistocene terrestrial ecosystem responses in western Central Europe**. 2021.

(2) Wang H H, Chu H L, Dou Q, et al. **Seasonal Changes in Pinus tabuliformis Root-Associated Fungal Microbiota Drive N and P Cycling in Terrestrial Ecosystem[J]**. *Frontiers in Microbiology*, 2021, 11:3352-.

(3) Le S, Wu Y, Guo Y, et al. **Game Theoretic Approach for a service function chain routing in NFV with coupled constraints[J]**. *Circuits and Systems II: Express Briefs, IEEE Transactions on*, 2021, PP(99):1-1.

(4) Li, H., Deng, J., Feng, P., Pu, C., Arachchige, D., and Cheng, Q., (2021) **Short-Term Nacelle Orientation Forecasting Using Bilinear Transformation and ICEEMDAN Framework**. *Front. Energy Res*. 9, 780928.

(5) Z Németová, S Kohnová. **Mathematical modeling of soil erosion processes using a physically-based and empirical models: Case study of Slovakia and central Poland[C].** *Adaptive Hardware and Systems. Central Library of the Slovak Academy of Sciences*, 2021.

(6) Wu Y, Guo Y, Toyoda M. **Policy Iteration Approach to the Infinite Horizon Average Optimal Control of Probabilistic Boolean Networks[J]**. *IEEE Transactions on Neural Networks and Learning Systems*, (99):1-15.

(7) Zhan Q, Zhao W, Yang M, et al. **A long-term record (1995-2019) of the dynamics of land desertification in the middle reaches of Yarlung Zangbo River basin derived from Landsat data[J]**. *Geography and Sustainability*, 2021, 2(1).

https://doi.org/10.17993/3cemp.2023.120151.165-184

(8) Zhang Y, Qian T, Tang W. **Buildings-to-distribution-network integration considering power transformer loading capability and distribution network reconfiguration[J]**. *Energy*, 2022, 244.

(9) Chen L. **Study on carbon fixation and oxygen release ability of urban greening tree species based on spatial and temporal dynamic analysis[J]**. *International Journal of Global Energy Issues*, 2020, 42(3/4):244.

(10) Li, H., Deng, J., Yuan, S., Feng, P., and Arachchige, D., (2021) **Monitoring and Identifying Wind Turbine Generator Bearing Faults using Deep Belief Network and EWMA Control Charts**. *Front. Energy Res*. 9, 799039.

(11) Hahn R G. **Renal water conservation and the volume kinetics of fluid induced diuresis; a retrospective analysis of two cohorts of elderly men[J]**. *Clinical and Experimental Pharmacology and Physiology*, 2020.

(12) Heinzelmann G, Sontheim P, Haas A, et al. **Hand-Portable Garden, Forestry and/or Construction Processing Device and Method for Operating a Hand-Portable Garden**, US20210291400A1[P]. 2021.

(13) Wang Y, Zhang D, Wang Y. **Evaluation Analysis of Forest Ecological Security in 11 Provinces (Cities) of the Yangtze River Economic Belt[J]**. *Sustainability*, 2021, 13.

(14) Maglyovana T, Dolin V. **KEY ISSUES FOR ECOLOGICAL MANAGEMENT OF RADIOACTIVE CONTAMINATED FOREST ECOSYSTEMS IN UKRAINE[J]**. 2020.

(15) Torres-Romero F, Acosta-Prado J C. **Knowledge Management Practices and Ecological Restoration of the Tropical Dry Forest in Colombia[J]**. *Land*, 2022, 11.

(16) Forum N R. **The concept delimitation, the value realization process, and the realization path of the capitalization of forest ecological resources**. 2021.

(17) Chen N, Qin F, Zhai Y, et al. **Evaluation of coordinated development of forestry management efficiency and forest ecological security: A spatiotemporal empirical study based on China's provinces[J]**. *Journal of Cleaner Production*, 2020:121042.

(18) Xiang M, Lin X, Yang X, et al. **Ecological Environment Evaluation of Forest Ecosystem Nature Reserves Using an Unweighted Cloud Model[J]**. *Water*, 2020, 12(7):1905.

(19) Yin C, Pan W. **Study on the Evaluation System of Forest Ecological Protection Using Big Data Technology and Adaptive Fuzzy Logic System[J]**. *Journal of Physics: Conference Series*, 2021, 1952(3):032030 (6pp).

(20) Jani H, Meder R, Hamid H A, et al. **Near infrared spectroscopy of plantation forest soil nutrients in Sabah, Malaysia, and the potential for microsite assessment[J]**. *Journal of Near Infrared Spectroscopy*, 2021, 29(3):148-157.

(21) Mitsuru, Toyoda, Yuhu. **Mayer-Type Optimal Control of Probabilistic Boolean Control Network With Uncertain Selection Probabilities[J]**. *IEEE transactions on cybernetics*, 2019.

(22) Lu C, Feng J, Chen Y, et al. **Tensor Robust Principal Component Analysis with A New Tensor Nuclear Norm[J]**. *IEEE Transactions on Pattern Analysis and Machine Intelligence*, 2020, 42(4):925-938.

https://doi.org/10.17993/3cemp.2023.120151.165-184

(23) Thiffault N, Hoepting M K, Fera J, et al. **Managing plantation density through initial spacing and commercial thinning: yield results from a 60-year-old red pine spacing trial experiment[J]**. *Canadian Science Publishing*, 2021(2).

(24) Tang S, Yang Y, Ma Z, et al. **Nearest Neighborhood-Based Deep Clustering for Source Data-absent Unsupervised Domain Adaptation[J]**. 2021.

(25) Ding Y, Liang A, Ma K, et al. **Research on Optimal Strategy of Residential Buildings Energy Based on Standardized Euclidean Distance Measure Similarity Search Method[J].** *IOP Conference Series Earth and Environmental Science*, 2021, 651(2):022052.

(26) Cai J, Dai X, Hong L, et al. **An Air Quality Prediction Model Based on a Noise Reduction Self-Coding Deep Network[J]**. *Mathematical Problems in Engineering*, 2020, 2020(3):1-12.

(27) Li B, Chen H, Tan T. PV **Cell Parameter Extraction Using Data Prediction–Based Meta-Heuristic Algorithm via Extreme Learning Machine[J]**. *Frontiers in Energy Research*, 2021, 9:693252.

(28) Ingraffia R, Amato G, Iovino M, et al. **Polyester microplastic fibers in soil increase nitrogen loss via leaching and decrease plant biomass production and N uptake**. 2022.

(29) Liu Z, Huang F, Wang B, et al. **Impacts of mulching measures on crop production and soil organic carbon storage in a rainfed farmland area under future climate[J]**. *Field Crops Research*, 2021, 273:108303-.

(30) KY Gülüt, Duymu E, Solmaz L et al. **Nitrogen and boron nutrition in grafted watermelon II: Impact on nutrient accumulation in fruit rind and flesh[J]**. *PLoS ONE*, 2021, 16(5):e0252437.

(31) Cla B, Wl A, Bl A, et al. C**omprehensive analysis of ozone water rinsing on the water-holding capacity of grass carp surimi gel[J]**. *LWT*, 2021, 150.

(32) Frayssinet, M., Esenarro, D., Juárez, F. F., y Díaz, M. (2021). **Methodology based on the NIST cybersecurity framework as a proposal for cybersecurity management in government organizations**. *3C TIC. Cuadernos de desarrollo aplicados a las TIC*, 10(2), 123-141. https://doi.org/10.17993/3ctic.2021.102.123-141

(33) Shen Siqi.(2021). **Multi-attribute decision-making methods based on normal random variables in supply chain risk management**. *Applied Mathematics and Nonlinear Sciences* (1). https://doi.org/10.2478/AMNS.2021.2.00147.

9. CONFLICT OF INTEREST

The authors declare that the research was conducted in the absence of any commercial or financial relationships that could be construed as a potential conflict of interest.

/09/

RESEARCH ON GEOLOGICAL ENVIRONMENT PROTECTION AND GEOLOGICAL DISASTERS CONTROL COUNTERMEASURES IN CHINA

Cheng Liu*

College of Artificial Intelligence, Dazhou Vocational and Technical College, Dazhou, Sichuan, 635001, China

liuchenglyl@163.com

Reception: 18/11/2022 **Acceptance**: 07/01/2023 **Publication**: 27/01/2023

Suggested citation:

L., Cheng (2023). **Research on geological environment protection and geological disasters control countermeasures in China**. *3C Empresa. Investigación y pensamiento crítico, 12(1)*, 186-205. https://doi.org/10.17993/3cemp.2023.120151.186-205

ABSTRACT

Geological disasters in mines, ecological environment and geology and geomorphology are closely bound up with each other. To reduce or avoid economic loss and to decrease the threat degree of geological disasters to life safety, the protection of geological environment are formulated in this study. Specifically, this includes taking mines that are dominated by thin bedded carbonate as the research objects. The goals of this study include prevention and control of geological disasters and protection of geological environment. The data are based on characteristics of geological strata in mines collected by the exploration, and combined with the characteristics of geomorphic environment, relevant rules aiming at the prevention and control of geological disasters. Then, pursuant to the selection of indicators, an evaluation system is constructed to verify the effectiveness of measures and strategies proposed, in which the score value is converted into the corresponding level to test the implementation effect of the measures and strategies proposed. Through comparing the changes of the utility levels before and after the implementation of measures and strategies proposed, it can be seen that the geological disaster levels of the five mining areas in the study region are respectively improved from the non-ideal levels V, IV, V, V, IV to II, I, I, II, II, with the tailings pond leakage times less than 4 times and collapse volume less than 5m3. And, the levels of geological environment are upgraded from levels IV, IV, IV, V, V to ideal levels II, II, II, I, II, accomplished by the vegetation coverage rate of the mine reaching more than 35%, as well as the recovery rate of exploitation and utilization rate of tailings both exceeding 85%, which indicates that the protection strategy proposed in this paper has good practicality and feasibility.

KEYWORDS

Geological characteristics; Geological disasters; Geomorphic environment; Linear weighted average method; Utility level; China

https://doi.org/10.17993/3cemp.2023.120151.186-205

PAPER INDEX

https://doi.org/10.17993/3cemp.2023.120151.186-205

1. INTRODUCTION

China is rich in mineral resources with huge reserves, and is one of the few large resource countries in the world. The demand for mineral resources has been accompanied by rapid economic development and has a long history of mining development [1-2]. In recent years, the scale of mining has been rapidly developed and expanded, and the development of mining resources has strongly disturbed the geological environment [3-5]. Mining resources are providing resources for urban construction and social development, providing industrial food for the national economy, and accelerating economic and social development. However, it has also triggered a series of frequent geological disasters such as ground collapse, cave-in, and roofing, leaving behind many mining geological environment problems [6-7]. Especially, the mining geological environment problems caused by open-pit mining are particularly serious, which put the lives of people at risk and property loss, and become one of the important elements threatening ecological security [8-10].

With the rapid advancement of industrialization and urbanization and the implementation of ecological civilization construction strategy, along with the massive mining and range expansion of mines, the geological environment problems of mines have become increasingly prominent and the degree of ecological damage has become more and more serious, leading to serious geological disaster problems in mines [11-14]. Especially on abandoned mines around urban areas and within the visual range along important traffic arteries, the resulting destruction of vegetation, exposed hills and land damage have a bad impact on the city image and ecological environment [15-19]. Mine geological hazards have become a hot issue of public concern and social attention, and gradually evolved into a major obstacle to social and economic development, making the prevention of geological hazards and ecological environment restoration and management increasingly a common demand [20-22].

Therefore, it is urgent to vigorously implement comprehensive remediation of mining geological environment, repair the ecological environment of mining areas, improve the level of scientific land use and further improve the image of the city. This has not only become a major issue concerning urban development and ecological civilization construction, but also an effective means to eliminate geological disasters and guarantee the safety of people's lives and properties. Besides, it is also an important initiative to make full use of mining resources, promote economic development, ensure social stability and improve ecological civilization construction [23-25].

The environmental problems of mining areas have been widely concerned and valued by societies in various countries. For example, the literature [26] explored the intensive use of magnetic resonance populations, taking Yangquan, China, as an example, from the scientific connotation of magnetic resonance populations, and proposed a dynamic improvement path to enhance the intensive use, thus filling the gap in this field. The background conditions of the mine and the basic cases of the corresponding mining enterprises, both of which are indicators presented by the resource itself in the process of converting minerals into useful products, constitute the basic framework for identifying and enhancing the intensive use of mineral

https://doi.org/10.17993/3cemp.2023.120151.186-205

resources. The results show that mining enterprises are the core of intensive utilization, the mining recovery rate contributes most to the intensive utilization of resources, and the mine size does have an impact on the intensive utilization of resources, but the impact will gradually decrease when a certain size is reached. Therefore, from the perspective of enterprise governance, a corresponding dynamic improvement path is adopted in an attempt to increase the degree of intensification. In the literature [27], a Bayesian belief network probabilistic prediction framework was developed to support practical and cost-effective decision making for decentralized disposal management. This approach allows the incorporation of expert knowledge in cases where data are insufficient for modeling. The performance of the model was validated using field data from actively managed mine sites and was found to be consistent in predicting soil erosion and ground cover. In the literature [28], stability studies were carried out for weathered toxic sand mine wastes of amorphous iron arsenate/pyrochlore using different doses of modifiers, as determined by X-ray diffraction and polarized light microscopy, to evaluate the effectiveness of such treatments using batch and column leaching methods. Under the equilibrium conditions imposed by the applied standard batch leaching tests, both treatments achieved significant reductions in leachable arsenic concentrations under their optimal conditions, making the mine wastes acceptable in controlled landfills as defined by international legislation. The literature [29] investigated dust pollution in open-pit coal mines in cold regions and explored its main influencing factors. The dust pollution characteristics were determined by statistical analysis, and the main influencing factors of dust concentration in different seasons were calculated using the integrated gray correlation. A hybrid single-particle Lagrangian integral trajectory model was used to simulate the dust pollution from the mine to the surrounding area. Based on the results of the study, an optimal mine design strategy was designed to better control dust in mining and adjacent areas, especially in winter. The literature [30] focused on underground mining in Pakistan, using the decision matrix risk assessment method to assess events based on their severity and probability, and based on the results of the resulting study, proposed management measures that would help avoid mining accidents by applying occupational safety and health regulations issued by the Ministry of Mines. The above approach is mainly manifested in the shift from static implementation of environmental policies and standards to the implementation of dynamic management. There is a shift from a single management tool to strengthening cooperation between government departments and mining companies and enhancing the environmental protection capacity of mining companies. However, with the huge impact of mining environmental problems on economic development, social progress and ecological environment, there is still a need to continuously carry out research on mining environmental problems.

The large-scale development and utilization of mineral resources has caused serious geohazards and geological environmental problems, and there is a certain connection between this problem and geomorphological feature. Based on this, this paper develops a geohazard prevention and control measure and geological environmental protection strategy consisting of three strategic points each, based on the geological and geomorphological features of the study area. Using the United

https://doi.org/10.17993/3cemp.2023.120151.186-205

Nations Commission on Sustainable Development's menu-based multi-indicator type indicator system approach, an evaluation indicator system for verifying the specific effectiveness of prevention and control measures and protection strategies is constructed for the reference of management and mining enterprises. The ultimate goal is to minimize the damage to the geological environment of mines and to restore it gradually.

2. GEOLOGICAL AND GEOMORPHOLOGICAL CHARACTERISTICS OF THE STUDY AREA

A mine with thin-layered carbonate rocks as the main mineral resource was selected as the study object, and the geological and geomorphological features of the mine are shown in Figure 1. The stratigraphy of the study area mainly includes Devonian, Carboniferous, Permian and Triassic. According to the lithological characteristics, the stratigraphy of the mine area can be divided into two sets of rock systems, namely the Triassic mud and sandstone rock system, and the carbonate rock system below the Triassic system. The primary sedimentary chain soil deposits are distributed in the stratum of carbonate rock system on the upper side, underlain by thick-layered carbonate rocks, and the rocks below the primary sedimentary chain soil deposits are light in color, pure and with little lithological variation. The rocks above the primary sedimentary silver earth ore layer are mostly thin-layered carbonate rocks with dark color, high lithological variation and muddy interlayer. The Triassic siltstone is mostly a fine-grained shoulder structure with tuffaceous components. The lithological characteristics of the mine stratigraphy can be summarized as the complete development process of the opening, expansion, interrupted surface and closing of the Right River Basin. The Right River Basin opened in the middle Devonian, and no pre-Devonian stratigraphic basement is exposed in the mine area, which cannot reflect the characteristics of the stratigraphic interface of the basin opening. The petrographic situation of the stratigraphy of the mine area indicates that the mine has a terrace tectonic nature and basically maintains a terrace shallow water depositional environment from the Devonian, although it also shows a temporary increase in water depth, but does not change the terrace nature. Therefore, the geography of the area generally belongs to a terrace environment in 31the Right River Basin.

The selected mines are located from southwest to northeast of the Right River, Bujian River and Pingzhi River, all of which are oriented in a northwesterly direction, forming a pattern of distribution between karst landforms and river landforms. On the southwest side of the Right River are the No. 1 and No. 2 mines, between the Right River and the Bujian River is the No. 3 mine, and between the Bujian River and the Pingzhi River are the No. 4 and No. 5 mines. The mining area is mainly divided into two types of landforms, karst and river valley. The karst landforms are mainly composed of mountainous positive terrain, and the river valley landforms are distributed in the negative terrain of the basin. The geomorphology of the mine area is mainly controlled by lithology and tectonics, and constitutes a combination of lithologic and tectonic geomorphology. The lithological control shows that the karst landform is

https://doi.org/10.17993/3cemp.2023.120151.186-205

developed in the carbonate stratum of the former Triassic, and the river landform is developed in the Triassic mudstone stratum. The tectonic control shows that the karst landforms are developed in the back-sloping core and the fluvial landforms are developed in the diagonal core. Since the geological and geomorphic features of the mine have not been discussed much in previous studies, the geology and geomorphology of the target area are combined in a comprehensive study to lay the foundation for the development of subsequent geological hazard prevention and control measures and geological environmental protection strategies.

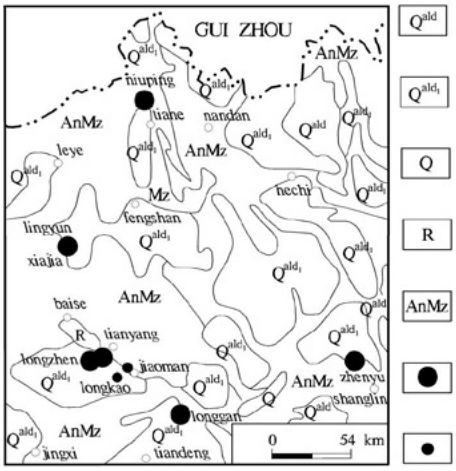

Figure 1 Schematic diagram of the geological features of the study area

3. MINE GEOLOGICAL HAZARD PREVENTION AND CONTROL AND GEOLOGICAL ENVIRONMENTAL PROTECTION STRATEGY DESIGN

Based on the geological features of the study area, the geological hazard prevention and control measures and geological environmental protection strategies shown in Table 1 are formulated.

Table 1 Mine geohazard prevention and control and geological environmental protection strategy

Strategic objectives	Strategy points
Geological disaster prevention and control	Disaster monitoring
	Landslide prevention and control
	Prevention and control of sudden water
Geological environmental protection	Fulfill regulatory responsibilities in accordance with the law and implement the main responsibility
	Improve the technology content and level of mine environmental protection
	Exploring new ways to develop and manage mines

https://doi.org/10.17993/3cemp.2023.120151.186-205

3.1. RULES FOR GEOLOGICAL HAZARD PREVENTION AND CONTROL MEASURES IN MINES

(1) Mine geological disaster monitoring is the basic work in mine geological disaster prevention and control. The main purpose of mine geological disaster monitoring is to understand the changes of mine geological environment in time and space, analyze the relationship between mining and mine geological environment changes, and provide basic reference information for formulating mine geological environmental protection measures and improving mine geological environment. In the specific mine geological disaster prevention and control process, reasonable and effective monitoring technology should be used according to the needs of mine geological environment monitoring, and mine terrain monitoring instruments should be developed. Introduce advanced mining geological environment monitoring technology, such as modern information collection technology, Zigbee wireless networking technology, modern network communication technology, etc., to effectively monitor and prevent mining geological disasters, so as to reduce the casualties and economic losses caused by mining geological disasters.

(2) In order to effectively manage mining geological hazards, it is necessary to do a good job of preventing and controlling crumbling. First, reduce the height of the steps. For areas where there are a lot of weathered and broken or soft structural surfaces, the self-weight should be reduced by using measures to lower the height or slow down the slope, and the height of the steps should be controlled within 9 meters. Second, interception of rolling rocks. For areas where rolling rocks occur frequently, not only do you need to set up warning signs, but you also need to set up intercepting structures at the foot of the slope. For example, production stripping can be dumped to stop rolling rocks and debris at a location away from the foot of the slope. Thirdly, when horizontal blasting operations are carried out at the end of mining, it is necessary to use slope residual cracking blasting and hole-by-hole seismic control blasting technology to alleviate blasting damage to the slope, thereby preventing the generation of crumbling disasters.

(3) The problem of sudden water is one of the key problems in mining geological hazards, which requires corresponding prevention and control measures, which can be carried out in the following aspects. First, mine-waterproofing. In the process of mine waterproofing, measures need to be taken to prevent water from flowing into the mine and to effectively control the inflow. In this way, it can reduce the amount of water gushing into the mine, save the cost of drainage, reduce the cost of coal production and prevent water damage from the root of the problem. Second, mine drainage. In order to remove mine water, drainage ditches, water bins and pumps in mine tunnels can be used.

https://doi.org/10.17993/3cemp.2023.120151.186-205

3.2. MINE GEOLOGICAL ENVIRONMENTAL PROTECTION STRATEGY RULES

(1) In order to effectively protect the mine geological environment, an annual treatment plan should be implemented and a sound monitoring network for the mine geological environment should be established. Dynamic monitoring of mine geological environment, regular reporting of mine geological environment to the competent natural resources department at the county level where the mine is located, and submission of real monitoring information. In addition, the relevant departments should target the mining right holder to fulfill the obligations of mine geological environmental protection and treatment and restoration. And establish a system of supervision and inspection, and use the results of supervision and inspection as the procedure for applying for the continuation, change and transfer of mining rights. In addition, the sampling of corporate information social disclosure should be a key review. The relevant departments also need to use remote sensing monitoring data of the mining geological environment to detect and dispose of illegal mining practices in a timely manner.

(2) Rely on scientific and technological progress and technological innovation to improve the level of geological environmental protection in mines. Strengthen the development and application of new technologies, new techniques and new methods, increase investment in science and technology, and promote technological progress in comprehensive utilization of resources. In addition, funding should also be strengthened for research fields such as mining environmental geology. Research on the impact of mine development on the geological environment and prevention and control technologies, research on the treatment of the three wastes of mining industry and waste recovery and comprehensive utilization technologies, and research on advanced mining and selection technologies and processing and utilization technologies, so as to achieve the purpose of protecting the geological environment of mines.

(3) Comprehensive consideration of mineral resources planning, mine geological environment protection and management planning, ecological environment planning, etc. Government departments should give priority to the geological environment management of mines within the visual range of the "three zones and two lines". For the remaining scattered resources, the mountain does not have the conditions for restoration and there are potential safety hazards, if it is in line with the mineral resources plan, the mining rights should be reset. If it does not conform to the mineral resources plan, it can be disposed of by the relevant government department where the mine is located in accordance with the principles of government-led, expert-evaluated, strict control and clear responsibility, and the corresponding residual resources will be used for geological environment treatment.

https://doi.org/10.17993/3cemp.2023.120151.186-205

4. EVALUATION SYSTEM FOR THE UTILITY OF GEOLOGICAL DISASTER PREVENTION AND CONTROL AND GEOLOGICAL ENVIRONMENTAL PROTECTION STRATEGIES

In order to effectively and accurately analyze the specific utility of the developed geohazard prevention and geological environmental protection strategies for the study area and to establish a reasonable evaluation index system, the prerequisite is to solve several problems. The first is the scientific nature of the indicators. The second is the operability and measurability of the indicators. The third is the conciseness of the metrics. Based on the above starting point, after fully considering the impact of the geological features of the mine on geological hazards and geological environment, reference is made to the sustainable development index system proposed by various units and departments. And using the method of the United Nations Commission on Sustainable Development menu-type multi-indicator type indicator system, it is proposed to construct the evaluation index system of mine geohazard condition and geological environmental level from two major first-level indicators and 13 second-level indicators. Thus, the specific utility of geological disaster prevention and control and geological environmental protection strategies can be verified. The weights of the indicators in this index system can also be obtained through hierarchical analysis [31-33]. For details, see Table 2.

Table 2 Evaluation system of the utility of geological disaster prevention and control and geological environmental protection strategies

Level 1 indicators	Secondary index
Level of geological hazards	Collapse volume/m^3
	Landslide volume/m^3
	Debris flow material source volume/t
	Ground collapse range/m^2
	Number of tailing pond leaks/time
Level of geological environment	Water quality index
	Soil quality index
	Vegetation coverage rate/%
	Land leveling degree
	Mining recovery rate/%
	Tailings utilization rate/%
	Mineral processing water reuse rate/%
	Ecological restoration rate/%

A percentage system was implemented, and the linear weighted average method was used for the calculation of the scores [34-35]. Based on the calculation principles

https://doi.org/10.17993/3cemp.2023.120151.186-205

and formulas of the weighted average method, a linear calculation model was established in turn. Based on the assessment team members' weights, the score of each index element in the lowest level index was calculated, and the calculation model was.

$$Q_j = \sum_{i=1}^{n} P_{ij} \cdot Q_{ij} \quad (1)$$

Where P_{ij} represents the rating of each member of the group for level j indicators; Q_{ij} represents the weight of the assessment group members for each indicator element of level j indicators; i represents the number of assessment group members, $i = 1, 2, ?n$.

Based on the index content weights, the weighted average score of each level index is calculated from bottom to top, and the calculation model is:

$$S_w = \sum_{c=1}^{n} P_{cw} \cdot Q_{cw} \quad (2)$$

Where P_{cw} represents the score of each indicator in level w; Q_{cw} represents the weight of each indicator in level w; c represents the number of indicators, $c = 1, 2, ?n$.

The index is scored according to the description of the index, and the score is written in the score column, and the full score of each level 2 index is 100. The score of each level 1 indicator can be calculated by adding up the scores of all level 2 indicators. Among them, the degree of geohazard is a negative indicator, and the smaller the value of the second-level indicator, the lower the degree of geohazard, and the larger the value of the first-level indicator. The specific scoring method for each indicator is described below.

(1) Collapse volume: full marks are given when the volume of collapse is below 5m^3, otherwise 0~90 marks are given as appropriate.

(2) Landslide volume: when the volume of landslide is less than 10m^3, full marks will be given, otherwise 0~90 marks will be given as appropriate.

(3) Mudslide source volume: full marks are given when the mudslide source volume is less than 3t, and 0~90 marks are given if the requirement is not met.

(4) The scope of ground collapse: when the ground collapse range of less than 6m^2 scored full points, otherwise 0 ~ 90 points as appropriate.

(5) tailing pond leakage number: full marks when the tailing pond leakage number is less than 4 times, otherwise 0~90 marks will be given as appropriate.

(6) Water quality index: full marks when the water quality index is above 7.9, and 0~90 marks when the requirement is not met.

(7) Soil quality index: full score when the soil quality index is greater than 8.2, and 0~90 points as appropriate when the requirement is not met.

https://doi.org/10.17993/3cemp.2023.120151.186-205

(8) Vegetation cover: full marks are given when the vegetation cover of the mine area reaches 35% or more, otherwise 0~90 marks are given as appropriate.

(9) Land leveling: full marks will be awarded when the land leveling exceeds 9, otherwise 0~90 marks will be awarded as appropriate.

(10) Mining recovery rate: full marks will be awarded when the mining recovery rate is above 85%, otherwise 0~90 marks will be awarded as appropriate.

(11) Tailings utilization rate: full marks are given when the tailings utilization rate is above 85%, and 0~90 marks are given as appropriate when the requirement is not met.

(12) Repeated utilization rate of mineral processing water: full marks will be given when the repeated utilization rate of mineral processing water is more than 80%, otherwise 0~90 marks will be given as appropriate.

(13) Ecological recovery rate: the ecological recovery rate of the geological environment is relative to the ecological damage. The destruction of the ecology of the mining environment can be understood as a change in the structure, degradation or loss of function of the ecosystem, and disturbance of relationships. Ecological restoration is about restoring the rational structure, efficient functions and harmonious relationships of the ecosystem [35]. Ecological restoration is essentially the process of orderly succession of the destroyed ecosystem, a process that makes it possible to restore the ecosystem to its native state [36]. However, due to the complexity of natural conditions and the influence of human society's orientation toward the use of natural resources, ecological restoration does not mean that the restored ecosystem can or must be left in its original state in all cases. Ecological restoration rate refers to the percentage of the restored area to the total area of the abandoned land after the implementation of ecological engineering for those abandoned land caused by mining stripping land, waste mine pits, tailing pits, tailings, slag, gangue, and wastewater sediment of ore dressing and washing. For the historical ecological problems, the indicator reaches 30% or more full marks [37]. For the area of mining and restoration at the same time, full marks will be given when the indicator reaches 70% or more; otherwise, 0~90 marks will be given as appropriate.

To sum up, when the final score range of the primary index is 90~100, the geohazard situation and geological environmental condition of the study target are excellent, and the disaster level and environmental level are set to class I [38-39]. It indicates that the strategy utility can be given full play, and has played an excellent prevention and protection effect. When the final score range is 80~90, the geohazard situation and geological environmental condition of the study target is good, and the grade is set to class II. It indicates that the prevention and protection effect of the strategy is strong. When the score range is 65~80, the geohazard situation and geological environmental condition of the mine is average, and the level of disaster and environmental level is set to class III. This indicates that the strategy has certain effect of geological disaster prevention and geological environmental protection. When the score range is 55~65, the geohazard situation and geological environmental condition of the area is poor, and the level is set to class IV, which

https://doi.org/10.17993/3cemp.2023.120151.186-205

means the developed strategy is not able to manage and protect the geohazard and ecological environment well. When the score range of the primary index is 0~55, the target's geohazard situation and geological environmental condition is extremely poor. The hazard level and environment level are set to class V, which means the developed strategy basically does not have any effect on the management and protection of geological hazards and ecological environment in the study area.

5. ANALYSIS AND DISCUSSION

By consulting the statistical yearbook of the city where the mine is located, the data of each index of the five divisions of the target mine were collected one year before and one year after the implementation of the strategy. After scoring with the utility evaluation system, the scores of geohazard degree and geological environmental level before and after the implementation of the strategy were obtained. After dividing the scores according to the levels, the utility evaluation results of the prevention and protection strategies were obtained as shown in Figure 2.

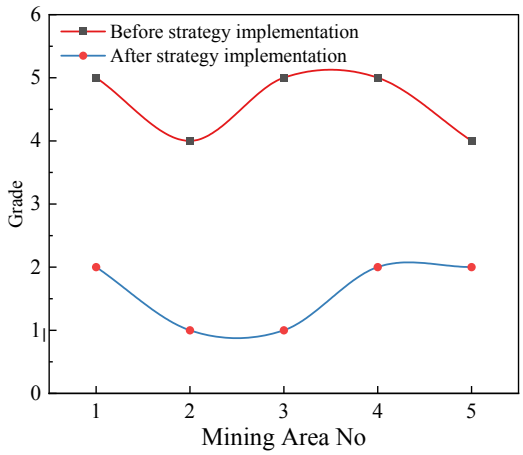

(a) Geological disaster prevention and control utility

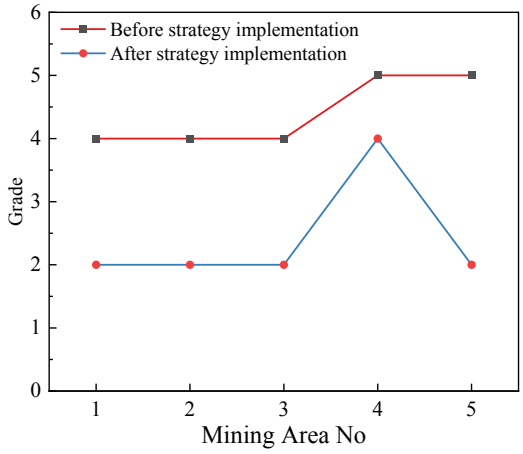

(b) Utility of geological environmental protection

https://doi.org/10.17993/3cemp.2023.120151.186-205

Figure 2 Schematic diagram of the utility of geohazard control and geological environmental protection strategies

By comparing the changes in the level of geological hazards before and after the implementation of the strategy in Figure 2(a), it can be seen that the level of geological hazards in the five mining areas in this study area before the geological hazard control measures were carried out were V, IV, V, V and IV levels. This indicates that the mine is characterized by geological lithology such as large changes in Devonian, Carboniferous, Permian and Triassic lithologies, increased muddy interlayers, fine-grained shoulder structure, tuff-bearing components and other geological lithologies, resulting in a large footprint for crumbling and slag disposal and a large impact area for ground collapse, leading to a relatively serious degree of geological disaster.

Through targeted and reasonable geological hazard prevention and control measures for different mining areas, the level of geological hazards in the target area is upgraded to class II, I, I, II and II.

For small collapse hazards in No.1 mine, the slope is cut to reduce the load and remove dangerous rocks to release the danger, and the large collapse is reinforced by anchor spraying method as a whole, paying attention to strengthen drainage. The surface of the collapsed mining area is re-leveled, the collapse pits and cracks are filled in, and interception ditches and drainage ditches are constructed to prevent the ground from pouring into the mine and causing landslides. The level of geological disaster was changed from V to II.

For the No. 2 mine, advanced mining technology is implemented, such as: using waste rock, slag or tailing sand to fill the mining area, which controls and slows down the surface subsidence and the collapse behavior and magnitude of the mining area, and also reduces the problem of massive land encroachment by slag and tailing sand, which changes the level of geological hazard from IV to I.

Due to the poor background conditions of the geological environment in mine site No. 3, the catchment area, landslide volume and relative height difference are large, and the tailings pond leakage breach is obvious. Therefore, anti-slip rock stacks, anti-slip retaining walls, anti-slip piles and anti-slip piles were constructed at different locations of the landslide body in the mine. The overall anchoring measures were taken to improve the friction and shear strength of the landslide body and enhance the overall stability of the landslide body. And plant trees and grass on the surface of the landslide body to prevent soil erosion and mudflow on the slope surface. During the operation of the tailing ponds, supervision and management were strengthened, and proper operation was carried out to prevent tailings sand overflow and dam failure more effectively. For tailings ponds that have breached or have the potential to breach, works were arranged to repair and reinforce them. When building new tailing ponds, extra attention was paid to site selection, and tailing ponds were built at locations higher than the highest flood level in the calendar year, and it was explicitly prohibited to dig and build tailing ponds on existing river floodplains. The tailing ponds were designed with safety and stability in mind, ensuring that the drainage and flood

https://doi.org/10.17993/3cemp.2023.120151.186-205

control systems were complete, and that quality and quantity were maintained during construction to prevent a recurrence of the dam failure and change the geological hazard level from V to I.

The main problem of No. 4 mine is the large size of the landslide, and part of the shed is built under the slag pile. When heavy rain comes, it will cause casualties, and there is a huge potential danger of collapse above the shed. Therefore, measures were taken to reduce the height or slow down the slope to reduce the self-weight, and the height of the steps was controlled within 9 meters, and intercepting structures were set at the foot of the slope, which greatly solved the problem of landslide and reduced the degree of geological disaster. The level of geological hazard was changed from class V to class II.

No. 5 mine is a large state-owned enterprise, according to the demand of mine geological environment monitoring, using reasonable and effective monitoring technology, developing mine terrain monitoring instruments, introducing advanced mine geological environment monitoring technology, constructing slag mudflow and accident pool collapse potential hazard management project, effectively monitoring and preventing mine geological disasters, controlling the magnitude of ground collapse, not only basically eliminating the previous existence of slag mudflow and accident pool collapse potential hazard, but also reducing the casualties and economic losses caused by mine geological disasters, changing the level of geological disasters from class IV to class II.

From the change of geological environmental level grade before and after the implementation of geological environmental protection strategy (see Figure 2(b)), it can be seen that before the implementation of geological environmental protection strategy, the geological environmental level grades of the five mining areas were class IV, IV, IV, V and V, with poor ecological and environmental benefits. And one year after the implementation of the geological environmental protection strategy, the level of geological environmental level in the study area increased dramatically to class II, II, II, I, II. It shows that the protection strategy has given full play to its effectiveness and has excellent protection and restoration effects. It has greatly improved the ecological environment of the mine and brought the ecology into balance gradually.

For example, the No. 1 mine area has a high number of mining pits, resulting in low vegetation coverage, serious soil erosion and high content of heavy metals in water and soil. By implementing the annual treatment plan, a sound monitoring network of mine geological environment is established. Dynamic monitoring of the geological environment of mines, regular to the mine location of the county-level natural resources authorities, report the geological environment of mines, submit real monitoring information. Using the remote sensing monitoring data of mine geological environment, illegal mining behaviors are detected and disposed of in a timely manner. It not only effectively protects the geological and ecological environment of mines, but also makes the mining and other activities of mines more standardized, so that the level of geological environment level rises from class IV to class II.

https://doi.org/10.17993/3cemp.2023.120151.186-205

In dealing with the geological environment of No. 2 mine, we based on the results of the surface engineering treatment. Considering the mineral resources planning, mine geological environment protection and treatment planning, ecological environment planning, etc., the geological environment treatment of the mine within the visual range of "three zones and two lines" was completed as a priority. The geological environment level of the mine has been upgraded from class IV to class II.

The heavy metal pollution of water and soil in No. 3 mine is more serious. On the basis of the project to raise and reinforce the tailing reservoir dike, the tailing sand was covered with soil 0.5~0.8m thick. Then trees, grass and crops were planted, so that the ecosystem of the mine was well protected. And gradually restored to a benign ecological level, so that the level of its geological environmental level rose from IV to II.

In response to the low vegetation cover in mine 4, the same conservation strategy as in mine 3 was adopted. Trees, grass and crops are planted in the 0.5~0.8m thick overburden. After mining, treatment and protection at the same time, the mine is reclaimed and re-greened in time to change the vicious ecosystem structure, restore the ecological function and stabilize the ecological balance. Make the ecosystem structure of the mine more reasonable, more efficient in function and more coordinated in relationship. Eventually, the level of geological environment will be upgraded from V to I.

For mine site No. 5, the accident pond is used for primary sedimentation treatment of mine pit wastewater. The suspended mineral dust in the water is retained and the pollution of surface water is reduced. A water purification system is also specially designed for the drainage outlet of the tailing pond to realize the recycling of water resources and the recovery of residual gold. Through the treatment of the three mining wastes and waste recycling, the purpose of protecting the geological environment has been truly realized, and the level of geological environment has been upgraded from V to II.

6. DISCUSSION

The geohazard prevention and control measures and geological environment protection strategies proposed in this paper for the geological features of mines, although certain research results have been achieved, there are still many shortcomings, mainly containing the following points.

(1) Only the geological and geomorphological characteristics of the study area were analyzed, which is not comprehensive. In future research, it is necessary to face several mines, summarize the geohazard prevention and control measures and geological environment protection methods of different mines, and propose remediation strategies suitable for universal mines.

(2) The geohazard prevention and control measures are mainly based on the management of geological hazards such as landslides, landslides and debris flows, and the geological environment protection strategy is mainly based on restoring the

https://doi.org/10.17993/3cemp.2023.120151.186-205

quality of water and soil, expanding vegetation coverage and improving resource utilization. Although the ecological environment of the mine is protected to a certain extent, the ways and means are too single, so in the future research, we should consider many aspects and integrate multiple perspectives to explore a more systematic protection scheme.

7. CONCLUSION

The large-scale development and utilization of mineral resources has made human beings enjoy the benefits brought by natural resources while also suffering from a series of bitter consequences such as environmental pollution, resource destruction and ecological degradation. Especially, some local mining areas with large-scale predatory mining have caused serious geological disasters and geological environment problems. Therefore, the research on the prevention and control of geological disasters and the protection of geological environment seems to be urgent. Therefore, based on the geological features of the study area, this paper formulates the details of the prevention and control measures for mine geological hazards and the protection strategy for mine geological environment, and uses the hierarchical analysis method to obtain the index weights of the utility evaluation system. The utility of the proposed measures and strategies was verified through the scoring results and ranking of the linear weighted average method, and the following research findings were obtained.

(1) According to the needs of mine geological environment monitoring, use reasonable and effective monitoring technology, develop mine terrain monitoring instruments, and introduce advanced mine geological environment monitoring technology, which can effectively monitor and prevent mines geological disasters.

(2) For the collapse phenomenon of geological disasters, the ground collapse magnitude can be greatly controlled by reducing the height of steps, intercepting rolling rocks, using slope residual cracking blasting and hole-by-hole seismic reduction control blasting technology, and preventing the occurrence of slope erosion, slope debris flow, tailing sand spill and dam failure. The volume of landslide is less than $10m^3$ and the ground collapse area is less than $6m^2$.

(3) the establishment of a sound mine geological environment monitoring network, regular to the county-level natural resources departments in charge of the mine location, report the mine geological environment. It can obtain the impact of mine development on the geological environment in real time and take relevant initiatives in time to increase the greening coverage of the collapse area, protect the ecosystem and restore it to a benign ecological level, and optimize the geological environment level from class IV, IV, IV, V, V to class II, II, I, II respectively. Raise the water quality index and soil quality index to above 7.9 and 8.2 respectively.

https://doi.org/10.17993/3cemp.2023.120151.186-205

8. DATA AVAILABILITY STATEMENT

The original contributions presented in the study are included in the article/ supplementary material, further inquiries can be directed to the corresponding author.

REFERENCES

(1) Meyer J M, Kokaly R F, Holley E. **Hyperspectral remote sensing of white mica: A review of imaging and point-based spectrometer studies for mineral resources, with spectrometer design considerations[J]**. *Remote Sensing of Environment*, 2022, 275:113000-.

(2) Toro N, E Gálvez, Saldaa M, et al. **Submarine mineral resources: A potential solution to political conflicts and global warming[J]**. *Minerals Engineering*, 2022, 179:107441-.

(3) Peng L I, Cai M F. **Challenges and new insights for exploitation of deep underground metal mineral resources[J]**. *Transactions of Nonferrous Metals Society of China*, 2021, 31(11):3478-3505.

(4) Shang Y, Lu S, Gong J, Liu R, Li X, Fan Q. **Improved genetic algorithm for economic load dispatch in hydropower plants and comprehensive performance comparison with dynamic programming method**. *Journal of Hydrology*, 2017, 554: 306-316.

(5) He F, Liu C, Liu H. **Integration and Fusion of Geologic Hazard Data under Deep Learning and Big Data Analysis Technology[J]**. *Complexity*, 2021.

(6) Lu S, Shang Y, Li W, Peng Y, Wu X. **Economic benefit analysis of joint operation of cascaded reservoirs**. *Journal of Cleaner Production*, 2018, 179:731-737.

(7) Kharisova O, Kharisov T. **Searching for possible precursors of mining-induced ground collapse using long-term geodetic monitoring data[J]**. *Engineering Geology*, 2021, 289:106173-.

(8) Liang Y, Chen X, Yang J, et al. **Analysis of ground collapse caused by shield tunnelling and the evaluation of the reinforcement effect on a sand stratum[J]**. *Engineering Failure Analysis*, 2020, 115:104616.

(9) Shang Y, You B, Shang L. **China's environmental strategy towards reducing deep groundwater exploitation**. *Environmental Earth Sciences*, 2016, 75:1439.

(10) Chernos M, Macdonald R J, Straker J, et al. **Simulating the cumulative effects of potential open-pit mining and climate change on streamflow and water quality in a mountainous watershed[J]**. *Science of The Total Environment*, 2022, 806:150394-.

(11) Zuo Z, Guo H, Cheng J, et al. **How to achieve new progress in ecological civilization construction? – Based on cloud model and coupling coordination degree model[J]**. *Ecological Indicators*, 2021, 127(1):107789.

(12) Poveda-Bautista R, Gonzalez-Urango H, E Ramírez-Olivares, et al. **Engaging Stakeholders in Extraction Problems of the Chilean Mining Industry through a Combined Social Network Analysis-Analytic Network Process Approach[J]**. *Complexity*, 2022, 2022.

(13) Zhang J, Shang Y, Cui M, Luo Q, Zhang R. **Successful and sustainable governance of the lower Yellow River, China: A floodplain utilization approach**

https://doi.org/10.17993/3cemp.2023.120151.186-205

for balancing ecological conservation and development, *Environment, Development and Sustainability*, 2022, 24：3014-3038.

(14) Mvdha B, Mbb C, Kd A, et al. **Changes in soil microbial communities in post mine ecological restoration: Implications for monitoring using high throughput DNA sequencing[J]**. *Science of The Total Environment*, 2020, 749.

(15) Chun S J, Kim Y J, Cui Y, et al. **Ecological network analysis reveals distinctive microbial modules associated with heavy metal contamination of abandoned mine soils in Korea[J]**. *Environmental Pollution*, 2021, 289:117851-.

(16) Yan Y, Mao K, Shen X, et al. **Evaluation of the influence of ENSO on tropical vegetation in long time series using a new indicator[J].** *Ecological Indicators*, 2021, 129:107872.

(17) Che D. **Investigation of Vegetation Changes in Different Mining Areas in Liaoning Province, China, Using Multisource Remote Sensing Data[J]**. *Remote Sensing*, 2021, 13.

(18) Yan M, Li T, Li X, et al. **Microbial biomass and activity restrict soil function recovery of a post-mining land in eastern Loess Plateau[J]**. *Catena*, 2021, 199(8):105107.

(19) Midor K, Biay W, Rogala-Rojek J, et al. **The Process of Designing the Post-Mining Land Reclamation Investment Using Process Maps. Case Study[J]**. *Energies*, 2021, 14.

(20) Xiao W, Zhang W, Ye Y, et al. **Is underground coal mining causing land degradation and significantly damaging ecosystems in semi-arid areas? A study from an Ecological Capital perspective[J]**. L*and Degradation & Development*, 2020, 31.

(21) Ross M, Nippgen F, Mcglynn B L, et al. **Mountaintop mining legacies constrain ecological, hydrological and biogeochemical recovery trajectories[J]**. *Environmental Research Letters*, 2021, 16(7):075004.

(22) Arifeen H M, Chowdhury M S, Zhang H, et al. **Role of a Mine in Changing Its Surroundings—Land Use and Land Cover and Impact on the Natural Environment in Barapukuria, Bangladesh[J]**. *Sustainability*, 2021, 13.

(23) Liu H, Yan F, Tian H. **Towards low-carbon cities: Patch-based multi-objective optimization of land use allocation using an improved non-dominated sorting genetic algorithm-II[J]**. *Ecological Indicators*, 2022, 134(4):108455.

(24) Bernatek-Jakiel A, Jakiel M. **Identification of soil piping-related depressions using an airborne LiDAR DEM: Role of land use changes[J]**. *Geomorphology*, 2021, 378.

(25) Wang Y, Yu L. **Can the current environmental tax rate promote green technology innovation? - Evidence from China's resource-based industries[J]**. *Journal of Cleaner Production*, 2020, 278(2):123443.

(26) Wei J, Zhang J, Wu X, et al. **Governance in mining enterprises: An effective way to promote the intensification of resources—Taking coal resources as an example[J]**. *Resources Policy*, 2022, 76:102623-.

(27) Ghahramani A, Bennett M L, Ali A, et al. **A Risk-Based Approach to Mine-Site Rehabilitation: Use of Bayesian Belief Network Modelling to Manage Dispersive Soil and Spoil[J]**. *Sustainability*, 2021, 13.

https://doi.org/10.17993/3cemp.2023.120151.186-205

(28) ALvarez-Ayuso E, Murciego A. **Stabilization methods for the treatment of weathered arsenopyrite mine wastes: Arsenic immobilization under selective leaching conditions[J]**. *Journal of Cleaner Production*, 2021, 283:125265.

(29) Wang Z, Zhou W, Jiskani I M, et al. **Annual dust pollution characteristics and its prevention and control for environmental protection in surface mines[J].** *Science of The Total Environment*, 2022, 825:153949-.

(30) Cheng X, Yang F, Zhang R, et al. **Petrogenesis and geodynamic implications of Early Palaeozoic granitic rocks at the Hongshi Cu deposit in East Tianshan Orogenic Belt, NW China: Constraints from zircon U–Pb geochronology, geochemistry, and Sr–Nd–Hf isotopes[J]**. *Geological Journal*, 2020, 55(3).

(31) JG López, Sisto R, Benayas J, et al. **Assessment of the Results and Methodology of the Sustainable Development Index for Spanish Cities[J]**. *Sustainability*, 2021, 13.

(32) Lee K H, Noh J, Khim J S. **The Blue Economy and the United Nations' sustainable development goals: Challenges and opportunities[J]**. *Environment international*, 2020, 137:105528.

(33) Karymbalis E, Andreou M, Batzakis D V, et al. **Integration of GIS-Based Multicriteria Decision Analysis and Analytic Hierarchy Process for Flood-Hazard Assessment in the Megalo Rema River Catchment (East Attica, Greece) [J]**. *Sustainability*, 2021, 13.

(34) Xie X, Xu Y, Dong Z Y, et al. **Multi-Objective Coordinated Dispatch of High Wind-Penetrated Power Systems against Transient Instability[J]**. *IET Generation Transmission & Distribution*, 2020, 14(19).

(35) Sun Q, Yang G, Zhou A. **An Entropy-Based Self-Adaptive Node Importance Evaluation Method for Complex Networks[J]**. *Complexity*, 2020, 2020(10):1-13.

(36) Chen A, Yang X, Guo J, et al. **Synthesized remote sensing-based desertification index reveals ecological restoration and its driving forces in the northern sand-prevention belt of China[J]**. *Ecological Indicators*, 2021, 131:108230-.

(37) Dong S, Wang G, Kang Y, et al. **Soil water and salinity dynamics under the improved drip-irrigation scheduling for ecological restoration in the saline area of Yellow River basin[J]**. *Agricultural Water Management*, 2022, 264.

(38) Kaseng, F., Lezama, P., Inquilla, R., y Rodriguez, C. (2020). **Evolution and advance usage of Internet in Peru**. *3C TIC. Cuadernos de desarrollo aplicados a las TIC*, 9(4), 113-127. https://doi.org/10.17993/3ctic.2020.94.113-127

(39) Che Xiangbei,Li Man,Zhang Xu,Alassafi Madini O. & Zhang Hongbin.(2021). **Communication architecture of power monitoring system based on incidence matrix model**. *Applied Mathematics and Nonlinear Sciences*(1). https://doi.org/10.2478/AMNS.2021.1.00098.

10. CONFLICT OF INTEREST

The authors declare that the research was conducted in the absence of any commercial or financial relationships that could be construed as a potential conflict of interest.

/10/

RESEARCH ON THE DEVELOPMENT AND APPLICATION OF CNN MODEL IN MOBILE PAYMENT TERMINAL AND BLOCKCHAIN ECONOMY

Hongyan Liu*

Suqian University, School of Foreign Studies, Suqian, Jiangsu, 223800, China

yanyanhong20221123@163.com

Reception: 17/11/2022 **Acceptance**: 17/01/2023 **Publication**: 15/02/2023

Suggested citation:

L., Hongyan (2023). **Research on the development and application of CNN model in mobile payment terminal and blockchain economy**. *3C Empresa. Investigación y pensamiento crítico, 12(1)*, 207-224. https://doi.org/10.17993/3cemp.2023.120151.207-224

ABSTRACT

As the most widely used payment method at this stage, mobile payment is more and more closely related to the blockchain economy. Traditional methods lack a certain degree of accuracy. This research proposes a feature-based and sequential-based Bilateral AM (BAM) and Convolutional Neural Network (CNN)-gated recurrent unit for the development and application of mobile payment and blockchain economy (Gated Recurrent Unit, GRU) hybrid model (BAM-CNN-GRU), select 5 feature parameters with high correlation with the blockchain for multivariate prediction. The introduction of BAM can automatically quantify the correlation between the input variables and the blockchain, and strengthen the expression of historical key information on the predicted output; the introduction of CNN can extract high-dimensional features that reflect the non-stationary dynamic changes of the blockchain. The proposed hybrid model achieves good results in both single-step and multi-step long-term series and multivariate input blockchain prediction. Compared with the other six methods, MAE is reduced by 75.45%, 64.74%, 62.84%, respectively. 59.41%, 45.54%, 44.16%. Compared with the BAM-GRU model, the CNN-GRU model, the GRU model, the LSTM model, the support vector machine SVM model and the BP model, the prediction accuracy of the hybrid model has been greatly improved, and it has a broader application prospect.

KEYWORDS

BAM-CNN-GRU; Mobile payment; Blockchain; Model comparison

https://doi.org/10.17993/3cemp.2023.120151.207-224

PAPER INDEX

https://doi.org/10.17993/3cemp.2023.120151.207-224

1. INTRODUCTION

Mobile payment refers to a network payment method in which users use mobile smart devices to complete transaction payments. According to different supporting technologies, mobile payment is roughly divided into two modes: remote payment and near-field payment. Common payment methods include online banking payment and QR code payment [1-2]. At present, the two major characteristics of mobile payment are convenience and security, among which the core factor affecting the development of mobile payment business is security [3-5]. Mobile intelligent terminals are usually bound by software and hardware disadvantages such as computing power and storage capacity, which lead to great restrictions on the data processing capacity of the terminal equipment [6]. Therefore, most mobile application software programs have to implement the corresponding functions of the client by invoking remote cloud services [7]. As far as mobile banking is concerned, the mobile banking APP of the mobile client must complete the application functions such as transfer and wealth management by calling the cloud service of mobile banking remotely [8]. Usually, in the process of invoking cloud services from a mobile application, the remote application server will first verify the identity of the end user and even the legitimacy of the device to ensure the security of the transaction process.

In some developed countries abroad, such as Japan, South Korea, Europe and the United States, the development of NFC payment is very rapid [9]. The mobile payment service provided by NTTDoCoM, the largest mobile communication operator in Japan, uses the Felica technology developed by Scmy, which uses mobile phones with Felica chips. Its virtual wallet has contactless payment functions such as ticket purchase and bus ride [10]. At the beginning of the promotion of mobile wallets, NTTDoCoM installed NFC card readers for merchants for free, and made profits in the form of monthly rent [11]. In the same year, NTTDoCoM acquired one-sixth of the shares of Sumitomo's credit card business, so that the virtual wallet can be bound one-to-one with bank cards. Bank card payment [12]. In 2006, the company extended the NFC mobile payment service to the consumer credit field and launched the DCMX mobile credit card. It can be said that mobile phones and wallets have been equated in Japan, and shops of all sizes support NFC mobile payment [13]. In Europe, Nokia and Philips are the main leaders of NFC mobile payment. The unified currency model in the euro area has removed many obstacles to mobile payment. Some operators have independent bank-authorized payment authority, which is very beneficial for banking services, making Europe's near-field communication technology research and development ahead of the world [14]. The first NFC experiment in Europe was launched in March 2005 at the Frankfurt Metro, where passengers can use a Nokia 3220 mobile phone equipped with an NFC module to purchase tickets at subway stations. The world's first multi-application NFC experiment began in October 2005. Smartphones embedded with Philips' NFC chips were distributed to hundreds of French citizens of Ona participating in the experiment. During the experiment, they can be used in specific shopping malls, hotels and cinemas. After swiping the phone to pay, the experiment went on for six months. In Munich, Germany, local residents can use mobile phones equipped with NFC chips to swipe their cards to travel or enter

https://doi.org/10.17993/3cemp.2023.120151.207-224

tourist attractions[15]. After Google released HCE technology in 2013, foreign markets responded quickly: Spanish bank Bankmeter was the first to announce HCE support earlier in 2014: TH coffee shop offered HCE-based NFC payments, and the coffee shop invested People praised that the American coffee chain SimplyTapp also received a large amount of investment to study the development of HCE and set out to standardize HCE [16]. In the field of card organization, Royal Bank of Canada has put the development of HCE on the agenda, Zaputal One of North America and Barclays of the United Kingdom have all adjusted and applied HCE technology. Apple launched the Apple Pay service in IOS8, which supports the NFC+AppleID transaction method, which greatly promoted the development of NFC payment [17-18].

This paper proposes a hybrid model based on Bilateral AM (BAM) and CNN-GRU (Gated Recurrent Unit) to make multivariate predictions on the blockchain, an important factor influencing mobile payment, and selects the same as the blockchain. Other relevant feature performance parameters are used as input [19-20] and the blockchain is used as output. First, a feature AM is introduced on the input side to quantify the relationship between performance parameters and blockchain output; then, through the powerful feature extraction capability of one-dimensional (One Dimensional, 1D-CNN), the local information between the input information is mined. Finally, a time-series feature AM is introduced on the output side to strengthen the expression of important information at historical moments for the prediction output [21]. The purpose is to establish a prediction model that depends on each performance parameter under the time node, explore the connection between mobile payment and blockchain, and accurately predict the impact of blockchain on mobile payment.

2. PRINCIPLES OF DEEP LEARNING MODELS

2.1. 1D-CNN

The convolutional neural network performs high-dimensional feature mapping on the original data through local connection and weight sharing, and mines the feature information of the original data. 1D-CNN is mainly used to process time series, and its internal structure is shown in Figure 1. For processing time series, the convolution layer extracts the translation features of the data in the direction, and extracts the effective feature vectors on the time series. From an accurate point of view, the analysis is to perform cyclic product and summation on the data. The specific expression is as follows:

$$y(\mu) = w(\mu) * v(\mu) = \sum_{\tau=0}^{N} w(\mu - \tau) v(\tau) M \quad (1)$$

where y, w, v are sequences, μ is the number of convolutions, and M is the length of v.

https://doi.org/10.17993/3cemp.2023.120151.207-224

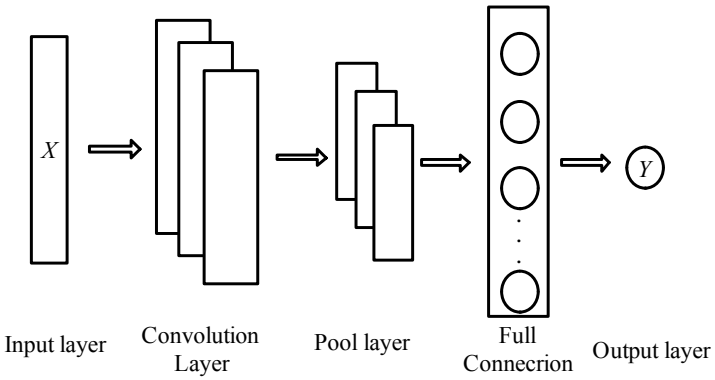

Fig.1 1D-CNN

2.2. ATTENTION MECHANISM (AM)

Attention mechanism (AM)is a reserve apportionment model that pretends the attention of the human brain. The human brain can pay attention to some important information of interest and ignore irrelevant information at a certain time node. The attention distribution of different information can be more important. The attention model assigns greater weight to important information through this probability distribution mode to different information, thereby improving the model's extraction of important information and improving the prediction accuracy of the model. In time series prediction, the AM can not only act on the input side to reflect the degree of correlation between each feature parameter and the predicted output, but also on the output side to weight the information at the historical moment to highlight the information related to the current prediction. Important time point information [22].

2.3. GRU

GRU network is an improved mode of LSTM network [23]. By optimizing the gate structure inside the LSTM network, the input gate and the forget gate are combined into an update gate, and the state of the neuron is mixed with the state of the hidden layer. The update gate inputs the combined matrix of the input vector and X_t and the state memory variable h_{t-1} of the previous moment into the update gate after the nonlinear transformation of the activation function, and determines the degree to which the information of the previous moment is retained to the current state [24]. The reset gate combines the previous state information with the current state information in the manner of $1 - z_t$ times h_{t-1} and z_t times $\tilde{h}_t$ as the output of the current state information. The GRU structure network is exposed in Fig. 2, and expression is revealed in Equation (2) [25].

https://doi.org/10.17993/3cemp.2023.120151.207-224

$$\begin{cases} r_t = \sigma\left(W_t \cdot \left[h_{t-1}, X_t\right]\right) \\ z_t = \sigma\left(W_z \cdot \left[h_{t-1}, X_t\right]\right) \\ \tilde{h}_t = \tanh\left(W_h \cdot \left[r_t \times h_{t-1}, X_t\right]\right) \\ h_t = \left(1 - z_t\right) \times h_{t-1} + z_t \times \tilde{h}_t \end{cases} \tag{2}$$

In Figure 2 and equation (2): X_t, h_{t-1}, r_t, z_t, $\tilde{h}_t$, h_t are the input information, the state information of the previous moment, the update gate, the reset gate, the input vector and the previous hidden layer state information, respectively. Summary, the output of the current hidden layer state; W_r, W_z, $W_{\tilde{h}}$ are the trainable weight matrices of each gate state; σ is represented as the Sigmoid function.

3. MOBILE PAYMENT AND BLOCKCHAIN PREDICTION MODEL BASED ON BAM AND CNN-GRU HYBRID MODEL

3.1. MOBILE PAYMENT AND BLOCKCHAIN PREDICTION MODEL

Mobile payment is not only carefully associated the operation of various components in the system, but also related to the blockchain environment, such as the sharing economy, etc., but these are external factors and will indirectly affect the operation status of each component in the system , and then make the mobile payment security change. Therefore, according to the internal operation rules of mobile payment, we select sharing economy N_1, Internet of Things N_2, cloud computing W_f, artificial intelligence p_o and digital economy T_o, five performance parameters that are highly correlated with mobile payment as input parameters, and establish the following parameters at each time point. The relevant performance parameters are dependent on the predictive model.

Note that the time series set of mobile payment is $Y = [y1, y2, \ldots, yT] \in RT$, and the time series of the five blockchain-related features of the input terminals N1, N2, Wf, po and To are X = [x 1， x 2， ...， xT] = [x(1)， x(2)， ...， x(5)]′, the specific expansion can be represented by equation (3). Where $xt = [xt(1), xt(2), \ldots, xt(5)]$ represents a set of five related feature parameter variables measured at time t, $x(k) = [x1(k), x2(k), \ldots, xT(k)]$ is represented as the measured value sequence of the k-th relevant feature parameter at T historical moments.

https://doi.org/10.17993/3cemp.2023.120151.207-224

$$X = \begin{bmatrix} x_1^{(1)} & x_1^{(2)} & ? & x_1^{(5)} \\ x_2^{(1)} & x_2^{(2)} & ? & x_2^{(5)} \\ ? & ? & ? & ? \\ x_T^{(1)} & x_T^{(2)} & ? & x_T^{(5)} \end{bmatrix} \in R^{T\times 5} \quad (3)$$

where k (1≤k≤5) of x(k) represents the number of features. (t 1≤t≤T) of xt represents the value of the corresponding feature at time t.

According to the five characteristic performance parameter variables related to the blockchain as the input, and the blockchain at the corresponding time as the output of the model, the multi-variable prediction of mobile payment in the future time and time is carried out. Let the mapping function of the entire model be Fθ, then the predicted value represents for:

$$x_{?1} = F_\theta\left(x_1, x_2, \ldots, x_T\right) \quad (4)$$

In order to obtain the relationship between each feature performance parameter and the blockchain at the current moment and the dependency in the time series information, a bilateral attention and CNN-GRU hybrid model combining the feature AM and the time series AM are adopted. Multivariate forecasting methods. A feature AM is presented on the input side to calculate the degree of correlation between the exhaust gas temperature value to be measured and other related performance parameters, so that the features with strong correlation are assigned greater weights, while the weak or irrelevant features are weakened. information. CNN mines the high-dimensional features of the input information through operations such as convolution pooling, and effectively reduces the error caused by manual feature extraction. The time series AM is introduced at the output, independently select the information of the historical key moment with high correlation with the current moment, and solve the problem of GRU network for long-term sequence.

3.2. FEATURE AM

In order to obtain the degree of correlation between the five feature parameters and the blockchain to be tested, a feature AM is introduced on the input side, and the multi-layer perceptron calculation method is used to quantify the attention weights of various features. The model is shown in Figure 2 [26]. ?

https://doi.org/10.17993/3cemp.2023.120151.207-224

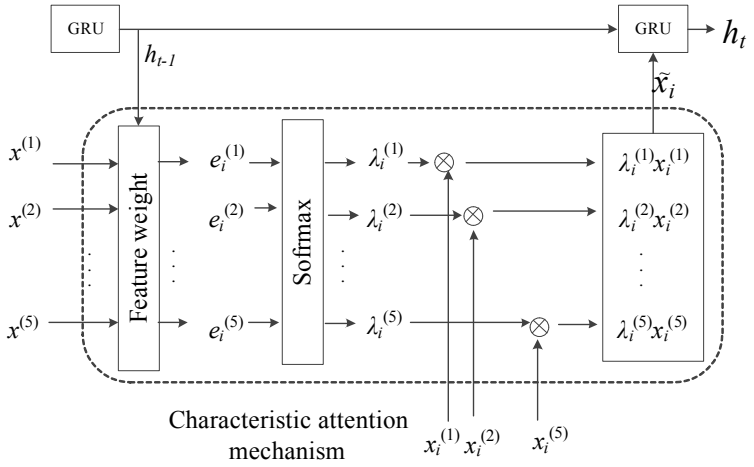

Fig. 2 Characteristic attention model

The five feature parameters at time t are combined with the hidden layer state ht - 1 at the preceding time as the input of the feature AM. The weight of each feature parameter at this time is calculated by formula (5), and the Softmax function is used. Normalize e(k) t according to formula (6), namely:

$$e_t^{(k)} = \boldsymbol{V}_{\mathrm{e}}^{\mathrm{T}} \operatorname{relu}\left(\boldsymbol{W}_{\mathrm{e}} \boldsymbol{h}_{t-1} + \boldsymbol{U}_{\mathrm{e}} x^{(k)} + \boldsymbol{b}_{\mathrm{e}}\right) \tag{5}$$

$$\lambda_t^{(k)} = \frac{\exp\left(e_t^{(k)}\right)}{\sum_{k=1}^{5} \exp\left(e_t^{(k)}\right)} \tag{6}$$

where V_e, W_e and U_e are the weight matrices of the feature AM, and be is the corresponding bias term.

The feature parameter weight λ(k) t assigned according to the feature AM is multiplied by the corresponding feature input x(k) t to obtain the associated features x̃ with different feature contribution rates, so as to perform strong and weak correlation for each feature Different expressions can be specifically expressed as:

$$\tilde{x}_t = \left(\lambda_t^{(1)} x_t^{(1)}, \lambda_t^{(2)} x_t^{(2)}, \ldots, \lambda_t^{(5)} x_t^{(5)}\right)^{\mathrm{T}} \tag{7}$$

Finally, the input information $\tilde{x}$ is iterated by formula (8) to ensure that the hidden layer state h_t at each time t contains the associated feature x:

$$\boldsymbol{h}_t = f_{\mathrm{GRU1}}\left(\boldsymbol{h}_{t-1}, \tilde{x}_t\right) \tag{8}$$

where f_{GRU1} represents the network unit of the input side GRU.

3.3. CNN LAYER

The introduction of the 1D-CNN network is to extract the feature of the relationship information processed by the feature AM, map the relationship information to the high-dimensional feature space, mine the deep-level feature information, and extract the

https://doi.org/10.17993/3cemp.2023.120151.207-224

key node information in the feature variables [27]. The convolutional layer extracts features, the pooling layer filters the information, and the dropout layer discards some neurons to prevent the network from over-fitting due to over-reliance on some local features [28]. In this paper, at the connection between 1D-CNN and GRU, the maximum pooling layer and dropout layer are used to replace the fully connected layer. This operation not only reduces the data dimension input to the GRU network, reduces the network training time, but also preserves the time series information of the input features to the greatest extent, ensuring the prediction accuracy of the model. The output feature vector Rφ of the 1D-CNN network can be expressed as:

$$\boldsymbol{C} = \mathrm{relu}\left(\boldsymbol{H} \otimes \boldsymbol{W} + \boldsymbol{b}_1\right) \tag{9}$$

$$\boldsymbol{P} = \left(\boldsymbol{C}\right) + \boldsymbol{b}_2 \tag{10}$$

where H is the set of hidden layers of the input side GRU, the outputs C and P are the outputs of the convolutional layer and the pooling layer, respectively; W and b_1 are the weights and bias terms of the convolutional layer; b_2 is the bias of the pooling layer. set item; the output of the CNN layer is:

$$\boldsymbol{R}_{\varphi} = \left[r_1, r_2, \ldots, r_{\mathrm{t},}, \ldots, r_{\varphi}\right] \tag{11}$$

3.4. TEMPORAL AM

Since the predicted value of the blockchain is greatly affected by the historical state, and the hidden layer state information at different times has different effects on the output of the current network, in addition, the network output is more inaccurate due to the increase in the length of the time series. In order to enable the predicted value to process historical state information autonomously and to strengthen the expression of important historical moment information with high output relevance at the current moment, this paper introduces a time-series AM for the output side of the GRU network. The specific structure is shown in Figure 4 [29].

https://doi.org/10.17993/3cemp.2023.120151.207-224

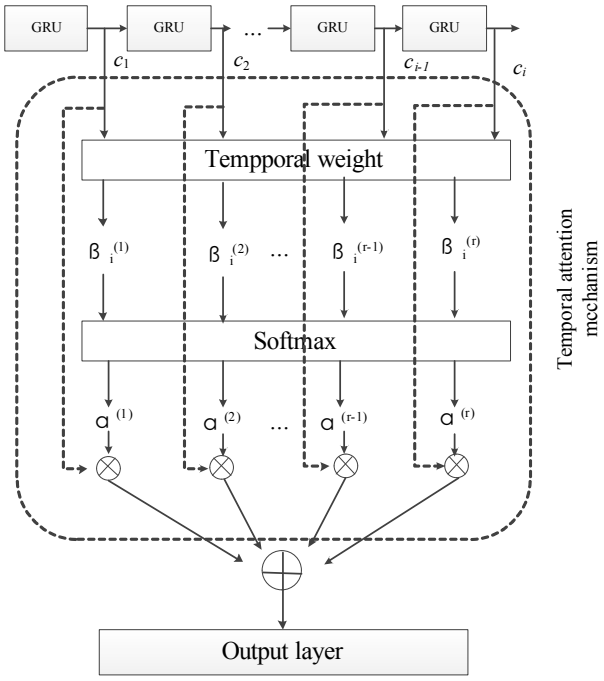

Fig.4 Temporal attention model

The time series information of the hidden layer state including the relationship information processed by the CNN is the vector Rφ, which is used as the input of the GRU network, and its output is expressed as C, and the output at time t is expressed as:

$$c_t = f_{\mathrm{GRU2}}\left(c_{t-1}^{'}, r_t\right) \tag{12}$$

where f_{GRU2} represents the network unit of the output side GRU.

The input of the time-series AM is the output vector C processed by the GRU network on the output side. According to the AM, the historical state information at each time point is weighted and expressed, and the Softmax function is continued to normalize the weight βtT, and record each moment in history. The correlation degree of the hidden layer state information to the output at the current moment is αφt [30].

$$\beta_t = \boldsymbol{V}_{\mathrm{c}}^{\mathrm{T}} \mathrm{relu}\left(\boldsymbol{W}_{\mathrm{c}} c_t + b_{\mathrm{c}}\right) \tag{13}$$

$$\alpha_t = \frac{\exp\left(\beta_t\right)}{\sum_{j=1}^{T} \exp\left(\beta_t\right)} \tag{14}$$

where V_c and W_c are the corresponding weight matrices of time-series attention, and b_c is the bias.

αt indicates that the correlation degree of each hidden layer state information in the history to the prediction output at the current time is quantified, and all α φt and the corresponding hidden layer state information are weighted and summed, and the output of the time series AM at time t is l_t express.

https://doi.org/10.17993/3cemp.2023.120151.207-224

$$l_t = \sum_{i=1}^{T} \alpha_t c_t \tag{15}$$

Finally, the output information is dimensionally transformed through the fully connected layer network, and the final blockchain prediction value ỹT + 1 is obtained:

$$\tilde{y}_{T+1} = F_\theta\left(x_1, x_2, \ldots, x_T\right) = \tanh\left(W_y l_t + b_y\right) \tag{16}$$

where W_y and b_y are the weights and biases for dimensional changes in the network.

3.5. HYBRID MODEL BASED ON BAM AND CNN-GRU

The structure of the entire prediction model is shown in Figure 5. After the input information is processed by the feature AM, relevant information with different weights is obtained, and then it enters the GRU network for learning. The output of the network is used as the input of 1D-CNN. In the processing of the pooling layer and dropout layer, the information enters the GRU network on the output side, and the hidden layer state is used as the input of the timing AM on the output side. . In the training process of this model, the Adam (Adaptive Moment Estimation) optimization algorithm is selected to update and learn various parameters, and the loss function of the model adopts the mse function, as shown in formula (17) [31].

$$Loss = \frac{1}{n}\sum_{i=1}^{n}\left(y_i - \tilde{y}_i\right)^2 \tag{17}$$

In the formula, n is the number of samples; y_i is the actual value of the blockchain, and $\tilde{y}_i$ is the blockchain value predicted by the model.

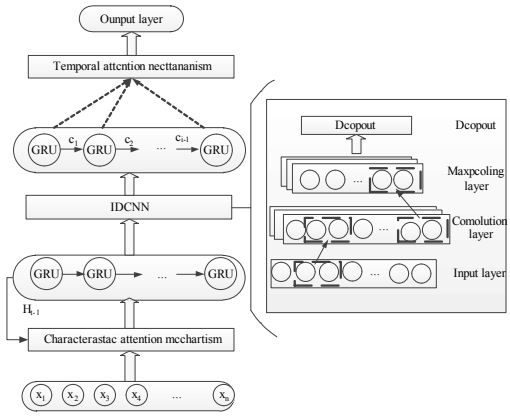

Fig.5 Model structure based on BAM and CNN-GRU

3.6. ERROR ANALYSIS

In this paper, Mean Absolute Error (MAE), Root Mean Square Error (RMSE) and Mean Absolute Percentage Error (MAPE) are used as indicators to evaluate the prediction accuracy of each model. The expressions are as follows shown [32]:

https://doi.org/10.17993/3cemp.2023.120151.207-224

$$MAE = \frac{1}{n}\sum_{i=1}^{n}|y_i - \hat{y}_i| \quad (18)$$

$$RMSE = \sqrt{\frac{1}{n}\sum_{i=1}^{n}(y_i - \hat{y}_i)^2} \quad (19)$$

$$MAPE = \frac{1}{n}\sum_{i=1}^{n}\frac{|y_i - \hat{y}_i|}{y_i} \times 100\% \quad (20)$$

4. MODEL PREDICTIONS

For the sample data, the mixed model of BAM and CNN-GRU, BAM-GRU model, CNN-GRU model, GRU model, LSTM model, BP model and SVM model proposed in this paper are used to predict the output. The training and test sets are split in a ratio of 4:1. The GRU network and LSTM network structure in the above models all use the same hyperparameters (the number of hidden layer neurons is 128, the sliding window is 6, the number of iterations is 400, and the batch_size is 256); the AM uses relu as the internal structure[33-34]. Activation function, and use Softmax function to normalize it; the convolution layer of CNN network is set to 64, the convolution kernel is 1, the maximum pooling layer is 4, and the dropout is 0.3; BP network adopts the number of hidden layer neurons is a network structure of 8; the SVM network adopts radial basis kernel function.

According to the three evaluation indicators selected in this paper, the prediction performance and accuracy of different models 566 are evaluated. The experimental comparison results are shown in Table 1.

Table 1 Comparison of prediction accuracy of different models

Model	AE	RMSE	MAPE
BP	4.48	4.57	0.67
SVM	3.12	3.76	0.48
LSTM	2.96	3.47	0.46
GRU	2.71	3.17	0.42
CNN-GRU	2.02	2.98	0.32
BAM-GRU	1.97	2.39	0.30
Proposed	1.10	1.81	0.17

From the information in Table 1, it can be concluded that the prediction accuracy of the algorithm in this paper is better than that of the other 6 algorithms. Compared with the other 6 methods, MAE is reduced by 75.45%, 64.74%, 62.84%, 59.41%, 45.54%, 44.16%; RMSE Compared with the other 6 methods, the reductions were 60.39%, 51.86%, 47.84%, 42.90%, 39.26%, 24.27%, respectively; compared with the other 6 methods, MAPE decreased by 0.50%, 0.31%, 0.29%, 0.25%, 0.15%, 0.13%.

https://doi.org/10.17993/3cemp.2023.120151.207-224

Comprehensive analysis, the algorithm in this paper has obvious reduction in the three error evaluation indicators, indicating that the algorithm in this paper has a relatively good prediction performance. According to the analysis of the error results, the machine learning methods (BP, SVM) are not as outstanding as the deep learning methods (LSTM, GRU, CNN-GRU, BAM-GRU, Proposed) in terms of prediction effect. From Table 1, it can be seen that the CNN-GRU model and the BAM-GRU model have a significant decrease in the three error evaluation indicators compared with the single deep learning model, indicating that the CNN network can be performed by the high-dimensional local dependence on the multivariate input performance parameters. Mining to improve the prediction performance of the model. By introducing BAM, the degree of correlation between input features and output is quantified on the input side, and the contribution rate of each performance feature is adaptively extracted, which effectively avoids the output expression of non-critical information and secondary feature information, and strengthens important information for prediction. The output side strengthens the correlation expression of historical important information for the current prediction output, reduces information omission and memory decay, and solves the prediction lag problem of LSTM and GRU single network models.

The comparison of the prediction output curves of each model on the test set is shown in Figure 6 and Figure 7. It can be seen from Figure 6 that the traditional machine learning method has a poor prediction effect, and the predicted output value has a low degree of fitting with the actual value. The error is large.

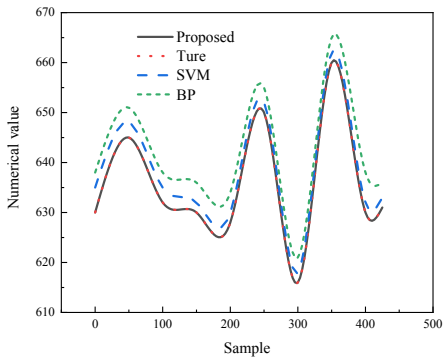

Fig. 6 Comparison of predicted values between the proposed model and the machine learning model

Figure 7 shows that the prediction output of the deep learning model has a high degree of fitting with the actual value, which proves the advantages of deep learning in time series prediction. The hybrid model of BAM and CNN-GRU proposed in this paper can not only accurately predict in a slightly smooth interval, but also accurately capture the changing law of mobile payment in high and low peak time periods. The other four learning methods can also accurately predict the blockchain in some intervals, but there is still a certain gap between their prediction performance and the method proposed in this paper when the blockchain peaks and fluctuates violently. It shows that the model proposed in this paper has good performance in establishing long-term dependencies of time series and effectively capturing the dynamic changes

https://doi.org/10.17993/3cemp.2023.120151.207-224

of blockchain. By accurately predicting the blockchain, the change rule of the blockchain can be known in advance, and compared with the corresponding baseline value to check whether the difference is within the maximum range allowed for operation, and then take the corresponding maintenance strategy. In addition, when it is found that there is a sudden and substantial rise and fall of the blockchain within a certain predicted time period, it is necessary to consider whether the mobile payment operation is normal, and investigate the reasons in time to avoid security accidents.

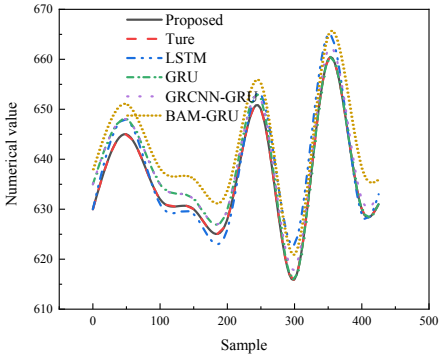

Fig. 7 Comparison between the predicted value of the proposed model and the deep learning model

5. CONCLUSION

Aiming at the relationship between mobile payment and blockchain economy, this paper proposes a hybrid model based on BAM and CNN-GRU to improve the prediction accuracy and stability of the long mobile payment model. The following conclusions are drawn: (1) The prediction accuracy of the hybrid model of BAM and CNN-GRU proposed in this paper is better than that of the other six algorithms. Compared with the other six methods, the MAE is reduced by 75.45%, 64.74%, 62.84%, respectively. 59.41%, 45.54%, 44.16%; (2) The hybrid model of BAM and CNN-GRU proposed in this paper can not only accurately predict in a slightly smooth interval, but also accurately capture the change law of mobile payment in high and low peak periods; (3) The CNN network can improve the prediction performance of the model by mining the high-dimensional local dependencies of multivariate input performance parameters.

6. CONFLICT OF INTEREST

The authors declared that there is no conflict of interest.

https://doi.org/10.17993/3cemp.2023.120151.207-224

REFERENCES

(1) Ayu, W., Siti, S., & Muhardono, A. (2021). **Consumer Behavior Toward Adoption of Mobile Payment: A Case Study in Indonesia During the COVID-19 Pandemic**. *Journal of Asian Finance Economics and Business*(4). https://doi.org/10.13106/JAFEB.2021.VOL8.NO4.0581

(2) Yang, S., Lu, Y., Gupta, S., Cao, Y., & Zhang, R. (2012). **Mobile payment services adoption across time: An empirical study of the effects of behavioral beliefs, social influences, and personal traits**. *Computers in Human Behavior*, 28(1), 129-142. https://doi.org/10.1016/j.chb.2011.08.019

(3) Fang, C. C., Liou, J., Huang, S. W., Wang, Y. C., & Tzeng, G. H. (2021). **A Hybrid, Data-Driven Causality Exploration Method for Exploring the Key Factors Affecting Mobile Payment Usage Intention**. https://doi.org/10.3390/math9111185

(4) Tao, & Zhou. (2013). **An empirical examination of continuance intention of mobile payment service**. *Decision Support Systems*. https://doi.org/10.1016/j.dss.2012.10.034

(5) Zhou, T. (2011). **An Empirical Examination of Initial Trust in Mobile Payment**. *Internet Research Electronic Networking Applications & Policy*, 77(2), 1519-1531. https://doi.org/10.1108/10662241111176353

(6) Chakraborty, D., Siddiqui, A., Siddiqui, M., Rana, N. P., Dash, G., & Timmermans, H. (2022). **Mobile payment apps filling value gaps: Integrating consumption values with initial trust and customer involvement**. *Journal of Retailing and Consumer Services*, 66. https://doi.org/10.1016/j.jretconser.2022.102946

(7) Handarkha, Y. D., Harjoseputro, Y., Samodra, J. E., & Irianto, A. (2021). **Understanding proximity mobile payment continuance usage in Indonesia from a habit perspective**. *Journal of Asia Business Studies*. https://doi.org/10.1108/JABS-02-2020-0046

(8) Zhao, Y., & Bacao, F. (2021). **How Does the Pandemic Facilitate Mobile Payment? An Investigation on Users' Perspective under the COVID-19 Pandemic**. *International Journal of Environmental Research and Public Health*, 18(3), 1016.https://doi.org/10.3390/ijerph18031016

(9) Fan, L., Zhang, X., Rai, L., & Du, Y. (2021). **Mobile Payment: The Next Frontier of Payment Systems? *- an Empirical Study Based on Push-Pull-Mooring Framework***. *Journal of Theoretical and Applied Electronic Commerce Research*, 16(2), 179-193. https://doi.org/10.4067/S0718-18762021000200112

(10) Becker, Michel, Stolper, Oscar and Walter, Andreas. **What Drives Mobile Banking Adoption? – An Empirical Investigation Using Transaction Data** *Zeitschrift für Bankrecht und Bankwirtschaft*, vol. 34, no. 1, 2022, pp. 1-11. https://doi.org/10.15375/zbb-2022-0103

(11) He, X., Gupta, S., Hu, Y., & Zhao, L. (2021). **Understanding the dual role of habit in cross-channel context: an empirical analysis of mobile payment**. *International Journal of Mobile Communications*, 19(1), 1. https://doi.org/10.1504/IJMC.2021.10034125

(12) Kang, D. (2021). **Research on Implicit Attitude and Behavioral Tendency of College Students to Mobile Payment**. *Psychology of China*, 3(2), 103-110. https://doi.org/10.35534/pc.0302014

(13) **Geomagnetic secular variation anomalies in relation to the recent crustal movement in the southwestern region of Japan: Sumitomo, Norihiko, 1981 Bull. Disaster Prevent. Res. Inst. Kyoto Univ., 30(4)(274):97–130**, *Deep Sea Research Part B. Oceanographic Literature Review*, Volume 28, Issue 12, 1981, Page 874, ISSN 0198-0254, https://doi.org/10.1016/0198-0254(81)91240-1

(14) Kim, H. R., Zhou, W., & Yun, S. (2021). **Mobile Payment Service Continuance Usage Intention and Network Externality: Focused on Self and Functional Congruity**. *THE JOURNAL OF SOCIAL SCIENCE*, 28(1), 176-197. https://doi.org/10.46415/jss.2021.03.28.1.176

(15) Ramli, F., & Hamzah, M. I. (2021). **Mobile payment and e-wallet adoption in emerging economies: A systematic literature review**. *Journal of Emerging Economies and Islamic Research*, 9(2), 1. https://doi.org/10.24191/jeeir.v9i2.13617

(16) Wong, D., Liu, H., Yue, M. L., Sun, Y., & Zhang, Y. (2021). **Gamified Money: Exploring the Effectiveness of Gamification in Mobile Payment Adoption among the Silver Generation in China**. *Information Technology & People, ahead-of-print(ahead-of-print)*. https://doi.org/10.1108/ITP-09-2019-0456

(17) Cacioppo, J. T., Petty, R. E., & Kao, C. F. (1984). **The efficient assessment of NFC**. *Journal of Personality Assessment*, 48(3), 306-307. https://doi.org/10.1207/s15327752jpa4803_13

(18) Sehaqui, H., Qi, Z., & Berglund, L. A. (2011). **High-porosity aerogels of high specific surface area prepared from nanofibrillated cellulose (NFC)**. *Composites Science & Technology*, 71(13), 1593-1599. https://doi.org/10.1016/j.compscitech.2011.07.003

(19) Christidis, K., & Devetsikiotis, M. (2016). **Blockchains and Smart Contracts for the Internet of Things**. *IEEE Access*, 4, 2292-2303. https://doi.org/10.1109/ACCESS.2016.2566339

(20) Yli-Huumo, J., Ko, D., Choi, S., Park, S., & Smolander, K. (2016). **Where Is Current Research on Blockchain Technology?—A Systematic Review**. *PLoS ONE*, 11(10), e0163477. https://doi.org/10.1371/journal.pone.0163477

(21) Wang, Y., Yan, J., Yang, Z., Wang, J., & Geng, Y. (2021). **A novel 1DCNN and domain adversarial transfer strategy for small sample GIS partial discharge pattern recognition**. *Measurement Science and Technology*, 32(12), 125118 (125110pp). https://doi.org/10.1088/1361-6501/ac27e8

(22) Palomino, A. J., Marfil, R., Bandera, J. P., & Bandera, A. (2011). **A Novel Biologically Inspired AM for a Social Robot**. *Eurasip Journal on Advances in Signal Processing*, 2011(1), 1-10. https://doi.org/10.1155/2011/841078

(23) Jiang, Y., Zhao, M., Zhao, W., Qin, H., Qi, H., Wang, K., & Wang, C. (2021). **Prediction of sea temperature using temporal convolutional network and LSTM-GRU network**. *Complex Engineering Systems*, 1(2), -. https://doi.org/10.20517/ces.2021.03

(24) Huang, G., Li, X., Zhang, B., & Ren, J. (2021**). PM2.5 Concentration Forecasting at Surface Monitoring Sites Using GRU Neural Network Based**

on Empirical Mode Decomposition. *Science of The Total Environment*, 768(3), 144516. https://doi.org/10.1016/j.scitotenv.2020.144516

(25) Xu, S., Li, J., Liu, K., & Wu, L. (2019). **A Parallel GRU Recurrent Network Model and its Application to Multi-Channel Time-Varying Signal Classification**. *IEEE Access*, PP(99), 1-1. https://doi.org/10.1109/ACCESS.2019.2936516

(26) Shen, X., Shao, Z., & Tian, Y. (2014). **Built-Up Areas Extraction by Textural Feature and Visual AM**. *Acta Geodaetica et Cartographica Sinica*. https://doi.org/10.13485/j.cnki.11-2089.2014.0131

(27) Razavian, A. S., Azizpour, H., Sullivan, J., & Carlsson, S. (2014). C**NN Features off-the-shelf: an Astounding Baseline for Recognition**. *IEEE*. https://doi.org/10.1109/CVPRW.2014.131

(28) Yan, C., Pang, G., Bai, X., Liu, C., Xin, N., Gu, L., & Zhou, J. (2021). **Beyond triplet loss: person re-identification with fine-grained difference-aware pairwise loss**. *IEEE Transactions on Multimedia*. https://doi.org/10.1109/TMM.2021.3069562

(29) Ning, X., Gong, K., Li, W., & Zhang, L. (2021). **JWSAA: joint weak saliency and attention aware for person re-identification**. *Neurocomputing*, 453, 801-811. https://doi.org/10.1016/j.neucom.2020.05.106

(30) Chen Wang, Xiang Wang, Jiawei Zhang, Liang Zhang, Xiao Bai, Xin Ning, Jun Zhou, Edwin Hancock, **Uncertainty estimation for stereo matching based on evidential deep learning**, *Pattern Recognition*, Volume 124, 2022, 108498, ISSN 0031-3203, https://doi.org/10.1016/j.patcog.2021.108498.

(31) Liu Ying, Zhang Qian Nan, Wang Fu Ping, Chiew Tuan Kiang, Lim Keng Pang, Zhang Heng Chang, Chao Lu, Lu Guo Jun & Ling Nam. **Adaptive weights learning in CNN feature fusion for crime scene investigation image classification**. *Connection Science*. https://doi.org/10.1080/09540091.2021.1875987

(32) Yu, Z., Li, S., Sun, L. N. U., Liu, L., & Haining, W. **Multi-distribution noise quantisation: an extreme compression scheme for transformer according to parameter distribution**. https://doi.org/10.1080/09540091.2021.2024510

(33) Dewani, A., Memon, M. A., y Bhatti, S. (2021). **Development of computational linguistic resources for automated detection of textual cyberbullying threats in Roman Urdu language**. *3C TIC. Cuadernos de desarrollo aplicados a las TIC*, 10(2), 101-121. https://doi.org/10.17993/3ctic.2021.102.101-121

(34) Guan Fuyu,Cao Jie,Ren Jie & Song Wenli.(2021). **The teaching of sports science of track and field-based on nonlinear mathematical equations**. *Applied Mathematics and Nonlinear Sciences*(1). https://doi.org/10.2478/AMNS.2021.2.00155.

/11/

THE IMPACT OF REFORM ON THE ECONOMIC GROWTH TRAJECTORY OF SUB-SAHARAN AFRICA

Islam Abdelbary*

Assistant Professor of Economics at the Arab Academy for Science and Technology, Alexandria 5310002, Egypt

l.abdelbary@aast.edu

Reception: 27/11/2022 **Acceptance**: 22/01/2023 **Publication**: 15/02/2023

Suggested citation:

A., Islam (2023). **The Impact of Reform on the Economic Growth Trajectory of Sub-Saharan Africa**. *3C Empresa. Investigación y pensamiento crítico, 12(1)*, 226-241. https://doi.org/10.17993/3cemp.2023.120151.226-241

ABSTRACT

The research examines why sub-Saharan African (SSA) nations have seen unsatisfactory economic development by assessing the reform programmes implemented during the last three decades. Based on an enhanced neoclassical growth model framework generated from a dynamic panel for 12 African nations from 1995 to 2019 using data from the LSDCV dynamic panel. The findings revealed that insufficient changes, particularly in governance and the institutional environment, had been implemented. Stability in the macroeconomic environment, structural reform, and physical infrastructure are all necessary for an efficient reform process and development of the developing world's growth prospects. Reform implies that it is political, social, and economical simultaneously. Political and economic reform should be carried out in tandem.

KEYWORDS

Development, Sub-Saharan Africa, institutions, reform policy, panel data, Economic growth

PAPER INDEX

https://doi.org/10.17993/3cemp.2023.120151.226-241

1. BACKGROUND

Sub-Saharan Africa (SSA) has lagged in growth performance and, consequently, income per capita compared to other world regions or even other developing regions [1]. There are also marked differences in income per capita across space and time in SSA. For instance, over the period 1970-2013, the average income per capita of the wealthiest state in the region, Seychelles, of US$ 7,100 was more than a factor of 54 of the poorest country, Ethiopia, whose average income per capita was only US$160.

Moreover, Africa's share in the global economy has dropped significantly during the past 50 years regarding the gross domestic product (GDP), exports, and foreign direct investment (FDI). For instance, its global GDP share declined from around 3.5% in 1950 to 2.5% in 2000 [2]. The decrease in Africa's share of world export and FDI is even more drastic. Export as a percentage of world export fell from about 7% to 2% (a 70% fall), while FDI declined from 5.5% to 1% in the same period. The deterioration of the continent's importance in the world economy appears in its global GDP share in purchasing power parity (PPP) terms, which dropped by more than 40% between 1950 and 2000 [1].

These poor economic indicators led to a series of socioeconomic and political reform programs in the 1980s. The domestic context for introducing policy reform was the deepening economic crisis. These development procedures have been implemented to improve the economic environment. These reforms included exchange rate liberalization, tariff reduction, and suspension of 'subsidies' [3]. The effects of these reforms were negligible. Paradoxically, the more African states attempted to impose controls, the more their ability to influence and direct the economy shrank as the informal economy expanded. The most important signal of this loss of state capacity was the tax base's weakening [4].

Therefore, despite various reforms implemented in Sub-Saharan Africa, the region has not experienced significant economic growth compared to other regions in the world. The paper seeks to examine the impact of these reforms on economic growth in the region and to determine the factors that contribute to the growth trajectory. This research seeks to understand better the challenges faced by Sub-Saharan Africa in achieving sustainable economic growth and help policymakers design more effective growth-enhancing policies.

The paper is organized as follows; Section 2 presents the literature review; Section 3 describes the empirical model and estimation approach. Section three explains the estimated results of the growth model, including different composite factors, followed by conclusions and policy implications.

2. LITERATURE REVIEW

The post-independence growth experience of the SSA has been episodic. The period from 1960 to the mid-1970s experienced high growth performance. However, after 1975 there was a sharp deterioration in the SSA economies, with a fall in the average annual per capita GDP growth rate of 1% during 1980-85. The decline

https://doi.org/10.17993/3cemp.2023.120151.226-241

continued reaching approximately 0.1%. Thus the 1980s could be considered as "Africa's lost decade" [5]. The falling trend in real per capita incomes coincided with widening domestic and external imbalances, climbing external debt burdens and debt servicing difficulties, worsening the plight of economically and socially vulnerable groups, sharp drops in world commodity prices and substantial losses in terms of trade of SSA countries. Regarding trade, virtually all African countries' export earnings were hugely concentrated on a few commodities, while for some countries, government revenues relied heavily on export taxes.

These poor economic indicators led to a series of socioeconomic and political reform programs in the 1980s. The domestic context for introducing policy reform was the deepening economic crisis [6]. These development procedures have been implemented to improve the economic environment. These reforms included exchange rate liberalization, tariff reduction, and suspension of 'subsidies' [3]. The effects of these reforms were negligible. Paradoxically, the more African states attempted to impose controls, the more their ability to influence and direct the economy shrank as the informal economy expanded. The most important signal of this loss of state capacity was the tax base's weakening [4].

The reform record was weak and limped along. Several arguments have been provided to explain this failure. Firstly, all SSA countries faced deep-rooted developmental constraints, rapid population growth, low human capital development, inadequate economic and social infrastructure, and structural rigidities. These factors also impede the private sector's development [7-9].

For instance, Nga Ndjobo and Certo Simões [10] re-examined the relationship between African institutions and the migration phenomena, specifically, the business start-up regulations and the brain drain from (SSA) countries towards those in OECD. They found that regulations controlling enterprise creation in SSA countries positively and significantly contribute to brain drain towards OECD countries. Thus, setting up regulations for effective enterprise creation may retain qualified individuals in Africa, mainly entrepreneurs who have in sight the creation of their own businesses. In addition, regulations, governance and the potential contribution of these entrepreneurs should be taken into account in setting up integrated national innovation systems in African countries. Abdelbary and Benhin [11] consistently examined the factors affecting economic growth, focusing on the role of governance based on a neoclassical growth framework for 97 countries. Results showed a positive impact of human capital and investment on growth but a negative impact on regulatory quality. Governance was found to have a significant positive effect on growth in advanced economies but a negative effect in developing countries. The study emphasized the importance of human capital and governance in improving growth prospects and reducing political and economic instability.

Secondly, this economic reform regime's conditional nature, controlled by leading donor countries, significantly inhibited attempts to remedy critical structural deficiencies in these economies. The reform programs with the World Bank and IMF institutions, especially the structural adjustment programs (SAPs) and poverty

https://doi.org/10.17993/3cemp.2023.120151.226-241

reduction strategy papers (PRSP), seem to have contributed to Africa's poor economic performance [12].

Moreover, factors such as ethnic conflicts, political instability, unfavorable security conditions, and protracted civil wars contributed to the region's dismal economic performance before the mid-1990s. The ineffective national government management of the mandated macroeconomic reforms was at the root of their failure. In nearly every SSA country, these development strategies were associated with a particular authoritarian regime type, referred to as "the development dictatorship". African development dictatorships promised high economic performance and rising living standards. In return, they gave themselves the right to maintain a centralized and authoritarian governance system [13].

Leadership problems plague many SSA countries. Besides being authoritarian, African leaders are noted for their high-level corruption and are in no position to promote development [14]. By changing the state's constitution or rigging elections, most African leaders continue to perpetuate themselves in office. For instance, according to Luiz and Charalambous [14], only 7% of African leaders between 1960 and 1999 had left office via free election compared to 60% overthrown in a coup d'état, war or by assassination with an average time in the office of 7.2 years compared to 3.2 years in Europe. Corrupt elongation of office tenure has negatively affected sufficient power, which is essential to building stable and efficient institutions for good governance.

Bräutigam and Knack [15] argue that institutions in many SSA countries are weak due to colonialism, which failed to develop domestic institutions to meet modern states' demands. Acemoglu, Johnson [16] also suggest that Africa is more inferior compared to the rest of the world due to European powers building "extractive colonies". This means the colonialists launched institutions devoid of rules to enforce accountability and transparency, a trend that has persisted even after political independence. Currently, the state in many SSA countries is significantly influenced by neo-patrimonial tendencies and poor policy choices, severely hindering state capacity [17]. These repressive regimes were associated with a lack of efficient political checks and balances systems. In addition, the absence of real electoral democracies had significantly retarded the region's economic performance and was a primary cause of the ineffective reform [18-20]

Furthermore, out of 26 African conflicts between 1963 to 1998, affecting 61% of the continent's total population, seven were classified as inter-state, while 19 happened within countries [14]. This political violence damages the state's capacity and destroys any efforts for serious reform. Also, it disrupts physical and human capital, reduces savings, diverts FDI from national economies, disrupts economic activities and leads to adverse structural change in government expenditures from the provision of civic services to military spending [21].

However, in recent years, especially starting from the mid-2000s, SSA economies have experienced a persistent increase in economic growth. The notable performance has been attributed to reduced conflict, slightly improved political stability, meaningful

https://doi.org/10.17993/3cemp.2023.120151.226-241

domestic economic reforms and a favourable foreign environment with more integration into the global economy [22-24]. Besides, better commodity prices have also been essential in driving growth.

3. METHODOLOGY

Based on the theoretical background of the Solow-Swan growth model and the empirical approach following "Barro-type regression" [25], the new aggregated reform indicators were generated using principal components analysis (PCA) to allow the computation and categorisation of macroeconomic variables into four separate groups.

These original indicators are: the Macroeconomic Stability (M) [26], the Business Environment (B) [27], Infrastructure (F) [28], and Political Institutions (I) [29]. Besides integrating the annual population growth rate ($POP_{i,t}$), and the percentage of oil rent to GDP ($oil_{i,t}$) to control variations in human and natural resource endowments across countries.

Real GDP per capita growth is empirically stated as follows:

$$(Y_{i,t}) = \alpha_0 + \varphi_1 ln(GDP_{i,t-1}) + \theta_1(M_{i,t}) + \theta_2(B_{i,t}) + \theta_3(F_{i,t}) + \theta_4(I_{i,t}) + \theta_5(oil_{i,t}) + \theta_6(POP_{i,t}) + \varepsilon_{i,t} \quad (1)$$

where, $Y_{i,t}$ represents the economic growth rate in the country *i* at time *t*; ln ($GDP_{i,t-1}$) is an *N x 1* vector of logs of initial GDP; α_0 is the intercept, θ_1 to θ_6, are parameters for convergence and the principal components, and $\varepsilon_{i,t}$ is the error term.

The study covered from 1995 to 2019 a host of economic, institutional and social indicators for 12 Sub-Saharan African countries (SSA) based on the data availability [30]. The sources of data include the World Development Indicators (WDI), the Economist Intelligence Unit (EIU) CountryData, UNCTAD, World Statistical Database, and the Worldwide Governance Indicators (WGI).

The analysis used the bias-corrected Least Square Dummy Variable (LSDVC) technique to undertake 100 repetitions to bootstrap the estimated standard errors to deal with endogeneity bias. This is applied because the generalised method of moments (GMM) estimators is not the most suitable procedure and will be highly unstable as the analysis period is relatively large compared to the number of observations. The Least Square Dummy Variable (LSDV) estimator has a relatively low variance and hence can lead to an estimator with a lower root mean square error after the bias is removed [34, 35].

4. EMPIRICAL RESULTS

Before estimating the research model as in Eq.(1), Levin, Lin, and Chu (LLC) and Im, Pesaran, and Shin (IPS) tests have been employed to determine each panel's integration characteristics. The results as reported in Appendix 1, indicate that none of the series has a panel unit root at the level, except for the Business Environment (B)

https://doi.org/10.17993/3cemp.2023.120151.226-241

series, which is stationary in the first difference, I (1). In addition, the Hausman test was used to determine the significance of unobservable individual effects, indicating that a fixed-effect simulation was appropriate instead of pooled OLS and random effects, as in Appendix 2.

Regarding estimating a conditional convergence equation for economic growth in SSA, Table 1, shows that Macroeconomic stability is highly significant and positively related to economic growth. In particular, the components of inflation and deficit. Empirical work such as Lin and Chu [36], Catao and Terrones [37] notes that fiscal deficits are likely to be inflationary only in lower-income countries where the restrictions on government borrowing are the most sharp. Especially in SSA, where the role of supply-side shocks is very critical because of the massive weight of agriculture in the GDP and the consumption basket, so variations of real GDP are expected to be strongly affected by environmental conditions that determine the quality of the harvest [38]. Inflation also shows a government's inability to balance its budget; therefore, the uncertainty of inflation affects the investment decision of foreign businesses [10, 39].

Concerning the Business Environment (B) indicator components, FDI plays a vital role in SSA to encourage growth, as shown in col. (3) Table 1. In many respects, Africa represents a frontier to global capital, seeking out new, growing and emerging markets. While Africa is considered a tiny player in the international market, it will attract foreign enterprises by addressing FDI-friendly policies.

African countries have seen an actual increase in FDI flows since 2000, which saw FDI flows to the region more than double from an average of US$ 14.9 billion (2001–2005) to US$ 30.3 billion (2006–2010). Also, SSA countries are an untapped market of 850 million people, and the returns on investment are already substantially higher here than anywhere else [40].

Table 1. Estimated panel data models for sub-Saharan African countries

	(1) FE Basic Model	(2) Model with M	(3) Model – with B	(4) Model – with P	(5) LSDVC Model with G	(6) LSDVC Model – with G
Macroeconomic stability (M)	**-0.701*** (0.216)**		**-0.76*** (0.179)**	**-0.64*** (0.178)**	**-0.489** (0.224)**	**-0.547** (0.221)**
Exchange rate		-0.071 0.045				
Deficit		**-0.18** (0.076)**				
Public debt		0.155 0.21				
Inflation		**-0.167** (0.084)**				
Unemployment		-0.041 0.466				

https://doi.org/10.17993/3cemp.2023.120151.226-241

Business Environment (B)	0.121 0.183	0.116 0.185		0.101 0.172	-0.009 0.226	-0.011 0.227
FDI			**0.105*** **(0.063)**			
Credit to the private sector			-0.086 0.149			
Concentration index			0.014 0.219			
Infrastructure (F)	0.247 0.17	0.243 0.204	0.051 0.094		0.161 0.224	**0.428**** **(0.257)**
Improved water source				**2.633***** **(0.988)**		
Electricity for the population				-0.507 (0.299)		
Improved sanitation facilities				-1.608 (0.913)		
Governance (G)					0.204 0.284	
Voice and accountability						**0.799*** **0.470**
Political stability						-0.149 (0.319)
Government effectiveness						**-0.975*** **(0.525)**
Regulatory quality						**1.192***** **(0.447)**
Rule of law						**1.384**** **(0.661)**
Control of corruption						-0.441 0.566
Initial GDP	-0.733 0.971	0.428 0.601	0.065 0.154	**0.518***** **(0.191)**	**-2.238***** **(0.603)**	**-2.072***** **(0.625)**
population growth rate	**1.146***** **(0.378)**	**1.038**** **(0.422)**	**0.616**** **(0.310)**	**1.262***** **(0.328)**	0.464 0.514	0.56 0.522
Oil rent to GDP	0.04 0.054	0.036 0.054	0.018 0.046	0.065 0.044	0.016 0.061	0.017 0.064
lag GDP per capita growth real					**0.223***** **(0.04)**	**0.229***** **(0.039)**
F statistic	4.31	3.65	4.96	4.94		
Adjusted R2	0.3	0.31	0.3	0.3		
#observations	288	288	288	288	288	288
#Countries	12	12	12	12	12	12

https://doi.org/10.17993/3cemp.2023.120151.226-241

***, **, and * indicate that the coefficient is significantly different from zero at 1%, 5%, and 10%, respectively

For the Political Institutions indicators, it is worth noting that more governance components are significant. The argument is that institutions are vital for the sustained increase in growth in SSF. Col. (6) shows the effect of the rule of law index, capturing a dimension of governance involving citizens' respect and the state for institutions that govern both social and economic interactions. Its coefficient is positive and statistically significant, with a one-standard-deviation change increasing income by 1.384. The result is firmly in line with Dollar and Kraay [41] and Rodrik, Subramanian [42]. They observed that the same index is positively associated with faster growth and higher per capita income. Therefore, it is acknowledged that enforcement of basic fundamental rights, such as human and property rights, can provide a conducive economic environment for factor accumulation in SSA.

The second dimension of Political Institutions involving the government's capacity to manage its resources and implement sound policies effectively is captured using the regulatory quality index. Its coefficient is positively signed and statistically significant, with a 1.192-factor improvement in income following a one standard deviation change. In other words, adopting less distortionary and market-friendly policies in trade and business is a stimulant for healthy competition and innovation, which are crucial for meaningful and sustainable development.

Excellent institutional quality plays an essential role in the process of economic development. A mixture of a firm rule of law, quality regulatory framework, and political stability are essential ingredients that governments should emphasise and prioritise at all stages of the development process, especially in SSA.

The more surprising finding in Table 1 is that neither the Infrastructure indicator nor its components, except the improved water source, are statistically significant. This outcome suggests that current levels and access to infrastructure in SSA countries have no relationship with economic growth. However, after introducing the governance indicators in col. (6), the infrastructure aggregate variable becomes highly significant. The result is in line with previous literature that found that the institutions and their quality boost economic growth determinants (e.g., Acemoglu, Johnson [43]). Consequently, the results of an insignificant effect of infrastructure access on growth might potentially be associated with Africa's relatively low institutional quality, which might have made infrastructure-less effective as a growth catalyst.

Finally, infrastructure and institution coefficients explain why the SSA region's growth performance has been unsatisfying. Mo [44] accentuates this relationship by associating low growth with corruption. He demonstrated that corruption raises investment costs and creates uncertainty about applying regulations for private investors. Corruption increases public enterprises' capital and operation expenditures of public enterprises, thus limiting private investment through insufficient and low-quality infrastructure [45]. The same outcomes have been drawn about the role of bureaucracy in businesses [46]. Furthermore, the above finding is consistent with

https://doi.org/10.17993/3cemp.2023.120151.226-241

Oyelere (2010) study, as he explained that Sub-Saharan Africa did not experience significant development because of a combination of inferior technology, bad governments, extractive institutions, ineffective policy choices, health crises and poor education.

5. CONCLUSIONS

The current study has confirmed that sub-Saharan African economic performance is improving, and it has highlighted numerous explanatory variables that have notably and favourably affected the post-2000 growth level. However, these rates are still insufficient to allow sub-Saharan African countries to catch up with other emerging economies. This paper seeks to address the possible explanation of why the region's growth performance has been unsatisfactory.

The findings of this study provide important insights into the drivers of economic growth in Sub-Saharan Africa (SSA). The results suggest that several key macroeconomic, business environment, infrastructure, and political institution indicators are significant determinants of economic growth in the region.

The analysis showed that Sub-Saharan African economies must significantly raise their real GDP per capita growth rate on a sustainable basis to be at least par with other developing countries. The regression results indicate that macroeconomic stability should play a vital role in the economic recovery of several Sub-Saharan African economies. It will also be essential to attract an increased inflow of FDI to sustain and broaden sub-Saharan economic growth performance. This can be accomplished by creating a favourable environment for private investment using appropriate macroeconomic policies, ensuring the availability of infrastructure needed and skilled workers and establishing and maintaining an efficient regulatory and justice system that adequately protects property rights.

Macroeconomic stability is one of the critical ingredients of economic growth. The theoretical framework discussed earlier has shown that the macroeconomic environment significantly accelerates economic growth and development. Therefore, sub-Saharan African governments must implement sound monetary and fiscal policies to sustain the growth acceleration episode, which started in the mid-1990s. Reducing the inflation rate and overall deficit may have influenced the recent economic growth acceleration favourably. Therefore, policies and measures that reduce inflation and overall deficit must be sustained to maintain the current economic growth acceleration. Government borrowing from the domestic economy must be limited to provide greater scope for the private sector's bank financing.

The results reveal that the Political Institutions indicators play a crucial role in economic growth in SSA. The rule of law index, which captures citizens' respect for institutions that govern both social and economic interactions, is positively and significantly associated with income. The regulatory quality index, which measures the government's capacity to manage its resources and implement sound policies effectively, is also positively and significantly associated with income. These findings

https://doi.org/10.17993/3cemp.2023.120151.226-241

align with previous literature and highlight the importance of governance quality in promoting economic growth.

The results also show that the infrastructure aggregate variable is insignificant until the governance indicators are introduced. This suggests that current infrastructure access levels in SSA countries have no relationship with economic growth, but the quality of governance may influence the relationship between infrastructure and growth. The finding that infrastructure is less effective as a growth catalyst in the presence of low institutional quality is consistent with previous literature on the relationship between corruption and economic growth.

Political conflicts in many sub-Saharan African countries have been reduced or eliminated. However, it is regrettable that several sub-Saharan African countries are still engulfed in political conflicts. Gains will be distributed widely throughout the continent and attempts to maintain effective macroeconomic policies and structural reforms will become more prosperous if regional and global steps are adopted to prevent future conflicts and settle the existing disputes that continue to erupt in Africa.

6. POLICY IMPLICATIONS

The findings of the study have important implications for policymakers in Sub-Saharan Africa. Firstly, governments should prioritize strengthening their governance structures to create a more conducive economic environment. This includes establishing a strong rule of law, improving the quality of regulation, implementing measures to increase transparency in government processes, reducing corruption, increasing public officials' accountability, and promoting political stability. These institutions are essential for creating a more stable and trustworthy political environment, thus, sustainable economic growth and development.

Secondly, the results suggest that investment in infrastructure is less effective as a growth catalyst in the absence of good governance. Therefore, policymakers should focus on improving governance quality in parallel with infrastructure investment. This would help to ensure that infrastructure projects are executed efficiently and effectively and that the benefits of such projects are more likely to be captured by the broader population. Policies aimed at improving infrastructure could include measures to improve transportation networks, energy supply, and telecommunication systems. For example, investing in roads, bridges, ports, and expanding energy production and distribution could help create a more favourable environment for businesses to operate.

Thirdly, the study highlights the importance of addressing corruption in promoting economic growth in SSA. Governments should prioritize efforts to reduce corruption and improve the overall business environment. This will help to create a more attractive investment climate and lower the costs of doing business, thereby promoting economic growth and development.

Finally, policy makers should prioritize measures that promote macroeconomic stability, such as monetary and fiscal policies that control inflation and manage public

https://doi.org/10.17993/3cemp.2023.120151.226-241

debt levels. Similarly, improvements in the business environment can be seen as key to attracting investment, promoting entrepreneurship, and boosting productivity. Thus, policies should be prioritised to enhance the business environment, such as reducing bureaucratic red tape, improving access to finance, and enhancing property rights protection.

In conclusion, this study's findings highlight the need to implement economic and political reforms concurrently. This is because genuine transformation is more than economic aspects. It is also a profit incentive, governance tool, property rights, allocation of resources, and income equality. Economic strategy formulations addressing these challenges are inextricably linked to their sociopolitical settings and repercussions. Political and economic reform should go together, especially if SSA attains significantly higher and sustained economic growth, which benefits the entire population.

7. STUDY LIMITATION

One of the limitations of this paper is that it primarily focuses on the macroeconomic, institutional, and infrastructure aspects of reform while giving less weightage to the social aspects. The lack of consideration for social indicators, such as social capital, human rights, and ethnic conflict, may lead to an incomplete representation of the whole picture of a country's reform efforts. However, it is possible to consider social aspects such as ethnic conflict and civil wars as part of the Political Institutions (I) indicator. The effect of these conflicts on FDI and infrastructure may also have been considered through the Macroeconomic Stability (M) and Business Environment (B) indicators. These limitations suggest that future studies should consider a more comprehensive approach that considers the social aspect of reforms to provide a more nuanced and accurate understanding of the relationship between reforms and economic growth.

REFERENCES

(1) Giavazzi, F., & Tabellini, G. (2005). **Economic and political liberalizations**. *Journal of monetary economics*, 52(7), 1297-1330.

(2) Tahari, A., Akitoby, B., & Aka, E. B. (2004). **Sources of growth in sub-Saharan Africa.**

(3) Bichaka, F., & Christian, N. (2010). **The Impact of Governance on Economic Growth: Further Evidence for Africa**. *Department of Economics & Finance working paper series, Middle Tennessee State University, Murfreesboro, Tanzania.*

(4) Gordon, D. (1994). **Sustaining economic reform in Sub-Saharan Africa: Issues and implications for USAID, Implementing policy change project (Working Paper No. 6).** *Washington, DC: US Agency for International Development.*

https://doi.org/10.17993/3cemp.2023.120151.226-241

(5) Dressel, B. (2007). **Constitutional Reform, Democratic Governance, and Budgetary Politics: Comparative Cases from Southeast Asia and Sub-Saharan Africa.** *(Doctoral dissertation, Johns Hopkins University).*

(6) Abdelbary, I. (2021). **Reviving Arab reform: Development challenges and opportunities.**

(7) Akpan, G. E., & Effiong, E. L. (2012). **Governance and development performance: a cross-country analysis of Sub-Saharan Africa**. *Governance*, 3(14), 54-67.

(8) Hammami, S. (2019). **Foreign direct investment inflows, intellectual property rights and economic freedom: Empirical evidence from middle- and low-income countries**. *African Journal of Science, Technology, Innovation and Development*, 11(7), 861-871.

(9) Abdelbary, I., & Benhin, J. K. (2019). **Political governance and sustainable development: The role of theory**. I*n Impacts of political instability on economics in the MENA region* (pp. 28-73). IGI Global.

(10) Nga Ndjobo, P. M., & Certo Simões, N. (2021). **Institutions and brain drain: The role of business start-up regulations**. *African Journal of Science, Technology, Innovation and Development*, 13(7), 807-815.

(11) Abdelbary, I., & Benhin, J. (2019). **Governance, capital and economic growth in the Arab Region**. *The Quarterly Review of Economics and Finance*, 73, 184-191.

(12) Markovits, M. T. (2010). **External actors, local participation, and political reform in Africa: Ghana and Senegal compared** *(Doctoral dissertation, University of Pennsylvania).*

(13) Jaunky, V. C. (2013). **Democracy and economic growth in Sub-Saharan Africa: a panel data approach**. *Empirical Economics*, 45, 987-1008.

(14) Luiz, J. M., & Charalambous, H. (2009). **Factors influencing foreign direct investment of South African financial services firms in Sub-Saharan Africa**. *International business review*, 18(3), 305-317.

(15) Bräutigam, D. A., & Knack, S. (2004). **Foreign aid, institutions, and governance in sub-Saharan Africa**. *Economic development and cultural change*, 52(2), 255-285.

(16) Acemoglu, D., Johnson, S., & Robinson, J. A. (2001). **The colonial origins of comparative development: An empirical investigation**. *American economic review*, 91(5), 1369-1401.

(17) Ndulu, B. J., & O'Connell, S. A. (1999). **Governance and growth in sub-Saharan Africa**. *Journal of economic Perspectives*, 13(3), 41-66.

(18) Cowen, M., & Laakso, L. (2002). **Multi-party elections in Africa.**

(19) Lindberg, S. I. (2006). **Opposition parties and democratisation in sub-Saharan Africa**. *Journal of contemporary African studies*, 24(1), 123-138.

(20) Qureshi, J. A. A., Memon, S. B., & Seaman, C. (2021). **Women entrepreneurial leaders as harbingers of economic growth: evidences from an emerging market of South Asia**. *3c Empresa: investigación y pensamiento crítico*, 10(3), 137-169. https://doi.org/10.17993/3cemp.2021.100347.137-169

https://doi.org/10.17993/3cemp.2023.120151.226-241

(21) Collier, P. (2007). **Africa's economic growth: opportunities and constraints**. *African Development Review*, 19(1), 6-25.

(22) Vañó, F. L., & Pina, J. A. T. (2013). **Repercusión económica y eficiencia de una empresa cultural: El caso del Marq**. *3c Empresa: investigación y pensamiento crítico*, 2(3), 4.

(23) Ndikumana, L., Brixiová Schwidrowski, Z., & Abderrahim, K. (2010). **Working Paper 117-Supporting Africa's Post-Crisis Growth: The Role of Macroeconomic Policies**. *African Development Bank*.

(24) Lundvall, B. Å., & Lema, R. (2014). **Growth and structural change in Africa: development strategies for the learning economy**. *The learning economy and the economics of hope*, 327.

(25) Barro, R. J., & Sala-i-Martin, X. (1995). **Economic growth.**

(26) **Including: exchange rate, budget deficit, public debt, unemployment, and inflation**.

(27) Including: foreign direct investment, credit to the private sector by banks, and the concentration exports index.

(28) Including: improved water source, improved sanitation facilities, and access to electricity for a population.

(29) Including: voice and accountability, political stability, government effectiveness, regulatory quality, the rule of law and control of corruption.

(30) Angola, Algeria, Egypt, Kenya, Namibia, Nigeria, South Africa, Sudan, Zambia, Zimbabwe, Ghana, and Senegal.

(31) (2019). **he Worldwide Governance Indicators (WGI),** *World Bank: Washington, D.C.*

(32) (2015). **World Bank, World Development Indicators.** *Washington, D.C.*

(33) (2018). **The Economist Intelligence Unit London**. *EIU, CountryData.*

(34) Pérez, I. P. (2018). **Mujeres rurales emprendedoras, detonadoras de desarrollo económico: binomio colaboración-empoderamiento**. *3C Empresa: investigación y pensamiento crítico*, 7(2), 26-43. http://dx.doi.org/10.17993/3cemp.2018.070234.26-43/

(35) Abonazel, M. R. (2017). **Bias correction methods for dynamic panel data models with fixed effects**. *International Journal of Applied Mathematical Research*, 6(2), 58-66.

(36) Lin, H. Y., & Chu, H. P. (2013). **Are fiscal deficits inflationary?**. *Journal of International Money and Finance*, 32, 214-233.

(37) Catao, L. A., & Terrones, M. E. (2005). **Fiscal deficits and inflation**. *Journal of Monetary Economics*, 52(3), 529-554.

(38) Odusola, A., & Abidoye, B. (2015). **Effects of temperature and rainfall shocks on economic growth in Africa**. *Available at SSRN 3101790.*

(39) Haikal, G., Abdelbary, I., & Samir, D. (2021). **'Lazy Banks': the case of Egypt**. *Macroeconomics and Finance in Emerging Market Economies*, 1-11.

https://doi.org/10.17993/3cemp.2023.120151.226-241

(40) Okafor, G. (2014). **Determinants of foreign direct investment into sub-saharan Africa and its impact on economic growth** *(Doctoral dissertation, Bournemouth University).*

(41) Dollar, D., & Kraay, A. (2001). **Trade, growth, and poverty**. *Available at SSRN 632684.*

(42) Rodrik, D., Subramanian, A., & Trebbi, F. (2004). **Institutions rule: the primacy of institutions over geography and integration in economic development**. *Journal of economic growth*, 9, 131-165.

(43) Acemoglu, D., Johnson, S., & Robinson, J. A. (2005). **Chapter 6 Institutions as a Fundamental Cause of Long-Run Growth**, in *Handbook of Economic Growth*, 385-472. P. Aghion and S.N. Durlauf, Editors. Elsevier.

(44) Mo, P. H. (2001). **Corruption and economic growth**. *Journal of comparative economics*, 29(1), 66-79.

(45) Tanzi, V., & Davoodi, H. (1998). **Corruption, public investment, and growth**. In *The Welfare State, Public Investment, and Growth: Selected Papers from the 53 rd Congress of the International Institute of Public Finance* (pp. 41-60). Springer Japan.

(46) Rauch, J. E., & Evans, P. B. (2000). **Bureaucratic structure and bureaucratic performance in less developed countries**. *Journal of public economics*, 75(1), 49-71.

https://doi.org/10.17993/3cemp.2023.120151.226-241

APPENDICES

Appendix 1. Panel unit root tests for variables in level (intercept is included)

Tests / Variables	Levin, Lin & Chu (LLC)	Im, Pesaran and Shin (IPS)
Initial GDP	-11.6460 (0.000)	-15.7851 (0.000)
Macroeconomic Stability (M)	3.73479 (0.001)	2.66146 (0.0039)
Business Environment (B)	-7.33402 (0.0000)	0.32819 (0.6286)
Infrastructure (F)	-8.28406 (0.0000)	1.10117 (0. 8646)
Political Institutions (I)	-8.5056 (0.0000)	-3.526 (0. 0002)

Source: Authors' calculations.

Appendix 2. Estimated panel data models for the sub-Saharan African

Dependent variable: Growth rate of GDP per capita	Pooled OLS	Fixed Effects	Random Effects
Initial GDP	-0.003 0.163		0.262 0.186
population growth	**0.817***** **(0.282)**	**1.486***** **(0.386)**	**1.183***** **(0.287)**
oil rent	0.062 0.046	0.045 0.052	**0.076**** **(0.038)**
Macroeconomic Stability (M)	**0.802***** **(0.182)**	**0.573***** **(0.200)**	**0.712***** **(0.185)**
Business Environment (B)	0.181 0.176	0.095 0.211	0.183 0.196
Infrastructure (F)	0.038 0.089	0.107 0.176	-0.007 0.09
Political Institutions (I)	0.045		
F statistic	**5.1*****	**5.23*****	
Adjusted R2	0.22	0.22	0.18
chi2			**66.17*****
Hausman, chi2		**34.81*****	
LM test, chi2			**8.67*****
#observations	190	167	167
#Countries	10	10	10

***, **, and * indicate the coefficient is significantly different from zero at 1%, 5%, and 10%, respectively.

Source: Authors' calculations

https://doi.org/10.17993/3cemp.2023.120151.226-241

/12/

MIXED SYMMETRY STATES IN ^{96}MO AND ^{98}RU ISOTONES IN THE FRAMEWORK OF INTERACTING BOSON MODEL

Heiyam Najy Hady*

Kufa University. Education College for girls, Physics department

hiyamn.alkhafaji@uokufa.edu.iq

Ruqaya Talib Kadhim

Kufa University. Education College for girls, Physics department

Reception: 06/12/2022 **Acceptance**: 28/01/2023 **Publication**: 15/02/2023

Suggested citation:

N. H., Heiyam and T. K., Ruqaya (2023). **Mixed symmetry states in ^{96}Mo and ^{98}Ru isotones in the framework of interacting boson model**. *3C Empresa. Investigación y pensamiento crítico, 12(1)*, 243-255. https://doi.org/10.17993/3cemp.2023.120151.243-255

https://doi.org/10.17993/3cemp.2023.120151.243-255

ABSTRACT

The software package IBM *code for interacting boson model-1 and Neutron Proton Boson* $NPBOS$ *code for interacting boson model-2 have been used to calculate energy levels for*, for *by estimating a set of parameters which are used to predict the behavior of even-even isotones within the current scope of work there is clear competition between the two parameters (*ε *and* a_2*) in* isotones, *as an inverse relationship. This means that vibrational qualities are continuous mixed with the rotational properties*. In interacting boson model-2 parameters($\varepsilon, \kappa, \chi_\pi$ and χ_ν) have been shown similarity with interacting boson model-1 expected. *The Majorana parameter effect (*ζ_2*) on the calculated excitation energy level* for isotones has been accomplished by vary the ζ_2 around the optimum-matches to practical data. The effect of increasing ζ_2 on mixing symmetry states is the same in all isotones but different from state to another, we find the state $J^+ = 2_3^+$ was the lowest mixing symmetry states still approximately constant in the all. In that time,isotones have $1^+, 3^+_1, 5^+_1$ mixed symmetry states, rapidly increasing with increasing ζ_2. The results of the calculated energy levels were in acceptable agreement with the experimental data. There is no pure vibrational property of these isotones

KEYWORDS

Interacting boson model-1&2, MSS's, IBM code and $NPBOS$ code

PAPER INDEX

https://doi.org/10.17993/3cemp.2023.120151.243-255

INTRODUCTION

Even-even isotones considered as medium nuclei mass number, which are always referred to be as vibrational nuclei, due to the small bosons number outside the closed N and Z shells, probably what appears from the sequence of energy levels in the modern experimental decay schemes are stay away from their values of typical harmonic oscillator (pure vibration), which indicates to energy levels distortion such as 0_2^+, 2_2^+ , $4_1^+$and 6_1^+. For this reason, isotones have been re-examined in modern experimental decay schemes. The interacting boson model, suggests that the collective behavior rises from the coupling, through the interaction of the nucleon-nucleon of the isolated low-lying systems of valence protons and neutrons that is definite in accordance to the respect of the major shell closure. It is capable of describing nuclear characteristics such as energies and spins of the levels, decay probabilities for the emission of gamma quanta, probabilities of electromagnetic transitions and their reduced matrix elements for different transitions, multipole moments, and mixing ratios[1-3]. IBM special cases are existed named “dynamic symmetries”[4-8]. They correspond to the well-known “limits”, vibrational, rotational, and gamma unsteady nuclei. The concept of dynamic symmetry is of a basic significance in the IBM, because it permits the exact and analytic solution of the associated eigenvalue problem for a restricted class of boson Hamiltonians.The interacting boson model is suitable for describing the low-lying collective states in even (N,Z) nuclei by a system of interacting s and d-bosons carrying angular momentum’s 0 and 2 respectively [9].The structure of medium mass nuclei are a focus of nuclear structure research [10-13]. The structure of nuclei with proton numbers 42,44 and 46 and the number of neutrons greater than 50 was for many years a challenge to theoretical explanations because of the fluctuating transition of nuclear properties between the vibrational features and weak-rotational features within$IBM1$ and $IBM2$[14,16].

INTERACTING BOSON MODEL-1

Realizing that there is only one body and two body parts in the interacting boson paradigm, formation ($s^\dagger$, $d_m^\dagger$) and destruction (s,dm) actions are introduced with the index m=0,±1,±2. When considering on-boson terms in the boson-boson contact, the greatest Hamiltonian is [1-4].

$$H = \varepsilon_s\left(s^\dagger s\right) + \varepsilon_d \sum_m d_m^\dagger d_m + V \ldots . (1)$$

The boson-boson interacting energy is introduced by $\varepsilon_s, \varepsilon_d$are the s and d boson dynamisms and V. The greatest extensively recycled method of $IBM1$ Hamiltonian is [2-5].

$$H = \varepsilon n_d + a_0 P^\dagger P + a_1 L \,.\, L + a_2 Q \,.\, Q + a_3 T_3 T_3 + a_4 T_4 T_4 \ldots (2)$$

In order to simplify it, sometimes the boson $\varepsilon = \varepsilon_d - \varepsilon_s$, $\varepsilon_s$vigor value is set to zero. In addition, the forte of the quadruple points only $\varepsilon = \varepsilon_d$ appears

https://doi.org/10.17993/3cemp.2023.120151.243-255

$a_0, a_1, a_2, a_3, and a_4$ is determined by the angular momentum that results from the interaction of the bosons. Thus, the five and six bosons are lengthy by their solitary constituent. In cases where the number of bosons is fixed, it is signified by the group $U(6)$ (As for the round oscillator. Correspondingly, it is shaped by the three apertures, which are $U(5)$, $SU(3)$ and $O(6)$ [14-16], these symmetries are related to the geometrical idea of the spherical vibrator, deformed rotor and a symmetric ($\gamma-$soft) deformed rotor, respectively.

INTERACTING BOSON MODEL-2

The interacting boson model-2, is a further step in the development of the interacting boson model. It is an approach which gives the collective nuclear states as described by interacting boson -1,a microscopic foundation, since the interacting boson model-2 can in principle be derived from the shell model. This development, which is based on the concept of the generalized fermion seniority [1,2], has been introduced by Arima et. al. [3-8]. The model has given the bosons a direct physical interpretation as correlated pairs of particles with $J^{\pi} = 0$ and $J^{\pi} = 2$.The Hamiltonian operator in interacting boson model-2 will have three parts: one part for each of proton and neutron bosons and a third part for describing the proton-neutron interaction[17-19].

$$H = H_{\pi} + H_{\nu} + V_{\pi\nu} \ldots\ldots (3)$$

A simple schematic Hamiltonian guided by microscopic consideration is given by[17-19]:-

$$H = \varepsilon\left(n_{d\pi} + n_{d\nu}\right) + \kappa Q_{\pi} . Q_{\nu} + V_{\pi\pi} + V_{\nu\nu} + M_{\pi\nu} \ldots (4)$$

where

$$Q_{\rho} = (d_{\rho}^{\dagger} s_{\rho} + s_{\rho}^{\dagger} d_{\rho})_{\rho}^{2} + \chi_{\rho}(d_{\rho}^{\dagger} d_{\rho})_{\rho}^{2} \quad \rho = \pi, \nu \ldots (5)$$

$$V_{\rho\rho} = \sum_{L=0,2,4} \frac{1}{2}(2L+1)^{\frac{1}{2}} C_{L}^{\rho}\left[(d_{\rho}^{\dagger} d_{\rho}^{\dagger})^{(L)} . (d_{\rho} d_{\rho})^{(L)}\right]^{(0)} \ldots (6)$$

$\varepsilon_{\pi}, \varepsilon_{\nu}$ are proton and neutron energy respectively, they are assumed equal $\varepsilon_{\pi} = \varepsilon_{\nu} = \varepsilon$. The last term in Eq.(4) contains the Majorana operator $M_{\pi\nu}$ and it is usually added in order to remove states of mixed proton neutron symmetry. This term can be written as[18-21]:-

$$M_{\pi\nu} = \zeta_2 (s_{\nu}^{\dagger} d_{\pi}^{\dagger} - d_{\nu}^{\dagger} s_{\pi}^{\dagger})^{(2)} . \left(s_{\nu} d_{\pi} - d_{\nu} s_{\pi}\right)^{(2)} + \sum_{k=1,3} \zeta_k (d_{\nu}^{\dagger} d_{\pi}^{\dagger})^{(k)} - \left(d_{\nu} d_{\pi}\right)^{(k)} \ldots (7)$$

If there is empirical proof of the existence of the so-called "mixing symmetrical condition," the Majorana factor is changed in order to adjust the placement of these levels in the continuum. Due to this approximation, a system of neutron and proton bosons is taken into consideration. In the interacting boson model2, the microscopic interpretation of the boson number $N = N_{\pi} + N_{\nu}$fixes the total number of bosons, N, which was previously treated as a parameter in the interacting boson model 1. It is

https://doi.org/10.17993/3cemp.2023.120151.243-255

possible to determine the levels of energy by diagonalizing Hamiltonian Eq. (4) and experimenting with the parameters $\varepsilon, \kappa, \chi_\pi, \chi_\nu$ and C_L to find the best match to the observed spectrum. One form of boson can be used to produce spectra that resemble those of the interacting boson model1 [20,21]. When $(\varepsilon \gg \kappa)$, $(\varepsilon \ll \kappa$ and $\chi_\pi = \chi_\nu = -\sqrt{7}/2)$, and($\varepsilon \ll \kappa$ and $\chi_\nu = -\chi_\pi$)are present, respectively. The U(5) limit, SU(3) limit, and O(6) limits are present. Most nuclei fall halfway between two of these three limiting instances rather than strictly falling under one of them. The interactive boson framework enables for a streamlined process between the restrictive conditions for different isotopes. The systematics of energy ratios of successive levels of collective bands in even –even medium and heavy mass nuclei were studied for vibrational and rotational limits for a given band for each I the following ratio were constructed to define the symmetry of excited band[22].

$$r\left(\frac{(J+2)}{J}\right) = \frac{R\left(\frac{(J+2)}{J}\right)exp. - \left(\frac{(J+2)}{J}\right)vib.}{R\left(\frac{(J+2)}{J}\right)rot. - \left(\frac{(J+2)}{J}\right)vib.}$$

$$= \frac{R\left(\frac{(J+2)}{J}\right)exp. - \left(\frac{(J+2)}{J}\right)}{2(J+2)/J(J+1)} \ldots . (8)$$

where $R((J+2)/J)exp.$ denotes the ratio's experimental value. For vibrational nuclei, the value of energy ratios, r, has vibrates to (0.1r0.35); for transitional nuclei, (0.4r0.6) and for rotating nuclei, (0.6r1).

CALCULATIONS AND RESULTS

The isotones have neutron number $N = 54$ which equivalent(two particles bosons) and atomic number $(Z = 42\ and\ 44)$ respectively, which equivalent $(4,3\ and\ 2)$ hole proton boson number. By calculating a number of variables specified in the formulas for the Hamiltonian component equations(2)&(3), the energy levels for have been calculated using the software packages $IBM-code$ computer code for interacting boson model-1 and Neutron Proton Boson $NPBOS-code$ for interacting boson model-2 [5]. Table (1) and Figure (1) provide the anticipated results for the computations of the stimulated energy state for three isotones that are conducted low-lying.

https://doi.org/10.17993/3cemp.2023.120151.243-255

Table 1. The parameters have been used in the interacting boson model1&2 Hamiltonian for even-even isotones (in MeV).

IBM1-Parameters in MeV, except χ		
Isotopes / **The parameters**	**^{96}Mo**	**^{98}Ru**
N	6	5
ε	0.44	0.57
a_0	0.0	0.0
a_1	0.02	0.008
a_2	-0.04	-0.018
a_3	0.001	0.001
a_4	0.001	0.001
χ	-0.8	-0.8
$IBM2$**-Parameters in MeV, except** χ		
Isotopes / **The parameters**	**^{96}Mo**	**^{98}Ru**
N_π	4	3
N_ν	2	2
ε_d	0.9	0.86
κ	-0.08	-0.08
χ_ν	-0. 8	-0. 8
χ_ν	-0. 8	-0. 8
ζ_2	0.01	0.01
$\zeta_{1,3}$	0.001	0.001
C_ν^L	(-0.6,0.8,0.1)	(-0.4,0.8,0.1)
C_π^L	(-0.56,0.8,-0.08)	(0.6,0.8,-0.08)

https://doi.org/10.17993/3cemp.2023.120151.243-255

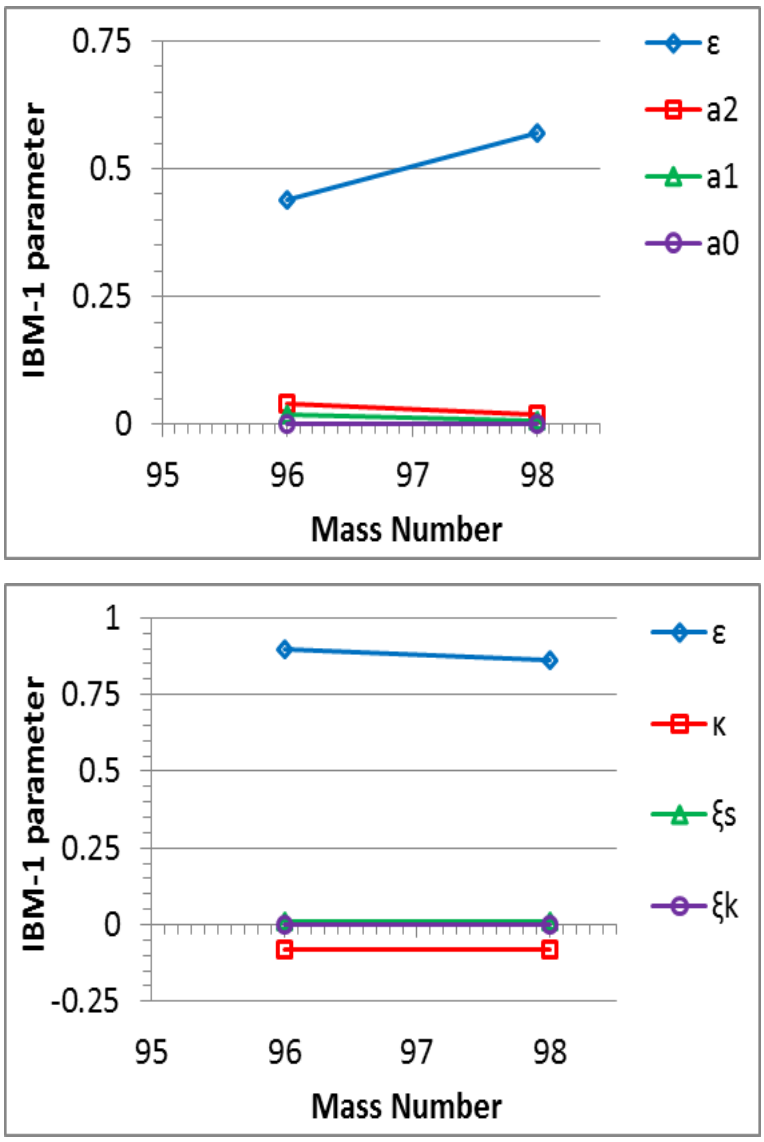

Figure 1. For even-even isotones, the parameters (in MeV)have been employed in the interacting boson model-1&2 Hamiltonian as a function of mass numbers

Calculation of energy ratios of $(\mathrm{E}4_1^+/\mathrm{E}2_1^+)$, $(\mathrm{E}6_1^+/\mathrm{E}2_1^+)$, $(E8_1^+/E2_1^+)$ and r ratios for all examined isotones have been calculated and are shown in figure (2).Figure (3) shows the estimated energy levels for the isotones in comparison to the experimental data[23-25].

https://doi.org/10.17993/3cemp.2023.120151.243-255

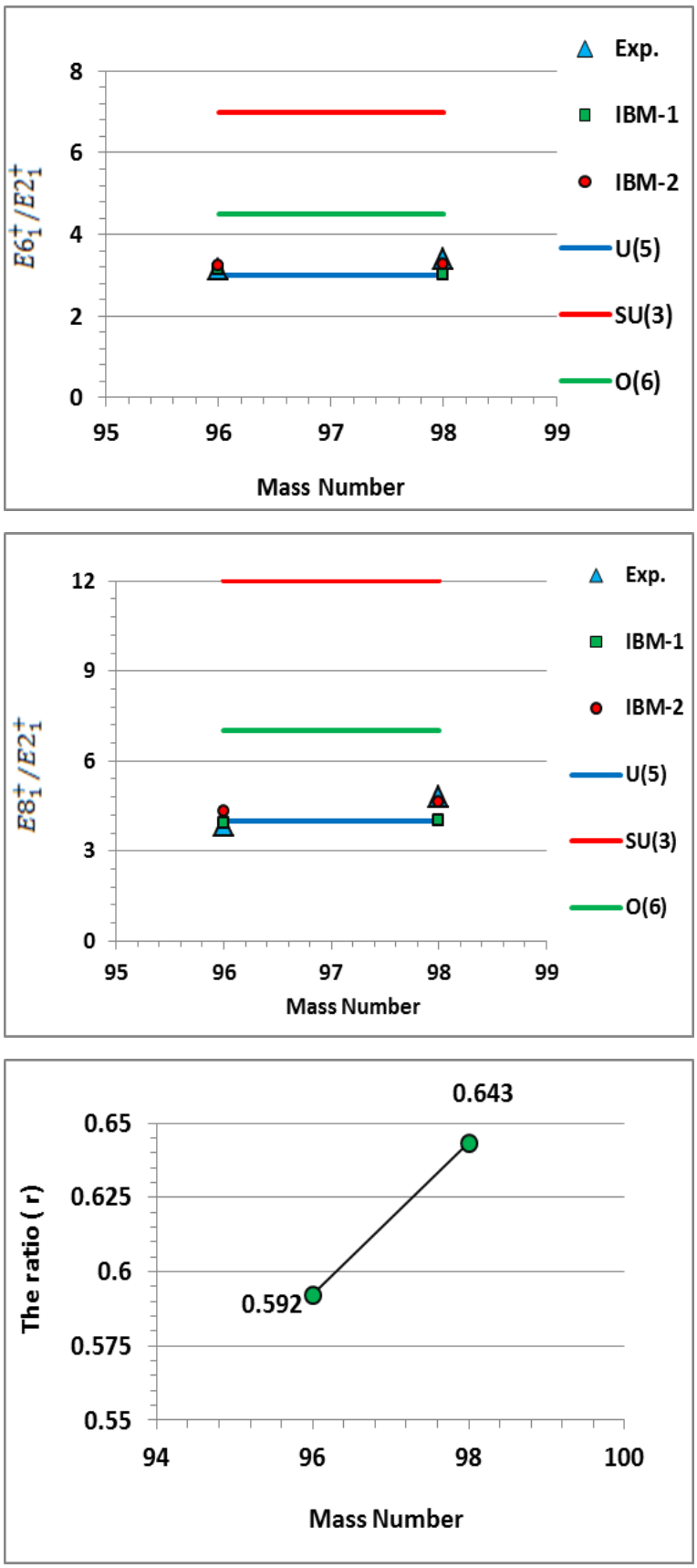

Figure 2 The experimental [23-25], theoretical and standard [1,2] energy ratios $(\mathrm{E4_1^+/E2_1^+}, \mathrm{E6_1^+/E2_1^+}, , E8_1^+/E2_1^+)$ and r ratio[22]respectively as a function of mass numbers for even-even isotones

https://doi.org/10.17993/3cemp.2023.120151.243-255

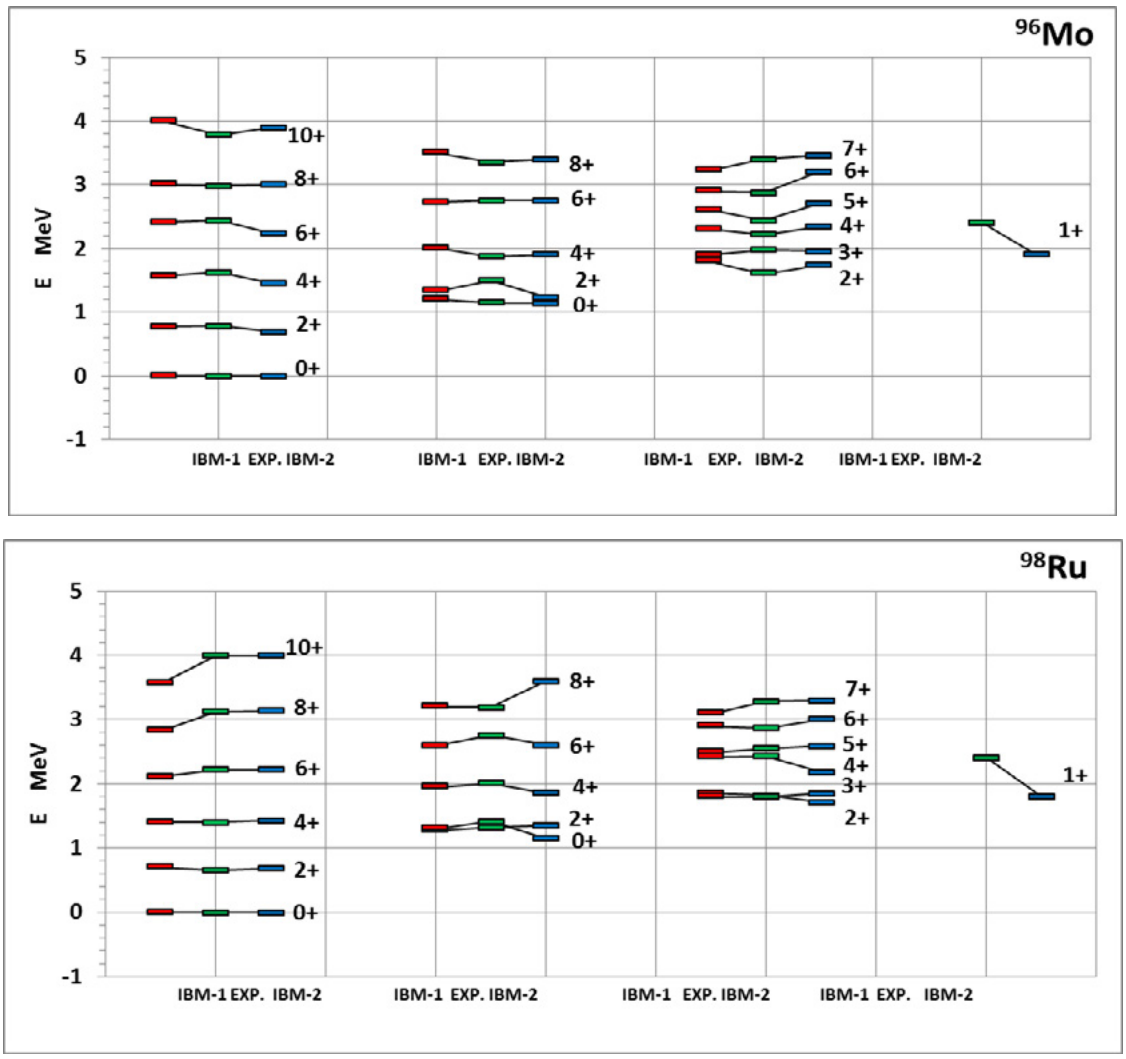

Figure 3 Comparison of the estimated and experimental[23-25] states for isotones,

For isotopes, the effect of Majorana parameters ($\zeta_{1,3}$, and ζ_2) on the levels of the calculated excitation energy for isotones has been conducted for all by vary the ζ_2 around the best-fitted with experimental data[23-25] for the states (2_3^+, 3_1^+ , $5_1^+$and 1_1^+). Figure (4) stated the variation of the energy of these states as the Majorana parameter function ζ_2.

https://doi.org/10.17993/3cemp.2023.120151.243-255

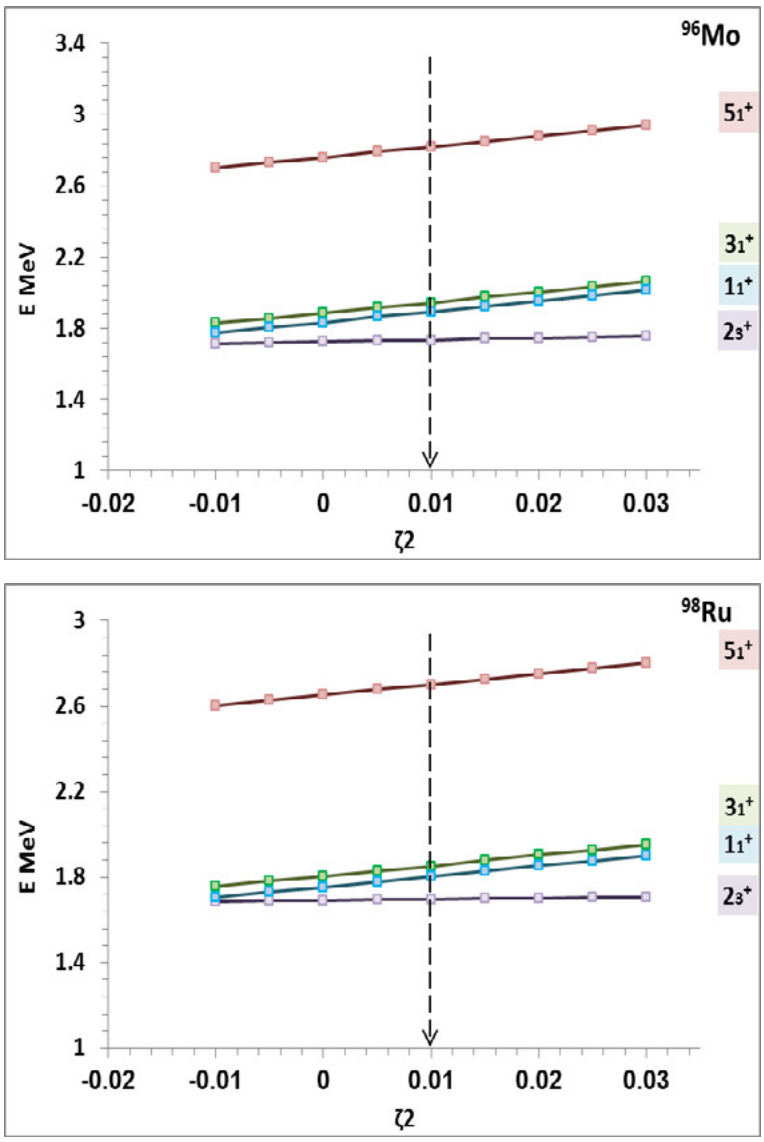

Figure 4 Mixed symmetry states MSS in even-even isotones.

DISCUSSION AND CONCLUSIONS

There are two approaches theoretical nuclear models $IBM1$ and $IBM2$which are used to predict the behavior of even-even isotones. The spectra of medium mass nuclei are usually characterized by the occurrence of low lying collective quadruple states. In this research, we discuss all results in term of dynamic symmetries, energy ratio, mixed symmetry states. The relatively medium mass nuclei nearly the mass number 100 which are located above the double closed $\mathrm{N} = 50$ and $\mathrm{Z} = 28$ have a few previous studies. The systematic excitation energy of low lying states mix the vibrational behavior and rotational behavior as illustrated by energy ratio $(\mathrm{E4}_1^+/\mathrm{E2}_1^+)$, $(\mathrm{E6}_1^+/\mathrm{E2}_1^+)$, $(\mathrm{E8}_1^+/\mathrm{E2}_1^+)$ and r in figure (2).

In the context of the interacting boson model-1, the competition between the two parameters ($\varepsilon$and a_2) is observed in the isotones of, where increases inε are correlated with decreases in a_2. This indicates that the opposite of the rotational

https://doi.org/10.17993/3cemp.2023.120151.243-255

properties, the vibrational features are continuously increasing. They emerge as a transition between the limits of vibration and rotation. The variants $\varepsilon, \kappa, \chi_\pi$ and χ_ν in the interacting boson model-2 represent the resemblance with the interacting boson model-1 anticipated as planned in table (1) and figure (1). The most significant element of the interactive boson paradigm is the potential to describe composite symmetrical conditions in even-even nuclei formed from a combination of the capabilities of the protons and neutrons waveforms. The lowest MS states are those with $J^+ = 2^+$ in more vibrational and gamma soft nuclei, while they are detected as $J^+ = 1^+$ states in rotational nuclei. By varying the Majorana parameter effect (ζ_2) around the optimum-fitted to experimental data, it has been possible to determine the calculated excitation energy level for the isotones. It has been discovered that the state $\mathrm{J}^+ = 2_3{}^+$ has the lowest mixing symmetry state that is still roughly constant in all isotones. The effect of raising $, a_2$ on mixing symmetry states is the same in all isotones but varied from state to state. isotones contain $1^+, 3^+{}_1, 5^+{}_1$ mixed symmetry states at that moment, which rapidly increase as ζ_2 increases. The collective states location of mixed proton-neutron symmetry is one of the most remarkable open experimental difficulties in the study of collective features of nuclei. The experimental value[23-25] of the first 1^+ for isotones are $\left(2.794 \text{ and } 2.406\right)$ MeV represented spin and parity as $(1^+ \text{and } (1^+, 2^+))$ respectively, somewhat higher than the values in the best fitting $(1.9027 \text{and } 1.8012)$ MeV in addition to energy levels values for the 3_1^+ state have a clear mixed symmetry state (MSS) increasing with increase the Majorana parameters ζ_2, the experimental values[23-25] of the first 3_1^+ for isotones are $(1.978 \text{ and } 1.797)\mathrm{MeV}$, very similar to the exact fitted values$(1.9539 \text{ and} 1.85)$ MeV, the same notification applies to 5_1^+ state with an excellent affinity between practical values and the best fitted.

REFERENCES

(1) F. Iachello and A. Arima. (1987). **The Interacting Boson Model.** *The Syndicate Press of the University of Cambridge, England.*

(2) R. Casten and D. Warner. (1988). **The Interacting Boson Approximation.** *Rev. Mod. Phys.*, 60, 389.

(3) A. Arima and F. Iachello. (1975). **Collective Nuclear States as Representations of a Group.** *Physical Review Letters*, 35, 16.

(4) A. Arima and F. Iachello. (1976). **Interacting Boson Model of Collective States I. The Vibrational Limit.** *Ann. Phys. NY,* 99, 253.

(5) A. Arima and F. Iachello. (1978). **Interacting Boson Model of Collective Nuclear States II.** *The Rotational Limit, Ann. Phys.,* 111, 201.

(6) A. Arima and F. Iachello. (1979). **Interacting Boson Model of Collective Nuclear States IV. The Limit.** *Ann.Phys.*, 123, 468.

(7) A. Arima, T. Otsuka, F. Iachello and I. Talmi. (1977). **Collective nuclear states as symmetric couplings of proton and neutron excitations.** *Physics Letters, B* 66, 205.

https://doi.org/10.17993/3cemp.2023.120151.243-255

(8) F. Iachello. (1979). **Interacting Boson in Nuclear Physics.** *Plenum, New York.*

(9) H. Najy Hady and M. Kadhim. (2021). **Investigation of transition symmetry shapes of 160- 168Yb nuclei using IBM.** *Iraqi Journal of Science*, 62, 4.

(10) H. Najy Hady. (2012). **Investigation of the low-lying energy levels structure of the rich neutron isotopes 96-104Mo**, *Journal of Kerbala University,* 10, 1, Scientific.

(11) Ch. Mu and Da. Zhang. (2018). **Description of Shape Coexistence and Mixed-Symmetry States in 96Mo Using IBM-2.** *Chin. Phys. Lett.* 35, 6.

(12) S. Thakur, P. Kumar, V. Thakur, V. Kumar and S. Dhiman. 2021. **Shape transitions and shell structure study in zirconium, molybdenum and ruthenium**, *Nuclear Physics A*, 1014, 122254.

(13) A. Yilmaz and and M. Kuruoglu, (2006). **Investigation of Even-Even Ru Isotopes in Interacting Boson Model-2.** *Commun. Theor. Phys. (Beijing, China)*, 46, 4.

(14) T. Thomasab, V. Wernerbc, J. Joliea, K. Nomurade, T. Ahnbf, N. Cooperb, H. Duckwitza A. Fitzlera, C. Fransena, A. Gadea1, M. Hintonb, G. Ilieb, K. Jessena, A. Linnemanna, P. Petkovagh, N. Pietrallac and D. Radecka. (2016). **Nuclear structure of 96,98Mo: Shape coexistence and mixed-symmetry states.** *Nuclear Physics A*, 947.

(15) P. Van Isacer and G. Puddu. (1980). **The Ru and Pd isotopes in the proton – neutron interacting boson model.** *Nuclear Physics,* A348.

(16) I. Ahmed, H. Abdullah, S. Ahmed, I. Hossain, M. Kasmin, M. Saeed and N. Ibrahim. (2012). **The evolution properties of even-even 100−110Pd nuclei**, *International Journal of Modern Physics E*, 21, 12.

(17) F. Iachello and A. Arima. (1974). **Boson symmetries in vibrational nuclei.** *Physical Letters*, 53, 4.

(18) F. Iachello, G. Puddu and O. Scholten. (1974). **A Calculation of low -lying collective state in even-even nuclei.** *Physical Letters*, 89B, 1.

(19) V. Hellemans, P. Van Isacker, S. De Baerdemacker and K. Heyde. (2007). **Phase transitions in the configuration mixed interacting boson model – mixing.** *Acta Phys. Polonica B*, 38, 4.

(20) J. Engel and F. Iachello. (1987). **Interacting boson model of collective octupole states (I). The rotational limit.** *Nuclear Physics A*, 472.

(21) R. Casten,and R. Cakirli. (2016). **The evolution of collectivity in nuclei and the proton–neutron interaction.** *Physica Scripta*, 91, 033004.

(22) A. Khalaf and A. Ismail. (2013). **Structure Shape Evolution in Lanthanide and Actinide Nuclei.** *Progress in physics*, 2.

(23) D. Abriola and A. Sonzogni. (2008). **Nuclear Data Sheets for A= 96.** *Nuclear Data Sheets*, 109(11), 2501-2655.

(24) K. Howard, U. Garg, M. Itoh, H. Akimune, M. Fujiwara, T. Furuno, Y. Gupta, M. Harakeh, K. Inaba, Y. Ishibashi, K. Karasudani, T. Kawabata, A. Kohda, Y. Matsuda, M. Murata, S. Nakamura, J. Okamoto, S. Ota, J. Piekarewicz, A. Sakaue, M. ¸Senyigit, M. Tsumura and Y. Yang. (2020). **Compressional-mode resonances in the molybdenum isotopes: Emergence of softness in open-shell nuclei near A = 90.** *Physics Letters B*, 807, 135608.

https://doi.org/10.17993/3cemp.2023.120151.243-255

(25) J. Chen and B. Singh. (2020). **Nuclear Data Sheets for A = 98**, *Nuclear Data Sheets*, 164(1), 1-477.

https://doi.org/10.17993/3cemp.2023.120151.243-255

/13/

ARTIFICIAL NEURAL NETWORKS MODELLING FOR AL-RUSTUMIYA WASTWATER TREATMENT PLANT IN BAGHDAD

Dalia H. aldahy*

Civil Engineering Department, College of Engineering, Al-Nahrain University, Baghdad, Iraq

st.dalia.hussein@ced.nahrainuniv.edu.iq

Mohammed A. Ibrahim

Civil Engineering Department, College of Engineering, Al-Nahrain University, Baghdad, Iraq

Reception: 03/12/2022 **Acceptance**: 27/01/2023 **Publication**: 13/02/2023

Suggested citation:

H. A., Dalia and A. I., Mohammed (2023). **Artificial Neural Networks Modelling For AL-Rustumiya Wastwater Treatment Plant in Baghdad** . *3C Empresa. Investigación y pensamiento crítico, 12(1)*, 257-271. https://doi.org/10.17993/3cemp.2023.120151.257-271

ABSTRACT

In the present research, Artificial Neural Networks (ANNs) were developed for modelling the performance of Al-Rustamiya wastewater treatment plant, Baghdad, Iraq. There were created two models and the outputs were the removal efficiency of BOD and COD parameters. Four main input parameters were selected for modelling, namely Total suspended solids (TSS), Total dissolved solids (TDS), chloride ion (Cl-), and pH. Influent and effluent concentrations of the parameters were collected from Mayoralty of Baghdad for the period from 2011 to 2021. The results of the modelling were in terms of mean square error (MSE) and correlation coefficient (R). The results indicated that the ANNs models were accurately able to predict the removal of the BOD, and COD, and the optimum topology of the ANNs is obtained at 13 neurons in the hidden layer for both with 3.09 MSE, 0.96 and 4.28 MSE, 0.96 R for BOD and COD respectively.

KEYWORDS

ANNs, BOD, COD, modelling, wastewater

PAPER INDEX

https://doi.org/10.17993/3cemp.2023.120151.257-271

INTRODUCTION

The change in the life styles due to urbanization and industrial practices has resulted in increasing production of wastewater that adversely impacts on human lives [1]. Water can be contaminated by human utilization in any mixture of mechanical, residential, businesses, storm water, surface overflow, and inflow of sewers [1, 2]. Wastewater treatment plants (WWTPs) are considered as significant infrastructure for a society. With the realization of the importance of such plants, the achievement of integrated and efficient units demands adequate operational and maintenance practices. Wastewater treatment plants mainly consist of three process, primary, secondary, and tertiary treatments. The combinations of these processes depends on the characteristics requirements of effluent [3]. Typically, the reduction degree in the biological oxygen demand (BOD) as well as chemical oxygen demand (COD) represent the basic indicator of the effectiveness of the plant [4, 5].

Moreover, modelling of WWTPs represents a difficult task as the treatment involves complex processes. The physical, biological, and chemical stages of the treatment plants provide non-linear performance which is complicated to presented in linear models. Thus, providing an efficient monitoring technique can be accomplished by the development of non-linear model to predict the performance of the treatment plant under previous observed water characteristics. Artificial neural networks (ANNs) represent computerized non-linear models for simulating the decision-making and functions of the brain of humans. It is being used for many wastewater quality issues. It has also been properly used in the modelling of the WWTPs for predicting wastewater characteristics, controlling stages of treatments, and providing estimation of effluent characteristics [6-9].

ANNs are usually used for predicting the parameters of water quality. It solves an issue through the development of a memory with the ability to relate large input data with a set of outputs [10]. A significant feature of the ANNs is its ability to handle considerable and complicated systems with various related parameters [11]. ANNs forms the basis of deep learning where the modelling algorithms are inspired by the brain structure of humans. After taking in the data, the ANNs train themselves for the recognition of data patterns and providing outputs. The model consists of grouped artificial neurons representing the core units of the modelling process [12]. The model represents an alternative method to conventional water quality models through the provision of advanced predictions and forecasts [13, 22].

In Baghdad, the capital city of Iraq, Al-Rustumiya WWTP is one of the main sewage water treatment facilities in the country. The plant recently has been expanded (3rd expansion) with the construction of nearby new plant for increasing capacity purposes. It releases the treated waters in Diyala River and then into the Tigris River [14, 15]. This study aims to at develop an ANNs model in MATLAB for investigating correlation between pairs of parameters to predict the performance of the 3rd expansion plant in terms of the removal efficiency of BOD, and COD. This work can assist in facilitating assessment or process control of effluent quality.

https://doi.org/10.17993/3cemp.2023.120151.257-271

WORK METHOD

1. DESCRIPTION OF THE STUDY AREA

Baghdad is the capital city of Iraq with an area approximately equals 800 square miles and population of 7.145 million according to the water and sewage sector report [16]. Three significant central WWTPs were built in Baghdad., namely Al-Karkh wastewater treatment plant, Southern Al-Rustumiya WWTP numbered 0, 1, and 2, and Northern Al-Rustumiya WWTP (3rd expansion). The effluent from the old plant being discharged in Tigris River while for the 3rd expansion, it is being discharged in Diyala River (also known as Sirwan River). The 3rd expansion of the plant began in 1984. Approximately third of the population in the city depends on the Al-Rustumiya WWTP [17]. The plant lies on the south-east part of Baghdad, Iraq, on Diyala River with longitudinal coordinate of 44˚32´05˝E and latitudinal coordinate of 33˚17´15˝N. The plant was mainly designed for the treatment of domestic wastewater which serves a population of 1500000 [17]. The plant consists of conventional activated sludge for biologically treating carbon compounds with average wastewater influent capacity equals 300MLD [17]. Figure 1 showed the 3rd expansion of the plant.

Figure 1. Al-Rustumiya WWTP3rd expansion in Baghdad, Iraq [14].

https://doi.org/10.17993/3cemp.2023.120151.257-271

2. DATA COLLECTION

The required data were obtained from Al-Rustamiya WWTP administration Office Mayoralty of Baghdad, over the period of ten years from January 2011 and December 2021 on a monthly basis. Two locations were selected: at entrance of the plant, and after secondary treatment. The selected physiochemical parameters included the biochemical oxygen demand (BOD5), chemical oxygen demand (COD), chloride (Cl-) and Total dissolved solids(TDS), and total suspended solids (TSS). The Removal efficiency of BOD, and COD were determined using Equation (1):

$$\text{Removal efficiency (\%)} = \frac{\text{input value} - \text{output value}}{\text{input value}} x\ 100 \qquad (1)$$

3. ANNS MODELLING IN MATLAB

The ANNs were created in MATLAB. This software allows creation, usage, export, and input of neural networks. Two models were created, with 4 inputs and 1 output. The modelling procedure and equations were based on Tümer and Edebali [18], Ammari [19] and Alsulaili and Refaie [20].

The ANNs architecture was defined by its number of layers and their neurons. Feedforward multi-Layered perception ANNs consist of various artificial neurons known as nodes, or processing elements (PEs). These are normally arranged in three layers, input, hidden or intermediate, and output layers. As was indicated in Figure 2 that for each processing element, the input from a layer (xi) was multiplied by an adjustable connection weight (wij). The summation was performed for the weighted inputs with the addition of a threshold value (θj). The resulted combined input was then transferred to activation function (f(ij)) for generating the output (yj). This output was then used as input for the next layer. The activation function represents the nonlinear mapping tool in the network before delivering the output to the next layer.

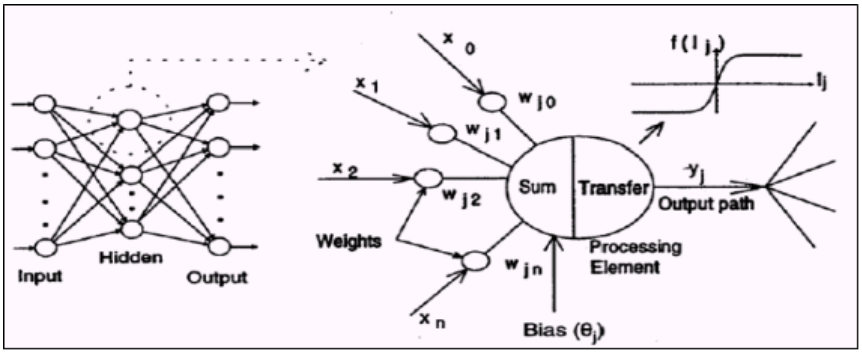

Figure 2. Typical structure and operation of ANNs [21].

The summary of the process was indicated in Equations (1 & 2) as follows:

$$\text{Summation f(IJ)} = \sum \text{Wij Xi} + \theta\text{j} \qquad (2)$$

$$\text{Transfer (yj)= f(Ij)} \qquad (3)$$

https://doi.org/10.17993/3cemp.2023.120151.257-271

Where,

f(IJ) is the level of activation at j node,

Wij is the weight of the connection between the nodes i and j,

xi is the i node input and equals 0, 1,2, …,n,

θj is the threshold for j node,

j is the j node output, and

f(ij) is the activation function.

Backpropagation algorithm is normally used for excellent results and easy application. The ANNs data propagation began at the input layer at which the information was provided. In order for the weights to be assigned, the network utilized the presented information and learning rule for the production of input and output maps with negligible errors. This is called training or learning which was divided into supervised and unsupervised learnings. Feedforward ANNs usually works with supervised learning. In this, model inputs and desired outputs were provided to the network. Errors were determined through the network by comparing the desired and actual ANNs produced outputs. These errors were then utilized for adjusting the weights given to the connections between the input and the outputs for reducing the errors between the actual output and the desired ones. Thus, the network learns for the presented data for adjusting the weights and capturing the relationship between the input and the output without the need of any previous knowledge about such relationship. Thus it regulates the bias and weights of the Multi-Layered perception ANNs. In order to evaluate the efficiency of the treatment plant, the backpropagation algorithm was improved by the incorporation of Levenberg-Marquadrt algorithm. This algorithm is a local optimization algorithm with a gradient basis. The advantage of its utilization over normal backpropagation is the better stability, advanced performance, and faster and advanced training and convergence properties.

Several forms are available for the activation function. The most commonly known were used in this research which was hyperbolic tangent transfer and logistic sigmoid functions. The functions are presented in Equations (4 & 5):

Hyperbolic tangent transfer function $$f(I_j) = \frac{e^{(I_j)} - e^{-(I_j)}}{e^{(I_j)} + e^{-(I_j)}} \quad (3)$$

logistic sigmoid function $$f(I_j) = \frac{1}{1 + e^{-(I_j)}} \quad (4)$$

https://doi.org/10.17993/3cemp.2023.120151.257-271

RESULTS AND DISCUSSION

1. REMOVAL EFFICIENCY OF BOD AND COD

Figures 3 presented the average yearly removal efficiency of BOD and COD from Al-Rustumiya WWTP. The figure indicated that the removal efficiencies were variable for both water parameters, mostly more than 80% and having approximately the same trend. The greatest removal efficiency occurred in 2020 with about 93% for BOD and 95% for COD. Generally, the removal efficiency of the plant increased from 2015 onwards. The lowest BOD and COD removals occurred in 2012. This could be attributed to the improper aeration in the aeration basin, or the measurement of high concentration of settling microbial mass in the secondary clarifier.

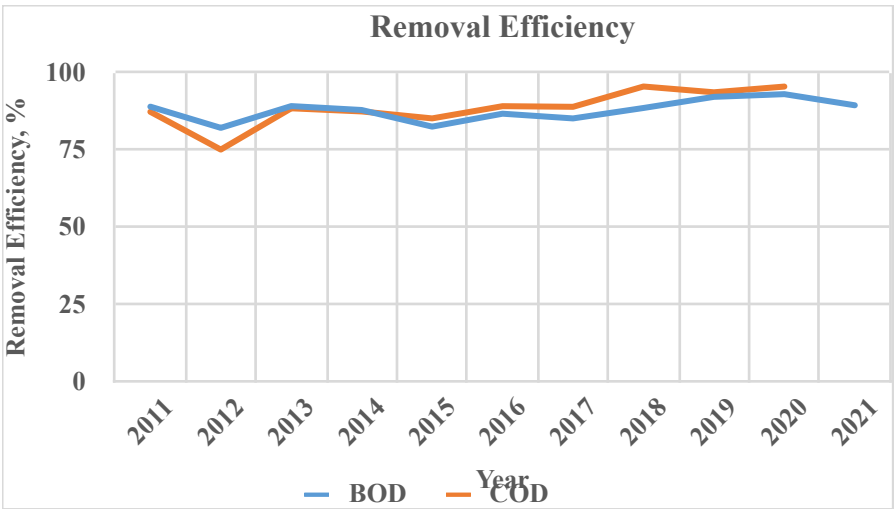

Figure 3. Removal efficiency of BOD and COD from Al-Rustumiya WWTP.

2. ANNS

The results of the ANNs modelling were evaluated in terms of Mean Square Error (MSE) and correlation coefficient (R) The functions are presented in Equations (6&7):

$$\text{Correlation coefficient (R)} = \frac{\sum_{i=1}^{n}\left(X-\bar{X}\right)\left(Y-\bar{Y}\right)}{\sqrt{\sum_{i=1}^{n}\left(X-\bar{X}\right)^{2}\left(Y-\bar{Y}\right)^{2}}} \quad (6)$$

$$\text{Mean Square Error (MSE)} = \frac{\sum_{i=1}^{n}(X-Y)}{2} \quad (7)$$

where X= observed yt , $\bar{X}$ = mean of X, Y= predicted yt, $\bar{Y}$= mean of Y, and n= number of observations.

https://doi.org/10.17993/3cemp.2023.120151.257-271

These are the most common criteria for the evaluation of a model's performance. The MSE provides the difference between the outputs and the targets. The R coefficient reflects how well the created model fits with used outputs. An R equaling 1 means a very close relationship while an R equaling 0 means a random relationship. Models were carried out for the removal efficiency of both BOD and COD. They represent the main parameters for evaluating organic pollution. They provide measurements of organic matter and oxygen demands.

2.1. ANNS FOR BOD MODELLING

The modelling results in terms of the MSE with the number of hidden layers are shown in Figure 4. and Table 1. The results indicated that the MSE was significantly decreased with the increase in the number of hidden neurons from 2 to 9 and the minimum MSE result is obtained at 13 hidden neurons. Afterward, training was stopped when reached 90 epochs for the Levenberg–Marquardt algorithm as shown in Figure 5. This is because of the difference between the training and validation errors increases. A plot of Levenberg–Marquardt algorithm regression for training, validation, and testing with R is shown in Figure 6. This revealed that the R values were 0.98, 0.94, 0.88, and 0.96 for training, validation, testing, and for all data respectively. Thus, the optimum topology of the ANNs is obtained at 13 neurons in the hidden layer with 3.09 MSE and 0.96 R. The architectural model of the optimum topology is shown in Figure 7. This is 4:13:1, indicating the input layer with the used four parameters, thirteen neurons at the hidden layers, and the output layer in terms of the removal efficiency of the BOD.

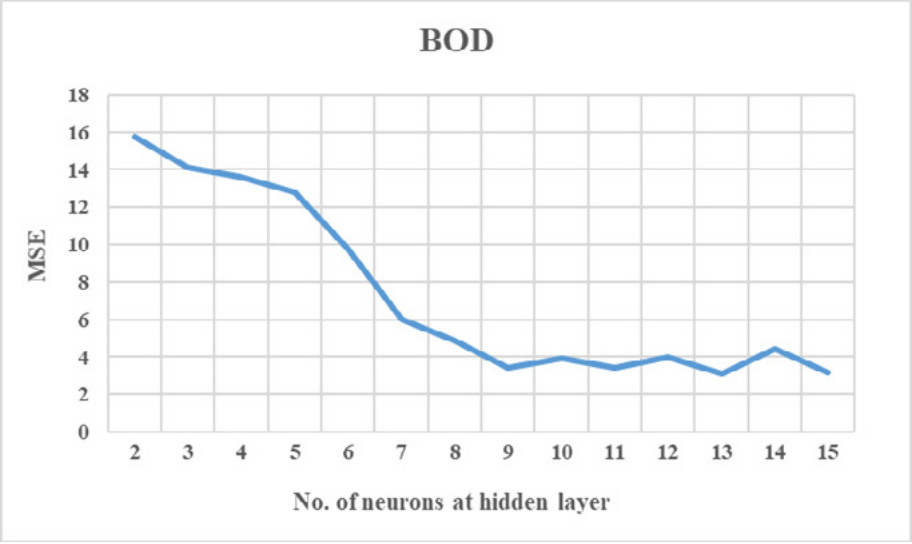

Figure 4. Mean Square Error (MSE) with different numbers of neurons at the hidden layers for ANNs modelling of BOD output.

https://doi.org/10.17993/3cemp.2023.120151.257-271

Table 1. ANNs details for BOD modelling.

BOD			
Model No.	**No. of neurons at hidden layers**	**MSE**	**Correlation Coefficient (R)**
1	2	15.72	0.80
2	3	14.13	0.83
3	4	13.59	0.83
4	5	12.83	0.84
5	6	9.75	0.88
6	7	6.00	0.93
7	8	4.87	9.43
8	9	3.42	0.96
9	10	3.96	0.95
10	11	3.41	0.96
11	12	4.00	0.95
12	13	3.09	0.96
13	14	4.43	0.95
14	15	3.21	0.96

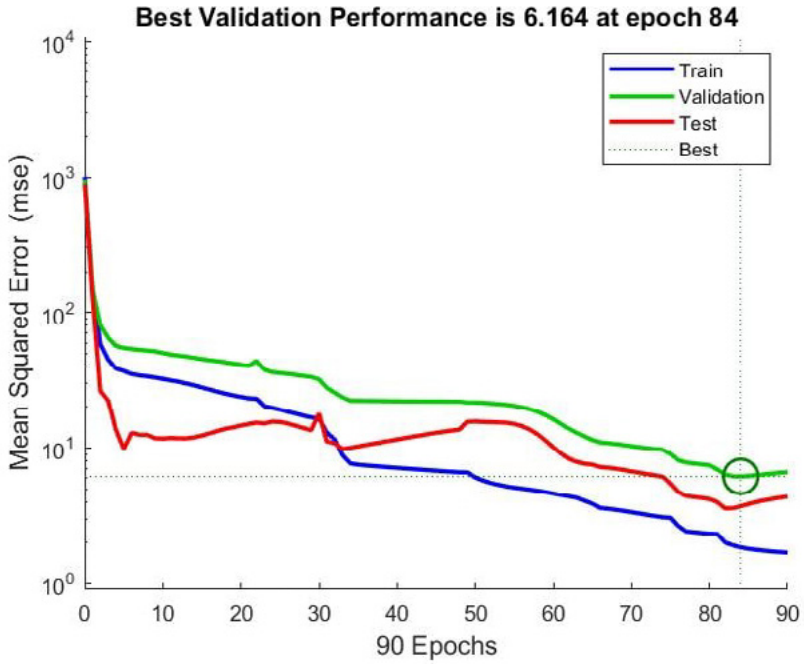

Figure 5. Training, validation, and test mean square errors for the Levenberg–Marquardt algorithm for BOD removal.

https://doi.org/10.17993/3cemp.2023.120151.257-271

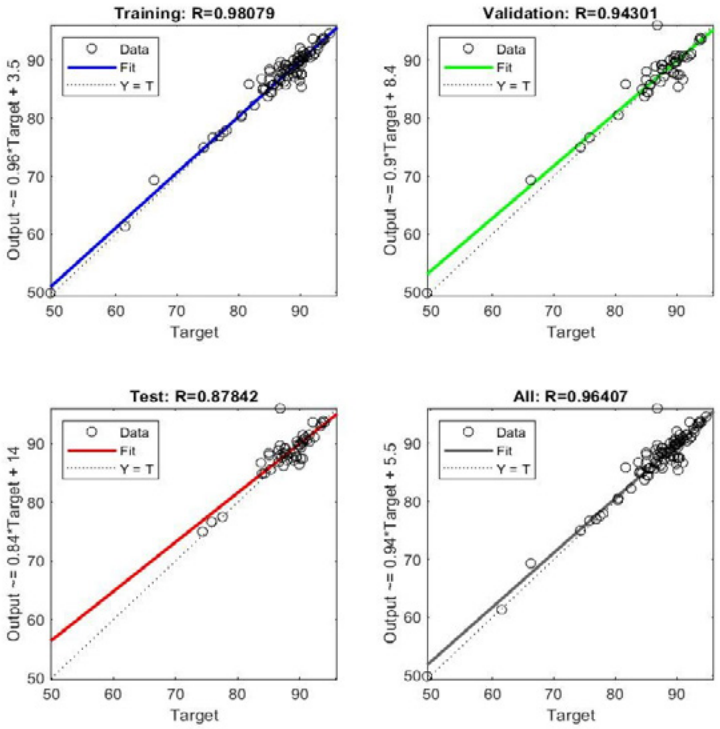

Figure 6. Training, validation and testing regression for the Levenberg–Marquardt algorithm for BOD removal.

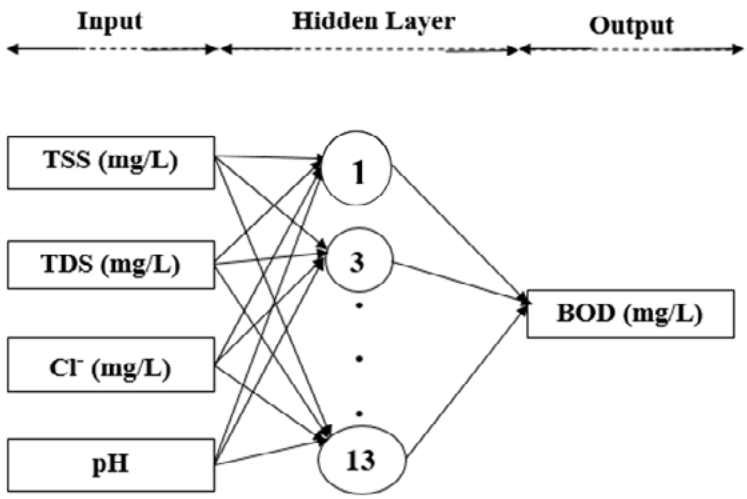

Figure 7. The architecture of the ANN model for the prediction of BOD removal.

2.2. ANNS FOR COD MODELLING

The modelling results in terms of the MSE with the number of hidden layers are shown in Figure 8. and Table 2. The results indicated that the MSE was significantly decreased with the increase in the number of hidden neurons from 2 to 11 and the minimum MSE result is obtained at 13 hidden neurons. Afterward, training was stopped when reached 78 epochs for the Levenberg–Marquardt algorithm as shown in Figure 9. This is because of the difference between the training and validation

https://doi.org/10.17993/3cemp.2023.120151.257-271

errors increases. A plot of Levenberg–Marquardt algorithm regression for training, validation, and testing with R is shown in Figure 10. This revealed that the R values were 0.96, 0.94, 0.96, and 0.96 for training, validation, testing, and for all data respectively. Thus, the optimum topology of the ANNs is obtained at 13 neurons in the hidden layer with 4.28 MSE and 0.96 R. The architectural model of the optimum topology is shown in Figure 11. This is 4:13:1, indicating the input layer with the used four parameters, thirteen neurons at the hidden layers, and the output layer in terms of the removal efficiency of the COD.

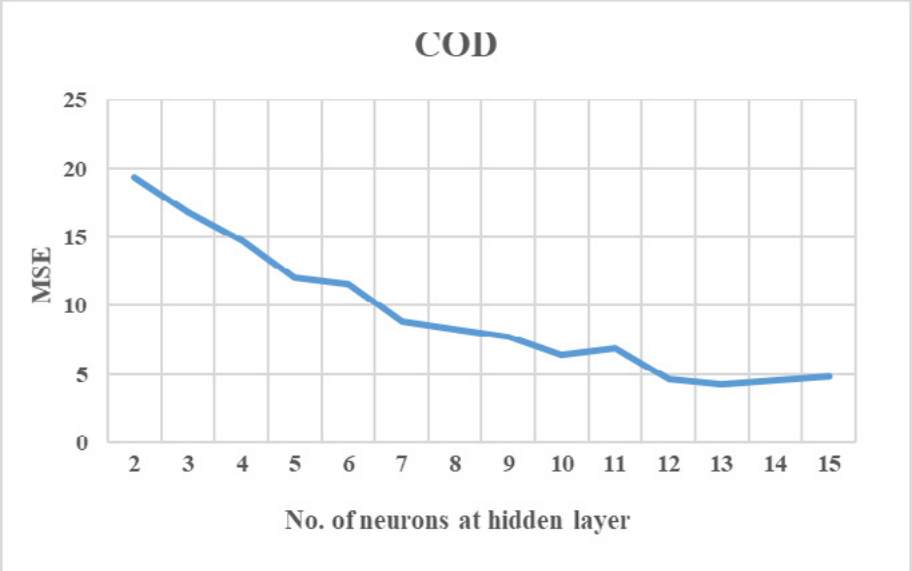

Figure 8. Mean Square Error (MSE) with different numbers of neurons at the hidden layers for ANNs modelling of COD output.

Table 2. ANNs details for COD modelling.

COD			
Model No.	**No. of neurons at hidden layers**	**MSE**	**Correlation Coefficient (R)**
1	2	19.34	0.79
2	3	16.79	0.82
3	4	14.74	0.84
4	5	12.03	0.87
5	6	11.58	0.88
6	7	8.81	0.91
7	8	8.31	0.90
8	9	7.68	0.91
9	10	6.36	0.93
10	11	6.85	0.93
11	12	4.61	0.95

https://doi.org/10.17993/3cemp.2023.120151.257-271

12	13	4.28	0.95
13	14	4.50	0.95
14	15	4.86	0.95

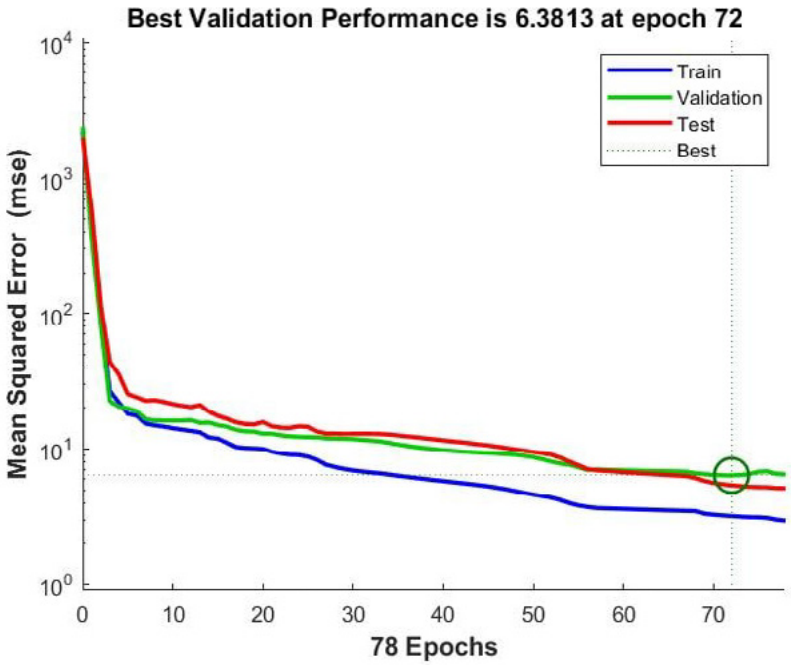

Figure 9. Training, validation, and test mean square errors for the Levenberg–Marquardt algorithm for COD removal.

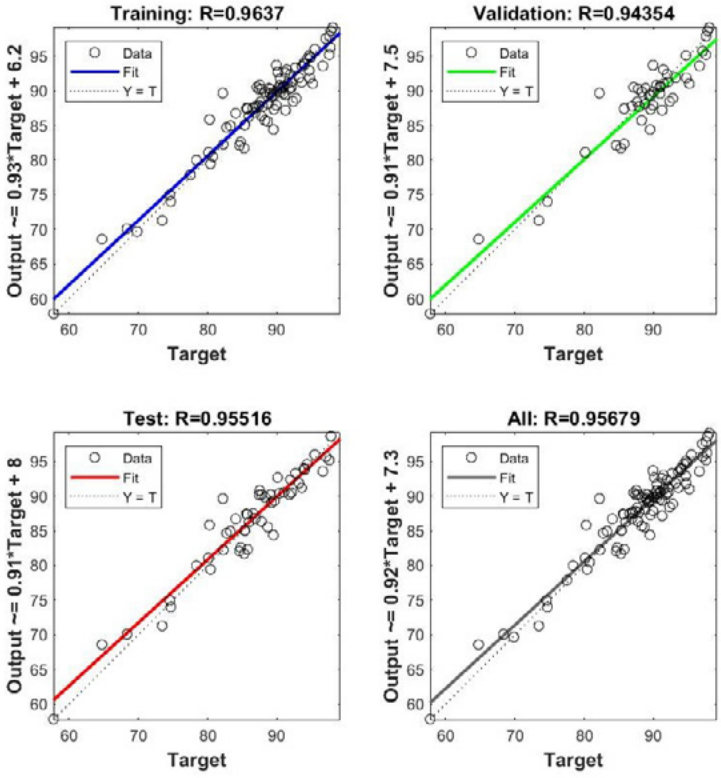

Figure 10. Training, validation and testing regression for the Levenberg–Marquardt algorithm for COD removal.

https://doi.org/10.17993/3cemp.2023.120151.257-271

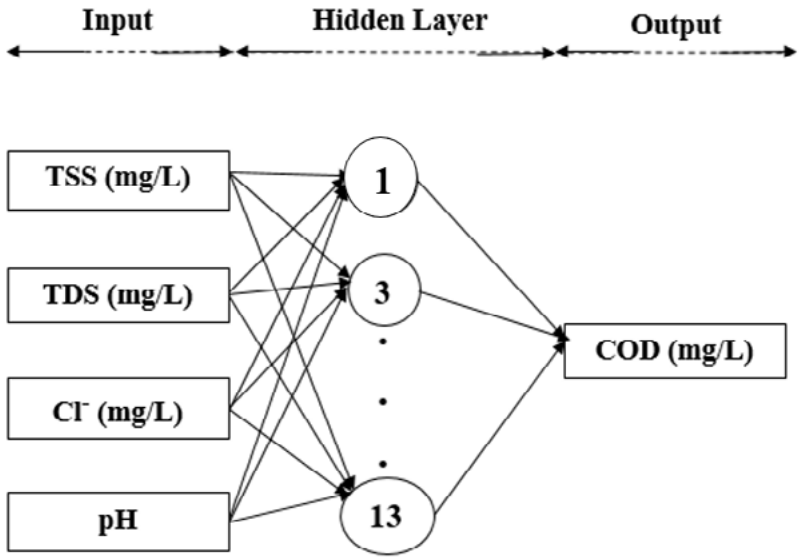

Figure 11. The architecture of the ANN model for the prediction of COD removal.

CONCLUSION

The results of the ANNs modelling for the prediction of BOD, and COD provided several advantages over the traditional calculation methods. The models were accurately able to determine the removal efficiency of the BOD, and COD of Al-Rustumiya WWTP by the use of raw dataset. The developed models can be considered as simple, fast, and most accurate determination tools. This proved that the developed MLP network trained with backpropagation incorporated with Levenberg–Marquardt algorithm was adequate in predicting the performance of Al-Rustamiya WWTP. For BOD and COD, the best results were obtained with 13 neurons at 3.09 MSE and 0.96 R for BOD and 4.28 MSE and 0.95 R for COD.

ACKNOWLEDGEMENTS

This research was carried out in Civil Engineering at Al-Nahrain University, Baghdad, Iraq. The assistance and support of Al-Rustamiya WWTP Administration Office Mayoralty of Baghdad are gratefully acknowledged.

CONFLICT-OF-INTEREST STATEMENT

The authors declare no conflict of interest for this research

REFERENCES

(1) Fahad A., Mohamed R. M. S., Bakar R., and Al-Sahari M. (2019). **Wastewater and its Treatment Techniques: An Ample Review.** *Indian Journal of Science and Technology*, 12(25).

https://doi.org/10.17993/3cemp.2023.120151.257-271

(2) Kılıç Z. (2021). **Water Pollution: Causes, Negative Effects and Prevention Methods.** *IZU Journal of the Institute of Science and Technology,* 3(2).

(3) Al-Attar R. T., Faris H. Al-Ani, and Al-Khafaji M. S. (2022). **SWOT-Based Assessment of the Maintenance Management of the Wastewater Treatment Plants in Iraq.** *Engineering and Technology Journal*, 40(5), 677-694.

(4) G. Sin, S. W. H. Van Hulle, D. J. W. De Pauw, A. van Griensven and P. A. Vanrolleghem. (2005). **A critical comparison of systematic calibration protocols for activated sludge models: A SWOT analysis.** *Water Research,* 39(12), 2459–2474.

(5) A. A. Abbas, Y. T. Yousif and H. H. Almutter. (2022). **Evaluation of Al-Thagher Wastewater Treatment Plant.** *Periodica Polytechnica Civil Engineering*, 66(1), 112–126.

(6) Han H. G., Qiao J.F., and Chen Q.L. (2012). **Model predictive control of dissolved oxygen concentration based on a self-organizing RBF neural network, Control.** *Eng. Pract.*, 20(4), 465–476.

(7) Olyaie E., Banejad H., Chau K.W., and Melesse A.M. (2015) **A comparison of various artificial intelligence approaches performance for estimating suspended sediment load of river systems: A case study in United States.** *Environ. Monit. Assess.,* 187(4),189.

(8) Seo Y., Kim S., and Singh V.P. (2018). **Comparison of different heuristic and decomposition techniques for river stage modelling.** *Environ. Monit. Assess.*, 190(7), 392.

(9) Shamshirband S., Jafari Nodoushan E., Adolf J.E., Abdul Manaf A., Mosavi A., and Chau K.W. (2019). **Ensemble models with uncertainty analysis for multi-day ahead forecasting of chlorophyll a concentration in coastal waters.** *Eng. Appl. Comp. Fluid.*, 13(1), 91–101.

(10) Ahmed A. A. M., Hossain M. I., Rahman M. T. and Chowdhury M. A. I. (2013). **Application of artificial neural network models for predicting dissolved oxygen concentration for Surma River, Bangladesh.** *Journal of Applied Technology in Environmental Sanitation*, 3(3), 135–140.

(11) Nourani V., Kisi O., and Komasi M. (2011). **Two hybrid Artificial Intelligence approaches for modeling rainfall runoff process.** *Journal of Hydrology*, 402, 41-59.

(12) Mohammed N. Y. (2016). **Assessment and Modelling of the Performance of Al Wahda Water Treatment Plant.** *Master Thesis: University of Baghdad*.

(13) Abrahart R., Kneale P. E. and See L. M. (2004). **Neural networks for hydrological modelling**. *CRC Press.*

(14) Ali ZH., Abd. Salman K., and Abd-Alateef K.A. (2001). **Evaluating the efficiency of the filter in AlRustamiya wastewater treatment plant.** *Almustansriyah J.*, 12, 200-212.

(15) Rasheed Kh. A. (2016). **Study the Efficiency of two waste Treatment Plants in the Al-Karkh and Al-Rusafa of Baghdad Region in 2015.** *J. Int. Environmental Application & Science*, 11(2), 176-179.

(16) Dunia Frontier Consultants. (2013). **Water and Sewage Sectors in Iraq: Sector Report. A report for JCCME prepared by Dunia**.

https://doi.org/10.17993/3cemp.2023.120151.257-271

(17) Amanat Baghdad. (2021). **Baghdad Water Supply and Sewerage Improvement Project**. https://amanatbaghdad.gov.iq/page.php?link=World%20Bank%20ads&lang=en

(18) Tümer A. E. and Edebali S. (2015). **An Artificial Neural Network Model for Wastewater Treatment Plant of Konya.** *International Journal of Intelligent Systems and Applications in Engineering*, 3(4), 131-135.

(19) Ammari A. (2016). **MATLAB Code of Artificial Neural Networks Estimation.** *ResearchGate*.

(20) Alsulaili A. and Refaie A. (2021). **Artificial neural network modeling approach for the prediction of five-day biological oxygen demand and wastewater treatment plant performance.** *Water Supply*, 21(5), 1861-1877.

(21) Shahin M. A. (2003). **Use of artificial neural networks for predicting settlement of shallow foundation on conhesionless soils**. *The university of Adelaide school of civil and environmental engineering*, 6-37.

(22) Ibrahim M. A., Mohammed-Ridha M. J., Hussein H. A., and Faisal A. A.H. (2020). **Artificial Neural Network Modeling of the Water Quality Index for The Euphrates River in Iraq.** *Iraqi Journal of Agricultural Sciences,* 51(6), 1572-1580.

https://doi.org/10.17993/3cemp.2023.120151.257-271

/14/

LEVEL OF LIPID PROFILE AND LIVER ENZYME OF DIABETIC MALE RATS INDUCED BY STREPTOZOTOCIN TREATED WITH FORXIGA

Wala'a. H. Hadi
College of Nursing, National University of Science & Technology, Iraq
wala.h.hadi@nust.edu.iq - https://orcid.org/0000-0001-9940-4539

Teeba T. Khudair
College of Nursing, National University of Science & Technology, Iraq
taiba.th.khudair@nust.edu.iq - https://orcid.org/0000-0001-8701-797X

Prof. Dr. Khalid G. Al-Fartosi
College of Nursing, National University of Science & Technology, Iraq
khalidalartosi@yahoo.com

Reception: 31/10/2022 **Acceptance**: 05/01/2023 **Publication**: 23/01/2023

Suggested citation:

H. H., Wall's, T. K., Tea and G. A., Khalid (2023). **Level of lipid profile and liver enzyme of diabetic male rats induced by streptozotocin treated with forxiga**. *3C Empresa. Investigación y pensamiento crítico, 12(1)*, 273-288. https://doi.org/10.17993/3cemp.2023.120151.273-288

ABSTRACT

The present study including study Level of lipid profile and liver enzyme of diabetic male rats induced by streptozotocin The study was carried out in the animal house of the Biology Department, College of Science, University of Thi-Qar ,Iraq. Thirty lab male rats were used in this study, and divided into five groups (6 rats for each group).

Thirty male rats (190-210 gm) were randomly divided into five groups and placed in cages according to the groups, containing 6 rats per group as following. Group1, considered as the negative control group, given food and water for a period of 30 days. Group 2, served as the diabetic positive control, given streptozotocin were injected I.P. 60 mg/kg b.w. as a single dose with food and water for 15 days. Group 3, received streptozotocin were injected I.P (60 mg/kg) with food and water for 15 days, then treated with forxiga 1mg/kg administrated orally every day for a period of 15 days. Group 4, given were injected I.P streptozotocin (60 mg/kg) with s food and Water for 30 days. Group 5, received streptozotocin were injected I.P (60 mg/kg) with food and water. Then treated with forxiga1mg/kg administrated orally every day for a period of 15 day. At the end of experimental, all rats were euthanized, blood sample were obtained for bio chemical parameters.

KEYWORDS

Lipid profile, liver enzyme ,Streptozotocin, Diabetic rats, forxiga

https://doi.org/10.17993/3cemp.2023.120151.273-288

PAPER INDEX

https://doi.org/10.17993/3cemp.2023.120151.273-288

1. INTRODUCTION

Diabetes mellitus (DM), a disarray of carbohydrate metabolism, is a medical and endocrinological set of symptoms characterized by hyperglycemia, high glycated hemoglobin, and a high risk of morbidity and humanity (1). It is caused by absence or diminish efficiency of endogenous insulin or the inappropriate use of insulin by goal cells, and is characterized by unbalanced metabolism, hypertension, and squeal principally distressing the vasculature (2). Experimental models in animals are used to study a variety of aspects associated to the disease, such as its symptom, development, and complication. They have also been second-hand in pharmacological tests in the exploration for more successful drugs and treatments.

The diabetes model most often use absorb the supervision of a single high dose of streptozotocin(STZ) or alloxan (ALX) to fully developed animals, which lead to the damage of pancreatic β cells and reason hyperglycemia as a express consequence of undersupplied insulin production (3). Forxiga exerts its glucose-lower property through awkwardness of the SGLT2 protein in the kidney proximal tubule, resultant in the excretion of glucose and calories into the urine(4). This lackluster energy balance consequences in dapagliflozin treatment-associated weight loss, as has been confirmed in a number of clinical Studies(5,6). Diabetic patients recurrently display a progressive decline in muscle mass and impair muscle serviceable quality(7), which are caused by concentrated insulin sensitivity and decreased mitochondrial role payable underline pathogenesis of T2DM(8).Regarding SGLT2i induced weight reduction, clinical concern has been raise over the event of sarcopenia(decrease in muscle mass)(9 ,10) and clinical studies are therefore needed to establish the weight loss efficacy and any belongings on muscle mass of dapagliflozin treatment in T2DM patients(11).

Aim of this study to elevated Level of lipid profile and liver enzyme of diabetic male rats induced by streptozotocin Treated with Forxiga.

2. MATERIAL AND METHODS

2.1. INDUCTION OF DIABETES MELLITUS

The male rats intraperitoneally injected by a single dose STZ (Sigma, Chemical), 60 mg/kg body wt, dissolved in sodium citrate buffer (0.1 mol/liter, pH 4.5) at a concentration of 20 mg/ml immediately before use. In order to prevent the onset of severe hypoglycemia they have received a solution of 10% glucose instead of normal drinking water over the 24 hours following the treatment. Streptozotocin induces diabetes within 3 days by destroying the beta cells and a mean blood glucose > 250 mg/dL. Diabetic animals and non-diabetic control group were kept in metabolic cages individually and separately and under feeding and metabolism control. Glucose in the blood of diabetic rats exceeded that of the non-diabetic control ones. Diabetes rats were treatment were with Forxiga drug (1mg /1kg/day) orally for 15 day. Animals used

https://doi.org/10.17993/3cemp.2023.120151.273-288

as normal control received standard rat pellet with ad libitum, distilled water till the end of the experiment.

2.2. EXPERIMENTAL DESIGN

Thirty male rats (190-210 gm) were randomly divided into five groups and placed in cages according to the groups, containing 6 rats per group as following.

1-Group1 :(Control group) considered as the negative control group, given food and water for a period of 30 days.

2-Group 2: (DM group for 15 day) served as the diabetic positive control, given streptozotocin were injected I.P.60 mg/kg b.w. as a single dose with food and water for 15 days.(12).

3-Group 3: (DM+ forxiga group for 15) received streptozotocin were injected I.P(60 mg/kg) with food and water for 15 days, then treated with forxiga 1mg/kg administrated orally every day for a period of 15 days. (13).

4-Group4:(DM group for 30 day) given were injected I.P streptozotocin(60 mg/kg) with s food and Water for 30 days

5- Group 5: (DM+ forxiga group for 30) received streptozotocin were injected I.P (60 mg/kg) with food and water. Then treated with forxiga1mg/kg administrated orally every day for a period of 30 day.

At end of experiment measured body weight of animals and then sacrificed.

2.3. BLOOD SAMPLES

Blood were drawn from each animal in the experimental groups, by heart puncture method after 12 hours fast and sacrificed by inhalation milddiethyl ether. Blood samples were obtained by means of heart puncture. Using 5cc sterile syringes, the sample was transferred into clean tube, left at room temperature for 15 minutes for clotting, centrifuged at 3000 rpm for 15 minutes, and then serum was separated and kept in a clean tube in the refrigerator at (-20$_o$C) until the time of assay.

2.4. MEASUREMENT OF GLUCOSE LEVEL (MG/DL)

Test principle

Enzymatic situation method through hexokinase.4,5 Hexokinase (HK) catalyzes the Phosphorylation of glucose through ATP to formglucose-6-phosphate and ADP. To follow the response, a second enzyme, glucose-6-phosphate dehydrogenase (G6PDH) is use to catalyze oxidation of glucose-6-phosphate by NADP+ to form NADPH (Titetz, 2006).

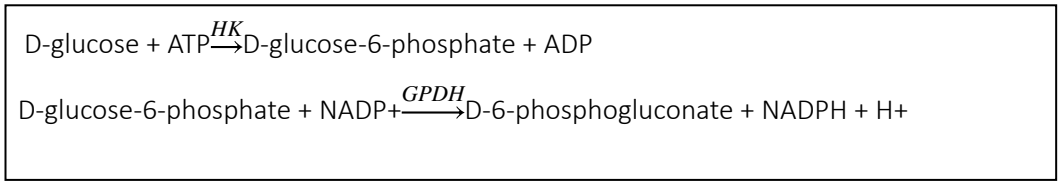

https://doi.org/10.17993/3cemp.2023.120151.273-288

The attentiveness of the NADPH formed is directly proportional to the glucose concentration. It is determined by measuring the raise in absorbance at 340 nm.

Reagents - working solutions

R1	MES buffer: 5.0 mmol/L; pH 6.0; Mg2+: 24 mmol/L; ATP: ≥ 4.5 mmol/L; NADP+: ≥ 7.0 mmol/L
SR	HEPES buffer: 200 mmol/L; pH 8.0; Mg2+: 4 mmol/L; HK (yeast):≥ 300 µkat/L; G6PDH (microbial): ≥ 300 µkat/L

2.5. MEASUREMENT OF LIPID PROFILE

2.5.1. TOTAL CHOLESTEROL LEVEL (TC) (MG/DL)

Enzymatic, colorimetric technique Cholesterol esters are cleave by the action of cholesterol esterase to yield free cholesterol and fatty acids. Cholesterol oxidize then catalyzes the oxidation of cholesterol to cholest-4-en-3-one and hydrogen peroxide. In the attendance of peroxides, the hydrogen peroxide formed effects the oxidative coupling of phenol and 4-aminoantipyrine to form a red quinone-imine dye.

Cholesterol esters + H2O $\xrightarrow{CE}$ cholesterol + RCOOH

Cholesterol + O2 $\xrightarrow{CHOD}$ cholest-4-en-3-one + H2O2

2 H2O2 + 4-AAP + phenol $\xrightarrow{POD}$ quinone-imine dye + 4 H2O

The color concentration of the dye formed is directly proportional to the cholesterol concentration. It is determined by measuring the increase in absorbance at 512 nm.

Reagents - working solutions

R	PIPESa) buffer: 225 mmol/L, pH 6.8; Mg2+: 10mmol/sodium cholate: 0.6 mmol/L; 4-aminoantipyrine: ≥ 0.45 mmol/L; phenol: ≥ 12.6 mmol/L; fatty alcohol polyglycol ether: 3 %; cholesterol esterase (Pseudomonas spec.): ≥ 25 µkat/L (≥ 1.5 U/mL); cholesterol oxidase (E. coli): ≥ 7.5 µkat/L (≥ 0.45 U/mL); peroxidase (horseradish): ≥ 12.5 µkat/L (≥ 0.75 U/mL); stabilizers; preservativea) PIPES = Piperazine-1,4-bis(2-ethanesulfonic acid.

https://doi.org/10.17993/3cemp.2023.120151.273-288

Pipetting parameters

Diluent (H2O)

R 47 µL70 µL

Sample 2 µL23 µL

Total volume 142 µL

Calculation

$$Result = \frac{Abs(Assay)}{Abs(standard)} x Standard\,concentration\left(\frac{mmol}{L}\right)$$

2.5.2. TRIGLYCERIDES LEVEL(TG) (MG/ML)

Test principle

Enzymatic colorimetric test (sidelet al .,1993).

triglycerides + 3 H2O $\xrightarrow{LPL}$ glycerol + 3 RCOOH

glycerol + ATP $\xrightarrow{GK}$ glycerol-3-phosphate + ADP

glycerol-3-phosphate + O2 $\xrightarrow{GPO}$ dihydroxyacetone phosphate + H2O2

H2O2 + 4-aminophenazone + 4-chlorophenol $\xrightarrow{Peroxidase}$

4-(p-benzoquinone-monoimino)-phenazone + 2 H2O + HCl

Reagents - working solutions

R	PIPES buffer: 50 mmol/L, pH 6.8; Mg2+: 40 mmol/L;sodium cholate: 0.20 mmol/L; ATP: ≥ 1.4 mmol/L; 4-aminophenazone: ≥ 0.13 mmol/L; 4-chlorophenol: 4.7 mmol/L; LPL (microbial): ≥ 83 µkat/L; GK (microbial): ≥ 3 µkat/L; GPO (microbial): ≥ 41 µkat/L; POD (horseradish): ≥ 1.6 µkat/L; preservative; stabilizers

R is in position B

Pipetting parameters

Diluent (H2O)

R 120 µL

Sample 2 µL28 µL

Total volume 150 µL

https://doi.org/10.17993/3cemp.2023.120151.273-288

Calculation

$$\text{Result} = \frac{Abs(Assay)}{Abs(standard)} x Standard\ concentration(200) mg/dl$$

2.5.3. HIGH DENSITY LIPOPROTEIN LEVEL (HDL) (MG/ML)

Test principle

Homogeneous enzymatic colorimetric assay. In the attendance of magnesium ions and dextran sulfate, water-soluble complexes with LDL, VLDL, and chylomicrons are form which are resistant to PEG-modified enzymes. The cholesterol special management of HDL cholesterols single-minded enzymatically by cholesterol esterase and cholesterol oxides couple with PEG to the amino groups (approximately40 %). Cholesterol esters are busted down quantitatively into gratis cholesterol and fatty acids by cholesterol esterase. In the presence of oxygen, cholesterol is oxidized by cholesterol oxides to Δ4cholestenoneand hydrogen peroxi.

HDL-cholesterol esters + H2O $\xrightarrow{PEG - cholesteol\ esterase}$ HDL-cholesterol+ RCOOH

HDL-cholesterol + O2 $\xrightarrow{PEG - cholesteol\ oxidase}$ Δ4-cholestenone + H2O2

2 H2O2 + 4-aminoantipyrine + HSDA a) + H+ + H2O $\xrightarrow{peroxidase}$ purple blue pigment + 5 H2O

a) Sodium N-(2-hydroxy-3-sulfopropyl)-3,5-dimethoxyaniline.The color intensity of the blue quinoneimine dye formed is directly proportional to the HDL-cholesterol concentration. It is determined by measuring the increase in absorbance at 583 nm.

Reagents - working solutions

R	HEPES buffer: 10.07 mmol/L; CHES: 96.95 mmol/L, pH 7, sulfate: 1.5 g/L; magnesium nitrate hexahyd rat> 11.7 mmol/L; HSDA: 0.96 mmol/L; as corbate oxides (Eupenicillium sp., recombinant): > 50 µ/L; per oxides (horseradish): > 16.7 µt/L; preservative
RS	HEPES buffer: 10.07 mmol/L, pH 7.0; PEG cholesterol esterase(Pseudomonas spec.): > 3.33 µ /L; PEG cholesterol oxides (Streptomycin sp., recombinant): > 127 µ/L; per oxidize(horseradish): > 333 µ/L; 4-amino-antipyrine: 2.46 mmol/L; preservative

R1 is in position B and SR is in position C.

Pipetting parameters

Diluent (H2O)

R1 150 µL

https://doi.org/10.17993/3cemp.2023.120151.273-288

Sample 2.5 µL7.0 µL

SR 50 µL

Total volume 209.5 µL

Calculation

$$Result = \frac{Abs(sample)}{Abs(Stander)} \times 50 \times 2$$

2.5.4. LOW DENSITY LIPOPROTEIN LEVEL (LDL) (MG/DL)

Serum LDL concentration can be calculated by the following equation (Ram,1996).

L D L = Cholesterol con. – (HDL +TG/5) = $(mmol/L)$

2.5.5. VERY LOW DENSITY LIPOPROTEIN (MG/ML)

By the following function:

VLDL= (TG\5)

2.6. MEASUREMENT OF LIVER ENZYME

2.6.1. ALANINE AMINOTRANSFERASES LEVEL (ALT)(U/L)

Test principle

Method according to the International Federation of Clinical Chemistry (IFCC), but without pyridoxal-5'-phosphate.3,4ALT catalyzes the reaction between L-alanine and 2-oxoglutarate(Schumann et al .,2002). The pyruvate formed is reduced by NADH in a reaction catalyzed by lactatedehydrogenase (LDH) to form Lactate and NAD+ Lalanine + 2-oxoglutarate$ALT \rightarrow$ pyruvate + Glutamate

pyruvate + NADH + H+$LDH \rightarrow$ Lactate + NAD+

The rate of the NADH oxidation is directly proportional to the catalytic ALT activity. It is determined by measuring the decrease in absorbance at340 nm.

Reagents - working solutions

R1	TRIS buffer: 224 mmol/L, pH 7.3 (37 °C); Lalanine: 1120mmol/L; albumin (bovine): 0.25 %; LDH (microorganisms): 45µkat/L; stabilizers; preservative
RS	2Oxoglutarate: 94 mmol/L; NADH: ≥ 1.7 mmol/L;preservate

R1 is in position B and SR is in position C.

https://doi.org/10.17993/3cemp.2023.120151.273-288

Pipetting parameters

Diluent (H2O)

R1 59 µL10 µL

Sample 11 µL26 µL

SR 17 µL9 µL

Total volume 132µL

2.6.2. ASPARTATE AMINOTRANSFERASES LEVEL(AST) (U/L)

Test principle

Method according to the International Federation of Clinical Chemistry(IFCC), but without pyridoxal-5'-phosphate.3,4AST in the sample catalyzes the transfer of an amino group between Aspartame and 2-oxoglutarate to form oxaloacetate and Glutamate. The oxaloacetate then reacts with NADH, in the presence of malatedehy drogenase (MDH), to form NAD+

Aspartate + 2oxoglutarate$\xrightarrow{AST}$ oxaloacetate + Glutamate
Oxaloacetate + NADH + H+$\xrightarrow{MDH}$ malate + NAD+

The rate of the NADH oxidation is directly proportional to the catalytic AST activity. It is determined by measuring the decrease in absorbance at 340 nm.

Reagents - working solutions

R1	TRIS buffer: 264 mmol/L, pH 7.8 (37 °C); L-aspartate: 792 mmol/L;MDH (microorganism): ≥ 24 µ/L; LDH (microorganisms):≥ 48 µkat/L; albumin (bovine): 0.preservative
RS	NADH: ≥ 1 .7 mmol/L; 2-oxoglutarate: 94 mmol/L; preservative

R1 is in position A and SR is in position B and C.

Pipetting parameters

Diluent (H2O)

R140 µL29 µL

Sample 11 µL26 µL

SR 17 µL9 µL

Total volume 132µL

https://doi.org/10.17993/3cemp.2023.120151.273-288

2.6.3. ALKALINE PHOSPHATASE LEVEL(ALP) (U/L)

Test principle

Colorimetric assay in accordance with a standardized method. In the presence of magnesium and zinc ions, pnitrophenyl phosphate is cleaved by phosphatase into phosphate and pnitrophenyl.

pnitrophenyl phosphate + H2O$ALP \rightarrow$ phosphate + pnitrophenyl

The pnitrophenyl released is directly proportional to the catalytic ALP activity. It is determined by measuring the increase in absorbance at409 nm.

Reagents - working solutions

R1	2-amino-2-methyl-1-propanol: 1.724 mol/L, pH 10.44 (30 °C)magnesium acetate: 3.83 mmol/L; zinc sulfate: 0.766 mmol/L; N-(2-hydroxyethyl)-ethylenediaminetriacetic acid: 3.83 mmol/L
RS	p-nitrophenyl phosphate: 132.8 mmol/L, pH 8.5 (25 °C); preservatives

R1 is in position B and SR is in position C.

Pipetting parameters

Diluent(H2O)

R1 75 µL16 µL

Sample 2.75 µL20 µL

SR 17 µL10 µL

Total volume 140.75 µL

$$ALP = \frac{Abs\ sample - Abs\ blank}{Abs\ standard} \times \mathbf{n}$$ N=141,8 u/l

3. RESULTS

3.1. EFFECT OF FORXIGA ON GLUCOSE LEVEL OF DIABETIC MALE RATS

The results as presented in table 1 indicated a significant increase (P≤ 0.05) of glucose concentration in DM and DM +forxiga groups (2,3,4and5)compared with control group, while no significant different were recorded in STZ treated group for 15 days compare with group that treated for 30 days . However a significant (P≤ 0.05) increase in glucose level of group DM and DM +forxgia groups for 15 days. In addition, significant (P≤ 0.05) increase in glucose level of group DM and DM +forxgia groups for 30 days.

https://doi.org/10.17993/3cemp.2023.120151.273-288

Table 1. Effect of forxiga on glucose level of diabetic male rats.

Parameters Groups	Glucose (mg/dl)
Group 1 Control group	88.16 ± 8.75[c]
Group 2 DM group (15 days)	329.33 ± 62.25[a]
Group 3 DM +Forxiga (15 days)	150.50 ± 14.23[b]
Group 4 DM group (30 days)	427.33 ± 230.02[a]
Group 5 DM +Forxiga (30 days)	277.0 ± 42.70[b]
L.S.D	146.57

*Values expressed as Mean ± SD(n=6)

*Different small letters denote significant deference (P ≤ 0.05) between experimental groups.

3.2. EFFECT OF FORXIGA ON LIPID PROFILE LEVEL OF DIABETIC MALE RATS

The results of lipids profile that found in the present study showed a significant (P≤0.05) increase in serum concentrations of CHOL and TG level in groups(2,3,4and5) compared with control group. There was significant decrease in serum concentrations CHOL and TG in DM group compared with DM (group 2) + forxiga group for 15 days (group 3). The serum concentrations of CHOL and TG was significant decrease in STZ administration group(group 4)compared with DM+forxiga group(5).

In the table 2 the results indicated no significant changes in the serum concentration of HDL in group(2,3 and 5) compared with control group. There was no significant change in level of HDL in group(2)compared with group(3). While there was significant(P≤0.05) increase of HDL level in group(5) compared with group(4).

In same table 2 the results indicated a significant increase (P≤0.05) in the serum concentration of groups(2,3,4 and 5) compared with control group. The serum concentration LDL was no significant change in group(2) compared with group(3). But there was no significant change in group (4) compared with group (5).

https://doi.org/10.17993/3cemp.2023.120151.273-288

Lastly a significant increase (P≤0.05)of the serum concentration of VLDL in DM and DM+ forxiga groups(2, 3, 4, 5) compared with control group (1). The serum concentration of VLDL a significant decrease in DM group compared with DM + forxiga group for 15 days .A significant decrease (P≤0.05)of the serum concentration of VLDL in group administration of STZ (group 4) than those of administration of STZ and treated with forxiga for 30 days(group 5) .

Table 2. Effect of forxiga on lipid profile level of diabetic male rats

Parameters Group	Cholesterol (mg/dl)	TGs (mg/dl)	HDL (mg/dl)	LDL (mg/dl)	VLDL (mg/dl)
Group 1 Control group	88.0 ± 5.54^{a}	60.0 ± 8.80^{d}	33.33 ± 6.80^{ab}	41.55 ± 4.42^{c}	11.66 ± 1.52^{d}
Group 2 DM group (15 days)	128.83 ± 4.70^{b}	165.50 ± 6.09^{b}	31.50 ± 5.0^{ab}	64.23 ± 7.49^{ab}	33.10 ± 1.21^{b}
Group 3 DM +Forxiga (15 days)	122.50 ±4.59^{c}	140.0 ± 8.46^{c}	35.0 ± 6.44^{a}	60.50 ± 9.88^{b}	28.0 ± 1.69^{c}
Group 4 DM group (30 days)	138.83 ± 3.48^{a}	185.50 ± 8.50^{a}	29.66 ± 5.60^{b}	72.05 ± 6.50^{a}	37.11 ± 1.70^{a}
Group 5 DM +Forxiga (30 days)	133.66 ± 6.28^{b}	167.16 ± 5.94^{b}	36.0 ± 7.0^{a}	63.40 ± 13.98^{ab}	33.43 ± 1.18^{b}
L.S.D	4.94	7.56	6.24	8.94	1.46

*Values expressed as Mean ± SD (n=6)

*Different small letters denote significant deference (P ≤ 0.05) between experimental groups.

3.3. EFFECT OF FORXIGA DRUG ON LEVEL OF LIVER ENZYME OF DIABETES MALE RATS

The results represented in Table 3 revealed a significant increase (P≤0.05) in serum concentration of ALT, AST groups (2, 3, 4 and 5)compared with control group. A significant decrease (P≤0.05)in DM group(2) compared with DM +forxiga treated group for 15 days (group 3).

On the other hand, ALT and AST concentrations in were significant decrease(P≤0.05)in group(4) compared with group(5).

In same table 3, A significant increase (P≤0.05) in ALP concentration was recorded in serum of the groups (2, 3, 4 and 5) compared with control group. There was no significant change in group DM(group 2) compared with DM + forxiga treated group

https://doi.org/10.17993/3cemp.2023.120151.273-288

for 15 days(group 3) and no significant change in DM (group 4) compared with DM + forxiga treated group (group 5) for 30 days.

Table 3. Effect of forxiga drug on level of liver enzymes of diabetes male rats.

Parameters Groups	ALT(U/L)	AST(U/L)	ALP(U/L)
Group 1 Control group	46.83±6.24^{d}	31.83±2.13^{e}	47.0±4.56^{c}
Group 2 DM group (15 days)	123.33±5.53^{b}	62.16±7.62^{c}	70.33±4.41^{b}
Group 3 DM +Forxiga (15 days)	102.83±13.10^{c}	52.16 ±6.96^{d}	67.48±0.87^{b}
Group 4 DM group (30 days)	139.83±6.21^{a}	89.66±10.57^{a}	92.16±9.90^{a}
Group 5 DM +Forxiga (30 days)	126.16 ±4.79^{b}	74.0 ±12.31^{b}	88.80±1.14^{a}
L.S.D	7.67	8.53	5.22

*Values expressed as Mean ± SD (n=6)

*Different small letters denote significant deference(P ≤ 0.05) between experimental groups.

4. CONCLUSION AND DISCUSSION

Data in the present study showed administration of STZ alone cause significant increase in the glucose as compared to the control group while When use forxiga, glucose return to normal or close to normal compared with control groups.

Uncontrolled blood glucose levels cause conditions of high(hyperglycaemia) or low (hypoglycaemia) blood sugar (14). Diabetes symptoms identify by raised blood glucose, change lipids, carbohydrate, and enhance opportunity for diabetic difficulties and oxidative stress (15,16). Low dosage streptozotocin is known to induce rapid obliteration of pancreatic β-cells lead to impaired glucose-stimulated insulin make public and insulin resistance, both of which are marked features of type 2 diabetes. The result showed significant increase in serum concentration of CHOL, TG, VLDL and LDL in diabetic groups compared with control group, while there was a significant decrease in level of HDL. Forxiga drug lead to significant improvement of serum

https://doi.org/10.17993/3cemp.2023.120151.273-288

concentration of CHOL, TG, VLDL and LDL , but there was significant increase in level of HDL compared with diabetic groups.

Lipid and lipoprotein abnormality are frequent in the diabetic inhabitants due to the effects of insulin shortage and insulin resistance on key metabolic enzymes (17). Glucose tolerance, insulin resistance and plasma an insulin levels have been implicate in abnormal plasma lipoprotein levels and hyperinsulinemia has been associated with the development of atherosclerotic vascular complications in diabetic patients . The result showed a significant increase in levels of (AST ,ALT and ALP) in diabetic groups compared with control group but DM group which treated with forxiga drug caused a significant improvement and return of serum AST and ALT to normal, while no significant changes in serum ALP concentration compared with diabetic group.

The analysis of the activities of these enzymes in the serum was used to observe the condition of liver tissue and any damage might occur after being exposed to a certain pharmacological agent such as STZ. Liver as an insulin-dependent tissue plays a vital role in the metabolism of glucose and other substances. The damage of liver cells cause a leakage of the contents out of the tissue into the blood stream (18). reported that increased activities of serum AST, ALT and ALP level indicated that hepatic dysfunction may be induced due to hyperglycemia in diabetic rats(19-20).

REFERENCES

(1) Alqahtani, N.; Khan, WA.; Alhumaidi, MH.; Ahmed, YA. (2013). **Use of glycated hemoglobin in the diagnosis of diabetes mellitus and pre-diabetes and role of fasting plasma glucose, oral glucose tolerance test**. *International Journal of Preventive Medicine,* 4, 1025-1029.

(2) Agoramoorthy, G.; Chen, F.;Venkatesalu, V.; Kudo, DH.; Shea, PC. (2008). **Evaluation of antioxidant polyphones from selected medicinal plants of India**. *Asian Journal of Chemistry,* 20, 1311-1322.

(3) Correla-santos, AM.; Suzuki, A.; Anjos, JS.; Rego, TS.; Almeida, KCL. and Boavetura, GT. (2012). **Induction of Type 2 Diabetes by low dose of streptozotocin and high-fat diet-fed in wistar rats**. *Medicina (Ribeirão Preto),* 45(4), 436-444.

(4) Vivian, EM. (2015). **Dapagliflozin: A new sodium–glucose cotransporter 2 inhibitor for treatment of type 2 diabetes**. *American Journal of Health-System Pharmacy*, 72(5), 361-372.

(5) Bolinder, J.; Ljunggren, O.; Johansson, L. (2014). **Dapagliflozin maintains glycaemic control while reducing weight and body fat mass over 2 years in patients with type 2 diabetes mellitus inadequately controlled on metformin**. *Diabetes Obes Metab.* 16(2), 159–169.

(6) Scheerer, MF.; Rist, R.; Proske, O.; Meng, A. and Kostev, K. (2016). **Changes in HbA1c, body weight, and systolic blood pressurein type 2 diabetes patients initiating dapagliflozintherapy: a primary care database study**. *Diabetes Metab Syndr Obes*, 9, 337-345.

https://doi.org/10.17993/3cemp.2023.120151.273-288

(7) Bianchi, L. and Volpato, S. (2016). **Muscle dysfunction in type 2 diabetes: a major threat to patient's mobility and independence**. *Acta Diabetol,* 53, 879-889.

(8) Heerspink, H.J.L.; Kurlyandskaya, R.; Xu, J. (2016). **Differential effects of dapagliflozin on cardiovascular risk factors at varying degrees of renal function**. *Diabetes,* 65(1), A286.

(9) Fujita Y and Inagaki N. (2014). **Renal sodium glucose cotransporter 2 inhibitors as a novel therapeutic approach totreatment of type 2 diabetes: Clinical data and mechanism of action**. *J Diabetes Investig*, 5, 265-275.

(10) Bouchi, R.; Terashima, M.; Sasahara, Y.; Asakawa, M.; Fukuda, T.; Takeuchi, T.; Nakano, Y.; Murakami, M.; Minami, I.; Izumiyama,H.; Hashimoto, K,; Yoshimoto, T. and Ogawa, Y. (2017). **Luseogliflozin reduces epicardial fat accumulation in patients with type 2 diabetes: a pilot study**. *Cardiovasc Diabetol*, 16.

(11) Cetrone, M.; Mele, A. and Tricarico, D. (2014). **Effects of the antidiabetic drugs on the age-related atrophy and sarcopenia associated with diabetes type II.** *Current Diabetes Reviews,*10(4), 231-237.

(12) Niyomchan, A.; Sricharoenvej, S.; Lanlua, P. & Baimai, S. (2019). C**erebellar synaptopathy in streptozotocin-induced diabetic rats**. *Int. J. Morphol.*, 37(1), 28-35.

(13) Ling Chen, MD.; Lauren LaRocque, BS.; Orhan Efe, MD.; Juan Wang, MD.; Jeff, M.; Sands, MD. and Janet, D. Klein, PhD. (2017). **Effect of Dapagliflozin Treatment on Fluid and Electrolyte Balance in Diabetic Rats.** *The American Journal of the Medical Sciences*, 352(5), 517-523.

(14) Sacher, R.A.; Mcpherson, R.A. (2001). **Widmann's Clinical Interpretationof Laboratory Tests**. *11th Edn. F.A. Davis Company,* 13–79.

(15) Davis, S. (2006). I**nsulin, oral hypoglycemic agents and the pharmacology of endocrine pancreas.** *McGraw- Hill, Medical Publishing Division,* 1037–1058.

(16) Al-Assaf, A.H. (2012). **Antihyperglycemic and antioxidant effect ofginger extract on streptozotocin-diabetic rats.** *Paki, J. Nutriti.*, 11, 1107–1112.

(17) Gustafsson, I.; Brendorp, B.; Seibaek, M.; Burchardt, H.; Hildebrandt, P. (2004). **Influence of diabetes and diabetes - gender interaction on the risk of death in patients hospitalized with congestive heart failure**. *J. AM. Coll. Cardiol,* 43(5), 771 – 777.

(18) Ozlem- Ozsoy, S.; Yanardaga, R.; Orakb, H.; Ozgeya , Y.; Yaratc, A. and Tunalic, T. (2006). **Effects of parsley (Petroselinum crispum) extract versus glibornuride on the liver of streptozotocin-induced diabetic rats**. Journal of Ethnopharmacol, 104(1–2), 175-81.

(19) Sarfraz, M.; Khaliq,T.; Khan,J.A. and Aslam, B. (2017). **Effect of aqueous extract of black pepper and ajwa seed on liver enzymes in alloxan-induced diabetic Wistar albino rats**. *Saudi Pharmaceutical Journal,* 25, 449–452

(20) M. A. Kumbhalkar, K. S. Rambhad, Nand Jee K. (2021). **An insight into biomechanical study for replacement of knee joint**, Material Today: Proceedings, Elsevier,47(11), 2957-2965. https://doi.org/10.1016/j.matpr.2021.05.202

https://doi.org/10.17993/3cemp.2023.120151.273-288

/15/

SERUM LEVELS OF IFN-Γ, COMPLEMENT COMPONENT C3 C4 AND VITAMIN D3 IN THE PROGNOSIS OF PATIENTS WITH ALOPECIA AREATA PROSPECTIVE TEACHERS

Teeba T. Khudair

College of Nursing, National University of Science& Technology, Iraq

taiba.th.khudair@nust.edu.iq

Wala'a H. Hadi

College of Nursing, National University of Science& Technology, Iraq

Haneen Kadhim Zaid

College of Nursing, National University of Science& Technology,Iraq

Reception: 14/11/2022 **Acceptance**: 06/01/2023 **Publication**: 21/01/2023

Suggested citation:

T. K., Teeba, H. H., Wala'a and K. Z., Hanene. (2023). **Serum levels of ifn-γ, complement component c3 c4 and vitamin d3 in the prognosis of patients with alopecia areata prospective teachers**. *3C Empresa. Investigación y pensamiento crítico, 12(1)*, 290-299. https://doi.org/10.17993/3cemp.2023.120151.290-299

ABSTRACT

***Background**: Alopecia areata is a prevalent autoimmune skin disorder. The current investigation aims to evolve the function of serum IFN-, complement component C3 C4, and vitamin D3 levels in the prognosis of patients with alopecia areata. The blood sample was taken from twenty AA patients and twenty healthy controls. Interferon (IFN-) levels in serum were evaluated using the ELISA method, V.D3 was detected using the Roche electrochemiluminescence method, and C3 and C4 were detected using the immunoturbidimetry method. . In the current study observed elevated levels of IFN-γ (299±115.7 Pg/ml), while the control group was lowest 73±10.84 Pg/ml .This funding was highly significantly different (p-value 0.00). The Mean±SD Level of components C3 and C4 in the current study were (1.37±0.903) (0.29±0.029) Alopecia Areata cases were not statistically different from the usual range, however vitamin D3 levels were severely deficient. (6.86±4.03) when compared to normal range. Distribution of AA among male was highly observed in age group NO = 10 (50%) 1 - 19years follow by age group NO = 4(20%) 20-39 and (40-50) respectively while Alopecia Areata among females was the lowest distribution.*

KEYWORDS

Alopecia Areata, AA, IFN-γ, C3, C4, V.D3, HF.

https://doi.org/10.17993/3cemp.2023.120151.290-299

PAPER INDEX

https://doi.org/10.17993/3cemp.2023.120151.290-299

1. INTRODUCTION

Alopecia areata is an autoimmune disease of specific – organ that causes nonscarring hair loss by targeting hair follicles. Most frequently observed as circular regions of hair loss, but may also be widespread throughout the entire scalp or body (1) . Alopecia areata is categorized as patchy alopecia areata, alopecia areata totalis, and alopecia areata Universalis (2). Several different forms of hair loss can be used to identify it, including: patchy, ophiasis (band-like hair loss in the parieto-temporal-occipital area), ophiasis inversus-sisaipho (band-like hair loss in the fronto-parieto-temporal area), reticulate, and diffuse (2In the general community, the condition affects between 1% and 2% of people (3.4) Perifollicular and intrafollicular infiltrates, which are mostly composed of CD4+ T helper 1 (Th1) cells and CD8+ cytotoxic T cells, respectively, are features of alopecia areata. (5) . The disorder is thought to be an autoimmune, T-cell-mediated disease with a hereditary predisposition and an environmental trigger. (5) Interferon-gamma (IFN-) induce the ectopic expression of MHC class antigens and the over-expression of adhesion molecules in keratinocytes of hair follicles and dermal papilla cells (6) Other reasons include vitamin abnormalities such as excessive retinoic acid and low vitamin D, immune system problems with hair follicle damage, and autoantibodies against tyrosine hydroxylase and retinol-binding protein 4. (7) complement component have been implicated in a variety of autoimmune dermatologic pathologies, including angioedema systemic lupus erythematous, and blistering diseases

The aim of the study is to investigate the effect of serum IFN-, complement component C3 C4, and vitamin D3 levels in the prognosis of patients with alopecia areata.

2. MATERIAL AND METHOD

2.1. STUDY DESIGNED

This study was conducted at the dermatology department of al Nasiriya teaching hospital in Iraq Thi Qar from January 2022 to May 2022., The study included 20 patients with AA and 20 healthy individuals as a control for all data of age ,and gender . Family history, exposure to some chemical substances were recorded in our study . All patients were diagnosed with AA based on clinical signs, medical history and dermoscopic examination . Patients diagnostic with fungal examination or signs of bacterial infection and patients with a history of using systemic or topical treatment within the one month were excluded from the study.

2.2. SAMPLE COLLECTION

A total of4 ml of blood was drawn from the controls and patient groups. Blood samples were centrifuged at 4000 R.P.M and sera were stored at -20 C°. were obtained from all the Patients for (IFN-γ, C3 , C4 ,V.D3 assay) .

https://doi.org/10.17993/3cemp.2023.120151.290-299

2.3. ALOPECIA AREATA -RELATED BIOMARKERS

Complement C3, C4 , IFN-γ , V.D3 were measured in both case and controls group. ELISA Technique detected IFN-γ according to the manufacturer's instructions. Complement component V.D3 were detected by the Roche electrochemiluminescence method. C3, C4 were detected by immune turbidimetry method.

2.4. STATISTICAL ANALYSIS

The data were analyzed using description statistic (mean and standard deviation) independent sample t test the level significant was set at $p < 0.05$ SPSS (Statistical Packing for Social Sciences) version 20

3. RESULT

3.1. AGE GROUP OF PATIENTS INCLUDED IN THE STUDY.

The current study comprised forty patients with Alopecia Areata; the male age group had the highest prevalence of A A. NO = 10 (50%) 1 – 19 years follow by age group NO = 4(20%) 20-39 and (40-50) respectively while Alopecia Areata among females was lowest distribution as shown in Table 1.

Table 1. Show distribution of Alopecia Areata among males and females for different age group.

Patients	No = 20			
Gender	Males		Females	
Age group	Frequency	Percent (%)	Frequency	Percent (%)
1 - 19	10	50%	2	10%
20-39	4	20%	1	5%
40-50	3	15%	0	0%
Total	17	85%	3	15%

3.2. DISTRIBUTION OF C3, C4 AND V.D3 AMONG ALOPECIA AREATA CASES

The Mean±SD Level of complement components C3 and C4 in the current study were (0.37±0.103) and (0.09±0.029) show within the range of normal value in Alopecia Areata cases while the level of vitamin D3 recorded sever deficiency (6.86±4.03) when compared to the normal range as showed in below table.

https://doi.org/10.17993/3cemp.2023.120151.290-299

Table 2. Distribution of C3, C4 ,and V.D3 among Alopecia Areata cases.

Patients NO=20	C3	C4	Vitamin D3
	(1.37±0.903)	(0.29±0.029)	6.86±4.03
Normal Range	(0.9-1.8)g/L	(0.1-0.4) g/L	Deficiency : < 10 Insufficiency: 10 – 30 ng/ml Sufficiency : 30 - 100

3.3. MEAN ± SD SERUM LEVELS OF IFN-Γ IN CONTROLS AND PATIENTS GROUP.

The level of IFN-**γ** in patients was 299±115.7 **Pg/ml**, this value showed to be in AA while the control group was 73±10.84 **Pg/ml**. This funding was highly significantly different (p-value 0.00) as shown in table (4.3).

Table 3. The mean level of interferon_gamma inpatient controls health group .

	No	IFN-γ Pg/ml	P value
Patients	20	299±115.7	0.00
Controls	20	73±10.84	
Total	40		

3.4. THE MEAN±SD OF COMPLEMENT COMPONENT (C3 AND C4) , IFN-Γ AND V. D3 AMONG CASES GROUP.

The Mean±SD level of C3 and C4 were not a significantly different level of C3 , C4 current study than the normal range, the Mean±SD level of **IFN-γ** for A A was significantly higher when compared to the control healthy group, however the mean SD level of vitamin D3 in the cases group was lower when compared to the normal value, and the gap between cases and controls was acceptable. **P value=0.00**

Biochemical test	C3	C4	V.D3	IFN-γ	
				Case group	Controls group
Value	(1.37±0.903)	(0.29±0.029)	6.86±4.03 ng/ml	299±115.7 pg/ml	73±10.84 pg/ml
Normal range	(0.9-1.8)g/L	(0.1-0.4) g/L	Deficiency : < 10 Insufficiency: 10 – 30 Sufficiency : 30 - 100		
P value	0.00				

https://doi.org/10.17993/3cemp.2023.120151.290-299

4. DISCUSSION

4.1. DEMOGRAPHIC PROPERTY

Individuals with AA showed higher levels of IFN-, C3, and C4 in their blood, while having severe V.D3 insufficiency, according to the current study.. Comparison of the values in the normal range in AA patients. case-control research was conducted to identify the relationship between regulation of the IFN-, C3, and C4 of AA as it relates to age groups. According to Alkhalifah (1), who found that 60% of patients are under the age of 20 at initial presentation, and patients with ages 1 to 19 had a higher risk of AA.

4.2. IFN-Γ

Is one sort of proinflammatory process that, among other things, robs dermal papilla cells of their capacity to sustain anagen hair development. It causes various types of cytokines to be produced at the site of inflammation. perifollicular or follicular antigen-presenting cells. (8) We discovered a considerably elevated level of IFN- in our study, and this funding was in agreement with research done by (9) that confirmed E. Arca's findings that patients with AA had considerably higher blood levels of IFN-, (10) Research demonstrated considerably increased serum IFN- levels in individuals with alopecia totalis or alopecia universalis compared to controls, However, there is no discernible difference in IFN- levels between individuals with localized alopecia areata and those with more severe types. Damage to hair follicles (HF) is mediated by IFN- (11) IFN-γ can induce another cytotoxic effector molecule, inducible nitric oxide synthase iNOS (12) . CD4+ Th1 mediated response aberrantly expressed IFN-γ in alopecia areata . Despite the aforementioned, individuals with severe types of alopecia areata may have higher blood levels of the inflammatory protein IFN-, which might indicate the existence of inflammation. Serum IFN- levels may be used as a prognostic sign or to distinguish between those who are more prone to develop alopecia universalis and those who just have the local condition. It is suggested that future study will be able to measure how IFN- levels fluctuate in people who undergo spontaneous regression or disease progression. (10).

4.3. COMPLEMENT COMPONENT C3 AND C4.

Complement is important in the development of AA., Our findings reveal that the levels of C3 and C4 are not considerably different, and this result is consistent with previous studies (13). Findings reveal no difference in levels between patients with AA and healthy controls, and contradiction with the research of (14) that show Complement C4 and C3 were decreased in 67.4% (56/83) and in 9.6% (8/83) of patients, respectively. There were no statistically significant differences between the two groups. C3 deposits in the hyaline membrane of the hair bulb, as well as the connective tissue sheath of anagen hair follicles in both normal and AA-affected scalp, led to the hypothesis that C3 regulates the hair cycle (15) and is not acceptable with

https://doi.org/10.17993/3cemp.2023.120151.290-299

another study of Ribeiro (14) Complement C4 and C3 levels were reduced. in 67.4% (56/83) and in 9.6% (8/83) of patients, respectively.

4.4. VITAMIN D AND AA

The current study discovered that AA patients had considerably decreased blood vitamin D levels when compared to the normal range, which is consistent with other studies.. Aksu. (16), Yilmaz (17) that revealed considerably lower levels of vitamin D in AA patients compared to the control group (17-20) Low calcium and vitamin D levels cause transitory noncicatricial alopecia, implying a role for calcium and potentially vitamin D in postnatal HF cycling Several investigations have found that patients with AA had a much greater frequency of vitamin D deficiency than the control group.. V.D has a vital role in the hair cycle and suppresses the development of dendritic cells which in turn reduces the activation of T-cells and the T-cells mediated immune response. Vitamin D also increases the production of regulatory of CD4+ CD25+ regulatory T cells and enhances their inhibitory function which plays a very important role in self-tolerance and therefore in the prevention of autoimmunity (21) (Gorman et al.2007) Hair loss in AA is caused by the destruction of HF cycle. The significance of vitamin D in HF cycling, on the other hand, is unclear .VDR may function as a selective suppressor/de-repressor of gene expression in the absence of 1,25(OH)2D3 (22) (Lee SM et al.2016) . Wnt/β-catenin signaling is a key player in inducing the onset of anagen and maintaining the cycling transition during the initiation and regeneration of HFs (23) Reduced VDR expression in AA might be linked to diminished hair cycle-related signals. -Wnt/β-catenin signals (24) vitamin D may affect the HF cycling through its impact on autoimmunity in AA pathogenesis .

5. CONCLUSION AND RECOMMENDATION

The role of complement was a contributor to the diagnosis of AA. And the presence of a high level of IFN in the study played a role in increasing the infection due to its effectiveness, as its presence in a large percentage works to deprive the dermal papillary cells of their ability to maintain hair growth and the presence of a percentage of it works to stimulate cytokines in the sites of inflammation. It is also possible to stimulate a cytotoxic molecule called iNOS, and due to this role and its effect on injury, this helps in the future on how these values may change among individuals suffering from the development of the disease. The presence of the role of vitamin D is an influential factor in the role of hair cycling, and its deficiency leads to hair loss. Vitamin D supplementation may play a therapeutic role in reducing disease.

REFERENCES

(1) Alkhalifah A, Alsantali A, Wang E, McElwee KJ, Shapiro J. (2010). **Alopecia areata update: part Clinical picture, histopathology, and pathogenesis**. *J Am Acad Dermatol,* 62, 177-188. https:/doi.org/10.1016/j.jaad.2009.10.032.

https://doi.org/10.17993/3cemp.2023.120151.290-299

(2) Alkhalifah A. (2013). **Alopecia areata update**. *Dermatol Clin.*, 31, 93-108. http://doi.org/10.1016/j.det.2012.08.010.

(3) Safavi, K. (1992). **Prevalence of alopecia areata in the First National Health and Nutrition Examination Survey**. Arch. Dermatol., 128, 702.

(4) Mirzoyev, S.A., Schrum, A.G., Davis, M.D.P., Torgerson, R.R. (2014). **Lifetime incidence risk of alopecia areata estimated at 2.1% by Rochester Epidemiology Project, 1990–2009**. *J. Investig. Dermatol.,* 134, 1141–1142.

(5) Żeberkiewicz, M., Rudnicka, L., Malejczyk, J. (2020). **Immunology of alopecia areata**. *Cent. Eur. J. Immunol*. 45, 325–333.

(6) Giordano, C.N., Sinha, A.A. (2013). **Cytokine pathways and interactions in alopecia areata**. *Eur. J. Dermatol*., 23, 308–318.

(7) Dainichi T, Kabashima K. (2017). **Alopecia areata: What's new in epidemiology, pathogenesis, diagnosis, and therapeutic options?.** J *Dermatol Sci*., 86, 3-12.

(8) M. Sato-Kawamura, S. Aiba, and H. Tagami, (2003). **Strong expression of CD40, CD54 and HLA-DR antigen and lack of evidence for direct cellular cytotoxicity are unique immunohistopathological features in alopecia areata.** *Archives of Dermatological Research*, 294(12), 536-543.

(9) Tomaszewska, K., Kozłowska, M., Kaszuba, A., Lesiak, A., Narbutt, J., & Zalewska-Janowska, A. (2020). **Increased serum levels of IFN-γ, IL-1β, and IL-6 in patients with alopecia areata and nonsegmental vitiligo**. *Oxidative Medicine and Cellular Longevity*.

(10) E. Arca, U. Mus¸abak, A. Akar, A. H. Erbil, and H. B. Tas¸tan, (2004). **Interferon-gamma in alopecia areata.** *European Journal of Dermatology*, 14(1), 33-36.

(11) J. E. Harris. (2013). **Vitiligo and alopecia areata: apples and oranges?.** *Experimental Dermatology*, 22(12), 785-789.

(12) V. Ramirez-Ramirez, M. A. Macias-Islas, G. G. Ortiz. (2013). **Efficacy of fish oil on serum of TNF α, IL-1 β, and IL-6 oxidative stress markers in multiple sclerosis treated with interferon beta-1b.** *Oxidative Medicine and Cellular Longevity*, 2013, 709493, 8.

(13) Berrens L, Jankowski E, Jankowski-Berntsen I. (1976). **Complement component profiles in urticaria, dermatitis herpetiformis, and alopecia areata**. *Br J Dermatol*., 95, 145-152.

(14) Rajabi, F., Drake, L.A., Senna, M.M., Rezaei, N. (2018). **Alopecia areata: A review of disease pathogenesis**. *Br. J. Dermatol, 179(5), 1*033-1048.

(15) Igarashi R, Takeuchi S, Sato Y. (1979). **Deposits of complement C3 in the hair follicle of normal scalp and alopecia areata[J].** *Nihon Hifuka Gakkai Zasshi,* 89, 481-483.

(16) Yilmaz N, Serarslan G, Gokce C. (2012). **Vitamin D concentrations are decreased in patients with alopecia areata**. *Vitam Miner,* 1, 105-109.

(17) Aksu Cerman A, Sarikaya Solak S, Kivanc Altunay I. (2014). **Vitamin D deficiency in alopecia areata**. *Br J Dermatol*., 170, 1299-1304.

(18) Mahamid M, Abu-Elhija O, Samamra M, Mahamid A, Nseir W. (2014). **Association between vitamin D levels and alopecia areata**. *Isr Med Assoc J.,* 16, 367-370.

https://doi.org/10.17993/3cemp.2023.120151.290-299

(19) d'Ovidio R, Vessio M, d'Ovidio FD. (2013). **Reduced level of 25-hydroxyvitamin D in chronic/relapsing Alopecia Areata**. *Dermatoendocrinol*., 5, 271-273.

(20) Daroach M, Narang T, Saikia UN, Sachdeva N, Sendhil Kumaran M. (2018). **Correlation of vitamin D and vitamin D receptor expression in patients with alopecia areata: a clinical paradigm**. *Int J Dermatol,* 57, 217-222.

(21) Gorman S, Kuritzky LA, Judge MA, Dixon KM, McGlade JP, Mason RS. (2007). **Topically applied 1,25-dihydroxyvitamin D3 enhances the suppressive activity of CD4+CD25+ cells in the draining lymph nodes**. *J Immunol*, 179(9), 6273-83.

(22) Lee SM, Pike JW. (2016). **The vitamin D receptor functions as a transcription regulator in the absence of 1,25-dihydroxyvitamin D(3).** *J Steroid Biochem Mol Biol*.,164, 265-270.

(23) Zhang H, Nan W, Wang S, Zhang T, Si H, Yang F, Li G. (2016). **Epidermal growth factor promotes proliferation and migration of follicular outer root sheath cells via Wnt/β-catenin signaling**. *Cell Physiol Biochem*., 39, 360-370.

(24) Gerkowicz A, Chyl-Surdacka K, Krasowska D, Chodorowska G. (2017). **The role of vitamin D in non-scarring alopecia**. *Int J Mol Sci*., 18.

https://doi.org/10.17993/3cemp.2023.120151.290-299

/16/

ANTIBACTERIAL ACTIVITY OF SOME PLANTS EXTRACTS AGAINST PROTEUS MIRABILIS BACTERIA

Rawaa M. Mohammed

Ph.D. Microbilogy, Department of Medical physics, Al-Mustaqbal University College, Iraq

rawaamagid@Mustaqbal-college.edu.iq

Nidaa F. Aziz

M.Sc. Virology, Department of Medical physics, Al-Mustaqbal University College, Iraq

nidaa.fadhil@Mustaqbal-college.edu.iq

Reception: 13/11/2022 **Acceptance**: 10/01/2023 **Publication**: 08/02/2023

Suggested citation:

M. M., Rawaa and F. A., Nidaa. (2023). **Antibacterial activity of some plants extracts against proteus mirabilis bacteria**. *3C Empresa. Investigación y pensamiento crítico, 12(1)*, 301-309. https://doi.org/10.17993/3cemp.2023.120151.301-309

https://doi.org/10.17993/3cemp.2023.120151.301-309

ABSTRACT

***Background**: Medicinal plants are being looked at as potential new sources of medicines that could replace antibiotics in the treatment of antibiotic-resistant bacteria. The aim of this study is to measure the effect of plant extracts on Proteus mirabilis growth to determine the antibacterial activity of them .*

Methods: Experimental, in vitro, of Al-Mustaqabal University Collage, The effects of four plant extracts on Proteus mirabilis were assessed. At a concentration of 10%, the activity was assessed using the well diffusion method.

Result: Four aqueous plant extracts were tested for antibacterial activity (Peganum harmala, Piper nigrum, Syzygium aromaticum and Cinnamomum zeylanicum) has been evaluated against Proteus mirabilis (Isolated from urinary tract infection). The concentration was used for each type of extract 10mg\ml. In this concentration, the aqueous extract was effective against Proteus mirabilis with inhibition zones of 18 mm, 15 mm and 14 mm respectively, and extract of Cinnamomum zeylanicum shown no inhibition zone.

Conclusion: The aqueous extract of Peganum harmala against Proteus mirabilis, showed the highest inhibition of 18mm with the concentration 10%. Whereas, aqueous extract of Cinnamomum zeylanicum has no antibacterial activity against Proteus mirabilis.

KEYWORDS

Medicinal plant, Proteus mirabilis, antibacterial activity, aqueous extract

PAPER INDEX

https://doi.org/10.17993/3cemp.2023.120151.301-309

1. INTRODUCTION

In recent years, the world has turned its attention to the study of medicinal plants, many of which have been found to have inhibitory effect against pathogens. They have been used in the treatment of many diseases, since they contain effective compounds that are inhibitory and free from side effects compared with the drugs used which have side effects on health with increased resistance towards it by time. This has called for urgent and continuous need to search for new antimicrobials as a result of increase in disease cases. The other reason is increasing resistance to antibiotics and on a continuous basis (1).

Medicinal plants contain various types of natural active substances used in traditional medicine (alternative medicine) to treat diseases around the world, the efficiency of these medicinal plants or their extracts varies depending on the method of extraction, the type of extraction solvent employed and the microscopic organism (2).

According to the World Health Organization (WHO), there are over 20,000 species of all recognized medicinal plants utilized worldwide (3).

Some of the chemicals derived from these plants have proven to be an effective preventive medicine and have even been utilized to treat difficult illnesses like cancer (4). The critical necessities to use medicinal plants do not involving severe feature control concerning to safety and efficiency compared to the other drug types (5).

Aim of study: The goal of this study was to see how effective aqueous plant extracts were at killing bacteria (Peganum harmala, Piper nigrum, Proteus mirabilis is fought using Syzygium aromaticum and Cinnamomum zeylanicum.

2. MATERIALS AND METHODS

The following instruments, as indicated in the table, were utilized in this study table 1.

Table 1. Instruments, their manufacturer companies and its origins.

No.	Instruments	Manufacturer company and Origin
1	Centrifuge tube	NURE /turkey
2	Incubator	Biomerieux/USA
3	Autoclave	Hirayama/japan
4	oven	Biomerieux/USA
5	Sensitive balance	Precia/swesra
6	Petri dish	Al-hanoof/jordon
7	Loop	Al-rawan/china

https://doi.org/10.17993/3cemp.2023.120151.301-309

Chemicals and Biological Materials: The table below lists the chemicals and biological materials utilized in this study table 2.

Table 2. The chemicals and biological materials as well as their suppliers and origin.

No.	Name of material	Supplier / Origin
1	Muller Hinton agar	Oxoid /united kingdom
2	Nutrient agar	Oxoid /united kingdom

Samples: The plant materials were obtained from a local market in Babylon Province, and included:

Table 3. Scientific name of plant

No	Scientific name of plant
1	*Peganum harmala* (Harmal)
2	*Piper nigrum* (Black pepper)
3	*Syzygium aromaticum* (Clove)
4	*Cinnamomum zeylanicum* (Cinnamon)

The plant material was washed in distilled water and dried at room temperature in the shade. The plant material has been processed in a mill to produce fine powders after most of the moisture has been removed (6).

Study design (7)

All plants were convert to fine powder

↓

5 gm of plant powder

↓

50 ml D.W

↓

Concentrated the extract by using an oven at 40 c o

↓

1g\ 10ml of each plant extract against Proteus mirabilis

↓

By the well diffusion method 50µ

2.1. EXTRACT PREPARATION

We prepared the plant extracts of (Peganum harmala, Piper nigrum, Syzygium aromaticum and Cinnamomum zeylanicum) according (8) and (9), that include the following : All plants were convert to fine powder and freshly prepared at the day of

https://doi.org/10.17993/3cemp.2023.120151.301-309

experiment using distilled water . In this method, the dried powder plants (5g) were soaked 50 milliliters distilled water. The solvent was evaporated by using an oven at 40 c o and then stored the dry powder in the refrigerator for further use to test the effectiveness against the bacteria used in the experiment.

2.2. ANTIBACTERIAL ACTIVITY

The antibacterial activities of the plant extracts (Peganum harmala, Piper nigrum, Syzygium aromaticum and Cinnamomum zeylanicum) The well diffusion method was used to test Muller-Hinton plats. The medium was sterilized in an autoclave at 121oC (1.5 psi/inch 2) for 15 minutes, following the manufacturer's recommendations. 50 uL of the plant extract was poured into wells cut into the agar. The plates were then incubated at 37°C for 24 hours. The diameter of the inhibitory zone was used to assess antibacterial activity(10)and(11).

2.3. ANTIBACTERIAL ACTIVITY MEASUREMENT (AGAR WELL DIFFUSION METHOD)

Muller Hinton agar plates were prepared and infected with test organisms by using a sterile brush to disseminate the bacterial inoculum on the surface of the media. Wells were punched in the agar by using Cork borer . Extracts with concentrations (10 mg/ml) were added. The plates were incubated for 24 hours at 37°C (12). The antibacterial activity was measured in millimeters by measuring the diameter of the inhibitory zone.

3. RESULT AND DISSCUSSION

Results of antibacterial activity of four aqueous plant extracts (Peganum harmala, Piper nigrum, Syzygium aromaticum and Cinnamomum zeylanicum) against Proteus mirabilis (Isolated from urinary tract infection).

Table 4. The activity of aqueous extracts against Proteus mirabilis

Name of plant	Inhibition zone of diameter
Peganum harmala	18 mm
Piper nigrum	15 mm
Syzygium aromaticum	14 mm
Cinnamomum zeylanicum	No inhibition zone

https://doi.org/10.17993/3cemp.2023.120151.301-309

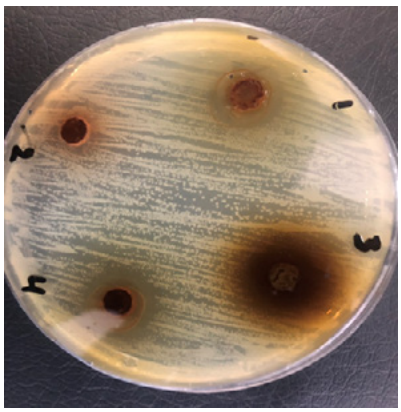

Figure 1. Inhibition zones of Proteus mirabilis growth on Mueller-Hinton agar produced by (1) black pepper (2) Cinnamon (3) clove (4) harmalcontained extract concentrations (10 mg/ml), whereas the central well contained 50 µl.

These results in table(1) revealed that this bacteria was sensitive to the concentrations of 10% in aqueous extract of harmal (Peganum harmala) with inhibition zone 18 mm, that agree with (13) ,which revealed the highest effect on bacterial growth since the hot extract reduced growth of most of bacterial isolates (Proteus mirabilis).(14), which obtained good antibacterial activity in harmal and pomegranate against Proteus mirabilis and Klebsiella using aqueous extract.

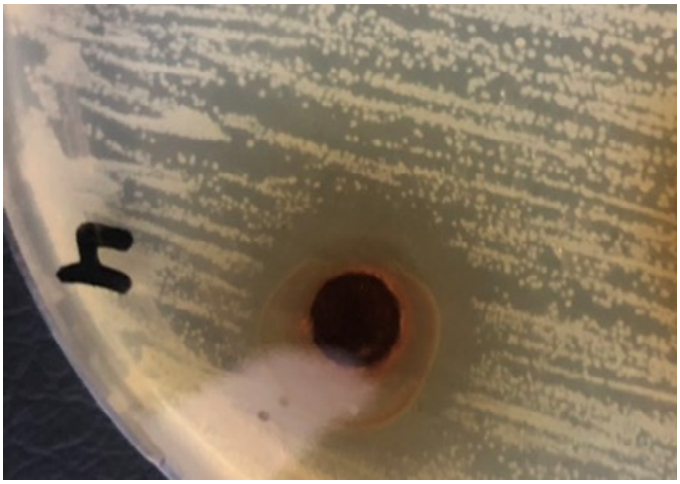

Figure 2. Inhibition zones of Proteus mirabilis growth produced by harmal contained extract concentrations (10 mg/ml), whereas the central well contained 50 µl.

And aqueous extract of black pepper (Piper nigrum) showed in Table1 that antibicrobial activity

against Proteus mirabilis with inhibition zone 15 mm, that agree with (15), reported the antibacterial

effect of piperine against Proteus mirabilis with inhibition zone (8mm). Also with (16), which he mentioned that black pepper (aqueous decoction) showed strongest antibacterial activity and in research against different bacterial isolates from oral cavity of two hundred individual volunteers.

https://doi.org/10.17993/3cemp.2023.120151.301-309

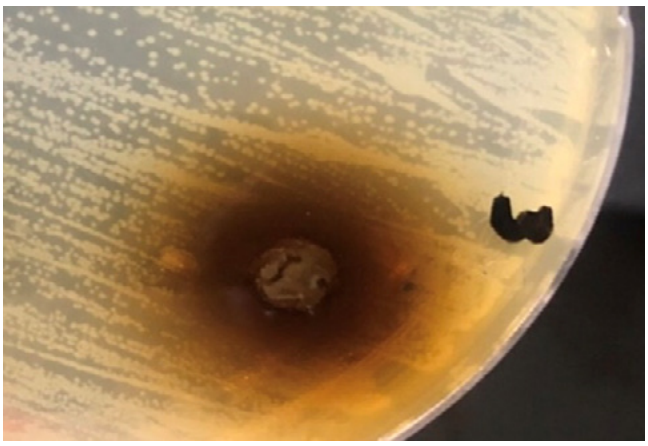

Figure 3. Inhibition zones of Proteus mirabilis growth produced by black pepper contained extract concentrations (10 mg/ml), whereas the central well contained 50 µl.

Our results of clove (Syzygium aromaticum) revealed antibacterial activity against Proteus mirabilis with inhibition zone 14 mm, that agree with, (17) which reported the result of antibacterial susceptibility to S.aromatic The average diameter zone of inhibition for S.aureus, Proteus mirabilis, and P.aeruginosa in aqueous extract was 31mm, 8mm, and 14.33mm, respectively. (18), provided additional support for these findings.

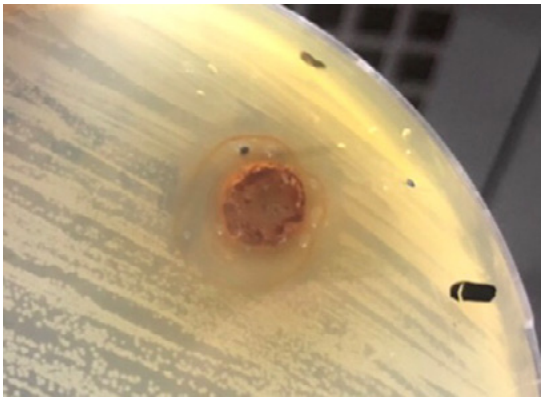

Figure 4. Inhibition zones of Proteus mirabilis growth produced by clove contained extract concentrations (10 mg/ml), whereas the central well contained 50 µl.

While Escherichia coli showed resistance against aqueous concentration extract of Cinnamon (Cinnamomum zeylanicum) as showed in table (1).

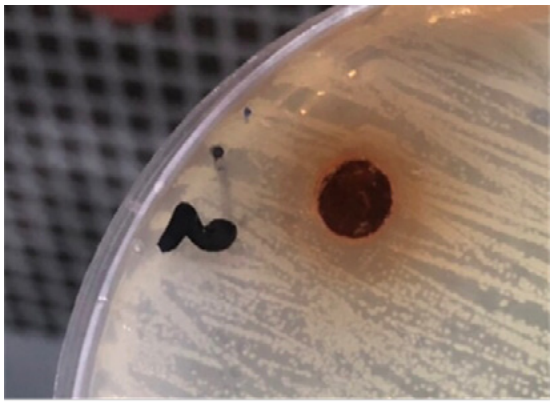

https://doi.org/10.17993/3cemp.2023.120151.301-309

Figure 5. Inhibition zones of Proteus mirabilis growth produced by Cinnamon contained extract concentrations (10 mg/ml), whereas the central well contained 50 µl.

4. CONCLUSIONS

1. Plant extracts have a complicated structure, with active components in the form of natural organic compounds.

2. The solubility of a component in the solvent determines the extraction method for that substance (water or organic solvent).

3. The extracts of the plants studied showed promising antibacterial properties. The prospect of developing antimicrobial chemicals from higher plants appears promising, as it could lead to the development of a phytomedicine that can combat multidrug-resistant bacteria.

4. The aqueous extract of Peganum harmala displayed the greatest inhibition of 18mm against Proteus mirabilis at a concentration of 10%. Cinnamomum zeylanicum aqueous extract, on the other hand, displays no antibacterial action against Proteus mirabilis.

REFERENCES

(1) Abid, M., Patra, A., Tirath, K., Khan, N. A., & Asad, M. (2008). **Subchronic toxicity study of alcoholic extract of pachyrrhizus erosus (linn.) seeds**. *Pharmacologyonline,* 3, 504-508.

(2) Hussein, N. and Hanon, N.A. (2017). **The Antimicrobial Activity of Some Medical Plants Extracts Used Against Some Types of Bacteria that Causes Urinary Tract Infection**. *Al-Mustansiriyah Journal of Science*, 28(3), 72-84.

(3) Harbone ,J.B.(1984). **Phyto chemical methods**. *2nd Ed. chapman Hull.*

(4) Foxman B. (2014). **Urinary tract infection syndromes occurrence, recurrence, bacteriology, risk factors, and disease burden**. *Infect. Dis. Clin. North Am.,* 28, 1-13. https://doi.org/10.1016/j.idc.2013.09.003.

(5) Dubey,. D., M.C. Sahu, S. Rath, B.P. Paty, N.K. Debata and R.N. Padhy. (2012). **Antimicrobial activity of medicinal plants used by aborigines of Kalahandi, Orissa, India against multidrug resistant bacteria**. *Asian Pac. J. Trop. Biomed.*, 2(2), 846-854.

(6) Dorman HJ, Deans SG. (2000). **Antimicrobial agents from plants: antibacterial activity of plant volatile oils**. *J Appl Microbiol,* 88(2), 308-316.

(7) Dorman HJ, Deans SG. (2000). **Antimicrobial agents from plants: antibacterial activity of plant volatile oils**. *J Appl Microbiol,* 88(2), 308-316.

(8) Diba K, Gerami Shoar M, Sharbatkhori M, Khorshivand Z. (2011). **Anti-fungal activity of alcoholic extract of Peganum harmala seed**. *J Med Plants Res.,* 5, 5550-5554.

(9) Dhuley JN. (1999). **Anti-oxidant effects of cinnamon (Cinnamomum verum) bark and greater cardamom (Amomum subulatum) seeds in rats fed high fat diet**. *Indian J Exp Biol.,* 37, 238-242.

https://doi.org/10.17993/3cemp.2023.120151.301-309

(10) Damanhouri ZA, Ahmad A. (2014). **A Review on Therapeutic Potential of Piper nigrum L. (Black Pepper): The King of Spices**. *Med. Aromat. Plants,* 3, 161.

(11) Chaieb K, Hajlaoui H, Zmantar T, et al. (2007). **The chemical composition and biological activity of clove essential oil, Eugenia caryophyllata (Syzigium aromaticum L. Myrtaceae): a short review**. *Phytother Res.,* 21(6), 501-6.

(12) Burt S. (2004) **Essential oils: their antibacterial properties and potential applications in foods – a review**. *Int J Food Microbiol,* 94, 223-253.

(13) Bhalodia, N. R., & Shukla, V. J. (2011). **Antibacterial and antifungal activities from leaf extracts of Cassia fistula l.: An ethnomedicinal plant**. *Journal of advanced pharmaceutical technology & research*, 2(2), 104-109. https://doi.org/10.4103/2231-4040.82956.

(14) Asgarpanah, J. and Ramezanloo Chemistry, F. (2012). **Chemistry, Pharmacology and Medicinal Properties of Peganum harmala L**. *African Journal of Pharmacy and Pharmacology*, 6, 1573-1580.

(15) Alsamarai AGM, Tawfeq B, Salih Y. (2016). **Teenage pregnancy complications in Samara city, Iraq**. *World J Pharm Pharmaceut Sci.*, 5, 142-163.

(16) Al-Sahlany, S.T.G. (2017). **Production of biodegradable film from soy protein and essential oil of lemon peel and use it as cheese preservative**. *Basrah J. Agric. Sci.*, 30(2), 27-35.

(17) Ahmad, N., Fazal, H., Abbasi, B. H., Farooq, S., Ali, M., & Khan, M. A. (2012). **Biological role of Piper nigrum L. (Black pepper): A review**. A*sian Pacific Journal of Tropical Biomedicine*, 2(3), S1945-S1953.

https://doi.org/10.17993/3cemp.2023.120151.301-309

/17/

FORECASTING PERFORMANCE IN IRAQI STOCK EXCHANGE FOR THE OIL PRICE THROW THE GM (1,2) MODEL AND THE IMPACTS ON ECONOMIC GROWTH

Heshu Othm Faqe Mahmood

University of sulaimany College of administration & Economics Statistics and informatics Dep.

heshu.faqe@univsul.edu.iq

Mohammed Aras Ali

University of sulaimany College of Commerce Economic Dep.

mohammed.aras@univsul.edu.iq

Zryan Jabar Raouf Ali

University of sulaimany College of Commerce Business Managment Dep.

zryan.raouf@univsul.edu.iq

Reception: 15/11/2022 **Acceptance**: 13/01/2023 **Publication**: 06/02/2023

Suggested citation:

F. M., Heshu Othm, A. A., Mohammed and R. A., Zryan Jabar (2023). **Forecasting Performance In Iraqi Stock Exchange For The Oil Price Throw The GM (1,2) Model And The Impacts On Economic Growth**. *3C Empresa. Investigación y pensamiento crítico, 12(1)*, 311-322. https://doi.org/10.17993/3cemp.2023.120151.311-322

ABSTRACT

Iraq's oil industry is the country's main source of income. Iraq's manufacturing sector has always been heavily dependent on the country's oil exports. Since the end of the Iraq War, Iraq has expanded its output and is currently the region's second-largest producer. For this investigation, the grey model was run using data on the monthly international price of Iraqi oil from October 2020 through September 2022. Researchers evaluated the MAPE and accuracy rate to choose which model to employ for oil price forecasting, and we found that the GM(2,1) model was the best fit for capturing the dynamics of the Iraqi oil market (precision rate = 96%, MAPE = 4%).

KEYWORDS

oil price, grey model, forecasting.

PAPER INDEX

https://doi.org/10.17993/3cemp.2023.120151.311-322

INTRODUCTION

Petroleum, commonly known as crude oil, is a naturally occurring liquid that may be converted into fuel and is found deep below the Earth's surface. Petroleum is a fossil fuel formed from the gradual breakdown of organic matter; it is burned to generate energy, heat buildings and machinery, and is also used in the production of plastics. As a result of its widespread use, the petroleum industry has significant sway in international affairs, and the wealth and business of countries such as Iraq, Saudi Arabia, and the United Arab Emirates are heavily invested in the sector. The study attempted to highlight the causal relationship between oil prices in the stock market and economic growth in Iraq. The study is based on the hypothesis that there is a bidirectional causal relationship between economic growth and global oil prices. Therefore oil prices will have a significant impact on the structure of economic growth in Iraq.

Iraq is one of the world's largest oil producers but is in an unstable political and economic situation. According to OPEC data, Iraq is rated fifth in the world, behind Venezuela, Saudi Arabia, Canada, and Iran. It should be noted that from 1986 until 2008, it was ranked second.

Oil was found inside Iraqi territory at the beginning of the twentieth century, and the first oil well was dug by the reigning British authorities in Iraq in 1902, but the notion of creating the global oil industry did not become popular until after World War II.

Since the sixties and seventies, Iraq's oil wealth has contributed to the country's rapid economic expansion, which in turn has contributed to the country's development and radical transformation. Iraq has some of the world's greatest oil reserves, with an estimated (147) billion barrels of known reserves. This amounts to over 20% of the world's total oil reserves. Oil is a lifeblood for Iraq, making it one of the world's most dependent nations. In the past ten years, oil sales have paid for more than 99 percent of exports, 85 percent of government spending, and 42 percent of GDP (GDP). This over-reliance on oil makes the economy vulnerable to fluctuations, and budget constraints limit room for manoeuvring in response to economic downturns. Iraq's unemployment rate in January 2021 was over 10 percentage points greater than it had been before COVID-19, at 22.7 percent, in a country of 40,2 million people. The oil and COVID-19 shocks of 2020 jolted the economy, but it is beginning to show signs of recovery. Following a significant decline of 11.3% in 2020, real GDP is predicted to have increased by 1.3% in 2021. As oil output rises and COVID19 limitations are relaxed, domestic economic activity is expected to return to pre-pandemic levels.

The oil sector worked to increase Iraqi revenues, which resulted in financial growth in the budget, which prompted the Iraqi government to increase spending on training, jobs, education, developing infrastructure, and increasing the salaries of government employees.

The grey system theory, of which Professor Deng is the proponent, includes grey prediction. A new model, GM(2,1), is presented to alter the linear structure of the GM(1,1) model and broaden the range of applications for grey prediction theory. Among the family of grey prediction models, it stands out as particularly significant.

https://doi.org/10.17993/3cemp.2023.120151.311-322

The GM(2,1) modeling approach is an offshoot of the GM(1,1) approach and satisfies the same mechanisms. The GM(1,1) model uses an accumulating generation operator (AGO) to reduce the noise in raw data and reveal hidden patterns.

1. LITERATURE REVIEW

Recent years have seen a proliferation of research aimed at advancing grey prediction theory, and as a result, numerous optimized algorithms have arisen, vastly increasing the range of grey prediction's potential applications. Here is a quick synopsis of relevant works:

The grey prediction technique, which Song, F., and et al (2014) employed, is a valuable tool for analyzing small datasets and making predictions for the near future. Among the many significant grey models, the GM(2,1) model stands out. They suggested a structure-optimized GM(2,1) model (SOGM(2,1)) to enhance accuracy and predictability. There are three new insights within grey prediction theory that have come out of this research. After constructing a new grey equation with an optimized structure using the background sequence and the inverse accumulating generated sequence, SOGM(2,1) model parameters are estimated using the method of least errors. Second, using the obtained temporal response function, a reflection equation is formed, and the process of solving it is derived. Finally, they proposed a different approach to determining the initial values of the temporal response function. A subsequent engineering evaluation uses the new model to anticipate highway settlement. The results demonstrate the efficacy and practicality of SOGM(2,1) compared to other models[1]. According to research by Junxu Liu et al (2020), load forecasting is crucial for ensuring the power system's reliability and efficiently allocating energy resources. In this study, we implement load forecasting of the power system using the grey model theory. In this study, we apply the grey model theory to implement medium- and long-term load forecasting. We also employ the posterior difference technique to evaluate the model's performance in this context.

At last, a case study is presented to evaluate the technique's effectiveness [2]. In addition, LiangZeng and ChongLiu (2023) created a novel approach to forecasting China's per capita living electricity consumption using the grey modelling technique, keeping in mind the aforementioned a variety of and mashup of shift patterns. As a result, this work provided an improved version of the DGM(2,1) model by introducing the polynomial component to investigate the growth patterns of different time-series sequences. This was accomplished by fixing the modeling error in the traditional DGM(2,1) model. This motivates the development of a brand-new model (denoted DGM(2,1,kn)) for estimating the future electricity needs of China's population. To help with the development of electrical power policies, forecasts of China's per capita living electricity consumption in 2020 and 2025 have been developed[3]. A brief overview of GM(1,1) models was provided by Evans, M. (2014), who also draws attention to a trend-based alternative to traditional grey prediction theory. This method provides an alternate strategy for estimating the parameters of the fundamental first-order differential equation of the GM (1,1). Parameter estimates obtained using this

https://doi.org/10.17993/3cemp.2023.120151.311-322

alternative method are demonstrated to be more accurate, and the method's straightforward graphical structure makes it simple to see. In this study, a more universal generalization of the Grey-Verhulst model is proposed. When applied to the intensity of steel use in the United Kingdom, yields very solid multi-step forward predictions.

2. METHODOLOGY

2.1. THE GM (2,1) MODELS

The appropriate grey one-by-one model is for exponential pattern sequences; also, it is used to show changes in monotonic patterns. While for other non-monotonic wave, such as development sequences or satiate sequences that is sigmoid, we are able to use GM two by one [5,6].

2.2. THE GM (2,1) MODEL

For raw data sequences $A^{(0)} = (a^{(0)}(1), a^{(0)}(2), \ldots\ldots, x^{(0)}(n))$, let it a generation accumulation and inverse accumulation generation be[5,7,8] $A^{(1)} = (a^{(1)}, a^{(1)}(1), a^{(1)}(2), \ldots\ldots, a^{(1)}(n))$ and $b^{(1)}A^{(0)} = (b^{(1)}a^{(0)}(2), \ldots\ldots, b^{(1)}a^{(0)}(n))$, where $b^{(1)}a^{(0)}(k) = a^{0}(k) - a^{(0)}(k-1),\ k = 2,3,\ldots,n$ and the adjacent sequence of neighbour mean a generation of$A^{(1)}$ $be\ Y^{(1)} = \left(y^{(1)}(2), y^{(1)}(3), \ldots\ldots, y^{(1)}(n)\right)$.

Then

$$b^{(1)}a^{(0)}(k) + b_1 a^{(0)}(k) + b_2 y^{(1)}(k) = c \quad (2.1)$$

Is show that GM(2,1) model ;

$$\frac{d^2 a^{(1)}}{dt^2} + \alpha_1 \frac{da^{(1)}}{dt} + b_2 a^{(1)} = c \quad (2.2)$$

Theorem: For the sequences$A^{(0)}A^{(1)}Y^{(1)}\ and\ b^{(1)}a^{(0)}$, as defined above, let

$$B = \begin{bmatrix} -a^{(0)}(2) & -y^{(1)}(2) & 1 \\ -a^{(0)}(3) & -y^{(1)}(3) & 1 \\ \cdots & \cdots & \cdots \\ -a^{(0)}(n) & -y^{(1)}(n) & 1 \end{bmatrix}$$

$$Y = \begin{bmatrix} b^{(1)}a^{(0)}(2) \\ b^{(1)}a^{(0)}(3) \\ \cdots \\ b^{(1)}a^{(0)}(n) \end{bmatrix} = \begin{bmatrix} a^{(0)}(2) - a^{(0)}(1) \\ a^{(0)}(3) - a^{(0)}(2) \\ \cdots \\ a^{(0)}(n) - a^{(0)}(n-1) \end{bmatrix}$$

https://doi.org/10.17993/3cemp.2023.120151.311-322

Also, in the least squares parametric sequence$\hat{a}$ have estimated the $= \left[b_1, b_2, c\right]^T$ Of the G.M (2,1) is used as follows:

$$\hat{\mathrm{b}} = \left(\mathrm{C}^{\mathrm{T}}\mathrm{C}\right)^{-1}\mathrm{C}^{\mathrm{T}}\mathrm{Y} \text{ (2.3)}$$

Theorem: For the solution of the G.M two by one winterization equation depend the steps [9,10]:

1. If $A^{(1)^*}$ is a unique solution of $\frac{d^2a^{(1)}}{dt^2} + b_1\frac{da^{(1)}}{dt} + b_2a^{(1)} = b$ and $\bar{A}^{(1)}$the general solution of the corresponding homogeneous equation $\frac{d^2a^{(1)}}{dt^2} + b_1\frac{da^{(1)}}{dt} + b_2a^{(1)} = 0$, Then $A^{(1)} + \bar{A}^{(1)}$ represents a universal method for solving the whitening equation for GM(2,1).
2. The general solution to the preceding homogeneous equation requires satisfying the following three conditions: (i) if the defining equation for a $r^2 + c_1r + b_2 = 0$ has two distinct real roots r_1, r_2,

$$\bar{A}^{(1)} = c_1e^{r_1t} + c_2e^{r_2t} \text{(2.4)}$$

when the repeated root r is the characteristic equation,

$$\bar{A}^{(1)} = e^{rt}(c_1 + c_2t); \text{(2. 5)}$$

when the two complex conjugate roots are the characteristic equation

$$r_1 = b + i\beta \; and \; r_2 = b - i\beta$$

$$\bar{X}^{(1)} = e^{\alpha t}(c_1cos\beta t + c_2sin\beta t) \text{(2.6)}$$

3. In particular, one of the following three scenarios may represent a solution to the winterization equation:

A. The characteristic equation root isn't zero,$A^{(1)^*} = C$.

B. In the characteristic equation, zero is one of the2 distinct roots of,$A^{(1)^*} = Ca$.

C. In the characteristic equation, zero is the only root of,$A^{(1)^*} = Ca^2$.

2.3. EVALUATE PRECISION OF FORECASTING MODELS

To test the accuracy and the performance of the proposed model used, some statistical tests and measurements, including residual test, MAPE, precision Rate and Posterior Ratio(c) [6,8].

2.3.1. RESIDUAL TEST

Step1: calculate the relative error and absolute percentage error presented as follows:

https://doi.org/10.17993/3cemp.2023.120151.311-322

$$\Delta^{(0)}(i) = \left| a^{(0)}(i) - \hat{a}^{(0)}(i) \right| \qquad i = 1,2,3,\ldots,n \text{(2.14)}$$

$$\varnothing(i) = \frac{\Delta^{(0)}(i)}{a^{(0)}(i)} \times 100\% \qquad i = 1,2,3,\ldots,n \text{ (2.15)}$$

Step 2: calculate the two-step minimum and maximum of the relative error:

$$\Delta_{min} = min \left| \Delta^{(0)}(i) \right| \text{ (2.16)}$$

$$\Delta_{max} = max \left| \Delta^{(0)}(i) \right| \text{ (2.17)}$$

Step 3: find grey incidence coefficient

$$\gamma\left(\hat{a}^{(0)}(k), a^{(0)}(k)\right) = \frac{\Delta_{min} + p \,.\, \Delta_{max}}{\Delta_{0i}(k) + p \,.\, \Delta_{max}} \text{ (2.18)}$$

Of which the distinguishing coefficient p is 0.5

Step 4: find the degree of grey incidence

$$\gamma\left(\hat{a}^{(0)}, a^{(0)}\right) = \frac{1}{n}\sum_{i=1}^{n} \gamma\left(\hat{a}^{(0)}(i), a^{(0)}(i)\right) \text{ (2.19)}$$

the GM model is qualified if

$$\gamma\left(\hat{a}^{(0)}, a^{(0)}\right) > 0.6, \; when \; p = 0.5$$

2.3.2. MEAN ABSOLUTE PERCENTAGE ERROR (MAPE)

To ensure that your forecasting model is as comprehensive as possible, you might use the Mean Absolute Percentage Error metric. Here is how we characterize it [7,9,10]:

$$MAPE = \frac{1}{n}\sum_{k=2}^{n} \left| \frac{a^{(0)}(k) - \hat{a}^{(0)}(k)}{a^{(0)}(k)} \right| \times 100\% \qquad \text{(2.20)}$$

Where $x^{(0)}(k)$: The actual value in period k

$\hat{x}^{(0)}(k)$: Estimated worth for a k-period forecast.

And there are four levels of MAPE achievement:

Precision rank	MAPE
Highly accurate	MAPE≤0.01
Good	MAPE≤0.05
Reasonable	MAPE≤0.1
Inaccurate	MAPE≤0.15

https://doi.org/10.17993/3cemp.2023.120151.311-322

The more depressed the MAPE, the higher the forecasting model's precision. In general, the MAPE below 0.01 is an exact model and the MAPE between 0.01 - 0.05 is a good model with passable accuracy.

2.3.3. PRECISION RATE(P)

For further information on how close the stated prediction quantity is to the actual value, see the section "Precision Rate" below, where p is the precision rate [7,11,12,13].

p = 1-MAPE (2.21)

Precision rank	MAPE
Highly accurate	MAPE≤0.99
Good	MAPE≤0.95
Reasonable	MAPE≤0.90
Inaccurate	MAPE≤0.90

The higher precision is the higher precision rate the forecasting model can achieve. In general, a precision rate greater than 0.99 is an exact model, and a precision rate between 0.99 -0.95 is a good model with fit accuracy.

3. APPLICATION

3.1. DATA DESCRIPTION

The data of this study has been taken from the world bank site, which demonstrates the monthly oil price of Saudi Arabia in the international market from Oct- 2020 to Sep- 2022.

Table 1. Represents the Monthly oil price of Saudi Arabia

	1	2	3	4	5	6	7	8	9	10	11	12
2018	69.05	65.78	70.27	75.17	77.59	79.44	74.25	77.42	82.72	75.47	58.71	53.8
2019	61.89	66.03	68.39	72.8	64.49	66.55	65.17	60.43	60.78	60.23	62.43	66

3.2. MODEL SPECIFICATION

In the previous section, the collected data has been described to perform the grey model GM (2,1).To make the appropriate model for forecasting the oil price.

https://doi.org/10.17993/3cemp.2023.120151.311-322

3.3. FITTING GM(2,1) MODEL

By using the OLS method, the parameters of the GM(2,1) model has been estimated depending on equation (2.3) with values of **a** and **b** (0.001734 and 0.00012), respectively.

$$\hat{a} = [a, b]^T = \begin{bmatrix} 0.001734 \\ 0.00012 \end{bmatrix}$$

Table 2. The actual predicted, and error values

Ordinality	Actual data $x^{(0)}(k)$	Model value $\hat{x}^{(0)}(k)$	Error $\varepsilon(k) = x^{(0)}(k) - \hat{x}^{(0)}(k)$	Relative error $\Delta_k = \frac{\lvert\varepsilon(k)\rvert}{x^{(0)}(k)}$
2	36.39	33.99	2.40	0.07
3	38.25	35.46	2.79	0.07
4	43.92	46.67	-2.75	0.06
5	49.47	51.99	-2.52	0.05
6	56.44	58.77	-2.33	0.04
7	60.43	65.27	-4.84	0.08
8	59.87	60.40	-0.53	0.01
9	62.8	58.78	4.02	0.06
10	68.58	74.31	-5.73	0.08
11	70.12	71.28	-1.16	0.02
12	65.68	64.18	1.50	0.02
13	69.09	67.01	2.08	0.03
14	78.51	76.09	2.42	0.03
15	76.45	79.83	-3.38	0.04
16	70.56	72.54	-1.98	0.03
17	80.33	78.04	2.29	0.03
18	89.41	91.95	-2.54	0.03
19	107.07	104.72	2.35	0.02
20	103.32	101.35	1.97	0.02
21	108.29	106.29	2.00	0.02
22	113.77	111.81	1.96	0.02
23	100.84	98.71	2.13	0.02
24	93.76	94.34	-0.58	0.01

https://doi.org/10.17993/3cemp.2023.120151.311-322

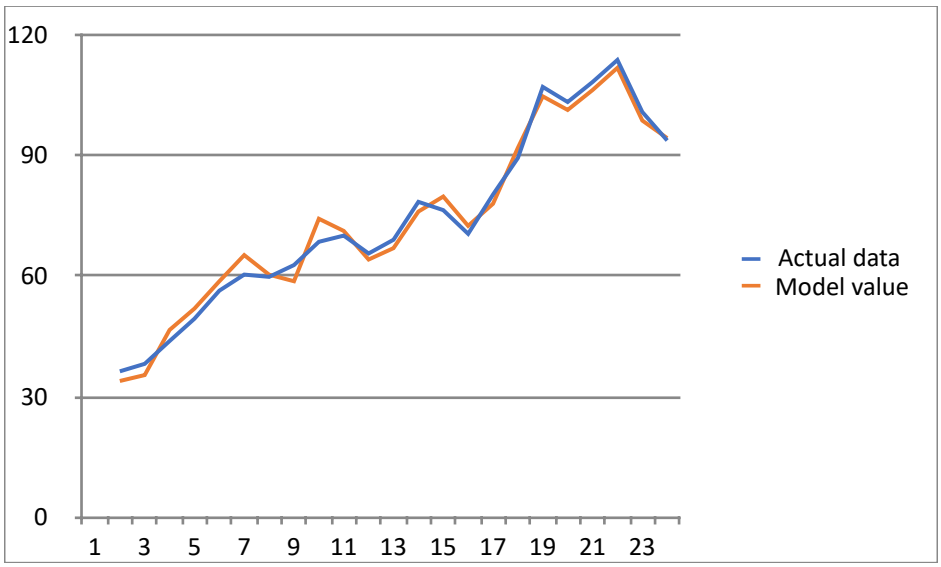

Figure 1. The scatter plot of the actual and predicted values of oil price

To test the performance of the proposed model, some statistical tests and measurements, including MAPE and precision Rate. from the above table represent model value and MAPE by GM(2,1) model, which is defined depending on eq (2.20).

Table 3. Represent the accuracy of the model

Test	GM (2,1)
MAPE	0.04
P	0.96

The data in the table above shows that the model has a high degree of accuracy, as measured by the precision rate, p, which is proportional to the degree of agreement between the forecasted amount and the actual value. p is specified as 0.96 in Eq. (2.21).

3.4. GOODNESS OF FIT

GM (2, 1) is a time series model then the goodness of fit of the model should be tested by using the Augmented Dickey-Fuller test statistic; the results were as follow:

Table 4. Represent ADF test for the monthly oil price

Test	t-Statistic	Prob.*
Augmented Dickey-Fuller test statistic	-4.258028	0.0034

Table 4 explains that the p-value of the ADF test equals (0.0034), and it is less than (0.05). This result indicates that the model is significant.

Table 5. Demonstrates the forecasted values for three periods of time.

Period	Forecasted	Confidence Interval	
Oct-22	95.76216	91.99667	99.52765

https://doi.org/10.17993/3cemp.2023.120151.311-322

Nov-22	98.3088	94.54331	102.0743
Dec-22	90.0592	86.29371	93.82469

4. CONCLUSIONS

From the results, we conclude that:

1. The petroleum sector constitutes approximately (85%) of budget revenues, (99%) of export revenues and (42%) of the gross domestic product (GDP) in Iraq, and any changes in oil prices will affect all economic activities in Iraq.
2. (GM(2,1) model is more adequate for the series that it has a few data to forecast in short terms).
3. From the results, it can be concluded that the GM(2,1) model is highly accurate to represent the behavior of the Oil price rate in Iraq.
4. The study shows that the MAPE for GM (2,1) model is equal to (0.04), which does not need large data and displays high prediction accuracy.
5. The model's great accuracy is indicated by the fact that the defined precision rate p equals (0.96), where p is the rate at which the statement of the forecast quantity matches the original value.
6. Depending on the Augmented Dickey-Fuller test statistic goodness of fit of the model has been tested; the p-value of the test equals (0.0034), and it is less than (0.05). This result indicates that the model is significant.

REFERENCES

(1) Xu, N., & Dang, Y. G. (2015). **An optimized grey GM (2, 1) model and forecasting of highway subgrade settlement**. M*athematical Problems in Engineering.*

(2) Song, F., Liu, J., Zhang, T., Guo, J., Tian, S., & Xiong, D. (2020). **The Grey Forecasting Model for the Medium-and Long-Term Load Forecasting**. *In IOP Conference Series: Materials Science and Engineering, 740(1),* 012076. IOP Publishing.

(3) Zeng, L., Liu, C., & Wu, W. Z. (2023). **A novel discrete GM (2, 1) model with a polynomial term for forecasting electricity consumption**. *Electric Power Systems Research*, 214, 108926.

(4) Evans, M. (2014). **An alternative approach to estimating the parameters of a generalized Grey Verhulst model: An application to steel intensity of use in the UK**. *Expert Systems with Applications*, 41(4), 1236-1244.

(5) Rahim, S. A., Salih, S. O., Hamdin, A. O., & Taher, H. A. (2020). **Predictions the GDP of Iraq by using Grey–Linear Regression Combined Model**. *The Scientific Journal of Cihan University–Sulaimaniya*, 4(2), 130-139.

(6) Ahmed, B. K., Rahim, S. A., Maaroof, B. B., & Taher, H. A. (2020). **Comparison Between ARIMA And Fourier ARIMA Model To Forecast The Demand Of**

https://doi.org/10.17993/3cemp.2023.120151.311-322

Electricity In Sulaimani Governorate. *QALAAI ZANIST JOURNAL*, 5(3), 908-940.

(7) Ahmed, L. S. T., & Tahir, A. L. H. A. (2021). **Comparison Between GM (1, 1) and FOGM (1, 1) Models for Forecasting The Rate of Precipitation in Sulaimani**. *journal of kirkuk University For Administrative and Economic Sciences*, 11(1).

(8) Asraa, A., Rodeen, W., & Tahir, H. (2018). **Forecasting the Impact of Waste on Environmental Pollution**. *International Journal of Sustainable Development and Science*, 1(1), 1-12.

(9) Majeed, B. N. (2022). **The Effect of Macroeconomic Variables on Stock Exchange Market Performance: Iraq Stock Exchange Market as an Example**. *Journal of Kurdistani for Strategic Studies*, 3.

(10) Li, G. D., Masuda, S., Yamaguchi, D., Nagai, M., & Wang, C. H. (2010). **An improved grey dynamic GM (2, 1) model**. *International Journal of Computer Mathematics*, 87(7), 1617-1629.

(11) Haijun, S., Yong, W., & Yi, S. (2011). **On Optimizing Time Response Sequence of Grey Model GM (2, 1)**. *Journal of Grey System*, 23(2).

(12) Mao, M., & Chirwa, E. C. (2006). **Application of grey model GM (1, 1) to vehicle fatality risk estimation**. *Technological Forecasting and Social Change*, 73(5), 588-605.

(13) Özdemir, A., & Özdagoglu, G. (2017). **Predicting product demand from small-sized data: grey models**. *Grey Systems: Theory and Application*.

https://doi.org/10.17993/3cemp.2023.120151.311-322

/18/

WATER - FOOD AND ENERGY NEXUS SYSTEMS ANALYSIS INTEGRATED POLICY MAKING TOOL

Noor Sabah
PhD student, University of Technology, Iraq.
bce.19.59@grad.uotechnology.edu.iq

Mustafa Al-Mukhtar
Civil Engineering Department, University of Technology, Iraq.
mmalmukhtar@gmail.com

Khalid Shemal
Civil Engineering Department, University of Technology, Iraq.
KhalidShemal@gmail.com

Reception: 05/11/2022 **Acceptance**: 13/01/2023 **Publication**: 31/01/2023

Suggested citation:

S., Noor, A., Mustafa and S. Khalid. (2023). **Water - food and energy nexus systems: analysis integrated policy making tool**. *3C Empresa. Investigación y pensamiento crítico, 12(1)*, 324-344. https://doi.org/10.17993/3cemp.2023.120151.324-344

ABSTRACT

This research discusses and analyses cutting-edge applications for water-energy-food nexus system analysis. It is axiomatic that substantial data should be acquired for a comprehensive model. The WEF nexus simulator may therefore be built to any extent by using simulated data future integral field spectroscopic (IFs and THENs) for WEF nexus interaction. The required data was then organized, and interactions (IFs and THENs) between the three subsystems were investigated. These IFs and THENs aid in our understanding of and ability to address the intricacy of the WEF. Given that the present study's objective is to review various solutions for WEF Nexus

We can now use these classifications to simplify the WEF nexus idea. In other words, the relationship between the three subsystems is demonstrated by the IFs and THENs variables. It would make sense to remove one of the following THEN variables from one subsystem if one of the IF variables in another subsystem remained. Because earlier Nexus initiatives did not provide information on how to initiate and discover interactions, it will be simple to determine interactions. This study demonstrates how a thorough nexus simulation model can access and communicate a wide range of data. The nexus model's interrelationships and interactions with other subsystems can be easily recovered thanks to this classification approach, and none of them will be missed because of ignorance of the nexus system. These IFs and THENs variables are also seen to be an excellent way to simplify the implementation of the Nexus system. The overall score for each project was then calculated by adding the weighted scores, which provided a methodical and objective way to rank the 29 irrigation and hydroelectric dam projects. This study is the first study in Iraq about water-energy and food nexus and helping to streamline decision-making at the nexus due to the size of the several sectors in the Iraqi human society

Following input from NWDS stakeholders, three new factors to take into account when deciding which irrigation project options to pursue were identified: a) Fighting poverty; b) Building irrigation projects close to Iraq's borders to ensure border security. 3) Rural Population Decline or Poverty Exodus. It's important to note that the nation places the highest priority on these three factors (Key Priorities National). Irrigation projects may now be planned in a deliberate manner that takes into account the observations of the relevant authorities thanks to the adoption of these aims together with the strategic assessment criteria. It takes scientific input to create "resource indexes."

KEYWORDS

Water, energy, and food (WEF) nexus; Sustainable livelihoods; policymaking, Food security

https://doi.org/10.17993/3cemp.2023.120151.324-344

PAPER INDEX

https://doi.org/10.17993/3cemp.2023.120151.324-344

1. INTRODUCTION

Currently, a number of interconnected, challenging concerns that pose major threats to human civilization must be addressed by the entire human society

must be addressed by the entire human society (Diamond, 2011). Several of these concerns are directly tied to the production, distribution, and use of food, energy, and water, especially in developing countries (WEF). According to Hague (2010), there are four resource pillars that underpin global security, prosperity, and equality. Despite this, little research has been done on how to streamline decision-making at the nexus due to the size of the several sectors and the challenge of weighing all three at once. As a result, laws and regulations frequently transmit mixed messages regarding problems with the economy, national security, or the environment. Also, when policy has been established by addressing more than one area, it is often done with a concentration on just two areas (Winpenny, 1992), and few methods have completely addressed the interdependencies in a larger context (McCornick et al., 2008).

The need for systems thinking is difficult to translate into government policy-making procedures (Forrester, 1994). The benefits of a more comprehensive approach to policy and regulation are anticipated to include economic efficacy, resource efficiency, enhanced livelihood possibilities, and public health. Negative outcomes may involve effects on communities, commodity pricing, sub-optimal infrastructure design, or environmental damage.

access to electricity, water, and food services of high quality. Over the past few years, the number of those adversely impacted by this has stayed mostly constant, and this trend appears to be expected to continue (at least in some areas). Security, economic, and social problems are only a few of the repercussions of this situation. Security, economic, and social problems are only a few of the repercussions of this situation. The problem of access is evident in both rural and urban contexts (Decker et al., 2000), and thus uses it as one lens through which to examine the WEF nexus.

Throughout this 2008 Worldwide Economic Forum annual conference (Forum), 2011), a "nexus" connecting water, energy, and food was established, and the WEF nexus has been classified as a global risk in 2011. (Hoff, 2011). "Initiating Generally Characterized by some combination for the Green Economy" marked a turning point by suggesting the energy security, food, and integration of water. The purpose of the conference was to ensure that the relationship between food security, energy, and water was "explicitly addressed in decision-making." Three years later, at the 'Sustainability in the Water–Energy–Food Nexus' meeting (Mohtar and DIE, 2014), policy and scientific communities from throughout the globe issued a call to action to create policies addressing a holistic nexus approach. Additionally, a nexus strategy that connects the Sustainable Development Goals (SDGs) is required (Weitz et al., 2014). Last but not least, UN Secretary-General Ban Ki-moon emphasized the significance of a "nexus" approach and suggested that environmental, social, and economic factors be combined (Caputo et al., 2021). The main forces behind the WEF nexus discussion are the strains currently affecting our global civilization along with new, related, and anticipated challenges. Due to population increase, the agricultural

https://doi.org/10.17993/3cemp.2023.120151.324-344

industry will need to treble its present food supply by 2050. (Wichelns, 2010). Currently, agriculture uses around 71% of all water withdrawals worldwide (Young and Esau, 2015) (Choudhari et. al, 2022). By 2050, the world's water consumption is expected to need to increase by 55% in order to keep up with expanding industry, power production, and home usage. The world's population is expected to grow by more than 40% while experiencing significant water stress (Zhongming and Wei, 2014). Finally, almost 15% of the world's water flows were utilized by the energy sector in 2010 (Van der Hoeven, 2013) and generated two thirds of the world's GHG emissions (Olejarnik, 2013). Techniques like desalination, pumping, and purification require a lot of energy to ensure alternative water supply. Between 2007 and 2013, the quantity of power used for desalination in the Middle East and North Africa region, which accounts for 38% of global desalination, quadrupled (IRENA, 2013). The development of biofuels accounted for two-thirds of the increase in worldwide maize production between 2003 and 2007 (Bank, 2008), which acted as a trigger for the 2008 jump in food prices, which were mostly brought on by subsidies for biofuels (Rudaheranwa, 2009).

Water, energy, and food security for the present and future generations is a challenging undertaking. Policymakers have a lot of power and duty when it comes to regulating the various pieces of the jigsaw puzzle. Although the scientific community has made progress in understanding and predicting future challenges, questions still exist regarding the most efficient way to convey this knowledge to the community of decision- and policy-makers. Lack of appropriate tools prevents decision-makers from taking into consideration different

resource allocation plans and understanding trade-offs between different systems. Existing tools handle certain nexus elements. Weap (Mroue et al., 2019), LEAP (Hoff, 2011), and MuSIASEM are a few examples of this (Giampietro et al., 2013) , and CLEWS (Ramos et al., 2021). WEAP (Water Evaluate and Plan) employs an integrated strategy to plan water resources. LEAP (Long-Range Energy Alternatives Planning System) is geared towards energy policy analysis and the assessment of climate change mitigation. MuSIASEM (MultiScale Integrated Analysis of Societal and Ecosystem Metabolism) is a technique for describing the fluxes of various societal systems. In order to determine the connections between interdependent sectors, CLEWS (Climate, Land, Energy, and Water Strategies) develops an integrated design methodology.

2. METHODOLOGY

A database was created that included publications that were published all across the world and were pulled from Google Scholar and the Web of Science. The following keywords were used as search terms: "water-energy nexus," "water-food nexus," "water-energy-food nexus," "climate change & food energy-water nexus," "bioenergy & water," "water-energy nexus & modelling." To pinpoint nexus applications in natural resource management, policy-related research has also attracted a lot of attention. We supplemented papers on environmental issues, resource recovery,

https://doi.org/10.17993/3cemp.2023.120151.324-344

water footprints, energy generation, and food consumption patterns in order to cover a broad spectrum of pertinent studies. Then, we weed out irrelevant studies by reviewing their conclusions and abstracts. The final sample included a large number of publications that provided rationale for addressing the nexus quantitatively and proposed a modelling methodology that would aid in the creation of effective laws and regulations. Brief case studies that highlight the need for this kind of research and the required institutional changes are also included. The current political focus on access issues offers an opportunity to reevaluate the requirement for successful inter-disciplinary assessments. The objective of this effort is to provide groundwork for more in-depth future research. As a result, we provide in-depth citations from the pertinent literature.

3. RESULTS AND DISCUSSION

There are other clear links between food and energy; consider biomass production, which uses plants a source of energy and has grown in popularity in countries such as Argentina and Brazil in recent years. This "new renewable" energy source uses water that would otherwise be used for irrigated agriculture for food production and relies on plant growth to produce energy, which could lead to a decline in food production (because of associated decreases in agricultural land for the production of food). The biological function of the forest may have been impacted by the biomass created from the forest waste. As a less anticipated result of using plants for energy, food prices could rise.

3.1. NEXUS TOOL

There are tight links between the food sector, energy, and water. As demands on these resources continue to rise, there is a rising necessity to develop, quantify, and comprehend the trade-offs involved with the future management and planning of these systems [Figure 1]. Water has been utilized to generate hydroelectricity and cool thermal power stations. Hydraulic fracturing has an effect on groundwater: gas and oil extraction pose the risk of polluting surrounding aquifers and reducing the availability of potable water or agriculture. Energy, on the other hand, is required for extracting groundwater and current irrigation methods, as well as for the whole urban water cycle, from transportation to delivery to treatment. The close relationship between water and food is most evident in agriculture's requirement for water and irrigation, in which the share of water utilized by the agricultural sector ranges from 70–80 percent to 80–90 percent. In many nations, the priority of water usage is regulated by law, and irrigation is often placed second to home consumption.

Food, energy, and water seem to be interdependent resource systems that confront several difficulties, such as a growing world publication, economic crises, hunger and poverty, and climate unpredictability. To address these issues, our traditional resource allocation model must undergo a paradigm shift to account for their intricate interdependencies. In pursuit of this objective, the authors have created a resource allocation plan evaluation platform (WEF Nexus Tool 2.0) that intends to assist

https://doi.org/10.17993/3cemp.2023.120151.324-344

decision-makers in establishing water-energy-food-informed sustainable resource management techniques.

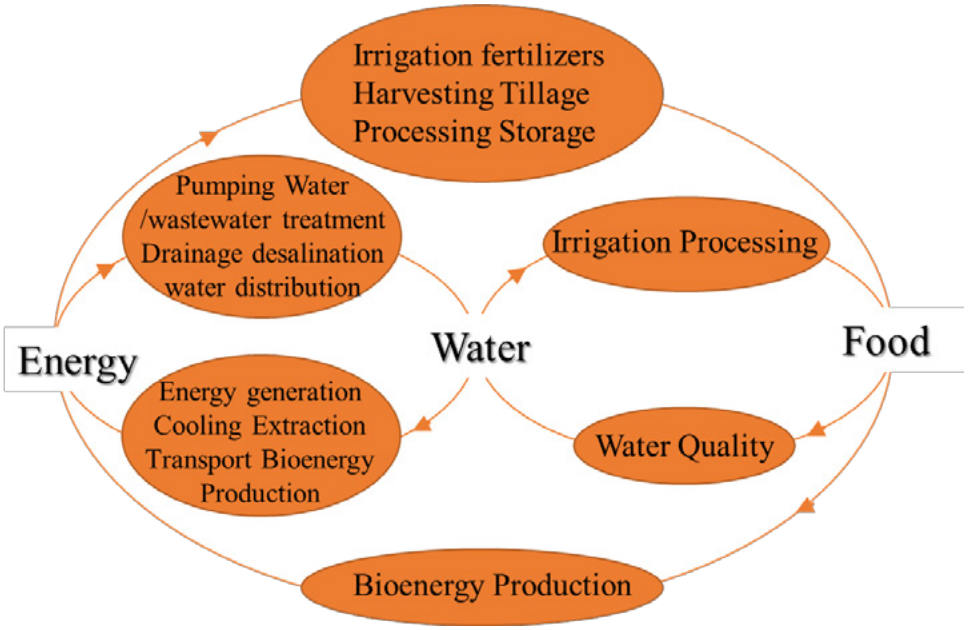

Figure 1. The resource management strategy Guiding Tools

The WEF Nexus Tool 2.0 is a shared platform that brings together scientific knowledge and policy input to detect present and predicted bottlenecks in resource allocation patterns, as well as potential trade-offs and possibilities to address resource stress concerns. The scenario-based approach aims to clearly quantify the relationships between the three sources while taking into account the consequences of population increase, climate change, changing policies and economies, and other stressors. It allows the user to construct scenarios for a certain nation by specifying the following parameters:

a) Water portfolio: identifying various water sources and the quantities needed for each.

b) Food portfolio: Assessing local food production vs. imports, as well as agricultural production technology.

c) Finding forms of energy for water and agricultural output as part of an energy portfolio.

Despite the fact that the water-energy-food framework seems general, the tool's situations seem to be location-specific and specified by the local variables of the research location. Local food yields, energy and water availability and needs, accessible technology, and land demands are only a few examples. The user defines the attributes, which allows

for the production of country-specific identities. The WEF Nexus Tool 2.0 allows users to view and evaluate resource needs across scenarios, as well as compute each scenario's sustainability index. The Sustainable Development Goals (SDGs) Acceleration Tool Kit from the United Nations Development Organization just included the tool. With the use of the application, users can simulate a variety of situations with

https://doi.org/10.17993/3cemp.2023.120151.324-344

varying degrees of food self-sufficiency, access to water and energy sources, and imports and exports. There is a description of the output, including the amount of water needed (m3), the amount of energy needed locally (kJ), the amount of carbon dioxide that needs to be released locally (tonne CO2), the amount of land needed (ha), the amount of money needed (QAR), the amount of energy needed to be imported (kJ), and the amount of carbon dioxide that needs to be imported (ton CO2). The user can look up and check how many resources are used in each of the available situations. The user might also be able to determine the relative relevance of each system (carbon through import, energy through import, financial, land, local carbon, local energy, and water).

3.2. ELEMENTS OF THE WEF NEXUS

The descriptive elements of the EWF nexus contain various elements that are simple to recognize, like (Global Risks, 2011):

a) Several billions of people lack access to all three factors (quality, quantity, or both).

b) All elements are in high demand across the world.

c) All elements are limited by resources.

d) All elements are "global goods," implying worldwide commerce and having global consequences.

e) All elements have variable geographical accessibility and supply and demand fluctuations.

f) Global warming and the environment are intertwined in all of them.

g) All these elements have serious security concerns because they are essential to society's functioning.

h) All of these elements work together in highly regulated markets. All of these things need the clear identification and handling of hazards.

3.3. SUSTAINIBILITY INDEX

Different scenarios can be created with the programme. For example, despite the fact that one scenario uses the least amount of land, it simultaneously uses the most water. The scenario that consumes the least amount of water is also likely to be the costliest. One of the most energy-intensive scenarios, for example, could be a less expensive option financially. How do we decide which scenario to pursue? What factors do we consider? How can we determine how much of the various resource demands we can handle? How may the tool's output be used to evaluate potential techniques? The answers aren't easy to find. To examine and compare conditions, the following aspects should be included in the construction of a sustainability report: (1) scientific data to aid in the quantification of system links and physical capabilities; and (2) policy input outlining policy options and strategies.

https://doi.org/10.17993/3cemp.2023.120151.324-344

The multidimensionality of the framework and instrument necessitates a deeper understanding and investigation of the results. Despite the conceptual framework's apparent scope, evaluations and solutions should be adapted to the specific problem at hand. The same outcomes and expenses for an idealised scenario are seen from varied perspectives by numerous governments, ministries, or decision-making organisations, and each must supply their own data. Each of the variables (carbon, energy, finance, water, or land) varies in relevance or sensitivity depending on the location. It may go beyond selecting the least resource-intensive solution to one that can be transformed into a cost-independent national goal or vision. A scenario's localized sustainability would be determined by figuring out its sustainability index using the two-step procedure shown below.

Iraq, on the other hand, the most difficult task at SWLRI is to find projects that maximize not only water and land utilization, but also food security, energy efficiency, and environmental conservation. These four areas — water, food, energy, and the environment – are so intertwined that every change in one has a direct impact on the others. The connection or interaction between these sectors emphasizes the importance of striking a delicate balance between competing uses of water, which is what this approach aims to achieve. The strategy is built around these four connections and examined in light of their interconnections. The following are the relationship categories. The water category encompasses the allocation of water across a variety of sectors, including municipalities, industry, agriculture, and the environment, as well as the numerous social and economic benefits that come with its use. Food: The food category represents the interdependence of water and food production, as well as agriculture's involvement in soil and river system health. Water and energy production in various forms, such as oil production and electricity generation in power plants, are all included in this category. The Statements Vision highlights the priorities, goals, and objectives of the ten ministries who participated in each of the four areas in the NWDS manifesto. The future vision statements (one for each of the following sectors: water, food, energy, and environment) describe the Iraqi government's goals for this sector on the page. They appear at the beginning of each chapter in this strategy. Not every chance can or should be taken. As a result, it was important to condense the lengthy list of possibilities into a more manageable set of priorities. To do so, a preliminary assessment was conducted to identify projects that are in the works or those are deemed critical to public safety. In actuality, it made sense to start with the ready-to-go projects, which are meant to be of the utmost significance to the Iraqi government. Both are established as constraints during the selection process, which means they are immediately added to the list of selected projects. The water dams and irrigation projects on the list were then evaluated using a multi-criteria screening approach. For a numerical representation of the technical, social, environmental, and economic aspects of opportunities, "strategic evaluation criteria," which are physical-factor-calculated values for hydroelectric dams and irrigation projects, were developed. The weights for each of the criteria were then determined based on the priorities specified by the NWDS stakeholder committees.

Finally, the sum of the weights was used to generate the total score for each project, providing an objective and systematic manner to rank the 29 hydroelectric dams and irrigation projects. Following feedback from NWDS stakeholders, three new elements to consider when selecting irrigation project possibilities were identified: a) Poverty alleviation 2) Developing irrigation projects near Iraq's borders to maintain national security at the border 3) The

https://doi.org/10.17993/3cemp.2023.120151.324-344

Exodus from Poverty: Rural population exodus or reduction. It's worth noting that these three criteria are the top priority for the country (see Key Priorities National). The adoption of these goals in conjunction with the strategic assessment criteria has allowed irrigation projects to be organised in a way that is both intentional and reflective of the appropriate authorities' observations. Creating "resource indices" requires scientific input as follows:

The index of Water (WI) = Wi/Wa,

The index of Land (LI) = Li/La,

The index of locally energy (EI) = Ei/Ea,

The index of locally carbon (CI) = Ci/Ca,

The index of financial (FI) = Fi/Fa,

The index of Energy IMP (EIMP I)=EIMPi/EIMPa, and

The index of Carbon IMP (CIMP I) = CIMPi/CIMPa.

Where index = resource amount essential by scenario/allowable capacity or limit.

Resource indices are computed to normalise the tool output and detect any exceeding local limitations. Each index represents the percentage of resources that the suggested scenario is allowed to use. Because they are unfavourable in terms of local input needs, scenarios with resource indices greater than 1 are less likely to be accepted. The 'local characteristics' of the territory under investigation include the local bounds. For example, the acceptable water limit (Wa) is a percentage of all available water resources that are allocated for agricultural production; similarly, for La, the percentage of arable land. This process depends on a combination of scientific inputs and an understanding of the available resources; part of this process may involve consultation with stakeholders (i.e., ministries, governmental organizations, etc.). Acceptable energy (Ea) is a measure of the amount of energy allotted to the agriculture industry and its related activities. A national commitment to reduce carbon emissions and corresponding quotas within the agricultural sector may have an impact on an acceptable carbon limit (Ca), which is a maximum ceiling on emissions connected to agriculture and activities associated with it (such as the use of water for agriculture).

The allowed financial limit serves as a representation of the state budget amount for the scenario (Fa). EIMP and CIMP are less relevant and might be more arbitrary when it comes to how they relate to energy consumption and carbon emissions in a global setting through the transportation of products. One step toward determining specific acceptable bounds would be done by cross-sector stakeholder engagement, representing diverse resource-consuming sectors with the use of scientific information. The precise amounts of resources that ought to be provided for carrying out diverse development plans across industries would be simpler to ascertain as a result of this.

Policy preference is shown in the identification of the importance coefficient. Combining scientific knowledge with policymaking is essential in order to establish sustainable policies. Both contributions must be taken into consideration. After determining the amount of resources needed for each scenario, policy-makers must provide their feedback. This entails determining the proportional value of lowering

https://doi.org/10.17993/3cemp.2023.120151.324-344

each resource need (water, energy, carbon, land, and financial). In other words, which expenses associated with a certain situation should be reduced more than others? Through focus groups, stakeholders would rank the relevance of each resource demand according to what their policies and plans thought should be decreased the most. This would be a reflection of governmental plans and objectives. The more important it is to choose a scenario with fewer required resources, the greater the significance coefficient. If minimizing water footprint is a higher priority than other footprints, Iw (importance of reducing water need) would be greater. The sustainability index of each scenario that is suggested is then determined. This index is the result of adding the "resource indices" and the "importance coefficients" that were given to them. The scenario is more beneficial if the assessment parameter index is lower since it shows how far the parameter is from the maximum specified limit. The relevance (and sensitivity) of the provided parameter decreases as the importance coefficient does. According to the decision-maker, the scenario with the lowest score is the most sustainable.

Scenario i:

$$S.I_i = \left[WI_i\left(100 - I_W\right) + LI_i\left(100 - I_L\right) + EI_i\left(100 - I_E\right) + CI_i\left(100 - I_C\right) + FI_i\left(100 - I_F\right) + E_{IMP}I_i\left(100 - I_{EIMP}\right) + C_{IMP}I_i\left(100 - I_{CIMP}\right)\right] \times 100$$

$$I_W + I_L + I_E + I_C + I_F + I_{EIMP} + I_{CIMP} = 100$$

where 'I' is the importance factor assigned for resource, which reflects the relative importance of reducing the consumption of this resource in a scenario.

Examples from an energy perspective-

It's difficult to address all three challenges without repeating popular statistics on growth, access, and so on, or without providing confusing recommendations. We briefly discuss a few particular domains where the EWF nexus is obvious yet underutilized by systems thinking at the moment. These are not case studies, but rather sections of the EWF nexus with distinct system boundaries on which future, more extensive research could be focused.

3.3.1. ENERGY ACCESS AND DEFORESTATION

For example, only 9% of Ugandans have access to electricity, a scarce resource (Taylor, 2010); and significant environmental issues, such as overgrazing, deforestation, and (typically) low-productivity agriculture practices, all contribute to soil erosion, a major barrier to growth. 93 percent of the nation's energy requirements are met by wood. Although the rate of ensuing deforestation has decreased significantly, from 67 percent loss of forests and woods between 1962 and 1977 to 7.7 percent loss between 1983 and 1993, it remains a serious issue (including effects on water systems) (Biswas et al., 2001; Liu et al., 2008; Viswanathan and Kumar, 2005; Zahnd and Kimber, 2009). Ethiopia experiences a lot of the same issues as well. Only 3% of natural forests are still intact due to extensive exploitation. Pressure has been put on

https://doi.org/10.17993/3cemp.2023.120151.324-344

particular basins as a result of the government's initiative to supply power to all inhabitants. The Awash Basin contains mixed crop and animal farming in its higher reaches; a mix of crops, livestock, and pastoral production in its middle region; and a nomadic pastoral system with some irrigation in its bottom segment. This is similar to how much of Ethiopia's highlands are farmed. The basin generates significant hydropower with 110 MW total at three plants, or 14% of the country's capacity, and a sizable tract of arable land. The basin must make severe trade-offs since there isn't enough water to fully support agriculture and power generation demands (McCornick et al., 2008).

3.3.2. BIOFUELS (AND UNCONVENTIONAL OIL AND GAS) PRODUCTION

It is evident that initiatives to create bioenergy substitutes for fossil fuels have frequently been implemented without a thorough knowledge of the costs and benefits from a variety of viewpoints, including: deforestation, biodiversity, water, energy, lifecycle emissions, and land use change. Many factors contributed to recent food price increases, including increased fertiliser and fuel prices, and thus transportation; increased demand for biofuels driven by energy security and climate change concerns; and changing consumption patterns (Galan-del-Castillo and Velazquez, 2010; Kaphengst et al., 2009; Lange, 2011; Méjean and Hope, 2010; Peters and Thielmann, 2008; Schut et al., 2010; UN, 2007). Although there are some price consequences, there appears to be sufficient land and water available globally to cultivate a sizable amount of biomass for the production of both food and bioenergy. Natural resources are distributed unevenly, leading to significant regional inequalities and severe land and water shortages in crucial places. For instance, more than 35% of the world's population resides in China and India, both of which have fully utilized the land and water resources available for agriculture. On the other hand, a significant portion of sub-Saharan Africa and South America still have the potential to increase areas used for agricultural production in addition to experiencing significant productivity gains for current land use. This is due to the availability of suitable land and exploitable water (Müller et al., 2008). Similar problems arise with unconventional sources of oil and gas. The exploitation of tar sands (Wu et al., 2009) and shale gas (Lee and Koh, 2002) utilizes a lot more water than traditional oil and gas, respectively, and can seriously pollute water.

3.3.3. IRRIGATION AND FOOD SECURITY

The connection between energy, irrigation, and food security in South Africa has become a serious issue (SA). Electricity rates increased by 31% between 2009 and 2010, and another 25% increase is anticipated over the next three years (Botterill, 2012; Setlhaolo et al., 2014). The agriculture industry, with its high energy requirements for irrigation, could be one of the most affected by rising energy prices. Irrigated land produces 25% of South Africa's main foods. Reduced irrigation and a move to rain-fed agriculture may jeopardise national food security, particularly during

https://doi.org/10.17993/3cemp.2023.120151.324-344

droughts. South Africa was a net food exporter from 1985 to 2008, but has since become a food importer due to population expansion and a slower increase in agricultural output. Another illustration would be Punjab, which barely makes up 1.5% of India's territory but produces 50% of the rice and wheat the government buys and distributes to feed the more than 400 million undernourished Indians. Farmers are "mining" (pumping) aquifers more quickly than they can be replenished, which is a significant problem. Since electricity is subsidized, this is partially due to insufficient price signals. As water levels drop, increased pumping is taxing an already brittle and overburdened electricity grid. In total, irrigation consumes between 15 and 20% of India's total power. Using distributed photovoltaic-powered water pumps, which can improve price signals, is one solution. PV irrigation systems are successfully used in this region when the right circumstances arise (Hussain et al., 2010; Purohit, 2007; Sallem et al., 2009).

Iraq, on the other hand, is a country wealthy in oil, with a medium income from the high law and a population of 36.4 million people in general in 2015, with 30.1 million of them living in refined regions. Despite the fact that it does not form until 5.7 in the water from local produce, the agricultural land sector is vital to the economy's survival. because of rapid urbanization, conflict, and the safe execution of execution. Furthermore, the cause of the colour shift is a reduction in water and a speeding up of the process. And these works are combined until the possibility of a distinct agricultural product is eliminated and the collection's ability to create a steady income is increased. Despite this difficulty, the country has a wonderful place for it. And, in Iraq, the national dominance line is being cultivated with the credit of the unit from the head parts in order to accelerate non-oil output, raise the distribution of the unit, and study gender equality.

3.3.4. HYDROPOWER

Hydroelectricity will continue to be the main source of power in Iraq and the Kurdistan Region. By 2030, the Kurdistan Regional Government wants to supply 15% of the region's electricity needs using hydropower. One percent of the rest of Iraq's electricity demands should be satisfied by hydropower. Five new medium-sized dams will be constructed in the Kurdistan Region by the year 2030, while ten new dams (ranging in size from small to medium) will be constructed throughout the remainder of the nation, largely along the Tigris River. Since the majority of these dams are primarily made to generate hydroelectric power, they will help conserve water and somewhat lessen floods. Some of them like the Taq Taq Dam on the Lower Zab will provide multi-purpose services. The construction of 30 new dams will increase the water storage capacity in Iraq by about 11 billion cubic meters by 2030.

The strategy's suggested dams represent Iraq's complete capacity for medium and large-scale reservoir construction. Alternative technologies, such as hydroelectric, solar, and wind energy, are another possible source of energy in Iraq. Iraq now generates electricity from hydroelectric power stations all around the country, despite their tiny output. According to the Ministry of Electricity MoEI in Baghdad, the

https://doi.org/10.17993/3cemp.2023.120151.324-344

production of hydroelectric power in Iraq in 2012 was the Republic of Iraq-Ministry of Water Resources Strategic Study of Water and Land Resources in Iraq 179 (excluding the Kurdistan Region) was 757.4 GW/year, or 1% of the total energy generated during the same year (2001; 21 GW/year). The average daily production of hydropower was 102 MW. Existing hydroelectric power plants can produce more, but it is limited by lower water levels at the top of the reservoirs, as well as the constraints imposed by the need to match irrigation expenses. The Ministry of Electricity estimates that power generation in Iraq, without the Kurdistan Region, for the year 2013 will be 46757 GWh/year.

The amount of water that is affected by the production of electricity is minimal (it only affects the amount of water lost through evaporation in the dams), but it may affect the timing of stream flows, both seasonally and hourly, because the timing of water releases is typically determined by the demand curve for electricity, subject to engineering and environmental limitations. Hydropower and downstream uses, such as irrigation, in-stream usage, and supporting ecosystems, may potentially conflict (Briscoe, 1999). A prominent instance of this type of conflict may be seen in Central Asia, where the Kyrgyz Republic must release water during the winter to produce energy, but South Kazakhstan and Uzbekistan want water during the summer for irrigation projects (Schmidt-Soltau, 2004). Jordan offers yet another intriguing scenario. The Jordan River and a few other river systems provide the country with the scant water it needs. Lifting, transferring, and purifying surface water—especially water from the Jordan Valley—requires energy. Importing energy has a substantial cost from a financial and foreign policy viewpoint (Scott et al., 2003). The cost of energy and water is another serious problem. Jordan is said to have utilized 25% of its power, which was mostly produced from imported oil, even before the current spikes in energy costs to manage its meager water supplies (McCornick et al., 2008).

3.3.5. DESALINIZATION

Several island communities, desalination is essential for agricultural and drinking water for large populations in North Africa and the Middle East. Desalination will become more necessary as subsurface water sources are exhausted and the human population grows. Reverse osmosis and thermally driven Multi-Stage Flash (MSF) are the two most used desalination techniques (RO), which, respectively, make about 44% and 42% of the world's capacity. Under the correct conditions, thermal desalination devices might be powered by solar energy, use distillation to separate fresh water from saline water. The brine is created when salty feed water is heated to Vaporization, enabling fresh water to steam off, leaving a highly salinized solution behind. The MSF technology has the ability to use extra thermal energy. As a consequence, huge volumes of energy and water may be produced at one station, thus meeting demand for both. Desalination energy demands are expected to rise substantially, particularly in dry areas. In the MENA area alone, water desalination is expected to increase from 8 million m3 currently to over 15 million m3 in 2030. According to research, integrated electricity and water plants might account for 33–67% of new power capacity expansions, depending on the nation (Blanco et al., 2009;

https://doi.org/10.17993/3cemp.2023.120151.324-344

Othmer, 1975; Peñate and García-Rodríguez, 2011; Publishing et al., 2005; Siddiqi and Anadon, 2011).There appear to be a number of alternate options, but the most of them still focus on the EWF nexus in two dimensions. The difficulty will almost probably be to create system limits that are large enough to handle the enormity of the interaction vectors while still being small enough to allow for realistic analysis. It's tough to locate examples of this approach in policy and regulation.

3.3.6. HOLISTIC WEF NEXUS SIMULATOR FRAMEWORK

Through the use of simulated data (IFs and THENs) for WEF nexus interaction, the WEF nexus simulator is scaleable. It's possible to alter the system boundaries and nexus elements by choosing various spatial sizes, but it's also crucial to keep in mind that shifting the spatial scale could result in altering nexus elements over time. All design factors would therefore overlap as the geographical scale is increased. The system borders of the WEF subsystems, which include a watershed, differ even though they confine the geographical scale to smaller limitations, with the energy subsystem's border being the greatest and the water subsystem's boundary being the lowest. Due to the significant physical constraints, each national WEF subsystem consists of its own components. Energy production is not limited to a single energy subsystem the size of a watershed or to a particular watershed, as it is in a watershed. Typically, it is made elsewhere and imported into the watershed. As a result, unless bigger geographic scales that encompass a variety of energy components could be included, it is hard to examine all of the interrelationships in the energy subsystem merely at the watershed size. Surface water and groundwater, on the other hand, are found in plenty in the watershed. As a result, these differences must be taken into account after setting system boundaries on a small spatial scale. Examining all of the linkages between WEF subsystems was the aim of this investigation. [Figure 2] depicts the WEF nexus simulator's IFs and THENs. The interactions in the WEF nexus system were given the names IFs and THENs because the output of one subsystem is thought of as an input for another subsystem. For instance, deep percolation appears to be an output of the food subsystem (THEN) that the water subsystem uses as an input (IF). Every simulation model in this class has independent THENs that are stand-alone outputs (THENs) that are not used by other subsystems. Non-nexus demands are met by the water subsystem's environmental water requirements, and non-agricultural byproducts have evolved into an example of independent outcomes in the WEF nexus system.

https://doi.org/10.17993/3cemp.2023.120151.324-344

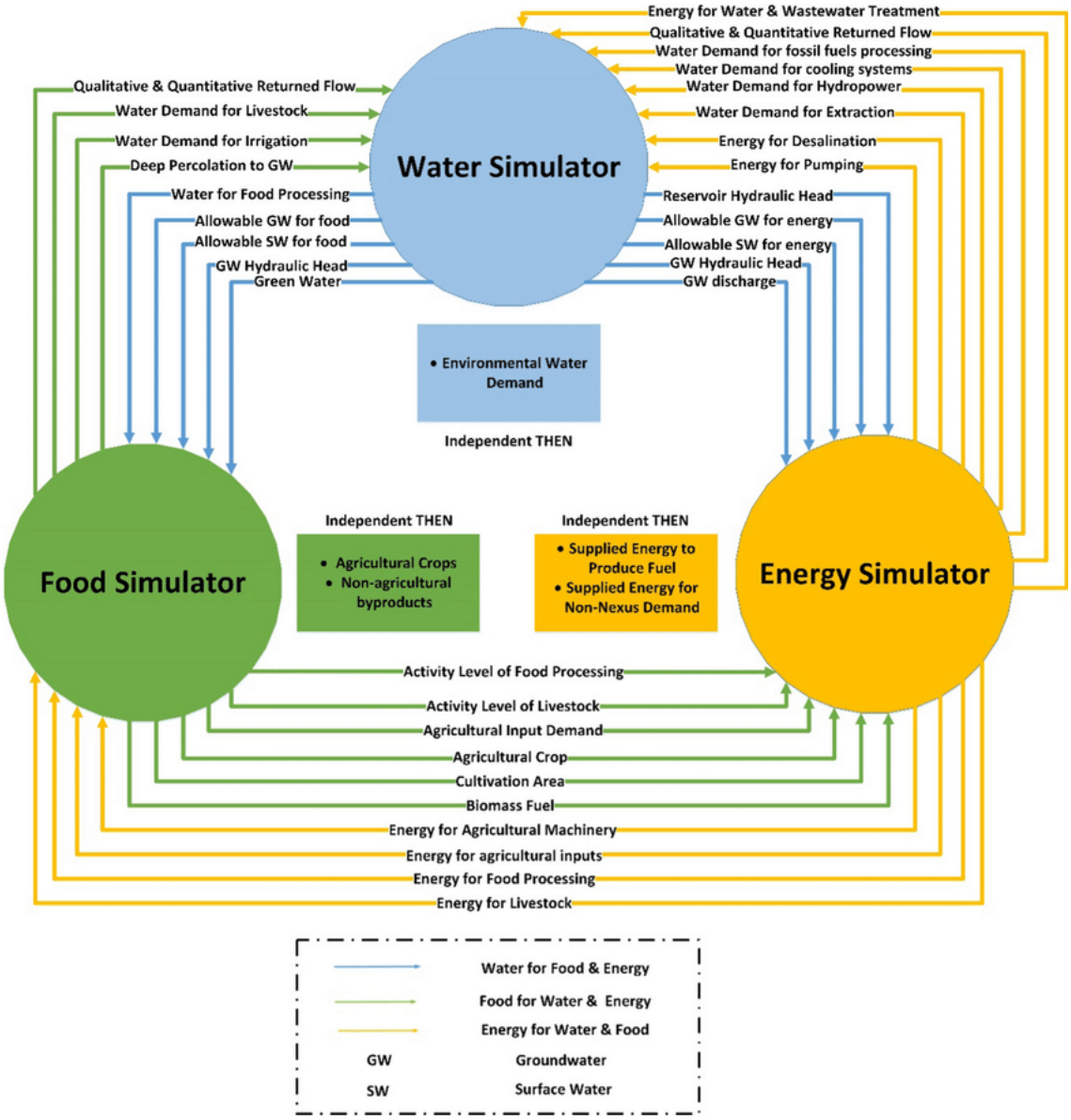

Figure 2. The interactions between the WEF nexus system (Afshar,A et al ,2012)

4. CONCLUSION

Energy modelling may benefit from a model that expands capabilities to other Nexus regions, but doing so would involve rigorous modelling concept design and the use of widely used tools. The present tools also have a lot of model overlap. These overlaps are not always bad because they allow for comparisons between different tools, shedding light on the significance of various presumptions or methods and enabling the risk/uncertainty evaluation of the model's output. In a number of European policy situations, this way of comparing model results is becoming more popular (Europea, 2015). The following are the consequences of the Nexus on energy modeling:

In the first place, to address cross-sector interdependence, resolve conflicts, and boost synergies between the energy sector and the nexus areas of climate, land, food, and water. By learning more about land markets, one can improve energy

https://doi.org/10.17993/3cemp.2023.120151.324-344

modeling, such as the solar and wind power potential. We need some form of creativity in food technology, engineering, and hydrology.

In order to resolve trade-offs and/or improve synergies amongst Nexus domains, governance is essential. Last but not least, transdisciplinary approaches enable the Nexus to be handled in a fashion that is driven by the needs of stakeholders (Siddiqi et al., 2013). Participatory approaches that unite business, government, academia, and civil society groups may enhance the relationship between science and policy. Comparing model results and setting a shared baseline could lead to model improvements. It is necessary to assess integrated modelling frameworks used at various scales. Nexus analysis is applicable to industrial processes as well as local, national, and international research. Increased modelling capabilities and the foundation for stronger policy recommendations could result from more Nexus research on the topic of energy modelling. If initiatives to encourage interdisciplinary team integration were coordinated, the development of spatial analysis consistency would be feasible.

5. RECCOMENDATION

There is little consensus on the most effective methods and tactics to utilize at various sizes and, most importantly, as more conferences concentrate on the complicated, developing issue of the WEF nexus, to achieve different goals. Without a doubt, there was a pressing need for fresh tools and procedures that could give personalized insights. In contrast, there are currently available technologies, such as those mentioned above, that provide in-depth analysis and critical insights for specific sectors or between any service areas in the nexus, such as water for food and energy for water. Connecting outputs and inputs among well-known models, followed by an analysis of the results at an integrated water-energy-food layer, was arguably the most difficult difficulty and demand. The water, energy, land-use, and climate strategies (CLEWS) framework is a step in the right direction and is now being tried in several locations. It entails the use of freely available technologies such as LEAP and WEAP from the Stockholm Environment Institute (respectively, the Long-Ranging Energy Alternative Planning Process and the Water Assessment and Master Plan). Integration of models across scales is also necessary to allow decision-makers to extract information and examine consequences at several scales. In order for the tools and approaches to be used in a range of global settings by informed (but not necessarily professional) practitioners, they must be readily accessible.

REFERENCES

(1) Afshar, A., Soleimanian, E., Akbari Variani, H., Vahabzadeh, M., & Molajou, A. (2021). **The conceptual framework to determine interrelations and interactions for holistic Water, Energy, and Food Nexus**. *Environment, Development and Sustainability*, 1-22.

(2) Bank, W. (2008). **World development report 2009: Reshaping economic geography. The World Bank**.

https://doi.org/10.17993/3cemp.2023.120151.324-344

(3) **Considering the energy, water and food nexus: Towards an integrated modelling approach**. *Energy Policy,* 39, 7896–7906.

(4) Blanco, J., Malato, S., Fernández-Ibañez, P., Alarcón, D., Gernjak, W., Maldonado, M.I. (2009). **Review of feasible solar energy applications to water processes**. *Renew Sustain Energy Rev,* 13, 1437–1445.

(5) Botterill, B.D. (2012). **South Africa's Electricity Crisis: The Need to Reconcile Environmental Policy Decisions with International Treaties**. *San Diego J Clim Energy L,* 4, 225.

(6) Briscoe, J., (1999). **The financing of hydropower, irrigation and water supply infrastructure in developing countries**. *Int J Water Resour Dev,* 15, 459–491.

(7) Caputo, S., Schoen, V., Specht, K., Grard, B., Blythe, C., Cohen, N., Fox-Kämper, R., Hawes, J., Newell, J., Poniży, L. (2021). **Applying the food-energy-water nexus approach to urban agriculture: From FEW to FEWP (Food-Energy-Water-People)**. *Urban For Urban Green,* 58, 126934.

(8) Chhipi-Shrestha, G., Hewage, K., Sadiq, R. (2017). **Impacts of neighborhood densification on water-energy-carbon nexus: Investigating water distribution and residential landscaping system**. *J Clean Prod,* 156, 786–795.

(9) Data, P. (2011). **The Emergence of a New Asset Class. An Initiative of the World Economic Forum January 2011**. *Collab with Bain Company, Inc*.

(10) Decker, E.H., Elliott, S., Smith, F.A., Blake, D.R., Rowland, F.S. (2000). **Energy and material flow through the urban ecosystem**. *Annu Rev energy Environ,* 25, 685–740.

(11) Diamond, J. (2011). **Collapse: how societies choose to fail or succeed: revised edition**. *Penguin*.

(12) Europea, C. (2015). **Commission staff working document Better Regulation Guidelines.**

(13) Forrester, J.W. (1994). **System dynamics, systems thinking, and soft OR. Syst Dyn Rev 10, 245–256.Forum**, *W.E.F. (World E., 2011. Water security: the water-food-energy-climate nexus, in: Conference: The Water, Energy and Food Security Nexus. Island Press Washington, DC, USA.*

(14) Galan-del-Castillo, E., Velazquez, E. (2010). **From water to energy: the virtual water content and water footprint of biofuel consumption in Spain**. *Energy Policy,* 38, 1345–1352.

(15) Giampietro, M., Aspinall, R.J., Bukkens, S.G.F., Benalcazar, J.J.C., Maurin, F.D., Flammini, A., Gomiero, T., Kovacic, Z., Madrid-Lopez, C., Martin, J.R. (2013). **An innovative accounting framework for the food-energy-water nexus: application of the MuSIASEM approach to three case studies.**

(16) Global Risks, W.E.F. (2011). A**n initiative of the risk response network, in: Geneva: World Economic Forum.**

(17) Hague, W. (2010). **The diplomacy of climate change. speech to Counc Foreign Relations.**

(18) Hoff, H. (2011). **Understanding the nexus.**

(19) Hussain, Z., Khan, M.A., Irfan, M. (2010). **Water energy and economic analysis of wheat production under raised bed and conventional irrigation**

https://doi.org/10.17993/3cemp.2023.120151.324-344

systems: A case study from a semi-arid area of Pakistan. *Soil Tillage Res,* 109, 61–67.

(20) IRENA, M. (2013). **Renewables Status Report.**

(21) Kaphengst, T., Ma, M.S., Schlegel, S. (2009). **At a tipping point? How the debate on biofuel standards sparks innovative ideas for the general future of standardisation and certification schemes**. *J Clean Prod,* 17, S99–S101.

(22) Lange, M. (2011). **The GHG balance of biofuels taking into account land use change**. *Energy Policy,* 39, 2373–2385.

(23) Lee, Y.E., Koh, K.-K. (2002). **Decision-making of nuclear energy policy: application of environmental management tool to nuclear fuel cycle**. *Energy Policy,* 30, 1151–1161.

(24) Liu, G., Lucas, M., Shen, L. (2008). **Rural household energy consumption and its impacts on eco-environment in Tibet: Taking Taktse county as an example**. *Renew Sustain energy Rev,* 12, 1890–1908.

(25) McCornick, P.G., Awulachew, S.B., Abebe, M. (2008). **Water–food–energy–environment synergies and tradeoffs: major issues and case studies**. *Water Policy,* 10, 23–36.

(26) Méjean, A., Hope, C. (2010). **Modelling the costs of energy crops: A case study of US corn and Brazilian sugar cane**. *Energy Policy,* 38, 547–561.

(27) Mohtar, R., DIE, I.D. (2014). **Sustainability in the water–energy–food nexus.**

(28) Mroue, A.M., Mohtar, R.H., Pistikopoulos, E.N., Holtzapple, M.T. (2019). **Energy Portfolio Assessment Tool (EPAT): Sustainable energy planning using the WEF nexus approach–Texas case**. *Sci Total Environ,* 648, 1649–1664.

(29) Müller, A., Schmidhuber, J., Hoogeveen, J., Steduto, P. (2008). **Some insights in the effect of growing bio-energy demand on global food security and natural resources**. *Water Policy,* 10, 83–94.

(30) Olejarnik, P. (2013). **World energy outlook 2013. Int Energy Agency Fr.**

(31) Othmer, D.F. (1975). **Fresh water, energy, and food from the sea and the sun.** *Desalination,* 17, 193–214.

(32) Peñate, B., García-Rodríguez, L. (2011). **Energy optimisation of existing SWRO (seawater reverse osmosis) plants with ERT (energy recovery turbines): Technical and thermoeconomic assessment**. *Energy,* 36, 613–626.

(33) Peters, J., Thielmann, S. (2008). **Promoting biofuels: Implications for developing countries**. *Energy Policy,* 36, 1538–1544.

(34) Publishing, O., Agency, I.E., Agency, I.E. (2005). **World Energy Outlook 2005: Middle East and North Africa Insights**. *Organisation for Economic Co-operation and Development.*

(35) Purohit, P. (2007). **Financial evaluation of renewable energy technologies for irrigation water pumping in India**. *Energy Policy,* 35, 3134–3144.

(36) Ramos, E.P., Howells, M., Sridharan, V., Engström, R.E., Taliotis, C., Mentis, D., Gardumi, F., de Strasser, L., Pappis, I., Balderrama, G.P. (2021). **The climate, land, energy, and water systems (CLEWs) framework: a retrospective of activities and advances to 2019**. *Environ Res Lett,* 16, 33003.

https://doi.org/10.17993/3cemp.2023.120151.324-344

(37) Rudaheranwa, N. (2009). **Biofuel subsidies and food prices in the context of WTO agreements.**

(38) Sallem, S., Chaabene, M., Kamoun, M.B.A. (2009). **Energy management algorithm for an optimum control of a photovoltaic water pumping system**. *Appl Energy,* 86, 2671–2680.

(39) Schmidt-Soltau, D. (2004). **Water energy nexus in Central Asia: improving regional cooperation in the Syr Darya Basin.**

(40) Schut, M., Slingerland, M., Locke, A. (2010). **Biofuel developments in Mozambique. Update and analysis of policy, potential and reality**. *Energy Policy,* 38, 5151–5165.

(41) Scott, C.A., El-Naser, H., Hagan, R.E., Hijazi, A. (2003). **Facing water scarcity in Jordan: reuse, demand reduction, energy, and transboundary approaches to assure future water supplies**. *Water Int,* 28, 209–216.

(42) Setlhaolo, D., Xia, X., Zhang, J. (2014). **Optimal scheduling of household appliances for demand response**. *Electr Power Syst Res,* 116, 24–28.

(43) Siddiqi, A., Anadon, L.D. (2011). **The water–energy nexus in Middle East and North Africa**. *Energy Policy,* 39, 4529–4540.

(44) Siddiqi, A., Kajenthira, A., Anadón, L.D. (2013). **Bridging decision networks for integrated water and energy planning**. *Energy Strateg Rev.,* 2, 46–58.

(45) Taylor, P. (2010). **Energy Technology Perspectives**. *Int Energy Agency*.

(46) UN, G. (2007). **Sustainable bioenergy: A framework for decision makers.**

(47) Van der Hoeven, M. (2013). **World energy outlook 2012**. *Int Energy Agency Tokyo, Japan*.

(48) Viswanathan, B., Kumar, K.S.K. (2005). **Cooking fuel use patterns in India: 1983–2000**. *Energy Policy,* 33, 1021–1036.

(49) Weitz, N., Nilsson, M., Davis, M. (2014). **A nexus approach to the post-2015 agenda**. *SAIS Rev Int Aff ,* 34, 37–50.

(50) Wichelns, D. (2010). **Agricultural Water Pricing: United States.**

(51) Winpenny, J.T. (1992). **Powerless and thirsty?: The outlook for energy and water in developing countries**. *Util Policy,* 2, 290–295.

(52) Wu, M., Mintz, M., Wang, M., Arora, S. (2009). **Water consumption in the production of ethanol and petroleum gasoline**. *Environ Manage,* 44, 981-997.

(53) Young, M., Esau, C. (2015). **CHARTING OUR WATER FUTURE: Economic frameworks to inform decision-making, in: Investing in Water for a Green Economy**. *Routledge*, 67–79.

(54) Zahnd, A., Kimber, H.M. (2009). **Benefits from a renewable energy village electrification system**. *Renew Energy,* 34, 362–368.

(55) Zhongming, Z., Wei, L. (2014). **United Nations World Water Development Report 2014: Water and Energy.**

(56) S. A. Choudhari, M. A. Kumbhalkar, D. V. Bhise, M. M. Sardeshmukh. (2022). **Optimal Reservoir Operation Policy Determination for Uncertainty**

https://doi.org/10.17993/3cemp.2023.120151.324-344

Conditions. *3C Empresa, Investigación y pensamiento crítico*, 11(2), 277-295. https://doi.org/10.17993/3cemp.2022.110250.277-295

https://doi.org/10.17993/3cemp.2023.120151.324-344

/19/

AN EXPERIMENTAL STUDY ON FRICTION STIR WELDING OF ALUMINUM-MAGNESIUM ALLOYS FOR IMPROVED MECHANICAL PROPERTIES OF TAILOR WELDED BLANKS

Manoj M. Joshi

Assistant Professor, Department of Mechanical Engineering, Sinhgad College of Engineering, Pune, Research scholar, Mechanical Engineering, SPPU, Rajarshi Shahu college of Engineering, Pune, India

manojmjoshi17@gmail.com

Dr. Amol Ubale

Professor, Department of Mechanical Engineering, Zeal College of Engineering, Pune, Research Guide, SPPU, Rajarshi Shahu college of Engineering, Pune, India

amol.ubale@zealeducation.com:

Reception: 20/11/2022 **Acceptance**: 14/01/2023 **Publication**: 12/02/2023

Suggested citation:

M. J., Manoj and U., Amol. (2023). **An Experimental Study On Friction Stir Welding Of Aluminum-Magnesium Alloys For Improved Mechanical Properties Of Tailor Welded Blanks**. *3C Empresa. Investigación y pensamiento crítico, 12(1)*, 346-359. https://doi.org/10.17993/3cemp.2023.120151.346-359

ABSTRACT

Tailor welded blanks (TWB) are used in automotive and aerospace industries as they offer weight saving followed by cost saving and improved fuel economy. Being light in weight and having low cost, Aluminum alloys have piqued the interest of scientists. Friction Stir Welding (FSW) is a well-known accepted technique used since 1991 worldwide for Aluminum and its alloys. Due to friction stir welding, mechanical changes occur due to stirring action at the joint. Also the inter-metallic compounds, kissing bond formation, onion ring formation etc. are defects encountered in the nugget zone of welding. Hence, a novel technique is suggested to carry out the friction stir welding using a blend of techniques viz. double sided friction stir welding and multi objective optimization of process parameters. For experimentation, AA 5182 and AA 5754-Aluminum Magnesium alloys of 5000 series are used with sheet size of 1.5 mm thickness. Experimentation was carried out on a vertical machining center, with circular, square, and triangular tool pin profiles with a tool rotational speed range between 1500 -1800 rpm and a welding speed range of 40 mm/min.-60 mm/min. For the analysis purpose, L9 orthogonal array was used and Grey Relational Analysis(GRA) was employed and ASTM standards were used for tensile testing. Base sample materials of AA 5182 and AA5754 are having ultimate tensile strengths of 289.58 N/mm2 and 220.75N/mm2respectively. The designed welded blank of the two materials recorded maximum ultimate tensile strength of 268.11N/mm2which was remarkable for FSW. Welded joint efficiency was found to be 92.73% and percentage elongation of TWB was found to be 44% as compared to the base metals.

KEYWORDS

Grey relational analysis, Double sided friction stir welding, Tensile Strength, Percentage Elongation.

PAPER INDEX

https://doi.org/10.17993/3cemp.2023.120151.346-359

1. INTRODUCTION

To achieve cost reduction and improved fuel efficiency, dissimilar materials of variable strengths can be employed at various locations in the automotive body. Nowadays, aluminum and its alloys are widely used in automobile body components. Due to the scarcity of aluminum in the market, it is frequently mixed with Magnesium to offer adequate strength. As custom welded blanks, aluminum-magnesium alloys with high specific strength, corrosion resistance, and a low weight-to-density ratio are employed. Due to metallurgical constraints, fusion welding of these Aluminum-Magnesium alloys is not practicable. Tailor Welded Blanks of dissimilar materials are frequently utilized to decrease cost, weight, and improve mileage in automobiles. Friction Stir Welding is a solid state joining technology that is more effective than fusion welding at joining dissimilar materials. A properly welded joint characteristics are dependent on a number of process parameters like, tool rotational speed, pin profile, shoulder shape, and welding speed [1]. Aluminum alloys, which are lighter in weight, more durable, and have better corrosion resistance, have largely supplanted steel in recent years.

Friction Stir Welding was invented by The Welding Institute in 1991.In the case of aluminum alloys, friction stir welding (FSW) has been found to be a better welding technique. However, as hardness increases in the weld zone, oxide formation is noticed in the Nugget Zone (NZ), residual stresses, kissing bond development, and production of intermetallic compounds are observed in the weld region. To establish a good welded joint is a difficulty that practically all researchers confront. FSW is being studied in order to improve welded joints. Many researchers have suggested multi-objective optimization of process parameters and double-sided friction stir welding approaches to solve faults in the welded connection.

Yuvaraj et al. [1] performed friction stir welding of dissimilar materials of AA7075-T651 and AA 6061 alloys using different FSW parameters and found that square pin profile gave higher strength, whereas Haribalaji et al. [2] used friction stir welding on input parameters and machine nature. Researchers Klos et al.[3] and Kaushik et al. [4] investigated the effects of tool pin profiles, feed rate, tool tilt angle, and welding speed, as well as a review of the mechanical and metallurgical characteristics of friction stir welded connections. They analyzed that there were micro structural changes which were found in AA 6063 when combined with SiC particles. The usage of interlayer material in dissimilar Aluminum and Magnesium alloys was studied by Kumar et al. [5]. But Cabibbo et al. [6] discussed two unique techniques: double-sided friction stir welding and RT type pin arrangement. The utility of aluminum magnesium alloys was explored in depth, as well as the metallurgical changes that occur and the utility of these Al-Mg alloys in diverse applications such as marine, automotive, and aerospace [7,8] was studied. Different materials to reduce weight of automotive parts were discussed by Miklos Tisza et al. [7]. Rahmatian et al. [9] investigated double-sided friction stir welding on AA 5083 in terms of various process factors. Das B. et al. [10] employed temperature signal as an approach and experimented with different tool pin profiles. Researchers [2,11,12,13] also discussed and utilized Grey Relational Analysis (GRA) to optimize process parameters for a better weld joint. Microstructural

https://doi.org/10.17993/3cemp.2023.120151.346-359

analysis using X-ray diffraction (XRD) and Scanning Electron Microscopy(SEM) confirmed that the joint was successful.

Some statistical process parameters were studied by few researchers and evidences were found in the open literature. The Taguchi method of optimization was utilized to optimize process parameters for Al- Mg-Si-Cu) alloys of the Aluminum 5000 and 6000 families for future automotive applications by researchers and researchers have focused on double friction stir welding technique and microstructure analysis at nugget zone [14,15,16,17]. During mechanical testing, Lee et al. [18] produced a hybrid composite material from carbon reinforced polymers on CR 340 plates and discovered epoxy leaks and significant gaps. Marco Parente et al. [11] concluded that TWB (Tailor Welded Blank) formability was reliant on weld line orientation, and its formability was lowered. A pin with a square pin profile was proven to be more effective than any other tool pin profile [19]. Kesharwani et. al. [16] used a Taguchi grey-based technique to multi-objective optimizes two sheet samples of AA 5052-H32 and AA 5754-H22. Experiments were designed using the L9 orthogonal array. Babu K. V., et al. [20] designed an expert system based on Artificial Neural Network (ANN) to analyze deep drawing behavior of Aluminum. Homola et al. [21] suggested the use of laminate plate at areas where lower load is applied to reduce weight in aircrafts. It was observed that lot of work was investigated on FSW but still there is a scope available on developing a novel FSW technique. Hence, using blend of techniques a new method is developed which will improve the mechanical properties of the joint to suit the requirements of the various applications.

Process factors such as tool rotational speed (rpm), worktable translational speed (mm/min), tool geometry, tool material, and tool tilt angle can all be changed, and by optimizing the process parameters, a good welded junction with good tensile strength and percentage elongation can be created. Double sided friction stir welding and multi objective optimization of process parameters are the methodologies which are blended to develop new Friction Stir Welding(FSW) method. The mechanical qualities and formability of this FSW joint are excellent.

Taking cognizance of all above discussions based on research literature availability, it was finalized to use an innovative combination of AA 5182, AA 5754 materials of 1.5 mm thickness to prepare a tailor welded blank and in order to get better mechanical properties of the tailor welded blanks, it was decided to use a novel technique of using double sided fiction stir welding with multi objective optimization of a

few prominent and important process parameters viz. tool rotational speed (rpm), worktable translational speed (mm/min), tool geometry to get better welded joint with better mechanical properties.

2. MATERIAL AND EXPERIMENTAL METHOD

By taking application into consideration, Aluminum-Magnesium Alloys Viz. AA 5182 and AA 5754 are used for experimentation purpose. These materials possess high specific strength, a low weight-to-density ratio, and a moderate strength, ductility and corrosion resistance. As pure Aluminum is scarce in the market, it is frequently mixed

https://doi.org/10.17993/3cemp.2023.120151.346-359

with Magnesium. They have moderate strength, high ductility, and very good corrosion resistance, wrought Al-Mg alloys are used as structural materials mainly in automobile industries.

Aluminum is soft and brittle by itself, but it can be strengthened by adding minor amounts of copper, magnesium, and silicon to the alloy. The Audi A8, Rolls Royce Phantom, and BMW Z8 all use the 5182 aluminum alloy [21]. Magnesium and manganese are minor components in the 5182 aluminum alloy. The aluminum alloy 5182 is used in the automobile industry to make a variety of parts.5754 Aluminum alloy is a common material in the automotive sector (vehicle doors, moulds, and seals). Magnesium is abundant in the 5000 class of aluminum alloys, which are non-heat treatable. Aluminum is soft and brittle in its pure form, but it can be strengthened by adding minor amounts of magnesium, copper, and silicon [21]. The Al-Mg-Si alloy 5182 is a type of aluminum alloy. It's a moderately strong alloy with good corrosion resistance, weld ability, and cold processing properties. The 5754 aluminum alloy has a medium strength, excellent processing properties, excellent corrosion resistance, weld ability, and ease of processing and forming. AA 5754 is Al-Mg alloy and AA 5754 is widely used in the automotive industry.

Experimentation was carried out on the material chosen and lab testing of base metal is done. The properties of the sample are shown in table 1 as follows:

Table 1. Composition of Elements of Aluminum Sheets

Elements	AA 5182		AA5 754	
	% Observed	% Specified	% Observed	% Specified
Copper	0.005	0.15 max.	0.004	0.10 max
Magnesium	5.82	4.00/5.00	3.09	2.6
Silicon	0.059	0.20 max	0.199	0.40 max
Iron	0.126	0.35 max	0.492	0.40 max
Manganese	0.449	0.20	0.030	0.5 max
Zinc	0.006	0.25 max.	-	-
Titanium	0.009	0.10 max	-	-
Chromium	0.063	0.30 max	0.179	0.30 max
Aluminum	93.26	93.2 max	95.71	87.1

2.1. TENSILE TEST

Tensile test specimens of the basic material: AA 5182 and AA 5754 sheets are taken according to ASTM E8M standards, as illustrated in fig. 1. Composition of the parent Aluminum alloys is enlisted in Table 1. Tensile tests were performed on AA 5182 and AA 5754 materials. Figure 1 shows the sample sizes obtained which adhere to ASTM E8 M standards. As shown in figure 2, a friction stir welding tool made up of

https://doi.org/10.17993/3cemp.2023.120151.346-359

High speed steel was used. Table 2 lists the mechanical properties found for the basic materials. A 100 kN computerized universal testing machine is employed to carry out the tensile test.

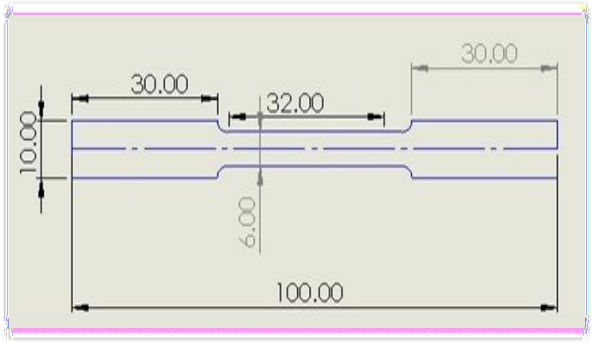

Figure 1. ASTM E8 Tensile Testing Specimen

Figure 2. Friction Stir Welding(FSW)Tool

Table 2. Tensile test result of AA 5182 and AA 5754 sheets

Parameter	AA 5182	AA5754
Specimen Type	Flat	Flat
Cross section area(mm2)	62.850	62.850
Original gauge Length	50	50
Final gauge Length	50	50
Preload(%)	0.2	0.2
Ultimate tensile load(kN)	18.200	14.44
Ultimate Tensile Strength (N/mm2)	209.577	229.752
Displacement at Ultimate load(mm)	12	5.5
Maximum Displacement(mm)	13.2	7.9
Percentage Elongation(%)	22.2	13.240
Breaking Load (kN)	17.240	12.920
Breaking Stress(N/mm2)	274.302	205.667
Yield Load(kN)	11.920	12.120
Yield stress(N/mm2)	189.658	192.840

Electro discharge machining is used to cut 18 samples of size 200 mm x 100 mm from 1.5 mm thick sheets of AA 5182 and AA 5754. Different cross sections of tool pins, such as circular, square, and triangular, are utilized as shown in figure 3. Double-sided friction stir welding is done for making test samples ready for further testing. The advancing side (A.S.) (Al Alloy AA5182) is the side when the tool rotation and welding directions are the same, whereas the retreating side is the opposite (R.S.) (Al alloy AA 5754) (shown in fig. 4). The samples were welded in the rolling direction of the sheet metals throughout the welding process as shown in fig.5 (A and B) for clear understanding about advancing and retreating side.

https://doi.org/10.17993/3cemp.2023.120151.346-359

As indicated in table 3, the Taguchi L_9 orthogonal array is utilized which consist of the factors and levels to apply design of experiments. The various process parameters used during experimentation are shown in table 4. Double Sided Friction Stir Welded (DSFW) samples of200 mm x 100 mm are cut from each of these materials, ASTM E8 specimens for tensile testing are obtained from each of these samples using the process parameters row wise. The results are tabulated in table 4 whereas figure 5 is showing tensile test specimens.

Circular Profile Square Profile Triangular Profile

Figure 3. Different tool pin profiles

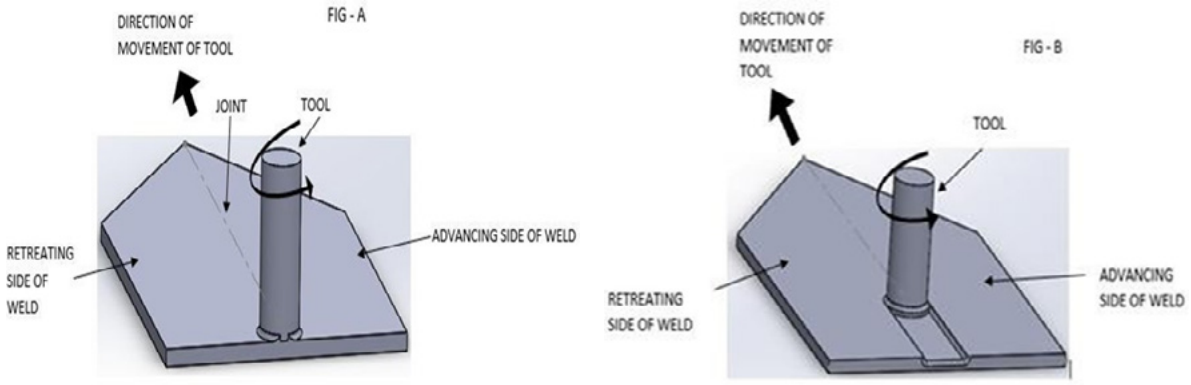

Figure 4 (*A & B*). Advancing and retreating side in Friction Stir Welding

Table 3. Factors and Levels

Sr. No.	RotationalSpeed of tool (rpm)	Worktablefeed (mm/ min.)	Cross SectionalShape ofpin
Level 1	1500	40	Circular
Level 2	1650	50	Triangular
Level 3	1800	60	Square

https://doi.org/10.17993/3cemp.2023.120151.346-359

Figure 5. Tensile test specimen of TWB

Table 4. Taguchi L9 orthogonal input array

Sr.No.	Rotational Speedof tool (rpm) (A)	Work table feed(mm/ min.)(B)	Cross sectional shape	FSW designation
1	1500	40	Circular	L_9_1111
2	1500	50	Triangular	L_9_1222
3	1500	60	Square	L_9_1333
4	1650	40	Square	L_9_2123
5	1650	50	Circular	L_9_2231
6	1650	60	Triangular	L_9_2312
7	1800	40	Triangular	L_9_3132
8	1800	50	Square	L_9_3213
9	1800	60	Circular	L_9_3321

3. RESULTS AND DISCUSSIONS

Grey Relational Analysis (GRA) is used in the multi-objective optimization of process parameters, and all samples are prepared using double-sided friction stir welding. The samples with the best ultimate tensile strength and percent elongation are determined.

Experimental readings are normalized in the range from zero to one. The two output parameters, weld strength and ductility values, are dealt with in the grey relational analysis. The results of the tests should be normalized in the range of 0 to 1. Grey relational coefficients and then grey relational grades are computed after normalizing. The higher value of grey relational grade is used to determine the optimal level of each process parameter. The most important controllable element and less important controllable parameters are determined by this technique.

https://doi.org/10.17993/3cemp.2023.120151.346-359

3.1. GREY RELATIONAL COEFFICIENT CALCULATION

Table 5. GRA Grey Relational Analysis Data Set

(I) GRA GREY RELATION ANALYSIS DATA SET						
	UTS			% Elongation		
SR.NO.	A	B	C	D	E	F
1	243.716	268.11	238.47	5.87	3.33	5.33
2	51.667	21.333	88.667	0.83	1.13	2.66
3	98.333	10.889	90.367	1.14	2.31	2.65
4	146.667	160.78	208.743	3.56	3.12	4.01
5	222.556	182.89	73.446	3.43	2.71	0.61
6	234.754	186.44	237.333	0.88	4.35	10.53
7	124.778	241.89	75.956	2.04	10.86	11.8
8	157.444	233.11	61.222	2.34	10.32	0.28
9	192.222	235.22	233.889	2.62	8.38	8.62

Table 5 is giving the experimental results obtained. Three such sets of readings of Ultimate Tensile strength and % elongation corresponding to the set of parameters used sequentially from Taguchi L9 orthogonal input array(table 4) are shown in table no.5.

Table 6. Normalized data

A	B	C	D	E	F
1.0000	1.0000	1.000	1.0000	0.2261	0.4384
0.0000	0.040	0.1548	0.0000	0.0000	0.2066
0.2430	0.000	0.1644	0.0615	0.1213	0.2057
0.4947	0.582	0.8323	0.5417	0.2045	0.3238
0.8898	0.668	0.0690	0.5159	0.1624	0.0286
0.9533	0.682	0.9936	0.0099	0.3309	0.8898
0.3807	0.898	0.0831	0.2401	1.0000	1.0000
0.5508	0.863	0.0000	0.2996	0.9445	0.0000
0.7319	0.872	0.9742	0.3552	0.7451	0.7240

Table 6 indicates the normalized values. Both ultimate tensile strength and % elongation are better if they are larger. Normalization values are obtained using formula with the help of data available from table 5.

$$v0_i k = 1 - \frac{max.x0_i(k) - x0_i(k)}{maxx0_i(k) - min.x0_i(k)} \quad (1)$$

https://doi.org/10.17993/3cemp.2023.120151.346-359

Here, k = 1 to n and k = 1 to n and i =trial number which is 1 to 9. n = performance characteristic, y=value in normalized data table, x=value from table 1

Table 7. Deviation sequence

A	B	C	D	E	F
0.0000	*0.0000*	*0.0000*	*0.0000*	*0.7739*	*0.5616*
1.0000	*0.9594*	*0.8452*	*1.0000*	*1.0000*	*0.7934*
0.7570	*1.0000*	*0.8356*	*0.9385*	*0.8787*	*0.7943*
0.5053	*0.4173*	*0.1677*	*0.4583*	*0.7955*	*0.6762*
0.1102	*0.3313*	*0.9310*	*0.4841*	*0.8376*	*0.9714*
0.0467	*0.3175*	*0.0064*	*0.9901*	*0.6691*	*0.1102*
0.6193	*0.1019*	*0.9169*	*0.7599*	*0.0000*	*0.0000*
0.4492	*0.1361*	*1.0000*	*0.7004*	*0.0555*	*1.0000*
0.2681	*0.1279*	*0.0258*	*0.6448*	*0.2549*	*0.2760*

Deviation sequence in Table 7 is obtained by formula,

$$Z0_ik = max.y0_ik \quad (2)$$

Z=Value in deviation sequence table 7, y=value in normalized data table, k = 1 to n and i =trial numberwhich is 1 to 9. n = performance characteristic

Table 8. Grey relation coefficient

Grey relation coefficient					
1.0000	*1.0000*	*1.0000*	*1.0000*	*0.3925*	*0.4710*
0.3333	*0.3426*	*0.3717*	*0.3333*	*0.3333*	*0.3866*
0.3978	*0.3333*	*0.3744*	*0.3476*	*0.3627*	*0.3863*
0.4973	*0.5451*	*0.7488*	*0.5217*	*0.3860*	*0.4251*
0.8194	*0.6015*	*0.3494*	*0.5081*	*0.3738*	*0.3398*
0.9146	*0.6116*	*0.9873*	*0.3356*	*0.4277*	*0.8193*
0.4467	*0.8306*	*0.3529*	*0.3969*	*1.0000*	*1.0000*
0.5267	*0.7861*	*0.3333*	*0.4165*	*0.9001*	*0.3333*
0.6509	*0.7964*	*0.9509*	*0.4367*	*0.6624*	*0.6443*

Grey relation coefficient is calculated by following formula

$$u0_ik = \frac{min.z0_ik + 0.5(max.z0_ik)}{z0_ik + 0.5(max.z0_ik)} \quad (3)$$

Here, u=values of grey relation coefficients. Z=Value in deviation sequence table 7. y=value in normalized data table, k = 1 to n and i =trial number which is 1 to 9. n = performance characteristic

https://doi.org/10.17993/3cemp.2023.120151.346-359

Table 9. Grey Relational Grade

(GRG) Grey Relational Grade	Rank
0.8106	*1*
0.3501	*9*
0.3670	*8*
0.5207	*6*
0.4987	*7*
0.6827	*3*
0.6712	*4*
0.5494	*5*
0.6903	*2*

Grey relational grade is obtained by taking average of all grey relational coefficients for a particular set of parameters. The process parameters that correspond to the greater value of grey relational grade are found to be optimal. [20]

The analysis is done on a cutting-edge welding method. Tool rotational speed, worktable translational speed, and tool pin geometry were chosen as process parameters for multi-objective optimization. The ultimate tensile strength and percent elongation are two essential tensile test results that have been calculated to determine the utility of these Aluminum alloys in terms of strength and ductility. Whereas the other characteristics of the welded joints like micro grain structure, distortion etc. are out of scope of this article.

- Using grey relational analysis, it was discovered that using **tool rotational speed of 1500 rpm, worktable translational speed of 40 mm/min, circular tool pin profile, and double sided friction stir welding, the maximum ultimate tensile strength obtained was 268.11 N/mm2 and the maximum percent elongation was 5.87 %.**
- The reason behind getting **92.73% weld joint efficiency as compared with the base metals** is due to proper intermixing of the material at the joint due to optimized process parameters and due to double sided friction stir welding. The material reaches everywhere leaving no space for oxide formation.
- **The basic metals AA 5182 and AA 5754 have ultimate tensile strengths of 289.58 N/mm2 and 220.75 N/mm2, respectively.**
- So, using double sided friction stir welding and optimizing the critical process parameters, such as tool rotational speed, tool pin profile, and welding speed, substantial strength and percentage elongation of custom welded blanks could be accomplished.

https://doi.org/10.17993/3cemp.2023.120151.346-359

4. CONCLUSION

- By using double sided friction stir welding for joining the dissimilar materials the harder material was kept on advancing side. The prominent parameters chosen in this experimentation were tool rotational speed, welding speed and tool geometry. **Tool rotational speed range was 1500 rpm, 1650 rpm and 1800 rpm. The worktable feed values chosen were 40mm/min., 50 mm/min.,60mm/min.**
- At the nugget zone, the mechanical properties are grossly varying as compared to the other zones, viz. thermos mechanically affected zone, heat affected zone and parent metal zone.
- While **the tool profiles chosen were circular, square, triangular with tool material as HSS. Taguchi grey relational analysis** was chosen to find out the optimized process parameters. Weld strength and ductility values were the output parameters used in GRA, it was found that **tool rotational speed of 1500 rpm, worktable translational speed of 40mm/min., circular tool pin profile were found to be the best process parameters when double friction stir welding was employed.**
- **Further, for the tailor welded blank, the maximum weld strength i.e. tensile strength obtained was 268.11 N/mm2which is 92.73% and the ductility i.e. maximum percentage elongation was 44% compared to base metal.**
- Double sided welding ensures that there are no voids at the joint and the new stirred material is leaving no voids at the nugget zone and optimized process parameters ensure that the welding at the nugget zone is best possible with the optimized process parameters.
- This novel blended technique of multi objective optimization of prominent process parameters and use of double sided friction stir welding with harder material on advancing side of the tool can overcome the usual metallurgical problems.
- Tailor welded blanks can give a better welded joint as the intermixing of the material is proper at the nugget zone with this technique and oxide formation associated with brittleness at the joint is also significantly low. Tunnel defect due to improper heat generation, cavity formation due to uneven mixing of the material, oxide formation at the joint is reduced to provide weld joint.

Further, Electron Backscatter Diffraction (EBSD) is proposed to check the micro structure for analysis of lesser ductility which will be the area of Industrial interest.

ACKNOWLEDGMENT

Authors would like to thank MIT World Peace University for offering ACE make Vertical Machining Centre and Computerized Universal Testing Machine to carry out friction stir welding and tensile testing. Special thanks to Dr. Ganesh Borikar and Dr. Anil Mashalkar at MITWPU, Pune for their valuable support. Also, authors would like to thank Dr. Sagar V. Wankhede, Assistant Professor, School of Mechatronics Engineering, Symbiosis Skills and Professional University, Pune and Mr.

https://doi.org/10.17993/3cemp.2023.120151.346-359

Soumyaranjan Nayak-Research Scholar at IIT-B, Dr. R.S. Hingole at D.Y. Patil College of Engineering, Akurdi, Punefor their valuable inputs.

REFERENCES

(1) Yuvaraj, K. P., Varthanan, P. A., Haribabu, L., Madhubalan, R., & Boopathiraja, K. P. (2021). **Optimization of FSW tool parameters for joining dissimilar AA7075-T651 and AA6061 aluminium alloys using Taguchi Technique**. *Materials today: proceedings*, 45, 919-925. https://doi.org/10.1016/j.matpr.2020.02.942

(2) Haribalaji, V., Boopathi, S., & Asif, M. M. (2022). **Optimization of friction stir welding process to join dissimilar AA2014 and AA7075 aluminum alloys**. *Materials Today: Proceedings*, 50, 2227-2234. https://doi.org/10.1016/j.matpr.2021.09.499

(3) Klos, A., Kahrimanidis, A., Wortberg, D., & Merklein, M. (2017). **Experimental and numerical studies on the forming behavior of high strain Al-Mg-Si (-Cu) sheet alloys**. *Procedia Engineering*, 183, 95-100. https://doi.org/10.1016/j.proeng.2017.04.017

(4) Kaushik, N., Singhal, S., Rajesh, R., Gahlot, P., & Tripathi, B. N. (2018). **Experimental investigations of friction stir welded AA6063 aluminum matrix composite**. *Journal of Mechanical engineering and sciences*, 12(4), 4127-4140. https://doi.org/10.15282/jmes.12.4.2018.11.0357

(5) Kumar, M., Das, A., & Ballav, R. (2020). **Influence of interlayer on microstructure and mechanical properties of friction stir welded dissimilar joints: A review**. *Materials Today: Proceedings*, 26, 2123-2129. https://doi.org/10.1016/j.matpr.2020.02.458

(6) Cabibbo, M., Forcellese, A., Santecchia, E., Paoletti, C., Spigarelli, S., & Simoncini, M. (2020). **New approaches to friction stir welding of aluminum light-alloys**. *Metals*, 10(2), 233. https://doi.org/10.3390/met10020233

(7) Tisza, M., & Czinege, I. (2018). **Comparative study of the application of steels and aluminium in lightweight production of automotive parts**. *International Journal of Lightweight Materials and Manufacture*, 1(4), 229-238. https://doi.org/10.1016/j.ijlmm.2018.09.001

(8) Singh, V. P., Patel, S. K., Ranjan, A., & Kuriachen, B. (2020). **Recent research progress in solid state friction-stir welding of aluminium–magnesium alloys: a critical review**. *Journal of Materials Research and Technology*, 9(3), 6217-6256. https://doi.org/10.1016/j.jmrt.2020.01.008

(9) Rahmatian, B., Mirsalehi, S. E., & Dehghani, K. (2019). **Metallurgical and mechanical characterization of double-sided friction stir welded thick AA5083 aluminum alloy joints**. *Transactions of the Indian Institute of Metals*, 72(10), 2739-2751. https://doi.org/10.1007/s12666-019-01751-8

(10) Das, B., Pal, S., & Bag, S. (2019). **Probing defects in friction stir welding process using temperature profile.** *Sādhanā*, 44(4), 1-9. https://doi.org/10.1007/s12046-019-1068-2

(11) Parente, M., Safdarian, R., Santos, A. D., Loureiro, A., Vilaca, P., & Jorge, R. M. (2016). **A study on the formability of aluminum tailor welded blanks**

produced by friction stir welding. *The International Journal of Advanced Manufacturing Technology*, 83(9), 2129-2141. https://doi.org/10.1007/s00170-015-7950-0

(12) Lee, M. S., Kim, S. J., Lim, O. D., & Kang, C. G. (2014). **Effect of process parameters on epoxy flow behavior and formability with CR340/CFRP composites by different laminating in deep drawing process**. *Procedia Engineering*, 81, 1627-1632. https://doi.org/10.1016/j.proeng.2014.10.202

(13) Singh, R., Rizvi, S. A., & Tewari, S. P. (2017). **Effect of friction stir welding on the tensile properties of aa6063 under different conditions**. *International Journal of Engineering*, 30(4), 597-603. https://doi.org/10.5829/idosi.ije.2017.30.04a.19

(14) GN, S. (2022). **Friction stir welding of dissimilar alloy combinations—A Review**. *Proceedings of the Institution of Mechanical Engineers, Part C: Journal of Mechanical Engineering Science*, 09544062211069292. https://doi.org/10.1177/09544062211069292

(15) Nguyen, V. N., Nguyen, Q. M., Thi, H. T. D., & Huang, S. C. (2018). **Investigation on lap-joint friction stir welding between AA6351 alloys and DP800 steel sheets**. *Sādhanā*, 43(10), 1-7. https://doi.org/10.1007/s12046-018-0930-y

(16) Kesharwani, R. K., Panda, S. K., & Pal, S. K. (2014). **Multi objective optimization of friction stir welding parameters for joining of two dissimilar thin aluminum sheets**. *Procedia Materials Science*, 6, 178-187. https://doi.org/10.1016/j.mspro.2014.07.022

(17) Shaik, B., Harinath Gowd, G., & Durga Prasad, B. (2019). **Investigations and optimization of friction stir welding process to improve microstructures of aluminum alloys**. *Cogent Engineering*, 6(1), 1616373. https://doi.org/10.1080/23311916.2019.1616373

(18) Lee, M. S., & Kang, C. G. (2017). **Determination of forming procedure by numerical analysis and investigation of mechanical properties of steel/ CFRP hybrid composites with complicated shapes**. *Composite structures*, 164, 118-129. https://doi.org/10.1016/j.compstruct.2016.10.021

(19) Nadikudi, B. K. B., Davidson, M. J., Akasapu, N. R., & Govindaraju, M. (2015). **Formability analysis of dissimilar tailor welded blanks welded with different tool pin profiles**. *Transactions of Nonferrous Metals Society of China*, 25(6), 1787-1793. https://doi.org/10.1016/s1003-6326(15)63784-0

(20) Babu, K. V., Narayanan, R. G., & Kumar, G. S. (2010). **An expert system for predicting the deep drawing behavior of tailor welded blanks**. *Expert Systems with Applications*, 37(12), 7802-7812. https://doi.org/10.1016/j.eswa.2010.04.059

(21) Homola, P., Kadlec, M., Růžek, R., & Šedek, J. (2017). **Fatigue behaviour of tailored blank thermoplastic composites with internal ply-drops**. *Procedia Structural Integrity*, 5, 1342-1348. https://doi.org/10.1016/j.prostr.2017.07.144

/20/

EXPERIMENTAL AND THEORETICAL INVESTIGATION OF SINGLE SLOPE SOLAR STILL COUPLED WITH ETC WITH STAINLESS-STEEL REFLECTOR WITH CENTRAL V-GROOVE

Bhushan L. Patil

Department of Mechanical Engineering, JSPM'S Rajarshi Shahu College of Engineering, S. P. Pune University, Pune,

patilb6982@gmail.com - https://orcid.org/0000-0003-4810-0708

Jitendra. A. Hole

Department of Mechanical Engineering, JSPM'S Rajarshi Shahu College of Engineering, S. P. Pune University, Pune,

jahole1974@gmail.com - https://orcid.org/0000-0002-0158-6221

Sagar V. Wankhede

School of Mechatronics Engineering, Symbiosis Skills and Professional University, Kiwle, Pune

sagarwankhede8890@gmail.com - https://orcid.org/0000-0002-2341-3110

Reception: 27/11/2022 **Acceptance**: 18/01/2023 **Publication**: 13/02/2023

Suggested citation:

L. P., Bhushan, A. H., Jitendra and V. W., Sagar. (2023). **Experimental And Theoretical Investigation Of Single Slope Solar Still Coupled With Etc With Stainless-Steel Reflector With Central V-Groove**. *3C Empresa. Investigación y pensamiento crítico, 12(1)*, 361-380. https://doi.org/10.17993/3cemp.2023.120151.361-380

ABSTRACT

Due to population, industrial, and agricultural growth as well as the rising demand for potable water, there is currently shortage of water in many region of the world. Desalination of brackish and salty water is one of the simplest and economical processes to convert it into potable or drinkable water. But solar still has a low productivity device as its main flaw. Mechanisms for heat exchange play a significant part in increasing the daily yield. The output of any solar desalination system is influenced by the water temperature. The productivity rises as the basin's water temperature rises. A series of experiments were conducted for four different cases in the current study, and it was discovered that the still combined with a parabolic concentrator and stepped basin is the most productive and efficient. The results were verified using mathematical modeling, and it was discovered that in all of these instances, the percentage RMS values range from 10% to 40% and the coefficient of correlation is varies in between 0.8 to 0.99. The overall thermal efficiency of 16.54% is obtained for the integrated system when coupled with evacuated tube collector.

KEYWORDS

Solar stills, Thermal modeling, ETC, Parabolic Reflector, V-groove, stepped basin solar still

https://doi.org/10.17993/3cemp.2023.120151.361-380

PAPER INDEX

https://doi.org/10.17993/3cemp.2023.120151.361-380

1. INTRODUCTION

Numerous authors have studied solar stills to enhance their performance. Some of the most important elements to get noticeable system improvements are heat exchange mechanisms [1]. (TES) and PCM materials further increase the internal energy of the solar distillation system (PCM). Creating temperature gradient between the surface of glass and the temperature of the top cover is another effective way to encourage evaporative heat transfer. Manokar et al. [2] provided basic principle of working evaporation and condensation in solar still. They claimed that the wind speed and glass cover configuration have a significant impact on the condensation process. The rate of condensation and yield are significantly influenced by the variation in wind velocity. A few other factors were also discovered to affect the evaporation rate. Similar findings that an increase in ambient air velocity has a significant impact on convective heat transfer were reported by Dimriet al. [3]. A study by Murugavel et al. [4] presented a connection of solar still's output with the tilt of the glass cover. Based on the location's latitude and known seasonal variations in productivity, Khalifa[5] proposed a correlation for the best inclination and concluded that the ideal inclination of glass cover should be closer to the location's latitude. The solar still's cover material has an impact on heat transfer rate as well. Cover materials like plain glass, plexiglass, and polyethylene sheet were tested by Jones et al. [6] they claimed that glass-covered solar stills have higher water temperatures and distilled water yield. The effect of water depth in a basin has been the subject of numerous studies, and it has been concluded that the yield and efficiency decreases with increase in the water depths [7, 8]. According to Taghvaei et al. [9], the yield is inversely proportional to the water depth. Water depth optimization is therefore a cost-effective method because it can achieve acceptable performance without additional investment. Similar findings were also reported by Ahmed et al. [10], who showed a strong dependence between distillate yield and water depth. Similar studies [11–12] have been conducted in great numbers to find variation of productivity with water depth of solar still. Solar still with additional reflector and stepped basin can improve the productivity by 34% [13]. External and internal reflector with stepped basin improves the efficiency by 125% the the reference case [14]. As an alternative to adding more energy to the still, Xie et al. [15] suggested using energy recovered from condensed vapour. Estahbanati et al. [16] showed how adding more stages can significantly increase the productivity of the system. Additionally, it was stated that by using this technique, the desalination yield and performance ratio could increase to 0.91 and 1.81, respectively [17]. Matrawy et al methods of using dark-colored (black) clothing works on the principle of capillary effect resulted in a 75% increase in overall productivity. Black rubber and gravel rocks were used by Nafey et al. [7] as practical heat storage mediums, increasing the still's yield. Other researchers have proposed new, inventive designs for solar stills, including those with pulsating heat pipe-type solar stills [21], stepped solar stills [19], conical solar stills [20], and solar stills with semicircular trough-absorber and baffles [18]. These modern systems have higher efficiencies and show a significant increase in distillate output. However, the system's overall cost as well as its installation and operation complexity both rises concurrently. These solutions necessitate the

https://doi.org/10.17993/3cemp.2023.120151.361-380

attachment of devices and a greater input of energy; consequently, additional capital or operating costs must be incurred.

2. EXPERIMENTAL SETUP AND PROCEDURE

A solar still is fabricated to perform experimental work. The figure.5 shows a stepped basin solar still, compound parabolic concentrator with ETC and storage tank. The experimental work is carried out at Indrayaninagar, Bhosari Pune (latitude 18.63o, longitude 73.84o) facing towards south.

Solar still made up of 0.7mm thick galvanized steel sheet with dimensions 1.41m x 0.70m also secondary stepped basin made up of 0.7mm thick galvanized steel sheet. Black paint is applied to improve absorptivity of solar still and secondary stepped basin. Cover glass is made up of toughened glass 4mm thickness.

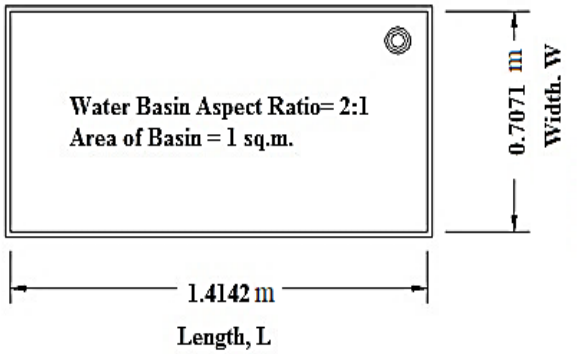

Figure 1. Basin area of solar still with aspect ratio 2:1

Figure 2. Stepped absorber plate

To build the solar still, gauge 22 galvanized iron sheet is used. The basin area is maintained at 1 m2, with a 2:1 aspect ratio. This is consistent with the findings of El-Swify and Metias[43], who found aspect ratio of 2:1 results in the solar still's best ability to capture solar energy. It is necessary to paint the interior of the basin black in order to effectively absorb solar energy. A condensing cover made of plain glass and inclined at an 18° angle (approximately equal to latitude location) is used to cover the basin. The solar still is facing towards the south to ensure maximum amount of solar energy incident on the still.

https://doi.org/10.17993/3cemp.2023.120151.361-380

Figure 3. Steel parabolic concentrator

3. INSTRUMENTATION AND OBSERVATION

The different measurements were taken to calculate the hourly yield such as temperature of water, glass cover temperature, inside and outside glass temperatures, atmospheric temperature and solar intensity. The temperatures were recorded using a probe type digital thermometer with L.C of 0.10C and the hourly productivity is calculated by using a measuring jar of L.C 10ml. the experiment were conducted from 8 A.M to 7 P.M. A computer program using Microsoft Excel was made to find inner glass, outer temperature of glass, temperature of water from basin and yield.

4. RESULTS AND DISCUSSIONS

In this study four cases are examined.

1. Single slope solar still with constant flow rate.
2. Single slope solar still with secondary stepped basin.
3. Single slope solar still coupled with compound parabolic concentrator.
4. Single slope solar still with secondary stepped basin coupled with compound parabolic concentrator.

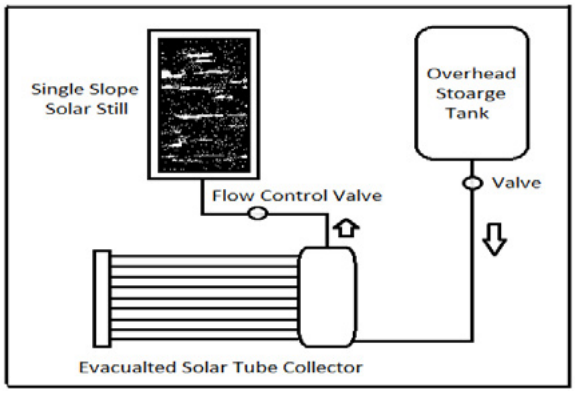

Figure 4. Schematic diagram of solar still coupled with evacuated tube solar collector.

https://doi.org/10.17993/3cemp.2023.120151.361-380

Figure 5: Experimental setup

CASE 1. SINGLE SLOPE SOLAR STILL WITH CONSTANT FLOW RATE (REFERENCE CASE)

Figure 6 shows variation of temperatures of various parts of the solar still such as temperature at outer, inner side of the glass temperature of basin, temperature of water and vapor with respect to the time of the day and found that the maximum temperature of 49.30C is obtained at the basin at around 3:00P.M. The figure 7 shows the relationship between hourly productivity and found that the maximum yield of 200ml is obtained at 3:00P.M.

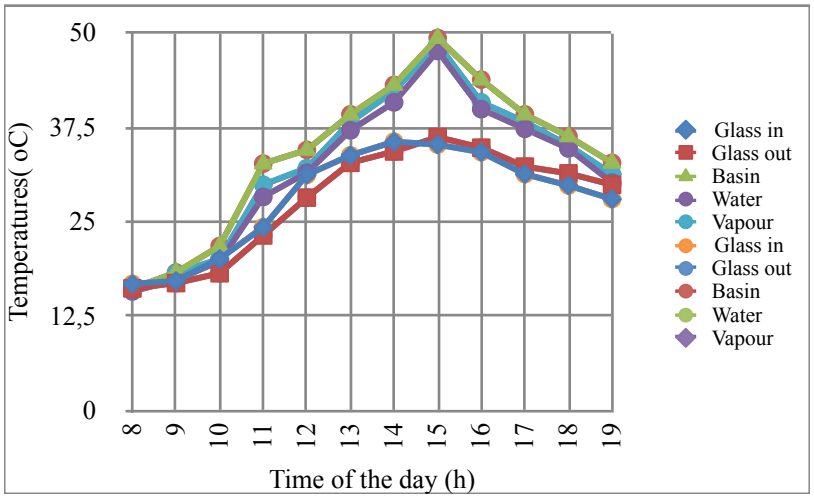

Figure 6. Relationship between various temperatures of solar stills with time.

https://doi.org/10.17993/3cemp.2023.120151.361-380

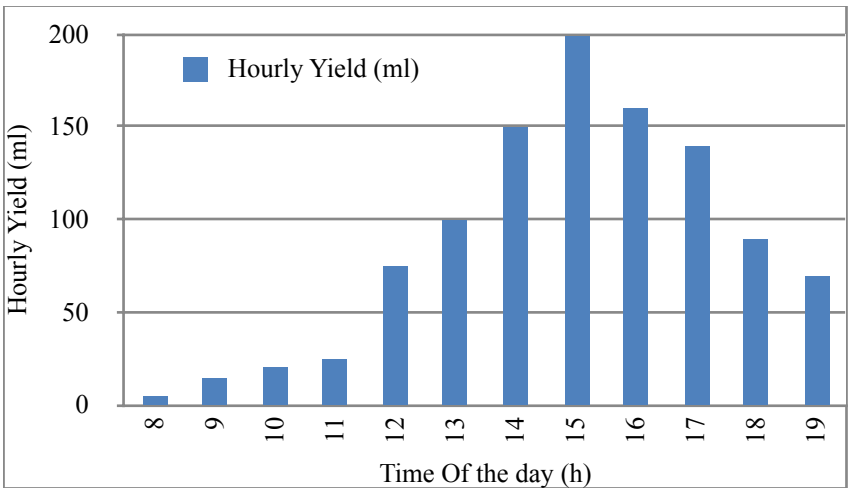

Figure 7. Relationship between hourly productivity with time.

CASE 2. SOLAR STILL WITH A SINGLE SLOPE WITH A SECONDARY STEPPED BASIN

Figure 8 and figure 9 shows change of temperatures and hourly yield respectively when the secondary stepped basin is used with solar still and found that the maximum temperature of 59.150C and maximum yield of 250ml is obtained at around 3:00P.M.

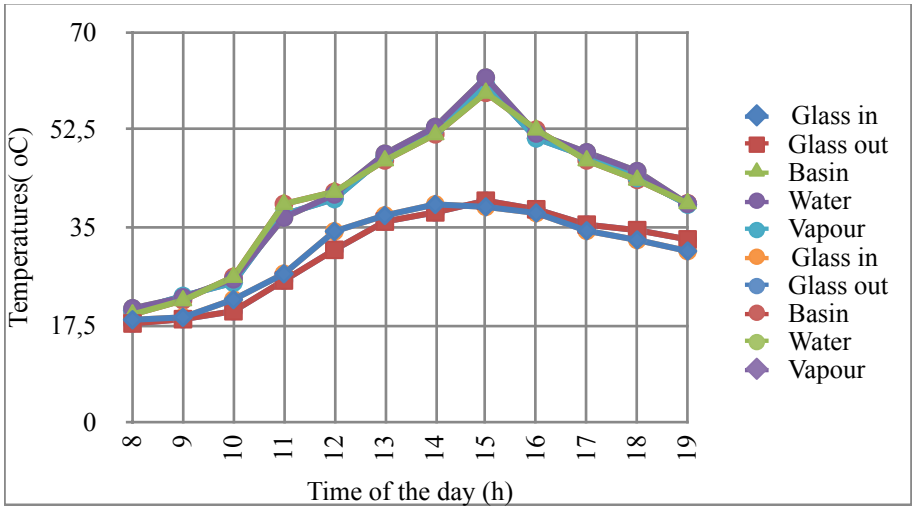

Figure 8. Relationship between solar still temperatures with time.

https://doi.org/10.17993/3cemp.2023.120151.361-380

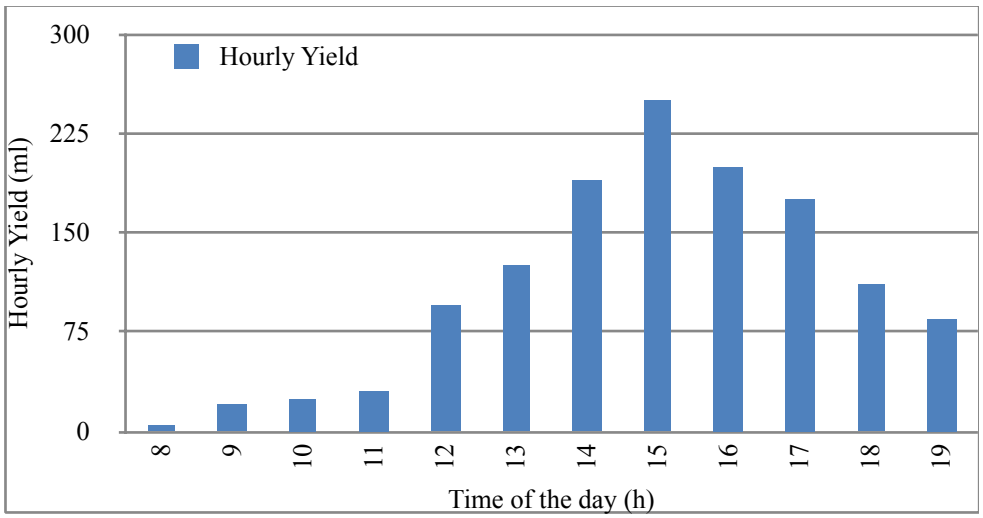

Figure 9. Relationship between hourly productivity with time.

CASE 3. SOLAR STILL WITH A SINGLE SLOPE AND A COMPOUND PARABOLIC CONCENTRATOR

Figure 10 and figure 11 shows variation of temperatures and hourly yield respectively when the still is coupled with ETC and found that the maximum temperature of 62.50C and maximum yield of 280ml is obtained at around 3:00P.M.

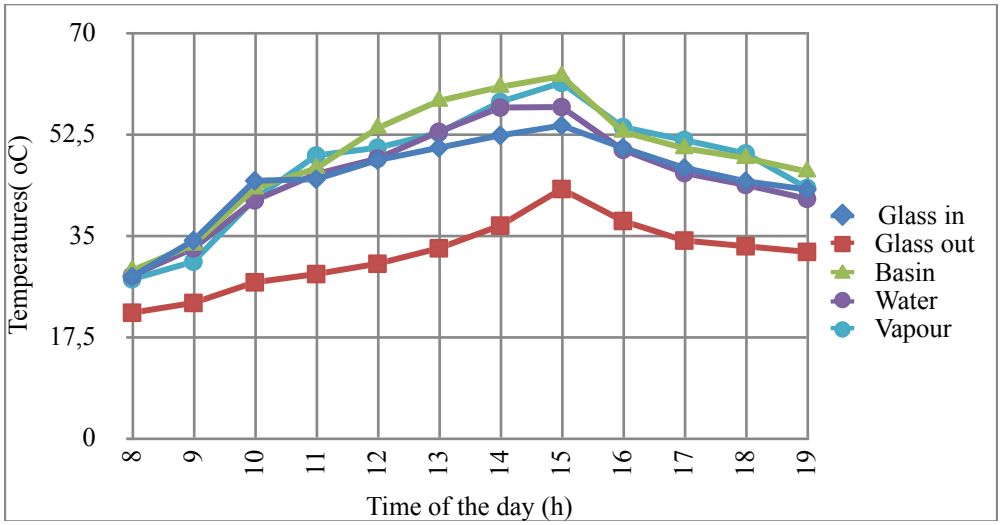

Figure 10. Relationship between solar still temperatures with time.

https://doi.org/10.17993/3cemp.2023.120151.361-380

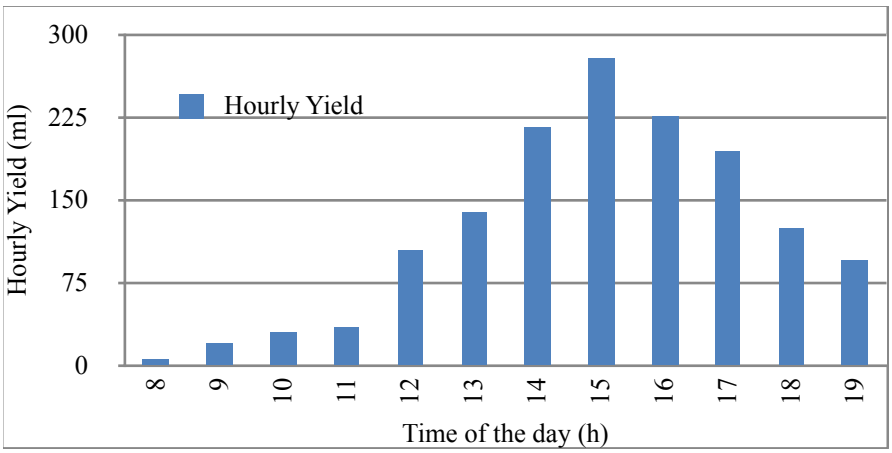

Figure 11. Relationship between hourly productivity with time.

CASE 4: SOLAR STILL WITH SECONDARY STEPPED BASIN AND COMPOUND PARABOLIC CONCENTRATOR

Figure 12 and figure 13 shows change of temperatures and yield respectively when the solar still is equipped with secondary stepped basin and coupled with parabolic concentrator with V-groove and found that the maximum temperature of 70.20C and maximum yield of 320ml is obtained at around 3:00P.M. Figure 14 shows the variation of atmospheric temperature with respect to the time of day on various days of experimentation.

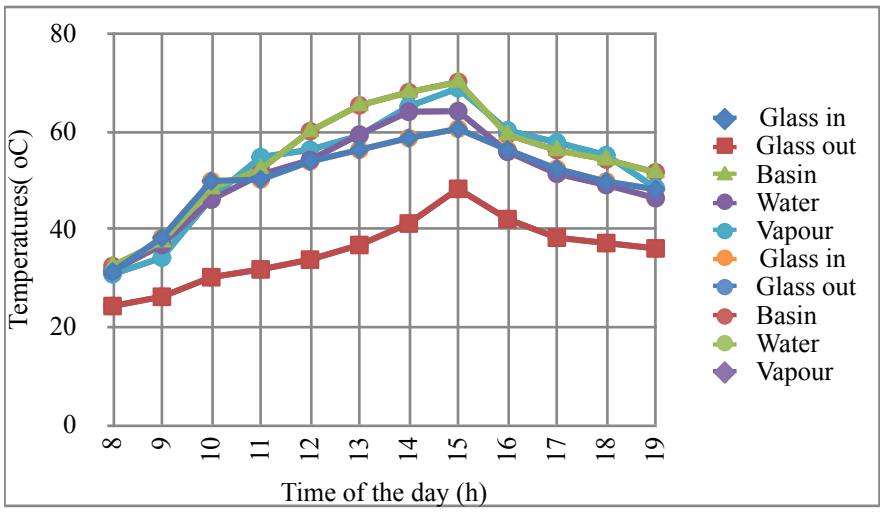

Figure 12. Relationship between solar still temperatures with time.

https://doi.org/10.17993/3cemp.2023.120151.361-380

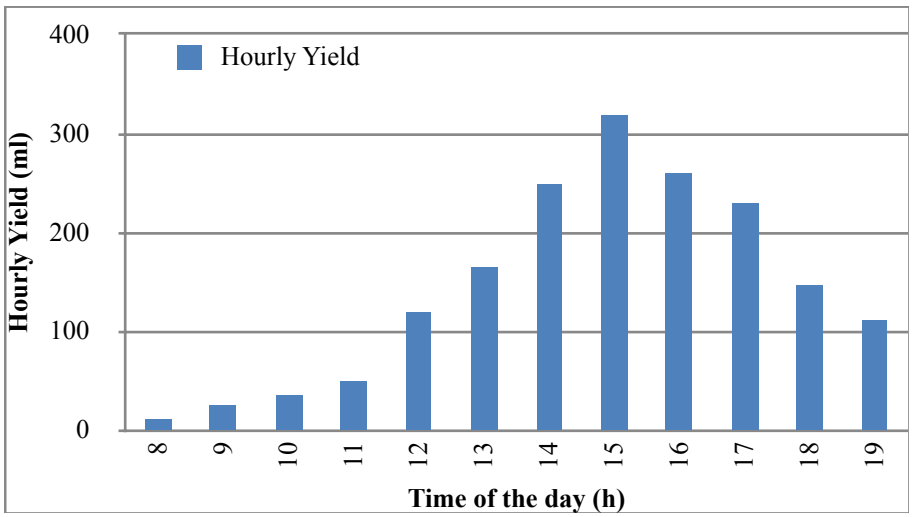

Figure 13. Relationship between hourly productivity with time.

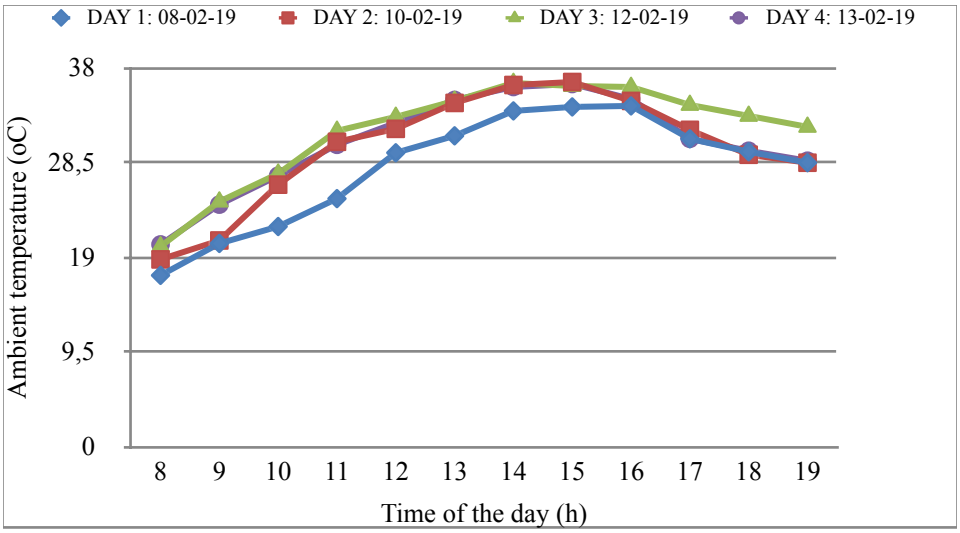

Figure 14. Relationship between ambient temperatures with time on the different days of experimentation.

5. THERMAL MODELING

Mathematical modeling of various parameters of still is performed by using the concept of validation of temperature of inner, outer glass, temperature of basin and yield of the solar still.

For inner glass

$$\propto {}'_{g} I_{effs} + h_{1w}(T_w - T_{gi}) = \frac{K_g}{L_g}(T_{gi} - T_{go}) \qquad (1)$$

For outer glass

https://doi.org/10.17993/3cemp.2023.120151.361-380

$$\frac{K_g}{L_g}(T_{gi} - T_{go}) = h_{1g}(T_{go} - T_a) \quad (2)$$

Temperature inside the glass is given by

$$T_{gi} = \frac{\alpha'_g I_{effs} + h_{1w}T_w + \frac{K_g}{L_g}T_{go}}{h_{1w} + \frac{K_g}{L_g}} \quad (3)$$

Temperature at outside of the glass is given by

$$T_{go} = \frac{\alpha'_g I_{effs} h_k + U_{wo}T_w + h_{1g}T_a}{h_{1g} + U_{wo}} \quad (4)$$

For basin liner

$$\alpha'_b \left(1 - \alpha'_g\right)(1 - \alpha'_w)I_{effs} = h_w(T_b - T_w) + h_b(T_b - T_a) \quad (5)$$

Temperature at the bottom of the basin liner is given by

$$T_b = \frac{\alpha'_{-b} I_{effs} + h_w T_w + h_b T_a}{h_w + h_b} \quad (6)$$

For water mass

$$\dot{Q}_u + \alpha'_w\left(1 - \alpha'_g\right)I_{effs} + h_w(T_b - T_w) = (MC)_w\frac{dT_w}{dt} + h_{1w}(T_w - T_{go}) \quad (7)$$

Where,

$$\dot{Q}_u = A_c F_R \left[(\alpha\tau)_c\right]I_c - U_{LC}(T_w - T_a) \quad (8)$$

Rate of evaporation is given by

$$\dot{q}_{ew} = h_{ew}(T_w - T_g)$$

And the hourly output is given by

$$\dot{m}_{ew} = \frac{h_{ew}(T_w - T_g)\ X\ 3600}{L} \quad (kg/m^2h)$$

6. RESULTS AND DISCUSSION

Various parameters from table 1 are used to find the values of basin, water, inner and outer glass temperature the figure 14 shows variation of atmospheric temperature on different days of experimentation. The atmospheric temperature, glass and water temperature are used as input parameters to calculate convective, evaporative and total heat transfer coefficient of the system. These heat transfer coefficient with initial basin and glass temperature are further used to calculate inner and outer glass temperature and also the temperature of basin The hourly yield in kg/m2h is also

https://doi.org/10.17993/3cemp.2023.120151.361-380

calculated theoretically and experimentally and we found that the coefficient of correlation varies in between 0.9 to 0.99 and RMS values lies between 10% to 40%.

Table 1. Various parameters for design of single slope solar still.

Parameter	Values
A_b	$1m^2$
C	0.54
C_w	$4190J/kg^0C$
G	9.81 m/sec
K_g	$0.78W/m^0C$
$L_c/L_g/L_p$	0.003m
$\propto'_g$	0.05
$\propto'_b$	0.8
$\propto'_w$	0.05
$\propto'_p$	0.05
h_w	135
μ	$17.8Ns/m^2$
ρ	$995.8kg/m^3$
σ	$5.67x10^{-8}W/m^2K^4$

Case 1. Experimental v/s Theoretical variation of different temperatures of solar stills with time of day. Figure 15, 16 and 17 shows the experimental and theoretical values of the temperature at inner, outer side of the glass and temperature of basin respectively for the single basin solar still.

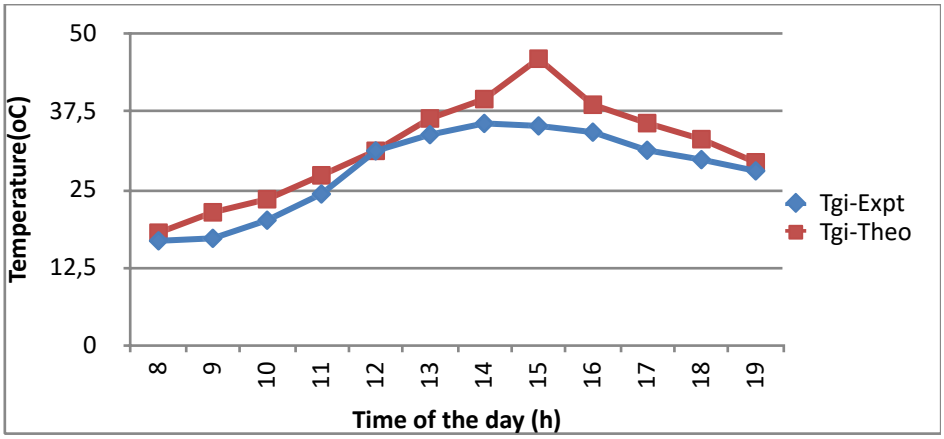

Figure 15. Experimental v/s Theoretical variation of glass inside temperatures.

https://doi.org/10.17993/3cemp.2023.120151.361-380

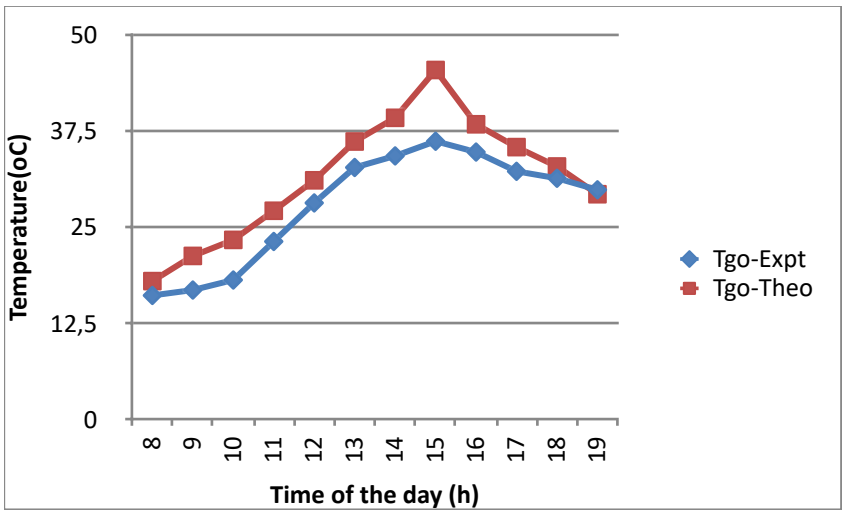

Figure 16. Experimental v/s Theoretical variation of glass outside temperatures.

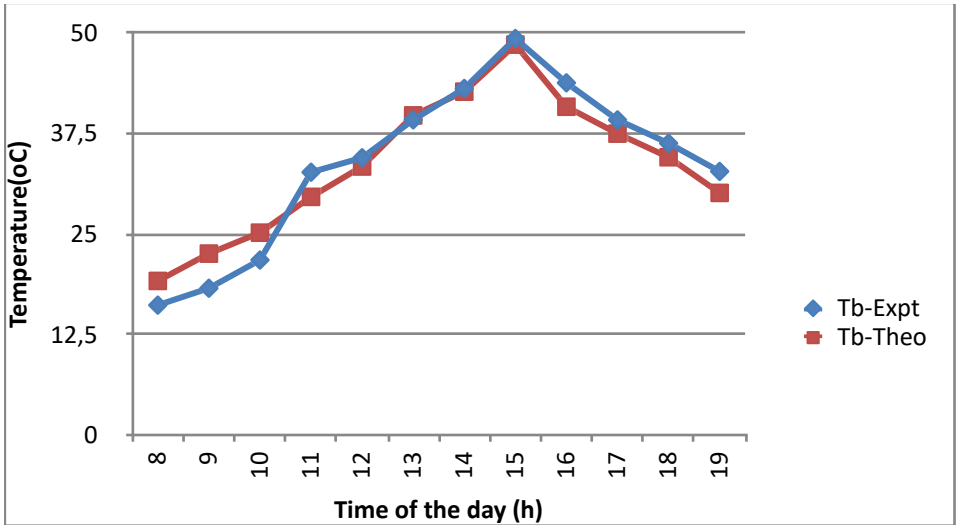

Figure 17. Experimental v/s Theoretical variation of basin temperatures.

Case2. Experimental v/s Theoretical variation of temperatures of the elements of still. Figure 18, 19 and 20 shows the experimental and theoretical values of the temperature at inner, outer side of the glass and basin respectively for the single basin solar still equipped with secondary basin.

https://doi.org/10.17993/3cemp.2023.120151.361-380

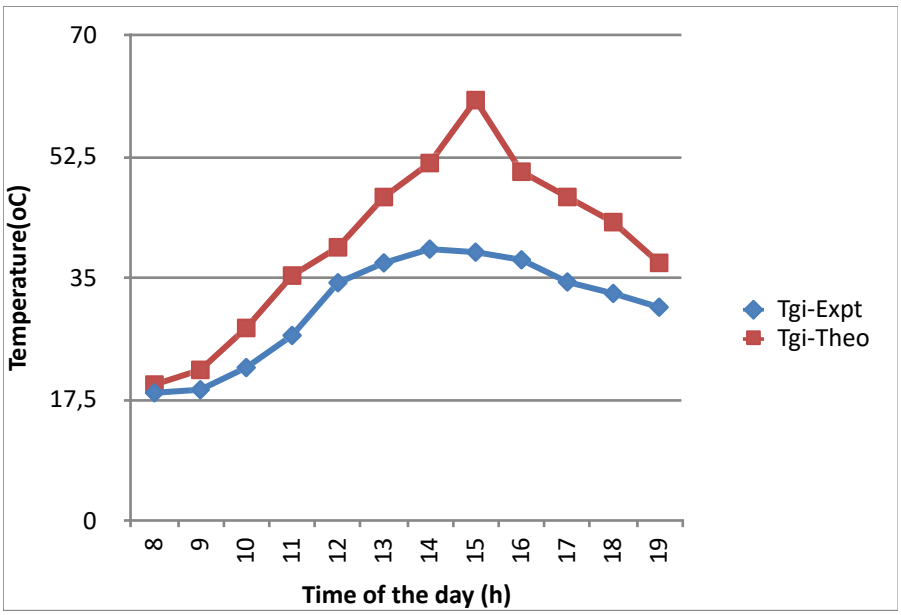

Figure 18. Experimental v/s Theoretical variation of glass inside temperatures.

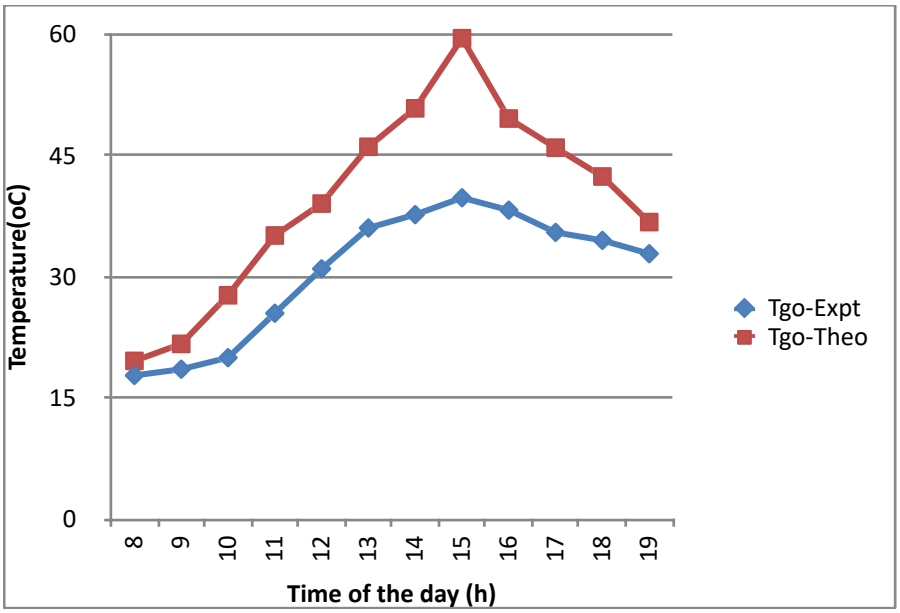

Figure 19. Experimental v/s Theoretical variation of glass outside temperatures.

https://doi.org/10.17993/3cemp.2023.120151.361-380

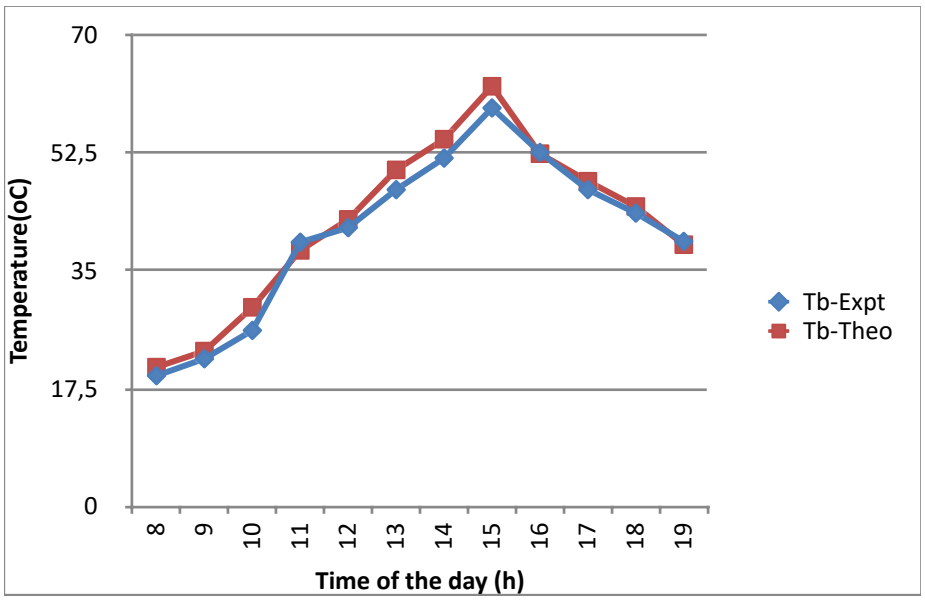

Figure 20. Experimental v/s Theoretical variation of basin temperatures.

Case 3. Experimental v/s Theoretical variation of temperatures of the elements of still. Figure 21, 22 and 23 shows the experimental and theoretical values of the temperature at inner, outer side of the glass and temperature of basin respectively for the single basin solar still coupled with parabolic collector.

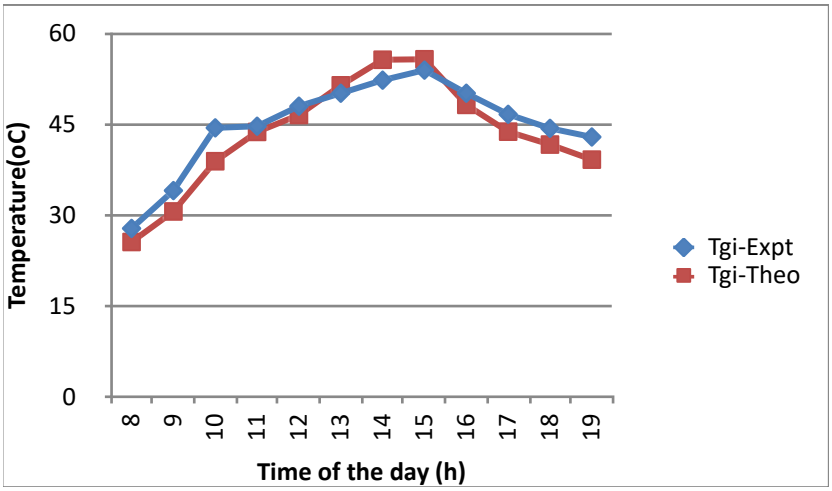

Figure 21. Experimental v/s Theoretical variation of glass inside temperatures.

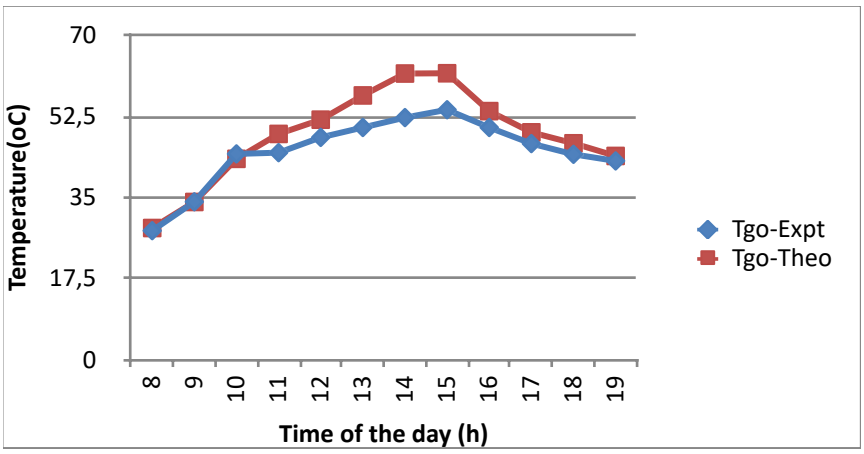

Figure 22. Experimental v/s Theoretical variation of glass outside temperatures.

https://doi.org/10.17993/3cemp.2023.120151.361-380

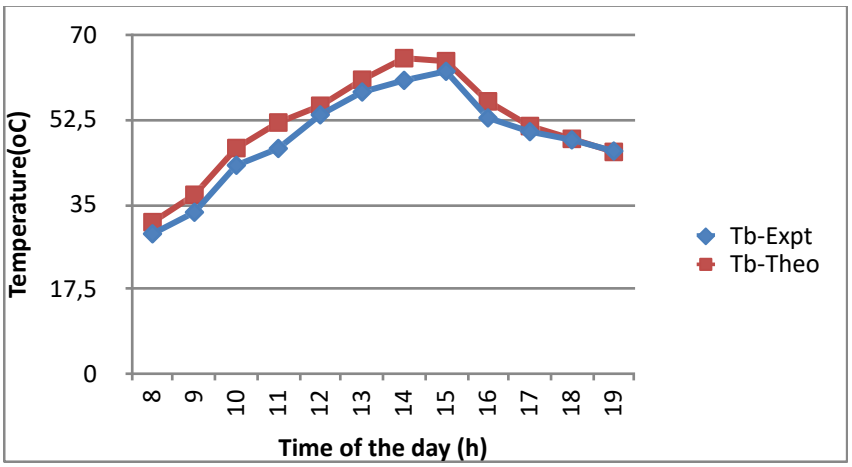

Figure 23. Experimental v/s Theoretical variation of basin temperatures.

Case 4. Experimental v/s Theoretical variation of temperatures of elements of still. Figure 24, 25 and 26 shows the experimental and theoretical values of the temperature at inner, outer side of the glass and temperature of basin respectively for the single basin solar still equipped with secondary basin and coupled with parabolic collector.

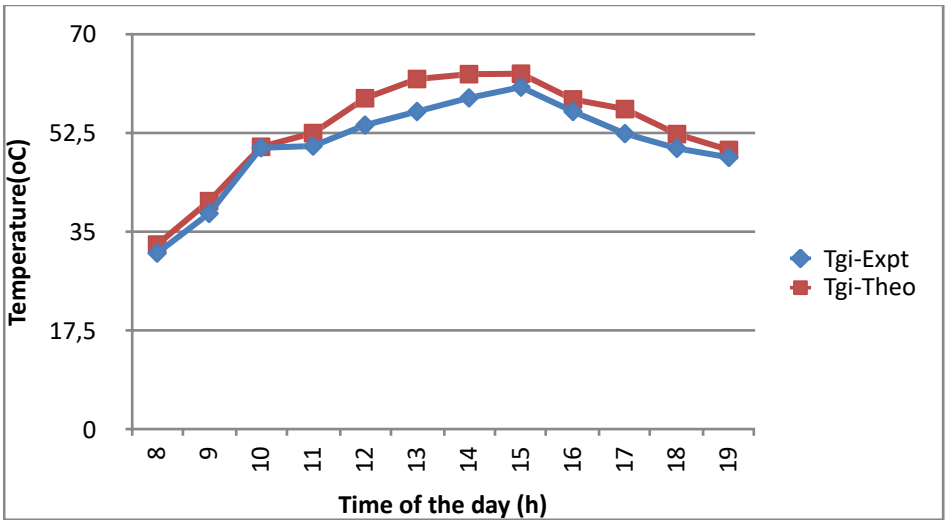

Figure 24. Experimental v/s Theoretical variation of glass inside temperatures.

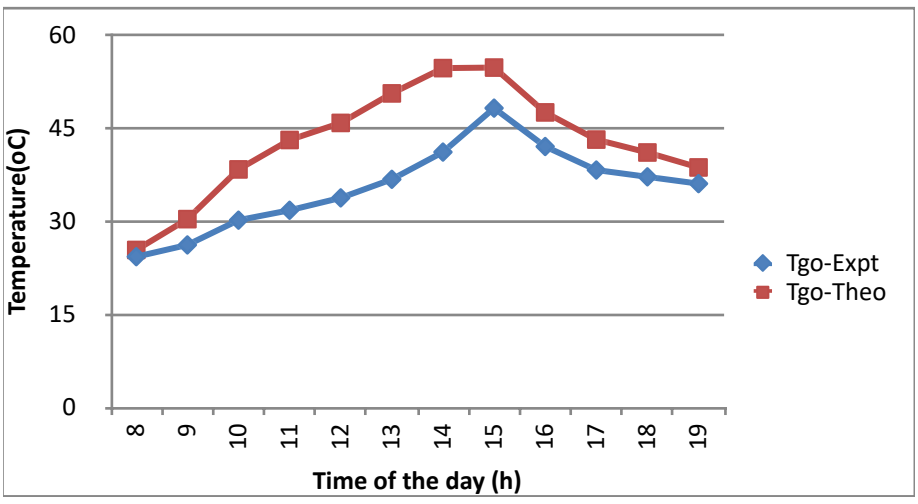

https://doi.org/10.17993/3cemp.2023.120151.361-380

Figure 25. Experimental v/s Theoretical variation of glass outside temperatures.

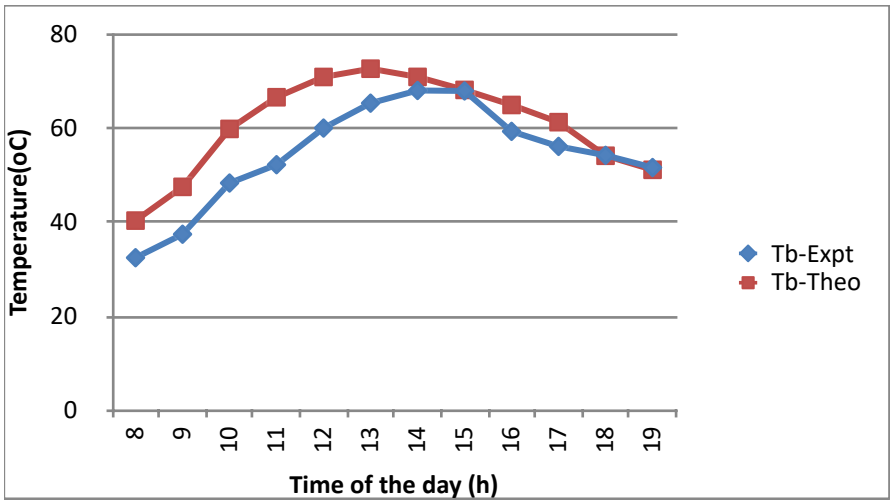

Figure 26. Experimental v/s Theoretical variation of basin temperatures.

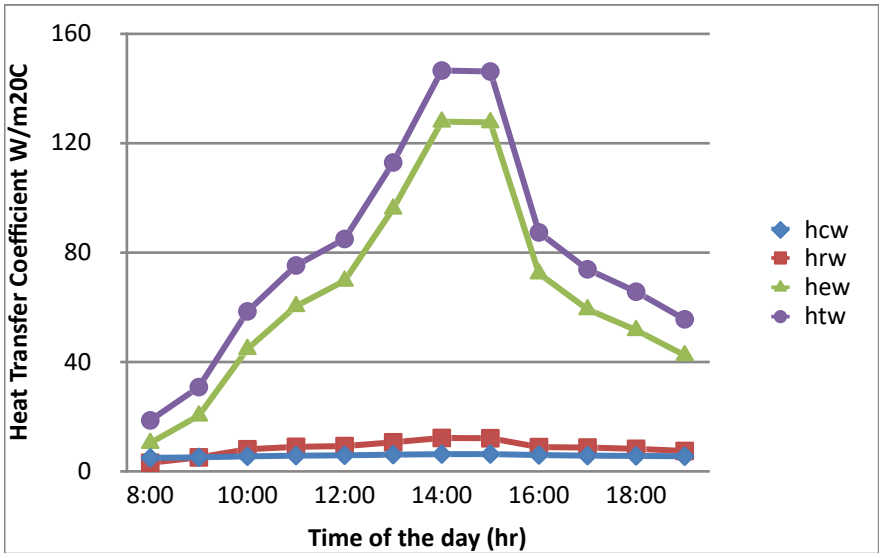

Figure 27. Heat transfer coefficient for solar still coupled with evacuated tube collector.

Figure 27 shows the variation of (h_{cw}), (h_{rw}), (h_{ew}), and (h_{tw}) heat transfer coefficient for the system when equipped with secondary stepped basin and coupled with evacuated tube collector with parabolic concentrator. The values of convective and radiative heat transfer coefficients are nearly identical. Figure 28 shows the comparison between theoretical and experimental hourly variation of yield for the integrated system when equipped with secondary stepped basin and coupled with evacuated tube collector with parabolic concentrator.

https://doi.org/10.17993/3cemp.2023.120151.361-380

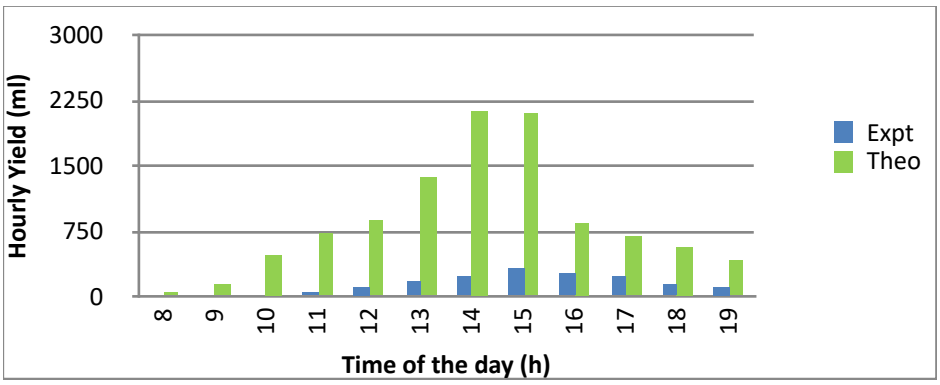

Figure 28. Hourly variation of theoretical and experimental yield for solar still coupled with evacuated tube collector.

7. CONCLUSION

The modeling of solar still with secondary basin and coupled with Tubular Parabolic concentrator using the concept of comparison of inner, outer glass temperature and temperature of basin has been validated experimentally. The experiments were carried out for four cases and found that the still coupled with parabolic concentrator and stepped basin is having maximum efficiency and productivity. Overall thermal efficiency of 16.54% is obtained for the integrated system when coupled with evacuated tube collector. The results were validated using mathematical modeling and found that the coefficient of correlation varies in between 0.9 to 0.99 and percentage RMS values lies in the range of 10% to 40%.

REFERENCES

(1) S.W. Sharshir, Nuo Yang, GuilongPeng, A.E. Kabeel. (2016). **Factors affecting solar stills productivity and improvement techniques: A detailed review.** *Appl. Therm. Eng*. 100, 267-284.

(2) A.M. Manokar, K.K. Murugavel, G. Esakkimuthu. (2014). **Different parameters affecting the rate of evaporation and condensation on passive solar still-a review.** *Renew.Sust.Energ.,* 38, 309–322.

(3) V. Dimri, B. Sarkar, U. Singh, G.N. Tiwari, (2008). **Effect of condensing cover material on yield of an active solar still: an experimental validation.** *Desalination,* 227, 178–189.

(4) K. Murugavel, K.K.S. Chockalingam, K. Srithar. (2008). **Progresses in improving the effectiveness of the single basin passive solar still**, *Desalination,* 220, 677–686.

(5) A.J.N. Khalifa. (2011). **On the effect of cover tilt angle of the simple solar still on its productivity in different seasons and latitudes.** *Energy Convers. Manag.,* 52, 431–436.

(6) J.A. Jones, L.W. Lackey, K.E. Lindsay. (2014). **Effects of wind and choice of cover material on the yield of a passive solar still.** *Desalin.Water Treat.,* 52, 48–56.

https://doi.org/10.17993/3cemp.2023.120151.361-380

(7) A.S. Nafey, M. Abdelkader, A. Abdelmotalip, A. Mabrouk. (2000). **Parameters affecting solar still productivity.** *Energy Convers. Manag.,* 41, 1797-1809.

(8) [A.K. Tiwari, G.N. Tiwari. (2008). **Effect of cover inclination and water depth on performance of a solar still for Indian climatic conditions.** *ASME J. Sol. Energy Eng.,* 130(2), 024502-024505.

(9) H. Taghvaei, H. Taghvaei, K. Jafarpur, M.R.K. Estahbanati, M. Feilizadeh, M. Feilizadeh, A.S. Ardekani, **A thorough investigation of the effects of water depth on the performance of active solar stills.** *Desalination,* 347, 77-85.

(10) M.I. Ahmed, M. Hrairi, A.F. Ismail. (2009). **On the characteristics of multistage evacuated solar distillation.** *Renewable Energy,* 34(6), 1471-1478.

(11) M. Feilizadeh, M.R.K. Estahbanati, A. Ahsan, K. Jafarpur, A. Mersaghian. (2016). **Effects of water and basin depths in single basin solar stills: an experimental and theoretical study.** *Energy Convers. Manag.,* 122, 174-181.

(12) B.A. Akash, M.S. Mohsen,W. Nayfeh. (2000). **Experimental study of the basin type solar still under local climate conditions.** *Energy Convers. Manag.,* 41, 883-890.

(13) M.R.K. Estahbanati, A. Ahsan, M. Feilizadeh, K. Jafarpur, S.A. Ashrafmansouri, M. Feilizadeh. (2016). **Theoretical and experimental investigation on internal reflectors in a single-slope solar still.** *Appl. Energy,* 165, 537-547.

(14) Z.M. Omara, A.E. Kabeel, M.M. Younes. (2014). **Enhancing the stepped solar still performance using internal and external reflectors.** *Energy Convers. Manag.,* 78, 876-881.

(15) G. Xie, J. Xiong, H. Liu, B. Xu, H. Zheng, Y. Yang. (2015). **Experimental and numerical investigation on a novel solar still with vertical ripple surface.** *Energy Convers. Manag.,* 98, 151-160.

(16) M.R.K. Estahbanati,M. Feilizadeh, K. Jafarpur,M. Feilizadeh, M.R. Rahimpour. (2015) **Experimental investigation of a multi-effect active solar still: the effect of the number of stages.** *Appl. Energy,* 137, 46-55.

(17) J. Xiong, G. Xie, H. Zheng. (2013). **Experimental and numerical study on a new multi-effect solar still with enhanced condensation surface**, *Energy Convers. Manag.,* 73, 176-185.

(18) R. Sathyamurthy, P.K. Nagarajan, S.A. El-Agouz, V. Jaiganesh, P.S. Khanna. (2015). **Experimental investigation on a semi-circular trough-absorber solar still with baffles for fresh water production.** *Energy Convers. Manag.,* 97, 235-242.

(19) S.A. El-Agouz. (2014). **Experimental investigation of stepped solar still with continuous water circulation.** *Energy Convers. Manag.,* 86, 186-193.

(20) H.E. Gad, Sh. Shams El-Din, A.A. Hussien, Kh. Ramzy. (2015). **Thermal analysis of a conical solar still performance: an experimental study.** *Sol. Energy,* 122, 900-909.

(21) H.K.S. Abad, M. Ghiasi, S.J. Mamouri, M.B. Shafii. (2013). **A novel integrated solar desalination system with a pulsating heat pipe**, *Desalination,* 311, 206-210.

https://doi.org/10.17993/3cemp.2023.120151.361-380

/21/

UPGRADING THE ENVIRONMENTAL PROPERTIES OF KIRKUK KEROSENE USING GLACIAL ACETIC ACID

Serwan Ibrahem Abdulkhader

Department of Chemical and Petrochemical Engineering, College of Engineering, University of Salahaddin, Erbil, Kurdistan Region, Iraq.

serwan.abdulkhader@su.edu.krd

Dr. Mohammed Jawdat Barzanjy

Department of Chemical and Petrochemical Engineering, College of Engineering, University of Salahaddin, Erbil, Kurdistan Region, Iraq.

Reception: 03/12/2022 **Acceptance**: 18/01/2023 **Publication**: 17/02/2023

Suggested citation:

I. A., Serwan and J. B., Mohammed. (2023). **Upgrading The Environmental Properties Of Kirkuk Kerosene Using Glacial Acetic Acid**. *3C Empresa. Investigación y pensamiento crítico, 12(1)*, 382-390. https://doi.org/10.17993/3cemp.2023.120151.382-390

ABSTRACT

Glacial acetic acid was used to improve Kirkuk kerosene samples and decrease their aromatics contents. Two sets of experimental processes were performed: the first set included more process steps (mixing by orbital shaker, heating, centrifugation, and stabilization over many days). This set of experiments showed its maximum improvement when 1 mL of glacial acetic acid was added to 10 mL of Kirkuk kerosene sample to get a 42% improvement in the aniline point and a 12.5% improvement in the smoke point. The smoke point test values gave confusing results when the stabilization was increased to 4 days; the reason may be the chemical cracking of single-ring aromatic components into polyromantic components like naphthalene, which reduced the quality of the kerosene samples. The second set of experiments included only mixing and leaving the processed kerosene sample with 2 mL mixtures of glacial acetic acid and distilled water to set for 5 minutes. The greatest improvement was obtained when 1.8 mL of water containing 0.2 mL of glacial acetic acid was mixed with 10 mL of kerosene samples, resulting in a 19% improvement in aniline point and a 45% improvement in smoke point. The total sulfur percent and flashpoint tests revealed that the second set also had an acceptable chemical effect on kerosene samples by reducing 4.8% for the total sulfur test and increasing 11.7% for the flashpoint test. As a number, the first set of experiments showed better improvements in comparison with the second set, but to scale up these experiments and apply them industrially will be very difficult and expensive, and some steps are difficult to apply like centrifugation because of its high cost and because the stabilization step consumes a lot of time. Therefore, the second set of results will be more acceptable from an engineering point of view.

KEYWORDS

Kirkuk kerosene, Aniline point, Smoke point, Aromatics content, and Glacial acetic acid.

PAPER INDEX

https://doi.org/10.17993/3cemp.2023.120151.382-390

1. INTRODUCTION

Kerosene, also known as kerosine, paraffin, or paraffin oil, varies in color depending on its quality. It is a light yellow or colorless oily flammable liquid. It has an odor and volatile in the range of gasoline and gasoline/diesel oil and distills between 125°C and 260°C (Speight, 2019). When burnt in a wide lamp, kerosene's flash point of around 25°C makes it acceptable for use as an illuminant. The heat of combustion of gasoline ranges between 11,000 and 11,500 calories per gram, whereas that of kerosene (and diesel fuel) is between 10,500 and 11,200 calories per gram. Finally, the heat of combustion for fuel oil ranges between 9500 and 11,200 calories per gram (El-Gendy and Speight, 2015).

Kerosene is primarily utilized as a fuel for residential water heaters and air conditioning systems equipped with kerosene engine heat pumps (KHPs), as well as it used as a heating oil (Fuse et al., 2004).

On the other hand, domestic combustion is a significant cause of indoor air pollution in poor nations, and has been highlighted as a significant health concern influencing hundreds of millions of people, particularly women, children, and the elderly. The smoke produced by household combustion instruments or devices has been linked to respiratory disorders such as chronic bronchitis, emphysema, expectorative coughing, and dyspnea. Exposure to unvented indoor cooking smoke may result in the development of cancer, most notably lung cancer (Kim Oanh et al., 2002).

To produce kerosene that burns cleanly, the aromatic content must be kept low. This quality is defined by the smoke point standard. The flash point is used to provide the front end of the distillation specification, whereas the freeze point is used to specify the back end (Holbrook, 1996).

In the petroleum industry and petroleum products, polycyclic aromatic hydrocarbons (PAHs) such as fluorene, anthracene, and fluoranthene are recognized to be harmful by-products of combustion that are hazardous to human health. PAHs are classified as persistent organic pollutants, which means they are able to stay in the environment for an extended period of time (POPs). These are organic pollutants that are resistant to degradation and can therefore persist in the environment for extended periods of time if not properly managed (Wild and Jones, 1995, Sankoda et al., 2013). Scientists have rarely questioned the concept that polycyclic aromatic hydrocarbons (PAHs) are inert substances even at high temperatures (Necula and Scott, 2000). PAHs are known to damage air, soil, and water resources at even low concentrations, and they have a high thermal stability and persistence in soil and groundwater, making them a significant threat to human health (Nelkenbaum et al., 2007).

For further information, particulate matter (PM), carbon monoxide (CO), and organic compounds are the primary contaminants in smoke from residential combustion instruments or devices. The latter is composed of a diverse array of components. Among the organic chemicals released, polycyclic organic matter (POM) and formaldehyde are of particular importance. POM is a chemical group composed

https://doi.org/10.17993/3cemp.2023.120151.382-390

of at least two benzene rings. The polycyclic aromatic hydrocarbons are one class of POM that have been identified as carcinogens or mutagens. The majority of PAH found in the environment are a result of incomplete combustion of organic molecules. PAH undergo changes in the environment, and the resulting derivatives are often more hazardous than the original PAH, hence increasing the potential for adverse health impacts (Kim Oanh et al., 2002).

The smoke point of aviation turbine fuels and kerosenes is a property that shows a fuel's tendency to burn with a smoky flame. Increased aromatic content in a fuel results in a smoky flame and energy loss owing to thermal radiation. The smoke point (SP) of a fuel is the highest flame height at which it can be burned without smoking in a standard wick-fed lamp. It is measured in millimeters, and a high smoke point signifies a fuel with a low tendency for smoke production(Baird, 1981). The ASTM D 1322 technique are used to determine the smoke point (Riazi, 2005, Speight, 2015).

The term "aniline point" refers to the lowest temperature at which equal amounts of aniline and oil are totally miscible. The procedure for determining the aniline point of petroleum products is detailed in ASTM D 611. The aniline point reflects the fraction's degree of aromaticity. The aniline point is inversely proportional to the aromatic concentration. As a result, the aromatic concentration of kerosene and jet fuel can be estimated using the aniline point(Jenkins and Walsh, 1968).

$$\%A = 692.4 + 12.15(SG)(AP) - 794(SG) - 10.4(AP)$$

where % A denotes the aromatic content, SG denotes the specific gravity, and AP is the aniline point in degrees Celsius (Riazi, 2005).

In general, the purpose of this research is to determine how adding GAA affects the quality of kerosene samples by lowering the aromatic content. more specific, improving the burning properties of local kerosene to meet Iraqi quality control standards for kerosene oil used for heating by improving specifications such as the smoke point and aniline point using simple processes and low-cost and safe chemicals.

2. MATERIALS AND METHODS

This study used a local kerosene sample known commercially as Kirkuk kerosene in the local market, which was of low grade and was sold as low-quality kerosene for house heating purposes in the local market. In this study, two experimental sets of processing were dependent. Four standard ASTM tests were used in both sets of experiments, including the smoke point, aniline point, total sulfur content ratio, and flash point, to compare the effects of the treatments, as explained in the following section.

The first set of experiments consisted of the following steps:

1. Heidolph® Unimax 2010 orbital shaker was used to mix a 10-mL of the kerosene sample with different milliliters of glacial acetic acid (0.5,0.75,1,2,3,4,5,and 6 mL) for 3 minutes.

https://doi.org/10.17993/3cemp.2023.120151.382-390

2. By using a mental heater, heat the mixtures for 15 minutes at 35 degrees Celsius.
3. Centrifuging the mixtures at 2000 rpm for 15 minutes
4) The mixtures were allowed to stabilize for two time durations (2 days and 4 days).

The second set of experiments consisted of the following steps:

1. 2 mL of pure water with different amounts of glacial acetic acid (5, 10, 15, and 20%) were prepared.
2. The water with GAA mixtures manually were mixed with 10 mL of the kerosene sample.
3. The final mixtures were mixed with Heidolph® Unimax 2010 orbital shakers for 20 minutes.
4. The treated kerosene samples were left for 5 minutes before analysis.

It is clear that the first set was more complicated than the second and consumed more time. The aniline point (ASTM-D611) and smoke point (ASTM-D1322) standard tests were used as main tests for both sets of experiments to compare the results of kerosene samples before and after acetic acid treatment to determine the effect of acetic acid treatment on the aromatic content of the kerosene samples. The total sulfur weight percentage (ASTM-D4294) and flash point (ASTM-D93-20) tests were used in the second set beside the main tests.

3. RESULTS AND DISCUSSION

The increasing aniline point (aniline mixing temperature in oC) and smoke point (height of smokeless fire in millimeters) directly indicate a decrease in the aromatic content of treated or processed kerosene samples. Table (1) and Figure (1) show confusing results for the first set at most points. This unstable data may be due to the existence of multiple steps as chemical influencers on the kerosene samples (high centrifugation power, long stabilization time, and heating), in addition to the existence of GAA. The maximum improvement of the first set was satisfied when 1mL added in GAA was added to the kerosene samples with (29 oC of aniline point, (42%) of improvement and in the smoke point, 5 mm (12.5%)). Adding more GAA affected the results negatively for both 2 and 4 days duration of stabilization.

https://doi.org/10.17993/3cemp.2023.120151.382-390

Table 1. First set of experiments results

Test no.	GAA mixing volume (mL)	Smoke point (mm)	Aniline point (°C)	Stand for time(days)
0	Zero	40	69	0
1	0.5	47	71	2
2	0.75	45	63	2
3	1	45	98	4
4	2	40	88	4
5	3	37	88	4
6	4	35	84	4
7	5	30	68	4
8	6	28	71	4

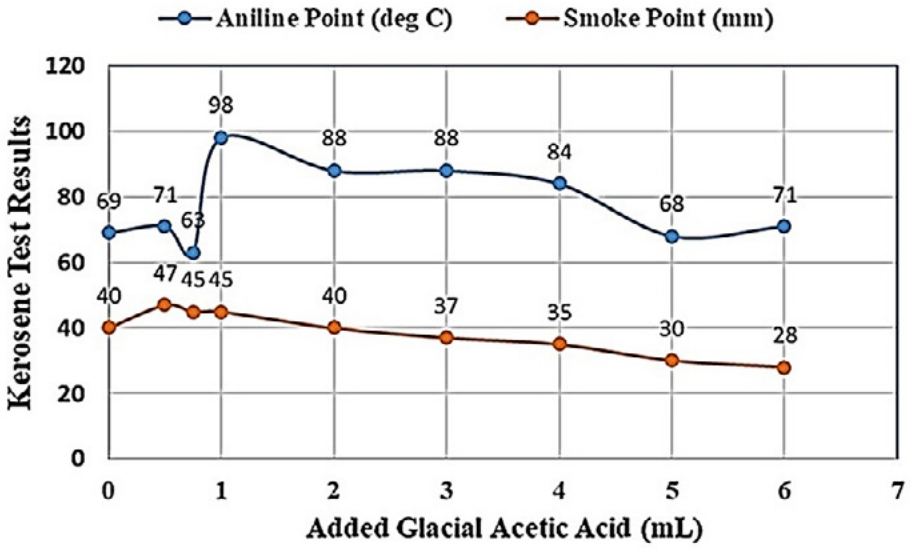

Figure 1. First set of experiments results

The results of the second set are more reasonable (Table (2) and Figure (2)). Although the heating, centrifugation, and stabilization time factors were canceled. The results of both the aniline point and the smoke point were improved in this set of experiments. These improvements will support our opinion that the long stabilization time is a reason for the confusing results of the first set of experiments. Here, the second test point (2 mL) of used water mixed with 0.2 mL of GAA increased the aniline point temperature by 13 oC (19% improvement), the smoke point by 10 mm (45% improvement), the flash point by 5 mm (11.6% improvement), and the total sulfur by 110 ppm (4.8% improvement). In addition to that, these experiments were performed at ambient conditions for temperature and pressure and mixed for only 20 minutes. It is expected that the polarity of water played an important role in these improvements, at least as an absorbing agent or washing agent for kerosene sample impurities.

https://doi.org/10.17993/3cemp.2023.120151.382-390

Table 2. Second set of experiments results

Test no.	GAA volume ratio in 2 mL of pure water (mL)	Aniline point (°C)	Smoke point (mm)	Total Sulphur ratio w/w %	Flash point (°C)
0	Original sample	68	40	0.229	43
1	5%	76	42	0.225	46
2	10%	81	58	0.218	48
3	15%	69	43	0.218	45
4	20%	71	56	0.219	46

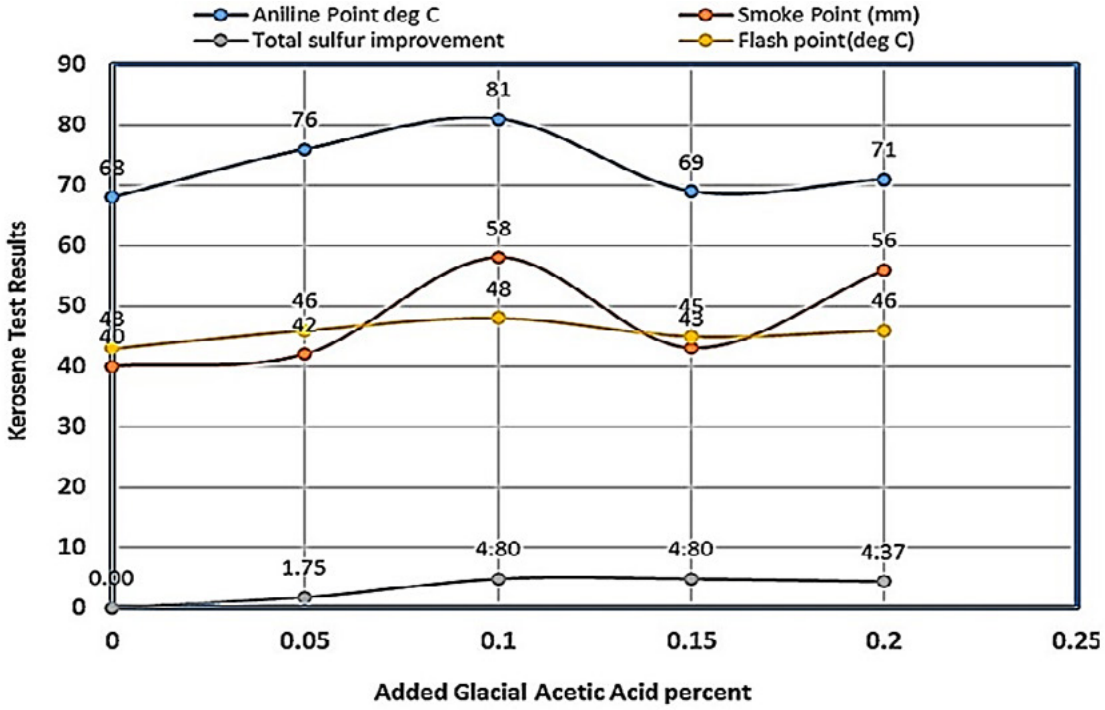

Figure 2. Second set of experiments results

The first study used a high temperature and pressure range hydrotreating lab unit (275-350 oC and 32-62 kPa), a catalyst (Ni w/-Al2O3), and a high purity hydrogen gas source (H2/HC ratios of 200-500). All of these improved the kerosene's aromatic content by only 1 to 12.8%(Hussein et al., 2018).

Another study worked on removing the aromatics components from hydrotreated kerosene from the Al-Dura refinery by using an organic solvent with a high mixing volume (solvent/fuel = 1). The solvents were methanol, glycerol, and sodium thiosulfate as surfactants. According to the study, the maximum aromatics percent satisfaction was around 47%. The problem with this study is that it is not cost-effective; they isolated 47% of aromatics from kerosene samples that contained 21% aromatics using organic solvents that are difficult to separate again to recover their value. In addition, these isolated aromatics caused a volume loss of about 10% for kerosene samples (Algawi et al., 2018).

https://doi.org/10.17993/3cemp.2023.120151.382-390

The present study used acetic acid and water at ambient operating conditions. For both sets of experiments, the maximum ratio of used GAA to kerosene was 0.1 for the first set to increase 42% of the aniline point and 0.02 for the second set with a 19% improvement in the aniline point by using the mixing for 20 minutes. Comparing the present study results and the simplicity of the experimental processing with other studies, which worked on Iraqi hydrotreated kerosene (Al-Dura refinery), demonstrates the preference for the present study and the quality of its results.

Finally, it is clear that the processing of the Kirkuk kerosene samples did not have a big impact on the sulfur and paraffinic components because of the greater stability that these components possess in comparison to the aromatic components. When taking into account the relatively low amounts of glacial acetic acid that were used, these relatively minor shifts in total sulfur weight percent and flash points are still regarded as significant improvements. Increasing the flash point can regarded as a guide that the cracked aromatics converted chemically to saturated and long straight paraffins by more specified lab analyzers.

4. CONCLUSIONS

1. Even with a low mixed volume ratio, GAA showed a good effect on aromatics content of Kirkuk kerosene samples. The water supported the chemical effect of the GAA, and it supported the process economically because it is free.
2. The positive effect of using water with GAA encouraged us to use commercial-grade glacial acetic acid instead of an analytical grade in the future, which means lowering the final cost of processing more and more.
3. Aniline point test results were more reliable than smoke point test results because the latter had manual steps that made errors more likely in comparison to the aniline point test.
4. All of the reviewed references ensured that the smoke point is generally related to the aromatics content of kerosene, but this does not prevent the fact that the high existence of PAH effects the smoke point values negatively..
5. Reducing the quantity of aromatics is not the end of the story. To get a better smokeless fire, the quality of aromatics will also be affected. Less PAH means the best quality of fire and the best smoke point value.
6. The second set of tests is easier to apply industrially and with low cost scale-up plant.
7. Other tests (total sulfur percent, flash point), even though they had a slight effect, can be used as make-up processing for kerosene samples that need a slight improvement to be salable commercially.

REFERENCES

https://doi.org/10.17993/3cemp.2023.120151.382-390

(1) ALGAWI, R., JAFFAR, S. & KHALAF, Z. (2018). **Effect of Cosolvents And Surfactant in The Extraction of Aromatics from Kerosene**. *IOP Conference Series: Materials Science and Engineering,* IOP Publishing, 012178.

(2) BAIRD, C. (1981). **Crude oil yields and product properties.** *Ch. De la Haute-Belotte*, 6.

(3) EL-GENDY, N. S. & SPEIGHT, J. G. (2015). **Handbook of refinery desulfurization**, *CRC Press*.

(4) FUSE, T., HIROTA, Y., KOBAYASHI, N., HASATANI, M. & TANAKA, Y. (2004). **Characteristics of low vapor pressure oil ignition developed with irradiation of mega hertz level ultrasonic**. *Fuel*, 83, 2205-2215.

(5) HOLBROOK, D. (1996). **Handbook of petroleum refining processes**. *RA Meyers (Edi,) McGraw Hill.*

(6) HUSSEIN, H. Q., ALI, S. M., ALTABBAKH, B. A. A., HUSSEIN, S. J., ALI, Y. M. & KARIM IBRAHIM, S. (2018). **Hydrodesulfurization and Hydrodearomatization of Kerosene over high metal loading Ni w/γ-Al2O3 Catalyst**. *Journal of Petroleum Research and Studies*, 8, 28-46.

(7) JENKINS, G. & WALSH, R. (1968). **Quick measure of jet fuel properties**. *Hydrocarbon Processing*, 47, 161.

(8) KIM OANH, N. T., NGHIEM, L. H. & PHYU, Y. L. (2002). **Emission of polycyclic aromatic hydrocarbons, toxicity, and mutagenicity from domestic cooking using sawdust briquettes, wood, and kerosene**. *Environmental science & technology*, 36, 833-839.

(9) NECULA, A. & SCOTT, L. T. (2000). **High temperature behavior of alternant and nonalternant polycyclic aromatic hydrocarbons**. *Journal of Analytical and Applied Pyrolysis*, 54, 65-87.

(10) NELKENBAUM, E., DROR, I. & BERKOWITZ, B. (2007). **Reductive hydrogenation of polycyclic aromatic hydrocarbons catalyzed by metalloporphyrins**. *Chemosphere*, 68, 210-217.

(11) RIAZI, M. (2005). **Characterization and properties of petroleum fractions**, *ASTM international.*

(12) SANKODA, K., NOMIYAMA, K., KURIBAYASHI, T. & SHINOHARA, R. (2013). **Halogenation of polycyclic aromatic hydrocarbons by photochemical reaction under simulated tidal flat conditions**. *Polycyclic Aromatic Compounds*, 33, 236-253.

(13) SPEIGHT, J. G. (2015). **Handbook of petroleum product analysis.** J*ohn Wiley & Sons.*

(14) SPEIGHT, J. G. (2019). **Handbook of industrial hydrocarbon processes.** *Gulf Professional Publishing.*

(15) WILD, S. R. & JONES, K. C. (1995). **Polynuclear aromatic hydrocarbons in the United Kingdom environment: a preliminary source inventory and budget**. *Environmental pollution*, 88, 91-108.

(16) DHIRAJ S. PATIL, DATTATRAY A. CHOPADE, MANOJ A. KUMBHALKAR. (2018). **Experimental investigation of effect of cerium oxide nanoparticles as a fuel additive in cottonseed biodiesel blends.** *MAYFEB Journal of Mechanical Engineering*, 1, 1-12.

https://doi.org/10.17993/3cemp.2023.120151.382-390

/22/

METAL OXIDE COATING ON BIODEGRADABLE MAGNESIUM ALLOYS

Pralhad Pesode

School of Mechanical Engineering, Dr. Vishwanath Karad MIT-World Peace University, Pune-411038, Maharashtra, India

pralhadapesode@gmail.com - https://orcid.org/0000-0001-5604-5740

Shivprakash Barve

School of Mechanical Engineering, Dr. Vishwanath Karad MIT-World Peace University, Pune-411038, Maharashtra, India

shivprakash.barve@mitwpu.edu.in - https://orcid.org/0000-0002-5372-6310

Sagar V. Wankhede

School of Mechatronics Engineering, Symbiosis Skills and Professional University Kiwle, Pune-412101, MS, India

svw8890@gmail.com - https://orcid.org/0000-0002-2341-3110

Amar Chipade

Dr. D. Y. Patil Institute of Technology, Pimpri Pune-411018, Maharashtra, India.

amar.chipade@dypvp.edu.in - https://orcid.org/0000-0002-2200-0752

Reception: 22/11/2022 **Acceptance**: 19/01/2023 **Publication**: 18/02/2023

Suggested citation:

P., Pralhad, B., Shivprakash, V. W., Sagar and C., Amar (2023). **Metal Oxide Coating On Biodegradable Magnesium Alloys**. *3C Empresa. Investigación y pensamiento crítico, 12(1)*, 392-421. https://doi.org/10.17993/3cemp.2023.120151.392-421

ABSTRACT

Magnesium is a biodegradable metal that has potential in orthopaedics. It has several advantages over other metallic materials because it is biocompatible and degradable now being used for biomedical applications, including elimination of stress shielding effects, enhancing degradation properties and enhancing biocompatibility concern in vivo, eliminating the second surgery for implant removal. Bioabsorbable magnesium (Mg) and related alloys have been limited in their usage because of its lower corrosion resistance. Surface alteration and functionality, in addition to basic alloying, is an important technique to deal with Mg and its alloys' reduced corrosion resistance. Magnesium's rapid depreciation however is a double-edged sword because it's critical to match bone renewal to material corrosion. As a result, calcium phosphate coatings have been proposed as a way to slow down corrosion. There are various possible calcium phosphate phases and their coating methods and can give a few distinct properties to various applications. Despite magnesium's lower melting point and greater reactivity, calcium phosphate coatings require precise settings to be effective. Because of their toxicity, non-biodegradability, and much higher cost, the recently used inorganic conversion coatings are less appealing and their application is limited. Conversion coatings are a viable alternative technology that is based on a cost-effective, environmentally friendly, and biodegradable organic component. Surface chelating functional groups in these compounds allow them to link with the magnesium/surface hydroxide layer while also providing anchoring groups for the polymer topcoat. Nanoreservoirs with multilayer inhibitors for active self-healing corrosion resistance thrive in this environment. This study examines the organic conversion coatings for Mg and its alloys in depth.

KEYWORDS

Magnesium, Calcium phosphate coating, Conversion coating, Biodegradable, Biocompatible.

https://doi.org/10.17993/3cemp.2023.120151.392-421

PAPER INDEX

https://doi.org/10.17993/3cemp.2023.120151.392-421

1. INTRODUCTION

To replace and repair damaged body tissue implants are broadly utilized in biomedical field [1,4]. Depending on type of material use, implants can be differentiated into three classes [5,6]: (i) ceramic, (ii) metal, and (iii) polymer. Metallic implants have excellent mechanical properties and good biocompatibility, due to which they are broadly utilized in dental, cardiovascular and orthopaedics applications [1]. Conventional metallic implant materials incorporate Ti alloy, Co-Cr alloy and SS [7, 131]. However, there is a stress shielding issue because of the substantial difference in modulus of elasticity of metallic implants and human bone, as indicated in table 1, which leads to osteoporosis and bone fusion [1]. Also, metallic implant generates metallic irons due to corrosion or erosion near to implant if these implants have been there for longer period of time, this might prompt issues, like inflammation of tissue [8]. At last, additional medical surgery may require to eliminate implants [6]. Availability of biodegradable materials have prompted new improvements in implant innovation.

Table 1. Cortical bone mechanical properties as well as implant materials [1].

Materials	Young's Modulus (GPa)	UTS (MPa)	Yield strength (MPa)	% Elongation
Cortical bone	5-23	35-283	--	1.07-2.10
Stainless steel	193-200	480-620	190	40
Titanium alloys	100-125	550-985	420-780	12-16
Pure iron	195-230	200	150	40
Co-Cr alloys	210	450-960	310-440	10.7-18.5
Pure Mg (As-cast)	41-45	90-190	20.9	7
DL-PLA	70-120	40-200	--	3.10

The primary purpose of biodegradable implants is to encourage tissue development, cure specific injuries, and then vanish in vivo by a breakdown process with little tissue damage [1]. Among orthopaedic application, bone screw and metallic bone plates are ordinarily used to fix crack sites before new bone development [5]. During rehabilitation, it has been discovered that the implant's strength gradually diminishes as the strength of the new bone grows [1,132]. Magnesium-based alloys are currently getting a lot of consideration and are being explored as more recent types of biodegradable material [8,9]. This is due to a number of factors. For starters, magnesium-based alloys have superior mechanical qualities for load-bearing applications than polymers, including high strength and malleability, in addition, they are biodegradable in vivo [9, 10]. Second, magnesium-based alloys have modulus of elasticity that are near to natural bone as compared to ordinary metallic implants, eliminating the stress shielding effect [11]. Magnesium-based alloys offer excellent in-vivo degradability; hence, using magnesium alloy to remove a temporary implant can avoid the need for additional medical operations, so significantly reducing a patient's suffering [7]. Magnesium-based alloys also exhibit good biocompatibility, osteogenesis induction, anti-inflammatory characteristics, and other bio functional qualities [12,13].

https://doi.org/10.17993/3cemp.2023.120151.392-421

Furthermore, it containing specific elements, for example Cu, Ag, Ga, and Sn may likewise have good antibacterial characteristics [14,15]. It indicates that magnesium-based alloys have extraordinary development potential as biodegradable materials.

Researchers and industry interest in magnesium- based alloy as biodegradable materials emphatically grown in the course of the last many years. Magnesium based alloys possess very good biocompatibility, excellent corrosion behaviour, and excellent mechanical properties when proper process parameters and right alloying elements are utilized. Likely uses of magnesium-based alloys are temporary cardiovascular devices and structural alloys for orthopaedic applications. Once these implants have served their limited purpose, the body consumes them, such as scaffolding, mechanical support and attaching to living tissue. Researchers and industry are exceptionally talking about the connection between magnesium-based alloys in-vitro and in-vivo characteristics, that could assist in reducing animal testing and backing simulations to choose alloys. Mechanical characteristics are typically portrayed by hardness test and tensile test. Additionally, information on stress corrosion and fatigue is anticipated to give a complete idea of stability over the course of degradation. Alloys made with magnesium are prone to pitting corrosion. A consistent corrosion morphology needs to be given special consideration since corrosion pits increase the intensity of stress during mechanical strain and contribute to the premature failure of implants [2, 132]. First and primarily, the mechanical and physical characteristics of magnesium-alloys do not yet match that of implant materials, and their rapid disintegration can cause mechanical instabilities before the bone healing process is completed [9,16]. Second, the rate of breakdown of magnesium-based alloys is very quick, particularly in a chloride medium like a human physiological fluid. The degradation product of Mg alloys is probably going to create some issues, for example, tissue inflammation [17]. Finally, corrosion of magnesium-based alloys is not uniform, which could lead to premature implant failure [18]. Various tests have been carried out to date with the goal of breaking through these barriers. Regardless of this advantageous property, magnesium alloys used in biomedical applications must be carefully monitored for their ability to corrode when in contact with ECF containing Cl iron. Due to low electronegativity of magnesium alloy, their corrosion rate is high in in-vivo. From one viewpoint, this implies that according to a thermodynamic perspective, a biomedical implant developed from magnesium alloy probably won't be viewed as a reasonable alternative in the exceptionally corrosive body fluid.

In general, three methods can be used to protect biomedical magnesium against in vivo corrosion: (i) adding defensive coatings to isolate body fluid and implant. (ii) alloying with biocompatible elements to protect surface from corrosion (iii) microstructural surface alteration. During initial phase of implantation, high corrosion resistance, and even the establishment of a homogeneous, controlled, and anticipated corrosion rate, are critical. Surface modifications of magnesium alloy for corrosion control includes micro arc oxidation (MAO), hydrothermal treatments, anodization, electrophoretic deposition (EPD), physical vapor deposition (PVD), electrochemical deposition (ECD), sol-gel deposition, magnetron sputtering, and a few other, less

https://doi.org/10.17993/3cemp.2023.120151.392-421

known process for example, electrospinning, cold gas dynamic showering (CGDS), phosphatization, laser cladding [3,19,20]. However, regardless of numerous multi-pronged methodologies towards improvements of magnesium alloy for biomedical applications, significantly more exploration is needed to overcome their insufficiencies in demanding biomedical field. This argument is supported by the astounding amount of effort, resources, funds, and research capacity put into adapting a chemical like magnesium, which is fundamentally inappropriate for use in medicinal applications. At the end, simply by applying protective coatings along with suitable alloying elements, it became conceivable to use Mg alloy in biomedical applications because of its promising mechanical and natural properties as a cutting-edge biomaterial. Currently, much research and development is focused on the development of magnesium alloy for cutting-edge biomaterials, To address the stress shielding effect, future isoelastic arthroplastic implants could be employed [3, 21–25] if they have lower young's modulus and are acceptable with the nearby cortical bone. Paper is focusing on metal oxide coating on magnesium alloy to improve its performance in biomedical applications.

2. CONVERSION COATINGS ON MAGNESIUM AND ITS ALLOYS

Surface coating is formed by electrochemical or chemical treatment in the conversion coating process. Coating transforms a metal's or alloy's surface layer into a thin coating of metallic oxide or any other chemically related substances. The coating creates a corrosion-resistant surface that better adheres to the topcoat. A successful conversion coating should be (i) inert/insoluble (ii) self-healing (iii) resistant to mechanical damages, (iv) impermeable to liquids/gas (v) eco-friendly (vi) cost effective. Chemical conversion coatings are manufactured via non-electrolytic chemical reactions without the use of electricity, whereas electrochemical conversion coatings use an electrolyte and electricity [26]. The primary benefits of chemical conversion coatings are process speed, simplicity, low capital and working expenses, lower energy utilization, low-temperature process, high efficiency and less treatment time [26,27]. It was found that corrosion fatigue properties were improved by conversion coating [28]. A conversion coating, in general, functions by driving interfacial reactions and resultant coating/precipitation formation. A reduction in pH and a rise in Mg2+ concentration at the solution/metal contact initiate the interaction. The chemical has a minor dissolving effect on the hydroxide/oxide layer, which will aid further solution penetration into the layer. Many variables have impacts on the quality of conversion coating, for example, phase or compound structure, types of pre-treatment processes, concentration and composition of bath solution, pH of bath, temperature of bath, time of immersion, degree of stirring, and condition of post treatment [29]. By and large, different functional additives are used to accelerate coating formation and to control bath pH value. By changing experimental condition, thickness of coating can be varied from several hundred nano meter to a micro meter. The thickness of the coating might range from a few hundred nanometers to a few micrometres, depending on the trial circumstances used. It was observed that

https://doi.org/10.17993/3cemp.2023.120151.392-421

thickness of coating can be varied by addition of nanoparticles to the conversion solutions.

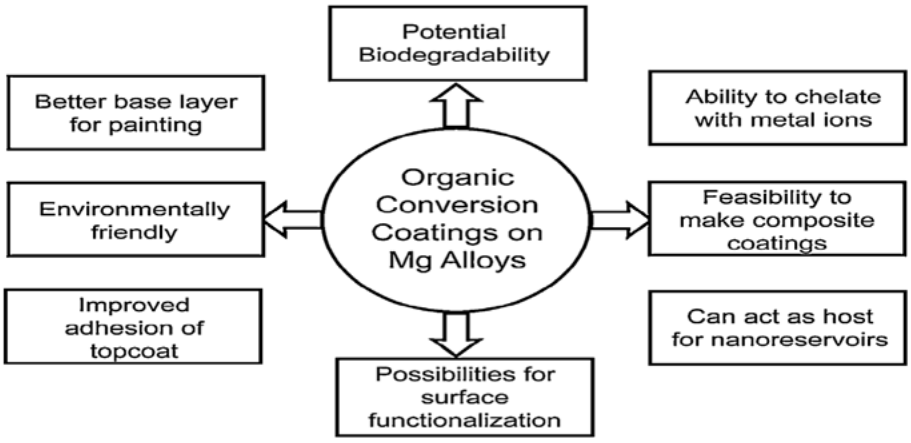

Figure 1. Potential advantages of organic conversion coatings [26]

Inorganic coatings, in which the chemical reacting with the surface of metal to generate highly adhesive coatings and corrosion resistance coatings, are among the various chemical conversion coatings explored and used in practise. Figure 1 depicts the most widely used inorganic conversion coatings on magnesium alloy. Chrome manganese, phosphate treatments, chrome-pickle, dichromate and ferric nitride pickle are most normal industrial conversion coatings. For biomedical applications fluoride and calcium phosphate containing conversion coatings are significant [27]. Chemical breakdown of rare earth and phosphate-based conversion coatings occurs at acidic and alkaline pH levels, respectively [30]. Phosphates in water may also promote nutritional replenishment. Molybdate conversion coatings decreased oxidising capacity isn't up to par. Heavy metal contamination is the main source of worry. When reactive magnesium comes into contact with certain inorganic materials, it can become anodic. As a result, research into non-toxic and environmentally acceptable conversion coatings for magnesium and related alloys is crucial. In this case, organic conversion coatings (OCCs) are crucial. Precipitation and chemical dissolution interact to form chemical conversion coatings. Chemical conversion coating generally carried out in bath of phosphate, fluoride, chromate and carbonate [32]. Because of its low cost and convenience of application, conversion coating can be employed in a various biomedical field. Regardless of the fact that chromate-based coatings offer outstanding corrosion resistance to Mg alloys, they have been outlawed because of concerns about the human health and environment. As a result, biomedical applications of phosphate conversion coatings [33, 34], fluoride [35], and MAO coating have gotten a lot of interest. Figure 2 depicts a few phosphate-based conversion coatings, which are typically Zn, Mg, Mn, Ce, Sr, and Ca phosphates. Ce, Sr, K, F, and Ca doped phosphates are rare. Regrettably, several conversion coatings have riverbed-like topologies on surfaces, limiting their robustness. In this case, it's also necessary to change the coating. Due to high biocompatibility, high temperature resistance, insoluble in water and chemical stability of calcium phosphate and zinc phosphate, they have been accounted as a possible option in contrast to chromate coating for biomedical applications [36]. The morphology and structure of those layers

https://doi.org/10.17993/3cemp.2023.120151.392-421

exceptionally relies upon the temperature of process, composition of conversion bath and pH value [37].

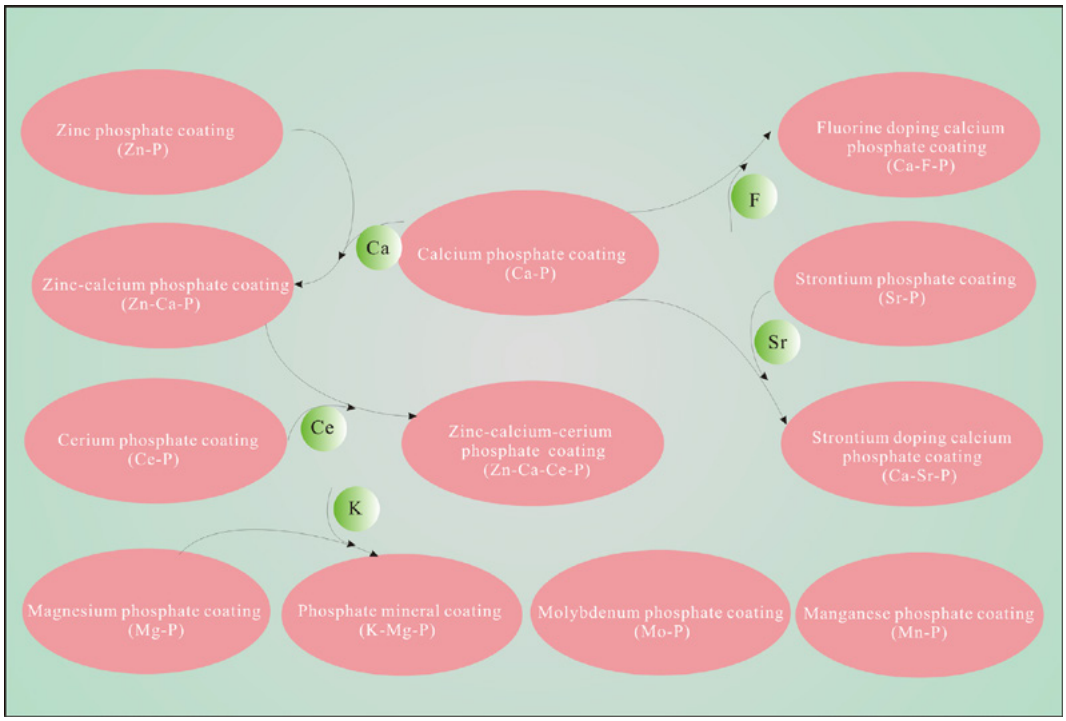

Figure 2. Mg alloys with phosphate-based conversion coatings [31]

A lot of strategies have been utilized for improving Mg-based biomedical implants and devices. Calcium phosphate (Ca-P) coatings are non-toxic and have excellent osteoconductivity. As a result, numerous researchers are concentrating their efforts on Ca-P coatings in bone replacement, orthopaedics, and other fields. The elements P and Ca combine to develop a HA layer and is the primary component of natural bone. The critical aspect is changing the phase and increasing the concentration of HA in Ca-P coatings, which are fundamentally non-crystalline and contain relatively lesser amount of HA. HA can develop across specified range of Ca/P proportions under sub-alkaline and neutral circumstances, as per calculation of the thermodynamic chemical reaction [34], HA is exclusively produced in a narrow range of Ca/P proportions in sub-alkaline and neutral circumstances.

One of the researchers [38] established a Ca-P coating on magnesium consisting of Mg (H2 PO4)2, Ca3(PO4)2, Ca (H2 PO4)2, and Mg 3 (H2 PO4)2 to reduce corrosion of AZ31B in SBF. The morphology of the surface, EDS finding, and cross-sectional area of the Ca-P coating on a surface with a thickness of roughly 20 m reveal a regular petal-like crystal made up of small long blocks. In comparison to its substrate, the Ca-P coating has a corrosion current density that is two times lower. As the immersion period in SBF grows, the hemolytic rate of AZ31B increases without and with coating at first, then reduces to a safe level. The load bearing capacity of the Ca-P coating for AZ31B decreases noticeably while submerged in SBF, and after 120 days of submersion, the loading capacity was reduced to 85%. Even yet, it's impossible to say which elements are significant in the progression of corrosion resistance.

https://doi.org/10.17993/3cemp.2023.120151.392-421

To seal the structural design, one of the researchers [39] applied a Ca-P coating to MAO oxidised Mg by immersing it in a Ca-P bath. The upper layer is made up of dicalcium phosphate dihydrate (DCPD) and HA, according to the findings. At various temperatures, flake-like and round-shaped morphologies appeared on the surface of the substrate, demonstrating that temperature has an impact on coating structure. The volume of hydrogen produced in MAO and soaked MAO after 300 hours of immersion in SBF was around 17.75 and 1.11 mL/cm2, respectively. After submerging the coated specimen in SBF, bone-like apatite formed. The thickness was about 42 m after 4 weeks of soaking in SBF Ca-P coatings. It has been observed that corrosion performance of coating enhanced. Instead of the Zn-P coating's dry-riverbed-like structure, one of the researchers [36] coated Mg alloy AZ31 with a Ca-doped zinc phosphate (Zn-Ca-P) coating that had a flower-like structure. The structure of Zn-Ca-P coatings were found to be tightly connected to the microstructure, including particle size and secondary phases, as well as the chemical composition of the substrate [40]. Form, orientation, and size of AlMn particles were discovered to take a significant effect on Zn-Ca-P coatings characteristics. Corrosion of the -Mg network near an upright AlMnSi particle almost likely results in an obstructed and deeper hole. Horizontal particles, on the other hand, may form a flat, open, and shallow trench. Because of this, small pits rather than deeper holes are where phosphate nuclei can easily accumulate. The outer layer of AM30 therefore develops a coarse grain coating. Under magnetic field, one of the researchers [41] developed Mn-P conversion coating on AZ91D Mg alloy. The findings demonstrated that, during the production of the phosphate conversion layer, superpositioning magnetic fields might speed up the synthesis of minute hydrogen gas bubbles as well as their speedy desorption from the surface. Following that, it was discovered that Mg2+ cations are evenly distributed throughout the alloy, regardless of its microstructure. Immersion in a solution treatment bath can provide a smooth and homogeneous phosphate conversion coating when the magnetic field is delivered perpendicular to the substrate rather than parallel to the substrate. It's worth mentioning that Ce-P, Zn-Ca-Ce-P, and Mn-P coatings have yet to be shown biocompatible. The biocompatibility of Sr-p ZnCaP and CaP coatings, on the other hand, is excellent [33,42].

2.1. FLUORIDE CONVERSION COATING

The use of fluoride conversion coatings as biomaterials appears to be a viable option [43, 44]. Fluoride conversion coating is created by a chemical reaction with Mg alloys in a hydrofluoric acid (HF) solution bath. Fluorine in bones can help with calcium and phosphorus digestion and improve bone strength. The major component of fluoride conversion coatings, magnesium fluoride (MgF2), is water insoluble and binds to the Mi-alloys surface satisfactorily. Because of their great biocompatibility, outstanding corrosion resistance, and cell responsiveness, magnesium alloys with MgF2 coatings have been explore in the biomedical appplications [45]. It has been observed that HF concentration has great impact on protective efficiency and performance of coating. One of the studies [46] suggested that a MgF2 coating on the LAE442 alloy could decrease the corrosion rate in-vivo. Despite the fact that the

https://doi.org/10.17993/3cemp.2023.120151.392-421

substrate was slightly protected, the MgF2 layer deteriorated completely after a month of implantation. Despite this, fluoride levels in the adjacent bone did not rise over the first six weeks after implantation. In MgF2 coated Mg implants, there was restricted pitting erosion but no subcutaneous gas pits. Regardless of the fact that fluoride conversion coating could offer safety during the initial phases of implantation, due to the relatively thin coating, in terms of prolonged use, it must be very effective. The detrimental effects of high fluoride on bone are also present at the same time, fluoride release during Mg implants breakdown and its harmfulness for implanted tissue has been unclear yet. One of the researchers [47] used a novel method to make fluoride conversion coatings by immersing an AZ61 sample in Na [BF4] liquid salt for varied durations of time at 430°C and 450°C, then heating the sample to eliminate any remaining salts and external layer. The two-layer structure of the 2-μm coating made of a larger interior MgF2 layer and a minor exterior NaMgF3 layer [47]. As the treatment period increases from 2 h at 450 °C, the corrosion current density, i corr, of the coatings decreases, implying higher corrosion resistance in SBF. The untreated substrate had an i corr that was around four times lower than the material that had been treated for 12 hours at 450°C. Even though a few deformities are seen on the surface of coating, these imperfections don't arrive at the substrate. The coatings are a superior alternative for fluoride treatments of magnesium alloys because they are finer than standard conversion coatings. The biocompatibility of the coating still has to be established. To increase the corrosion resistance of the conversion coating, researchers [45] employed a two-step immersion approach to develop a uniform and thinner MgF 2/polydopamine (PDA) coating on Mg-Zn-Y-Nd alloy. Dopamine and tris-hydrochloric acid (tris-HCl) bath treatments followed by Mg alloy immersion in HF bath. The coating is made up of two layers, each of which is roughly 100 nm thick: a PDA outside layer and a MgF2 inner layer.

2.2. IONIC CONVERSION COATING

Ionic fluids (ILs) are molten organic salts formed entirely of ions at normal temperature [48]. Because of the combination of a charge delocalized anion and a big cation, the salts are defined by weak interaction. ILs have been classified as ecologically friendly or biocompatible compounds in the past. Mg alloys can stay stable over longer periods time without corroding due to the absence of free H+ or even other metal cations in ILs, providing ideal environment for active metal film development control [49]. One of the research groups created an IL film on the basis of interaction of ILs with highly pure Mg [50], which led to the use of ILs in the creation of Mg alloy composite films. Various ILs conversion coatings have been proposed in the past [51-54]. Because of their biocompatibility, phosphonate derivative-containing coatings have been investigated as a new chemical for Mg alloy corrosion protection. To decrease deterioration in the human body, it been recommended that the AZ31 Mg alloy be surface treated in compatible phosphate-based ionic fluids [55]. IL coating's corrosion resistance and cytotoxicity were investigated, and it was observed that treatment times have a considerable impact on corrosion resistance. A more homogenous IL film was generated when the ZE41 Mg alloy was exposed to the IL of

https://doi.org/10.17993/3cemp.2023.120151.392-421

trihexyl phosphonium diphenyl phosphate at a potential of 200 mV [52]. Because of the protic ammonium-phosphate and trihexyl tetradecyl phosphonium cation mixed with organophosphate, it was suggested that ILs, or (CF3SO2)2N- anions, might reacting with Mg alloy surface to develop an excellent corrosion protection coating [50,56,57]. The metal phosphates, metal oxides, and carbonaceous compounds in the IL 300°C conversion coating have a double layer structure having 70-80 nm thickness and outstanding passivation performance in a 1 wt. percent NaCl. Deep eutectic solvents (DESs), are another type of ecologically friendly IL [58]. Because they are non-reactive with water, DESs are easier to synthesise in a pure condition than conventional ILs. Most of them seem to be biodegradable, and the component's toxicological qualities are well known [58]. One of the research groups [59] focused on the creation of DES-based Mg alloy conversion coatings. At 160 degrees Celsius, the interaction of a ChCl-urea mixture-based DES with the AZ31B Mg alloy was proposed as a new ionothermal method for generating a corrosion resistant layer. Mg alloy and DES reacted to produce a MgH2 and MgCO3 conversion coating that replaced a dangerous process. The conversion coating was also found to be superhydrophobic after additional reaction with stearic acid. According to electrochemical polarisation experiments [59], the Mg alloy's corrosion resistance could be increased by the DESs conversion coating. An electric field was also used by the same research group to induce the disintegration of DES, which aided the reactivity of the DES/Mg alloy interface [49]. Surprisingly, the proposed anodic treatment in DESs produced conversion films on Mg alloy substrates with different nanostructures. It was discovered that a more corrosion-resistant conversion coating can be created by increasing anodic current density. On the resulting conversion layer, superhydrophobic and sliding surfaces can be made to even further improve corrosion resistance [49]. Excellent conversion coatings with double capacity of super-hydrophobicity and self-healing may also be produced on the AZ31B Mg alloy in DES-based media [60]. Using varied external fields at the IL/substrate contact to build more effective coatings on Mg alloy could be promising.

2.3. BIOMIMETIC COATINGS

Phases of CaP are precipitated out of solution and developed on the necessary sample in simulated bodily fluids (SBF) under close physiological conditions in biomimetic techniques for CaP coating deposition [62,63]. CaP coatings made with this approach can be seen in SEM images of a biomimetically synthesised hydroxyapatite coating on a Mg-alloys at higher and lower magnification. The technique offers an affordable option to coat a large number of specimens at once with a uniform coating and is easy to set up and operate. When compared to CaP coatings made using non-physiological pH, composition, and temperature, coatings created in physiological circumstances are expected to produce CaP crystalline structures that are more similar to bone minerals [64]. According to ongoing research [65], altering the coating solution's pH and temperature can help some CaP phases form more quickly than others. Furthermore, it was discovered that the geometry of the specimen to be coated has an impact on the CaP phases that form on sample

https://doi.org/10.17993/3cemp.2023.120151.392-421

surface [66]. Although the concentration of the SBF used in the publications is typically concentrated, it can range from 1 to 10 SBF [63,67-69]. Additionally, immersion times fluctuate significantly between established protocols, and can be somewhere around 2 h to 20 days [68,70-73]. While using a biomimetic technique, pH and temperature appear to have been explored consistently, staying within physiological range, to be specific at 37 °C and 7.4, respectively. Pre-treatment is typically necessary in this process to affect the coating properties, the Mg reactivity, and the coated specimen's surface reactivity. To achieve this, most studies utilise an alkaline solution, such as NaOH, at various concentrations [74,75], or an acidic solution, such as HCl [77] or HF [76], at various concentrations. In biomimetic norms, however, many investigations have focused on temperature pre-medicines [76,78], or acidic or soluble post-medicines [79]. Covering magnesium and similar alloys using biomimetic technologies has shown to be a successful solution. Some researchers have raised concerns about biomimetic coatings on non-biodegradable substrates like titanium, however they haven't considered the influence of the SBF immersion period on substrate degradation. Previous research has demonstrated that very lengthy immersion in SBF can result in thick coating development if phosphate and calcium ions are abundant [73]. Researchers discovered that a second immersion in a new SBF solution is effective in these circumstances [73]. Numerous researchers have found that it is beneficial to modify the biomimetic convention for biodegradable specimens like Mg and its alloys, by shortening the period spent incubating in SBF, hence minimising the possibility of coating disintegration [80]. Furthermore, as indicated by horizontal CaP crystal binding across the coating, biomimetic CaP coatings on Ti have been labelled as thick, comprehensive, homogenous, and non-porous [81]. According to one of the studies [82], coating formation took place around hydrogen bubbles that were developed on magnesium surface while submerge, resulting in irregular and porous CaP coatings on Mg samples. The non-uniform and porous CaP coating on Mg alloy, according to several studies, is caused by the specimen's non-uniform shape [77] and the presence of Mg^{2+} ions, which prevent crystal formation [83]. Porosity production on degradable metals like Mg is another key disadvantage of a biomimetic coating method. Until now, no modification or variation of this procedure has been successful in achieving strong cohesiveness between the specimen and the CaP coating. For biomedical applications, such as orthopaedic applications, it is critical to develop an extremely strong adhesive covering with a long-life span and the ability to endure surgeries.

Biomimetically developed apatite coating on a pure Mg specimen to improve corrosion protection were explored by one researcher [73]. In SBF, they used either single-coated or double-coated substrates, with pure Mg as a control. Other investigations found that coating Mg alloys AZ91D and AZ31 with this method before doing in vitro immersion testing, electrochemical [84] and SBF solution [85] provided similar corrosion resistance. Recent investigations on biomimetic CaP-coated pure Mg, on the other hand, have shown corrosion protection and enhanced cell adhesion [75,79]. The biomimetic method has most likely been studied as a viable strategy for employing CaP on Mg specimens, as previously indicated. Given this, and as reported

https://doi.org/10.17993/3cemp.2023.120151.392-421

in the literature, further refinement of these methods is required if they are to be used as a viable CaP coating approach on magnesium and its alloys.

2.4. HYDROTHERMAL COATING

The uncoated Mg alloy's outer layer lacks adsorption sites associated with Ca-P crystal formation. In the absence of a chelating specialist in hydrothermal coatings method, high-temperature corrosion would produce a significant number of Mg2+ ions, leading to the creation of Mg(OH)2 and aggressive absorption of a Ca2+ ions. Similarly, coating a Mg alloy with a very pure Ca-P coating is difficult, because the binding strength between the specimen and the coating is poor, reducing the implant's mechanical stability in the body. Several conjugates, polymers, and chemicals are utilised as precursors or inducers to ramp up the formation of calcium phosphate in attempt to optimise phase purity, bonding strength, and density of Ca-P coatings [86-88]. EDTA is an organic compound that promotes HA nanocrystal nucleation and growth by binding to divalent metallic cation and reacting with calcium ion. On the other hand, MEA is an aminol that speeds up the synthesis of hydroxyapatite crystal and increases the solvency of reactants in hydrothermal reactions [89,90]. Because it contains -NH2, -COOH, and -SH, L-cysteine was discovered to get a decent capacity to suppress metallic corrosion. Using a hydrothermal technique, one of the researchers [91] created an L-cysteine CaP coatings on AZ31 which is bioinspired. Addition of L-cysteine increased corrosion resistance, illustrated in Fig.3, which depicts the Ca-PL-Cys-coating development mechanism. A hydrothermal technique was used to coat the exterior layer of Mg alloy with HA, with in the centre, PDA acts as a glue. PDA's catechol functional group is very sensitive to metal iron absorption, which helps generate the HA coating by binding Ca2+ ions and subsequently drawing PO43- to develop hydroxyapatite nuclei, allowing for cross-connection with hydroxyapatite. The interactions of the polyhydroxyl unit of glucose with Ca2+ ions in fluid solution may enable the formation of Ca-P crystals on the pure magnesium surface [92].

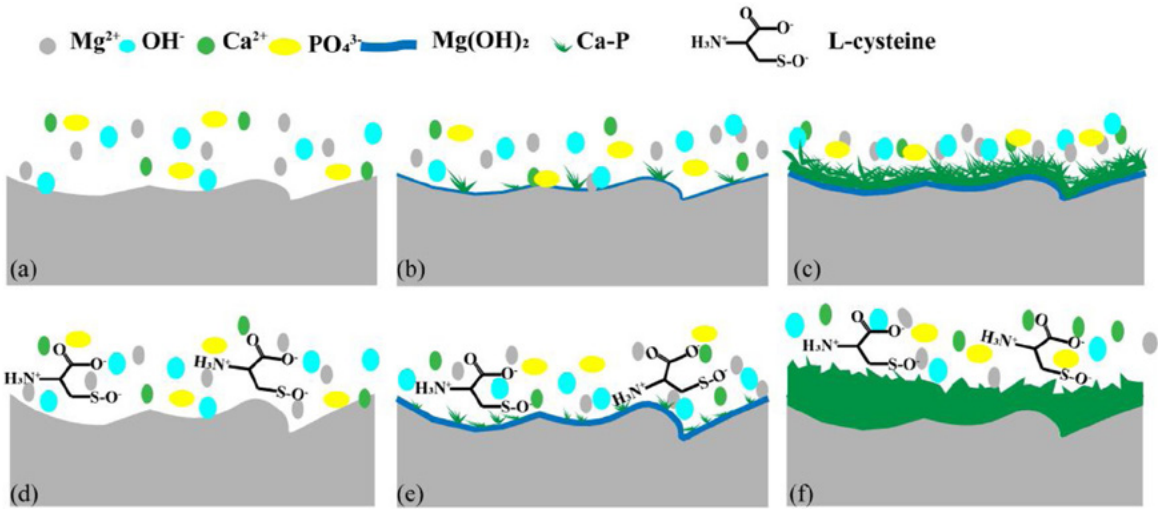

Figure 3. Ca-P coating formation mechanism (a-c) and Ca-PL-Cys coating creation technique (d-f) [92]

https://doi.org/10.17993/3cemp.2023.120151.392-421

According to one of the researchers [93], glucose can be used as a catalyst to convert gluconic acid into a carboxyl group under hydrothermal treatment, creating a negative charged magnesium surface that draws in Ca2+ ions and advancing the creation of a corrosion protective Ca-P coatings while also significantly reducing the Mg substrate's anodic dynamics in Hank's solution. The glucose-initiated compound coating of Mg (OH)2 and Ca-P provoked by hydrothermal treatment of pure Mg is depicted schematically in Fig. 3. Table 2 lists the characteristics, structure, and composition of chelating agents utilised in the recent creation of Ca-P coatings on Mg alloy surfaces using the hydrothermal process.

Table 2. Recent investigations on chelating compounds, related active groups, and coating characteristics.

Chelating agent	Specimen	Conditions of hydrothermal reaction	Coordination ion	Active group	Coating composition	Properties of coating	Ref
Glucose	pure Mg	500 mM glucose, 250 mM Ca(NO3)2 • 4H2O 250 mM KH2PO4 120 ◦C, 24 h, pH = 10	Ca2+ ion	Carboxyl group transformed from aldehyde group	Mg(OH)2 DCPA HA CDPA	Corrosion protection is enhanced by a denser coating morphology that uses several large single particles as its building blocks.	93
L-cysteine	Mg alloy AZ31	0.15 g/L L-cysteine, 0.25 M of CaCl2 and KH2PO4, 60◦C, 30min	Ca2+ ion	sulfenyl)-SH(amino)-NH2 (carboxyl)- COOH	Ca(10-x) (HPO4)x (PO 4)(6-x) (OH)2-x MgHPO4 • 3H2O, Ca10 (PO4)6(OH)2	The morphology of the coating has been greatly enhanced in terms of uniformity and integrity. Coating thickness twice that of the control group; enhanced corrosion resistance.	92

https://doi.org/10.17993/3cemp.2023.120151.392-421

Polydopamine (PDA)	Mg alloy AZ31	5 M NaOH 60 ◦C 3 h 2 mg/ mL dopamin e hydrochl oride14 mM Ca(NO3) 2 8.4mM NaH2PO 4 4mM NaHCO 3,393K 4 h	Ca 2+ ion	Catechol	PDA/HAp	Increased adhesion, proliferation , and dispersion of osteoblasts; Denser coating structure; Lower corrosion rate	126
Deoxyribonuclei c acid (DNA)	Mg alloy AZ31	1g/L DNA, 14 mM Ca(NO3) 2 8.4mM NaH2PO 4 4mM, NaHCO 3 150 ◦C,4h	Ca 2+ ion	Base pair and deoxyribo se double helix	tricalcium phosphate (TCP), dicalcium phosphate anhydrous (DCPA) and calcium-deficient hydroxyapa tite (CDHA)	By fine-tuning the coating grain, researchers can increase bonding with sample. Improve the resistance to corrosion	127
Polyacrylic acid (PAA)	Mg alloy AZ31	1 M NaOH 60 °C for 1h, ,14 mM Ca(NO3) 2 8.4mM NaH2PO 4 4mM NaHCO 3 ,90 ◦C,4 h	Ca 2+ ion	COO-	Mg(H2PO4)2; (Ca, Mg)3 (PO4)2; and HA	Good corrosion resistance; denser stereoscopic blade structure; 10.69 N adhesive force	128

https://doi.org/10.17993/3cemp.2023.120151.392-421

Phytic acid (PA)	Mg alloy AZ31	0.70 wt. % phytic acid ,4.90 wt. % Ca(NO3) 2 •4H2O and 0.89 wt.% P2O5 at 40 C for 40 min, pH = 4.5	Ca 2+ ion	COO-	Phytic acid/ HA	24.3 ± 1.7 MPa bonding strength; good corrosion resistance	129
Ciprofloxacin hydrochloride (CIP)/ Polyacrylamide hydrochloride (PAH)	Mg alloy AZ31	5 M NaOH 30 min 14 mM Ca(NO3) 2 , 8.4 mM NaH2PO 4 , 4 mM NaHCO 3 , 150 ◦C, 240 min	Ca 2+ ion	COO-	CIP/PAH/ HA; composite coating	Excellent corrosion protections; CIP discharge that may be controlled; Antibacteria l activity is excellent, and cytocompati bility is adequate.	130

2.5. ALKALI-HEAT TREATED CONVERSION COATING

To remove oil and other impurities from Mg and Mg alloy alkali heat treatment is an important step. Coatings are typically used as a pre-treatment to improve corrosion resistance of adjacent layer to strengthen the bond between outer layer and the sample. The sample was submerged in an extremely saturated solution of NaHCO3 - MgCO3 having a pH of 9.3 for 24 hours before being heated at 500 °C for 10 hours for alkali-heat treatments [94]. The coating in SBF has a high level of corrosion resistance. Simultaneously, in an early cytotoxicity investigation, it shows no cytotoxicity by cell development, with no morphological changes on cells or inhibitory effect. One of the researchers [95] used alkali heat pre-treatment to create LbL assembled coatings, which boosted the binding force between the sample and LbL layer and improved corrosion protection. The benefits of alkali heat treatment coating are its good biocompatibility and excellent corrosion resistance. In any event, the coatings are exceedingly thiner and therefore could not be utilised as a topcoat, or even as a primer.

3. MAO COATING

Plasma Electrolytic Oxidation is another name for micro arc oxidation (MAO) (PEO), is a greener alternative to anodization [96,97]. MAO has lately been popular

https://doi.org/10.17993/3cemp.2023.120151.392-421

for covering magnesium alloys with oxide-ceramic coatings [98]. In the PEO technique, the cathode is a cylindrical SS container, and the anode is a Mg alloy. Due to the higher temperature induced by the high voltage, an oxide coating developed on the outer layer of the Mg alloy at first, and vigorous gas development could be seen. The voltage then continues to rise, although at a slower rate, and the oxide film is broken at the weaker portion, with the thickness of the coating gradually increasing. Due to exceptionally powerful discharges on the surface of the specimen [99], discharge channels emerged, and the electrolyte fused into these channels. A combination of high voltage and high temperature in the discharge channel converts a few of the Mg on the specimen external layer and an electrolyte within channels to plasma, which is subsequently transformed to plasma through a plasma chemical process. Metallic ions generated by the magnesium alloy are expelled and moved away from it, whereas oxygen ion moved in reverse direction. The oxide is subsequently deposited on the outer layer [100] as a result of an interaction between magnesium metallic ions and oxygen ions. The applied electric field pushes anions from the MAO electrolyte, such as SiO32- or PO43-, toward the anode, where they reacting with Mg2+ions from the discharge channels of Mg specimen [101]. A ceramics-like covering with better corrosion resistance, bonding strength and wear resistance is formed by MAO process. Fig. 4 depicts the MAO coatings on Mg alloy production procedure and structure. At the start of the MAO process, a dense and thin coating is applied to magnesium alloy. Because of this, the MAO coatings have a two-layered microstructure with a thick inside layer and a porous outside layer [102].

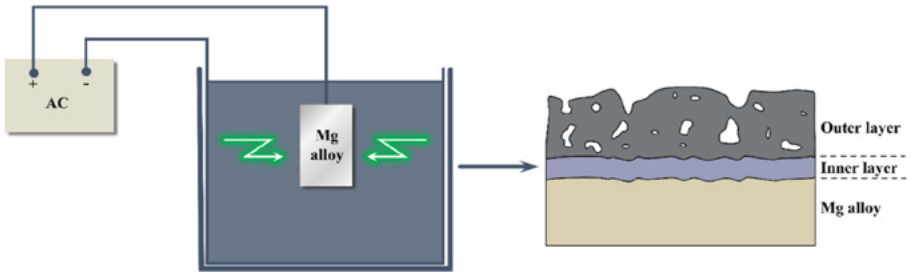

Figure 4. Schematic example of MAO coating preparation and structure on Mg alloy [96].

The two-layered structure of MAO coatings can be seen using scanning electron microscopy (SEM). Thermal strains induced by quick solidification of molten oxide in a gradually cooling electrolyte form small pores, whereas miniature fractures are formed by thermal stresses caused by quick solidification of molten oxide in a gradually cooled electrolyte [103]. MAO coating act as physical barriers, successfully isolating the Mg sample from hostile environments and lowering its corrosion resistance [104]. The corrosive Cl- iron penetrates the exterior layer through micropores during the initial phase of submersion in physiological environment. Simultaneously, the coating's main ingredient (MgO) reacts with H2O to form Mg (OH)2 as per Eq. (1) [105]. The hydrated substance partly fills the pores in the coating, whereas the rest settles on the outer layer [106]. Notwithstanding its volatile chemical characteristics, Mg (OH)2 could be converted to dissolvable MgCl2 through Cl-as per Eq. (2), releasing hydroxyl ions [107]. After then, as per Eq. (3) [105], a Ca-P layer structure arises as the OH- interacts with various chemicals and ions. During this period, the MAO coating's breakdown is slowed by the outside porous layer. The corrosion zone expands as the

https://doi.org/10.17993/3cemp.2023.120151.392-421

submersion duration rises, and the pores get deeper and larger, facilitating electrolyte infusion into the inward dense layer [108]. The innermost thick layer is useful in stopping aggressive medium from reaching and touching magnesium substrate, and if this layer is removed, corrosive medium would penetrate and touch the magnesium substrate. Because of its high inherent corrosion characteristics in aqueous solution, Mg corrosion occurs quickly when the electrolyte meets the substrate [109]. During this time, the MAO coatings' corrosion resistance is primarily dependent on the interior dense layer. The MAO coating's two-layered structure, as illustrated above, can greatly increase the corrosion protection of Mg alloys. Figure 3 depicts the biodegradation process of the MAO coating on Mg alloy.

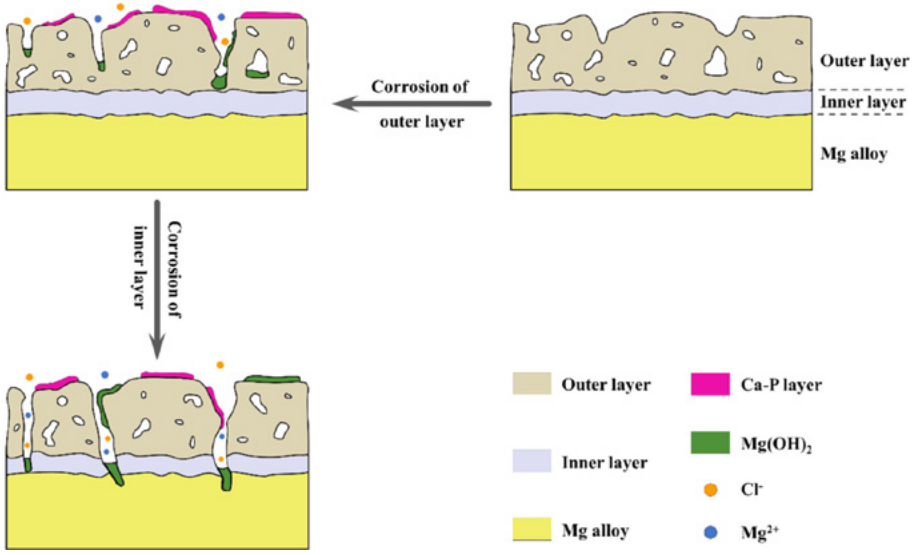

Figure 5. MAO coating on Mg alloy biodegradation process [96]

$$MgO + H_2OMg\,(OH)_2 \quad (1)$$

$$Mg\,(OH)_2 + 2Cl^- = MgCl_2 + 2OH \quad (2)$$

$$Ca^{2+} + HPO^{2-}{}_4 + OH^- = Ca - Player + H_2O \quad (3)$$

3.1. ANTIBACTERIAL MAO COATINGS ON MG ALLOYS

Mg's antibacterial capabilities have been revealed in a number of previous studies [110,110]. The results demonstrated that Mg was effective towards methicillin-resistant Staphylococcus aureus when it was injected into rats with implant-related infection (MRSA). One of the researchers used pure Mg, glass slides, and polyurethane stents to grow Escherichia coli (E. coli). After 16 hours of coculturing with pure Mg, the bacterial cell density was at its lowest, indicating that Mg has a very powerful antibacterial impact. Mg has also been shown to have outstanding antibacterial properties in the past [112]. The alkaline rise caused by Mg's breakdown in solution is responsible for its antibacterial effect [113]. It was observed that AZ31 and pure Mg along with silicon and fluorine coatings created by chemical conversion technique lost their antibacterial activities because of its dense coating on the surface [114]. Coating Mg alloy with antibacterial coatings, in this way, could be a potential methodology for increasing antibacterial effects and corrosion resistance of the magnesium alloy

https://doi.org/10.17993/3cemp.2023.120151.392-421

concurrently. For development of antibacterial coating on the metal surface MAO technique is effective, economical and extensively used method [115].

The MAO approach produces coatings that are largely made up of substrate oxides, but they also contain electrolyte components [116]. As a result, altering the electrolyte composition can efficiently vary the composition of the MAO coating [117]. Furthermore, significant antimicrobial activity is known for Zn, Cu, and Ag, and these antibacterial metallic components kill bacteria by denatureing proteins, damaging membranes, and generating oxidative stress [118-121]. Antibacterial coatings can be made using this metal complex or by merely putting micro/nanoparticles of these metals to MAO electrolyte [122].

4. BIOCOMPATIBILITY OF CONVERSION COATINGS

CaP type coatings have good biocompatibility, according to the cell survival test findings shown in Fig. 6, which can be attributed to their DCPD content.

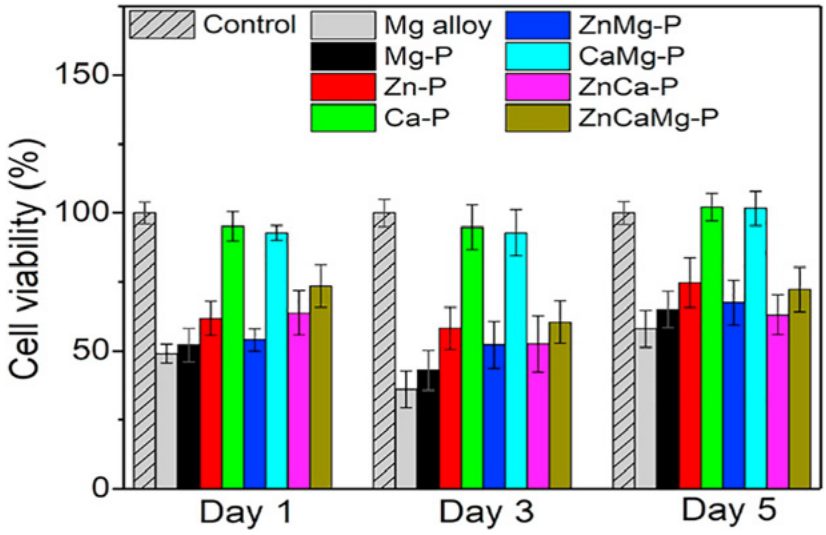

Figure 6. After 1, 3, and 5 days of incubation, cell feasibility of all treated specimen and bare AZ31 [123].

Because of its outstanding biocompatibility and biodegradability [125], DCPD is an essential biomaterial in the field of bone cement [123,124], and its degradation products can supply vital calcium and phosphorus supplies for bone tissue regeneration. The effects of CaP, ZnP, and MgP coating types on the precipitation of Ca3(PO4)2 and Mg3(PO4)2 have not been thoroughly investigated.

According to the different morphologies of all conversion coating after a 15-day soaking, there are more precipitations on CaP and MgP type conversion coatings than on ZnP type conversion coatings. The divergence of phosphates, magnesium, and calcium precipitation on diverse types of coatings can be explained by two factors:

1. CaP type and MgP type coatings have a higher solubility than ZnP type coatings. As a result, the alkalization of the Hanks' solution near the magnesium complex sample and the precipitation of phosphates magnesium and calcium is accelerated by the breakdown of conversion coatings.

https://doi.org/10.17993/3cemp.2023.120151.392-421

2. The CaP and MgP coatings have the same composition as the phosphate precipitation from Hanks' solution, that minimises the principal factor driving precipitation nucleation and development and, as a result, speeds up precipitation during the immersion test [123].

5. CONCLUSION

In vivo corrosion of biomedical magnesium can be controlled by alloying magnesium with by alloying it with biocompatible elements, by changing surface microstructure and applying protective coating to isolate implant and body fluid.

Because of the lower cost and easiness in operation conversion coating can be generally utilized in biomedical fields. Chemical conversion coatings are created by interaction of precipitation and chemical dissolution. Fluoride conversion coating can give safety during the initial phases of implantation due to its thin coating, however it must be employed for long-term applications. Fluoride leak during Mg implants corrosion and its cytotoxicity for tissue are unknown, and it would have a negative impact on bone, necessitating additional investigation. Alkali heat treatment coating has good biocompatibility and excellent corrosion resistance; however, coatings are extremely thin and cannot be used as topcoat.

It was observed that Zn, Cu and Ag have excellent antimicrobial capacity, and these antibacterial metallic components kill microorganisms through protein denature, membrane destroy and oxidative stress. MAO is another technique used for bioactive and antibacterial coating on magnesium and its alloys. Antibacterial coatings can be made by mixing micro/nanoparticles of these metals with MAO electrolyte.

ACKNOWLEDGEMENTS

For the research, authoring, and/or publication of this article, the author(s) received no financial funding.

REFERENCES

(1) Li, H., Wen, J., Liu, Y., He, J., Shi, H., & Tian, P. (2020). **Progress in research on biodegradable magnesium alloys: a review**. *Advanced Engineering Materials*, 22(7), 2000213.

(2) Maier, P., & Hort, N. (2020). **Magnesium alloys for biomedical applications**. *Metals*, 10(10), 1328.

(3) Heimann, R. B. (2021). **Magnesium alloys for biomedical application: Advanced corrosion control through surface coating**. *Surface and Coatings Technology*, 405, 126521.

(4) Chakraborty Banerjee, P., Al-Saadi, S., Choudhary, L., Harandi, S. E., & Singh, R. (2019). **Magnesium implants: prospects and challenges**. *Materials*, 12(1), 136.

https://doi.org/10.17993/3cemp.2023.120151.392-421

(5) Touri, M., Kabirian, F., Saadati, M., Ramakrishna, S., & Mozafari, M. (2019). **Additive manufacturing of biomaterials− the evolution of rapid prototyping**. *Advanced Engineering Materials*, 21(2), 1800511.

(6) Bordbar-Khiabani, A., Yarmand, B., & Mozafari, M. (2019). **Emerging magnesium-based biomaterials for orthopedic implantation.**

(7) Li, J., Qin, L., Yang, K., Ma, Z., Wang, Y., Cheng, L., & Zhao, D. (2020). **Materials evolution of bone plates for internal fixation of bone fractures: A review.** *Journal of Materials Science & Technology*, 36, 190-208.

(8) Sun, Y., Wu, H., Wang, W., Zan, R., Peng, H., Zhang, S., & Zhang, X. (2019). **Translational status of biomedical Mg devices in China**. *Bioactive materials*, 4, 358-365.

(9) Riaz, U., Shabib, I., & Haider, W. (2019). T**he current trends of Mg alloys in biomedical applications—A review**. *Journal of Biomedical Materials Research Part B: Applied Biomaterials*, 107(6), 1970-1996.

(10) Pesode, P., & Barve, S. (2022). **Additive manufacturing of metallic biomaterials and its biocompatibility**. *Materials Today: Proceedings.*

(11) Nayak, S., Bhushan, B., Jayaganthan, R., Gopinath, P., Agarwal, R. D., & Lahiri, D. (2016). **Strengthening of Mg based alloy through grain refinement for orthopaedic application.** *Journal of the mechanical behavior of biomedical materials*, 59, 57-70.

(12) Costantino, M. D., Schuster, A., Helmholz, H., Meyer-Rachner, A., Willumeit-Römer, R., & Luthringer-Feyerabend, B. J. C. (2020). **Inflammatory response to magnesium-based biodegradable implant materials**. *Acta Biomaterialia*, 101, 598-608.

(13) Henderson, S. E., Verdelis, K., Maiti, S., Pal, S., Chung, W. L., Chou, D. T., . & Almarza, A. J. (2014). **Magnesium alloys as a biomaterial for degradable craniofacial screws**. *Acta biomaterialia*, 10(5), 2323-2332.

(14) Gao, Z., Song, M., Liu, R. L., Shen, Y., Ward, L., Cole, I., ... & Liu, X. (2019). **Improving in vitro and in vivo antibacterial functionality of Mg alloys through micro-alloying with Sr and Ga**. *Materials Science and Engineering: C*, 104, 109926.

(15) Jiang, W., Wang, J., Liu, Q., Zhao, W., Jiang, D., & Guo, S. (2019). **Low hydrogen release behavior and antibacterial property of Mg-4Zn-xSn alloys**. *Materials Letters*, 241, 88-91.

(16) Munir, K., Lin, J., Wen, C., Wright, P. F., & Li, Y. (2020). **Mechanical, corrosion, and biocompatibility properties of Mg-Zr-Sr-Sc alloys for biodegradable implant applications.** *Acta biomaterialia*, 102, 493-507.

(17) Noviana, D., Paramitha, D., Ulum, M. F., & Hermawan, H. (2016). **The effect of hydrogen gas evolution of magnesium implant on the postimplantation mortality of rats.** *Journal of Orthopaedic Translation*, 5, 9-15.

(18) Bommala, V. K., Krishna, M. G., & Rao, C. T. (2019). **Magnesium matrix composites for biomedical applications: A review**. *Journal of Magnesium and Alloys*, 7(1), 72-79.

(19) Heimann, R. B., & Lehmann, H. D. (2017). **Recent research and patents on controlling corrosion of bioresorbable Mg alloy implants: Towards next generation biomaterials**. *Recent Patents on Materials Science*, 10(1), 2-19.

https://doi.org/10.17993/3cemp.2023.120151.392-421

(20) Pesode, P., Barve, S., Wankhede, S. V., Jadhav, D. R., & Pawar, S. K. (2022). **Titanium alloy selection for biomedical application using weighted sum model methodology**. *Materials Today: Proceedings.*

(21) Zhao, D., Witte, F., Lu, F., Wang, J., Li, J., & Qin, L. (2017). **Current status on clinical applications of magnesium-based orthopaedic implants: A review from clinical translational perspective**. *Biomaterials*, 112, 287-302.

(22) Li, X., Liu, X., Wu, S., Yeung, K. W. K., Zheng, Y., & Chu, P. K. (2016). **Design of magnesium alloys with controllable degradation for biomedical implants: From bulk to surface**. *Acta biomaterialia*, 45, 2-30.

(23) Li, L., Zhang, M., Li, Y., Zhao, J., Qin, L., & Lai, Y. (2017). **Corrosion and biocompatibility improvement of magnesium-based alloys as bone implant materials: a review**. *Regenerative biomaterials*, 4(2), 129-137.

(24) Esmaily, M., Svensson, J. E., Fajardo, S., Birbilis, N., Frankel, G. S., Virtanen, S., ... & Johansson, L. G. (2017). **Fundamentals and advances in magnesium alloy corrosion**. *Progress in Materials Science*, 89, 92-193.

(25) Prakasam, M., Locs, J., Salma-Ancane, K., Loca, D., Largeteau, A., & Berzina-Cimdina, L. (2017). **Biodegradable materials and metallic implants—a review.** *Journal of functional biomaterials*, 8(4), 44.

(26) Saji, V. S. (2019). **Organic conversion coatings for magnesium and its alloys.** *Journal of Industrial and Engineering Chemistry*, 75, 20-37.

(27) Thakur, B., Barve, S., & Pesode, P. (2022). **Investigation on mechanical properties of AZ31B magnesium alloy manufactured by stir casting process**. *Journal of the Mechanical Behavior of Biomedical Materials*, 105641.

(28) Khan, S. A., Miyashita, Y., & Mutoh, Y. (2015). **Corrosion fatigue behavior of AM60 magnesium alloy with anodizing layer and chemical-conversion-coating layer**. *Materials and Corrosion*, 66(9), 940-948.

(29) Duan, G., Yang, L., Liao, S., Zhang, C., Lu, X., Yang, Y., ... & Wang, F. (2018). **Designing for the chemical conversion coating with high corrosion resistance and low electrical contact resistance on AZ91D magnesium alloy**. *Corrosion Science*, 135, 197-206.

(30) Su, Y. H., Chiang, F. C., Chang, C. C., Lin, S. T., Chen, C. T., Chen, T. W., & Chen, S. M. (2020). **Trivalent Chromium Based Conversion Coating Contains Zinc/Zn (OH) 2 on Iron Substrates for the Detection of Uric Acid in Biological Samples and Control of Dyeing**. *Int. J. Electrochem. Sci*, 15, 2935-2947.

(31) Yin, Z. Z., Qi, W. C., Zeng, R. C., Chen, X. B., Gu, C. D., Guan, S. K., & Zheng, Y. F. (2020). **Advances in coatings on biodegradable magnesium alloys**. *Journal of Magnesium and Alloys*, 8(1), 42-65.

(32) Li, Z., Yuan, Y., & Jing, X. (2017). **Composite coatings prepared by combined plasma electrolytic oxidation and chemical conversion routes on magnesium-lithium alloy**. *Journal of Alloys and Compounds*, 706, 419-429.

(33) Chen, X. B., Nisbet, D. R., Li, R. W., Smith, P. N., Abbott, T. B., Easton, M. A., ... & Birbilis, N. (2014). **Controlling initial biodegradation of magnesium by a biocompatible strontium phosphate conversion coating**. *Acta biomaterialia*, 10(3), 1463-1474.

https://doi.org/10.17993/3cemp.2023.120151.392-421

(34) Chen, X. B., Yang, H. Y., Abbott, T. B., Easton, M. A., & Birbilis, N. (2014). **Corrosion protection of magnesium and its alloys by metal phosphate conversion coatings**. *Surface engineering*, 30(12), 871-879.

(35) Pereda, M. D., Alonso, C., Gamero, M., Del Valle, J. A., & De Mele, M. F. L. (2011). **Comparative study of fluoride conversion coatings formed on biodegradable powder metallurgy Mg: The effect of chlorides at physiological level**. *Materials Science and Engineering*: C, 31(5), 858-865.

(36) Zeng, R., Lan, Z., Kong, L., Huang, Y., & Cui, H. (2011). **Characterization of calcium-modified zinc phosphate conversion coatings and their influences on corrosion resistance of AZ31 alloy**. *Surface and Coatings Technology*, 205(11), 3347-3355.

(37) Zeng, R. C., Sun, X. X., Song, Y. W., Zhang, F., Li, S. Q., Cui, H. Z., & Han, E. H. (2013). I**nfluence of solution temperature on corrosion resistance of Zn-Ca phosphate conversion coating on biomedical Mg-Li-Ca alloys**. *Transactions of Nonferrous Metals Society of China*, 23(11), 3293-3299.

(38) Wang, Q., Tan, L., Xu, W., Zhang, B., & Yang, K. (2011). **Dynamic behaviors of a Ca–P coated AZ31B magnesium alloy during in vitro and in vivo degradations**. *Materials Science and Engineering: B*, 176(20), 1718-1726.

(39) Liu, G., Tang, S., Li, D., & Hu, J. (2014). **Self-adjustment of calcium phosphate coating on micro-arc oxidized magnesium and its influence on the corrosion behaviour in simulated body fluids**. *Corrosion science*, 79, 206-214.

(40) Zeng, R. C., Zhang, F., Lan, Z. D., Cui, H. Z., & Han, E. H. (2014). **Corrosion resistance of calcium-modified zinc phosphate conversion coatings on magnesium–aluminium alloys**. *Corrosion Science*, 88, 452-459.

(41) Zhao, M., Li, J., He, G., Xie, H., & Fu, Y. (2013). **An investigation of the effect of a magnetic field on the phosphate conversion coating formed on magnesium alloy**. *Applied surface science*, 282, 499-505.

(42) Zou, Y. H., Zeng, R. C., Wang, Q. Z., Liu, L. J., Xu, Q. Q., Wang, C., & Liu, Z. W. (2016). **Blood compatibility of zinc–calcium phosphate conversion coating on Mg–1.33 Li–0.6 Ca alloy**. *Frontiers of Materials Science*, 10(3), 281-289.

(43) Mao, L., Yuan, G., Niu, J., Zong, Y., & Ding, W. (2013). **In vitro degradation behavior and biocompatibility of Mg–Nd–Zn–Zr alloy by hydrofluoric acid treatment**. *Materials Science and Engineering: C*, 33(1), 242-250.

(44) Yan, T., Tan, L., Zhang, B., & Yang, K. (2014). **Fluoride conversion coating on biodegradable AZ31B magnesium alloy**. J*ournal of Materials Science & Technology*, 30(7), 666-674.

(45) Liu, X., Zhen, Z., Liu, J., Xi, T., Zheng, Y., Guan, S., ... & Cheng, Y. (2015). **Multifunctional MgF2/polydopamine coating on Mg alloy for vascular stent application**. *Journal of Materials Science & Technology*, 31(7), 733-743.

(46) Witte, F., Fischer, J., Nellesen, J., Vogt, C., Vogt, J., Donath, T., & Beckmann, F. (2010). **In vivo corrosion and corrosion protection of magnesium alloy LAE442**. *Acta biomaterialia*, 6(5), 1792-1799.

(47) Fintova, S., Drabikova, J., Pastorek, F., Tkacz, J., Kubena, I., Trsko, L., ... & Ptacek, P. (2019). **Improvement of electrochemical corrosion characteristics**

https://doi.org/10.17993/3cemp.2023.120151.392-421

of AZ61 magnesium alloy with unconventional fluoride conversion coatings. *Surface and Coatings technology*, 357, 638-650.

(48) Dusastre, V. (Ed.). (2010). **Materials for sustainable energy: a collection of peer-reviewed research and review articles from Nature Publishing Group**. *World Scientific*.

(49) Zhang, J., Gu, C., Yan, W., Tu, J., & Ding, X. (2018). **Fabrication and corrosion property of conversion films on magnesium alloy from deep eutectic solvent**. *Surface and Coatings Technology*, 344, 702-709.

(50) Birbilis, N., Howlett, P. C., MacFarlane, D. R., & Forsyth, M. (2007). **Exploring corrosion protection of Mg via ionic liquid pretreatment**. *Surface and Coatings Technology*, 201(8), 4496-4504.

(51) Huang, P., Latham, J. A., MacFarlane, D. R., Howlett, P. C., & Forsyth, M. (2013). **A review of ionic liquid surface film formation on Mg and its alloys for improved corrosion performance**. *Electrochimica Acta*, 110, 501-510.

(52) Efthimiadis, J., Neil, W. C., Bunter, A., Howlett, P. C., Hinton, B. R., MacFarlane, D. R., & Forsyth, M. (2010). **Potentiostatic control of ionic liquid surface film formation on ZE41 magnesium alloy**. *ACS applied materials & interfaces*, 2(5), 1317-1323.

(53) Howlett, P. C., Khoo, T., Mooketsi, G., Efthimiadis, J., Macfarlane, D. R., & Forsyth, M. (2010). **The effect of potential bias on the formation of ionic liquid generated surface films on Mg alloys**. *Electrochimica acta*, 55(7), 2377-2383.

(54) Forsyth, M., Neil, W. C., Howlett, P. C., Macfarlane, D. R., Hinton, B. R., Rocher, N., ... & Smith, M. E. (2009). **New insights into the fundamental chemical nature of ionic liquid film formation on magnesium alloy surfaces**. *ACS applied materials & interfaces*, 1(5), 1045-1052.

(55) Zhang, Y., Liu, X., Jamali, S. S., Hinton, B. R., Moulton, S. E., Wallace, G. G., & Forsyth, M. (2016). **The effect of treatment time on the ionic liquid surface film formation: Promising surface coating for Mg alloy AZ31**. *Surface and Coatings Technology*, 296, 192-202.

(56) Elsentriecy, H. H., Qu, J., Luo, H., Meyer III, H. M., Ma, C., & Chi, M. (2014). I**mproving corrosion resistance of AZ31B magnesium alloy via a conversion coating produced by a protic ammonium-phosphate ionic liquid**. *Thin Solid Films*, 568, 44-51.

(57) Elsentriecy, H. H., Luo, H., Meyer, H. M., Grado, L. L., & Qu, J. (2014). **Effects of pretreatment and process temperature of a conversion coating produced by an aprotic ammonium-phosphate ionic liquid on magnesium corrosion protection**. *Electrochimica Acta*, 123, 58-65.

(58) Smith, E. L., Abbott, A. P., & Ryder, K. S. (2014). **Deep eutectic solvents (DESs) and their applications**. *Chemical reviews*, 114(21), 11060-11082.

(59) 59. Gu, C. D., Yan, W., Zhang, J. L., & Tu, J. P. (2016). **Corrosion resistance of AZ31B magnesium alloy with a conversion coating produced from a choline chloride—Urea based deep eutectic solvent**. *Corrosion Science*, 106, 108-116.

https://doi.org/10.17993/3cemp.2023.120151.392-421

(60) Zhang, J., Gu, C., Tong, Y., Yan, W., & Tu, J. (2016). **A Smart Superhydrophobic Coating on AZ31B Magnesium Alloy with Self-Healing Effect**. *Advanced Materials Interfaces*, 3(14), 1500694.

(61) Shadanbaz, S., & Dias, G. J. (2012). **Calcium phosphate coatings on magnesium alloys for biomedical applications: a review**. *Acta biomaterialia*, 8(1), 20-30.

(62) Kim, H. M. (2003). **Ceramic bioactivity and related biomimetic strategy**. *Current opinion in solid state and materials science*, 7(4-5), 289-299.

(63) Habibovic, P., Barrere, F., Van Blitterswijk, C. A., de Groot, K., & Layrolle, P. (2002). **Biomimetic hydroxyapatite coating on metal implants**. *Journal of the American Ceramic Society*, 85(3), 517-522.

(64) Duan, K., Tang, A., & Wang, R. (2009). **A new evaporation-based method for the preparation of biomimetic calcium phosphate coatings on metals**. *Materials Science and Engineering: C*, 29(4), 1334-1337.

(65) Lu, X., & Leng, Y. (2005). **Theoretical analysis of calcium phosphate precipitation in simulated body fluid**. *Biomaterials*, 26(10), 1097-1108.

(66) Reiner, T., & Gotman, I. (2010). B**iomimetic calcium phosphate coating on Ti wires versus flat substrates: structure and mechanism of formation**. *Journal of Materials Science: Materials in Medicine*, 21(2), 515-523.

(67) Silva, C. C. G., Rigo, E. C. D. S., Marchi, J., Bressiani, A. H. D. A., & Bressiani, J. C. (2008). **Hydroxyapatite coating on silicon nitride surfaces using the biomimetic method**. *Materials Research*, 11, 47-50.

(68) Yang, L., Hedhammar, M. Y., Blom, T., Leifer, K., Johansson, J., Habibovic, P., & van Blitterswijk, C. A. (2010). **Biomimetic calcium phosphate coatings on recombinant spider silk fibres**. *Biomedical materials*, 5(4), 045002.

(69) Majid, K., Tseng, M. D., Baker, K. C., Reyes-Trocchia, A., & Herkowitz, H. N. (2011). **Biomimetic calcium phosphate coatings as bone morphogenetic protein delivery systems in spinal fusion**. *The Spine Journal*, 11(6), 560-567.

(70) Stigter, M., De Groot, K., & Layrolle, P. (2002). **Incorporation of tobramycin into biomimetic hydroxyapatite coating on titanium**. *Biomaterials*, 23(20), 4143-4153.

(71) Muller, F. A., Jonášová, L., Cromme, P., Zollfrank, C., & Greil, P. (2004). **Biomimetic apatite formation on chemically modified cellulose templates**. *In Key Engineering Materials*, 254, 1111-1114. *Trans Tech Publications Ltd.*

(72) Bigi, A., Boanini, E., Bracci, B., Facchini, A., Panzavolta, S., Segatti, F., & Sturba, L. (2005). **Nanocrystalline hydroxyapatite coatings on titanium: a new fast biomimetic method**. *Biomaterials*, 26(19), 4085-4089.

(73) Zhang, Y., Zhang, G., & Wei, M. (2009). **Controlling the biodegradation rate of magnesium using biomimetic apatite coating**. *Journal of Biomedical Materials Research Part B: Applied Biomaterials: An Official Journal of The Society for Biomaterials, The Japanese Society for Biomaterials, and The Australian Society for Biomaterials and the Korean Society for Biomaterials,* 89(2), 408-414.

(74) Gray-Munro, J. E., & Strong, M. (2009). **The mechanism of deposition of calcium phosphate coatings from solution onto magnesium alloy AZ31**. *Journal of Biomedical Materials Research Part A: An Official Journal of The*

https://doi.org/10.17993/3cemp.2023.120151.392-421

Society for Biomaterials, The Japanese Society for Biomaterials, and The Australian Society for Biomaterials and the Korean Society for Biomaterials, 90(2), 339-350.

(75) Lorenz, C., Brunner, J. G., Kollmannsberger, P., Jaafar, L., Fabry, B., & Virtanen, S. (2009). **Effect of surface pre-treatments on biocompatibility of magnesium**. *Acta Biomaterialia*, 5(7), 2783-2789.

(76) Lopez, H. Y., Cortes-Hernandez, D. A., Escobedo, S., & Mantovani, D. (2006). **In vitro bioactivity assessment of metallic magnesium**. *In Key Engineering Materials,* 309, 453-456. *Trans Tech Publications Ltd.*

(77) Gray-Munro, J. E., Seguin, C., & Strong, M. (2009). **Influence of surface modification on the in vitro corrosion rate of magnesium alloy AZ31**. *Journal of Biomedical Materials Research Part A: An Official Journal of The Society for Biomaterials, The Japanese Society for Biomaterials, and The Australian Society for Biomaterials and the Korean Society for Biomaterials,* 91(1), 221-230.

(78) Cortes-Hernández, D. A., Lopez, H. Y., & Mantovani, D. (2007). **Spontaneous and biomimetic apatite formation on pure magnesium.** *In Materials science forum,* 539, 589-594. *Trans Tech Publications Ltd.*

(79) Keim, S., Brunner, J. G., Fabry, B., & Virtanen, S. (2011). **Control of magnesium corrosion and biocompatibility with biomimetic coatings**. *Journal of Biomedical Materials Research Part B: Applied Biomaterials*, 96(1), 84-90.

(80) Chen, Y., Mak, A. F., Li, J., Wang, M., & Shum, A. W. (2005). **Formation of apatite on poly (α-hydroxy acid) in an accelerated biomimetic process**. *Journal of Biomedical Materials Research Part B: Applied Biomaterials: An Official Journal of The Society for Biomaterials, The Japanese Society for Biomaterials, and The Australian Society for Biomaterials and the Korean Society for Biomaterials*, 73(1), 68-76.

(81) Barrere, F., Van Der Valk, C. M., Dalmeijer, R. A. J., Van Blitterswijk, C. A., De Groot, K., & Layrolle, P. (2003). **In vitro and in vivo degradation of biomimetic octacalcium phosphate and carbonate apatite coatings on titanium implants**. J*ournal of Biomedical Materials Research Part A: An Official Journal of The Society for Biomaterials, The Japanese Society for Biomaterials, and The Australian Society for Biomaterials and the Korean Society for Biomaterials*, 64(2), 378-387.

(82) Cui, F. Z., Yang, J. X., Jiao, Y. P., Yin, Q. S., Zhang, Y., & Lee, I. S. (2008). **Calcium phosphate coating on magnesium alloy for modification of degradation behavior**. *Frontiers of Materials Science in China*, 2(2), 143-148.

(83) Liu, Y., Layrolle, P., de Bruijn, J., van Blitterswijk, C., & de Groot, K. (2001). **Biomimetic coprecipitation of calcium phosphate and bovine serum albumin on titanium alloy**. *Journal of Biomedical Materials Research: An Official Journal of The Society for Biomaterials, The Japanese Society for Biomaterials, and The Australian Society for Biomaterials and the Korean Society for Biomaterials*, 57(3), 327-335.

(84) Hu, J., Wang, C., Ren, W. C., Zhang, S., & Liu, F. (2010). **Microstructure evolution and corrosion mechanism of dicalcium phosphate dihydrate**

https://doi.org/10.17993/3cemp.2023.120151.392-421

coating on magnesium alloy in simulated body fluid. *Materials Chemistry and Physics*, 119(1-2), 294-298.

(85) Yang, J. X., Cui, F. Z., Yin, Q. S., Zhang, Y., Zhang, T., & Wang, X. M. (2009). **Characterization and degradation study of calcium phosphate coating on magnesium alloy bone implant in vitro**. I*EEE Transactions on plasma science*, 37(7), 1161-1168.

(86) Ling, L., Cai, S., Li, Q., Sun, J., Bao, X., & Xu, G. (2022). **Recent advances in hydrothermal modification of calcium phosphorus coating on magnesium alloy**. *Journal of Magnesium and Alloys*, 10(1), 62-80.

(87) Xu, Y., Li, H., Wu, J., Yang, Q., Jiang, D., & Qiao, B. (2018). **Polydopamine-induced hydroxyapatite coating facilitates hydroxyapatite/polyamide 66 implant osteogenesis: an in vitro and in vivo evaluation**. *International Journal of Nanomedicine*, 13, 8179.

(88) Park, S. Y., Kim, K. I., Park, S. P., Lee, J. H., & Jung, H. S. (2016). **Aspartic acid-assisted synthesis of multifunctional strontium-substituted hydroxyapatite microspheres**. *Crystal Growth & Design*, 16(8), 4318-4326.

(89) Zhou, H., Yang, Y., Yang, M., Wang, W., & Bi, Y. (2018). **Synthesis of mesoporous hydroxyapatite via a vitamin C templating hydrothermal route**. *Materials Letters*, 218, 52-55.

(90) Suchanek, K., Bartkowiak, A., Perzanowski, M., Marszałek, M., Sowa, M., & Simka, W. (2019). **Electrochemical properties and bioactivity of hydroxyapatite coatings prepared by MEA/EDTA double-regulated hydrothermal synthesis**. *Electrochimica Acta*, 298, 685-693.

(91) Suchanek, K., Perzanowski, M., Suchy, K., Lekka, M., Szaraniec, B., & Marszałek, M. (2019). **Assessment of phase stability and in vitro biological properties of hydroxyapatite coatings composed of hexagonal rods**. *Surface and Coatings Technology*, 364, 298-305.

(92) Fan, X. L., Li, C. Y., Wang, Y. B., Huo, Y. F., Li, S. Q., & Zeng, R. C. (2020). **Corrosion resistance of an amino acid-bioinspired calcium phosphate coating on magnesium alloy AZ31**. *Journal of Materials Science & Technology*, 49, 224-235.

(93) Li, L. Y., Cui, L. Y., Liu, B., Zeng, R. C., Chen, X. B., Li, S. Q., ... & Han, E. H. (2019). **Corrosion resistance of glucose-induced hydrothermal calcium phosphate coating on pure magnesium**. *Applied Surface Science*, 465, 1066-1077.

(94) Li, L., Gao, J., & Wang, Y. (2004). **Evaluation of cyto-toxicity and corrosion behavior of alkali-heat-treated magnesium in simulated body fluid**. *Surface and Coatings Technology*, 185(1), 92-98.

(95) Kunjukunju, S., Roy, A., Ramanathan, M., Lee, B., Candiello, J. E., & Kumta, P. N. (2013). **A layer-by-layer approach to natural polymer-derived bioactive coatings on magnesium alloys**. *Acta biomaterialia*, 9(10), 8690-8703.

(96) Lin, Z., Wang, T., Yu, X., Sun, X., & Yang, H. (2021). **Functionalization treatment of micro-arc oxidation coatings on magnesium alloys: A review**. *Journal of Alloys and Compounds*, 879, 160453.

https://doi.org/10.17993/3cemp.2023.120151.392-421

(97) Pesode, P., & Barve, S. (2021). **Surface modification of titanium and titanium alloy by plasma electrolytic oxidation process for biomedical applications: A review**. *Materials Today: Proceedings*, 46, 594-602.

(98) Wang, D. D., Liu, X. T., Su, Y., Wu, Y. K., Yang, Z., Han, H. P., ... & Shen, D. J. (2020). **Influences of edge effect on microstructure and corrosion behaviour of PEO coating**. *Surface Engineering*, 36(2), 184-191.

(99) Fattah-alhosseini, A., Babaei, K., & Molaei, M. (2020). **Plasma electrolytic oxidation (PEO) treatment of zinc and its alloys: A review**. *Surfaces and Interfaces*, 18, 100441.

(100) Zhang, Z. Q., Wang, L., Zeng, M. Q., Zeng, R. C., Kannan, M. B., Lin, C. G., & Zheng, Y. F. (2020). **Biodegradation behavior of micro-arc oxidation coating on magnesium alloy-from a protein perspective**. *Bioactive materials*, 5(2), 398-409.

(101) Zhang, Y., Chen, Y., Duan, X. Y., Zheng, W. Q., & Zhao, Y. W. (2019). **Long time corrosion test of AZ31B Mg alloy via micro-arc oxidation (MAO) technology**. *Materials Research Express*, 6(12), 126416.

(102) Shen, Y., He, L., Yang, Z., & Xiong, Y. (2020). **Corrosion behavior of different coatings prepared on the surface of AZ80 magnesium alloy in simulated body fluid**. *Journal of Materials Engineering and Performance*, 29(3), 1609-1621.

(103) Shi, P., Niu, B., Shanshan, E., Chen, Y., & Li, Q. (2015). **Preparation and characterization of PLA coating and PLA/MAO composite coatings on AZ31 magnesium alloy for improvement of corrosion resistance**. *Surface and Coatings Technology*, 262, 26-32.

(104) Kaseem, M., Hussain, T., Rehman, Z. U., & Ko, Y. G. (2021). **Stabilization of AZ31 Mg alloy in sea water via dual incorporation of MgO and WO3 during micro-arc oxidation**. *Journal of Alloys and Compounds*, 853, 157036.

(105) Wang, Z. X., Chen, G. Q., Chen, L. Y., Xu, L., & Lu, S. (2018). **Degradation behavior of micro-arc oxidized ZK60 magnesium alloy in a simulated body fluid**. *Metals*, 8(9), 724.

(106) Liu, C., Yuan, J., Li, H., & Jiang, B. (2019). **Role of substrates in the corrosion behaviors of micro-arc oxidation coatings on magnesium alloys**. *Metals*, 9(10), 1100.

(107) Staiger, M. P., Pietak, A. M., Huadmai, J., & Dias, G. (2006). **Magnesium and its alloys as orthopedic biomaterials: a review**. *Biomaterials*, 27(9), 1728-1734.

(108) Lee, C. Y., Chen, K. L., Xu, Z. M., & Lee, H. B. (2020). **Corrosion and Biocompatibility Behavior of the Micro-Arc Oxidized AZ31B Alloy in Simulated Body Fluid**. *Int. J. Electrochem. Sci*, 15, 6405-6424.

(109) Amaravathy, P., & Kumar, T. S. (2019). **Bioactivity enhancement by Sr doped Zn-Ca-P coatings on biomedical magnesium alloy**. *Journal of Magnesium and Alloys*, 7(4), 584-596.

(110) Zaatreh, S., Haffner, D., Strauß, M., Wegner, K., Warkentin, M., Lurtz, C., ... & Bader, R. (2017). **Fast corroding, thin magnesium coating displays antibacterial effects and low cytotoxicity**. *Biofouling*, 33(4), 294-305.

https://doi.org/10.17993/3cemp.2023.120151.392-421

(111) Zeng, J., Ren, L., Yuan, Y., Wang, Y., Zhao, J., Zeng, R., ... & Mei, X. (2013). **Short-term effect of magnesium implantation on the osteomyelitis modeled animals induced by Staphylococcus aureus**. *Journal of Materials Science: Materials in Medicine*, 24(10), 2405-2416.

(112) Yu, X., Ibrahim, M., Liu, Z., Yang, H., Tan, L., & Yang, K. (2018). **Biofunctional Mg coating on PEEK for improving bioactivity**. *Bioactive materials*, 3(2), 139-143.

(113) Ma, R., Wang, W., Yang, P., Wang, C., Guo, D., & Wang, K. (2020). **In vitro antibacterial activity and cytocompatibility of magnesium-incorporated poly (lactide-co-glycolic acid) scaffolds**. *BioMedical Engineering OnLine*, 19(1), 1-12.

(114) Ren, L., Lin, X., Tan, L., & Yang, K. (2011). **Effect of surface coating on antibacterial behavior of magnesium based metals**. *Materials Letters*, 65(23-24), 3509-3511.

(115) Fattah-alhosseini, A., Molaei, M., Attarzadeh, N., Babaei, K., & Attarzadeh, F. (2020). **On the enhanced antibacterial activity of plasma electrolytic oxidation (PEO) coatings that incorporate particles: A review**. *Ceramics International*, 46(13), 20587-20607.

(116) Chen, H., Lv, G., Zhang, G., Pang, H., Wang, X., Lee, H., & Yang, S. (2010). **Corrosion performance of plasma electrolytic oxidized AZ31 magnesium alloy in silicate solutions with different additives**. *Surface and Coatings Technology*, 205, S32-S35.

(117) Mashtalyar, D. V., Sinebryukhov, S. L., Imshinetskiy, I. M., Gnedenkov, A. S., Nadaraia, K. V., Ustinov, A. Y., & Gnedenkov, S. V. (2020). **Hard wearproof PEO-coatings formed on Mg alloy using TiN nanoparticles**. *Applied Surface Science*, 503, 144062.

(118) Pesode, P. A., & Barve, S. B. (2021). **Recent advances on the antibacterial coating on titanium implant by micro-Arc oxidation process**. *Materials Today: Proceedings*, 47, 5652-5662.

(119) Davidović, S., Lazić, V., Miljković, M., Gordić, M., Sekulić, M., Marinović-Cincović, M., ... & Nedeljković, J. M. (2019). **Antibacterial ability of immobilized silver nanoparticles in agar-agar films co-doped with magnesium ions**. *Carbohydrate polymers*, 224, 115187.

(120) Kasi, G., Viswanathan, K., & Seo, J. (2019). **Effect of annealing temperature on the morphology and antibacterial activity of Mg-doped zinc oxide nanorods**. *Ceramics International*, 45(3), 3230-3238.

(121) Giachino, A., & Waldron, K. J. (2020). **Copper tolerance in bacteria requires the activation of multiple accessory pathways**. *Molecular microbiology*, 114(3), 377-390.

(122) Rizwan, M., Alias, R., Zaidi, U. Z., Mahmoodian, R., & Hamdi, M. (2018). **Surface modification of valve metals using plasma electrolytic oxidation for antibacterial applications: A review**. *Journal of Biomedical Materials Research Part A*, 106(2), 590-605.

(123) Zai, W., Zhang, X., Su, Y., Man, H. C., Li, G., & Lian, J. (2020). **Comparison of corrosion resistance and biocompatibility of magnesium phosphate (MgP),**

https://doi.org/10.17993/3cemp.2023.120151.392-421

zinc phosphate (ZnP) and calcium phosphate (CaP) conversion coatings on Mg alloy. *Surface and Coatings Technology*, 397, 125919.

(124)Hamanishi, C., Kitamoto, K., Tanaka, S., Otsuka, M., Doi, Y., & Kitahashi, T. (1996). **A self-setting TTCP-DCPD apatite cement for release of vancomycin**. *Journal of Biomedical Materials Research: An Official Journal of The Society for Biomaterials and The Japanese Society for Biomaterials*, 33(3), 139-143.

(125)LeGeros, R. Z. (2008). **Calcium phosphate-based osteoinductive materials**. *Chemical reviews*, 108(11), 4742-4753.

(126)Zhou, Z., Zheng, B., Gu, Y., Shen, C., Wen, J., Meng, Z., ... & Qin, A. (2020). **New approach for improving anticorrosion and biocompatibility of magnesium alloys via polydopamine intermediate layer-induced hydroxyapatite coating**. *Surfaces and Interfaces*, 19, 100501.

(127)Liu, P., Wang, J. M., Yu, X. T., Chen, X. B., Li, S. Q., Chen, D. C., ... & Cui, L. Y. (2019). **Corrosion resistance of bioinspired DNA-induced Ca–P coating on biodegradable magnesium alloy**. *Journal of Magnesium and Alloys*, 7(1), 144-154.

(128)Cui, L. Y., Cheng, S. C., Liang, L. X., Zhang, J. C., Li, S. Q., Wang, Z. L., & Zeng, R. C. (2020). **In vitro corrosion resistance of layer-by-layer assembled polyacrylic acid multilayers induced Ca–P coating on magnesium alloy AZ31**. *Bioactive Materials*, 5(1), 153-163.

(129)Zhang, M., Cai, S., Shen, S., Xu, G., Li, Y., Ling, R., & Wu, X. (2016). **In-situ defect repairing in hydroxyapatite/phytic acid hybrid coatings on AZ31 magnesium alloy by hydrothermal treatment**. *Journal of Alloys and Compounds*, 658, 649-656.

(130)Ji, X. J., Gao, L., Liu, J. C., Jiang, R. Z., Sun, F. Y., Cui, L. Y., ... & Wang, Z. L. (2019). **Corrosion resistance and antibacterial activity of hydroxyapatite coating induced by ciprofloxacin-loaded polymeric multilayers on magnesium alloy**. *Progress in organic coatings*, 135, 465-474.

(131)Thakur, B., Barve, S., & Pesode, P. **Magnesium-Based Nanocomposites for Biomedical Applications**. *In Advanced Materials for Biomechanical Applications,* 113-131. CRC Press.

(132)Pesode, P., & Barve, S. Magnesium **Alloy for Biomedical Applications**. I*n Advanced Materials for Biomechanical Applications,* 133-158. CRC Press.

https://doi.org/10.17993/3cemp.2023.120151.392-421

/23/

USE OF VALUE CHAIN ANALYSIS TO IMPROVE THE QUALITY OF HEALTH SERVICE

Seror Naji Mohsen aldouri

College of Administration and Economics, University of Samarra, Iraq

seror.n.m@uosamarra.edu.iq

Manoj A. Kumbhalkar

Department of Mechanical Engineering, JSPM Narhe Technical Campus, Pune, India

manoj.kumbhalkar@rediffmail.com - https://orcid.org/0000-0003-2289-6373

Reception: 27/11/2022 **Acceptance**: 20/01/2023 **Publication**: 05/02/2023

Suggested citation:

Seror Naji Mohsen Aldouri and Manoj A. Kumbhalkar. (2023). **Use the Value Chain Analysis to Improve the Quality of Health Service**. *3C Empresa. Investigación y pensamiento crítico, 12(1)*, 423-438. https://doi.org/10.17993/3cemp.2023.120151.423-438

ABSTRACT

Quality is currently one of the most important strategies adopted by WHO in to gain time to please and deal with the client for the greatest possible benefit to auditors, In health service, quality and value have become convergent ideas, and the importance of patients as clients has grown as a result of a focus on quality management and value delivery.The supply chain idea also aids marketing by showcasing the ties that make up a network of firms that manufacture products for customers, as well as shifting the attention away from individual transactions and toward a more holistic view of the entire system. The value chain idea in marketing broadens the perception of the supply chain in a significant way. It describes the value created at each level of the chain and, for marketers, is a critical tool in satisfying customers for a portion of the value chain. This research looks at numerous value approaches that are critical for the value chain's success, then identifies key aspects of the value chain and follows them as they relate to services. Finally, it looks at one of the most complicated services, the health services system. Finally, the research reveals some crucial implications for health-service marketers by evaluating the critical aspects determining the performance of the health-service process.

KEYWORDS

Value Chain, Analysis, Quality Enhancement, Health Service

https://doi.org/10.17993/3cemp.2023.120151.423-438

PAPER INDEX

https://doi.org/10.17993/3cemp.2023.120151.423-438

1. INTRODUCTION

Measuring beneficiary satisfaction with health service has become one of the most significant indicators of service quality. These organizations now operate in a world that is unquestionably marked by numerous challenges as a result of significant developments associated with increased domestic, regional, and international competitiveness, as well as the significant effects of modern technologies, which have altered many of the issues associated with the management and functioning of institutions in comparison to previous times.

In light of this, these institutions' management should be concerned about long-term competitive strategy. In the area of strategic management of institutions, in particular, the development and expansion of their use were initiated by Porter's contributions as one of the leading researchers in this field, which were accompanied by contemporary developments in the management sciences and business management of enterprises in general.

Value chain analysis is an economic development strategy aimed at reducing poverty by improving SMEs' integration into competitive markets. It provides a basis for understanding the linkages between enterprises in a certain sector by looking at the chain's performance or rationale and determining the circumstances under which it might perform better. The series of transactions that move a product from the point of origin to the end consumer is determined by the same value chain. The value chain framework aids in the identification of services and solutions vital to an industry's productivity and competitiveness, as well as helping micro, small, and medium businesses to enhance the quality of their services, products, and overall productivity (Kula & Farmer, 2004) As a result, the value chain analysis considers both macro and micro issues, addressing policy restrictions to economic development, trade, and competitiveness as well as domestic restraints encountered by businesses and people.

The value chain for the manufacturing process is theoretically easier to define than the value chain for the service process (Evans & Berman, 2001). The level of customization supplied by the service, the degree of engagement of a partner or consumer, and the uncertainty underlying the underlying process are all essential elements to consider from a value chain viewpoint. Many of these aspects are backed by formulae and metrics that allow for a degree of precision in the field of industrialization. Because measurements are less precise in services, the value chain of services might be more complicated.

This paper examines the critical factors affecting the success of the health service process and focuses on one of the most complex services, the health service delivery system. It describes the value chain of health services and describes the critical factors affecting the success of the health service process. Finally, some major implications for health service marketers are suggested.

https://doi.org/10.17993/3cemp.2023.120151.423-438

2. INVESTIGATE THE VALUE CHAIN

2.1. THE CONCEPT "VALUE CHAIN ANALYSIS" HAS A LONG HISTORY

One of the terminologies used in business management to convey the chain of actions that might help improve the value of final goods is the value chain.

Lawrence Mill coined the phrase Value Chain in the 1950s, and Porter expanded on it in his publications, which focused on the search for sources of competitive advantage and their origins by focusing on the performance of diverse operations at the company level.

2.2. THE VALUE ANALYSIS CHAIN'S IDEA, GOALS, AND SIGNIFICANCE

2.2.1. VALUE CHAIN ANALYSIS AS A CONCEPT

The value chain is a chain of activities that runs from the use of raw materials to the delivery of the product to the final consumer (Porter & Millar, 1985).

They were defined by (Miles, 2015; Fard et al., 2013) as a comprehensive approach for identifying and addressing variables that do not contribute effort or expense to goods, processes, or services. This approach makes use of all available technology, information, and abilities to quickly discover any expenditures and efforts that aren't contributing to the client's needs and desires.

He said (K. L. Smith, 2000) that a giant organization that seeks likeness or excellence in its work must guarantee the principle of doing too much (Doing more with less), so it is a tool that helps us achieve that.

Describes (Ranjbaran & Moselhi, 2014) as a comprehensive mission to manage problems: take alternative design objectives, cost estimation, and draft and organization inappropriate selection criteria. Quantity methods are used and know-based decisions to improve job satisfaction for owners with help reduce unnecessary costs.

They are (the talents and resources necessary to carry out each of the Organization's actions to supply products or offer services through marketing outlets), according to (Day, 1999).

According to (Ansari et al., 1997), a value chain is the interaction of numerous parties, including the processor, the organization's sections, the distributor, and all those parties who offer value at various stages to the value chain's activities.

It can be said that according to the above definition, the value chain is a method or analysis that entails examining all of an institution's internal and external activities, as

https://doi.org/10.17993/3cemp.2023.120151.423-438

well as organizing them by the organizational structure and the selection of effective human resources.

2.2.2. VALUE CHAIN ANALYSIS OBJECTIVES

One of the objectives of the organizations' adoption of the value chain analysis concept is:

1. Improve quality by increasing the function of the product (the level of performance the client receives from the product) while making resources stable (which are considered raw materials, human resources, price, and time) or by lowering resources while stabilizing the function, or by both enhancing the function and reducing resources.
2. They may be used to increase efficiency and find the optimal balance between the cost, functionality, quality, dependability, and performance of a product or service, as well as to finish processes as soon as possible without increasing costs or lowering quality (Taghipour et al., 2015).
3. Besides using them efficiently and logically with collective wisdom and experience, they can reduce the potential risks involved in implementing a project (Kalluri & Kodali, 2017).
4. Identify the function of the product or service by determining the equivalent of this function, find alternatives through creative thinking, provide required functions to achieve the project's original objective, reliability, and at the lowest cost of life cycle without compromising the project's quality, maintenance, conservation, or environmental requirements.
5. Use all available technologies, information, and abilities to determine expenses and efforts that aren't in line with the client's objectives and needs. "Their influence makes it easier for perform better"(Carter & Price, 2017).

2.2.3. IMPORTANCE OF VALUE CHAIN ANALYSIS:

The following is a summary of the importance of value chain analysis (Bogale, 2013):

a) Reducing operational costs is aided by solving the value chain.

b) The analysis aids in the organization's performance planning.

c) Assists the organization in identifying chances to expand its work.

d) Assists the organization in determining performance metrics for management information systems.

e) Assists you in making better decisions.

https://doi.org/10.17993/3cemp.2023.120151.423-438

2.3. VALUE CHAIN ANALYSIS ACTIVITIES

2.3.1. THE MAIN ACTIVITIES ARE:

a) Input: This includes the processing of raw materials, inspecting and storing raw materials as well as receiving and storing materials, inventory control, and distribution of inputs used in the manufacture of goods or the provision of services.

b) Production Operations: Are concerned with quality, cost, consumable services, delivery, and reaction time. Production processes encompass the acquisition, design, and operation of machinery, as well as the control of production (Foss & Robertson, 2007).

c) Output: Many operations entail distribution, companies rely on brokers to dispose of their goods or sell them to consumers. Distribution systems are a critical component of an organization's resources. that must be handled, and a distribution strategy connected with the selection and determination of distribution channels is required (Hitt et al., 2016).

d) Marketing and selling: Marketing is a significant activity that contributes to understanding consumer wants or uncovering new marketing possibilities, as well as aiming to establish a balance between market needs and the organization's capabilities and hence the organization's competitive advantage (Mohamad & Bakar, 2018).

e) Service: It includes after-sales services such as maintenance and client delivery. According to the researcher, distribution is intended to be a component of marketing and selling.

2.3.2. SUPPORT ACTIVITIES

a) The buying department is in charge of supplying raw materials and equipment to the company required for the manufacturing process, and the Purchasing Department must have a high capacity in order to achieve maximum benefit from cost reduction while maintaining the quality components of the good or service.

b) Technology development: Refers to all actions aimed at improving production techniques and complying to total quality standards and new ISO systems that need the use of computers in the job to be done (Forcht, 1996).

c) Human Resource Management: Active employees are the human resources that the organization’s management has to pay great attention to because they are largely reflected in its activities.

d) The organizational fundamental structure is made up of all organizational levels that are responsible for carrying out the organization's numerous duties, such as public administration, strategic planning, accounting, legal affairs, public relations, and industrial security. As a result, all of the organizational structure's contents are

https://doi.org/10.17993/3cemp.2023.120151.423-438

compatible with the organization's core thinking qualities, which may be updated and altered in response to developments and changes.

2.4. VALUE CHAIN AND APPLICATION

The value chain framework attempts to overcome limitations by identifying the many entry points and links in the production or supply chain, allowing SMEs to take advantage of the full range of activities needed to change a product or service from concept to end use, including design. While production, marketing, distribution and delivery to the final consumer can be contained within one large firm in an economy with few cross-border transactions and dispersed production inputs and assets, they are more likely to be shared by specialized firms of different sizes and cost structures operating in different locations.

The competitiveness and growth of a company, as well as the strength of the whole industry chain, are determined by how it participates in the industry's production process. This strength is defined by two types of corporate ties, vertical and horizontal, according to the literature on value chains. Vertical linkages are at the heart of every manufacturing process, connecting providers of inputs, producers, retailers and distributors of a certain service or product.The value chain's fundamental skills are defined by these linkages. Collateral linkages are frequently associated, lowering overall efficiency and transaction costs. Individual organizations can be included in the network, and commercial service providers can be partnered with to obtain economies of scale.

3. THE VALUE CHAIN FOR HEALTH SERVICES

Health services are a market with many similarities to traditional markets, such as market segments that can be identified by common characteristics, they also have clients and patients, and similar problems, such as increased customer identification and governance structures that are revenue and cost conscious, implying that the health service does not differ and should not differ in its interest in customer satisfaction.

By mapping and responding to the restrictions and possibilities presented by health care institutions in specific markets, value chain analysis may be used to improve health sector efficiency. In developing nations, the size and complexity of the health sector is expanding, and health sector reforms and cuts to the government's health budget have resulted in a greater role for private health in the delivery of health services (E. Smith et al., 2001). In this setting, public health practitioners and the donor community must work to improve access and quality of services.

The interactions between diverse service providers, product suppliers, manufacturers, policymakers, government agencies, and customers show the intricacies of the health industry. The formulation of plans to improve sector growth and raise demand for health services and goods requires sector-wide analyses of health care delivery and product distribution. The value chain framework might be

https://doi.org/10.17993/3cemp.2023.120151.423-438

used for this purpose, serving as a tool for identifying supply chain bottlenecks in the health sector and leveraging synergies among service providers, professional organizations, manufacturers, distributors, and other stakeholders. Figure 1 depicts the health value chain scheme.

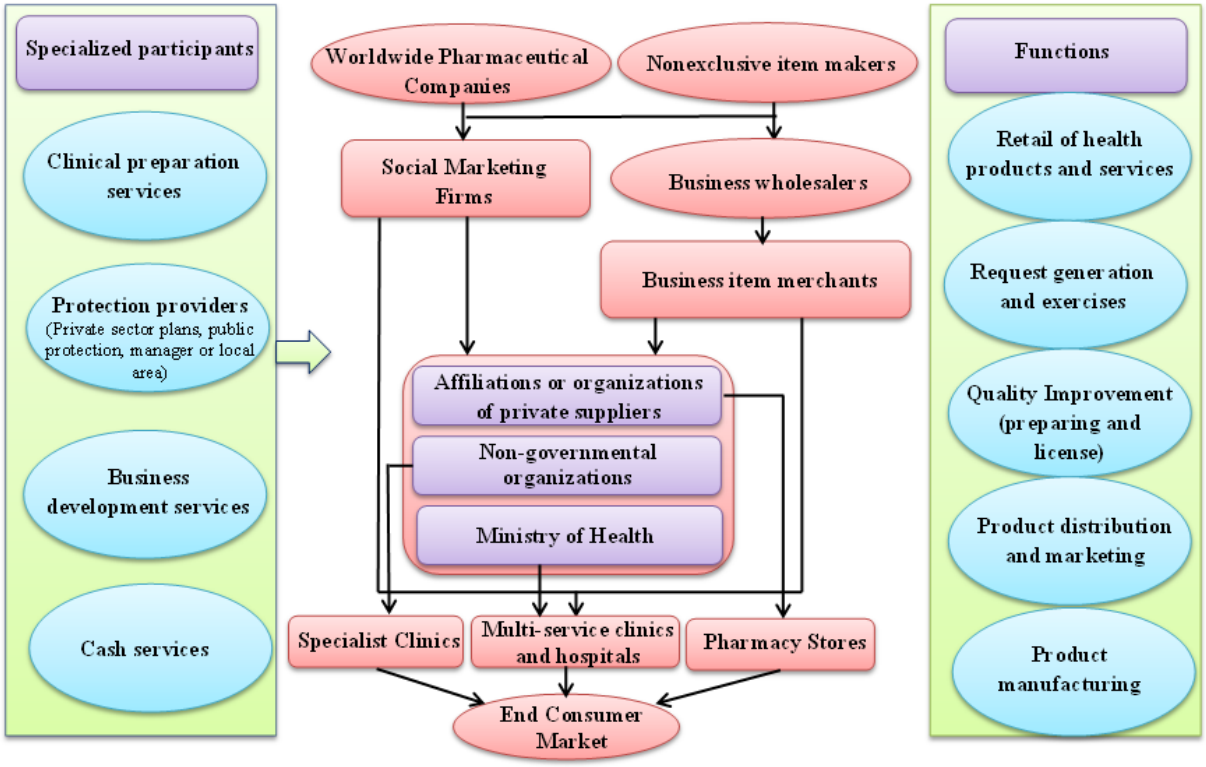

Figure 1. Health services value chain for products and services

Figure 2 depicts some of the players in the health services value chain who link the many stakeholders in the health services system as a model of the health services value chain. These value chains must be understood to be non-linear, non-continuous, periodic, and recurring. The flow of information is usually governed by a specialized communication network among many parties. The value chain will be damaged or interrupted if communication is stopped, information sent is delayed, or worse, fraudulent information is sent, placing one or more players at risk. Patients (and their health) are the most vulnerable, but other parties may suffer reputational harm or face litigation directly.

The shortest value chain of patients and their interactions with health professionals or physicians is formed by the initial participants. Patients often begin the exchange procedure and obtain the anticipated health advantages at the conclusion. They prefer to share essential information with their doctor, especially if they believe it will help the doctor make the best diagnosis possible. Sharing information entails confidence that the doctor will protect the information's integrity and that the exposed patient will utilize it for the intended purpose. Another crucial part of this information sharing is the patient's trust in the accuracy and relevance of the information presented. Patients may provide information and describe symptoms that are unrelated to the patient's

https://doi.org/10.17993/3cemp.2023.120151.423-438

current problem, which can cause confusion rather than help a doctor. Assuming that they have the correct information from their patients, health providers must first make the correct diagnosis and then develop the treatment plan, thus contributing to the value chain. Figure 2 shows the first and second numbers in the series.

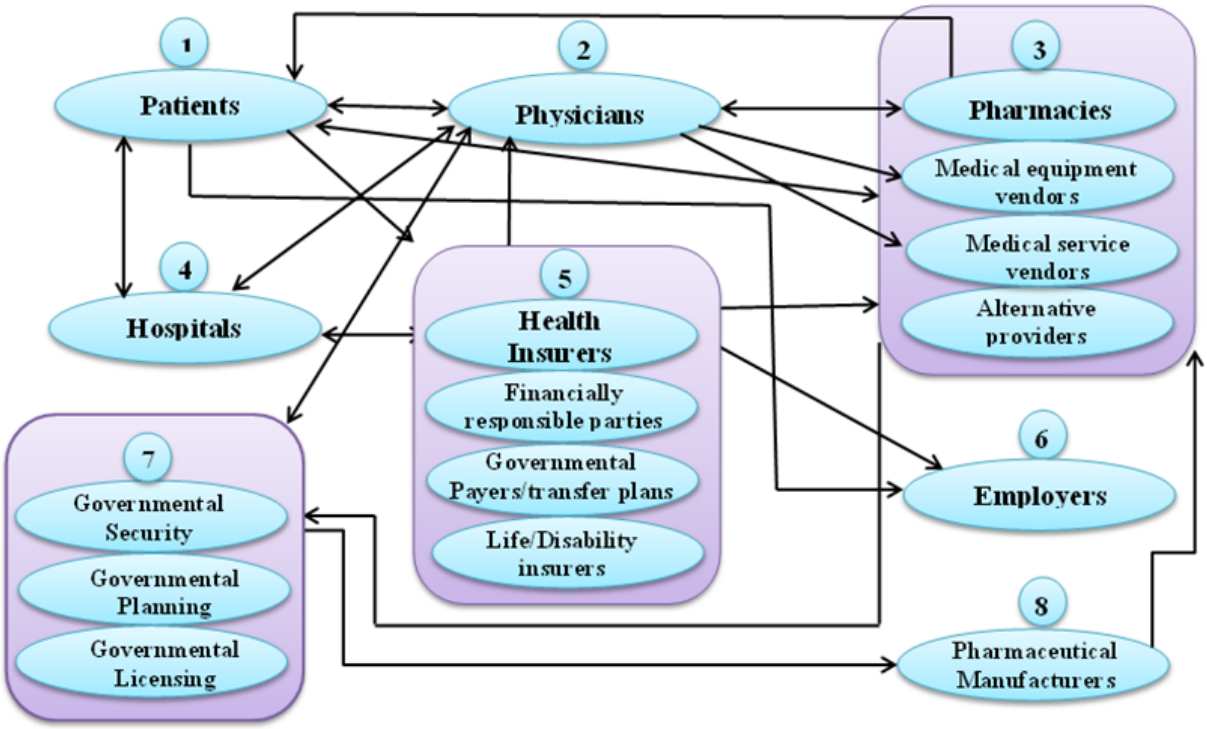

Figure 2. The health service value chain's relationships

In many cases, a diagnosis includes a treatment plan, which includes a prescription, as well as the pharmacist's dose schedule, which includes doses and other pertinent information; the pharmacist may or may not be aware of the patient's other medications, and it is possible that the last prescription will be filled. Pharmacies are an obvious entry point within the value chain and introduce a new variable. Figure 2 shows the expanded value chain in figures 1, 2, and 3.

By asking patients for extra information or offering a mechanism for patients to contribute further information, a third value chain is created, even if the patient offers a correct description of their symptoms. Additional material may include a description of a diagnostic test. Once this diagnostic test is detailed, more participants enter the process. Naturally, they should be aware of the expectations placed on them and aware of the need of obtaining accurate information about their role in the value chain. Medical laboratories, equipment makers, and diagnostic providers are now part of the value chain.

Suppliers of inclusivity are another possible value chain, as described above. An increasing number of alternative health services professionals, such as acupuncturists and herbalists, have recently entered the value chain. There may be four to seven actors in the new value chain, and information is passed back and forth frequently in

https://doi.org/10.17993/3cemp.2023.120151.423-438

sequence. One or more actors, such as those depicted in figure 2a, 2b, or 2c, have now been added to the value chain (2).

In addition to serving as major repository of medical records, hospitals have a considerable impact on the value chain because of the involvement of patients. Fourth-generation health service delivery chains revolve around patients, just way products do as they travel up and down value chains. Patients' health and responsiveness to therapy are heavily influenced by the value chain, which currently includes numbers 1 to 4 in figure 2 A new categories of health care services is created as a result of this value chain.

A new link was added to the value chain with the development of health insurance in the late 1800s. The availability of resources, affordability, and insurance theoretically adds a lot to the value chain. They also need access to formerly confidential information. Before paying for a test ordered by a medical professional, the insurance company, for example, could ask for diagnostic information. Procedures that are too complicated may be denied by insurers who prefer to utilize simpler methods to examine a problem. Figure 2 shows that the value chain now includes numbers 1 to 5.

Employees and their families in the United States have access to health insurance through their workplace and a collective bargaining agreement, which is generally the product of talks between the employee's firm and the insurance carrier. In this way, huge corporations may be able to get better terms for themselves, such as reduced premiums or greater coverage for their employees. When it comes to employee benefits, it's all part of an overall strategy of equalizing the risks. Refusing to cover employees who are qualified for benefits is almost never an option. Numbers 1 to 6 have been added to the sixth value series of health services shown in figure 2.

The capacity to pay out of pocket for health services promotes the idea of everlasting value for health service providers as a result of insurance interference in health care transactions. All insured people who do not register health service providers in their insurance schemes fall under this group, regardless of whether or not they are uninsured. Consumption is considered as a way for customers to make their own choices, which might possibly shorten the value chain while also altering its overall structure.

Affordability may have a role in a variety of factors, including health service demands and the appropriateness of different providers. Figure 2 shows the impact on the value chain of a patient's inability to pay for or need to find a lower-cost medication prescribed by their doctor, which we classify as a third variable in the value chain.

https://doi.org/10.17993/3cemp.2023.120151.423-438

4. APPLICATION OF THE VALUE CHAIN FRAMEWORK FOR HEALTH SERVICES

With this value chain method, it is possible to discover various aspects of the health service market and identify prospective areas where public health care services and products might be strengthened.

1. One of the best ways for small businesses to achieve a competitive edge is by improving their overall efficiency and quality of service. There have been technological advances as well as advancements in the clinical capabilities of medical facilities.
   Health service providers can boost their competitiveness and productivity by boosting service quality and stock or decreasing operational expenses. Smaller healthcare providers can boost productivity by offering a wider range of services, such as specialized therapeutic or diagnostic care. Large health service providers can instead create expensive laboratories in order to continue internalization services.

2. Horizontal links guarantee that small businesses collaborate to cut transaction costs and benefit from economies of scale.

   Individual service providers can benefit from economies of scale and easier access to training and supplementary services, such as loans, business development, or marketing, when structured into subsidiaries or networks. It is possible for the network to have a variety of service providers, depending on the situation. Small businesses can benefit from referrals between professional service providers, such as retail pharmacies and midwifery clinics, in order to guarantee that consumers are aware of respected service providers and have easy access to a high-quality package of health service. A unified procurement agreement might be used to recruit high-quality manufacturers into the supply chain through the network.

3. The use of vertical connections is critical in fostering growth by increasing efficiency and enhancing a company's ability to compete. A direct link between input supply and ultimate consumer markets is shown by these links, which may be restricted to domestic boundaries or linked to global markets

   Connections between various sorts of health care institutions. Relationships between various professional service providers, such as laboratory or diagnostic services, which are directly integrated into the supply chain, should be reinforced to increase overall supply chain efficiency.

4. In many developing nations, the existing market for support services will have a significant impact on the strength of the value chain of health service.

   Small and medium-sized enterprises (SMEs) must have access to financial services, cutting-edge technology, and information on clinical and other health training in order to keep up with the times and remain competitive.

https://doi.org/10.17993/3cemp.2023.120151.423-438

An major element in increasing the usage of preventative service is the health insurance market. Consumers who are unwilling to pay for preventative treatments up front may be reluctant to pay service providers to deliver those services as part of ad hoc programs. The employer or the business sector contributes to private patient funds. Some of the strategies to stimulate the use and supply of health service include national insurance schemes and community risk-sharing partnerships with providers.

5. The engagement of governments and donors in policy formation and formulation is essential to establish an enabling climate for the supply of health service.

   Individual health service providers, whether small businesses or major hospitals, must enhance the quality of their health services in order to adopt and control health quality standards. By offering training and clinical assistance, national standards may be a stimulus for local market development organizations.

   Private health service providers, large and small, must be encouraged to participate in the delivery of services by the larger policy environment. For example, private health insurance subsidies and contracts with private providers within the national health insurance plan can serve as methods for licensing and regulating the operations of health services.

   As a result, the health sector will be constrained in its expansion and may need to enter into joint ventures with public producers in order to boost supply and lower prices for end users. The reduction of import duties or the negotiation of long-term agreements with certain pharmaceutical businesses might serve as incentives to foster collaboration between these nations and regional manufacturers in countries where drug makers do not have a local market.

6. Demand generating strategies must be institutionally connected to their provision in order to enhance the final market potential. Demand and service delivery are interdependent, and demand generation strategies must be linked to their provision.

   Partnerships with a wide range of stakeholders might include: Preventive health services can be promoted by the public sector, major enterprises, schools, community organizations, and so on. For the purpose of boosting their market share, commercial pharmaceutical corporations might team up with non-governmental organizations (NGOs) to conduct educational programs targeted at certain consumer groups.

   Funding strategies based on need: In order to entice clients who are less inclined or who have a tight budget, targeted vouchers or savings-based micro-

https://doi.org/10.17993/3cemp.2023.120151.423-438

insurance products might be employed. There will be a rise in demand for other types of insurance and risk-sharing systems that are based on the private sector or employers.

Increase demand for preventative health service by offering urgently required services provided by small service providers. Providers of these diagnostic and therapeutic services make more money.

5. EFFECTS ON MARKETERS

While the value chain is built on the notion of a supply chain, this study investigates how value is produced for the final consumer at each point along the way.

Business components, such as the value delivery network, and consumer business components, which complement the value chain, are recognized as distinct in the value chain idea. That value chains will compete with others and that members of the value chain must shift away from transaction models and recognize that their well-being resides in a successful value chain.

For enterprises that want to develop a value chain for health services, each member of the service chain must be carefully selected and evaluated. The whole value delivery network and patient outcomes are impacted when a value chain component fails. As a result of an incorrect diagnosis or operation, the health care delivery system will suffer greatly.

To ensure the success of the series as a whole, each member must achieve on his or her own while also contributing to the success of the group as a whole. This, for example, will improve the efficiency of the value chain and raise the perceived value of customers.

The long-term success of the chain is more important than the short-term success of a single transaction for organizations who want to maximize their own interests. Clearly, the argument that everyone should win is a waste of time. Instead, they should put their money into things that they both care about. More efficient health-care value chains will benefit from stronger government and third-party cost management, while those that lack efficiency and efficacy will eventually perish.

Enterprises must express their efforts to avoid difficulties before they become problems in order to avoid being blamed by consumers for unforeseen issues that hamper the success of their services. Reorganization of the workplace or medical facility may be necessary in some circumstances in order to accommodate this sort of engagement. Organizational value and the perception of value can be supported by patient representative concepts in hospitals.

Value chain organizations are critical to the service's success. There are several factors to consider when deciding which organizations should be given the most attention by marketers. Previously key partners may become less significant as the value chain develops.

https://doi.org/10.17993/3cemp.2023.120151.423-438

The first step in maximizing earnings for health providers is to estimate the worth of the patient. Following their initial treatment, some patients may be sent for more expensive options including fitness and health training, physiotherapy, or even cosmetic surgery. Patients like these must be prioritized as appointment candidates in order to safeguard and preserve the lives of the most important patients.

6. CONCLUSIONS

This case study shows how the value chain concept can be used in a health service setting. It benefits health service managers because it requires them to disaggregate their health service function and evaluate its efficacy, as well as to identify alternate strategies for obtaining present results and consider future possibilities. Value chain analysis allows for an intra- and inter-organizational examination of resource application costs, which motivates both medical staff and management to consider alternate techniques and structures for accomplishing goals. This research yielded a lot of options and opportunities. The idea of employing staff abilities to propose preventative measures to industry and the wider community was considered, as was the possibility of expanding collaboration arrangements.

ACKNOWLEDGMENTS

The author wishes to express gratitude to the University of Samarra, College of Administration and Economics, for supporting them in completing this paper.

REFERENCES

(1) Ansari, S. A., Ansari, S. L., & Bell, J. (1997). **Target costing: the next frontier in strategic cost management.** *Irwin Professional Pub.*

(2) Bogale, E. (2013). **Advanced management accounting techniques in manufacturing firms in Ethiopia**. *Research Journal of Finance and Accounting*, 4(16), 9-17.

(3) Carter, M. W., & Price, C. C. (2017). **Operations research: a practical introduction**. *CRC Press.*

(4) Day, G. S. (1999). **The market driven organization: understanding, attracting, and keeping valuable customers**. *Simon and Schuster.*

(5) Evans, J. R., & Berman, B. (2001). **Conceptualizing and operationalizing the business-to-business value chain**. *Industrial Marketing Management*, 30(2), 135-148.

(6) Fard, A. B., Rad, K. G., Sabet, P. G. P., & Aadal, H. (2013). **Evaluating effective factors on value engineering implementation in the context of Iran**. *Journal of Basic and Applied Scientific Research*, 3(10), 430-436.

(7) Forcht, K. A. (1996). **Doing business on the Internet: marketing and security aspects**. *Information Management & Computer Security*.

https://doi.org/10.17993/3cemp.2023.120151.423-438

(8) Foss, N. J., & Robertson, P. L. (2007). **Resources, technology and strategy (Vol. 11)**. *Psychology Press.*

(9) Hitt, M. A., Ireland, R. D., & Hoskisson, R. E. (2016). **Strategic management: Concepts and cases: Competitiveness and globalization.** *Cengage Learning.*

(10) Kalluri, V., & Kodali, R. (2017). **Component cost reduction by value engineering: a case study**. *Journal of The Institution of Engineers (India): Series C*, 98(2), 219-226.

(11) Kula, O., & Farmer, E. (2004). **Mozambique Rural Financial Services Study.** *Submitted to USAID for AMAP Knowledge & Practice.*

(12) Miles, L. D. (2015). **Techniques of value analysis and engineering**. M*iles Value Foundation.*

(13) Mohamad, B., & Bakar, H. A. (2018). **Corporate communication and strategic management: history, operational concept and integration.** *Advances in Social Science, Education and Humanities Research (ASSEHR)*, 186.

(14) Porter, M. E., & Millar, V. E. (1985). **How information gives you competitive advantage**. *Harvard Business Review Reprint Service.*

(15) Ranjbaran, Y., & Moselhi, O. (2014). **4D-based value engineering**. *Construction Research Congress 2014: Construction in a Global Network*, 1606-1615.

(16) Smith, E., Brugha, R., & Zwi, A. (2001). **Working with private sector providers for better health care: an introductory guide**. *London School of Tropical Medicine London, UK.*

(17) Smith, K. L. (2000). **Applying value analysis to a value engineering program.** *VALUE WORLD*, 23(3), 14-17.

(18) Taghipour, M., Nokhbefallah, M., Nosrati, F., Yaghoubi, J., & Nazemi, S. (2015). **Evaluation of the effective variables of the value engineering in services (Qazvin post center case study)**. *Journal of Applied Enviromental and Bilogical Science*, 5(12), 319-322.

(19) M. M. Sardeshmukh, Shradha Kulkarni, M. A. Kumbhalkar, S. A. Choudhari, D. V. Bhise, Dr. S. W. Shaikh, (2019) **Smart Ai-Based Online Proctoring.** *Journal of the Gujarat Research Society*, 21(16).

(20) Sajid Shaikh, M. M. Sardeshmukh, S. A. Choudhari, M. A. Kumbhalkar, D. V. Bhise, (2019) **A comparative study on Utilization and Benefits of Wireless Mobile Networks.** *Journal of the Gujarat Research Society*, 21(17).

https://doi.org/10.17993/3cemp.2023.120151.423-438

/24/

REDUCING THE COSTS OF SUSTAINABLE DEVELOPMENT IN INDUSTRIAL COMPANIES (AN APPLIED STUDY)

Khaleel Radhi Hasan Alzlzly
Alfurat Alawsat Technical University, Technical Institute of Samawa
ins.khl2@atu.edu.iq - khlznb2016@gmail.com

Reception: 18/11/2022 **Acceptance**: 20/01/2023 **Publication**: 14/02/2023

Suggested citation:

H. A., Khaleel Radhi. (2023). **Reducing the costs of sustainable development in industrial companies (an applied study)**. *3C Empresa. Investigación y pensamiento crítico, 12(1)*, 440-461.
https://doi.org/10.17993/3cemp.2023.120151.440-461

ABSTRACT

The research aims to reduce the costs of sustainable development through the use of strategic cost management methods, characterizing the cost system used to reduce costs in these companies, as well as studying the relationship between the use of modern methods of strategic cost management and reducing the costs of sustainable development, as well as studying the role of reduced costs in achieving the competitive advantage of companies. In addition to its role in assisting in making strategic decisions.

The research methodology relies on the deductive approach, which is the researcher relying on books, letters, dissertations, and scientific articles to enrich the theoretical aspect of the study, formulating the research problem and the research hypothesis, and the inductive approach through designing a questionnaire as a tool for the field study, which was distributed to workers in cement and brick factories in Al-Muthanna Governorate in Iraq. Where the number of the distributed questionnaire reached (200) questionnaires, 175 of which were retrieved, and the validity and reliability of the questionnaire questions and the correlation between all the axes of the questionnaire were calculated, and the values of the correlation coefficient were a statistical function at a significant level (0.05).

The most important findings of the researcher were the existence of a significant positive relationship between the use of strategic cost management methods and reducing the costs of sustainable development, as well as the existence of a positive significant relationship between reducing the costs of sustainable development and achieving competitive advantage and making strategic decisions for companies.

The most important recommendations were that there is a need to pay attention to reducing the costs of sustainable development by adopting strategic cost management methods in cement and brick factories in Al-Muthanna Governorate.

KEYWORDS

Strategic cost management, cost reduction, sustainable development.

https://doi.org/10.17993/3cemp.2023.120151.440-461

PAPER INDEX

https://doi.org/10.17993/3cemp.2023.120151.440-461

1. INTRODUCTION

As a result of the increasing interest in sustainable development by all countries, the interest in the dangers of pollution or environmental deterioration and social responsibility on economic units has increased due to industrial progress in addition to human behavior. The environmental and social dimension in addition to the economic dimension of industrial companies has become a distinctive event and an important topic that many address in their writings. The field of modern administrative, accounting and economic thought.

As a result of the international fear of the risks of environmental degradation, interest in sustainable development issues has increased at the local, regional and global levels. Governments and various international organizations have begun to charge environmental and social costs to companies and factories. Many binding laws and regulations have been put in place to implement sustainable development standards in these companies and factories. Here The problem of reducing the costs of sustainable development began to pose a challenge to accountants in these companies in order to preserve the company's reputation and maintain the company's competitive advantage in the local and international markets.

Sustainable development has important dimensions, which are the economic dimension, the social dimension, and the environmental dimension, in addition to the technological and institutional dimensions. It has become the basis for a new philosophy that governs the performance of industrial companies, which puts company managers in a new challenge in achieving high profits, and in turn, taking into account social responsibility towards society in reducing costs.

Through the foregoing, companies in developing countries in general and in Iraq in particular are facing a challenge in reducing the costs of sustainable development as a result of the mandatory directives of developed countries and the systems of international trade policies. Where these countries set standards on the level of products in terms of characteristics and specifications, as well as standards for production methods and methods used, and all companies must adhere to comprehensive quality standards and international standards that guarantee product quality, environmental safety, and compatibility with international standards of sustainability.

All this contributed to increasing the obligations and increasing the environmental costs borne by the industrial companies and has an impact on the competitive position of these companies, and the emergence of new challenges for accountants in how to reduce these costs, and therefore it is necessary to practice or use modern cost methods that help and contribute to reducing these costs and increasing the competitive advantage of these companies in the global and local markets.

2. RESEARCH METHODOLOGY:

2.1. RESEARCH PROBLEM:

https://doi.org/10.17993/3cemp.2023.120151.440-461

Due to the adoption by many business organizations of the concept of sustainable development as a result of the rapid developments in the modern business environment, this led to the necessity of developing cost accounting systems and management accounting, and then the need to develop methods and methods used appropriate to the new reality of industrial companies and the competition market in order to keep pace with the rapid modern developments of the concept of sustainable development.

Accordingly, the research problem is represented in the inability of industrial companies to reduce the costs of sustainable development, due to the inability of traditional systems to address these costs, which are considered various and indirect costs. Therefore, the research problem is summarized in the following questions:

First question: Do the traditional cost systems in companies and factories help reduce the costs of sustainable development?

Second question: Does the application of modern methods and systems of costs help in reducing the costs of sustainable development?

Third question: Does reducing the costs of sustainable development contribute to achieving a competitive advantage for industrial companies?

2.2. IMPORTANCE OF RESEARCH:

The importance of the research lies in the urgent need to implement the sustainable development program in the Iraqi industrial companies at the present time in order to reduce the costs of sustainable development at the local and global levels. As the use of strategic cost management methods in order to reduce the costs of sustainable development is one of the important things that industrial companies need in the competition market in order to know these costs and how to reduce them while maintaining the quality of products, as well as assisting in planning and control, which leads to achieving sustainability.

It also leads to the expansion of academic studies among researchers in order to delve into this field in developing countries, including Iraq, due to the weakness of sustainable development in this country, whether at the economic, social or environmental level.

2.3. RESEARCH OBJECTIVES:

The main objective of this research is how to reduce the costs of sustainable development in industrial companies by using strategic cost management methods, and there are sub-objectives of the research summarized as follows:

1. Studying the relationship between strategic cost management methods and reducing the costs of sustainable development in Iraqi industrial companies.
2. Studying the relationship between reducing the costs of sustainable development and achieving the competitive advantage of Iraqi industrial companies.

https://doi.org/10.17993/3cemp.2023.120151.440-461

3. Studying the relationship of reducing sustainable development and making strategic decisions in Iraqi industrial companies.

2.4. RESEARCH HYPOTHESIS:

The research is based on a main hypothesis:

There is an effect of strategic cost management methods in reducing the costs of sustainable development, achieving competitive advantage, and assisting in strategic decision-making in Iraqi industrial companies.

From this hypothesis, the following hypotheses are derived:

1. There is a significant relationship between the methods of strategic cost management and reducing the costs of sustainable development.
2. There is a significant relationship between reducing the costs of sustainable development and achieving competitive advantage.
3. There is a relationship between reducing the costs of sustainable development, making strategic decisions and improving the quality of industrial companies.

2.5. RESEARCH LIMITS:

A. Spatial limits: The research is limited to conducting an applied study and comparison between each of the cement factories and the brick factories in Al-Muthanna Governorate / Iraq, due to the nature of the production operations carried out by these factories, which cause damage and pollution to the environment on the one hand, and the depletion of natural resources on the other hand. And through the use of strategic cost management methods, which are (activity-based costing, value engineering, target costing, benchmarking, continuous improvement, production on time, balanced scorecard, value chain).

B. Temporal limits: The research covers the time period from 2014-2022 for the purpose of finding out the extent to which companies and factories are committed to applying sustainable development standards, applying laws and legislation to account for the costs of sustainable development, and the extent to which these companies are committed to disclosing environmental and social performance.

3. THEORETICAL FRAMEWORK OF SUSTAINABLE DEVELOPMENT:

3.1. THE CONCEPT OF SUSTAINABLE DEVELOPMENT:

The term sustainable development appeared for the first time in a publication issued by the National Union for Environmental Protection in 1980, but it was widely circulated only after it was reused in the report "Our Common Future" known as the "Brundtland Report" issued in 1987 by the World Environment Committee. and

https://doi.org/10.17993/3cemp.2023.120151.440-461

development of the United Nations. The report defined sustainable development as "development that responds to the needs of the present without endangering the ability of future generations to meet their own needs." (International Commission for Development and Sustainability, 1989: 83).

Barbier defined it in a more general way, which includes the establishment of a social and economic system that guarantees support for achieving the following goals: an increase in real income, an improvement in the level of education, and an improvement in the health of the population. (Ismail, 2015: 44).

As for Robert Solow, he defined it as “not harming the productive capacity of future generations and leaving it on the situation inherited by generations.” (Same source, 2015: 44).

Sustainable development was defined as “preserving opportunities for future generations, with a general idea that justice is intertwined between generations.” (Khudair, 2015: 341).

Sustainable development was defined by the Food and Agriculture Organization of the United Nations in 1989 (FAO), where sustainability was defined as “managing and protecting the natural resource base and directing technical and institutional changes to ensure the permanent satisfaction of present and future human needs, provided that this development is protected (in the agricultural and forestry sector and residential resources (land, water, animal and plant genetic resources), while being environmentally harmless, technically appropriate, economically feasible, and socially acceptable (FAO, 1989:7).

And defined sustainable development at the United Nations Conference held in Rio Janeiro 1992 and emphasized that the human being is the cornerstone of sustainable development, with the necessity for people to have a healthy and productive life in a manner that is compatible with the environment, and justice is achieved when meeting the developmental and environmental needs of the present and the future (UNCED, 1992: 1).

Sustainable development for developed countries means a reduction in the level of consumption of energy and resources, while for developing countries it means employing resources in order to raise the standard of living for citizens and reduce poverty, and in a more comprehensive manner ensuring the development of per capita income in the future not less than the current generation. (Ciegis, R. 2008: 17).

3.2. SUSTAINABLE DEVELOPMENT GOALS: (ABDUL-GHANI, 2020: 423).

The 17 Sustainable Development Goals and 169 targets demonstrate the breadth and ambition of this global agenda. The aim of these goals and objectives is to continue the march of the Millennium Development Goals and to accomplish what has not been achieved within their framework. It is very important to point out that these goals and objectives are the result of public consultations and extensive contacts conducted over more than two years in all parts of the world with civil society and

https://doi.org/10.17993/3cemp.2023.120151.440-461

other accompanying parties, in which special attention was paid to the voices of the poorest and weakest groups. The general objectives (United Nations, September 2015) included:

1. End poverty in all its forms everywhere.
2. Eradicating hunger, providing food security and improved nutrition, and promoting sustainable agriculture.
3. Ensure the enjoyment of healthy lifestyles and well-being for all at all ages.
4. Ensure inclusive and equitable quality education and promote lifelong learning opportunities for all.
5. Achieving gender equality and empowering all women and girls.
6. Ensure the availability of water and sanitation services for all and their sustainable management.
7. Ensure universal access to affordable, reliable and sustainable energy services.
8. Promoting sustained, inclusive and sustainable economic growth, full and productive employment, and decent work for all.
9. Build resilient infrastructure, stimulate inclusive and sustainable industrialization, and encourage innovation.
10. Reducing inequality within and between countries.
11. Make cities and human settlements inclusive, safe, resilient and sustainable.
12. Ensure sustainable consumption and production patterns.
13. Take urgent action to address climate change and its impacts.
14. Conserving and sustainably using the oceans, seas and marine resources to achieve sustainable development.
15. Protect, restore and promote sustainable use of terrestrial ecosystems, sustainably manage forests, combat desertification, halt and reverse land degradation, and halt biodiversity loss.
16. Promote peaceful and inclusive societies for sustainable development, provide access to justice for all, and build effective, accountable and inclusive institutions at all levels.
17. Strengthening the means of implementation and revitalizing the global partnership for achieving sustainable development. It is worth noting that the goals and objectives are integrated and indivisible, achieving a balance between the three dimensions of sustainable development, and are intended to be implemented until 2030. They also confirm the results of all major conferences and summits held by the United Nations, which laid a solid foundation for sustainable development and contributed to the formation of this The new plan. These include the Rio Declaration, the World Summit on Sustainable Development, the World Summit for Social Development, and the Program of Action of the International Conference on Population and Development. (United Nations, September 2015).

https://doi.org/10.17993/3cemp.2023.120151.440-461

3.3. DIMENSIONS OF SUSTAINABLE DEVELOPMENT:

There are many approaches and aspects to the study of sustainable development, but the various literatures in the field of economics all indicate that the concept of sustainable development emerges from its normative framework from three basic dimensions: economic and social development and environmental sustainability. Before dealing with these dimensions, we confirm that they converge and intertwine together in multiple fields. As for the other derived aspects, the most famous of them are the institutional aspect, the technological aspect, the administrative aspect, and the human development aspect, and these aspects also emerge from other branches aspects (Al-Kubaisi et al., 2019: 4-8).

The first dimension: focuses on the economic aspect to explain the concept of sustainable development, which is more profound as it focuses on the optimal use of resources to obtain the maximum benefits in light of preserving the diversity and use of resources and does not lead to a reduction in real income in the future. In this regard, developed countries are interested in reducing their consumption of energy and resources, while developing countries seek optimal use of resources in order to raise the standard of living of citizens and curb poverty, in other words ensuring the development of per capita income in the future so that it is not less than per capita income in the current generation. During the 1990s, the trend increased to include the environmental dimension in the field of economics, thus changing the concept of economic development from increasing the exploitation of scarce economic resources to satisfy multiple and renewable human needs to the concept of sustainable economic development, which does not prevent the intensive exploitation of economic resources such as water, oil or forests, but rejects The unfair exploitation of these resources so as to affect the share of future generations of these depleted or non-renewable resources, and the concept of pure economic development emerged that does not take into account the environmental dimension and is considered a subject of criticism from all circles and global economic institutions; To the extent that some called it “black development” (Al-Harbi, 2019: 5-6).

The economic dimension aims to continuously improve the level of quality of goods and services and achieve economic efficiency through the optimal use of resources. (Harries, Johthan, 2003: 2).

The second dimension: It is the social dimension, so it focuses on the human being and his mutual relationship, non-discrimination, and improving the standard of living through education, health, equality, and providing opportunities for freedom and political participation. In all cases, it is concerned with the government sector and civil society (Al-Juhani, 2015: 9).

Sustainability from a social perspective means focusing primarily on providing opportunities for access to decent work, public services, and how to achieve growth, which takes into account health issues, the elimination of epidemics and diseases, levels of poverty issues, education, training and social justice, and includes social development also of all kinds and the elimination of hunger, Shelter and quality of life

https://doi.org/10.17993/3cemp.2023.120151.440-461

issues, social security, population growth, and the number of deaths, especially in the early stages of life.

The social dimension aims to achieve social justice in the distribution of economic and natural resources, respect for human rights, the development of cultures, diversity and participation in decision-making (Othman Muhammad, Magda Ahmed, 2007: 39).

The third dimension: focuses on the environmental aspect, which looks at sustainable development on the basis of the use of renewable natural resources, in a manner that does not lead to their annihilation, deterioration, or diminishing of their capacity for future generations, and to maintain a stable balance of natural resources that does not diminish.

The institutional dimension: It aims to pay attention to a number of issues, the most important of which are the institutional framework, the institutional capacity of the parties concerned with sustainable development, and the extent of commitment to implementing binding international agreements (Stefanie.2005,:81).

Technological dimensions: It aims to use cleaner and more efficient technology in industrial facilities, and to reduce emissions of gases and fuels that lead to global warming.

In view of the association of each of the economic, environmental and social dimensions with a group of activities, where economic activity generates economic costs, environmental activity environmental costs, and social activity social costs, and these costs are collectively called the costs of sustainable development.

3.4. THE CONCEPT OF COST REDUCTION:

Cost reduction can be defined as an attempt to reduce cost. Cost reduction implies a real and permanent reduction in the unit cost of goods manufactured or services rendered without prejudice to the suitability of their products for their intended use. (Devilal Sharma, 2017: 47).

Cost reduction is a process aimed at reducing the unit cost of a product being manufactured or providing a service without affecting its quality. This can be done by using new and improved methods and technologies, achieved through alternative methods to reduce the unit production cost. (https://vmec.org/cost-reduction-strategies).

Cost reduction aims to reduce the objectives themselves. In other words, the objective of cost reduction is to see if there is any possibility of savings in cost incurred, labor, overheads, etc. According to the cost accounting terminology of the Institute of Cost Accountancy and Management in London, cost reduction should be understood as the success of a real and unchanging reduction in unit costs of manufactured goods without affecting their suitability for their intended use. Thus, the term cost reduction refers to real or explicit savings in production, management, selling and sharing costs resulting from the elimination of wasteful and unnecessary elements from product design and from the technologies and practices implemented in connection therewith. The necessity of cost reduction arises when profit margin has

https://doi.org/10.17993/3cemp.2023.120151.440-461

to be increased without increase in sales turnover, for the same volume of sales, cost has to be reduced. (Akeem, 2017: 22-23).

Cost reduction is not related to setting objectives and standards, but to improving standards. It is a continuous process that can be applied to all the activities involved. It focuses on two main areas:

1. Reducing expenses: A decrease in expenses in the specified production volume leads to a decrease in the unit cost.
2. Increased productivity: the general decrease in unit cost by increasing production for specific expenditures.

Cost reduction can be achieved by combining these factors. Moreover, it is somewhat difficult to know what contribution each factor has made to the increase in savings (increased profit for the firm).

"Cost reduction is a process aimed at reducing the unit cost of a product being manufactured or providing a service without affecting its quality. This can be done by using new and improved methods and technologies, achieved through alternative methods to reduce the unit production cost." (https://vmec.org/cost-reduction-strategies).

3.5. CLASSIFICATION OF SUSTAINABLE DEVELOPMENT COSTS:

There are many classifications of environmental costs from the point of view of environmental organizations and those interested in their costs, as it is possible to define the classification of environmental costs into three groups: (Al-Razzaq, 2012: 436).

A. Environmental before production: It includes all the sacrifices incurred by the economic unit in the pre-production stage or the operation of the system, and includes the costs of equipment, product design, evaluation of equipment alternatives, and environmental protection measures.

B. Periodic environmental costs during the operating stages: These include all costs incurred by the economic unit during the production and marketing stages of the product in order to improve the level of environmental performance, such as examination, measurement, evaluation and timely removal of damages.

C. Dimensional environmental costs: It includes all costs that are confirmed as well as likely to occur in the future, such as the costs of waste treatment and disposal, the costs of environmental compatibility and compliance with environmental legislation.

https://doi.org/10.17993/3cemp.2023.120151.440-461

3.6. REASONS FOR CARING ABOUT THE COSTS OF SUSTAINABLE DEVELOPMENT:

One of the studies adopted by the US Environmental Protection Agency (EPA) indicates that the reasons for concern about environmental costs are: Goetsch & Stanley, 2010: 339).

1. Many costs can be reduced or avoided because these costs do not add value to the products
2. These costs may be implicitly included in the indirect costs that are not ignored.
3. Reconsidering existing operating systems and understanding environmental costs helps the establishment to provide more accurate information to the establishment about environmental costs and pricing of its products, and then design products with better profitability specifications.
4. Achieving competition for the company's products by promoting products with better environmental specifications.
5. Understanding the environmental costs helps in supporting the environmental management system that many companies seek to develop as a means to obtain the ISO (14001) certificate related to the environment.

4. THEORETICAL FRAMEWORK OF STRATEGIC COST MANAGEMENT :

4.1. THE CONCEPT OF STRATEGIC COST MANAGEMENT:

Strategic cost management is an integrated approach that includes a set of tools and methods that integrate together to build and maximize the competitive position of companies in the competition market, help in decision-making, as well as improve the quality of products in industrial companies. There are many definitions of the concept of strategic cost management, including:

1. Cooper & Slagmulder defined it as “the management’s use of cost information to prepare and develop strategies and reduce costs in order to achieve a competitive advantage for the company” (Cooper & Slagmulder, 2003:23).
2. Wilson defined it as “representing one of the modern administrative approaches, which is concerned with analyzing cost in a broad framework, and using its information in formulating and developing strategies and choosing the best ones for differentiation and enhancing competitive advantage (Sorour, 2019: 3).
3. Anderson defined it as “analyzing, structure and behavior of the costs of the organization in the light of its strategic objectives and controlling its strategic performance in order to improve the decision-making process” (Anderson, 2005: 354).

https://doi.org/10.17993/3cemp.2023.120151.440-461

4. Strategic cost management is a process through which the cost is tracked and controlled throughout the life cycle of the product in all its stages to reach the cost to the lowest possible level, with a focus on analyzing the elements of the internal and external environment of the company in order to provide products with specifications and characteristics that meet the needs of customers and reflect value to them from one point of view. Their vision is to improve the strategic position of the company and to create a continuous competitive advantage by using technical methods and tools to track and control costs. (Mahmoud, 2010: 15).
5. Strategic cost management is defined as “a cost analysis, but on a large scale, by paying attention to the strategic objectives, using cost data to reach the best strategies that help achieve competitive advantages for the company.” (Khalaf, 2004: 76).

Through the above definitions, we conclude that strategic cost management is a comprehensive approach that adopts tools and methods that work in an integrated and coordinated manner in order to support the competitive advantage of the company because it focuses on the following: (Ahmed, 2017: 31).

A. Corporate strategy.

B. Cost driving factors.

C. Continuous cost reduction and competitive advantage.

4.2. THE OBJECTIVES OF STRATEGIC COST MANAGEMENT:

There are many goals for the strategic cost management approach, summarized as follows: (Khalifa et al., 2018: 474).

1. Focusing on the external environment and interacting with it to identify and respond to the renewed desires of customers, and monitoring the performance of cost management in other companies in order to address and confront competitors' threats and increase productivity.
2. Focusing on multiple analytical concepts that improve the strategic activities of the company, as these concepts provide a broader understanding of cost management due to its dependence on the strategic dimension of cost, and its various methods lead to improving profitability, rationalizing costs, and achieving competitive advantage.
3. Focusing on gaining customer satisfaction, achieving an increase in profits, and maximizing the company's competitiveness.
4. Activate the role of senior management in consolidating and supporting the achievement of the desired strategic objectives to improve the strategic position of the company.

4.3. THE IMPORTANCE OF STRATEGIC COST MANAGEMENT:

https://doi.org/10.17993/3cemp.2023.120151.440-461

The importance of strategic cost management lies in the following: (previous source, 2018: 474).

1. Helps management to plan properly, whether in the short or long term.
2. Contribute to increasing the company's ability to face intense competition.
3. It helps the company to have a continuous competitive advantage.
4. Enables the company to use resources effectively.
5. Availability of opportunities for the participation of all administrative levels in the decision-making process.
6. Develop strategic thinking among managers and make them take the initiative to make events and not be recipients of them.

4.4. METHODS OF STRATEGIC COST MANAGEMENT:

The methods of strategic cost management work to reduce the costs of sustainable development in industrial companies through a set of methods that work with each other through the different stages of the product life cycle. These methods are: (Ahmed, 2017: 37) and (Khalifa et al., 2018: 476).

A. The target costing method: It is a system that begins with designing the desired characteristics of the product and the appropriate price for the product, then the project activities are controlled, which helps to reach the allowable cost that enables the company to achieve its profits. This method works to reduce costs with an emphasis on ensuring the achievement of product quality, by studying all the ideas proposed to reduce costs during the early stages of the product's life (product planning design stage).

B. The value engineering method: It is a systematic application of specific methods through which product functions are determined, the value of each function, and an attempt to reach the best job performance at the lowest cost. This method works to identify marginal jobs that do not add value to customers and get rid of them. It also provides the company with a modern way of thinking and dealing with the modern industrial environment by focusing on its most important stages, which is the design stage, through which at least 80% of the cost is pledged. Product cost.

C. Activity-based cost method: It is a methodology for addressing indirect industrial costs by identifying the activities necessary to perform operations in the company, allocating resources to activities, and then reallocating activity costs to products according to the consumption of each activity. This method seeks to reduce costs and optimal use of available resources without extravagance. It takes a broader dimension through the analysis of activities, and thus it bypasses the drawbacks of traditional methods by providing detailed information about activities, costs and their causes, and excluding valueless activities.

D. Just-in-time production method: It is a philosophy of inventory management, which focuses on policies, procedures, and attitudes by managers that result in the

https://doi.org/10.17993/3cemp.2023.120151.440-461

efficient production of high-quality goods while maintaining the lowest possible level of inventory. This method works to reduce costs by getting rid of the quantities of inventory and reaching its lowest level, and as a result, the money invested in inventory decreases and the costs associated with this investment decrease. Optimum utilization of production capacity and without wastage.

E. The method of total quality management: It is the concerted efforts of managers and employees in a distinct manner to achieve the expectations of customers, by focusing on the quality of performance in the first stage, in order to reach the required quality at the lowest cost and the least time. This method works to reduce costs by searching for high levels of quality that lead to lower costs and getting rid of defective production, which will undoubtedly cost the company additional costs, so the total quality management method is the essence of the reduction process that leads to cost reduction without compromising the quality the product.

F. Benchmarking method: It is the process by which the company's performance is compared with other companies with outstanding performance in the same sector. This method works to reduce costs by adopting some of the methods used by competitors in managing costs, and this method is an incentive and a catalyst for generating ambition in the company's management for the purpose of reaching the level of competition with other companies.

G. The balanced scorecard method: It is a tool to stimulate the performance of the business unit by focusing on four main perspectives, including the financial perspective, the customers perspective, the operations perspective, and the education and growth perspective. New perspectives have been added to the balanced scorecard, namely the risk perspective and the societal perspective, to become six perspectives, which gives a balanced picture of the current operating performance and the causes of future performance.

The balanced scorecard method seeks to reduce costs in all its dimensions by reducing waste of resources, reducing costs, providing high quality products, focusing on the production process, innovation and development of products according to the wishes of customers and within the appropriate time.

The following figure shows the methods of strategic cost management:

https://doi.org/10.17993/3cemp.2023.120151.440-461

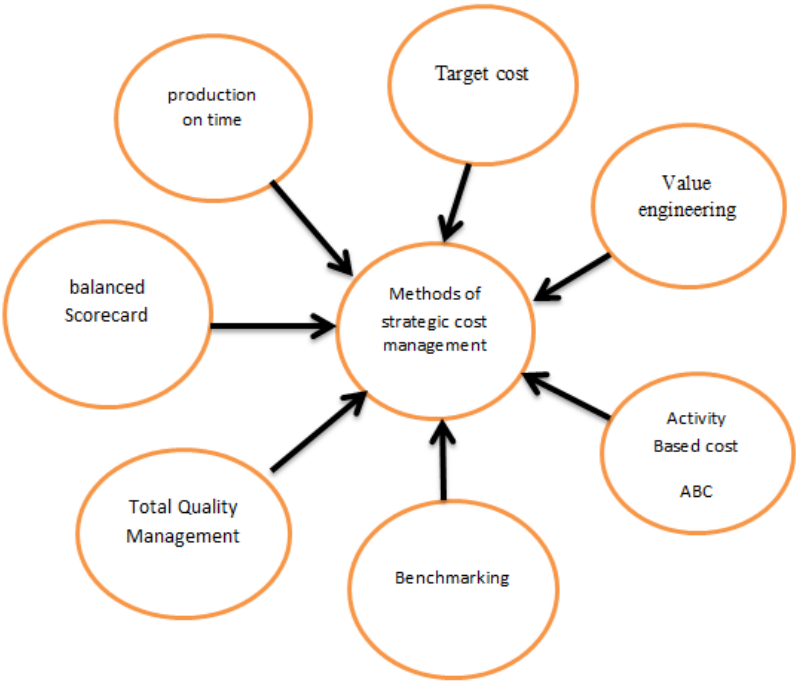

Figure 1. Methods of strategic cost management. (Source: Prepared by the researcher)

4.5. RESEARCH TOOLS:

A questionnaire was designed for the purpose of obtaining appropriate and accurate answers, and the following matters were taken into account when designing the questionnaire:

1. A five-point Likert scale was used and weights were given to the answers as follows:
   (Strongly agree 5, agree 4, neutral 3, disagree 2, strongly disagree 1).
2. The reliability was tested by calculating the alpha value of the variables, and all of them were greater than (0.9), and this indicates the consistency of the variables.
3. The validity and reliability of the questionnaire was calculated according to the correlation factor (Pearson) between all the axes of the questionnaire, and the values of the correlation factor were at the level of significance (0.5).
4. The SPSS program was approved for data analysis.

4.6. THE STUDY POPULATION AND THE STUDY SAMPLE:

Cement factories and brick factories were selected in Al-Muthanna Governorate / Iraq. (200) questionnaires were distributed, and the number of questionnaires retrieved from them was (175) questionnaires.

The following table shows the number of questionnaires distributed and the percentage of each:

https://doi.org/10.17993/3cemp.2023.120151.440-461

Table 1. Forms distributed to workers in laboratories

Samples	Number	Ratio
Cement plants	95	54%
Bricks plants	80	46%
Total	175	100%

The previous table shows the following:

1. The number of correct questionnaires for cement plants is (95), with a rate of 54%.
2. The number of correct questionnaires for the brick plants is (80), with a rate of 46%.

4.7. RESULTS OF HYPOTHESIS TESTING:

First Hypothesis: There is a relationship between the use of strategic cost management methods and the reduction of sustainable development costs:

Table 2. Choose the simple regression coefficient to determine the effect of using strategic cost management methods in reducing the costs of sustainable development

Samples	Pearson correlation factor	Regression factor	Difference
Cement plants	0.975	0.963	0.037
Bricks plants	0.980	0.975	0.025

Table 3. ANOVA analysis of variance

Samples	Freedom degree	F value	Sig.	Ratio of Regression	Difference Ratio
Cement Plants	1 94	1665.592	0.000	96.3%	3.7%
Bricks Plants	1 79	3330.126	0.000	97.5%	2.5%

Through the simple regression analysis table, we find that the value of the correlation factor between the two variables is (0.975) for the cement plants, and (0.980) for the bricks plants. It is a significant value at the level of significance (0.05) and at the level of significance (0.000). Through the results of the regression factor, we find that there is a direct relationship between the methods of strategic cost management and reducing the costs of sustainable development by (96.3%) for the cement plants and by (97.5%) for the brick plants. Significance level (0.05).

This confirms the significance of the regression. Thus, we conclude that the strategic cost management methods work to reduce the costs of sustainable development in each of the cement and brick plants.

https://doi.org/10.17993/3cemp.2023.120151.440-461

Second Hypothesis: There is a relationship between reducing the costs of sustainable development and achieving competitive advantage:

Table 4. Testing the simple regression coefficient to determine the effect of achieving competitive advantage in reducing the costs of sustainable development

Samples	Pearson correlation factor	Regression factor	Difference
Cement plants	0.948	0.935	0.065
Bricks plants	0.984	0.952	0.028

Table 5. ANOVA analysis of variance

Samples	Freedom degree	F value	Sig.	Ratio of Regression	Difference Ratio
Cement Plants	1 94	6010.512	0.000	93.5%	6.5%
Bricks Plants	1 79	5435.510	0.000	95.2%	2.8%

Through the simple regression analysis table, we find that the value of the correlation between the variables amounted to (0.935) for the cement plants and (0.952) for the brick plants at the level of significance (0.05) and the level of significance (0.000). By determining the regression factor, we find that there is a direct and significant relationship between Achieving the competitive advantage and reducing the costs of sustainable development by (93.5%) for the cement coefficient and (95.2%) for the brick factor, at the level of significant significance (0.05), depending on the F value, which reached (6010.512) for the cement plants and (5435.510) for the plants of bricks.

Thus, we conclude that reducing the costs of sustainable development leads to achieving a competitive advantage for each of the cement and brick plants.

Third Hypothesis: There is a relationship between reducing the costs of sustainable development and making strategic decisions:

Table 6. Testing the simple regression coefficient to determine the impact of strategic decision-making in reducing the costs of sustainable development

Samples	Pearson correlation factor	Regression factor	Difference
Cement plants	0.945	0.924	0.076
Bricks plants	0.979	0.965	0.035

https://doi.org/10.17993/3cemp.2023.120151.440-461

Table 5. ANOVA analysis of variance

Samples	Freedom degree	F value	Sig.	Ratio of Regression	Difference Ratio
Cement Plants	1 94	320.722	0.000	92.4%	7.6%
Bricks Plants	1 79	4325.120	0.000	96.5%	3.5%

Through the previous table for simple regression analysis, we find that the value of the correlation factor for the cement plants was (0.945) and for the brick plants was (0.979) with a significant (0.05) and at the level of significance (0.000), and through the results of the regression factor we find that there is a direct relationship between taking Strategic decisions and reducing the costs of sustainable development, as the percentage reached (92.4%) for cement plants and (96.5%) for brick plants, with a significant (0.05) and at the level of significance (0.000), depending on the value of F, which amounted to (320.722) for cement plants, amounting to (4325.120). for brick plants.

Thus, we conclude that reducing the costs of sustainable development leads to assistance in making strategic decisions for each of the cement and brick plants.

5. CONCLUSIONS AND RECOMMENDATIONS

5.1. CONCLUSIONS:

1. There is a direct relationship between the methods of strategic cost management and reducing the costs of sustainable development in industrial companies.
2. There is a direct relationship between reducing the costs of sustainable development and achieving the competitive advantage of industrial companies.
3. There is a direct relationship between reducing the costs of sustainable development and making strategic decisions in industrial companies.
4. Reducing the costs of sustainable development in the Iraqi industrial environment is important and leads to raising the level of quality of products and achieving an increase in the competitive process between companies.
5. Assisting senior management in making strategic decisions for the purpose of achieving sustainable development at the lowest costs, which achieves long-term benefits.
6. Reducing the costs of sustainable development requires working as one team within companies and building a good relationship between managers and employees, which serves to achieve the goal of sustainability.
7. The existence of a good cost system through the use of modern methods that are in line with developments that have taken place in the contemporary business environment leads to a reduction in the costs of sustainable development.

https://doi.org/10.17993/3cemp.2023.120151.440-461

8. Adopting the achievement of sustainable development requires the state to put in place laws and legislations that are binding to protect and preserve the environment, as well as preserve natural resources and encourage factories to achieve sustainable development through the use of modern and environmentally friendly equipment.

5.2. RECOMMENDATIONS:

1. The senior management of industrial companies should use modern cost strategic management methods to reduce costs, because these methods provide accurate, reliable and timely information that helps management in making various decisions and achieving competitive advantage.
2. The senior management should provide adequate support to the departments to ensure the achievement of sustainable development practices, with the aim of raising production efficiency, improving the quality of products and reducing their costs.
3. Work to intensify academic and applied research and studies on the methods of strategic management of modern costs, due to their ability to reduce the costs of sustainable development and keep abreast of developments that have taken place in the contemporary industrial environment.
4. Workers in all departments must be trained in order to raise awareness of the importance of sustainable development at the state level and at the level of economic units.
5. Holding courses, conferences and workshops, which helps in creating sustainable awareness among all officials, workers and citizens, which helps in solving many economic, environmental and social problems.
6. Integrating the economic, environmental and social dimensions of sustainable development in factories, which leads to a comprehensive improvement in production processes and the preservation of the environment and the social environment.
7. The need to improve and develop production systems and techniques by defining product specifications that meet the economic, environmental and social requirements and fulfill the desires of customers, and then compare them with the production standards of international factories and benefit from their experiences.

REFERENCES

(1) Ahmed, Khalifa Saud and others. (2018). **A proposed accounting framework to rationalize the costs of sustainable development. A** *comparative study, research published in the Journal of Environmental Sciences, Institute of Environmental Studies and Research, Ain Shams University*, 44, Part Two.

https://doi.org/10.17993/3cemp.2023.120151.440-461

(2) Sorour, Manal Jabbar. (2019). **Strategic Cost Management.** *University of Baghdad, College of Administration and Economics, Department of Accounting, second edition, Al Jazeera Printing and Publishing, Al Waziriyah, Baghdad, Iraq*.

(3) Ahmed, Mohamed Othman Ibrahim. (2017). **Strategic cost management and its role in controlling costs and making administrative decisions.** *A doctoral thesis submitted to the Sudan University of Science and Technology, College of Graduate Studies.*

(4) Zorob, Hamdi Shehdeh Mahmoud. (2013) **An integrated approach to strategic cost management to support the competitiveness of service sector companies.** *A field study, research published in the Journal of the Islamic University for Economic and Administrative Studies, 21(1), 29-77.*

(5) Al-Kubaisi, Amer Khader and others. (2019). **Studies on Entrances to Sustainable Development.** *Naif University Publishing House, 2019, Riyadh, Naif Arab University Press for Security Sciences.*

(6) Abdul-Ghani, Muhammad Mufti. (2020). **The development of the concept of sustainable development, its dimensions and results.** *Scientific Journal of Economics and Trade, Beni Suef University*, 401-468.

(7) The United Nations. (2015). **Transforming Our World.** *The 2030 Agenda for Sustainable Development.*

(8) Al-Harbi, Abdulaziz Selim. (2019). **The Economic Approach: Studies on the Approach to Sustainable Development.** *Naif University for Security Sciences, Riyadh.*

(9) Al-Taher, Muhammad Qadri. (2010). **Sustainable Development in the Arab Countries between Theory and Practice.** *Dar Al-Hussein, Dar Hanna for Publishing and Distribution, Amman.*

(10) Ghoneim, Othman Muhammad, Abu Zant, Magda Ahmed. (2007). **Sustainable development, its philosophy, methods of reducing it, and methods of measuring it.** *Dar Al-Safaa, Amman.*

(11) Al-Razzaq, Asmaa Muhammad Abd. (2012). **The Relationship of Environmental Costs and Product Life Cycle with Application in the General Company for Batteries Industry**. *A research published in the Journal of the College of Administration and Economics, University of Baghdad, Journal of Economic and Administrative Sciences*, 18(68).

(12) The International Committee for Environment and Development. (1989) **Our Common Future** (translated by Muhammad Kamel Aref). *World of Knowledge Series*, 142. National Council for Culture, Arts and Literature, Kuwait.

(13) Mahmoud, Ali Ashraf Hassan. (2010). **Strategic Cost Management to Maximize the Value of the Firm and Strengthen Competitive Advantages.** *Exploratory Study, Master's Thesis, Alexandria, Alexandria University, Faculty of Commerce*, 15.

(14) Khalaf, Abdel-Mahmoud Hamida. (2004). **The role of value chain analysis in cost management in educational facilities.** *Benha, Zagazig University, Faculty of Commerce, Benha, Journal of Commercial Studies and Research*, 1(76).

(15) Food and Agriculture organization (FAO). (1989). **Frost rehabilitation, technology transfer, environmental policies.** *Environmental degradation deforestation. Tropical forests.*

https://doi.org/10.17993/3cemp.2023.120151.440-461

(16) United Nations, conference on environmental and development (UNCED). (1992). **Earth summit report.**

(17) Anderson, Shannon,W. (2005). M**anagement costs and cost structure throughout the value chain.** *International journal of Quality and reliability management*, 22(4).

(18) Barbire, E. (1987). **The concept of sustainable economic development**. *Environmental conservation*, 14(2), 101-110.

(19) Harris, jonathan, M. (2003). **Sustainability and sustainable development.** *International society for ecological economics journal.*

(20) Stefanie, pfahl. (2005). **Institutional sustainability.** *International journal for sustainable development*, 8.

(21) Devilal, Shama. (2017). **Application of cost Reduction Tools in Manufacturing organization at pokhara.** *Janaprya. journal of international studies*, 6(Dec 14), 45-59.

(22) Akeem, Lawal Babatunde. (2017). **Effect of cost control and cost Reduction Techniques in organizational performance.** *International Business and Management*, 14(3).

(23) Goetsch, David L. Davis, Stanley B. (2010). **Quality Management for organization Excellence.** *Introduction to total Quality, 6th ed, pearson eduction, New Jersey. USA.*

(24) https://vmec.org/cost-reduction-strategies.

https://doi.org/10.17993/3cemp.2023.120151.440-461

/25/

THE INFLUENCE OF USING SUSTAINABLE MATERIALS ON PAVING COST OF AL-KUT-MAYSAN HIGHWAY USING COST-BENEFIT ANALYSIS

Sajjad Hashim*

College of Engineering, Al-Nahrain University, Baghdad, Iraq

sajjadhashimm2@gmail.com

Hasan Al-Mosawe

College of Engineering, Al-Nahrain University, Baghdad, Iraq

Reception: 21/11/2022 **Acceptance**: 20/01/2023 **Publication**: 08/02/2023

Suggested citation:

H., Sajjad and A., Hasan. (2023). **The Influence of Using Sustainable Materials on Paving Cost of AL-Kut-Maysan Highway Using Cost-Benefit Analysis**. *3C Empresa. Investigación y pensamiento crítico, 12(1)*, 463-478. https://doi.org/10.17993/3cemp.2023.120151.463-478

ABSTRACT

Paving is regarded as one of the essential layers in the construction of a road since it directly affects traffic loads and is subject to environmental factors. As a result, appropriate asphalt mixes that can support the designed traffic loads and environmental conditions must be developed. From an economic and environmental aspect, recycling the waste from the old pavement is a good step in this regard. This paper comprises detailed laboratory work that tested the impact of using different recycled asphalt pavement (RAP) content in addition to 3% crumb rubber (CR). The (CR) is used as fine aggregate. The tests were evaluated based on the response of hot asphalt mixes (HMA). The objectives of this study are to analyze the volumetric or weight change in hot mix asphalt of the different percentages and then analyse the costs of Kut-Maysan Road as a case study in case of using the different percentages of RAP and CR. The results show that the cost analysis of using RAP reduces the cost of a produced ton of HMA. On the other hand, the use of CR increases the cost of producing HMA. Using 10% RAP reduces the cost of one ton of HMA by 0.64 $ while using 20% RAP reduces the cost by 1.10 $, and the cost is reduced by 1.41 $ when using 30% RAP. On the other hand, the use of 3% CR with 10% RAP increased the production cost of one-ton HMA by 1.47 $. While decreased by 0.82 $ with 20% RAP content and by 0.28 $ with 30% RAP.

KEYWORDS

Sustainable Materials, pavement costs, cost-benefit analysis, Recycled asphalt pavement, crumb rubber

https://doi.org/10.17993/3cemp.2023.120151.463-478

PAPER INDEX

https://doi.org/10.17993/3cemp.2023.120151.463-478

INTRODUCTION

A road pavement in both types (flexible and rigid) is a structure which is made of multi-layers of processed and compacted materials, which have different thicknesses due to a special design consideration that is found in both bound and unbound forms. These forms are forming a structure that has a primary mission that is supporting the loads applied by vehicles in addition to providing a smooth riding quality [1]. Flexible pavements are most commonly used [2]. When bituminous material is added to granular materials to be bounded and then placed over granular layers such as base and sub-base layers that are supported by a sub-grade layer, this is called a flexible pavement System. The loads applied by vehicles are distributed with depth after being absorbed [1]. Paving is regarded as one of the essential layers in the construction of a road since it primarily affects traffic loads and is exposed to environmental factors. Asphalt mixtures must therefore be made in a way that is capable to manage the designed traffic loads and weather conditions. In this light, the process of recycling the waste of the previous paving is a useful move from an economic and environmental point of view. reusing recycled paving materials RAP was first used in 1915, but its extensive use began in 1970 during the Arab oil embargo, which increased the price of virgin bitumen and was the major reason for the rise in the usage of RAP in significant amounts [3,4]. RAP is regarded as one of the greatest aggregate choices for the production of asphalt paving using hot, cold, or warm mixing processes. RAP can be recycled using plants or on the job site. The previous researches show that using RAP when making asphalt mixture resulted in superior mechanical qualities than using the regular mixture.

RECYCLED ASPHALT PAVEMENT (RAP) AS A SUSTAINABLE MATERIAL

The majority of US institutes state that adding RAP in amounts of 15% or less to asphalt mixtures does not affect whether bitumen is added., i.e. RAP is regarded as black rocks, but if its percentage exceeds this limit (15%), the amount of bitumen must be adjusted, therefore RAP is no longer regarded as a black rock. [4,5]. produced an asphalt mixture containing 50% of RAP and 50% virgin materials and made a hot asphalt mixture but added the proportion of bitumen half the calculated percentage assuming that the RAP contained bitumen to evaluate the performance of asphalt mixtures containing RAP materials [6]. reported that adding 20% of RAP to the hot asphalt mixture of the surface layer with the addition of a regeneration agent of 10% by weight of bitumen resulted in higher rutting resistance than the reference mixture, as the rutting depth of the mixture containing 20% of RAP was (7.6) mm, while the rutting depth of the reference mixture was (8.2) mm after (20000) passes which made the mixture containing RAP had higher resistance to rutting than the reference mixture. In Iraq, RAP has not been used in road construction or maintenance yet, but there are laboratory studies from several researchers in Iraq to support the use of RAP and to get benefit from it applying these research outcomes [7]. used an advanced technique, Nano-indentation to investigate the level of blending between

https://doi.org/10.17993/3cemp.2023.120151.463-478

RAP and virgin materials for a mixture incorporating some warm additives such as; Sasobit, Rediset WMX and Rediset LQ and concluded that RAP cannot be considered as black rocks even with the inclusion RAP materials up to 40%. Furthermore, a novel protocol was reported to find a complete blend between RAP and virgin materials [8]

CRUMB RUBBER (CR) AS A SUSTAINABLE MATERIAL

Modifying asphalt pavement materials have been begun many decades ago. The use of asphalt pavement incorporating rubber first appeared in the 1840s aimed to test the ability of rubber to make paving surfaces last longer due to its flexibility [12, 13]. Using recycled rubber for tires (crumb rubber CR) in the flexible pavement enhances asphalt pavement performance, sustainability and cost. In the last decades, considerable attention has been growing to the use of CR. Several previous studies have indicated several improvements in the flexible pavement, such improvements were resistance to pavement rutting, reduced costs of pavement construction and maintenance, and enhancing the ability of pavement to resist fatigue cracks [14]. CR is then added to modify the physical and chemical characteristics of asphalt cement that is utilized to produce pavements containing rubber. There are two methods adopted to add CR dry process and the wet process. in a comparison of these methods, the dry method is simpler and more limited than the wet method [13,14].

PAVEMENT STRUCTURAL DESIGN

The method of constructing the most cost-effective mix of pavement layers, taking into account both type of material and depth to fit the soil foundation and vehicular load throughout the design phase, is known as pavement design. The design of pavement constructions might well be carried out with a variety of techniques. One of the widely authorized design methods is the AASHTO design procedure. The AASHO design procedure was established as a result of empirical equations that were developed as a result of the AASHO Road Test, which was conducted in Ottawa, Illinois, from 1956 to 1960. Experience and experimentation are key components of an empirical approach. This means that experiment, experience, or a mix of the two are used to determine the relationship between the input factors and the design thicknesses. As a result, the AASHTO methodology is limited to the circumstances and material types used in the AASHO Testing [9].

THE COST-BENEFIT ANALYSIS

The cost analysis was completed by calculating the savings of implementing RAP in each highway application. It must be recognized that this approach to cost analysis primarily aims to identify material cost savings. When adding RAP and CR to the mix, it simply considers the decrease in resources such as aggregate and asphalt cement. Decreased usage of large quantities of these expensive materials results in savings. Based on the similarity in these procedures between recycled and virgin materials, the costs associated with transporting, milling, placing, and compacting are not included

https://doi.org/10.17993/3cemp.2023.120151.463-478

in this cost analysis. Additionally ignored are social and environmental benefits, whose worth is hard to quantify and differ between projects [15].

STUDY OBJECTIVES

The objectives of this study can be summarized as follow:

1. To seek out Marshall test response in case of the addition of RAP and CR as an aggregate replacement in Hot Mix Asphalt HMA.
2. For determining Marshall stability of asphaltic mixes as well flow, and bulk density. These mixtures are containing three percentages of RAP which are 10%, 20% and 30% then adding 3% CR to these percentages.
3. To estimate the optimum asphalt content by conducting a Marshall Stability test for virgin mix, 20% RAP-containing mix, and 30% RAP-containing mix.
4. To analyze the volumetric or weight change in hot mix asphalt of the different percentages.
5. Cost analysis calculation of Kut-Maysan Road as a case study in case of using the different percentages of RAP and CR.

MATERIALS

The material used in this research are all available in local areas and are widely utilized for pavement construction nationally. One asphalt concrete was used in this study which was a binder course. One type of asphalt binder, one type of aggregate gradation, and one type of mineral filler were used. The properties of the materials selected are described in the following subsections.

MINERAL AGGREGATE USED

The mineral aggregate utilized in the tests of this study was natural aggregate collected from Badra quarries in Wassit Governorate. To fulfil the binder course degree as expected by the SCRB standards [13].

Table 1. Physical properties of aggregate

Physical properties	Specification no.	Coarse Aggregate	Fine Aggregate
Bulk Specific Gravity	ASTM C-127 and C-128	2.583	2.668
Apparent Specific Gravity	ASTM C-127 and C-128	2.546	2.633
(%) Water Absorption	ASTM C-127 and C-128	0.369	0.48
Los Angelo's	ASTM C 131	13	-

https://doi.org/10.17993/3cemp.2023.120151.463-478

This aggregate is commonly used for asphaltic mixes in Kut city- Wassit Province in Iraq. Aggregates in both gradations (fine and coarse) which were used in this work had been sieved and remixed to the right extent. To assess the physical characteristics, typical standard tests were conducted on the aggregate. Table 1 above shows the summary of the test results. The results of these tests show that the aggregate being chosen met the specifications for the SCRB.

MINERAL FILLER

Fine-grained mineral aggregates that are either normally found in the aggregate system or that are added externally to it make up the mineral filler utilized in asphalt mixes. The percentage of aggregates that pass through a 0.075 mm sieve is a common definition for it. The filler utilized herein stands for Portland cement produced from Crista Factory in north Iraq. The characteristics of filler are illustrated in Table 2 below which shows that all results are acceptable and dependable

Table 2. Physical characteristics of the filler

Property	Result
Specific gravity	3.14
Per cent passed No.200 sieve (0.075mm)	100%

ASPHALT CEMENT AC

In this work, penetration of (40-50 mm) asphalt cement grade was utilized. Which was brought from the refinery that lies in Al-Duarah, southern side of Baghdad, with PG (64-16). The physical properties of this asphalt cement are described in Table 3 below. The results show that the physical properties of asphalt cement used met the requirements of the specification.

Table 3. Physical characteristics of asphalt cement AC

Test	Standard	Unit	Result	Specification Requirement
Penetration of bitumen At 25˚C,100 gm,5 sec. (0.1mm).	ASTM D 5-06	1/10mm	44.6	40-50
Ductility of bitumen at 25˚C, 5cm/ min, (cm).	ASTM D 113-07	(cm)	108	≥100
Flash Point (Cleveland open cup)	ASTM D 92-05	(˚C)	280	≥230
Bitumen's specific gravity (25 ˚C).	ASTM D 70-08	----	1.02	----
Softening Point	----	(˚C)	48	Not Limited

THE RECYCLED ASPHALT PAVEMENT (RAP)

The recycled (or reclaimed) asphalt pavement (RAP) that was utilized in the study was excavated from a road lying in Al-Kut city, Wassit Province in Iraq. RAP used was

https://doi.org/10.17993/3cemp.2023.120151.463-478

15 years in service which claimed from different layers of pavement (service layer, binder layer, and base layer). The RAP was also sieved and recombined in the right proportion of gradation for the binder layer. The graduated recycled asphalt pavement was added to the asphalt mixture with (10%, 20%, and 30%) percentages.

THE CRUMBED RUBBER (CR)

One of the sustainable materials used in the study is the polymer, represented by crumbed rubber of cars' tires as waste materials, which was brought from a hashing factory in Al-Diwanyeh town in Iraq. The crumbed rubber was used as a 3% replacement from 2.36 mm and 300 µm. of fine aggregate gradation which will be referred to later as 3% CR. This replacement is used as a combination addition with the 10%, 20%, and 30% RAP as a virgin aggregate replacement. Table 4 Below shows the physical properties of the crumb rubber used.

Table 4. Physical characteristics CR used.

Property	Result
Colour	black
Moisture content (%)	< 0.75
Textile Content	< 0.65
Max. Density ; C.N.R UNI-1, ASTM C128, UNE 12597-5:2009	(%Ø0.4-2.36mm ; %Ø2.36-4.75mm)
Max. specific gravity for rubber (gm/cm3)	1.16

STUDY METHODOLOGY

The study methodology can be summarized in 4 states as follows:

1. Specimens of the virgin mix and recycled mixtures were prepared depending on the Marshall mix design method (ASTM D1559). 15 samples were prepared for the virgin mix with 100% virgin aggregate using (4%, 4.3%, 4.6%, 4.9%, and 5.2%) asphalt cement per cent for every 3 samples. Then the optimum binder content OBC was determined. The same procedure was followed for mixtures containing 20% RAP, and 30% RAP. Then the Marshall test was conducted for 3 samples of mixtures mixed with the OBC for comparison.
2. Calculation of the depth of binder course for a segment of 6 km. of Kut-Missan highway as a case study.
3. Calculation of asphalt concrete materials quantities to be used in Kut-Missan highway as a case study.
4. Cost analysis of the materials used

https://doi.org/10.17993/3cemp.2023.120151.463-478

MARSHALL SPECIMEN SAMPLING

1. After washing the aggregate it was dried in the oven at 110 Cº for 24 hours for wiping moisture content as it may increase falsely the weight of aggregate.
2. Sieving the aggregate and distributing it as binder course gradation as it separated into groups as retained on each of the following sieves (25 mm, 19 mm, 12.5 mm, 9.5 mm, 4.75 mm, 2.36 mm, 300 am, 75 µm, and pan) using dry sieve analysis.
3. Weigh of aggregate retained on the pan has been replaced with mineral filler (Portland cement).
4. Each sample of Marshall specimen is weighing 1200 gm. Which means that 3600 gm. For every 3 samples, An addition of 2000 gm. aggregate was added to conduct volume-specific gravity (Gmm).
5. This procedure was used to determine the O.B.C. for the control specimen, 20% RAP and 30% RAP. Then depending on the result of this step the OBC that has been determined has been used for the virgin mix and mix with 10% RAP.

MARSHALL SPECIMEN MIXING

Marshall Tests were conducted to calculate the volumetric properties of mixes. The volumetric properties included mass/bulk density, sample air voids (AV), voids filled with bitumen (VFB), Marshall Stability, and flow. The Optimum asphalt content (OBC) for the reference mix and RAP were settled from the plots of stability, AV, VFA, flow, density, and VMA. The bulk specific gravity of every sample was entirely settled by test techniques D2726, D1188, or D6752.

CASE STUDY

The case study of this research was a highway that lies in Kut city, Wassit province of Iraq, which is a highway that is supposed to be reconstructed due to a huge failure in serviceability. The highway information is listed in table 5 below:

Table 5. AL-Kut-Maysan Highway information

property	information
Location information	Lies in Wassit Province and it is considered as Al-Kut city entrance from Maysan Province
Coordinates of the centre line	N 576723 E 358049 N 584771 E 3603902
length	10 km
Number of lanes	3 per direction
Length width	3.75

https://doi.org/10.17993/3cemp.2023.120151.463-478

STRUCTURAL DESIGN OF LAYERS USING PCASE APPLICATION

PCASE is mandated for all vehicle types operating from outside the United States and its territories and possessions, as well as for highways and parking lots. Anyone can utilize PCASE, which is a computer software designed by the Engineer Research and Development Center (ERDC) of the United States Army Corps of Engineers (USACE). The criteria for compaction and pavement thickness may be determined using PCASE. This program was used to calculate the thickness of the binder course asphaltic concrete layer. (CODE,2016)

QUANTITIES AND COSTS ANALYSIS

After the determination of the depth of the binder course, the quantities required for preparing asphalt concrete that was required to surface the highway were calculated depending on the volumetric analysis and on the properties of asphalt concrete individuals that are conducted practically in the laboratory. The cost of individual materials was adopted depending on local prices (according to the local Government and Al-Kut Municipality) but converted to American dollars. Cost analysis of different layers was calculated depending on (NAPA, 2007)

EXPERIMENTAL RESULT

RESULTS OF USING RAP AND CR

The result of using RAP and CR after conducting the optimum binder content OBC is shown in Table 6 below:

Table 6. Effect of RAP on Marshall characteristics

Sample	OBC (%)	Stability (kN)	Flow (mm)	Density (gm/cm3)	AV%	VFA %	VMA %
Virgin	4.55	11.28	3.305	2.329	3.741	68.92	12.04
10 % RAP	4.55	18.03	2.197	2.327	3.653	70	12.14
RAP+CR	4.55	17.467	2.623	2.324	3.705	69.69	12.22
20 % RAP	4.336	18.65	2.143	2.297	3.367	74.62	13.27
RAP+CR	4.336	14.733	2.343	2.275	4.401	68.75	14.08
30 % RAP	4.167	19.53	3.087	2.304	3.212	75.32	13.02
RAP+CR	4.167	16.033	3.267	2.278	4.573	67.22	13.95

The result shows that Marshall stability continued to increase with any addition of RAP while decreasing slightly with the addition of CR, the same response appeared in percentages of voids filled with asphalt VFA% and voids in mineral aggregate VMA%.

https://doi.org/10.17993/3cemp.2023.120151.463-478

The value of density, air voids and flow decreased dramatically when using RAP concerning the virgin mix while increasing with the addition of CR.

DEPTH OF BINDER COURSE CALCULATION

According to the relationship between Marshall stability and resilient modulus of asphaltic mixtures that are found in AASHTO the following equation can be derived for values exceeding those in the chart:

$$M_r(psi) = \text{Marshall Stability in}(Kg) \times 483$$

When Mr: Resilient Modulus

The Mr. values were converted to (Mpa.) as a requirement for PCASE application entries. The other entries are shown in table 7 below as the information was taken from Al-Kut Municipality as a formal reference.

Table 7. PCASE application entries

Category	PCASE entry
PCASE Version:	24-08-2022 7.0.4
Design Name:	Binder
Layer Model Name:	Binder Course
Drainage Station:	Not selected
Frost Station:	Not selected
Pavement Use:	Roadway
Design Type:	Flexible
Traffic Area:	Road Areas
Analysis Type:	LED
Wander Width (mm):	847

The calculation of depth using the virgin mix gave the following results which are shown in Table 8:

Table 8. depth calculation of binder course layer for the virgin mix

Layer Type	Material Type	Analysis	Thickness (mm)	Modulus (MPa)	Poisson's Ratio	Bond
Asphalt Concrete	Asphalt Cement	Compute	197	3830.49	0.35	Fully Bonded
Subbase	Unbound Aggregate	Manual	300	107	0.35	Fully Bonded
Natural Subgrade	Cohesionless Cut	Manual	102	42	0.4	Fully Bonded

https://doi.org/10.17993/3cemp.2023.120151.463-478

QUANTITIES/COSTS ANALYSIS PROCEDURE

The quantities and costs related that are required for the 10 km of Al-Kut Maysan highway were determined depending on the following procedure :

1. The volume needed to be filled is calculated by the equation below

$$\text{Volume } (\text{m}^3) = \text{length (m)} \times (\text{lane width } \times \text{number of lanes}) \times \text{depth of layer (m)}$$

2. The mass of the mix is calculated in the equation below

$$\text{mass (ton)} = \frac{\text{Volume } (\text{m}^3) \times \text{specimen density } (\text{kg/m}^3)}{1000}$$

3. The mass of materials has been distributed by multiplying the weight per cent of individual material by the whole mass of the mix in step 2.
4. The cost of individual materials has been calculated according to the cost of unit mass or unit volume depending on local agencies' prices.
5. Calculating the approximate reduction in the cost of using RAP in Hot Mix Asphalt is explained in table 9 below:

Table 9. the approximate reduction in the cost of using RAP equations (NAPA, 2007)

A	Savings from Asphalt Cement: **New AC $/ton ( ) x AC % in Mix ( ) x % of RAP in Mix ( )**	$/ton
B	Savings from Fine Aggregate: $\left(\text{New Fine Agg.} \frac{\$}{\text{ton}}(\,)\text{x \% Fine Agg. in Mix }(\,)\text{x \% of RAP in Mix }(\,)\right) +$ $\left(\text{New Fine Agg.} \frac{\$}{\text{ton}}(\,)\text{x \% Fine Agg. in Mix }(\,)\text{x of CR in Mix }(\,)\right)$	$/ton
C	Savings from Coarse Aggregate: $\left(\text{New Coarse Agg.} \frac{\$}{\text{ton}}(\,)\text{x \% Coarse Agg. in Mix }(\,)\text{x \% RAP in Mix }(\,)\right) +$ $\left(\text{New Coarse Agg.} \frac{\$}{\text{ton}}(\,)\text{x \% Coarse Agg. in Mix }(\,)\text{x \% CR in Mix }(\,)\right)$	$/ton
D	Total Gross Savings per ton of Hot Mix (Add A + B + C)	$/ton
E	Less Acquisition Cost of RAP and CR (includes Trucking Cost): $\left(\text{Less Acq. Cost of RAP} + \text{Acq. Cost} \frac{\$}{\text{ton}}(\,)\text{x \% of RAP in Hot Mix }(\,)\right) +$ $\left(\text{Less Acq. Cost of CR} + \text{Acq. Cost} \frac{\$}{\text{ton}}(\,)\text{x \% of CR in Hot Mix }(\,)\right)$	$/ton
F	Less Additional Processing/Crushing of RAP and CR : $\left(\text{Less Add. Processing of RAP} + \text{Process Cost} \frac{\$}{\text{ton}}(\,)\text{x \% of RAP in Hot Mix }(\,)\right)$ $+\left(\text{Less Add. Processing of CR} + \text{Process Cost} \frac{\$}{\text{ton}}(\,)\text{x \% of CR in Hot Mix }(\,)\right)$	$/ton

https://doi.org/10.17993/3cemp.2023.120151.463-478

G	Less any Additional Miscellaneous Costs of RAP and CR : $\left(\text{Misc. Cost of RAP} + \text{Misce. Cost}\frac{\$}{\text{ton}}(\,)\text{x \% of RAP in Hot Mix}\,(\,)\right)+ \left(\text{Misce. Cost of CR} + \text{Misce. Cost}\frac{\$}{\text{ton}}(\,)\text{x \% of CR in Hot Mix}\,(\,)\right)$	$/ton
H	Net Savings per ton of Hot Mix Asphalt (D less E, F & G)	$/ton

QUANTITIES/ COSTS ANALYSIS

The results show quantities to be used in the project for any alternative of (virgin mix, 10% RAP, 10% RAP and 3% CR, 20% RAP, 20% RAP and 3% CR, 30% RAP or 30% RAP and 3% CR) are shown in the table below:

Table 10. quantities distribution of materials of the mixtures

mix	Mass of mix (ton)	Coarse aggregate (ton)	Fine aggregate (ton)	Filler (ton)	RAP (ton)	CR (ton)	Asphalt Cement (ton)
Virgin	103255.09	49355.93	43470.39	5926.84	0.00	0.00	10579.52
10 % RAP	103135.41	44390.00	39064.19	5919.97	9272.80	0.00	10547.86
RAP+CR	103037.90	44348.03	38016.14	5914.38	9264.03	1011.11	10537.89
20 % RAP	101814.53	39043.53	34349.98	5844.15	18345.65	0.00	9943.34
RAP+CR	100852.67	38664.60	33154.00	5788.94	18172.34	881.55	9849.40
30 % RAP	102107.07	34307.87	30201.13	5860.95	27642.32	0.00	9598.78
RAP+CR	101007.81	33938.52	29092.07	5797.85	27344.73	773.82	9495.45

The prices of materials in asphalt mixture in American dollars are shown in the table below:-

Table 11. prices of materials in asphalt mixture

Material	Price $ / ton
Coarse aggregate	6.06
Fine aggregate	3.85
filler	72
RAP	1.25
CR	175
Asphalt Cement	308

Depending on the prices in table 12 above the cost of every individual material can be calculated by the following equation.

$$\text{cost of material}\,(\$) = \text{weigh of individual material}\,(\text{ton})\ \text{x Price}\ \ (\$/\text{ton})$$

the results are shown in Table 13 below:

https://doi.org/10.17993/3cemp.2023.120151.463-478

Table 12. The cost of every individual material used in the asphalt mixtures is shown in the table below

mix	Coarse aggregate/ $	Fine aggregate/ $	Filler/$	RAP/$	CR	Asphalt Cement/$	Sum/$
Virgin	299126.86	167301.06	426732.6	0.00	0.00	1386591.9	2279752.4
10 % RAP	269030.28	150343.25	426238.0	11591.0	0.00	1382443.5	2239646.0
RAP+CR	268775.91	146309.71	425835.0	11580.0	176944.4	1381136.4	2410581.5
20 % RAP	236627.45	132200.05	420779.0	22932.0	0.00	1303212.0	2115750.7
RAP+CR	234330.88	127597.20	416803.9	22715.4	154271.8	1290900.4	2246619.7
30 % RAP	207926.51	116232.69	421988.1	34552.9	0.00	1258053.4	2038753.6
RAP+CR	205688.02	111964.34	417445.0	34180.9	135418.6	1244509.5	2149206.5

Now we can calculate the approximate reduction in costs of using RAP by using equations in table 10 and the procedure is shown in table 14 below:

Table 13. the approximate reduction in costs when using RAP and

	10 % RAP	RAP & CR	20 % RAP	RAP & CR	30 % RAP	RAP & CR
Savings from Asphalt Cement:	1.21	1.21	2.31	2.31	3.34	3.34
Savings from Fine Aggregate:	0.13	0.13	0.23	0.23	0.31	0.31
Savings from Coarse Aggregate:	0.23	0.23	0.42	0.42	0.55	0.55
Total Gross Savings per ton of Hot Mix	1.57	1.57	2.96	2.96	4.20	4.20
Less Acquisition Cost of RAP/CR	0.54	0.55	1.08	1.10	1.62	1.64
Less Additional Processing/ Crushing	0.25	1.92	0.5	2.02	0.76	2.08
Less any Additional Miscellaneous Cost:	0.13	0.58	0.27	0.66	0.41	0.75
Net Savings per ton of Hot Mix Asphalt	0.64	-1.47	1.10	-0.82	1.41	-0.28

As it is clear from table 13 above the use of RAP reduces the cost of a produced ton of HMA. As the use of 10% RAP reduces the cost 0.64 $ per ton. And any increase in RAP content will decrease the cost of a produced ton of HMA as it is reduced by 1.10 $ per ton when using 20% RAP and reduced by 1.41 $ per ton when using 30% RAP. The reverse effect of using RAP is shown by using CR as using CR increased the cost of producing one ton of HMA by 1.47 $ then reduces to 0.82 $ when using 20% RAP with it and to 0.28 $ when using 30% RAP with it. This reduction is due to the increase in RAP content not for using CR itself.

https://doi.org/10.17993/3cemp.2023.120151.463-478

CONCLUSION

Finally, we can conclude the following:-

1) The results of laboratory testing for the physical characteristics of mixtures show that the materials' properties utilized in this study all met the required specification.
2) From the Marshall Test result, the OBC for the virgin mix is 4.55%, RAP 20 is 4.336%, and RAP 30 is 4.167%. The OBC for mixtures with RAP dropped as the content of RAP was raised, which is due to the effect of the remaining asphalt in the RAP.
3) The use of RAP and CR results had better performance in Marshall Stability. Compared to the virgin aggregate mix, CR increased AV and RAP decreased it. VFA dramatically raised with RAP, but CR reduced the VFA as it increased AV.
4) The cost analysis shows that the use of RAP reduces the cost of a produced ton of HMA. And the reverse effect of using RAP is shown by using CR as using CR increased the cost of producing one ton of HMA.
5) Using 10% RAP reduces the cost of one ton of HMA to 0.64 $ while using 20% RAP reduces the cost to 1.10 $, and the cost is reduced to 1.41 $ when using 30% RAP.
6) Using 3% CR with 10% RAP increased the production cost of one-ton HMA up to 1.47 $. While decreased to 0.82 $ with 20% RAP content and to 0.28 $ with 30% RAP.

REFERENCES

(1) Dhir, R. K., de Brito, J., Silva, R. V., & Lye, C. Q. (2019). **Sustainable construction materials: recycled aggregates**. *Woodhead Publishing.*

(2) Minkwan Kim, A.M.ASCE, ErolTutumluer, M.ASCE and Jayhyun Kwon. (2009). **Nonlinear Pavement Foundation Modeling for Three-Dimensional Finite-Element Analysis of Flexible Pavementsll.** *International Journal of Geomechanics*.

(3) KANDHAL, P. S. J. J. O. T. A. O. A. P. T. (1997). **Recycling of asphalt pavements-an overview.** 66.

(4) Abdalhameed, A. M., & Abd, D. M. (2021). **Rutting Performance of Asphalt Layers Mixtures with Inclusion RAP Materials**. *Anbar Journal of Engineering Sciences*, 9(2).

(5) Mcdaniel, r. S. & Anderson, r. M. (2001). **Recommended use of reclaimed asphalt pavement in the Superpave mix design method: technician's manual**. *National Research Council (US). Transportation Research Board*.

(6) OLIVER, J. W. (2001). **The influence of the binder in RAP on recycled asphalt properties**. *Road Materials and Pavement Design*, 2, 311-325.

(7) PRADYUMNA, T. A., MITTAL, A., JAIN, P. J. P.-S. & SCIENCES, B. (2013). **Characterization of reclaimed asphalt pavement (RAP) for use in bituminous road construction**. 104, 1149-1157.

https://doi.org/10.17993/3cemp.2023.120151.463-478

(8) ABD, D. M., AL-KHALID, H. & AKHTAR, R. J. J. O. M. I. C. E. (2018). **A novel methodology to Investigate and obtain a complete blend between RAP and virgin materials**. 30

(9) Bekele, A. (2011). **Implementation of the AASHTO pavement design procedures into MULTI-PAVE.**

(10) CODE, D. B. (2016). **UNIFIED FACILITIES CRITERIA (UFC).**

(11) Pavements, R. H. M. A. (2007). I**nformation Series 123**. *National Asphalt Pavement Association, NAPA: Lanham, MD.*

(12) Heitzman, M.A. State of the Practice (1992). **Design and Construction of Asphalt Paving Materials with Crumb Rubber Modifier.** *Research Report No. FHWA-SA-92-022, 1339; Federal Highway Administration: Washington, DC, USA*, 1-8.

(13) Alfayez, S. A., Suleiman, A. R., & Nehdi, M. L. (2020). **Recycling tire rubber in asphalt pavements: state of the art**. *Sustainability*, 12(21), 9076.

(14) SCRB. (2003). **State Commission of Roads and Bridges, Standard Specification for Roads & Bridges, Ministry of Housing & Construction, Iraq.**

(15) Franke, R., & Ksaibati, K. (2015). **A methodology for cost-benefit analysis of recycled asphalt pavement (RAP) in various highway applications**. *International Journal of Pavement Engineering*, 16(7), 660-666.

CONFLICT OF INTEREST

The authors declare that the research was conducted in the absence of any commercial or financial relationships that could be construed as a potential conflict of interest.

https://doi.org/10.17993/3cemp.2023.120151.463-478


3C
empresa
Investigación y pensamiento crítico